Criblage, efficacité et modes d'action de composés de biocontrôle microbiens sur le pathosystème blé-Zymoseptoria tritici

Rémi Platel

THÈSE DE DOCTORAT

Pour l'obtention du grade de

DOCTEUR DE L'UNIVERSITÉ DE LILLE

École doctorale Sciences de la Matière, du Rayonnement et de l'Environnement
Discipline : Ingénierie des Fonctions Biologiques
UMR-Transfrontalière n°1158 BioEcoAgro

Criblage, efficacité et modes d'action de composés de biocontrôle microbiens sur le pathosystème blé-*Zymoseptoria tritici*

Rémi PLATEL

Soutenue publiquement à Lille, le 3 juin 2021

Jury :

Marielle ADRIAN, Professeure, Université de Bourgogne (Présidente du jury, Rapportrice)

Alain HEHN, Professeur, Université de Lorraine (Rapporteur)

Marie-Noelle BRISSET, Directrice de recherche, INRAe Angers (Examinatrice)

Philippe JACQUES, Professeur, Université de Liège (Examinateur)

Ali SIAH, Professeur, Junia-Université de Lille (Directeur de thèse)

Philippe REIGNAULT, Professeur, Université du Littoral-Côte d'Opale-ANSES (Co-directeur de thèse)

Monica HÖFTE, Professeure, Université de Gand (Invitée)

Maryline MAGNIN-ROBERT, Maître de conférences, Université du Littoral-Côte d'Opale (Invitée)

RÉSUMÉ

La septoriose, causée par le champignon hémibiotrophe *Zymoseptoria tritici*, est l'une des maladies les plus préjudiciables sur les cultures de blé, responsable de pertes de rendement pouvant atteindre 50%. La lutte contre cette maladie repose essentiellement sur l'utilisation des fongicides conventionnels et, dans une moindre mesure, sur le recours aux ressources variétales. Toutefois, en raison des résistances développées par l'agent pathogène vis-à-vis de ces leviers et d'une demande sociale croissante pour limiter l'utilisation des intrants chimiques en agriculture, des alternatives agroécologiques, comme le biocontrôle, doivent être développées. L'objectif de ce présent projet de thèse se situe dans ce contexte et vise à identifier des composés de biocontrôle efficaces sur le pathosystème blé-*Z.tritici* et à caractériser leurs modes d'action. Tout d'abord, un criblage *in vitro* d'un panel de 181 composés microbiens (extraits fongiques ou bactériens, rhamnolipides, lipopeptides, *etc.*) a été réalisé pour évaluer leur activité antifongique directe vis-à-vis de l'agent pathogène. Les composés les plus actifs ont ensuite été sélectionnés pour vérifier leur efficacité de protection *in planta*. Une étude de relation structure-activité a été menée avec 19 rhamnolipides (RL) et a révélé que ceux présentant des liaisons éthers ou esters, avec une chaine carbonée hydrophobe de 12 carbones, sont les plus efficaces pour toutes les activités biologiques testées (activité biocide, élicitation des défenses du blé et efficacité de protection). Parmi eux, le Rh-Est-C12 s'est montré le plus prometteur, avec une efficacité de protection de 78,9%. Le potentiel de ce RL, ainsi que de la mycosubtiline, un lipopeptide efficace pour protéger le blé contre *Z. tritici*, pour stimuler les défenses du blé, a été étudié à l'aide d'une approche combinée de transcriptomique et de métabolomique. Le RL n'a pas déclenché de modifications majeures de la physiologie foliaire de blé ; celui-ci protégerait donc l'hôte principalement *via* son activité directe vis-à-vis du champignon, alors que la mycosubtiline semble présenter un mode d'action double, basé sur une activité antifongique directe et la potentialisation des défenses du blé. Cette induction des défenses pourrait résulter de l'interaction de la mycosubtiline avec les membranes cytoplasmiques du blé, conduisant à une accumulation de flavonoïdes dans les feuilles, mais aussi à d'autres réponses dépendantes de la voie de l'acide abscissique. Ces travaux ont, par ailleurs, permis de mettre en évidence de nouveaux mécanismes dans les réactions de défense du blé vis-à-vis de *Z. tritici*. Enfin, deux nouvelles souches isolées de *Bacillus velezensis* ont présenté une activité antifongique prometteuse contre l'agent pathogène, résultant probablement de la production de lipopeptides, comme la bacillomycine D, dont l'activité sur *Z. tritici* mériterait d'être explorée.

Mots clés : Blé, *Zymoseptoria tritici*, biocontrôle, biofongicides, induction de défenses, bioprotection.

ABSTRACT

Septoria tritici blotch, caused by the hemibiotrophic fungus *Zymoseptoria tritici*, is one of the most severe diseases on wheat, responsible for yield losses up to 50%. Currently, strategies used to control this disease rely mainly on the use of chemical fungicides, and to a lower extent, on the use of partially resistant cultivars. Nevertheless, because of the pathogen resistances and an increasing social demand to reduce conventional pesticides in agriculture, new agroecological alternative crop protection methods, like biocontrol, must be developed. The main purpose of this thesis project was, therefore, to identify new effective biocontrol compounds on the wheat-*Z. tritici* pathosystem and to decipher their modes of action. An *in vitro* screening of a set of 181 microbial compounds (fungal and bacterial extracts, rhamnolipids, lipopeptides, *etc*.) was performed to assess their antifungal activity towards the pathogenic agent. The most active compounds were selected for further experiments, such as verifying their protection activity *in planta*. The ability of 19 rhamnolipids (RLs) to control the pathogen was explored and a structure-activity relationship study revealed that bioinspired RLs with ether or ester links and a 12 carbon hydrophobic fatty acid tail were the most effective for all tested biological activities (biocide activity, wheat defense elicitation and protection efficacy). Among them, Rh-Est-C12 was the most promising compound, with a protection efficacy of 78.9%. The potential of Rh-Est-C12 as well as mycosubtilin, a lipopeptide also effective to protect wheat against *Z. tritici*, to induce host defenses, was investigated using a combined transcriptomic and metabolomic approach. The RL did not trigger any major disorganization of the wheat leaf physiology, hence it would protect the host mainly through its direct activity towards *Z. tritici*, while mycosubtilin would display a dual mode of action, antifungal effect and plant defense priming. Mycosubtilin could prime wheat by interacting with its plasma membranes leading to flavonoid accumulation and other abscisic acid dependent responses. Besides, new insights into wheat defense mechanisms towards *Z. tritici* were reported. Finally, two *Bacillus velezensis* strains, isolated from wheat phyllosphere, displayed promising antifungal effect towards the pathogen. A characterization of their metabolites was performed and the putative role of bacillomycin D as a potent *Z. tritici* antifungal lipopeptide was suggested.

Key-words : wheat, *Zymoseptoria tritici*, biocontrol, bio-fungicides, defense induction, bioprotection

AVANT-PROPOS

Le laboratoire d'accueil dans lequel j'ai réalisé mon projet de thèse fait partie de l'Unité Mixte de Recherche transfrontalière (UMR-t) INRAE 1158 BioEcoAgro qui fédère plusieurs acteurs académiques de la région transfrontalière franco-belge travaillant dans le domaine de l'ingénierie biologique appliquée à l'agriculture, la biotechnologie, l'agro-alimentaire et l'environnement. Ce laboratoire multi-site est composé de l'Université de Lille, l'Université de Liège, l'Université de Picardie Jules Verne, l'INRAE (tutelles principales) ainsi que de l'Université du Littoral-Côte d'Opale, l'Université d'Artois et Junia (tutelles associées). Les thématiques de recherche de cet UMR-t s'articulent autour de trois pôles, neuf équipes, ainsi que de 4 axes transversaux **(Figure i)**. Plus précisément, mon projet a été conduit sur le site ISA-Junia dans le cadre de l'équipe 5 « Métabolites secondaires d'origine végétale » et dans l'axe transversal « Biocontrôle ».

Certains travaux ont été réalisés en collaboration avec des partenaires internes et externes à l'UMR-t BioEcoAgro (Université de Lille, Université de Liège, Université du Littoral-Côte d'Opale, Université d'Artois, Université de Gand, INRAE de Colmar, Université Catholique de Louvain, Université de Reims Champagne-Ardenne, INRA de Kenitra).

Cette thèse a été réalisée du 1er novembre 2017 au 3 juin 2021, avec une interruption des travaux de mars à juin 2020, en raison des conditions sanitaires liées à la pandémie de la Covid-19.

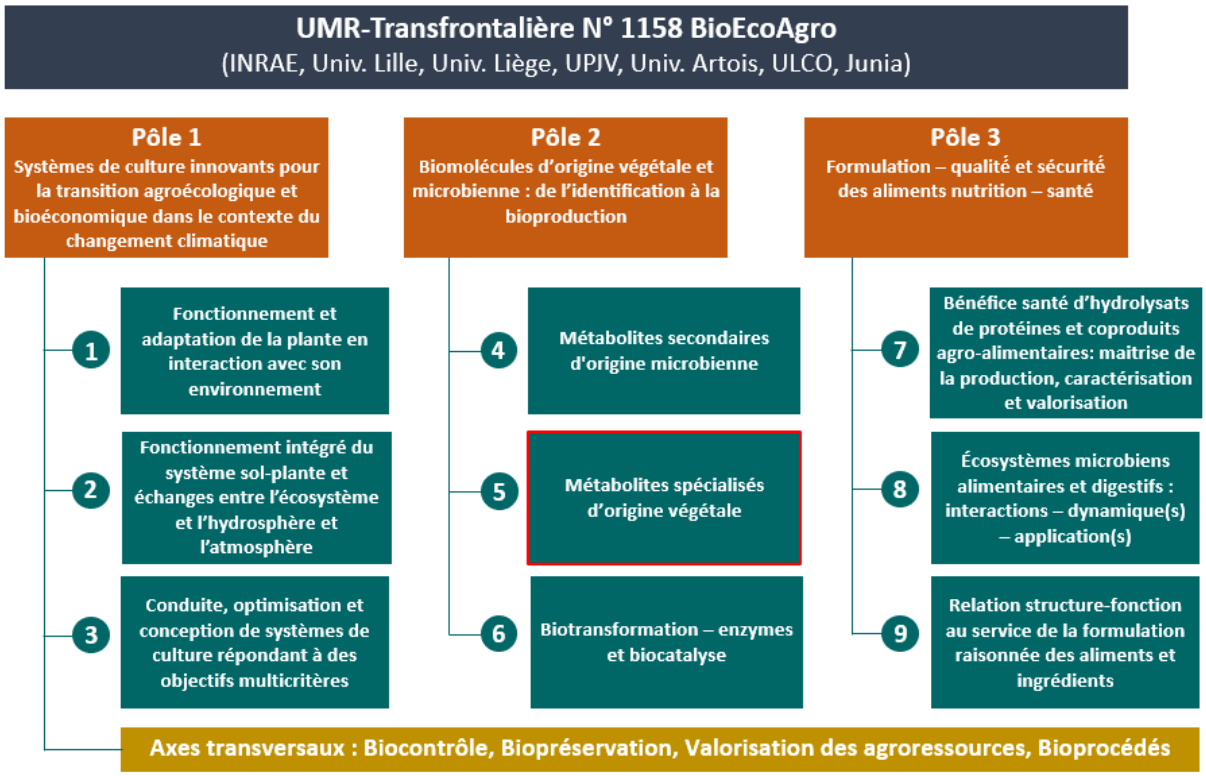

Figure i : Organisation des thématiques de recherche de l'UMR-t 1158 BioEcoAgro (www.bioecoagro.eu).

REMERCIEMENTS

Je tiens, tout d'abord, à remercier très sincèrement les différents membres du jury, dont Marielle Adrian et Alain Hehn qui ont accepté d'être les rapporteurs du manuscrit, Marie-Noëlle Brisset et Philippe Jacques qui auront le rôle d'examinateur, ainsi que Monica Höfte et Maryline Magnin-Robert en tant que membres invités. Merci Alain de boucler ainsi la boucle de mes études supérieures.

Mes remerciements vont ensuite au projet Bioscreen (portefeuille de projets Smartbiocontrol) qui m'a financé, aux porteurs du projet et surtout à tous ses acteurs avec qui j'ai eu l'opportunité de travailler pendant ces 3 années.

Un grand merci à Monica pour l'aide, les conseils et le temps octroyés pendant tout ce projet de thèse en tant que membre du comité de suivi de thèse, du jury, et en tant que collègue. Merci aussi à Rutger pour son sérieux et son énergie, j'ai hâte que notre collaboration se poursuive et bon courage à toi pour la poursuite de ta thèse. Merci à Maryline Calonne pour m'avoir accueilli et formé à l'UCLouvain. Mes remerciements vont aussi à l'équipe de l'Université d'Artois avec qui j'ai eu l'occasion de travailler. Merci aussi à François Coutte et à Philippe Jacques pour leur aide sur la partie lipopeptide.

J'adresse aussi mes remerciements à Marc Ongena pour son implication dans mon comité de suivi de thèse. En général, merci à ce comité qui a su me prodiguer d'excellents conseils ainsi qu'un support fort utile pour avancer plus sereinement dans cette thèse.

Merci à toute l'équipe de l'INRAe de Colmar, Philippe Hugueney, Raymonde Baltenweck et Alessandra Maia-Grondard pour son implication dans nos projets de recherche ainsi que son accueil. J'ai beaucoup appris grâce à vous.

Mes remerciements vont aussi à tous les collègues de l'Université de Lille avec lesquels j'ai pu interagir, en particulier Jean-Louis Hilbert, Alice Rochex, Alexandre Bricourt et Anca Lucau. Anca, encore un très grand merci à toi pour ton investissement plus que conséquent dans nos travaux et ta disponibilité.

Je salue aussi chaleureusement toute l'équipe de l'ULCO, en particulier Béatrice et Maryline, qui m'ont co-encadré avec sérieux et bienveillance pendant ces années, vous avez toujours été là en cas de besoin et je vous en remercie. Phillipe aussi, merci pour ta réactivité, tes corrections et tes conseils. Cela a été un vrai plaisir de travailler avec vous.

J'adresse évidemment tous mes remerciements aux différents collègues de Junia-ISA qui étaient présents durant ces trois années dernières années. Plus particulièrement, merci à tout le monde de l'équipe PPB pour leur compréhension, leur soutien et la bonne ambiance générale. Merci à Caroline Deweer pour son soutien pratique (sans qui tout aurait été plus compliqué). Merci à Caroline Choma, Jérôme et Ourida, pour le soutien moral, ainsi qu'aux plus récemment arrivées dans l'équipe, Marie et Pauline, merci d'ailleurs à cette dernière pour ses nombreuses corrections. Mes meilleurs sentiments vont aussi à Patrice qui m'a encadré pendant une partie de ma thèse, profite bien de ta retraite désormais.

Tous mes vœux de bonheur aux jeunes chercheurs qui sont là ou qui ont été là et qui ont permis de développer une vraie bonne ambiance de travail, Myriam, Maxime, Océane, Marlon, Mathias,

Mateus, Renata, Morgane, Robin, Alice, Morgane plus tous ceux que j'oublie, ils me pardonneront sans aucun doute. Quel dommage que nos sorties aient été impossibles ces derniers temps. Bon courage aux doctorant(e)s Marie-Astrid, Claire, Arthur et Anne-Sophie ! Je vous passe le témoin.

A Ali, mon directeur de thèse, ce fut un long voyage, parfois tumultueux, souvent exigeant, mais toujours intéressant et enrichissant. Merci pour tout, l'encadrement, les opportunités scientifiques, les nombreuses discussions, les débats ainsi que les demandes qui m'ont poussé à me dépasser. Ce fut un beau voyage, j'ai beaucoup appris et encore plus à encore apprendre mais il est temps maintenant de faire une petite halte avant de repartir, on a bien mérité de se reposer.

Merci à mes amis qui ont su me distraire et me stimuler quand il le fallait, heureusement que vous étiez là. J'ai hâte de vous revoir pour fêter ça comme il se doit une fois que les conditions le permettront.

Je pense évidemment à ma famille, ça n'a pas toujours été facile, les évènements qui ont eu lieu pendant ces trois ans n'ont pas toujours été joyeux, mais voilà une étape de franchie. Merci à vous d'avoir été là et j'espère bien avoir plus de temps pour profiter avec vous dans les mois à venir.

Enfin, je ne saurais jamais remercier suffisamment ma compagne pour tout son soutien, son aide et sa gentillesse, même dans les moments plus compliqués. Quoiqu'il arrive cette thèse nous aura permis de nous rencontrer et rien que pour ça, ça valait le coup. De nouvelles aventures nous attendent désormais.

TABLE DES MATIÈRES

TABLE DES FIGURES

TABLE DES TABLEAUX

LISTE DES ABRÉVIATIONS

4CL	4-coumarate-CoA ligase
ABA	Acide abscissique
ABC	*ATP-binding cassette*
ACS1	*ACC synthase*
AIM1	*Abnormal inflorescence meristem 1*
AMPc	Adénosine monophosphate cyclique
AOC	Allène oxyde cyclase
AOS	Allène oxyde synthase
AQP	*Aquaporin*
BA2H	*Benzoic acid 2-hydroxylase*
BR	Brassinostéroïdes
C3'H	*4-coumarate 3-hydroxylase*
C4H	Cinnamate 4-hydroxylase
CAD	*Cinnamyl alcohol dehydrogenase*
CAT	Catalase
CCoAOMT	*Caffeoyl CoA O-methyltransferase*
CCR	*Cinnamoyl CoA reductase*
CDPK	*Calcium dependant protein kinase*
CEBiP	*Chitin elicitor binding protein*
CERK1	*Chitin elicitor receptor kinase 1*
CI_{50}	Concentration inhibitrice à 50%
CIPK	*CBL-interacting protein kinase*
CK	Cytokinines
CLP	Lipopeptide cyclique
CM	Chorismate mutase
CMI	Concentration minimale inhibitrice
COMT	*Caffeic acid O-methyltransferase*
CWDE	*Cell wall degrading Enzymes* ; Enzymes de dégradation de la paroi cellulaire
DAM	*Differentially accumulated metabolite*
DAMP	*Damage-associated molecular patterns*
DEG	*Differentially expressed gene*
DMAP	*N,N*-dimethylpyridin-4-amine
DMF	*N,N*-dimethylformamide
DMI	*Demethylation inhibitors*
DMSO	*Dimethyl sulfoxide*
EDS5	*Enhanced disease susceptibility 5*
EPS1	*Enhanced pseudomonas susceptibility 1*
ESI	*Electrospray ionization*
ET	Ethylène
ETI	*Effector-triggered immunity*
ETS	*Effector-triggered susceptibility*
F5H	*Ferulate-5-hydroxylase*
FAO	*Food and Agriculture Organization*
FC	*Fold change*
FDR	*False discovery rate*
FLA15	*Fasciclin-like protein 15*
GA	Gibbérellines
HCN	Cyanide d'hydrogène

HCT	*Quinate/shikimate p-hydroxycinnamoyltransferase*
HR	*Hypersensitive response*
HrBP1-1	*Harpin binding protein 1-1*
HRGP	*Hydroxyproline-rich glycoproteins*
HSP	*Heat-shock protein*
IAA	*Indole-3-acetic acid*, Acide indole-acétique
IC	*Isochorismate*
ICS	*Isochrosimate synthase*
ID50	*Half-maximal inhibitory dilution*
IGS	*Isochorismoyl-glutamate synthase*
ISR	*Induced systemic resistance*
IWGSC	*International Wheat Genome Sequencing Consortium*
JA	*Jasmonic acid*, acide jasmonique
JA-Ile	*Jasmonoyl-isoleucine*
Jpi	Jours post inoculation
KB	*King's B*
KEGG	*Kyoto Encyclopedia of Genes and Genomes*
LACs	Laccases
LAR	*Local acquired resistance*, Résistance locale acquise
LB	*Lysogeny broth*
LLP	Lipopeptide linéaire
LOX	Lipoxygénase
MALDI-ToF	*Matrix assisted laser desorption Ionization-time of flight*
MAMP	*Microbe-associated molecular patterns*
MAPK	*Mitogen-activated protein kinases*
MDR	*Multi-drug resistant*
MeJA	Méthyl-jasmonate
MeSA	Méthyl-salicylate
MID	*Minimal inhibitory dilution*
MYB2	*Myeloblastosis 2*
NB-LRR	*Nucleotide binding leucine-rich repeat*
NIP	*Necrosis-inducing proteins*
NMR	*Nuclear magnetic resonance*
nsLTP	*Non-specific lipid transfert protein*
OAD	Outils d'aide à la décision
OPDA	Cis-*(+)-12-oxo-phytodienoic acid*
OXO	Oxalate oxydase
PAL	Phénylalanine ammonia lyase
PAMP	*Pathogen-associated molecular patterns*
PBS3	*AvrPphB susceptible 3*
PCA	*Plate count agar*
PDA	*Potato dextrose agar*
PDX1.1	*Pyridoxal biosynthesis protein 1.1*
POX	*Peroxidase* ; Péroxydase
PR1	*Pathogenesis-related protein 1*
PRR	*Pattern recognition receptors*
PTI	*PAMP-triggered immunity*
QoI	*Quinone outside inhibitors*
QTL	*Quantitative trait loci*
Rh-Est	Rhamnose Ester
Rh-Eth	Rhamnose Ether
Rh-Suc	Rhamnose succinate

RIN	*RNA intergity number*
RL	*Rhamnolipid*
ROS	*Reactive oxygen species*, Espèces réactives de l'oxygène
RT	*Retention time*
SA	*Salicylic acid*, Acide salicylique
SAR	*Systemic acquired resistance*, Résistance systémique acquise
SDHI	*Succinate dehydrogenase inhibitors*
SDP	Stimulateur de défense des plantes
SL	Strigolactones
SOD	Superoxyde dismutase
SRB	*Synthetic rhamnolipid bolaforms*
STB	*Septoria tritici blotch* ; Septoriose du blé
TaRH1	*Triticum aestivum RNA helicase 1*
TF	*Transcription factor*
TL4	*Thaumatin-like protein*
TLC	*Thin layer chromatography*
Tween 20	*Polyoxyethylene-sorbitan monoclaurate*
UE	Union Européenne
UHPLC-MS	*Ultra-high performance liquid chromatography-mass*
UN	*United nations* ; Organisation des nations unies
WCOR518	*Cold acclimation protein*
WZF1	*Zinc finger protein*

INTRODUCTION GÉNÉRALE

Selon les prévisions de l'Organisation des Nations unies (*United Nations,* UN), la population humaine devrait continuer à croître considérablement dans les décennies à venir, atteignant 9,7 milliards d'individus en 2050 et possiblement 11 milliards vers 2100 (UN, 2019). Dans ce contexte, il est crucial d'arriver à assurer une production suffisante et durable des principales denrées alimentaires. Les céréales regroupent des espèces végétales, appartenant principalement à la famille des graminées, cultivées pour leurs grains. Elles sont utilisées aussi bien pour la subsistance humaine que pour celle des animaux. Parmi toutes les céréales consommées et produites dans le monde, le blé occupe une place essentielle, tout particulièrement en Europe. Ingrédient principal pour de nombreuses sociétés au cours du temps, il a joué, et joue toujours, de nombreux rôles, que ce soit au niveau agronomique, industriel, économique, historique et même géopolitique. Le blé est ainsi l'une des plantes les plus cultivées et consommées dans le monde. Selon les estimations de la *Food and Agriculture Organization* (FAO), la production de blé aurait dépassé les 761 millions de tonnes sur la période 2018-2019 (FAO, 2020). Cette céréale est cependant soumise à des nombreuses contraintes biotiques et abiotiques pouvant impacter significativement son rendement.

En Europe de l'Ouest, la maladie foliaire la plus dévastatrice sur la culture de blé est la septoriose, causée par le champignon phytopathogène *Zymoseptoria tritici,* qui peut, selon les conditions, conduire à des pertes de rendement pouvant atteindre les 50% (Fones and Gurr, 2015). Les pertes économiques causées par cette maladie cryptogamique, chaque année, en Europe seulement, sont estimées à 400 millions de dollars, faisant de la septoriose du blé une problématique agronomique et économique majeure au niveau européen comme au niveau mondial (Yemelin *et al.*, 2017). Les principales méthodes employées pour contrôler cet agent phytopathogène au champ reposent majoritairement sur l'utilisation de produits phytopharmaceutiques de synthèse et, dans une moindre mesure, sur la lutte variétale. Cependant, en raison du développement fréquent de phénomènes de résistance aux fongicides chez l'agent pathogène et d'une demande sociale toujours plus croissante pour réduire l'utilisation des intrants d'origine chimique en agriculture, des méthodes alternatives de protection des cultures efficaces doivent être développées. L'une des alternatives possibles pour la gestion des maladies des cultures est le recours au biocontrôle. Celui-ci peut se définir comme un ensemble de méthodes de protection contre les bio-agresseurs des cultures, basées sur l'utilisation d'organismes vivants bénéfiques ou de substances d'origine naturelle (INRAE, 2016).

Dans le cadre de ce projet de thèse, nous avons cherché à identifier de nouveaux composés de biocontrôle efficaces pour protéger le blé vis-à-vis de *Z. tritici* et à caractériser leurs modes d'action. Dans le présent manuscrit, nous débuterons avec un état de l'art présentant les différentes facettes du sujet, puis viendra la description du contexte général dans lequel s'inscrit ce projet de thèse ainsi que les objectifs visés. Les principaux résultats obtenus seront ensuite décrits et discutés sous forme d'articles scientifiques. Enfin, une discussion générale, comprenant les perspectives des travaux, parachèvera ce manuscrit.

ÉTAT DE L’ART

1. LE BLÉ

1.1. Présentation générale et classification

Le blé est une plante angiosperme monocotylédone appartenant à la famille des *Poaceae* ou graminées **(Figure 1)**. Cette dernière regroupe un grand nombre d'espèces parmi les plus importantes sur les plans agronomique et économique, comme, outre le blé, le maïs (*Zea mays)*, l'orge (*Hordeum vulgare*), le riz (*Oryza sativa*), les millets ou encore le sorgho (*Sorghum bicolor*) qui constituent l'alimentation de base dans plusieurs régions à travers le monde. Dans cette famille, on retrouve le genre *Triticum*, qui comporte les deux espèces de blé les plus cultivées dans le monde, le blé dur et le blé tendre **(Figure 1)**. Le blé dur est majoritairement cultivé dans des régions chaudes et sèches comme celles du pourtour méditerranéen (*i.e.* Afrique du nord et Europe du sud) et sert principalement à la production de semoule et de pâtes alimentaires. Le blé tendre, aussi appelé froment, est cultivé dans des régions présentant des climats plus tempérés. Grâce aux propriétés visco-élastiques particulièrement intéressantes de sa farine, dû à la présence des protéines du gluten, il est utilisé majoritairement pour la fabrication du pain. Il peut aussi être utilisé pour l'alimentation animale, la mouture ou la production de biocarburant. Au niveau mondial, la culture du blé tendre représente plus de 90% de la production de blé (Shewry, 2009).

A

Règne	***Plantae***
Sous-règne	*Tracheobionta*
Division	*Magnoliophyta*
Classe	*Liliopsida*
Sous-classe	*Commelinidae*
Ordre	*Cyperales*
Famille	*Poaceae*
Sous-famille	*Pooideae*
Tribu	*Triticeae*
Genre	*Triticum*

B

Figure 1 : Présentation taxonomique et botanique du blé tendre. (A) Classification taxonomique du blé tendre et dur et (B) planche botanique du blé tendre (d'après Brandt *et al*., 1883)

1.2. Histoire évolutive du blé

Historiquement, le blé est l'une des premières plantes domestiquées par l'homme il y a environ 10 000 ans lors de l'apparition de l'agriculture dans le Croissant fertile. Le blé dur (*Triticum turgidum* ssp. *durum*) est un organisme tétraploïde possédant 14 paires de chromosomes (2n=4x=28 ; AABB). Il aurait été domestiqué par d'anciens cultivateurs du Moyen-Orient à partir d'une espèce sauvage locale tétraploïde, toujours existante aujourd'hui, appelée *Triticum dicoccoides*. Cette dernière est issue de l'hybridation de deux espèces graminées diploïdes sauvages, *Triticum urartu* (2n=2x=14; AA) et *Aegilops speltoides* (2n=2x=14; BB), suivie d'un doublement du nombre de chromosomes **(Figure 2)**. Ce croisement aurait eu lieu il y a plus de 500 000 ans. Le blé tendre (*Triticum aestivum*), quant à lui,

est un organisme hexaploïde possédant 21 paires de chromosomes (2n=6x=42; AABBDD). Cette espèce serait apparue il y environ 9500 ans. Les preuves génétiques et cytologiques accumulées ces dernières décennies suggèrent que ce blé est issu d'une espèce ancestrale hexaploïde appelée *Triticum spelta*. Cette dernière serait apparue à la suite d'une hybridation, suivie encore une fois d'un doublement des chromosomes, entre une espèce ancestrale tétraploïde de blé dur cultivé au Moyen-Orient à cette époque, *Triticum turgidum* (2n=4x=28 ; AABB), et une autre poacée sauvage diploïde, *Triticum tauschii* (2n=2x=DD) **(Figure 2)** (Shewry, 2009 ; Snape and Pánková, 2013).

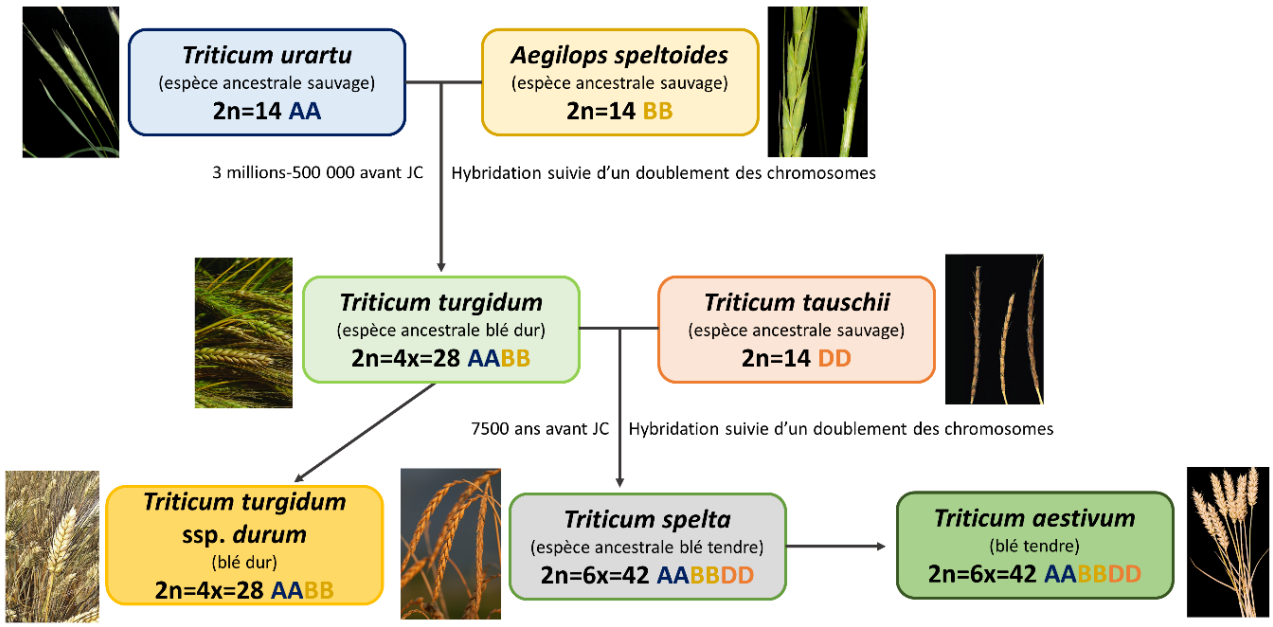

Figure 2 : Histoire évolutive et évènements génétiques ayant mené à l'émergence des deux espèces de blé les plus cultivées actuellement, le blé dur (*Triticum turgidum* ssp. *durum*) et le blé tendre (*Triticum aestivum*). Le blé dur est un organisme tétraploïde (sous-génomes AA et BB). Le blé tendre (sous-génomes AA, BB et DD) est, quant à lui, hexaploïde (modifié d'après **Snape and Pánková, 2013).**

1.3. Implantation du blé en Europe et en Asie

Après les premiers processus de domestication du blé dans le Croissant fertile, la culture de cette céréale a rapidement été introduite en Europe et en Asie *via* différentes routes **(Figure 3)**. Avant 4000 ans avant JC, le blé était implanté partout en Europe (Snape and Pánková, 2013). Il s'imposa ensuite comme une denrée essentielle des principales organisations territoriales et culturelles européennes. L'importance de cette denrée dans l'alimentation en fait une ressource majeure ; ainsi, son niveau de production a fortement influencé la stabilité sociale et politique des organisations européennes et ce dès l'antiquité. Durant l'époque romaine antique, il était fréquent que des pénuries de blé conduisent à des périodes de famines et de violence intenses frappant de plein fouet les bases mêmes des régimes politiques. Les régions hautement productrices devinrent des zones stratégiques majeures et furent au cœur de nombreux conflits à travers l'histoire. Ce fut le cas par exemple de l'Egypte au moment de la Rome antique (Evans, 1981).

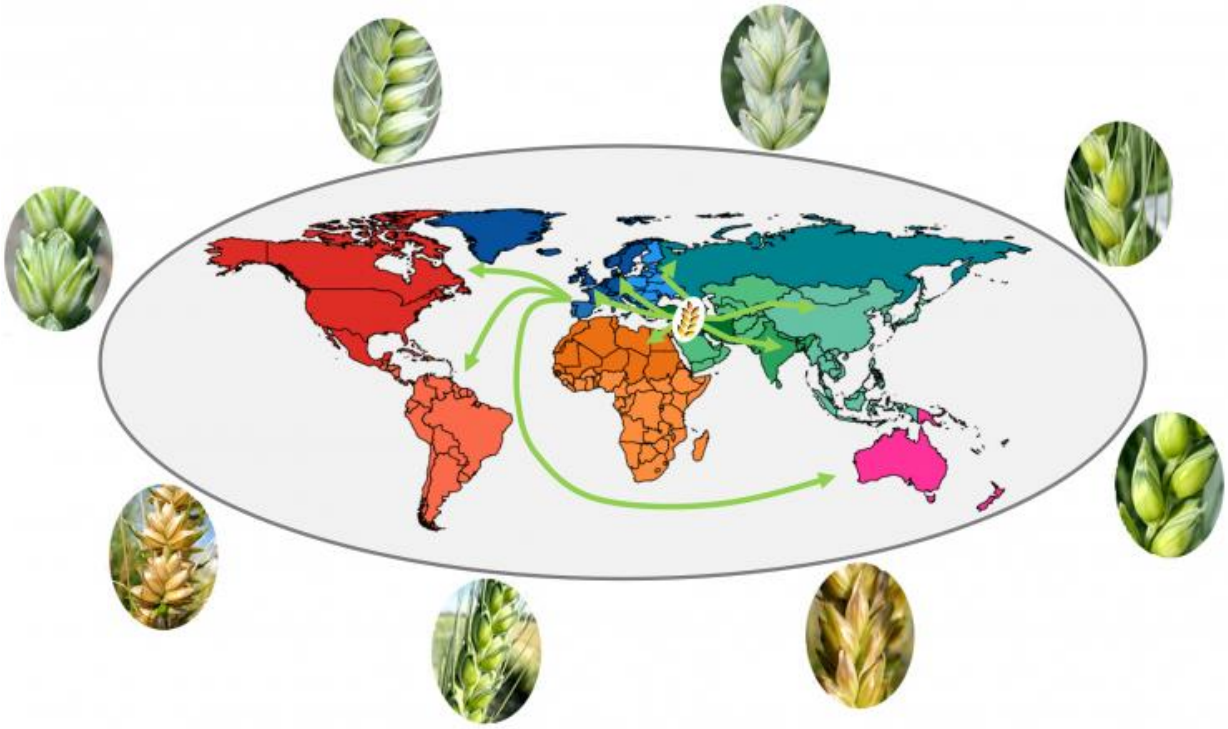

Figure 3 : Expansion de la culture blé depuis sa domestication au Croissant Fertile au Néolithique (d'après **INRAE, 2020**).

Le génome du blé tendre est l'un des génomes les plus complexes observés pour les organismes végétaux cultivés. Celui-ci est composé de trois sous-génomes différents (AA, BB et DD) du fait des multiples hybridations ancestrales ayant mené à l'hexaploïdie de cette espèce **(Figure 2)**. La taille particulièrement grande de ce génome ajoute encore à cette complexité. En effet, celui-ci comporte 17 gigabases (17 milliards de pairs de base), ce qui correspond à environ 5 fois la taille du génome humain ou à 35 fois celle du riz. Il a fallu plus de 10 ans de travaux au consortium *International Wheat Genome Sequencing Consortium* (IWGSC) pour réaliser le séquençage, l'assemblage et l'annotation complet du génome du blé tendre. Ce travail titanesque s'est terminé récemment, en 2018, et 107 891 gènes ont été identifiés avec un haut degré de confiance, avec une distribution relativement égale entre les différents sous-génomes (AA=35345, BB=35643 et DD=34212 gènes). Les résultats ainsi obtenus pourront être utilisés afin de mieux comprendre la biologie du blé et cibler de nouveaux gènes impliqués dans la régulation de différents caractères d'intérêt agronomique, tels que les résistances aux stress abiotiques et biotiques, le rendement, ou encore les caractéristiques nutritionnelles du grain. Il est à noter que si la taille du génome du blé est exceptionnellement élevé, celui-ci contient plus de 85% de séquences répétées (Consortium IWGSC, 2018).

1.4. Production mondiale de blé

De nos jours, le blé est l'une des cultures les plus produites et consommées dans le monde, avec le maïs et le riz, et constitue l'aliment de base pour plus d'un tiers de la population mondiale. Selon la *Food and Agriculture Organization* (FAO), la production de blé fut de 732 millions de tonnes pour la période 2017-2018 et atteindrait 761 millions de tonnes selon les récentes estimations pour la période 2018-2019 (FAO, 2020). Les cinq principaux producteurs de blé, sont, par ordre décroissant, l'Union

européenne (UE), la Chine, l'Inde, la Russie et les Etats-Unis **(Figure 4)**. Au niveau de l'UE, qui enregistra une production de 156 millions de tonnes pour l'année 2019 (FAO, 2020), les deux états-membres produisant le plus de blé sont la France, qui est aussi le premier pays exportateur de blé de l'UE, et l'Allemagne avec des productions respectives d'environ 34 et 20 millions de tonnes pour le blé tendre et 1,8 et 0,1 millions de tonnes pour le blé dur pour la période 2018-2019 (FranceAgriMer, 2020).

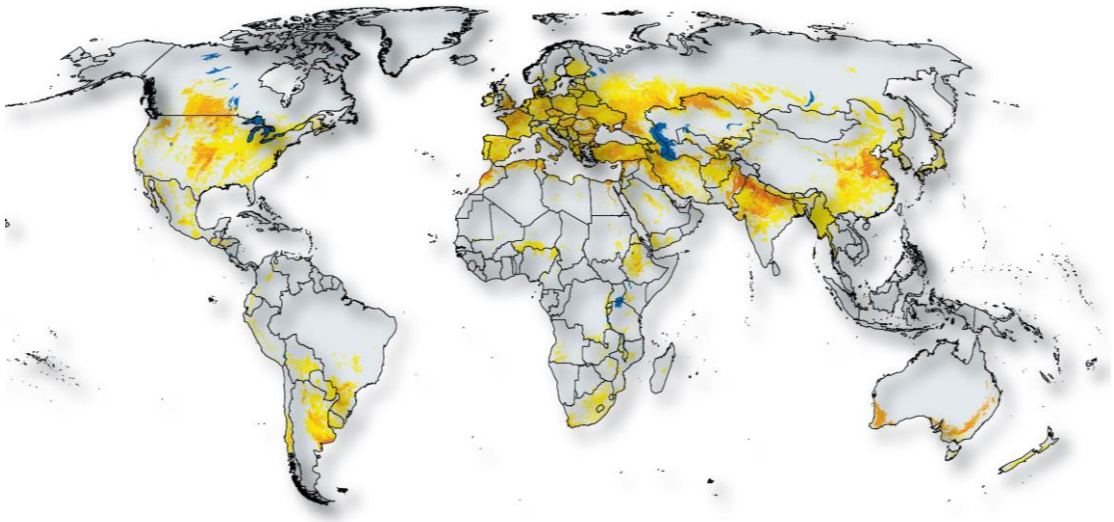

Figure 4 : Principales régions productrices de blé dans le monde en 2014 (modifié d'après **You *et al*., 2014**). Les couleurs plus foncées indiquent les zones où le blé est plus cultivé.

1.5. Cycle de développement du blé

Le blé est une plante annuelle dont le cycle de développement est décrit en plusieurs étapes principales, en allant de la germination du grain (le caryopse, c'est-à-dire le fruit du blé, caractéristique des céréales) à la formation de la génération suivante de grains au sein de l'épi et jusqu'à la sénescence de la plante. Ces étapes sont couramment décrites suivant un code décimal qui se base sur l'échelle de Zadoks *et al*. (1974) **(Figure 5)** (Lancashire *et al*., 1991). Brièvement, en premier lieu, le cycle débute par la germination du grain, suivie par une phase de développement végétatif de l'individu comprenant des phénomènes d'organogénèse racinaire et foliaire. Lors de cette phase, et lorsque la plante atteint le stade trois feuilles (environ 21 jours après germination), de nombreuses talles (tiges adventices émergeant de la plantule initiale) sont formées. S'en suit une extension importante de la tige et la montaison du blé. La phase reproductrice commence ensuite, lorsque la plante est suffisamment développée, avec les phénomènes d'initiation foliaire, de développement des épis et de production des gamètes. Après fécondation, la phase de formation et maturation des grains a lieu et ce jusqu'à leur déhiscence et sénescence de la plante **(Figure 5)**.

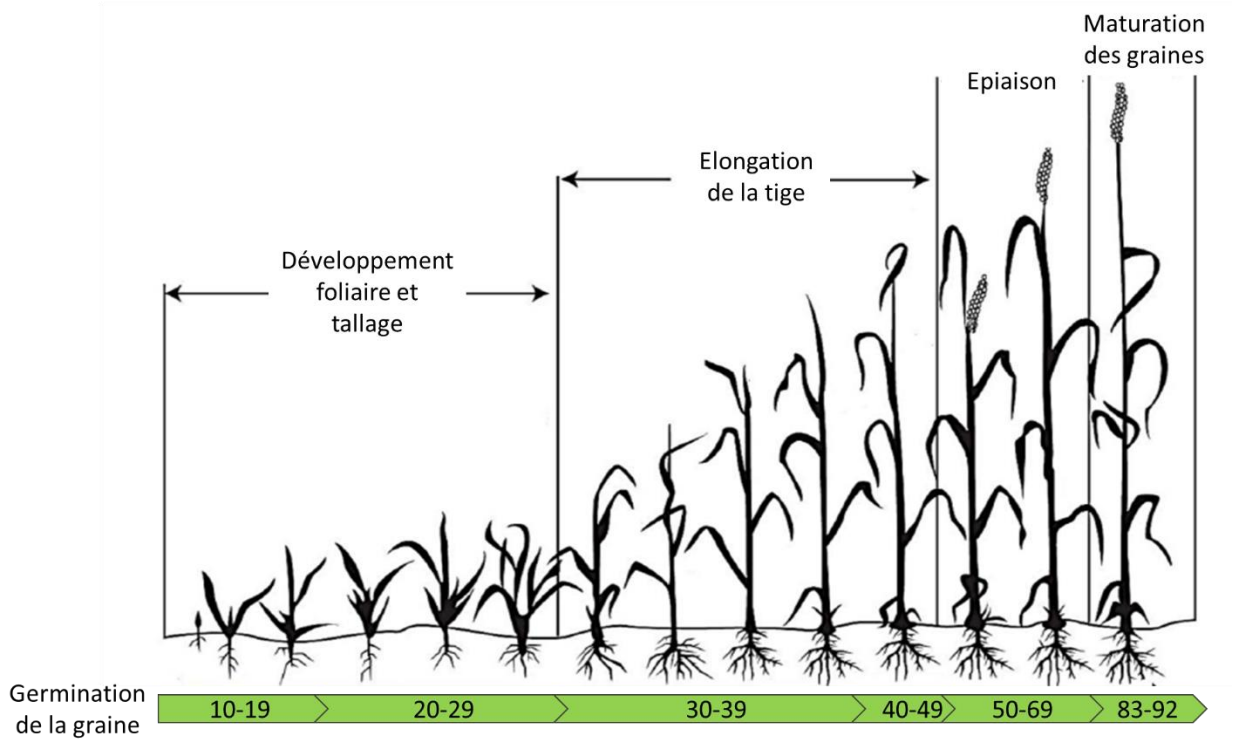

Figure 5 : Principales étapes du développement du blé selon l'échelle de Zadocks *et al*. (1974). Le premier chiffre de cette échelle décimale correspond au stade principal de développement, sous-divisé en étapes plus précises, indiquées par le deuxième chiffre. Stade 0, germination de la graine ; stade 1, développement des feuilles ; stade 2, tallage ; stade 3, élongation de la tige principale ; stade 4, montaison ; stade 5, épiaison ; stade 6, floraison ; stade 7, développement des grains ; stade 8, maturation des grains ; stade 9, sénescence.

1.6. Impact des stress environnementaux sur la culture du blé

Tout au long de son cycle de développement, le blé subit de nombreuses contraintes capables d'affecter sévèrement sa croissance et son rendement. Au niveau abiotique, par exemple, l'une des principales inquiétudes actuelles est l'impact que pourra avoir le réchauffement climatique sur la production du blé. En effet, de nombreuses études ont déjà reporté l'effet négatif de températures élevées (au-dessus de 30 °C) sur le rendement en grain, en particulier lorsque ces épisodes climatiques avaient lieu lors de la phase reproductrice (Girousse *et al*., 2018). Lobell *et al*. (2011) avaient déjà estimé l'impact de ce stress comme étant responsable chaque année de pertes de rendement d'environ 5,5 % et de pertes nettes de production de 35 millions de tonnes au niveau mondial. Au niveau biotique, les maladies du blé peuvent être causées par un large panel de bio-agresseurs, comme les champignons, les bactéries, les virus et les nématodes. Les maladies les plus fréquentes et causant le plus de dommages au niveau de la culture sont le plus souvent d'origine cryptogamique (Figueroa *et al*., 2018). En Europe de l'Ouest, la maladie considérée comme la plus menaçante pour la production de blé est la septoriose du blé (*Septoria tritici blotch*, STB) (Fones and Gurr, 2015).

2. *ZYMOSEPTORIA TRITICI*

2.1. Présentation et classification taxonomique

Zymoseptoria tritici (anciennement forme anamorphe *Septoria tritici* et téléomorphe *Mycosphaerella graminicola*) est un champignon ascomycète appartenant à la classe des *Dothideomycetes* (Quaedvlieg *et al*., 2011). Plus précisément, il appartient à l'ordre des *Dothideales* et la famille des *Mycosphaerellaceae*. Cette dernière est connue pour contenir un grand nombre d'espèces pathogènes des plantes tel que *Cercospora beticola*, l'agent responsable de la maladie foliaire la plus dévastatrice de la betterave, ou encore *Ramularia collo-cygni*, un agent pathogène très préoccupant sur la culture de l'orge (Groenewald *et al*., 2007 ; Walters *et al*., 2008). *Zymoseptoria tritici* est actuellement l'agent principal responsable de la STB, maladie foliaire capable d'affecter le blé tendre comme le blé dur, et considérée comme l'une des principales contraintes actuelles pour la production de cette denrée alimentaire majeure (O'Driscoll *et al*., 2014). Ce champignon aurait émergé en tant qu'agent phytopathogène spécialisé du blé il y a environ 10 000 ans, lors de la domestication de ce dernier dans le Croissant Fertile (Stukenbrock *et al*., 2007). Ce parasite se serait ensuite disséminé en accompagnant la migration du blé dans l'Eurasie et l'Afrique d'abord, puis, lors de l'époque des grandes découvertes dans le monde (Banke and McDonald, 2005). La forme anamorphe du champignon a été décrite pour la première fois en 1842 par Desmazières (Shipton *et al*., 1971) alors que sa forme téléomorphe, moins fréquente et plus complexe à observer, n'a été décrite et rattachée à *Septoria tritici* qu'un siècle plus tard, en 1972, en Nouvelle-Zélande (Sanderson, 1972). Depuis, la forme parfaite de ce champignon a été observée en France et dans plusieurs régions à travers le monde (Halama, 1996 ; Zhan *et al*., 2003 ; Hassine *et al*., 2019).

2.2. Importance économique de la septoriose du blé

La septoriose du blé a été rapportée dans toutes les régions du monde où le blé est cultivé. Il s'agit d'une maladie fongique exclusivement foliaire qui limite grandement le potentiel photosynthétique du blé, car il engendre des lésions (chloroses et nécroses) sur les feuilles **(Figure 6)**, des modifications dans le métabolisme primaire de son hôte et prélève à la plante ses ressources, incluant ses sucres et acides aminés (Shtienberg, 1992 ; Shetty *et al*., 2007). Cela entraîne des pertes de rendement qui se caractérisent notamment par une diminution du poids et de la qualité des grains (McKendry *et al*., 1995)

Dans certaines régions présentant des conditions agro-environnementales propices au développement de la maladie, celle-ci entraîne des pertes de rendement sévères pouvant atteindre les 50 % (Eyal *et al*., 1987). C'est le cas, tout particulièrement, pour une partie de l'Europe de l'Ouest, caractérisée par Bouma (2005) de « zone maritime », où règne un climat humide particulièrement favorable à la croissance et à la propagation de *Z. tritici*. Dans cette zone, les pays les plus affectés par septoriose sont la France, l'Allemagne et le Royaume-Uni, soit les principaux pays producteurs de blé de l'Union Européenne (UE). Les pertes annuelles engendrées par cette maladie sont estimées à 400 millions de dollars pour l'UE et 70 % des fongicides qui y sont utilisés annuellement ciblent uniquement ce champignon (Fones and Gurr, 2015 ; Yemelin *et al*., 2017).

Figure 6 : Symptômes de la septoriose du blé causés par le champignon ascomycète *Zymoseptoria tritici*. (A) Effet de la maladie sur un champ d'une variété de blé sensible (d'après **Rothamsted Research, Harpenden, UK**). (B) Observation de feuilles de blé infestées où sont apparentes les lésions nécrotiques et chlorotiques typiques de la maladie. Les zones nécrosées présentent des ponctuations noires, les pycnides, qui sont issues du mode de multiplication asexuée du champignon (d'après **Juina UMR-t 1158 BioEcoAgro**).

En France, les pertes de rendement causées annuellement par *Z. tritici* ont été en moyenne de 16,8 quintaux par hectare (q/ha) sur la décennie 2002-2012. La nuisibilité de la maladie diffère grandement au niveau régional. Ainsi, elle est généralement beaucoup plus importante dans le Nord-Ouest du pays. Les pertes moyennes de rendement ont, par exemple, été de 19,2 q/ha dans le Nord-Pas-de-Calais (Hauts-de-France) et ont atteint jusqu'à 24,1 q/ha en Bretagne. Dans d'autres régions, la nuisibilité a été bien moindre, comme en Auvergne, où les pertes ont été de 7,9 q/ha en moyenne **(Figure 7)** (Arvalis-Institut du végétal, 2013a).

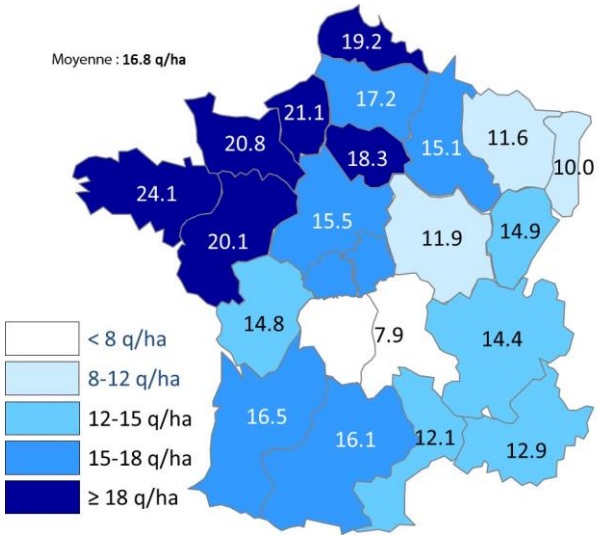

Figure 7 : Pertes de rendement annuel moyen causées par *Zymoseptoria tritici* en France métropolitaine sur la période 2002-2012. Les pertes de rendement sont indiquées en quintaux par hectares (q/ha) selon le découpage régional d'avant 2016 (d'après **Arvalis-Institut du végétal, 2013a**).

La sévérité de la maladie peut également grandement varier d'une année à l'autre. Différents facteurs interviennent dans cette variabilité, comme la quantité d'inoculum présent en début de saison, l'humidité, la température ou encore le stade de croissance du blé lors de l'infection (Holmes and Colhoun, 1974 ; Chungu *et al*., 2001). En raison de son impact agronomique et économique majeur, ainsi que pour toutes les caractéristiques biologiques particulières qu'il présente, *Z. tritici* a été classé parmi le top 10 des espèces de champignons phytopathogènes modèles (Dean *et al*., 2012).

2.3. Cycle épidémique

L'épidémie de septoriose commence le plus généralement en automne dès la levée du blé. L'inoculum responsable des contaminations du blé peut se présenter soit sous forme d'ascospores **(Figure 8)**, issues de la reproduction sexuée du champignon, soit sous forme de pycnidiospores **(Figure 9)**, issues de la multiplication asexuée.

2.3.1. Les ascospores, forme principale des infections primaires

Les ascospores sont considérées comme majoritairement responsables des premières infections au champ, jouant ainsi le rôle d'inoculum dit primaire. Elles peuvent provenir des résidus de culture de blé de l'année précédente, de repousses spontanées de la culture ou être produites sur d'autres espèces herbacées servant d'hôtes alternatifs pour le pathogène (Wenham, 1959 ; Shaw and Royle, 1989 ; Suffert *et al*., 2011). Certaines graminées adventices extrêmement communes, notamment en Europe, peuvent ainsi jouer le rôle de réservoir d'inoculum, c'est le cas, des rays-grass (*Lollium perenne, Lollium mutilflorum*), du vulpin des prés (*Alopercurus pratensis*), du pâturin annuel (*Poa annua*) ou encore du seigle (*Secale cereale*) (Williams and Jones, 1973 ; Ao and Griffiths, 1976; Haghdel and Banihashemi, 2005)

Les ascospores bicellulaires de *Z. tritici* résultent obligatoirement du croisement entre des souches présentant des *mating types* compatibles, MAT1-1 et MAT1-2 (Halama, 1996 ; Kema *et al*., 1996). Ce mode de reproduction assure une diversité génétique élevée des populations sur le terrain et favorise les flux de gènes ainsi que l'apparition rapide de résistance aux fongicides (Zhan *et al*., 2003 ; Zhan *et al*., 2006). Les ascospores sont abritées dans des structures spécialisées du champignon, appelées asques, qui sont eux-mêmes contenus dans des fructifications appelées périthèces ou pseudothèces **(Figure 8)**. Ces fructifications, localisées au niveau sub-épidermique des feuilles, présentent une paroi épaisse à double couche et sont de couleur brun foncé. Chaque pseudothèce peut contenir environ 26 asques qui abritent chacun 8 ascospores, les ascospores ainsi produites lors de l'épidémie sont transportées par le vent sur de très longues distances, pouvant dépasser les 100 km (Eriksen and Munk, 2003). Comme elles participent également à la propagation de la maladie pendant la saison, elles sont donc aussi responsables de contaminations dites secondaires (Eriksen and Munk, 2003).

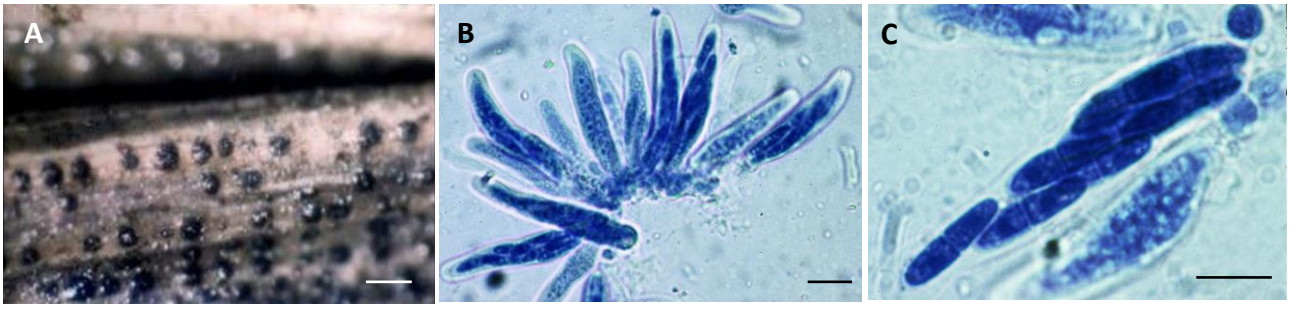

Figure 8 : Structures issues de la reproduction sexuée de *Zymoseptoria tritici*. (A) Observation de périthèces à la loupe binoculaire, barre d'échelle = 1 mm. (B) Asques contenant 8 ascospores observés au microscope optique. (C) Ascospores bicellulaires de *Z. tritici*. observées au microscope optique. Barre d'échelle = 10 µM pour (B) et (C) (d'après **Halama, 1996**).

2.3.2. Les pycnidiospores, forme principale des infections secondaires au niveau local

Les pycnidiospores, spores issues de la multiplication asexuée du champignon, peuvent aussi jouer le rôle d'inoculum primaire même si elles sont considérées moins importantes dans ce processus que les ascospores. Elles sont contenues dans des structures globuleuses, de couleur brune, les pycnides **(Figure 9)**. Les pycnidiospores sont produites dans une matrice mucilagineuse appelée cirrhe, qui leur donne la capacité de rester viable durant de longues périodes de conditions défavorables, comme la faible humidité et les températures extrêmes (Gough and Lee, 1985).

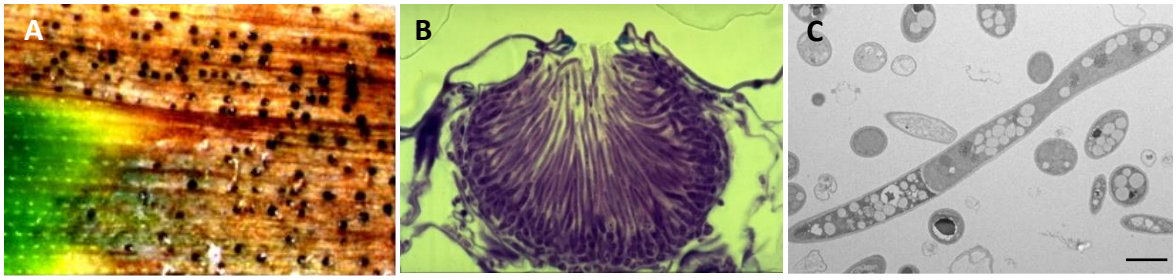

Figure 9 : Structures issues de la multiplication asexuée de *Zymoseptoria tritici.* (A) Lésions causées par le champignon sur une feuille de blé où sont observables les pycnides matures exsudant le cirrhe qui contient les pycnidiospores (d'après **Junia UMR-t 1158 BioEcoAgro)**. (B) Coupe transversale d'une pycnide mature observée au microscope optique contenant un grand nombre de pycnidiospores (d'après **Kema *et al*., 1996**). (C) Pycnidiospore cultivée en milieu liquide *yeast extract sucrose broth* observée au microscope électronique à transmission. Barre d'échelle = 2 µM (d'après **Francisco *et al*., 2019**).

Les pycnidiospores sont surtout impliquées dans la propagation de la maladie pendant l'épidémie et à un niveau local. A l'issue des premières infections, des pycnides se développent sur les premiers étages foliaires. Sous l'effet des éclaboussures de gouttelettes de pluie, les pycnidiospores contenues dans le cirrhe se dispersent et ensuite contaminent les étages foliaires supérieurs et les plantes adjacentes ; on parle alors du phénomène de *rain-splashing* **(Figure 10)** (Shaw, 1987). Après la récolte du blé, les spores de *Z. tritici* (pycnidiospores et ascospores) pourront contaminer les hôtes alternatifs, repousses de blé ou persister dans les résidus de culture, ce qui donnera naissance à l'inoculum primaire de la saison suivante **(Figure 10)** (Suffert *et al*., 2011). Par ailleurs, les populations de *Z. tritici* sont caractérisées par une très grande diversité génétique. En effet, à l'aide de marquages génétiques, Siah *et al*. (2018) ont estimé à 50 millions le nombre d'haplotypes différents présents dans un seul hectare de blé. Cette taille de population conséquente rend la maladie particulièrement difficile à contrôler.

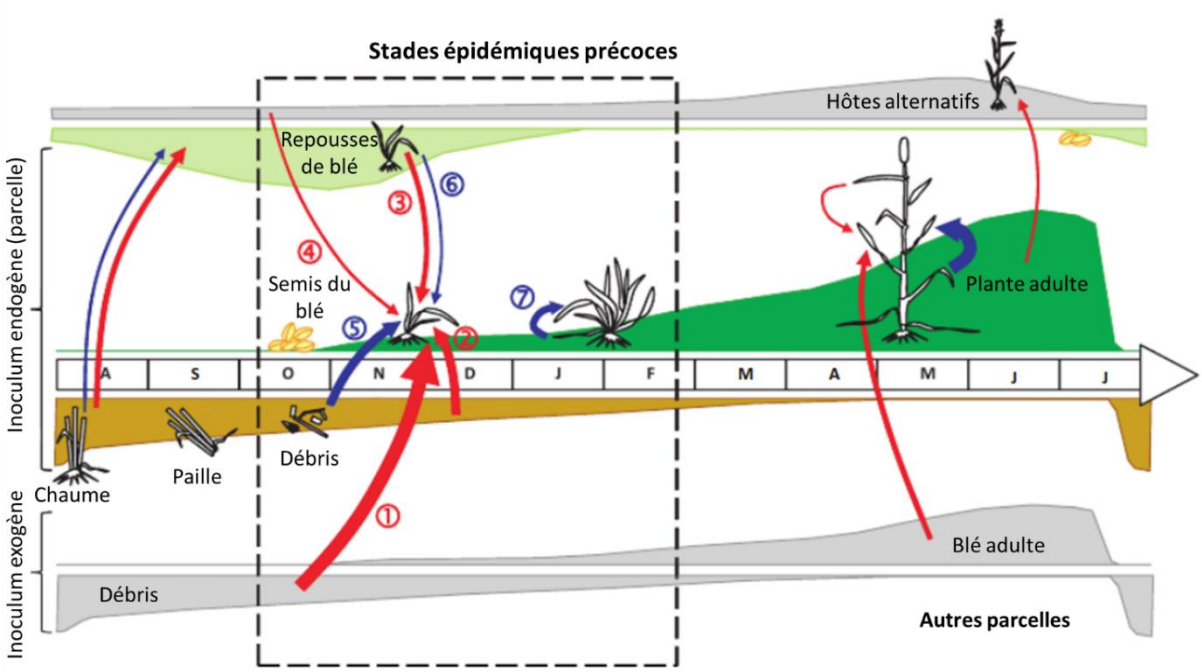

Figure 10 : Représentation schématique de la dynamique épidémique annuelle de la septoriose du blé. Les flèches rouges représentent les contaminations causées par les ascospores et les bleues celles causées par les pycnidiospores. Les ascospores sont disséminées par le vent et peuvent contaminer les cultures de blé sur de longues distances ; les pycnidiospores sont disséminées par *rain-splashing* sur de courtes distances. L'épaisseur des flèches est proportionnelle à l'impact supposé du mécanisme impliqué. Les stades épidémiques précoces principaux sont décrits plus précisément, avec 1 : contaminations par des ascospores provenant de débris de cultures de blé situés à longue distance ; 2 : ascospores provenant de débris de culture de blé proches ; 3 : ascospores provenant de repousses spontanées du blé ; 4 : ascospores provenant d'hôtes alternatifs ; 5 : pycnidiospores provenant de débris de blé ; 6 : pycnidiospores provenant de repousses de blé ; 7 : pycnidiospores provenant de feuilles basales infectées (d'après **Suffert *et al.*, 2011).**

2.4. Processus infectieux

Zymoseptoria tritici est un agent pathogène hémibiotrophe ; son cycle de développement se compose d'une phase biotrophe suivie d'une phase nécrotrophe.

2.4.1. Germination et pénétration

L'infection du champignon débute par la germination des spores (ascospores et/ou pycnidiospores) environ 12h après contact avec la feuille du blé. Cette étape est fortement dépendante du niveau d'humidité ambiante. Selon Ponomarenko *et al*. (2011), au moins 20h d'humidité relative élevée sont nécessaires pour la réussite de l'infection. Après germination, les tubes germinatifs deviendront des hyphes qui pourront ensuite s'insinuer dans les tissus foliaires **(Figure 11)** (Eyal, 1987 ; Duncan and Howard, 2000). Le mode de pénétration de *Z. tritici* a été le sujet de nombreux débats au sein de la communauté scientifique. Celle-ci a généralement lieu entre 24 et 48h après contamination. Néanmoins, Fones *et al*. (2017) ont récemment montré que la croissance épiphyte des hyphes du champignon pouvait durer plusieurs jours avant pénétration. Il a été rapporté que le champignon était capable de rentrer dans les tissus de l'hôte soit, *via* les stomates, soit , plus rarement, directement à travers l'épiderme de la feuille, généralement au niveau des parois anticlinales (Kema *et al*., 1996 ; Duncan and Howard, 2000 ; Shetty *et al*., 2003 ; Siah *et al*., 2010). Certains auteurs suggèrent que le champignon serait capable de reconnaître et de croître en direction des stomates

grâce à un signal thigmotropique encore inconnu (Duncan and Howard, 2000 ; Cousin *et al*., 2006). Cette hypothèse est toutefois loin d'être consensuelle, et de nombreux auteurs considèrent que la croissance des hyphes sur la surface des feuilles se déroule de manière aléatoire (Fones *et al*., 2017). Contrairement à d'autres champignons phytopathogènes, comme *Magnaporthe oryzae*, un agent pathogène majeur du riz, *Z. tritici* ne forme pas d'appressorium lors de cette étape de pénétration foliaire. L'absence de cette structure spécialisée est corrélée avec l'absence de plusieurs gènes impliqués dans sa formation dans le génome de *Z. tritici* (Goodwin *et al*., 2011). Toutefois,plusieurs équipes ont rapporté la formation de pseudo-appressoria, sous forme de renflements, localisés au niveau des zones de pénétration **(Figure 11)** (Kema *et al*., 1996 ; Duncan and Howard, 2000 ; Siah *et al*., 2010).

2.4.2. Phase biotrophe

Après pénétration, le champignon colonise les cavités stomatiques sans causer de symptômes apparents sur les feuilles. Cette période est appelée phase latente ou biotrophe et peut durer, selon la variété du blé, la souche de *Z. tritici* et les conditions environnementales, entre 6 et 36 jours au champ et entre 9 et 14 jours au laboratoire (Steinberg, 2015). Durant cette phase, *Z. tritici*, contrairement à d'autres champignons phytopathogènes, ne produit pas de structure spécialisée dans la nutrition (haustorium). Rudd *et al*. (2015) ont révélé que la source d'énergie principale du champignon provenait majoritairement de ses propres réserves lipidiques. Le pathogène est toutefois aussi capable d'utiliser les ressources de la plante, notamment les sucres présents dans l'apoplasme, mais aussi les composés issus de dégradation de la cuticule du blé, comme le suggère la surexpression de gènes codant pour des lipases et des cutinases par *Z. tritici* durant cette phase (Rohel *et al*., 2001 ; Palma-Guerrero *et al*., 2016). Pendant cette période, tout en évitant les défenses de la plante, les hyphes croissent et colonisent l'espace, ce qui aboutit à la formation des pré-pycnides **(Figure 11)** (Duncan and Howard, 2000).

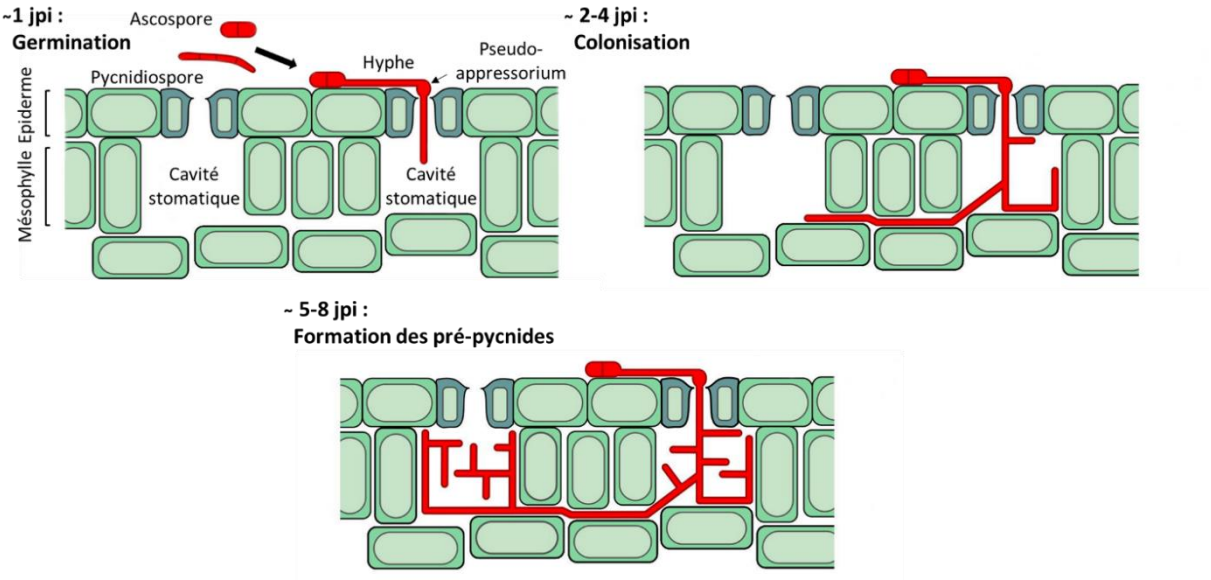

Figure 11 : Représentation schématique du développement de *Z. tritici* sur feuille de blé lors de la phase biotrophe. Après germination, les spores du champignon produisent des hyphes qui pourront infecter les tissus foliaires, soit directement *via* la cuticule, soit *via* les stomates. Le champignon se développe jusqu'à la formation de pré-pycnides. Aucun symptôme d'infection n'est apparent durant cette phase sur la feuille. Jpi : jours post inoculation (d'après **Steinberg, 2015)**.

2.4.3. Phase nécrotrophe

Environ deux semaines après contamination, *Z. tritici* entre dans sa phase nécrotrophe qui se traduit notamment par l'apparition des premiers symptômes sur la feuille, des lésions nécrotiques et chlorotiques, ainsi que par la maturation des pycnides (Kema *et al*., 1996 ; Steinberg, 2015) **(Figure 12)**. Durant cette phase, le champignon libère différentes molécules, comme des protéines effectrices riches en cystéines ou des protéines nécrosantes, qui entraîneront la mort des cellules du mésophylle du blé (Rudd *et al*., 2015) . Parmi les composés impliqués dans le processus d'apoptose, les enzymes de dégradation de la paroi cellulaire du blé (*cell wall degrading enzymes*, CWDE) jouent un rôle fondamental (Brunner *et al*., 2013). Ainsi, Siah *et al*. (2010) ont pu mettre en évidence, lors de la phase nécrotrophe, une forte corrélation entre l'activité de l'endo-β-1,4-xylanase, une CWDE, et le développement de la maladie (r = 0,94), pour 26 souches de *Z. tritici*. La mort des cellules entraîne la libération, dans l'apoplasme, de sucres et d'acide aminés libres, utilisés par le champignon pour augmenter grandement sa biomasse (Keon *et al*., 2007 ; Shetty *et al*., 2007). En parallèle, les pycnides matures contenant des pycnidiospores sont formées et ces dernières pourront alors infecter d'autres plantes de blé lorsque les conditions seront favorables (Shaw, 1987).

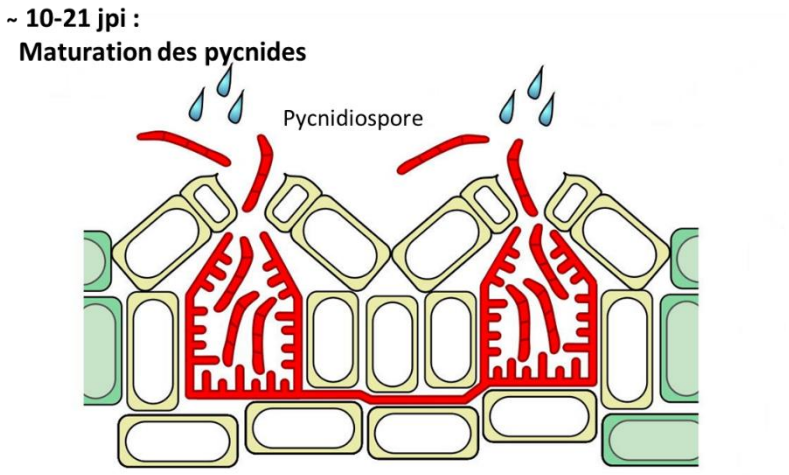

Figure 12 : Représentation schématique du développement de *Z. tritici* sur feuille de blé lors de la phase nécrotrophe. Lors de cette phase, le champignon produit des toxines qui initieront l'apoptose des cellules foliaires. Les ressources libérées sont utilisées par le pathogène comme source d'énergie. En parallèle, les pycnides se développent puis, sous l'effet des gouttelettes de pluie, les pycnides libèrent les pycnidiospores qui pourront contaminer d'autres feuilles ou plantes de blé. Jpi : Jours post inoculation (d'après **Steinberg, 2015**).

2.5. Organisation génomique

Zymoseptoria tritici est le premier champignon appartenant à la classe des *Dothideomycetes* dont le génome a été séquencé, en utilisant la souche de référence IPO323 isolée aux Pays-Bas. Les séquences des génomes nucléaire et mitochondrial de cette souche sont disponibles dans la base de données EnsemblFungi (Kema and van Silfhout, 1997 ; Goodwin *et al*., 2011 ; Flicek *et al*., 2014). La taille de son génome nucléaire assemblé est de 39,69 Mb, réparti sur 21 chromosomes qui présentent une grande variété de longueur, allant de 0,39 à 6,09 Mb (Mehrabi *et al*., 2007). Parmi les 21 chromosomes, treize ont été décrits comme indispensables à la survie et au développement de

l'organisme et sont présents chez toutes les souches de cette espèce. Les 8 autres décrits comme facultatifs ou accessoires , pouvant être présents, absents ou réarrangés selon les isolats, et font de *Z. tritici* l'espèce de champignon filamenteux phytopathogène présentant le plus grande nombre de chromosomes facultatifs (Goodwin *et al*., 2011 ; Yang *et al*., 2020). Chez *Z. tritici*, la taille des chromosomes accessoires varie de 0,39 à 0,77 Mb et ils représentent environ 12 % du génome total du champignon, tout en étant composés en majorité de séquences répétées (Wittenberg *et al*., 2009). Le rôle exact de ces chromosomes facultatifs reste encore à déterminer mais, selon Croll et McDonald (2012), ils pourraient, du fait de leur taux d'évolution rapide, servir de « berceau de l'évolution adaptative » pour le champignon et seraient un composant de sa redoutable plasticité sur le terrain. Ils seraient le siège de mutations rapides, fournissant ainsi au champignon des avantages phénotypiques lui permettant de répondre efficacement aux contraintes environnementales et aux réactions de défenses activées par l'hôte, tout en ayant, en conditions non-stressantes, un impact faible sur le métabolisme général du pathogène (Croll and McDonald, 2012 ; Testa *et al*., 2015). Par ailleurs, des expériences d'infections de différents cultivars de blé avec des souches de *Z. tritici* ayant perdu un ou plusieurs de ces chromosomes accessoires ont démontré que certains d'entre eux ont un rôle dans l'interaction spécifique hôte-pathogène et/ou dans le déclenchement du passage de la phase biotrophe à la phase nécrotrophe (Habig *et al*., 2017). Stewart *et al*. (2018), ont aussi récemment démontré l'association, significative mais faible, de quatre chromosomes accessoires avec des traits de virulence de *Z. tritici* grâce à une étude de cartographie de *quantitative trait loci* (QTL). Les deux études suggèrent ainsi le rôle potentiel des chromosomes accessoires dans la virulence du champignon et les interactions hôte-pathogène mais il reste encore beaucoup à comprendre sur le fonctionnement et le rôle de ces chromosomes facultatifs chez *Z. tritici*.

2.6. *Zymoseptoria tritici*, champignon dimorphe ou pléomorphe ?

Les champignons dimorphes sont des organismes ayant la capacité de changer entre deux morphologies, levure-*like* unicellulaire et hyphe pluricellulaire, lors de leur cycle de vie, en fonction des conditions environnementales **(Figure 13)** (Souza and Taborda, 2020). De nombreux champignons pathogènes majeurs, des animaux comme des végétaux, font partie de cette catégorie. C'est le cas par exemple de l'agent phytopathogène *Ustilago maydis,* responsable du charbon du maïs, ou des espèces appartenant au genre *Verticillium* (Ruiz-Herrera *et al*., 1995 ; Nadal *et al*., 2008). *Zymoseptoria tritici* est lui aussi considéré comme dimorphe, son nom de genre est basé notamment sur l'observation de sa morphologie de type levure, d'où le préfixe « *Zymo* » signifiant « levain, ferment » en grec (Quaedvlieg *et al*., 2011). Certains gènes impliqués dans la morphogénèse de *Z. tritici* ont été identifiés et caractérisés, comme par exemple des gènes codant pour des *mitogen-activated protein kinases* (MAPK) ou pour des protéines impliquées dans la voie de signalisation de l'adénosine monophosphate cyclique (AMPc) (Mehrabi *et al*., 2006a ; Mehrabi *et al*., 2009). Les différentes morphologies peuvent jouer différents rôles durant le processus infectieux. La morphologie de type levure permettrait une rapide augmentation de la taille de la population et favoriserait sa dispersion, facilitant ainsi la colonisation de nouveaux milieux (Lin *et al*., 2015). Chez *Z. tritici*, cette morphologie a surtout été observé *in vitro* et très rarement *in planta*. Récemment, Francisco *et al*. (2019), ont rapporté avoir observé ce mode de développement sur feuille de blé, mais sa contribution dans les processus infectieux et épidémique est encore inconnue. Les auteurs émettent l'hypothèse qu'il pourrait être

impliqué dans la dissémination de la maladie. Les hyphes sont, quant à eux, essentiels à la colonisation et à la pénétration du champignon dans les tissus foliaires ; les souches de *Z. tritici* incapables de produire des hyphes sont en effet incapables d'infecter la plante (Mehrabi *et al*., 2006b ; Steinberg, 2015). Les hyphes sont aussi associés à des mécanismes d'évitement des conditions stressantes comme le stress oxydatif, les températures élevées, ainsi que le manque de ressources disponibles (Francisco *et al*., 2019). Par exemple, Il a été démontré que la souche IPO323 de *Z. tritici* cultivée sur un milieu riche en nutriments avec des températures comprises entre 15°C et 18°C présente une morphologie levure-*like*, alors qu'elle se développe sous forme d'hyphe sur un milieu pauvre en ressources et avec des températures élevées, entre 25 et 28 °C (Motteram *et al*., 2011 ; King *et al*., 2017). La quantité de nutriments et leur biodisponibilité étant très limitées sur la surface des feuilles (Derridj, 1996), Francisco *et al*. (2019) suggèrent qu'après germination des spores sur la feuille de blé, celles-ci percevraient ce manque de ressources qui agirait comme un stimulus induisant la formation d'hyphes qui seraient plus à même d'explorer efficacement l'environnement à la recherche de sources d'énergie.

Récemment, Francisco *et al*. (2019) ont décrit deux autres morphologies exprimés par *Z. tritici*, les pseudo-hyphes, se différenciant des vrais hyphes par une absence de continuité cytoplasmique entre cellules-mères et filles, ainsi que des structures de type chlamydospores, cellules sphériques à parois épaisses riches en lipides **(Figure 13)** (Veses and Gow, 2009). Si le rôle des pseudo-hyphes reste encore inconnu, les chlamydospores, permettent au champignon, selon Francisco *et al*. (2019), de survivre dans des conditions stressantes (dessiccation, températures élevées ou choc de froid) beaucoup plus efficacement qu'en exprimant d'autres morphologies (levure-*like* et pseudo-hyphe). Selon ces auteurs, *Z. tritici* serait donc un champignon pléomorphe, capable de produire au moins quatre morphologies distinctes, chacune avec ses rôles spécialisés, en fonction des conditions environnementales. Cette caractéristique lui confère une plasticité phénotypique remarquable, qui associée à sa plasticité génétique et à son *fitness* élevé, le rendent difficile à contrôler au champ.

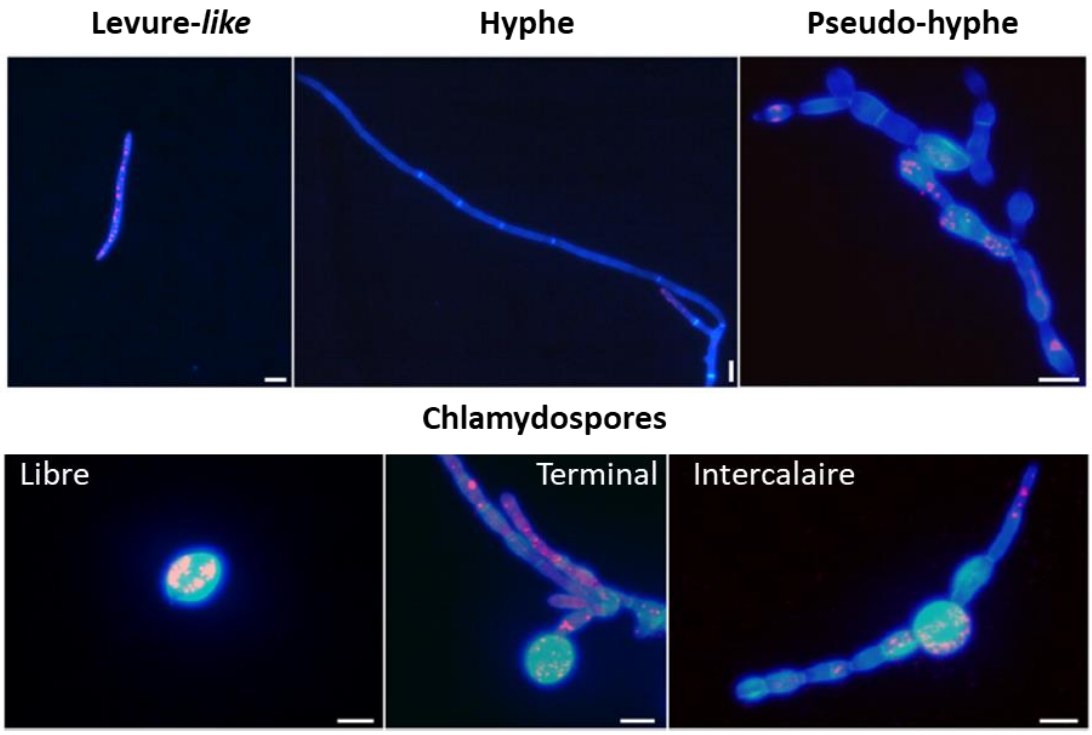

Figure 13 : Morphologies produites par *Zymoseptoria tritici in vitro* observées au microscope optique. La coloration bleue est due à l'utilisation de calcofluor white se liant à la chitine au niveau des parois cellulaires du champignon. Les gouttelettes lipidiques ont été colorées en rouge avec du rouge de Nil. Les structures de type chlamydospores ont été observées libres, situées aux extrémités terminales ou intercalées dans des hyphes ou des pseudo-hyphes (d'après **Francisco *et al*. 2019**).

3. INTERACTION BLÉ-*ZYMOSEPTORIA TRITICI*

Tout au long de leur cycle de vie, les plantes doivent faire face à un grand nombre d'agents pathogènes. Malgré l'absence d'un système immunitaire semblable à celui des animaux, les végétaux ont développé des mécanismes de défense interconnectés et complexes pour faire face aux diverses agressions extérieures. Ceux-ci reposent sur deux stratégies distinctes : les défenses constitutives et les défenses induites.

Les défenses constitutives, appelées aussi passives, correspondent aux barrières physiques (paroi, cuticule, trichome) et chimiques (métabolites secondaires) déployées par la plante, avant toute infection, pour se protéger des bio-agresseurs (Freeman and Beattie, 2008). Dans le cas du pathosystème blé-*Z. tritici*, ces défenses constitutives ne sont pas suffisantes pour protéger la plante de l'infection, les spores du champignon arrivant dans la majorité des cas à les contourner, germer et pénétrer dans les tissus foliaires (Shetty *et al.*, 2003). Les défenses induites, appelées aussi actives, correspondent aux réponses (production de composés toxiques, enzymes, mort cellulaire programmée, *etc*.) mises en place par les cellules végétales après perception de l'invasion par les agents pathogènes. Ces mécanismes de défense active sont souvent coûteux d'un point de vue énergétique (Freeman and Beattie, 2008). Les réactions de défense induites chez le blé contre la septoriose seront développées et détaillées par la suite.

Les interactions plante-pathogène peuvent se dérouler de trois manières différentes : (i) relation non-hôte, (ii) relation incompatible et (iii) relation compatible. Concernant la relation non-hôte, le bio-agresseur (quel que soit son biotype) est incapable de pénétrer et de se développer au sein du végétal (quel que soit le cultivar). Les relations « hôte » sont dépendantes de l'association entre une souche de pathogène et une variété de plante. Si l'agent pathogène parvient à contourner les défenses constitutives de la plante et pénétrer dans les tissus végétaux mais que sa croissance et son développement sont inhibés par les mécanismes de défense induits mis en place par l'hôte, il s'agit d'une relation incompatible. Aucun symptôme n'est engendré lors de cette infection avortée ; le pathogène est qualifié d'avirulent (Reignault and Sancholle, 2005). Dans le cas d'une relation compatible, le pathogène est capable d'infecter son hôte sans que les mécanismes de défense de la plante ne puissent l'empêcher. Les symptômes sont visibles, le pathogène est alors qualifié de virulent (Reignault and Sancholle, 2005).

3.1. Réactions de défense induites du blé vis-à-vis de *Zymoseptoria tritici*

3.1.1. Perception de la présence du pathogène

La mise en place de réponses de défense induites nécessite tout d'abord que l'hôte détecte la présence de l'envahisseur. Pour ce faire, les végétaux sont capables de reconnaître des signaux moléculaires, de compositions chimiques diverses, qui peuvent être classés en trois catégories selon l'origine des composés. Si les molécules sont originaires de l'organisme pathogène lui-même, elles sont appelées *pathogen-associated molecular patterns* (PAMP). Si elles proviennent d'autres micro-organismes non pathogènes, il s'agit alors de *microbe-associated molecular patterns* (MAMP). La troisième et dernière catégorie correspond aux composés et débris cellulaires libérés lors de l'attaque par l'agent pathogène et issus de la plante elle-même. Ceux-ci sont nommés *damage-associated molecular patterns* (DAMP) et proviennent des cellules mortes ou endommagées par les toxines et enzymes du bio-agresseur (Henry *et al.*, 2012). Ces signaux sont reconnus par des récepteurs transmembranaires, les *pattern recognition receptors* (PRR), ce qui engendre par la suite des cascades de signalisation aboutissant à l'activation de voies de défense chez la plante. La mise en place de ces mécanismes suivant la reconnaissance de PAMPs par la cellule végétale est appelée *PAMP-triggered immunity* (PTI). Ce mécanisme de défense est non-spécifique mais peut parfois suffire pour empêcher l'invasion de l'agent phytopathogène **(Figure 14)**. Celui-ci est toutefois capable de contourner la PTI en sécrétant des protéines effectrices. Celles-ci vont engendrer un phénomène appelé *effector-triggered susceptibility* (ETS) **(Figure 14)**. Les rôles de ces effecteurs sont multiples, ils peuvent, par exemple, dissimuler la présence du champignon, inhiber la PTI et dégrader les cellules végétales (Duba *et al.*, 2018). Le rôle de certaines de ces protéines sera présenté et développé par la suite **(voir partie 3.3 Les effecteurs de *Zymoseptoria tritici*)**. La plante peut, dans certains cas, reconnaitre spécifiquement ces effecteurs, ce qui déclenchera une nouvelle vague de défense appelée *effector-triggered immunity* (ETI) **(Figure 14)**. La reconnaissance de ces protéines nécessite des récepteurs appelés *nucleotide binding leucine-rich repeat* (NB-LRR), localisés à l'intérieur des cellules et codés par des gènes de résistance (*R*). L'ETI se révèle généralement plus rapide, plus efficace et plus spécifique que la PTI pour lutter contre l'envahisseur (Jones and Dangl, 2006). L'ETI s'accompagne souvent de mort cellulaire chez l'hôte au niveau des zones les plus infectées, mécanisme aussi appelé réponse hypersensible ou *hypersensitive response* (HR). le modèle en zigzag de Jones and Dangl (2006) intègre l'ensemble de ces interactions (PTI,ETS et ETI) **(Figure 14)**.

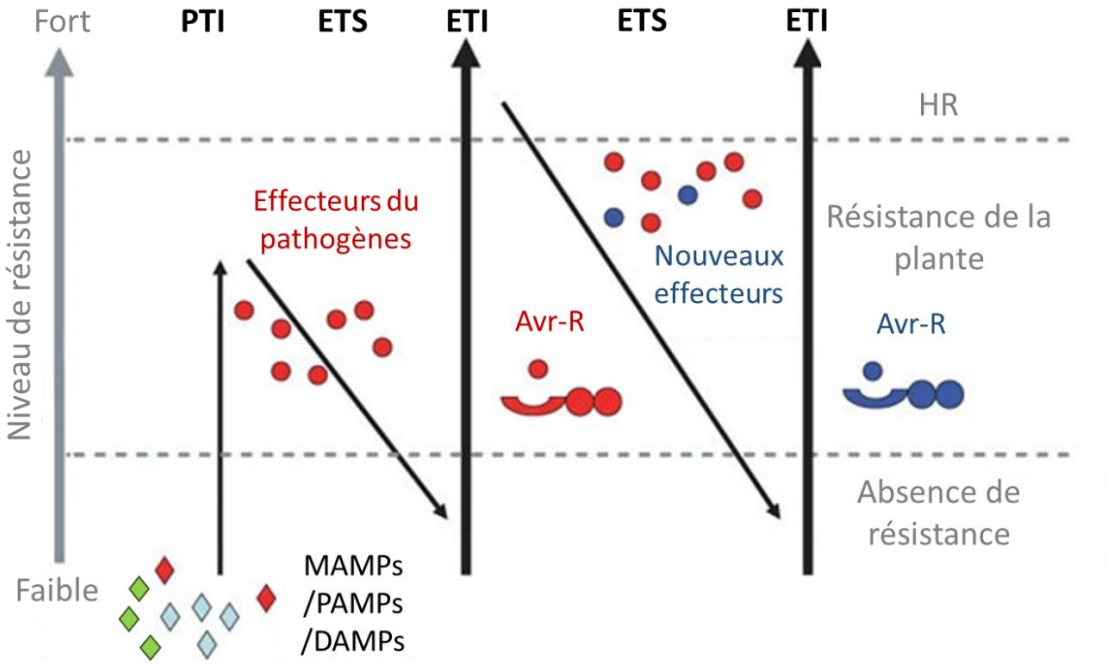

Figure 14 : Modèle en zigzag des interactions plante-pathogène. Avec, Avr-R : reconnaissance gène pour gène (Avr : gène d'avirulence du pathogène et R : gène de résistance de la plante), DAMPs : *damage-associated molecular patterns*, ETI : *effector-triggered immunity*, ETS : *effector-triggered susceptibility***,** HR : réponse hypersensible, MAMPs *: microbe-associated molecular patterns*, PAMPs : *pathogen-associated molecular patterns*, PTI : *PAMP-triggered immunity* (d'après **Jones and Dangl 2006**).

Dans le cas du pathosystème blé-*Z. tritici*, plusieurs PAMP ont été décrits, dont la chitine et le β-1,3-glucane qui sont tous deux des polymères glucidiques présents dans les parois fongiques et notamment celles de *Z. tritici* (Duba *et al.*, 2018). Shetty *et al.* (2009) ont ainsi mis en évidence que la reconnaissance de fragments de β-1,3-glucane, provenant de la paroi de *Z. tritici*, par le blé permettait sa protection vis-à-vis de la maladie. La chitine est, quant à elle, capable de déclencher la PTI chez de nombreuses espèces végétales (Sánchez-Vallet *et al.*, 2015). Chez le blé, la reconnaissance des fragments de ce polysaccharide nécessite deux protéines-clés, la *chitin elicitor binding protein* (CEBiP) et la *chitin elicitor receptor kinase 1* (CERK1) **(Figure 15)** (Lee *et al.*, 2014). Par homologie avec le mode de fonctionnement de ces protéines chez d'autres céréales, notamment le riz, il est suggéré qu'après fixation de la chitine par la CERK1, une cascade de phosphorylation impliquant la voie des MAPK est générée, entraînant par la suite de nombreuses réactions chez la plante (Shimizu *et al.*, 2010). *Z. tritici* est toutefois capable de contourner la PTI induite par la chitine en sécrétant des effecteurs, déclenchant ainsi le phénomène d'ETS. Marshall *et al.* (2011) ont ainsi montré que deux gènes codant pour des effecteurs présentant des motifs lysine, *Mg3LysM* et *Mg1LysM,* étaient fortement transcrits durant la phase asymptomatique du champignon. Ces deux protéines sont capables de se lier à la chitine, ce qui, d'une part, bloque la reconnaissance par les récepteurs CEBiP et CERK1 de la plante et les réactions qui en découlent et, d'autre part, protège le champignon des enzymes de la plante dégradant ce composé glucidique, les chitinases **(Figure 15)**. Les auteurs soulignent le rôle clé de la Mg3LysM, qui est à ce jour, la seule protéine décrite à pouvoir réprimer les défenses précoces du blé induites par la reconnaissance de la chitine.

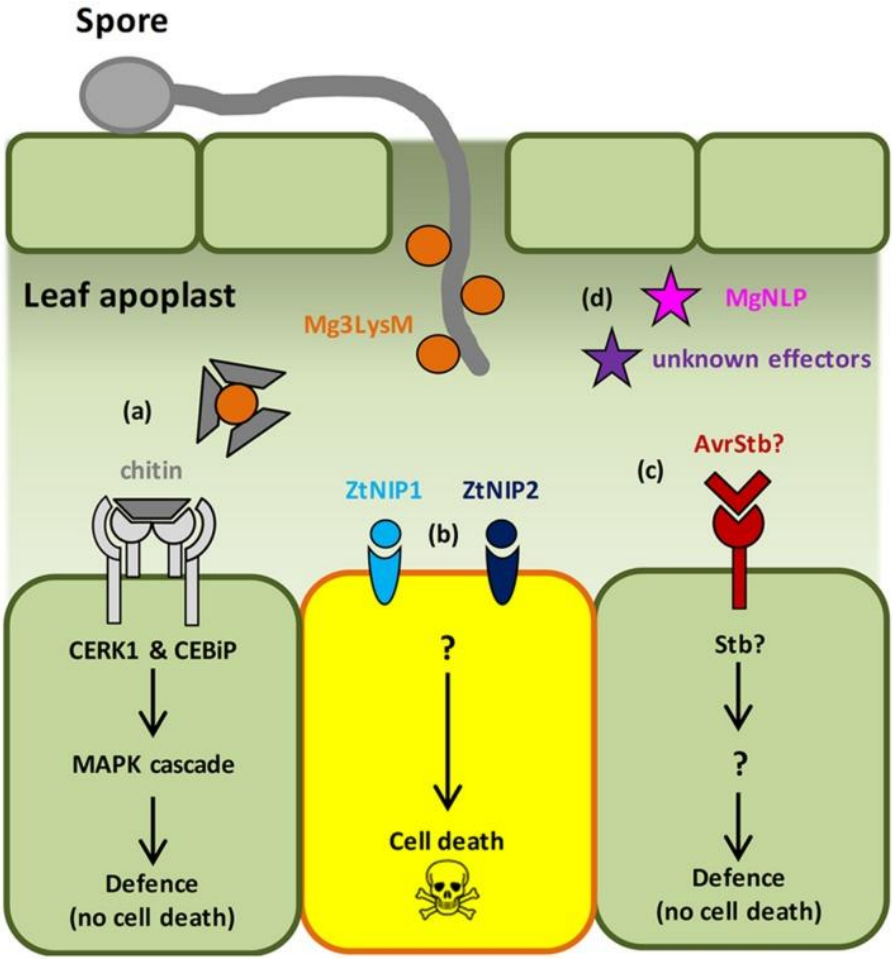

Figure 15 : Schéma des interactions moléculaires blé-*Z. tritici*. (a) La chitine est reconnue par les récepteurs membranaires *chitin elicitor binding protein* (CEBiP) et *chitin elicitor receptor kinase 1* (CERK1), déclenchant la PTI. L'effecteur Mg3LysM est capable de fixer la chitine inhibant l'immunité du blé et protégeant le champignon des chitinases de l'hôte. **(b)** Les effecteurs ZtNIP1 et ZtNIP, des facteurs nécrotiques, induisent la mort des cellules du blé *via* un mécanisme encore inconnu. **(c)** Gènes de résistance *Stb* possiblement induits après reconnaissance d'effecteurs (AvrSTB) sécrété dans l'apoplasme. Dans certains cas, ce mécanisme permet d'inhiber la croissance du pathogène. **(d)** Autres effecteurs impliqués dans l'infection de *Z. tritici*, comme la protéine *necrosis and ethylene-inducing peptide1* (NEP1), un autre potentiel facteur nécrotique (d'après **Kettles and Kanyuka, 2016**).

3.1.2. Réponses précoces du blé

A la suite de la reconnaissance des signaux moléculaires trahissant la présence de l'agent pathogène, des réponses induites précoces se mettent en place rapidement et localement chez la plante. Celles-ci nécessitent l'activation de cascades de phosphorylation qui impliquent notamment les MAPK **(Figure 15)**. En effet, du fait de la phosphorylation ciblée de certaines protéines-clés, notamment des enzymes et des facteurs de transcription, les MAPK peuvent réguler, entres autres, la synthèse d'hormones et de métabolites de défense, l'activation de gènes de résistance, la fermeture des stomates ou encore la HR (Meng and Zhang, 2013). Dans le cadre de l'interaction blé-*Z. tritici*, plusieurs équipes ont montré qu'une MAPK, codée par le gène *TaMPK3*, s'accumulait dans les feuilles juste avant l'apparition des symptômes causés par *Z. tritici* (Rudd *et al.*, 2008 ; Yang *et al.*, 2013). Selon Rudd *et al*. (2008), cette protéine serait impliquée dans le déclenchement local de la HR-*like* au niveau

de l'infection, une réaction qui serait liée au développement des lésions nécrotiques sur les feuilles de blé lors de la phase nécrotrophe du champignon.

Une autre des réactions précoces ayant lieu dans les tissus végétaux en réponse à une infection est la libération de messagers secondaires, tels que les ions calcium (Ca^{2+}) qui régulent de nombreux processus cellulaires. Ces derniers peuvent notamment entraîner très rapidement la production et l'accumulation d'espèces réactives de l'oxygène (*reactive oxygen species*, ROS) aux niveaux intra- et extracellulaires. Les ROS regroupent plusieurs formes de molécules, extrêmement oxydantes, comme le radical superoxide (O_2^-), le radical hydroxyle ($OH^\bullet$) et le peroxyde d'hydrogène (H_2O_2) (Görlach *et al.*, 2015). Le phénomène d'accumulation de ces composés au niveau cellulaire est souvent appelé *burst* oxydatif. Les ROS jouent différents rôles dans la réponse des plantes aux stress, qu'ils soient d'origine abiotique ou biotique. Dans le cadre des interactions plante-pathogène, les ROS peuvent présenter un effet direct antimicrobien, être impliqués dans l'induction de gènes de défense, la production de phytoalexines, le renforcement pariétal et la HR (Thordal-Christensen *et al.*, 1997 ; Gechev and Hille, 2005 ; Shetty *et al.*, 2007 ; Linley *et al.*, 2012 ; Lehmann *et al.*, 2015).

Dans le cas du pathosystème blé-*Z. tritici*, l'effet du H_2O_2 au niveau foliaire a été largement étudié. Shetty *et al.* (2003) ont ainsi démontré que chez les plantes résistantes, ce composé était accumulé rapidement et en grande quantité dès le début de l'infection. A l'inverse, chez les variétés sensibles, la concentration en H_2O_2 n'augmentait que lors du passage à la phase nécrotrophe du champignon. Les travaux de Shetty *et al.* (2007) ont aussi démontré que *Z. tritici* était sensible au H_2O_2 tout au long de son cycle de développement et qu'une accumulation importante de ce composé dans les tissus foliaires réduisait la colonisation, la production de biomasse fongique et allongeait la période de latence du champignon. Les auteurs ont toutefois noté que le champignon était plus tolérant au H_2O_2 lors du passage à la phase nécrotrophe, moment concomitant à la mort des cellules végétales et à la libération d'une grande quantité de ce composé.

Les ROS sont donc des composés majeurs de la défense des plantes. Toutefois, à fortes concentrations, ils sont hautement toxiques pour la plante elle-même. Une régulation fine de leur concentration cellulaire est donc nécessaire, rôle joué par de nombreuses enzymes comme la superoxyde dismutase (SOD), l'oxalate oxydase (OXO), la catalase (CAT) ou encore les péroxydases (POX). La SOD et l'OXO sont impliquées dans la formation du peroxyde d'hydrogène alors que la CAT et la POX interviennent dans sa détoxification et son utilisation en tant que substrat. Plus précisément, la SOD est une enzyme qui catalyse la dismutation du O_2^- en O_2 et H_2O_2, et constitue la première ligne de détoxification des ROS (Gill *et al.*, 2015). L'oxalate oxydase est impliquée dans la réponse des plantes à différents stress et catalyse la transformation de l'acide oxalique en H_2O_2 et CO_2 (Delisle *et al.*, 2001). La catalase, située dans les peroxysomes, permet la détoxification du H_2O_2 en eau et dioxygène. Les peroxydases, quant à elles, utilisent le H_2O_2 pour oxyder de nombreux substrats et sont impliquées dans de nombreuses réactions de défense majeures impliquant la lignification, l'oxydation de composés phénoliques et la subérisation (Pandey et al., 2017).

Les rôles de la CAT et de la POX dans la résistance du blé vis-à-vis de la septoriose ont été étudiés et ont des effets bien différents (Shetty *et al.*, 2003 ; Shetty *et al.*, 2007) . En ce qui concerne la CAT, on observe, chez les cultivars les plus résistants à la septoriose, une réduction de son activité après infection, corrélée avec un *burst* oxydatif précoce, suggérant un rôle négatif de cette enzyme dans la résistance du blé, lié probablement à la répression de l'accumulation de ROS en début d'infection

(Shetty *et al.*, 2007). L'augmentation de l'activité POX dans les plantes, après infection, a plusieurs fois été associée avec une résistance accrue contre les agents pathogènes, comme, par exemple, lors de l'interaction riz-*Magnaporthe oryzae* (Hiraga *et al.*, 2001 ; Reimers *et al.*, 1992). De même, Shetty *et al.* (2003) ont rapporté une implication de la POX dans la résistance du blé vis-à-vis de la septoriose. Les auteurs ont en effet observé, après inoculation avec *Z. tritici*, une augmentation significative de l'activité de cette enzyme chez une variété résistante (Cv. Stakado), ce qui n'était pas le cas chez la variété sensible (Cv. Flame).

3.1.3. Transduction du signal et phytohormones

Après l'établissement des réponses précoces, le signal de stress perçu par les cellules végétales est transmis aux cellules et tissus adjacents, induisant ainsi la mise en place de la résistance locale acquise (*local acquired resistance*, LAR) au niveau du site de l'infection et/ou la résistance systémique acquise (*systemic acquired resistance*, SAR) transmettant la résistance au reste de la plante. Les messagers chimiques impliqués dans la transduction du signal sont très souvent des phytohormones. Les principales familles d'hormones observées chez les plantes sont l'auxine ou l'acide indole-acétique (*indole-3-acetic acid*, IAA), l'acide abscissique (ABA), l'acide salicylique (*salicylic acid*, SA), l'acide jasmonique (*jasmonic acid*, JA), les brassinostéroïdes (BR), les cytokinines (CK), l'éthylène (ET), les gibbérellines (GA) et les strigolactones (SL). Celles-ci jouent des rôles fondamentaux, allant de la division cellulaire et la régulation du métabolisme primaire jusqu'à l'adaptation des plantes aux différents stress environnementaux (Robert-Seilaniantz *et al.*, 2011).

Dans le cas des interactions blé-*Z. tritici*, les études visant à caractériser le rôle des phytohormones ont principalement été focalisées sur le JA et le SA. La biosynthèse et la signalisation du JA ont souvent été rapportées comme centrales dans la défense des plantes contre les pathogènes nécrotrophes, à l'inverse du SA qui est, lui, bénéfique pour lutter contre l'invasion d'agents biotrophes ou hémi-biotrophes. Ce *crosstalk* hormonal entre ces deux molécules antagonistes a largement été discuté et parfois nuancé dans la littérature. De récentes études ont mis en lumière l'activation simultanée de ces deux voies hormonales dans certains cas, notamment durant l'ETI (Thaler *et al.*, 2012 ; Wasternack and Hause, 2013 ; Betsuyaku *et al.*, 2018).

La synthèse du JA dépend de la voie des octadécanoïdes et commence dans le chloroplaste avec un acide gras à 18 carbones, l'acide linoléique. Celui-ci est oxydé successivement par plusieurs enzymes clés de cette voie de biosynthèse, la lipoxygénase (LOX), l'allène oxyde synthase (AOS) et l'allène oxyde cyclase (AOC). Le produit de ces réactions est ensuite transféré dans le peroxysome où il est finalement transformé en JA. Dans le cytosol, la phytohormone peut ensuite être convertie en plus de 30 dérivés. Les composés considérés les plus actifs biologiquement sont le JA libre, le méthyl-jasmonate (MeJA), le *cis*-jasmone et le jasmonoyl-isoleucine (JA-Ile) (Wasternack and Hause, 2013 ; Ali and Baek, 2020).

La LOX joue un rôle prépondérant dans le cadre des interactions blé-*Z. tritici*. Ray *et al.* (2003) ont ainsi montré chez le blé une expression différentielle d'un gène codant pour une LOX en lien avec le niveau de résistance du cultivar infecté par *Z. tritici*. En effet, chez les cultivars résistants, les auteurs ont observé une diminution significative du nombre de transcrits plus rapidement que chez le cultivar sensible. Selon cette équipe, la LOX pourrait favoriser le développement et la colonisation du champignon chez l'hôte. L'inhibition de cette enzyme apporterait alors un avantage majeur à la plante

vis-à-vis du pathogène, faisant de ce mécanisme une caractéristique des variétés résistantes à la maladie.

Le SA, ou *2-hydoxybenzoic acid*, est un acide phénolique hydroxylé surtout connu pour son rôle en tant qu'hormone-clé des voies de défense chez les plantes. Ce composé est notamment impliqué dans la régulation des phénomènes HR et la mort cellulaire en réponse aux stress biotiques, ainsi que dans l'induction de la LAR et de la SAR (Malamy *et al.*, 1990 ; Gaffney *et al.*, 1993 ; Radojičić *et al.*, 2018). Le SA est généré à partir du chorismate, produit final de la voie du shikimate, et *via* deux voies métaboliques distinctes : celle de l'isochorismate (IC) et celle des phénylpropanoïdes (Ding and Ding, 2020) **(Figure 16)**.

- La voie de l'IC comprend trois enzymes principales ; la première est l'isochrosimate synthase (ICS1) qui catalyse la transformation du chorismate en ioschorismate dans le chloroplaste, son homologue proche ICS2 joue un rôle similaire (Strawn *et al.*, 2007 ; Garcion *et al.*, 2008). La deuxième est l'EDS5 qui est un transporteur localisé dans la membrane du chloroplaste et permettant le transport de l'IC du chloroplaste vers le cytosol (Serrano *et al.*, 2013). La troisième est la PBS3 présentant une fonction isochorismoyl-glutamate synthase (IGS), permettant la transformation de l'IC en isochorismoyl-9-glutamate, qui se fragmente ensuite spontanément pour former le SA (Ding and Ding, 2020).

- La voie des phénylpropanoïdes se déroule majoritairement dans le cytosol et débute avec la transformation de la phénylalanine, dérivant du chorismate, en acide trans-cinnamique grâce à l'action de la phénylalanine ammonia lyase (PAL), enzyme-clé de la voie. Le produit est ensuite transformé, *via* différentes enzymes, d'abord en acide benzoïque puis en SA (Huang *et al.*, 2010) **(Figure 16)**.Tout comme le JA, le SA peut ensuite être converti en plusieurs dérivés qui ont alors des rôles différents, comme le méthyl-salicylate (MeSA), une forme inactivée du SA qui pourrait servir de signal mobile déclencheur de la SAR, mais cette hypothèse reste toutefois à confirmer (Park *et al.*, 2007).

Les ROS peuvent influer sur l'accumulation du SA. L'H_2O_2 entraîne une accumulation de l'acide benzoïque, un des intermédiaires réactionnels de la biosynthèse du SA dans la voie des phénylpropanoïdes. En retour, l'augmentation de la concentration cellulaire en SA conduit à une inhibition de l'activité de la CAT, induisant une augmentation de la concentration en H_2O_2 (Vidhyasekaran, 2015). En parallèle, le SA intervient notamment sur l'expression de gènes de défense comme la *pathogenesis-related protein 1* (PR1) (Ali *et al.*, 2018).

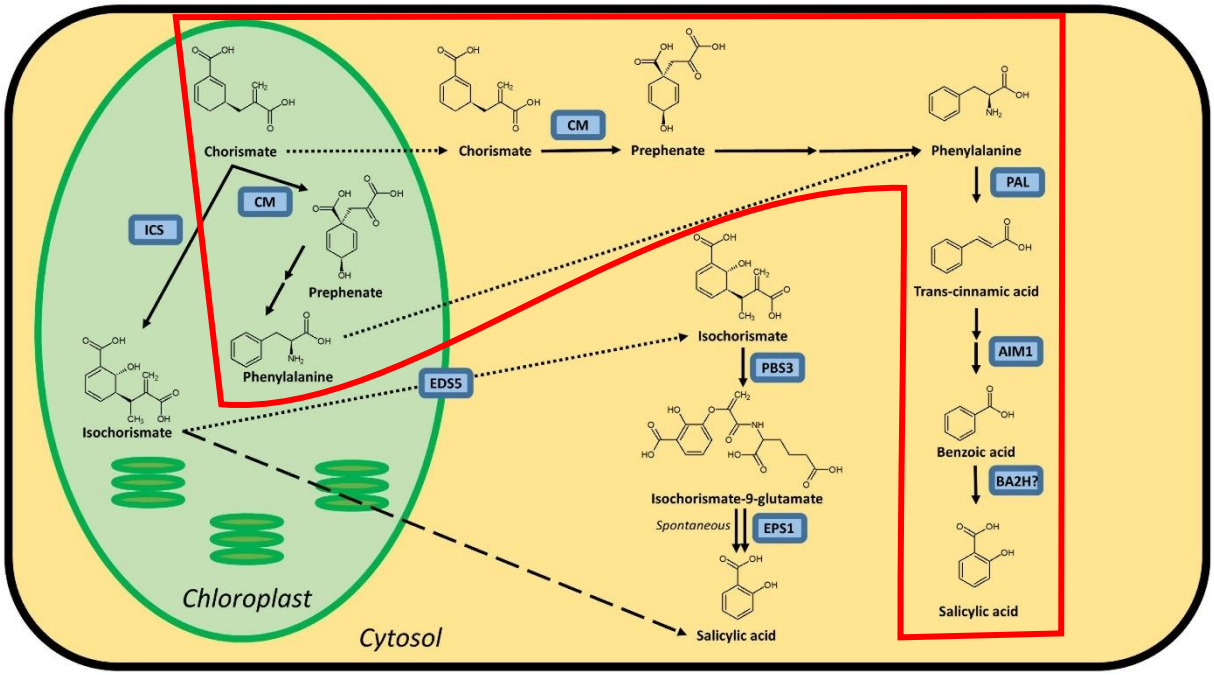

Figure 16 : Biosynthèse de l'acide salicylique. L'encart en rouge correspond à la voie des phénylpropanoïdes, les lignes en pointillées au transport de molécules du chloroplaste au cytosol et la ligne en tiret à une voie alternative encore inconnue, indépendante des voies connues (isochorismate et phénylpropanoïdes). AIM1 : *abnormal inflorescence meristem*, BA2H : *benzoic acid 2-hydroxylase*, CM : *chorismate mutase*, EDS5 : *enhanced disease susceptibility 5*, EPS1 : *enhanced pseudomonas susceptibility 1*, ICS : isochrosimate synthase, PAL : *phenylalanine ammonia lyase*, PBS3 : *AvrPphB susceptible 3* (d'après **Lefevere *et al.*, 2020**).

3.1.4. Réponses tardives du blé

Après reconnaissance de l'agent pathogène, l'établissement de réponses précoces et la transduction du signal aux niveaux local et systémique, *via* notamment les phytohormones, la plante infectée peut développer des réponses de défense dites tardives. Les principaux mécanismes impliqués sont (i) le renforcement des barrières physiques, (ii) la production de métabolites secondaires antimicrobiens et (iii) l'accumulation de protéines PR (*pathogenesis-related*).

Les renforcements pariétaux

Après l'attaque, la paroi des cellules végétales est modifiée, voire remodelée, en profondeur, dans le but, notamment, de résister aux toxines et aux CWDEs produites par l'agent pathogène. De nombreux composés de défense, de natures chimiques variées, y sont incorporés, allant des polysaccharides comme la callose, en passant par des phénylpropanoïdes comme la lignine et la subérine, jusqu'aux glycoprotéines structurales comme les *hydroxyproline-rich glycoproteins* (HRGP) (Deepak *et al.*, 2010). La callose est un polymère glucidique, composé majoritairement de β-1,3-glucane, dont la déposition est induite au niveau des sites d'infection et régulée en partie par le SA (Luna *et al.*, 2011). La lignine est un polymère de monolignols dont les trois principaux représentants sont l'alcool coniférylique, l'alcool sinapylique et l'alcool coumarylique **(Figure 17)**. Ces monolignols sont issus de la voie des phénylpropanoïdes, et leur synthèse nécessite l'intervention de plusieurs enzyme-clés, incluant la PAL, la *cinnamyl alcohol dehydrogenase* (CAD), la *caffeic acid O-*

methyltransferase (COMT) et bien d'autres **(Figure 17)**. L'assemblage des monolignols en lignine est ensuite catalysée par les laccases (LAC) et surtout les POX, qui utilisent des ROS comme substrats (Frei, 2013).

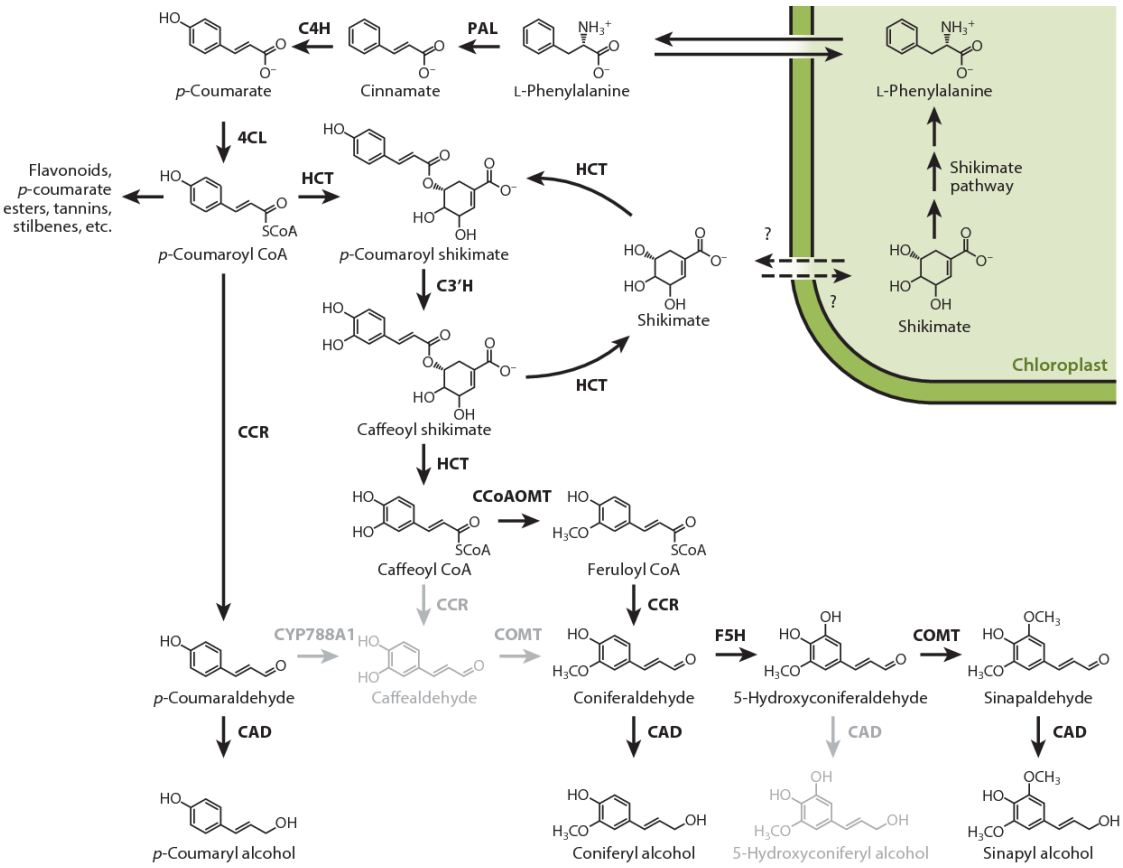

Figure 17 : Biosynthèse des monolignols, monomères de lignine. La production des monolignols débute avec la voie des phénylpropanoïdes, ces monomères sont ensuite polymérisés grâce à l'action de péroxydases et potentiellement de laccases. 4CL : *4-coumarate-CoA ligase*, C3'H : *4-coumarate 3-hydroxylase*, C4H : *cinnamate 4-hydroxylase*, CAD : *cinnamyl alcohol dehydrogenase*, CCoAOMT : *caffeoyl CoA O-methyltransferase*, COMT : *caffeic acid O-methyltransferase*, CCR : *cinnamoyl CoA reductase*, F5H : *ferulate-5-hydroxylase*, HCT : *quinate/ shikimate p-hydroxycinnamoyltransferase*, PAL : *phenylalanine ammonia lyase* (d'après **Bonawitz and Chapple, 2010**).

Dans le cadre des interactions blé-*Z. tritici*, le rôle capital de la callose dans la résistance du blé, a été démontré par Shetty *et al.* (2009). Une accumulation beaucoup plus importante de ce polysaccharide, jusqu'à 46 fois supérieure, a été détectée chez le cultivar résistant Stakado comparé au cultivar sensible Sevin, 9 jours après infection. Les auteurs ont observé que ce dépôt de callose était principalement localisé au niveau des cavités sous-stomatiques et du mésophylle, suivant ainsi la croissance du champignon. De même, Seybold *et al.* (2020) ont trouvé que la concentration en lignine chez une variété plus résistante (Chinese Spring) était significativement plus importante que chez une variété sensible après infection (Obelisk). Ces deux études soulignent le rôle du renforcement pariétal dans la résistance du blé vis-à-vis de *Z. tritici*.

Production de métabolites secondaires

Une autre des réponses tardives mises en place par la plante lors d'une agression est la synthèse et la libération de composés à faible poids moléculaire issus du métabolisme secondaire tels que les phénylpropanoïdes. Ces composés phénoliques sont impliqués dans la réponse aux stress qu'ils soient d'origine abiotique ou biotique. Cette famille regroupe, outre les monolignols qui interviennent dans la synthèse de la lignine, le SA et ses dérivés, les flavonoïdes et les phytoalexines.

Toutes ces molécules appartiennent à la voie des phénylpropanoïdes et leur synthèse nécessite souvent l'action de la PAL, une enzyme-centrale de cette voie. Adhikari *et al.* (2007) ont observé une augmentation significative du nombre de transcrits du gène codant pour la PAL très tôt, entre 3 et 6 heures après l'infection par *Z. tritici*, uniquement chez les variétés de blé résistantes (Tadinia and W7984), soulignant l'importance de ce gène dans la résistance de la plante à la maladie. Toutefois, Shetty *et al.* (2009) n'ont pas observé ce phénomène chez le cultivar résistant Stakado indiquant qu'il serait possiblement dépendant du cultivar. En ce qui concerne les flavonoïdes, et bien qu'ils soient connus pour leurs activités antifongiques, très peu de travaux se sont intéressés à leur rôle dans les interactions blé-pathogène (Mierziak *et al.*, 2014 ; Al Aboody and Mickymaray, 2020). Pour ce qui est des phytoalexines, seul un petit nombre a été observé et décrit chez le blé (Du Fall and Solomon, 2013).

Les protéines PR

Les protéines PR sont des molécules induites chez la plante en réponse à l'attaque d'agents pathogènes et sont des acteurs essentiels de la défense chez les plantes. Il s'agit de molécules à faible poids moléculaire, compris entre 6 et 43 KDa, s'accumulant principalement dans l'apoplasme et présentant des caractéristiques communes, notamment le fait d'être particulièrement stables. Elles sont ainsi thermostables, résistantes aux protéases et restent solubles en conditions acides (pH inférieur à 3) (Van Loon *et al.*, 1994). Ces protéines sont largement distribuées chez les plantes et ont été détectées dans tous les organes et particulièrement dans les feuilles où elles sont présentes en très grande quantité, représentant entre 5 et 10 % des protéines totales (Van Loon *et al.*, 1994). Les protéines PR ont des fonctions diverses et sont classées, selon celles-ci, en 17 catégories **(Tableau 1)** (Ali *et al.*, 2018). Il est à noter que le mode d'action exact de certaines de ces protéines, comme PR1, reste encore obscur à l'heure actuelle.

Tableau 1: Catégories, fonction et origine des protéines PR (d'après **Ali *et al.*, 2018**).

Protéine PR	Fonction	Origine	Référence
PR1	*Antifungal*	*Nicotiana tabacum*	Antoniw *et al.* (1980)
PR2	*β-1,3-glucanases*	*Nicotiana tabacum*	Antoniw *et al.* (1980)
PR3	*Class I, II, IV, V, VI, VII Chitinases*	*Nicotiana tabacum*	Van Loon (1982)
PR4	*Class I, II Chitinases*	*Nicotiana tabacum*	Van Loon (1982)
PR5	*Thaumatin-like proteins*	*Nicotiana tabacum*	Van Loon (1982)
PR6	*Proteinase inhibitor*	*Solanum lycopersicum*	Green and Ryan(1972)
PR7	*Endoproteinase*	*Solanum lycopersicum*	Vera and Conejero (1988)
PR8	*Class III Chitinase*	*Cucumis sativus*	Metraux *et al.* (1988)
PR9	*Peroxidase*	*Nicotiana tabacum*	Lagrimini *et al.* (1987)
PR10	*Ribonuclease-like proteins*	*Petroselinum crispum*	Somssich *et al.* (1986)
PR11	*Class I Chitinase*	*Nicotiana tabacum*	Melchers *et al.* (1994)
PR12	*Defensin*	*Raphanus raphanistrum*	Terras *et al.* (1995)
PR13	*Thionin*	*Arabidopsis thaliana*	Epple *et al.* (1995)
PR14	*Lipid-transfer protein*	*Hordeum vulgare*	Garcıa-Olmedo *et al.* (1995)
PR15	*Oxalate oxidase*	*Hordeum vulgare*	Zhang *et al.* (1995)
PR16	*Oxidase-like*	*Hordeum vulgare*	Wei *et al.* (1998)
PR17	*Antifungal and antiviral*	*Nicotiana tabacum*	Okushima *et al.* (2000)

Le rôle de certaines de ces protéines PR dans les interactions blé-*Z. tritici* a été étudié. Plusieurs travaux ont montré que le niveau d'expression des gènes *PR1, PR2, PR3, PR5* et *PR9* après infection différait selon le niveau de résistance du cultivar (Ray *et al.*, 2003 ; Adhikari *et al.*, 2007 ; Shetty *et al.*, 2009). Selon Adhikari *et al.* (2007), le gène codant pour la PR1 pourrait servir de biomarqueur pour distinguer un cultivar résistant d'un cultivar sensible selon son niveau d'expression à 12h après infection. Les PR2 et PR3 correspondent respectivement aux glucanases et chitinases, enzymes capables de dégrader les polymères de la paroi fongique, freinant ainsi son développement et libérant par la même occasion des fragments de chitine et de β-1,3-glucane qui pourront ensuite servir de PAMPs **(voir 3.1.1. Perception de la présence du pathogène)**. Les PR5 sont de petites molécules présentant une activité antimicrobienne (Wang *et al.*, 2010). Les PR9 correspondent aux péroxydases dont le rôle à déjà été présenté **(voir 3.1.2. Réponses précoces du blé)**. Ray *et al.* (2003) ont observé une augmentation significative du nombre de transcrits des *PR1, PR2* et *PR5*, 12h après infection, chez les cultivars les plus résistants comme les plus sensibles. Les auteurs indiquent, toutefois, une expression significativement plus marquée chez les cultivars résistants. Le niveau d'expression de ces protéines PR peut aussi varier durant le processus infectieux. En effet, Rudd *et al.* (2015) ont rapporté, un jour après infection une réduction de l'expression de gènes codant pour les PR1, PR2, PR3, PR4 et PR5 chez un cultivar sensible (Cv. Riband). Les auteurs émettent l'hypothèse que cette régulation négative serait causée par le champignon afin de manipuler et contourner les réactions de défense de la plante.

3.2. Résistance génétique structurale du blé vis-à-vis de *Zymoseptoria tritici*

Chez les plantes, la résistance peut être définie comme la capacité de la plante à empêcher ou réduire la colonisation ou la croissance d'un bio-agresseur dans ses tissus. D'un point de vue génétique, deux types de résistance existent : la résistance qualitative (spécifique) et la résistance quantitative (non-spécifique). Celles-ci ont, toutes deux, été observées dans le cas du pathosystème blé-*Z. tritici*.

3.2.1. La résistance qualitative

La résistance qualitative (spécifique) est contrôlée par un ou plusieurs gènes majeurs, appelés aussi gènes *R*, réagissant supposément selon la relation gène pour gène décrite par Flor (1971) **(Figure 14)**. Les effets de protection de ces gènes sont majeurs mais souvent limités dans le temps, à cause du contournement des résistances par les agents pathogènes. Chez le blé, 21 gènes impliqués dans la résistance qualitative du blé vis-à-vis de la septoriose ont été rapportés et cartographiés. Ils sont appelés *Stb* (pour *Septoria tritici blotch*) (Brown *et al.*, 2015) **(Tableau 2)**. Ces gènes sont fortement spécifiques et ne sont efficaces que contre un faible nombre de génotypes du champignon, généralement les avirulents. Parmi les 21 gènes identifiés, l'importance du *Stb6*, codant pour une *wall-associated recpetor kinase*, a été largement étudié (Saintenac *et al.*, 2018). Arraiano *et al.* (2009) ont ainsi montré que la présence de ce gène était associée à une réduction de la sévérité de la maladie en moyenne de 19 % chez de nombreuses lignées de blé. La résistance apportée par ces gènes *Stb* est toutefois fréquemment contournée par le pathogène. Ainsi, la résistance quantitative, plus durable, a gagné de plus en plus en intérêt pour les scientifiques et les sélectionneurs (Pilet-Nayel *et al.*, 2017).

Tableau 2: Principaux gènes *R* impliqués dans la résistance qualitative du blé vis-à-vis de *Z. tritici* (d'après **Brown *et al.*, 2015**).

Gène	Chromosme	Marqueur	Souche de *Z. tritici*	Cultivar de blé	Référence
Stb1	5BL	Xbarc74 (2.8cM), Xgwm335 (7.4cM)	IN95-Lafayette-1196-WW 1-4 et Purdue local	Bulgaria 88	Adhikari *et al.* (2004a)
Stb2	1BS	Xwmc406 (6cM), Xwmc230 (5cM)	Paskeville local et IPO92034	Veranopolis	Liu *et al.* (2013)
Stb3	7AS	Xwmc83	Paskeville local isolate	Israel 493	Goodwin and Thompson (2011)
Stb4	7DS	Xgwm111 (0.7cM)	IN95-Lafayette-1196-WW-1-4, I-89, IPBr1	Tadinia	Adhikari *et al.* (2004c)
Stb5	7DS	Xgwm44 (7.2cM)	IPO94269	Synthetic 6x	Arraiano *et al.* (2001b)
Stb6	3AS	Xgwm369 (2cM)	IPO323	Flame, Hereward	Brading *et al.* (2002)
Stb7	4AL	Xwmc313 (0.3 à 0.5cM), Xwmc219 (1cM)	MG2 et IPO87019	ST6	McCartney *et al.* (2003)
Stb8	7BL	Xgwm146 (3.5cM), Xgwm577 (5.3cM)	IN95-Lafayette-1196-WW 1-4	Synthetic W7984	Adhikari *et al.* (2003)
Stb9	2BL	Xfbb226 (3.6cM), Xwmc317, Xbarc0129	IPO89011	Courtot, Tonic	Chartrain *et al.* (2009)
Stb10	1Dc	Xgwm848	IPO94269 et ISR8036	Kavkaz-K4500	Chartrain *et al.* (2005c)
Stb11	1BS	Xbarc008 (1cM)	IPO90012	TE9111	Chartrain *et al.* (2005a)
Stb12	4AL	Xwmc219	ISR398 et ISR8036	Kavkaz-K4500	Chartrain *et al.* (2005c)
Stb13	7BL	Xwmc396 (7-9cM)	MG96-36, MG2	Salamouni	Cowling (2006)
Stb14	3BS	Xwmc500 (2cM), wmc632 (5cM)	MG2	Salamouni	Cowling (2006)
Stb15	6AS	Xpsr904 (14cM)	IPO88004	Arina, Riband	Arraiano *et al.* (2007b)
StbSm3	3AS	barc321 (1.9cM)	MG96-36, MG2	Salamouni	Cuthbert (2011)
Stb16q	3DL	Xgwm494 (4.3cM), Xbarc128 (9.9cM)	IPO88018 et IPO94218	SH M3	Tabib Ghaffary *et al.* (2012)
Stb17	5AL	Xhbg247 (3.1cM), Xgwm617 (38.3cM)	IPO88018	SH M3	Tabib Ghaffary *et al.* (2012)
Stb18	6DS	Xgpw5176, Xgpw3087	IPO323, IPO98022, IPO89011, IPO98046	Balance	Tabib Ghaffary *et al.* (2011)
StbWW	1BS	Xbarc119b (0.9–4.1cM)	79, 2, 1A	WW1842, WW2449, WW2451	Raman *et al.* (2009)
TmStb1	$7A^{m}S$	Xbarc174 (23.5cM)	IPO323	MDR043 (T. monococcum)	Jing *et al.* (2008)

3.2.2. La résistance quantitative

La résistance quantitative est gouvernée par l'action de différents ensembles de gènes et est généralement moins spécifique que la résistance qualitative, ce qui lui permet d'être souvent efficace contre un large panel de souches de *Z. tritici* et d'être plus difficilement contournée par le pathogène. Plusieurs travaux ont montré que la résistance qualitative chez le blé vis-à-vis de *Z. tritici* dépend de *quantitative trait loci* (QTL) qui ont pu être localisés et associés à certains marqueurs moléculaires (Eriksen *et al.*, 2003 ; Chartrain *et al.*, 2004 ; Brown *et al.*, 2015). Brown *et al.* (2015) rapportent que 89 régions génomiques, portant des QTL ou des méta-QTL, ont été identifiés comme étant impliqués dans la résistance du blé vis-à-vis de la maladie. Les auteurs indiquent que seul le chromosome 5D ne porte pas de QTL ou méta-QTL. Il est aussi à noter que plusieurs QTL et méta-QTL ont été cartographiés dans des régions du génome où des gènes de résistance spécifique (*Stb*) étaient présents. L'amélioration des connaissances sur la génétique des résistances qualitative et quantitative est d'une grande utilité pour les sélectionneurs pour développer des variétés plus résistantes à la maladie.

3.3. Les effecteurs de *Z. tritici*

Les effecteurs sont des protéines essentielles au bon déroulement de la colonisation et du développement de l'agent pathogène dans son hôte. Chez *Z. tritici*, des études de transcriptomique ont permis d'identifier une centaine de gènes candidats impliqués dans la virulence ou la pathogénicité (Rudd *et al.*, 2015 ; Kettles and Kanyuka, 2016). Aujourd'hui, plus d'une vingtaine de gènes codant pour des effecteurs ont été identifiés **(Tableau 3)** (Mirzadi Gohari *et al*., 2014 ; Kettles and Kanyuka, 2016; Tiley *et al.*, 2019)**.** Si beaucoup d'efforts ont été menés ces dernières décennies pour mieux comprendre le rôle de ces effecteurs, il reste encore beaucoup à découvrir pour mieux élucider leurs implications. Parmi les effecteurs majeurs identités, on peut citer MgAtr4, qui a été le premier effecteur découvert chez *Z. tritici* (Stergiopoulos *et al.*, 2003). Il s'agit d'un transporteur membranaire, membre de la famille des *ATP-binding cassette* (ABC) et dont le rôle serait de protéger l'envahisseur contre les molécules de défense produites par la plante hôte, comme les phytoalexines (Stergiopoulos *et al.*, 2003). La protéine MgHog1 est indispensable au champignon durant les débuts de l'infection, les mutants ne l'exprimant pas se révélant incapable de coloniser leur hôte. Mehrabi *et al.* (2006b) ont démontré qu'elle était impliquée dans la transition entre le tube germinatif et le développement de l'hyphe. MgSlt2 joue aussi un rôle fondamental, durant la phase asymptomatique, étant impliquée dans la ramification du mycélium, nécessaire à la colonisation des cavités sous-stomatiques (Mehrabi *et al.*, 2006a). D'autres travaux ont permis de mettre en évidence des effecteurs-clés de la phase nécrotrophe du champignon. Ainsi, M'Barek *et al.* (2015) ont montré que des filtrats de culture de *Z. tritici* contenaient des composés capables d'entraîner la mort des cellules foliaires quand elles étaient injectées dans les feuilles de blé. Les auteurs ont identifié deux effecteurs, potentiellement des *necrosis-inducing proteins,* nommés ZtNIP1 et ZtNIP2, qui viennent rejoindre le gène *NEP1* en tant que facteurs nécrotiques (Motteram *et al.*, 2009) **(Figure 15)** . Le gène *ZtWor1* est quant à lui impliqué dans plusieurs mécanismes tels que la colonisation du mésophylle et la fructification asexuée du champignon (Mirzadi Gohari et al., 2014). Plusieurs autres gènes de virulence sont impliqués dans la formation des pycnides, notamment *MgTpk2* et *MgBcy1* (Mehrabi and Kema, 2006). Très récemment, un nouvel effecteur a été identifié chez *Z. tritici*, il s'agit du gène de virulence *ZtvelB* qui est aussi

nécessaire pour la mise en place de pycnides. Il est à noter que celui-ci est aussi impliqué dans le développement du champignon sous forme levure-*like* (Tiley *et al.*, 2019).

Tableau 3: Liste de gènes codant pour des protéines effectrices chez *Z. tritici* (d'après **Gohari *et al.*, 2015**, modifié).

Gène	Catégorie	Référence
MgAtr4	*ABC Transporter*	Stergiopoulos *et al.,* 2003
MgFus3	*Mitogen-activated protein kinase (MAPK)*	Cousin *et al.*, 2006
MgSlt2	*MAPK*	Mehrabi *et al.*, 2006a
MgHog1	*MAPK*	Mehrabi *et al.*, 2006b
MgTpk2	*Protein kinase A catalytic subuniT*	Mehrabi et Kema, 2006
MgBcy1	*Protein kinase A regulatory subunit*	Mehrabi et Kema, 2006
MgSTE11	*MAPK kinase kinase*	Kramer *et al.*, 2009
MgSTE50	*Scaffold protein for MAPK signaling*	Kramer *et al.*, 2009
MgSTE12	*Transcription factor target of MAPK signaling*	Kramer *et al.*, 2009
MgSTE7	*MAPK kinase*	Kramer *et al.*, 2009
MgNLP	*Unknown*	Motteram *et al.*, 2009
MgGpa1	*G-protein alpha subunit*	Mehrabi *et al.*, 2009
MgGpa3	*G-protein alpha subunit*	Mehrabi *et al.*, 2009
MgGpb1	*G-protein alpha subunit*	Mehrabi *et al.*, 2009
MCC1	*c-type cyclin*	Choi and Goodwin, 2010
Mg3LysM	*Chitin binding effector protein*	Marshall *et al.*, 2011
MgAlg2	*Protein N-Glycosylation*	Motteram *et al.*, 2011
ZtWor1	*Transcription factor*	Gohari *et al.,* 2014
ZtNIP1	*Necrotic factor*	M'Barek *et al.*, 2015
ZtNIP2	*Necrotic factor*	M'Barek *et al.* 2015
Zt80707	*Unknown/Secreted*	Poppe *et al.*, 2015
Zt89160	*Unknown*	Poppe *et al.*, 2015
Zt103264	*Unknown*	Poppe *et al.*, 2015
ZtvelB	*Transcription factor*	Tiley *et al.,* 2019

4. LES MÉTHODES DE LUTTE CONTRE LA SEPTORIOSE

Actuellement, la lutte contre *Z. tritici* repose essentiellement sur l'utilisation des produits phytopharmaceutiques de synthèse mais aussi, dans une moindre mesure, sur le déploiement des résistances variétales (Torriani *et al*., 2015). La protection octroyée par la lutte génétique est toutefois limitée et, à ce jour, aucune variété totalement résistante à la septoriose n'a pu être obtenue. D'autres méthodes par ailleurs existent pour protéger la culture et seront discutées ci-dessous.

4.1. La lutte chimique

La lutte chimique reste encore, et de loin, la principale méthode employée au champ pour lutter contre la septoriose. Dans l'Union européenne, jusqu'à 70 % des fongicides épandus dans les parcelles sont utilisés pour protéger le blé contre cette maladie (Fones *et al*., 2017). Plusieurs familles de fongicides ont été utilisées pour contrôler *Z. tritici* au cours de ces dernières décennies.

Les premiers à avoir vu le jour sont les inhibiteurs multi-sites de contact, tels que le chlorothalonil ou le mancozèbe. Ces produits sont capables d'agir sur différentes cibles cellulaires du champignon et peuvent agir à la fois sur la germination des spores et la croissance mycélienne. Aucun phénomène de résistance marqué n'a été observé pour ces molécules, très probablement grâce à leur mode d'action non spécifique, ce qui leur confère un avantage certain (Leroux *et al*., 2007). Néanmoins, ces produits présentent de nombreux inconvénients qui limitent fortement leur utilisation. En effet, pour être efficace, ils doivent être appliqués à fortes doses et sont facilement lessivables lors des épisodes de précipitation, ce qui peut entraîner une pollution environnementale conséquente. Leurs risques aux niveaux toxicologique et éco-toxicologique ont récemment conduit à leur interdiction d'utilisation par l'UE, respectivement en 2020 pour le chlorothalonil et 2021 pour le mancozèbe (Anses, 2019).

A partir des années 1960, de nouvelles molécules fongicides ont été élaborées. Il s'agit cette fois-ci de produits systémiques, donc pénétrants dans la plante, efficaces à faible dose et faiblement écotoxiques. Ces produits présentent aussi une double activité, préventive et curative. Leur mode d'action est cependant uni-site (mode d'action spécifique), ce qui, couplé à une absence de stratégie globale sur l'utilisation des fongicides et sur la gestion des résistances, a conduit très vite à une émergence et à une sélection de souches résistantes de *Z. tritici*, en Europe comme dans le reste du monde. Les premiers produits systémiques uni-sites à avoir été employés, dès fin 1960, sont les antimitotiques. Ceux-ci sont capables d'empêcher la polymérisation des microtubules, inhibant *de facto* la division cellulaire. Fin 1970, une nouvelle catégorie de fongicides a été développée, les inhibiteurs de la 14α-déméthylase CYP51 (*demethylation inhibitors*, DMI), enzyme-clé de la biosynthèse de l'ergostérol, un lipide membranaire essentiel chez les champignons **(Figure 18)**. La famille des strobilurines, ou *quinone outside inhibitors* (QoI), qui sont capables d'inhiber la respiration du champignon en interagissant avec le complexe III de la chaîne de transporteurs d'électrons mitochondriale, sont utilisés, quant à eux, depuis la fin des années 1990. Enfin, la dernière grande famille de fongicides anti-*Z. tritici* à avoir vu le jour, dans les années 2000, est celle des inhibiteurs de la succinate déshydrogénase (*succinate dehydrogenase inhibitors*, SDHI), une protéine du complexe II de la membrane mitochondriale. Les SDHI sont donc aussi des inhibiteurs de la respiration cellulaire.

Aujourd'hui, la lutte chimique contre la septoriose repose majoritairement sur l'utilisation des DMI et des SDHI (Torriani et al., 2015). L'application de traitements foliaires de DMI et de SDHI en mélange, a aussi été recommandé par certains auteurs, dans le but notamment de limiter le développement des populations résistantes à ces produits (Drummond *et al*., 2015). Si aucun phénomène majeur de résistance n'a été observé chez *Z. tritici* contre les SDHI, ce n'est pas le cas pour les autres catégories de fongicides. Il n'aura fallu attendre que quelques années après le début de la commercialisation des QoI pour que des résistances à ce fongicide apparaissent dans des populations du Royaume-Uni et d'Irlande (McCartney *et al*., 2007). Cheval *et al*. (2017) ont récemment montré que dans le Nord de la France, tous les isolats actuels du pathogène récoltés au champ sont totalement résistants à ces molécules.

En ce qui concerne les DMI, plusieurs équipes ont rapportés des diminutions inquiétantes de leur activité, d'abord en Europe, puis très vite dans le reste du monde (Cools *et al*., 2013 ; McDonald *et al*., 2019). Trois mécanismes associés à la résistance de *Z. tritici* envers les DMI ont été décrit dans la littérature, (i) des mutations du gènes codant pour la protéine CYP51 engendrant une altération de

sa structure 3D, diminuant l'affinité entre le DMI et cette protéine et donc l'activité du fongicide, (ii) une surexpression du gène *CYP51* et (iii) une surexpression de gènes codant pour des transporteurs membranaires jouant le rôle de pompe à efflux permettant à la cellule d'évacuer les composés fongicides dans un objectif de détoxification **(Figure 18)** (Cools *et al*., 2013). Les populations exprimant ce dernier phénotype sont appelées *multidrug resistants* (MDR). Certaines populations sont mêmes capables de cumuler ces différents mécanismes, expliquant en partie l'érosion de l'activité des DMI (Kildea *et al*., 2019).

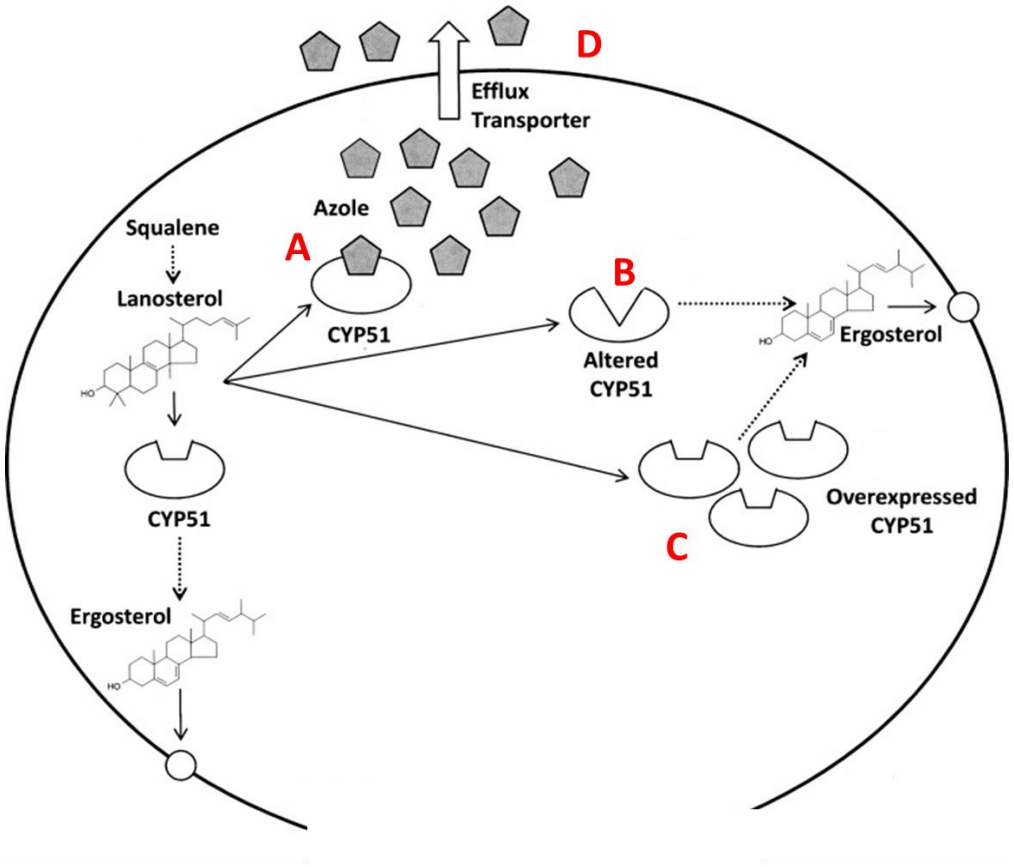

Figure 18 : Mécanismes de résistance aux DMI chez *Z. tritici*. La biosynthèse de l'ergostérol, composé lipidique membranaire majeur, nécessite l'activité de l'enzyme CYP51. (A) Inhibition de la protéine CYP51 par le fongicide DMI lorsque la souche n'est pas résistante. (B) CYP51 altérée et non-affectée par les DMI. (C) Surexpression du gène *CYP51* permettant la synthèse de l'ergostérol. (D) Surexpression de gènes codant pour des pompes à efflux (d'après **Parker *et al*., 2014**).

4.2. La lutte variétale

Les cultivars de blé commercialisés jusqu'à très récemment étaient au mieux modérément résistants à la maladie et au pire sensibles. La création de variétés résistantes ou tolérantes à la septoriose n'étant pas la priorité des sélectionneurs, les fongicides de synthèse employés ces dernières décennies protégeant efficacement de la maladie (Fraaije *et al*., 2012). Toutefois, avec le contexte sociétal et agroécologique actuel, le recours aux fongicides conventionnels se fait plus contraignant et les programmes d'amélioration du blé doivent désormais sérieusement prendre en compte cette maladie (Fraaije *et al.*, 2012). La tolérance à une maladie peut se définir comme la capacité d'un

cultivar à maintenir un rendement relativement élevé comparativement à un autre cultivar à niveau de sévérité égal (Bingham *et al*., 2009). Des variétés hautement tolérantes à la septoriose ont ainsi déjà vu le jour, mais aucune totalement résistante n'a pu être obtenue **(Tableau 4)** (Castro and Simón, 2016). Nous avions vu qu'il existe chez le blé deux types de résistance à la septoriose : la résistance quantitative et la résistance qualitative **(voir 3.2. Résistance génétique structurale du blé vis-à-vis de *Zymoseptoria tritici*)**. Les avancées récentes dans l'identification des QTL du blé associés à la résistance vis-à-vis de la maladie ont permis de faire des progrès majeurs dans l'amélioration des variétés commerciales de cette céréale (Brown *et al*., 2015). A l'inverse, les mécanismes de résistance qualitative, basés sur des gènes spécifiques, contournés de manière récurrente, n'ont pas permis d'aboutir à des cultivars résistants contre les populations de *Z. tritici* en Europe (Arraiano *et al*., 2009). Dans le but d'exploiter la diversité génétique des populations ancestrales de blé afin de découvrir et de valoriser de nouvelles sources de résistance, les sélectionneurs s'intéressent à la production d'hybrides synthétiques (Tabib Ghaffary *et al*., 2012).

Tableau 4 : Classement des variétés de blé tendre en France selon leur sensibilité à la septoriose, notée de 1 (variété sensible) à 9 (variété tolérante) (d'après **Arvalis-Institut du végétal**).

Très sensibles		**Moyennement sensibles**				**Peu sensibles**			
ADVISOR	5	ARKEOS	5,5	AUCKLAND	6	CAMPESINO	6,5	**LG ABSALON[2]**	**7,5**
BERGAMO	5	**BOREGAR[6]**	**5,5**	COMPLICE	6	COLLECTOR	6,5	AMBOISE	7
CELLULE[9]	**5**	CHEVRON	5,5	CONCRET	6	**FRUCTIDOR[3]**	**6,5**	**CHEVIGNON[1]**	**7**
OREGRAIN[5]	**5**	COSTELLO	5,5	CREEK	6	KWS DAKOTANA	6,5	CUBITUS	7
RUBISKO[4]	**5**	DIAMENTO	5,5	FLUOR	6	KWS TONNERRE	6,5	KWS EXTASE	7
APACHE	4,5	EXPERT	5,5	HYKING	6	LYRIK	6,5	RGT CESARIO	7
RGT VOLUPTO	4,5	FILON	5,5	MACARON	6	OXEBO	6,5	SY ADORATION	7
ALIXAN*	**4**	**NEMO[10]**	**5,5**	MONITOR	6	PASTORAL	6,5		
		OBIWAN	5,5	MUTIC	6	RGT PULKO	6,5		
		RGT KILIMANJARO	5,5	PROVIDENCE	6	SANREMO	6,5		
		RGT LEXIO	5,5	SORBET CS	6	SOPHIE CS	6,5		
		RGT LIBRAVO	5,5	TENOR	6				
		RGT SACRAMENTO[8]	**5,5**						
		UNIK	5,5						

(*) Le cultivar Alixan est celui qui sera utilisé dans le cadre des études décrites dans ce manuscrit.

([1-10]) Les numéros en exposant sur les variétés en gras, présentent le classement des variétés les plus cultivées en France, (d'après **FranceAgriMer, 2019**). La 7ème variété, Syllon, n'est pas inscrite dans ce tableau.

Les trois variétés de blé les plus cultivées au niveau de l'assolement français sur la période 2019-2020 sont, dans l'ordre décroissant, Chevignon, LG Absalon et Fructidor (FranceAgriMer, 2019). Ces cultivars sont tous les trois peu sensibles à la maladie, en particulier le cultivar LG Absalon qui est l'une des variétés les plus tolérantes à la septoriose actuellement disponible sur le marché, montrant l'intérêt croissant donné à *Z. tritici* dans les programmes de sélection ces dernières années **(Tableau 4)** (Arvalis-Institut du végétal, 2019). Malgré ces améliorations dans la résistance et la tolérance du blé vis-à-vis du pathogène, celles-ci ne sont pas suffisantes pour protéger totalement la culture et il convient de mettre en place d'autres méthodes de lutte, dont la prophylaxie.

4.3. Mesures agronomiques prophylactiques

Plusieurs stratégies peuvent être mises en place afin, tout d'abord, de limiter la présence du champignon pathogène en début de saison. Nous avions vu que *Z. tritici* pouvait persister d'une année à l'autre sous forme de pycnidiospores et, surtout, d'ascospores dans de multiples réservoirs, nommément, les résidus de culture, les repousses et les hôtes alternatifs**.** Afin de réduire la pression de cet inoculum primaire, il est recommandé d'enfouir, grâce à un travail adapté du sol, ou de détruire les résidus de culture après récolte contenant ces spores, afin que ces dernières ne puissent plus contaminer la parcelle. La rotation des cultures et l'élimination rapide des repousses du blé et des adventices qui pourraient servir d'hôtes alternatifs à l'agent infectieux permettent également de casser le cycle de vie du champignon et ainsi de réduire l'inoculum primaire présent à la saison suivante (Suffert *et al*., 2011). Décaler la date de semis est aussi recommandé, tout comme recourir à des variétés de blé plus tardives qui émergent en fin d'automne, quand les températures sont plus basses, limitant grandement la germination des spores et le niveau de sévérité final de la maladie (Gladders *et al*., 2001). La densité des semis est aussi un facteur à prendre en compte ; un nombre important de feuilles sur une surface réduite favorise les contaminations secondaires *via* le *rain-splashing* ou simplement par contact (Eyal and Center, 1987). De plus, une densité foliaire forte entretient un taux d'humidité élevé au niveau foliaire, propice au développement de *Z. tritici*. La taille du cultivar utilisé semble aussi jouer un rôle. Les variétés naines étant particulièrement sensibles à la maladie, il est recommandé de recourir à l'emploi de variétés non-naines (Brown *et al*., 2015). L'association de variétés en champ est, selon certains auteurs, une stratégie viable pour réduire l'impact de *Z. tritici*. Gigot *et al*. (2013) ont ainsi montré qu'un mélange de cultivars avec un ratio de 1:3 (cultivar sensible : cultivar résistant) diminuait la sévérité de la maladie d'un peu plus de 40 % pour le cultivar sensible. Cette association permettrait aussi de limiter la pression et la sélection de souches de *Z. tritici* virulentes sur les cultivars résistants.

4.4. Outils basés sur l'agriculture de précision

L'agriculture de précision vise à optimiser la gestion des intrants par les agriculteurs grâce à une meilleure compréhension de la variabilité intra-parcellaire associée à des outils d'aide à la décision (OAD). Dans la pratique, les parcelles sont scrutées à l'aide d'images satellites, de drones et/ou de différents senseurs. Les données obtenues sont ensuite analysées, et permettent d'avoir une vision globale de l'état des cultures, que ce soit au niveau du statut hydrique, des besoins azotés ou de la présence de pathogènes. Grâce à des modèles statistiques, les OAD permettent *in fine* aux agricultures d'apporter la dose optimale d'intrants, au moment opportun et uniquement sur les zones de la parcelle qui le nécessitent. Le but est ainsi de réduire la quantité d'intrants utilisés sans toutefois entraîner une baisse de rendements (Godwin *et al*., 2003 ; Tackenberg *et al*., 2016). Tackenberg *et al*. (2016) ont ainsi mis en place une méthode d'application de fongicides ciblée leur permettant d'économiser au total 8 % de produit comparé à une application conventionnelle uniforme. En ce qui concerne la septoriose, plusieurs OAD ont été développés pour lutter contre cette maladie (Ecophyto, 2018). Par exemple, le modèle d'Arvalis-Institut du végétal, Septo-LIS®, prend en compte la variété de blé cultivé, la date de semis, la localisation de la parcelle, les conditions météorologiques (*i.e* température et pluviométrie) ainsi que le stade de la culture et permet de déterminer des dates de traitements fongicides

recommandées (Arvalis-Institut du végétal, 2015). Les OAD peuvent aussi optimiser la fertilisation azotée, cette dernière étant connue pour accélérer le développement de la septoriose ; la réduction de ces intrants azotés aurait donc également un impact bénéfique sur la sévérité de la maladie (Simón *et al*., 2003).

4.5. Le biocontrôle : une méthode de lutte alternative

4.5.1. Définitions et catégories

D'après le ministère de l'agriculture et de l'alimentation français, le biocontrôle peut se définir comme « un ensemble de méthodes de protection des végétaux basé sur l'utilisation de mécanismes naturels ». Toujours selon eux, les produits de biocontrôle sont définis à l'article L. 253-6 du code rural et de la pêche maritime comme « des agents et des produits utilisant des mécanismes naturels dans le cadre de la lutte intégrée contre les ennemis des cultures. Ils comprennent en particulier : les macro-organismes ; et les produits phytopharmaceutiques qui sont composés de micro-organismes, de médiateurs chimiques tels que les phéromones et les kairomones, ou de substances naturelles d'origine végétale, animale ou minérale » (Ministère de l'agriculture et de l'alimentation, 2021). Actuellement, la place du biocontrôle dans le marché de la protection des cultures au niveau mondial ne représente que 5 %, soit environ 3 milliards de dollars, mais est en croissance continue chaque année (IBMA, 2017). De plus, considérant les limites de la lutte chimique et la mise en place de stratégies globales visant à réduire l'utilisation de produits phytopharmaceutiques de synthèse chimique en agriculture (plan Ecophyto 2025), il est fort probable que la croissance du marché du biocontrôle se poursuive dans les années à venir. Il existe quatre grandes catégories de produits de biocontrôle : les macroorganismes, les microorganismes, les médiateurs chimiques et les substances d'origine naturelle. En France, la législation définit cette dernière catégorie, de la manière suivante : « on entend par substance naturelle toute substance naturellement présente et qui a été identifiée en l'état dans la nature. Cette substance est soit extraite d'un matériau source naturel ; soit obtenue par synthèse chimique et strictement identique à une substance naturelle telle que décrite ci-dessus » (articles L.253-5 et L.253-7 du code rural et de la pêche maritime). Les produits de biocontrôle issus de cette dernière catégorie peuvent présenter différents modes d'actions, parfois complémentaires, pour protéger le cultures contre les agents pathogènes, notamment fongiques. Ils peuvent être, soit bio-fongicides, soit stimulateurs de défense des plantes (SDP), soit être les deux **(Figure 19)**.

Les bio-fongicides sont des substances d'origine naturelle agissant directement sur le champignon, en inhibant sa croissance et/ou son développement grâce à leur activité fongicide ou fongistatique. Les SDP sont, quant à eux, des composés, d'origine naturelle ou synthétique, qui agissent indirectement pour protéger la plante, en induisant ses réactions de défense. Seules les SDP d'origine naturelles sont classés parmi les produits de biocontrôle. Deux grandes catégories de SDP peuvent être différenciés selon leur mode d'action, les éliciteurs stricts et les potentialisateurs.

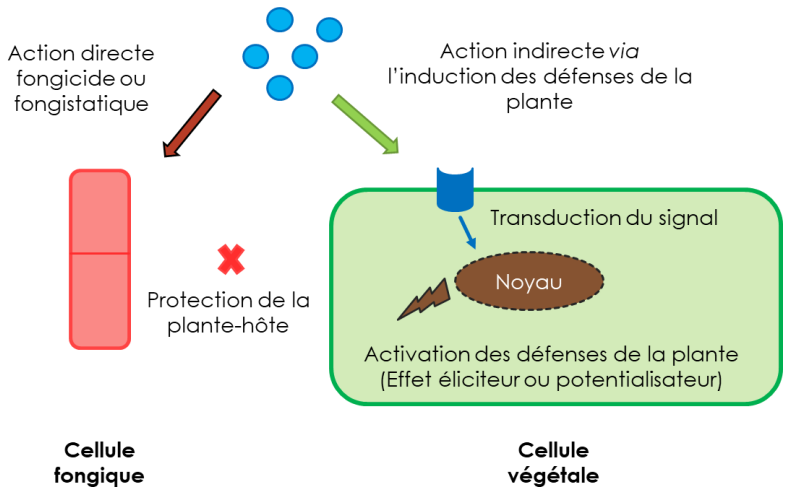

Figure 19 : Les modes d'action des produits de biocontrôle ciblant les agents pathogènes. Le produit (en bleu) peut agir directement sur le champignon, et/ou indirectement en stimulant les réactions de défense du végétal, conduisant à la protection de la plante contre l'agression.

4.5.2. Les éliciteurs stricts *versus* potentialisateurs

Après traitement avec un éliciteur strict et reconnaissance de ce composé par la plante, les voies de défense de cette dernière sont directement et fortement activées, qu'il y ait infection par la suite ou non. L'élicitation des défenses de la plante peut certes conduire à une protection de l'organisme végétal mais au prix d'un coût énergétique potentiellement conséquent et d'une réorientation métabolique pouvant nuire au rendement final de la culture. L'importance de ce coût dépend grandement du contexte environnemental et agronomique (Steppuhn and Baldwin, 2008 ; Cipollini *et al*., 2017).

Les composés potentialisateurs, quant à eux, protègent la plante par effet *priming*. Celui-ci est établi chez les plantes préalablement exposées à un stimulus, dit primaire, de niveau faible, qui seront capables de le mémoriser et de rentrer alors dans un « état d'alerte » ou *primed state*. Dans cet état, la plante est capable de réagir à une infection ou une agression, beaucoup plus rapidement et plus fortement qu'une plante non stimulée au préalable, appelée naïve, mais aussi de reconnaître la présence de l'agresseur à des niveaux de signaux beaucoup plus faibles **(Figure 20)**. Ce *primed state* dure souvent quelques jours à quelques semaines mais peut parfois durer plus longtemps et même être transmis à la descendance (Conrath *et al*., 2015 ; Hilker *et al*., 2016). Après le stimulus initial et durant l'« état d'alerte », et contrairement à l'effet que peuvent entraîner les éliciteurs stricts, seule une activation faible et transitoire, voire inexistante, est observée **(Figure 21)**. L'effet *priming* n'entraîne pas de modifications au niveau de l'ADN de la plante et est réversible.

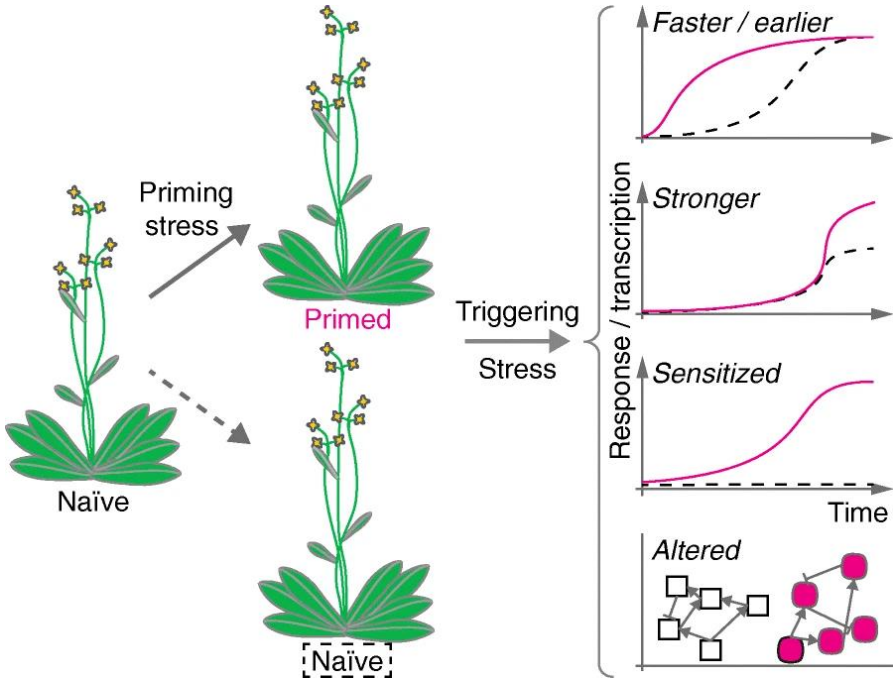

Figure 20 : Illustration de l'effet *priming* chez les plantes. Les plantes stimulées, *primed*, voient leurs réponses à une agression modifiées par rapport à des plantes naïves. Ces premières peuvent ainsi réagir plus vite ou plus fort ou à des niveaux plus faibles que les secondes. Les voies métaboliques engagées durant la réponse au bio-agresseur peuvent aussi différer entre une plante *primed* et une naïve. Des combinaisons de ces mécanismes peuvent avoir lieux lors de l'attaque par le pathogène. Les courbes en pointillées indiquent les réponses d'une plante naïve à l'infection et celles en rose correspondent aux réponses des plantes *primed* (d'après **Lämke and Bäurle, 2017**).

4.5.3. Les particularités des potentialisateurs

Dans le cas du *priming* par les potentialisateurs, les mécanismes liés à la mémorisation du signal et à cet état physiologique unique sont encore peu connus, mais des hypothèses ont pu être avancées par certains auteurs. Parmi celles-ci, Conrath *et al*. (2006) proposent comme mécanisme biologique l'accumulation de protéines signal, telles que les *calcium dependant protein kinases* (CDPK) ou les *heat-shock proteins* (HSP), qui seraient produites sous forme inactivée lors du stimulus initial et activées uniquement lors de l'attaque par le bio-agresseur. Les auteurs suggèrent aussi que l'accumulation de facteurs de transcription serait impliquée lors du phénomène de *priming* (Ptashne, 2008). Le stimulus initial modifie l'expression des gènes de la plante, dont les facteurs de transcription qui, à leur tour, pourront modifier l'expression d'autres gènes, notamment au moment de l'infection post-stimulus. Des mécanismes de boucles rétroactives impliquant ces facteurs de transcription pourraient aussi contribuer à la rémanence dans le temps de cet « état d'alerte » (Ptashne, 2008).

Selon Bruce *et al*. (2007), des régulations épigénétiques pourraient aussi jouer un rôle dans la mémorisation de cet état *primed*. La définition moderne d'épigénétique se réfère à l'étude des modifications agissant directement sur l'expression des gènes mais qui ne sont pas dues à des modifications dans la séquence de l'ADN (Gayon, 2016). Dans le cas du *priming*, le stimulus initial entraînerait notamment des changements dans la conformation 3D de l'ADN par méthylation, modifications des histones ou au niveau de la condensation de la chromatine, modifiant ainsi

l'accessibilité de certaines portions de l'ADN par les ARN polymérases et l'expression des gènes, sans toutefois altérer la séquence nucléotidique (Madlung and Comai, 2004).

Il est à noter que lors d'un effet *priming*, les tissus et organes n'ayant pas reçu le stimulus initial sont souvent aussi dans cet « état d'alerte » et ainsi plus résistants aux futures agressions, évoquant un phénomène de type SAR (Conrath *et al*., 2006). Les plantes stimulées (*primed*) expriment souvent des réponses modifiées de celles mises en places par les naïves lors de l'infection **(Figure 20)** (Lämke and Bäurle, 2017).

Les potentialisateurs présentent donc de nombreux avantages théoriques par rapport aux éliciteurs stricts, un coût énergétique *a priori* moindre et donc potentiellement moins impactant au niveau du rendement, ainsi qu'une mise en place plus rapide et/ou plus forte des mécanismes de défense permettant de contrer plus efficacement l'agent pathogène **(Figure 21)**. Ces molécules SDP capables de déclencher le *priming* chez les plantes sont donc particulièrement recherchées dans le cadre de la protection des cultures.

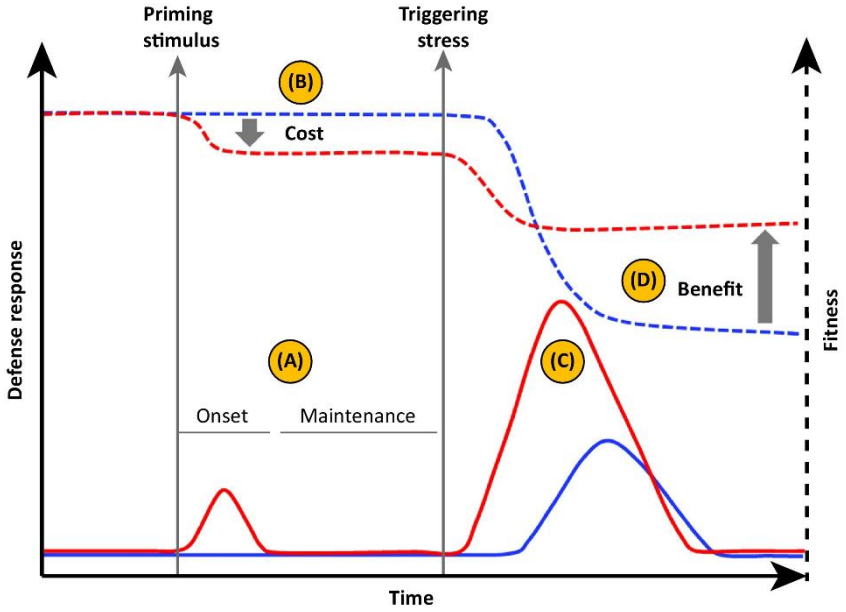

Figure 21 : Schéma de la relation entre *priming* (courbes pleines) et *fitness* (tirets) chez les plantes *primed* (en rouge) *versus* naïves (en bleu). (A) le stimulus initial déclenche de faibles, voire inexistantes, réactions de défense chez la plante qui est alors en « état d'alerte ». (B) Ces réactions de défense peuvent présenter un coût énergétique et métabolique significatif même si bien inférieur à celui causé par l'élicitation stricte des défenses. (C) Lors de l'infection, les plantes *primed* peuvent mobiliser leurs réactions de défense plus rapidement et plus fortement que les plantes naïves. (D) Les plantes *primed* sont plus à même de se défendre face à l'infection avec un ratio bénéfice/coûts > 1 (d'après **Martinez-Medina *et al*., 2016**).

Les SDP présentent des origines et des structures moléculaires très variées. Ils peuvent être d'origine synthétique (*i.e.* sulfamethoxazole), abiotique, comme les minéraux et leurs ions associés (*i.e.* cuivre ou phosphites) ou encore biotique (Bektas and Eulgem, 2015 ; Siah *et al*., 2018). Les composés provenant d'êtres vivants sont les plus variés et regroupent notamment des extraits de plantes (algues ou spermatophytes), des co-produits issus des industries agroalimentaires, des métabolites bactériens (rhamnolipides, lipopeptides, harpines, *etc*.), des extrais de parois et membranes microbiennes (chitosan, lipopolysaccharides, peptidoglycanes, flagellines,

exopolysaccharides, ergostérol, *etc*.) et encore d'autres catégories de molécules organiques tels que les vitamines, les acides aminés et les sucres (Siah *et al*., 2018b). Les SDP d'origine biotique peuvent aussi être classés selon leur origine au niveau des interactions plante-pathogène comme PAMP, MAMP ou DAMP.

4.5.4. Le biocontrôle de *Z. tritici*

A l'heure actuelle, très peu de produits de biocontrôle sont homologués et disponibles pour protéger les grandes cultures. Dans le cadre de la lutte contre la septoriose, à part le soufre, bio-fongicide bien connu, seul le Vacciplant® (précédemment Iodus 40®, Goëmar, Arista LifeScience, France), est homologué et est disponible sur le marché européen. Il s'agit d'un SDP d'origine biotique à base de laminarine, un polymère glucidique de β-1,3-glucane, extrait de l'algue brune *Laminaria digitata* (Renard-Merlier *et al*., 2007). Pour rappel, Shetty *et al*. (2009) ont montré que des extraits de β-1,3-glucane provenant de la paroi de *Z. tritici* permettait la mise en place de réactions de défense chez le blé conduisant à sa protection vis-à-vis de la septoriose. Plusieurs équipes ont par ailleurs rapporté une induction des défenses par cet SDP chez d'autres plantes, telles que la vigne et le tabac (Klarzynski *et al*., 2000 ; Aziz *et al*., 2003). Ainsi, Aziz *et al*. (2003) ont montré que la laminarine était, chez les feuilles de vigne, capable d'augmenter l'expression de gènes de défense comme ceux codant pour la β-1,3-glucanase, la chitinase ou encore d'inhibiteurs de protéases à sérine, et d'induire une protection partielle contre *Botrytis cinerea* et *Plasmopara viticola*.

Jusqu'en 2017, le Bion® (Syngenta, Suisse) contenant de l'acibenzolar-S-methyl, un analogue fonctionnel du SA synthétisé chimiquement, était aussi homologué comme éliciteur du blé et permettait de lutter contre la septoriose et d'autres maladies affectant cette culture, telles que l'oïdium et la rouille (Görlach et al., 1996a). Cet éliciteur n'a, toutefois, jamais été homologué comme produit de biocontrôle au niveau de la réglementation.

Les microorganismes bénéfiques

Les plantes peuvent dans certains cas coopérer avec des microorganismes épiphytes ou endophytes, vivants respectivement à l'extérieur ou à l'intérieur des tissus de l'hôte sans lui causer de dommages. Ces microorganismes symbiotiques peuvent fournir différents avantages à la plante, comme l'amélioration de sa croissance, son apport en eau et en composés minéraux et sa résilience face aux stress biotiques et abiotiques (Pérez-Montaño *et al*., 2014). Lors d'une attaque par un agent pathogène, les microorganismes bénéfiques peuvent intervenir dans la protection de la plante de différentes manières, notamment *via* la production de composés toxiques vis-à-vis du bio-agresseur, la compétition directe vis-à-vis du pathogène ou encore en activant les réactions de défense de la plante. L'induction de phénomènes de résistance par les microorganismes bénéfiques peut se produire au niveau de la rhizosphère et entraîner une résistance globale et durable chez la plante, phénomène alors appelé résistance systémique induite (*induced systemic resistance,* ISR). L'ISR a, pendant un temps, été considéré comme dépendante de la voie de biosynthèse et de la perception du JA/ET et n'induisant pas l'expression de protéines PR (Pieterse *et al*., 1998). Toutefois, des travaux ont pu mettre en évidence l'inverse ; lors de certains phénomènes d'ISR, la voie du SA était impliquée, ainsi que la production de protéines PR, mais pas celle du JA/ET (Barriuso *et al*., 2008). D'autres études ont

montré que les deux voies antagonistes, JA/ET et SA, pouvaient être induites ensemble durant l'activation de l'ISR (Walters and Bennett, 2014).

Dans le cadre de la lutte contre *Z. tritici*, plusieurs agents de biocontrôle potentiels ont été découverts ces dernières décennies. En ce qui concerne l'utilisation de bactéries vivantes, plusieurs espèces de *Pseudomonas* se sont révélées efficaces contre le champignon, que ce soit *in vitro* ou *in planta* (Levy *et al*., 1988 ; Levy *et al*., 1992 ; Kildea *et al*., 2008 ; Bricout, 2020). Par exemple, selon Flaishman *et al*. (1996), l'application de la souche de *P. putida*, BK8661, connue pour sécréter des sidérophores et du cyanide d'hydrogène (HCN), directement sur des feuilles de plantules de blé, est capable de réduire, en chambre de culture, la densité des pycnides de 20 % et la sévérité de la maladie de 71 %. Par ailleurs, le traitement de feuilles de blé avec des suspensions de *Paenibacillus polymyxa* et de *Bacillus cereus* ont montré des efficacités de protection allant jusqu'à 55 % en serre (Alippi *et al*., 2000). Plus récemment, Kildea *et al*. (2008) ont identifié la souche MKB135 de *Bacillus megaterium*, qui lorsque appliquée sur les feuilles de blé, réduit la sévérité de la maladie très fortement, jusqu'à 80 % au champ. Des bactéries lactiques ont aussi montré une efficacité de protection du blé vis-à-vis de la septoriose (Lynch *et al*., 2016). D'autres équipes se sont intéressées à l'utilisation de champignons et principalement aux effets potentiels des espèces de *Trichoderma*. En effet, Cordo *et al*. (2007) ont identifié plusieurs souches de *Trichoderma* sp., agissant comme éliciteurs des réactions de défense chez le blé vis-à-vis de *Z. tritici*, en stimulant notamment l'activité protéolytique antifongique des protéines situées dans l'apoplasme. Parmi les souches testées, *T. harzanium* Th5 était le plus efficace lorsqu'appliqué sous forme d'enrobage de semence avec une activité de protection d'environ 26 %. D'autres souches de *T. harzanium*, 123 et 170, se sont montrées encore plus prometteurs dans la lutte contre la septoriose, en réduisant la sévérité de la maladie respectivement de 80 % et 90 % (Stocco *et al*., 2016). Pour finir, des enrobages de semence avec des souches de *T. konigii* se sont aussi révélés efficaces pour réduire le développement de la maladie (Perelló *et al*., 2009). Plus récemment, le rôle potentiel de l'ISR induite par *Paenibacillus* sp. strain B2 dans la réduction de la biomasse fongique de *Z. tritici* a été rapporté (Samain *et al*., 2019).

Les substances d'origine naturelle

Les recherches menées par différentes équipes sur le pathosystème blé-*Z. tritici* ont permis d'identifier de nouvelles substances d'origine naturelle prometteuses, qu'elles soient bio-fongicides, SDP ou les deux. Ces composés sont d'origines végétale ou microbienne et peuvent même provenir de *Z. tritici* lui-même, comme le β-1,3-glucane provenant de la paroi du champignon (Shetty *et al*., 2009). Récemment, Le Mire *et al*., (2019) ont identifié de nouveaux SDP contre la septoriose, le λ-carraghénine (polysaccharide extrait d'algues rouges), le CpG-Oligo désoxynucléotide, la glycine bétaïne, l'ergostérol (composé essentiel des membranes fongiques) et la spiruline (*Spirulina platensis*). Leurs résultats ont montré que ces éliciteurs induisaient à la fois la voie du SA et du JA et permettait de protéger le blé de la septoriose jusqu'à 70 % en conditions semi-contrôlées, sans présenter d'activité antifongique. Les activités d'extraits de rhizomes de *Juncus maritimus* ont été testé pour leur activité directe *in vitro*. Les auteurs ont pu mettre en évidence un dérivé phénanthrène particulièrement efficace, l'effusol, qui présentait une concentration minimal inhibitrice (CMI) égale à 19 $mg.L^{-1}$ (Sahli *et al*., 2018). Bocquet *et al*. (2018) ont aussi rapporté une activité antifongique *in vitro* de la part d'extraits de cônes et d'huile essentielle de houblon, même si les concentrations requises

étaient relativement élevées. Le rôle des lipopeptides produit par *Bacillus subtilis* dans le biocontrôle de *Z. tritici* a récemment été souligné. En effet, Mejri *et al*., (2018) ont rapporté un effet bio-fongicide marqué de la mycosubtiline à la fois *in vitro*, CI_{50} = 1,4 mg.L^{-1} (concentration inhibitrice à 50 % de la croissance fongique), et *in planta*. A l'inverse aucun effet direct n'a été observé avec la surfactine et la fengycine. L'application foliaire de ces composés à 100 mg.L^{-1} a permis de montrer que les trois lipopeptides protégeaient le blé vis-à-vis de la septoriose, avec une efficacité de protection plus élevée conférée par la mycosubtiline. Au vu de leur absence d'activité *in vitro*, les auteurs suggèrent que le mode d'action de la surfactine et la fengycine est basé sur une activité SDP. Les travaux de Le Mire *et al*. (2018) confirment cette hypothèse et montrent que la surfactine extraite de la souche S499 de *Bacillus amyloliquefaciens* protège le blé en induisant les voies de défense dépendantes du SA et du JA de manière conjointe. D'autres extraits de bactéries, notamment de *Bacillus* spp. ont aussi pu montrer des activités directes antifongiques *in vitro*, soulignant l'intérêt potentiel de ces bactéries dans le biocontrôle de la septoriose du blé (Alippi *et al*., 2000 ; Kildea *et al*., 2008).

Les biosurfactants microbiens : des biomolécules prometteuses pour le biocontrôle

Les biosurfactants sont des molécules tensio-actives qui sont produites par un large panel de microorganismes. Les principales classes de biosurfactants sont représentées par les lipides mannosylérythritol, les tréhaloses dimycolates, les tréhalolipides, les sophorolipides, les rhamnolipides et les lipopeptides (Crouzet et al., 2020). Ces molécules peuvent présenter des structures très diverses mais sont toutes amphiphiles, composés d'une partie hydrophobe et d'une partie hydrophile qui leur donnent leurs caractéristiques physico-chimiques particulières. Ces composés sont utilisés dans une large gamme de champs d'applications tels que l'industrie alimentaire, la santé humaine, l'industrie cosmétique, l'industrie pétrolière, la remédiation des eaux et des sols contaminés, les nanotechnologies et, en ce qui nous concerne, l'agriculture (Sachdev and Cameotra, 2013 ; Lourith and Kanlayavattanakul, 2009 ; Singh *et al*., 2019). Les biosurfactants sont des composés prometteurs en biocontrôle car ils sont considérés comme facilement biodégradables, présentent une faible toxicité sur la santé humaine et l'environnement et plusieurs études ont déjà montré des effets significatifs de ces biomolécules en protection des plantes (Crouzet et al., 2020a). Les principales familles étudiées dans ce contexte sont les lipopeptides et les rhamnolipides, qui présentent de nombreux avantages, notamment leur production à une échelle industrielle, leur efficacité et leur faible rémanence dans l'environnement, faisant d'eux des candidats particulièrement intéressants en biocontrôle (Crouzet et al., 2020a). Certaines études se sont toutefois intéressées aux autres familles de biosurfactants en agriculture (Yoshida *et al*., 2015 ; Sen *et al*., 2017 ; Chen *et al*., 2020).

Les rhamnolipides

Les rhamnolipides sont des glycolipides, produits, notamment, par des espèces de *Pseudomonas* sp. et de *Burkholderia* sp., constitués d'une ou plusieurs têtes rhamnose hydrophiles et d'une ou plusieurs chaînes d'acide gras hydrophobes **(Figure 22)**. En protection de cultures, plusieurs études ont rapporté leurs activités antimicrobiennes et d'induction des voies de défense chez les plantes (Vatsa *et al*., 2010). Les rhamnolipides sont efficaces en tant que bio-fongicides et ont montré une activité

directe contre un large spectre d'agents phytopathogènes : *Botrytis* sp., *Rhizoctonia* sp., *Fusarium* sp., *Alternaria* sp., *Pythium* sp., *Phytophthora* sp., et *Plasmopara* sp. (Stanghellini and Miller, 1997 ; Abalos *et al*., 2001 ; Crouzet *et al*., 2020). Les rhamnolipides sont aussi capables d'induire des phénomènes de résistance chez les plantes comme chez la vigne, *Brassica napus* ou *Arabidposis thaliana*, notamment en déclenchant des influx de Ca^{2+}, l'accumulation de ROS, la déposition de callose ou la production d'hormones de défense **(Figure 23)** (Varnier et al., 2009 ; Sanchez *et al*., 2012 ; Monnier *et al*., 2018). Cette double activité des rhamnolipides, bio-fongicide et SDP, pourrait s'expliquer par la nature amphiphile de ces composés. Plusieurs auteurs émettent l'hypothèse que ces molécules seraient capables d'interagir avec les membranes des plantes comme celles des agresseurs fongiques (Monnier *et al*., 2019). Chez les champignons pathogènes, ces glycolipides s'intercaleraient dans leurs membranes, au niveau des bicouches de phosphatidylcholine et de phosphatidyléthanolamine, causant *in fine* leur déstabilisation et leur lyse cellulaire **(Figure 23)** (Stanghellini and Miller, 1997 ; Sánchez *et al*., 2010 ; Monnier *et al*., 2019). Chez les plantes, le mécanisme de reconnaissance des rhamnolipides est encore inconnu. Il est, cependant, suggéré que les molécules interagiraient aussi avec la membrane des plantes mais avec des conséquences moins radicales, entraînant seulement l'induction des voies de défense **(Figure 23)** Monnier *et al*., 2019).

Les lipopeptides

Les lipopeptides, produits par de nombreuses espèces de champignons et de bactéries, sont composés d'une chaine lipidique hydrophobe liée à un oligopeptide linéaire (LLP) ou cyclique (CLP) **(Figure 22)**. L'activité antimicrobienne de ces composés est très bien documentée et leur potentiel dans le domaine du biocontrôle n'est plus à démontrer (Ongena and Jacques, 2008 ; Geudens and Martins, 2018 ; Caulier *et al*., 2019). Les CLP bactériens sont de puissants biosurfactants qui sont supposément capables d'engendrer d'importantes déstabilisations membranaires, comme les rhamnolipides, conduisant à la perte d'intégrité cellulaire et ainsi à la mort des champignons pathogènes (**Figure 22**; Crouzet *et al*., 2020). Toutefois, d'après plusieurs équipes, l'activité antimicrobienne des CLP ne serait pas seulement due aux interactions avec les membranes, mais aussi à des modifications et des altérations des fonctions intracellulaires des microorganismes ciblés (Latoud *et al*., 1987 ; Qi *et al*., 2010). Plusieurs CLP sont aussi capables de stimuler les voies de défense chez les plantes. Il a ainsi été montré que la fengycine et/ou la surfactine protégeaient le haricot, la tomate, la laitue, le melon, le citron, le ray-grass, la vigne, la betterave, la fraise, le coton et, bien sûr, le blé contre différentes maladies (Ongena *et al*., 2007 ; Desoignies *et al*., 2013 ; García-Gutiérrez *et al*., 2013 ; Chowdhury *et al*., 2015 ; Waewthongrak *et al*., 2014 ; Han *et al*., 2015 ; Rahman *et al*., 2015 ; Yamamoto *et al*., 2015 ; Le Mire *et al*., 2018 ; Li *et al*., 2019). Chez le riz, des CLP comme le WLIP, la lokisin et l'entolysin ont réussi à induire des phénomènes de résistance contre *M. oryzae* (Omoboye *et al*., 2019). Ces CLP protégeraient les plantes vis-à-vis des infections principalement par l'intermédiaire de l'ISR. Les lipopeptides induiraient les réactions de défense chez les plantes d'une manière similaire aux rhamnolipides, en interagissant avec les membranes végétales **(Figure 23)** (Henry *et al*., 2011 ; Schellenberger *et al*., 2019). Il est à noter que dans le cas des rhamnolipides comme des lipopeptides, la structure de la molécule influe grandement sur les activités de ces molécules (Henry *et al*., 2011 ; Kawagoe *et al*., 2015 ; Luzuriaga-Loaiza *et al*., 2018 ; Robineau *et al*., 2020). Plusieurs espèces de *Bacillus* ont été identifiées comme prometteuses pour la production de lipopeptides pouvant

présenter des structures différentes, en particulier des CLP appartenant à 3 principales familles, les iturines (mycosubtiline, baccilomycine D), les surfactines et les fengycines **(Figure 22)**.

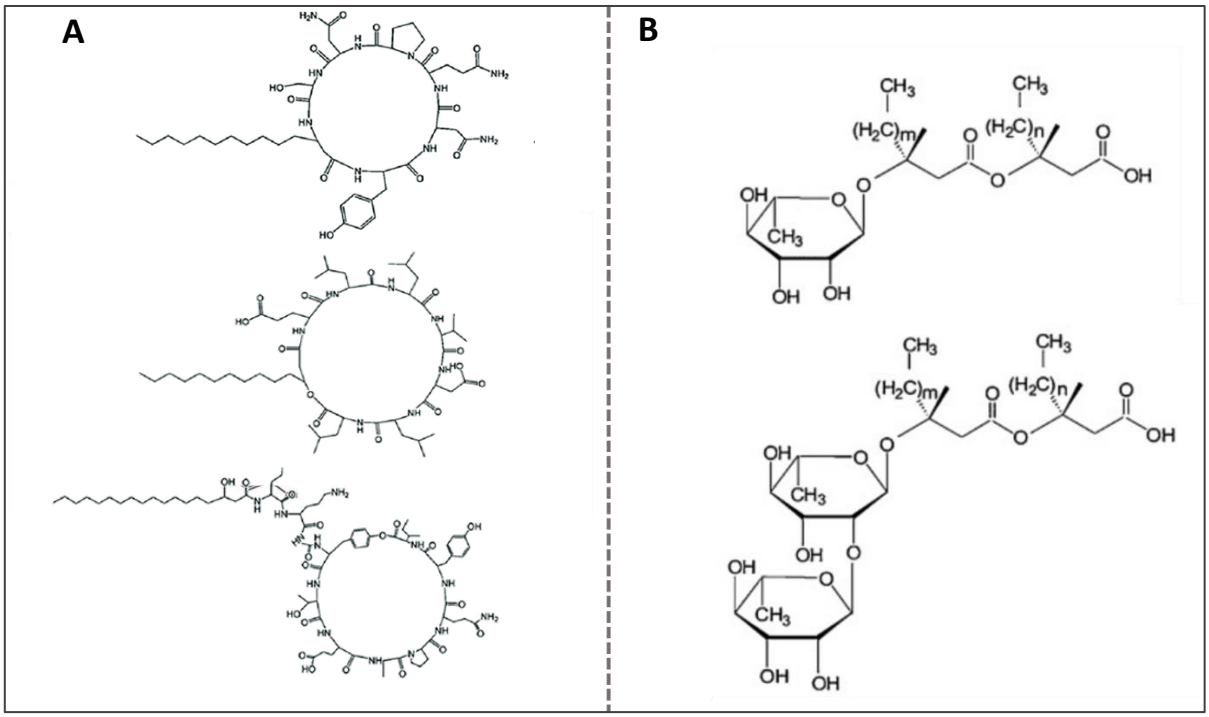

Figure 22: Structure générale des (A) principaux lipopeptides produits par *Bacillus* sp. et des (B) rhamnolipides. Avec, en (A) de haut en bas : la structure d'une iturine, d'une surfactine et d'une fengycine et en (B) en haut à droite, la structure générale des mono-rhamnolipides et en bas des di-rhamnolipides (d'après **Hamley et al., 2013 et Dobler et al., 2016**).

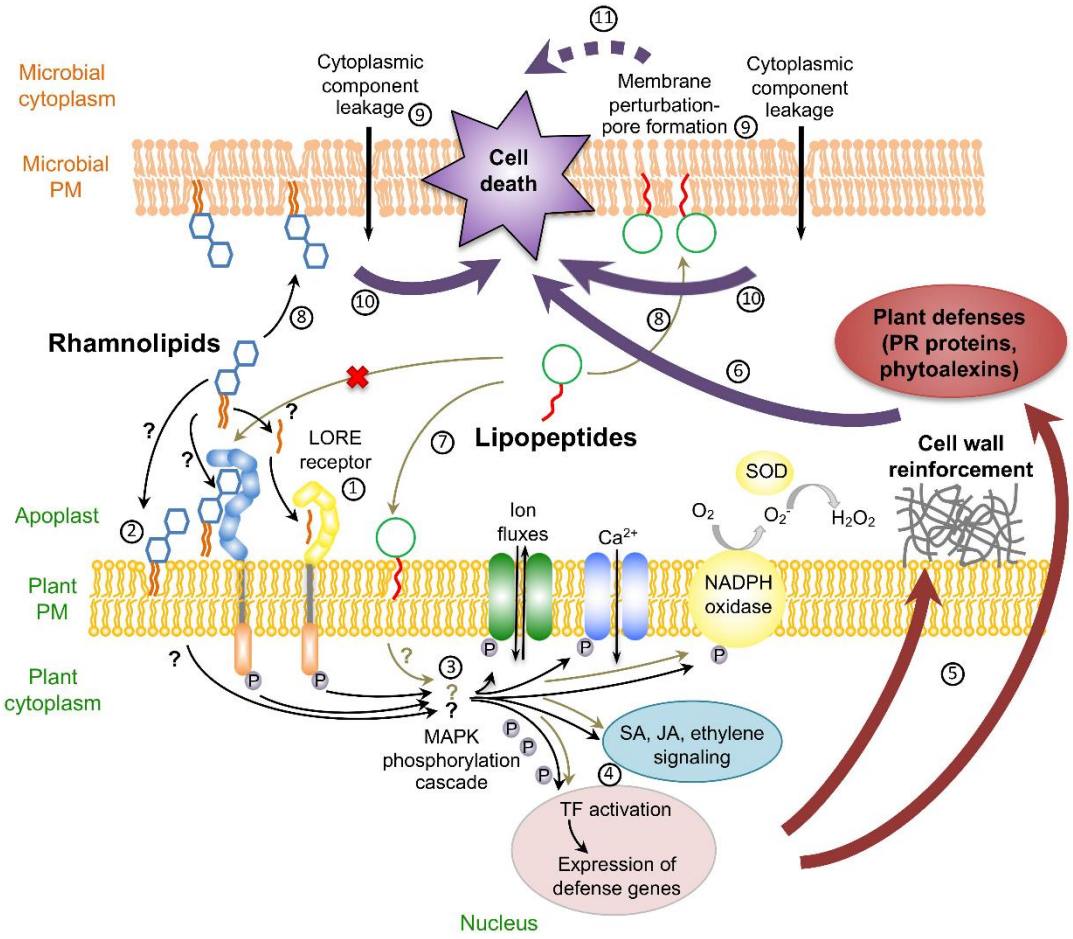

Figure 23 : Effets des rhamnolipides et des lipopeptides, à la fois direct sur l'agent pathogène et indirect *via* la stimulation des défenses de la plante. (1) La partie mc-3-OH-acyl du rhamnolipide est perçue par le récepteur LORE de la plante. (2) Le rhamnolipide pourrait être reconnu directement par la cellule de la plante au niveau de la membrane végétale. (3) La reconnaissance du rhamnolipide conduit à l'établissement de réponses précoces. (4) Mise en place d'une transduction du signal à l'issue de ces réponses précoces. (5) Etablissement des réponses tardives, comme l'expression de protéines PR et la production de phytoalexines permettant (6) l'inhibition de développement du pathogène. (7) Les lipopeptides peuvent aussi interagir avec la membrane plasmique de la cellule végétale pour induire les réactions de défense. (8) Les rhamnolipide s et les lipopeptides peuvent désorganiser directement la membrane du pathogène, ce qui (9) induit la formation de pores au niveau de la membrane plasmique et une perte d'intégrité cellulaire chez le microorganisme et finit par (10) conduire à la mort cellulaire de l'agent pathogène. (11) La mort cellulaire causée par les lipopeptides peut aussi être due à l'action de ces biomolécules sur d'autres mécanismes intra-cellulaires (d'après **Crouzet *et al.*, 2020**).

CONTEXTE ET OBJECTIFS GÉNÉRAUX DU PROJET DE THÈSE

Actuellement, la lutte contre *Z. tritici* sur les cultures de blé repose essentiellement sur l'utilisation des fongicides conventionnels. Toutefois, ces produits sont de plus en plus controversés à cause de leurs effets négatifs potentiels sur l'environnement et la santé humaine, mais aussi en raison de l'émergence fréquente de résistances à ces produits chez les populations de l'agent pathogène. La réduction de leur utilisation est ainsi fortement encouragée dans l'Union Européenne (UE). En France, le plan Ecophyto a été mis en place et s'inscrit dans cette démarche. Celui-ci, qui a débuté en 2008, visait tout d'abord à réduire de 50% l'utilisation des produits phytosanitaires de synthèse pour 2018. Le plan fut révisé en 2015, l'objectif est maintenu mais désormais à l'horizon 2025 (Ecophyto II, 2016). A l'heure actuelle, 70% des fongicides épandus dans l'UE le sont pour lutter uniquement contre *Z. tritici* (Fones and Gurr, 2015a). Au vu de la quantité de fongicides utilisés contre cette maladie, il est urgent de développer d'autres méthodes de lutte pour y faire face. Une alternative prometteuse à l'utilisation des pesticides conventionnels dans la gestion des agents phytopathogènes est le recours aux agents ou produits de biocontrôle. Actuellement, seuls le soufre et le Vacciplant® sont homologués en tant que produits de biocontrôle contre la septoriose du blé. L'identification de nouveaux composés ou principes actifs de biocontrôle ciblant la septoriose du blé est ainsi fortement encouragée pour offrir aux agriculteurs de nouvelles bio-solutions leur permettant de lutter durablement contre cette maladie. Par ailleurs, si certains travaux menés par la communauté scientifique ont permis de mettre en évidence des microorganismes et des substances naturelles prometteurs pour contrôler la septoriose du blé, leur nombre reste toutefois limité (*e.g.* Lynch *et al*., 2016 ; Stocco *et al*., 2016 ; Bocquet *et al*. 2018 ; Le Mire *et al*., 2018 ; Mejri *et al*. 2018 ; Le Mire *et al*., 2019 ; Ors *et al*., 2019 ; Samain *et al*., 2019). Par ailleurs, les connaissances sur les mécanismes de résistance induite déclenchés chez le blé, contre cette maladie, par les microorganismes bénéfiques et les composés éliciteurs ou potentialisateurs, restent, aujourd'hui encore, largement lacunaires (Le Mire *et al*., 2018 ; Le Mire *et al*., 2019; Ors *et al*., 2019; Samain *et al*., 2019). En outre, aucune étude à l'aide d'outils Omics n'a été jusqu'ici été conduite pour caractériser plus finement ces mécanismes chez le blé vis-à-vis de la septoriose. Seuls quelques travaux ont utilisé ces approches pour décrypter les mécanismes de résistance induite chez le blé vis-à-vis des agents pathogènes, comme *Blumeria graminis* (Chain *et al*., 2009) et *Xanthomonas translucens* (Fiorilli *et al*., 2018). Ce manque d'information concernant les modes d'action des produits de biocontrôle dans leur ensemble constitue actuellement un frein au développement de leur utilisation.

Les objectifs principaux de ce projet de thèse étaient donc d'identifier de nouveaux produits de biocontrôle efficaces sur le blé vis-à-vis de la septoriose et de caractériser leurs modes d'action, en particulier au niveau de l'induction des mécanismes de défense de l'hôte.

Cette thèse s'inscrit dans le cadre du portefeuille de projets Smartbiocontrol, financé par Interreg V, qui vise à promouvoir l'utilisation et le développement de produits de biocontrôle sur les cultures d'intérêt présentes au niveau de la région transfrontalière franco-belge (Smartbiocontrol, 2017). Plusieurs pathosystèmes y ont été ciblés, dont, celui qui nous intéresse ici, le pathosystème blé-*Z. tritici*. Ce portefeuille de projets est mené en collaboration entre 26 partenaires français et belges,

dont l'UMR Transfrontalière BioEcoAgro site ISA-Junia **(Figure 24)**. Smartbiocontrol est composé de cinq projets :

- Bioscreen : Criblage et identification de nouveaux composés de biocontrôle
- Bioprod : Optimisation de la production et de la formulation des composés
- Bioprotect : Optimisation de l'application des composés en serre et au champ
- Biosens : Détection des agents pathogènes au champ pour optimiser le positionnement
- Biocomgest : Coordination

Plus précisément, mon projet de thèse s'inscrit dans le projet Bioscreen, qui vise principalement à cribler et identifier de nouveaux composés de biocontrôle (bio-fongicides et/ou inducteurs de résistance). Le coût complet du projet Bioscreen est de 3 097 785 €, avec une aide de 1 703 781 € par le FEDER (le budget octroyé à l'ISA-Junia est de 143 991 € pour un coût complet de 261 801 €). Dans le cadre de mes travaux, j'ai eu accès, grâce notamment aux différents partenaires de Bioscreen, à une bibliothèque de 181 composés d'origines variées (extraits microbiens purifiés ou non, molécules synthétiques bio-inspirées, *etc*.). Dans un premier temps, un criblage de leurs activités biologiques sur le pathosystème d'intérêt blé-*Z. tritici* a été réalisé, principalement sur la base de leur activité antifongique directe *in vitro*. L'efficacité de protection des composés les plus prometteurs a ensuite été vérifiée *in planta* en serre. Enfin, parmi les 181 composés initialement mis à disposition, deux molécules (*i.e.* un lipopeptide et un rhamnolipide) se sont révélées particulièrement actives pour protéger le blé contre *Z. tritici*, supposément grâce à leur double activité (antifongique et activation des défenses de l'hôte). Les mécanismes liés à leurs modes d'action ont finalement été caractérisés, en particulier concernant leur activité possible de stimulation des défenses du blé. Les principaux résultats obtenus dans le cadre de ces travaux sont ou seront valorisés sous forme d'articles scientifiques présentés ci-après.

Figure 24: Carte présentant les 26 partenaires franco-belges du portefeuille de projets Smartbiocontrol, financé par Interreg V (www.smartbiocontrol.eu/fr).

RÉSULTATS

RESUMÉ DU CRIBLAGE DES COMPOSÉS D'ORIGINE MICROBIENNE ÉTUDIÉS

Un total de 181 composés (bactéries, molécules ou extraits) a été fourni par les différents partenaires du projet Bioscreen, afin de réaliser un criblage de leurs activités biologiques sur le pathosystème blé-*Z. tritici*. L'objectif était de déterminer quels composés pouvaient être les plus prometteurs pour lutter contre la septoriose du blé. Si ces composés ont tous des origines, des niveaux de pureté et des propriétés physico-chimiques bien différents, ceux-ci présentent toutefois une même caractéristique commune, celle de provenir de micro-organismes bactériens ou fongiques ou alors de mimer des métabolites provenant de ceux-ci. Nous avions ainsi à disposition :

- 146 extraits d'espèces fongiques différentes provenant de la mycothèque de l'Université Catholique de Louvain, Belgique.
- 2 souches de *Bacillus velezensis*, 1 souche de *B. amyloliquefaciens* et 2 souches de *Paenibacillus polymyxa*, fournies par l'Institut National de la Recherche Agronomique (INRA) de Kenitra, Maroc.
- 8 lipodepsipeptides cycliques extraits et purifiés de *Pseudomonas* spp., fournis par l'Université de Gand, Belgique.
- 1 lipopeptide, la mycosubtiline, extrait et purifié à partir d'une souche de *Bacillus subtilis*, fournis par Lipofabrik, France.
- 21 rhamnolipides et molécules associées, dont 18 bio-inspirés et synthétisés par chimie verte, ainsi qu'un mix de rhamnolipides naturels produits par *P. aeruginosa* et deux molécules associées, fournis par l'Université d'Artois, France.

L'activité *in vitro* antifongique directe des différents composés a été déterminée en mesurant la croissance des colonies de *Z. tritici* sur milieu solide (*potato dextrose agar*, PDA), en plaques 12 puits, contenant les molécules ou extraits d'intérêt. Les tests d'activité antifongique ont tous été réalisés vis-à-vis de la souche T02596 de *Z. tritici*, virulente sur le cultivar de blé Alixan (Mejri *et al*., 2018). Les concentrations initiales des composés étaient de 30% pour les surnageants bactériens et fongiques, de 50 $\mu g.ml^{-1}$ pour les métabolites microbiens purifiés (lipodepsipeptides cycliques et mycosubtiline) et de 1500 µM pour les rhamnolipides bio-inspirés. Les observations ont été effectuées 10 jours après inoculation des plaques avec la suspension de spores du champignon (5.10^5 spores/mL) et les résultats obtenus sont présentés en **Annexe 1**. Ce criblage a permis de mettre en évidence un nombre conséquent de composés efficaces *in vitro* contre l'agent pathogène. Sur les 146 extraits fongiques testés, 11 ont montré une inhibition totale de la croissance fongique et 12 un taux d'inhibition allant de 80 à 99% (concentration de 30% (v/v)). Six rhamnolipides et molécules associées ont aussi induit son inhibition totale à la concentration de 1500 µM. Aucun effet significatif n'a été observé avec les six lipodepsipeptides cycliques extraits de *Pseudomonas* spp., contrairement à la mycosubtiline, qui a montré une activité inhibitrice totale de la croissance du champignon à la concentration de 50 $\mu g.mL^{-1}$. Les surnageants de cinq souches de *Bacillus* spp. ont, quant à eux, tous inhibé à 100% la croissance de l'agent phytopathogène **(Annexe 1)**.

Afin de caractériser plus finement l'activité antifongique des composés les plus efficaces *in vitro* vis-à-vis de *Z. tritici*, leur concentration minimale inhibitrice (CMI) et d'inhibition à 50% (CI_{50}) ont été déterminées dans les mêmes conditions que précédemment, avec une concentration maximale de 1500 µM pour les rhamnolipides, 100 µg/mL pour la mycosubtiline et 30% (v/v) pour les extraits

(fongiques et bactériens) **(Tableau 5)**. La CMI représente la concentration minimale d'un composé empêchant totalement la croissance de *Z. tritici*, alors que la CI_{50} correspond à la concentration théorique inhibant 50% de la croissance. Les CI_{50} des extraits fongiques présentés ci-dessous ont été calculées à l'aide du logiciel XLSTAT (Addinsoft, France) alors que les autres CI_{50} (pour les filtrats de culture bactériens, rhamnolipides, mycosubtiline) l'ont été avec le logiciel GraphPad Prism (USA).

Tableau 5 : Résumé des CI_{50} et CMI des composés les plus efficaces in vitro contre *Z. tritici*

Composés	CI_{50}	CMI
Extraits fongiques		
Penicillium griseofulvum	2.1%	7.5%
Trichoderma Virens	2.9%	15%
Aspergillus niger	3.6%	15%
Myrothecium verrucaria	4.5%	15%
Lecanicillium longisporum	5.9%	30%
Penicillium cyclopium	6.0%	15%
Trichothecium roseum	7.3%	15%
Emericella rugulosa	8.0%	>30%
Paecilomyces lilacinus	15.3%	>30%
Penicillium aurantiogriseum	16.3%	>30%
Penicillium purpurogenum	19.5%	>30%
Sporothrix insectorum	19.9%	>30%
Talaromyces flavus	22.6%	>30%
Laetiporus sulphureus	29.6%	>30%
Penicillium brevicompactum	33.7%	>30%
Chaetomium globosum	43.4%	>30%
Surnageants bactériens		
***Bacillus velezensis* S1**	1.4%	3.7%
***Bacillus velezensis* S6**	7.4%	15%
***Paenibacillus polymyxa* M2**	Nd*	30%
***Paenibacillus polymyxa* AMESA**	Nd*	15%
***Bacillus amyloliquefaciens* I3**	26.7%	30%
Rhamnolipides et molécules associées		
Rhamnose-Ester-C12	75 µM	133 µM
Rhamnose-Ether-C12	81 µM	450 µM
Acide laurique	109 µM	200 µM
Rhamnose-Ether-C10	158 µM	200 µM
Dodécanol	164 µM	200 µM
Rhamnose-Succinate-C8	1399 µM	1500 µM
Lipopeptide cyclique purifié		
Mycosubtiline	0.57 $\mu g.mL^{-1}$	0.78 $\mu g.mL^{-1}$

*Les CI_{50} des surnageants bactériens de *Paenibacillus polymyxa* n'ont pas pu être déterminées en raison des faibles rendements en filtrats obtenus avec ces souches.

Plusieurs composés ont ainsi montré une activité antifongique significative dans ces conditions. Parmi ceux-ci, huit extraits fongiques (*Penicillium griseofulvum*, *Trichoderma virens*, *Aspergillus niger*, *Myrothecium verrucaria*, *Lecanicillium longisporum*, *Penicillium cyclopium*, *Trichothecium roseum*, *Emericella rugulosa*) ont présenté des CI_{50} inférieures à 10% (v/v). Après élimination des candidats fongiques pouvant potentiellement produire des métabolites toxiques, notamment pour l'homme, trois espèces semblaient prometteuses pour lutter contre la septoriose du blé, *Trichoderma virens, Lecanicillium longisporum* et *Emericella rugulosa*. Les surnageants bactériens provenant des souches S1 et S6 de *Bacillus velezensis* se sont révélés particulièrement efficaces *in vitro*, avec des CI_{50} de 1,4% et de 7,4%, respectivement. Les CI_{50} des surnageants bactériens provenant des deux souches de *Paenibacillus polymyxa* n'ont pas pu être calculées en raison d'une quantité trop limitée de filtrats utilisables. En effet, la viscosité de leurs milieux de culture après quelques heures était beaucoup trop élevée. Pour produire des surnageants provenant de ces souches en quantité et qualité convenable, il serait donc recommandé d'optimiser les conditions de culture (milieux, température, pH, *etc*.). En ce qui concerne les rhamnolipides et molécules associées, seuls six ont présenté une activité antifongique significative *in vitro*. Nous avons aussi retrouvé une CI_{50} et une CMI particulièrement basse pour la mycosubtiline, confirmant les résultats rapportés par Mejri *et al*. (2018) **(Tableau 5)**.

Les composés les plus prometteurs au cours de cette étape ont ainsi été sélectionnés pour de plus amples analyses visant à (i) vérifier leur activité de protection *in planta*, (ii) déterminer si certains d'entre eux étaient capables d'induire les défenses du blé vis-à-vis de la septoriose, (iii) comprendre leurs modes d'action et (iv) caractériser leurs composants principaux dans le cas des surnageants bruts. Les méthodologies utilisées, les caractéristiques des biomolécules et extraits ainsi que les principaux résultats obtenus seront présentés et discutés dans les chapitres suivants :

- Dans le **chapitre 1**, nous nous intéresserons aux activités biologiques (antifongique, élicitation des défenses du blé et activité de protection) des rhamnolipides naturels et bio-inspirés et verrons, grâce à l'étude de leur relation structure-activité, l'importance de la longueur de la chaîne carbonée dans leur efficacité.
- Dans le **chapitre 2**, le potentiel du rhamnolipide le plus efficace pour protéger le blé contre *Z. tritici*, le Rhamnose-Ester-C12 (Rh-Est-C12), de stimulation des défenses de l'hôte, sera exploré à l'aide d'une approche combinée de transcriptomique et de métabolomique.
- Dans le **chapitre 3**, l'activité élicitrice et potentialisatrice de, cette fois-ci, la mycosubtiline, sera étudiée à l'aide d'approches transcriptomiques, métabolomiques, mais aussi cytologiques.
- Dans le **chapitre 4**, la caractérisation métabolique des souches S1 et S6 de *Bacillus velezensis*, présentant les plus fortes efficacités directes *in vitro* et dont les surnageants sont aisés à produire, sera abordée en lien avec leurs activités antifongiques.

CHAPITRE 1

Importance de la chaine C12 dans les activités biologiques des rhamnolipides sur le pathosystème blé-*Zymoseptoria tritici*

Les rhamnolipides sont des métabolites secondaires amphiphiles, produits par plusieurs espèces bactériennes appartenant, notamment, aux genres *Pseudomonas* et *Burkholderia*. Cette famille de glycolipides, généralement considérée comme faiblement toxique et écotoxique, a déjà montré des activités antimicrobiennes significatives vis-à-vis d'autres agents pathogènes ainsi que des activités inductrices de défense chez certains organismes végétaux (Vatsa *et al.*, 2010 ; Crouzet *et al*., 2020). Leur potentiel en tant que produit de biocontrôle n'avait toutefois jamais été exploré sur le pathosystème blé-*Z. tritici*. Lors du criblage initial, nous avons mis en évidence que seule une partie des rhamnolipides à notre disposition était capable d'inhiber significativement la croissance du champignon pathogène *in vitro*, ceux présentant une chaine carbonée longue de 10 ou 12 carbones. Afin d'aller plus loin, nous avons décidé de déterminer les activités biologiques (antifongique, élicitation des défenses du blé et activité de protection) de ces composés et d'étudier ainsi leur relation structure-activité. Les résultats obtenus sont présentés et discutés dans l'article suivant. Brièvement, nous avons pu monter que les rhamnolipides présentant des liaisons éthers ou esters et avec des chaînes carbonées à 12 carbones étaient globalement les plus efficaces pour toutes les activités biologiques étudiées. Aussi, nous avons mis en évidence que le groupement rhamnose était essentiel pour l'activité de ces composés, notamment de protection. Le Rhamnose-Ester-C12 (Rh-Est-C12) s'est révélé être le composé le plus prometteur parmi de tous ceux dont nous disposions et des analyses supplémentaires ont été réalisées afin d'explorer plus en profondeur son potentiel pour protéger le blé vis-à-vis de *Z. tritici*, notamment sa capacité à inhiber la croissance de souches de l'agent pathogène hautement résistantes (*multi-drug resistants*, MDR) aux fongicides de synthèse de la famille des inhibiteurs de la déméthylation (DMI).

Les travaux de ce chapitre sont publiés dans l'article : Platel et al. (2021). Importance of the C12 carbon chain in the biological activity of rhamnolipids conferring protection in wheat against Zymoseptoria tritici*.* Molecules*, 26, 1: 40. doi.org/10.3390/molecules26010040 (IF = 3,27).*

molecules

MDPI

Article

Importance of the C12 Carbon Chain in the Biological Activity of Rhamnolipids Conferring Protection in Wheat against *Zymoseptoria tritici*

Rémi Platel [1], Ludovic Chaveriat [2], Sarah Le Guenic [2], Rutger Pipeleers [3], Maryline Magnin-Robert [4], Béatrice Randoux [4], Pauline Trapet [1], Vincent Lequart [2], Nicolas Joly [2], Patrice Halama [1], Patrick Martin [2] , Monica Höfte [3], Philippe Reignault [4], Ali Siah [1,*]

[1] Joint Research Unit N° 1158 BioEcoAgro, Junia, Univ. Lille, INRAE, Univ. Liège, UPJV, Univ. Artois, ULCO, 48, boulevard Vauban, BP 41290, F-59014, Lille cedex, France ; remi.platel@junia.com (R.P.) ; pauline.trapet@junia.com (P.T.) ; patrice.halama@junia.com (P.H.)

[2] Univ. Artois, UniLasalle, ULR 7519 – Unité Transformations & Agroressources, F-62408 Béthune, France ; sarah.leguenic@univ-artois.fr (S.L.) ; vincent.lequart@univ-artois.fr (V.L.) ; nicolas.joly@univ-artois.fr (N.J.) ; patrick.martin@univ-artois.fr (P.M.)

[3] Ghent University, Lab. Phytopathology, Dept. Plants & Crops, B-9000 Ghent, Belgium ; Rutger.Pipeleers@UGent.be (R.P.) ; Monica.Hofte@UGent.be (M.H.)

[4] Unité de Chimie Environnementale et Interactions sur le Vivant (EA 4492), Université du Littoral Côte d'Opale ,CS 80699, F-62228, Calais cedex, France ; maryline.magnin-robert@univ-littoral.fr (M.M-R.) ; beatrice.randoux@univ-littoral.fr (B.R.) ; philippe.reignault@univ-littoral.fr (Ph.R.)

* Correspondence: ali.siah@junia.com ; Tel.: +33 (0)3 28 38 48 48 , Co-correspondence: ludovic.chaveriat@univ-artois.fr ; Tel.: +33 (0)3 21 63 23 20

Abstract: The hemibiotrophic fungus *Zymoseptoria tritici*, responsible for Septoria tritici blotch, is currently the most devastating foliar disease on wheat crops worldwide. Here, we explored, for the first time, the ability of rhamnolipids (RLs) to control this pathogen, using a total of 19 RLs, including a natural RL mixture produced by *Pseudomonas aeruginosa* and 18 bioinspired RLs synthesized using green chemistry, as well as two related compounds (lauric acid and dodecanol). These compounds were assessed for *in vitro* antifungal effect, *in planta* defence elicitation (peroxidase and catalase enzyme activities), and protection efficacy on the wheat-*Z. tritici* pathosystem. Interestingly, a structure-activity relationship analysis revealed that synthetic RLs with a 12 carbon fatty acid tail were the most effective for all examined biological activities. This highlights the importance of the C12 chain in the bioactivity of RLs, likely by acting on the plasma membranes of both wheat and *Z. tritici* cells. The efficacy of the most active compound Rh-Est-C12 was 20-fold lower in *planta* than *in vitro*; an optimization of the formulation is thus required to increase its effectiveness. No *Z. tritici* strain-dependent activity was scored for Rh-Est-C12 that exhibited similar antifungal activity levels towards strains differing in their resistance patterns to demethylation inhibitor fungicides, including multi-drug resistance strains. This study reports new insights into the use of bio-inspired RLs to control *Z. tritici*.

Keywords: Wheat, *Zymoseptoria tritici,* rhamnolipids, elicitors, structure-activity relationship

1. Introduction

Wheat is one of the most produced and consumed crops worldwide along with maize and rice. For the 2018-2019 period, the Food and Agriculture Organisation estimated that global wheat production

reached 732.1 million tons [1]. This crop is cultivated in many different geoclimatic areas and ecosystems, and it is vastly used for human food as well as livestock feed. Hence, ensuring a safe and sufficient production of this cereal is a vital matter. Although wheat is susceptible to various pathogenic agents, Septoria tritici blotch (STB), caused by the hemibiotrophic fungus *Zymoseptoria tritici*, is considered as the most impacting foliar disease on wheat and is of major concern for wheat production worldwide. Currently, strategies to control this phytopathogen rely mainly on the application of conventional fungicides and, to a lower extent, on the use of partially resistant cultivars. In Western Europe, where the climate is particularly conducive for fungal development, STB is of critical importance, both agronomically and economically, leading to yield losses up to 50%. Thus, 70% of fungicides applied in the European Union are used for the control of this disease, for a cost of approximately 1.2 billion dollars per year [2,3].

The main conventional fungicides used currently for STB control are (i) succinate dehydrogenase inhibitors (SDHIs), carboxamide molecules inhibiting succinate dehydrogenase of the fungal mitochondrial respiratory chain, and (ii) demethylation inhibitor (DMI) fungicides, which target the 14 α-demethylase CYP51 protein involved in the biosynthesis of ergosterol, a major lipid compound of fungal plasma membrane. Although the decreasing sensitivity in *Z. tritici* populations to SDHIs in the field is still being contained, reports regarding the resistance of this fungus towards DMIs have increased in the recent years. Indeed, serious breakdowns in azole fungicide efficacy appeared, firstly in Europe and then all over the world [4-6]. Concerning DMI resistance, three mechanisms of resistance have been described: (i) alteration of the CYP51 protein due to mutations in the corresponding gene, causing a decrease of affinity between the fungicide and its target, the protein CYP51, (ii) overexpression of the *CYP51* gene, and (iii) enhanced efflux activity in fungal cells due to the overexpression of genes coding for membrane transporters, leading to populations exhibiting multi-drug resistance (MDR) phenotypes [4]. Because of this fungicide resistance issue and the increasing societal demand to implement a more sustainable agriculture, there is a strong need to develop alternatives to control STB in the field.

In the last decades, many studies have highlighted the potential of green surfactants in agriculture. Biosurfactants are surface-active compounds produced by a wide range of microorganisms. Even though they may be chemically very diverse, they are all amphiphilic molecules, consisting of hydrophobic and hydrophilic moieties. They may be used in agriculture for different applications like bioremediation, stimulating interactions between plants and beneficial microorganisms, as well as in crop protection by acting as biofungicides or/and as plant resistance inducers [7-9]. Rhamnolipids (RLs) are secondary metabolites with biosurfactant properties, naturally produced by bacteria belonging to the genera *Pseudomonas* sp. and *Burkholderia* sp. They are naturally biosynthetized as a mixture of compounds with one or two rhamnose residues (mono- or di-RLs), forming a polar hydrophilic head and linked through a beta-glycosylic bond to one or two 3-hydroxy fatty acids, as hydrophobic tails. Rhamnolipids are one of the most intensively studied classes of surfactant glycolipids. Like other biosurfactants, they may potentially be used in a broad range of areas, including medicine, cosmetics, food processing, petroleum industries, and agriculture [10-12]. In crop protection, previous studies reported the antimicrobial properties of natural RLs, as well as their capacity to induce plant resistance mechanisms, as reviewed by Vatsa et al. [13]. For instance, they were demonstrated to inhibit the growth of various phytopathogenic fungi, such as *Botrytis cinerea* and *Fusarium solani*, and to control oomycete phytopathogens, such as *Phytophtora* sp., by lysing zoospores [14-17]. Natural RLs are also able to protect plants, such as grapevine and *Brassica napus*, against *B. cinerea*, by triggering defense responses, such as ROS production [17,18]. Natural RLs were also reported to induce defense mechanisms in *Arabidospis thaliana* against three phytopathogens, including *Pseudomonas syringae* pv. *tomato*, *Hyaloperonospora arabidopsidis*, and *B. cinerea* [19]. RLs are considered as easily biodegradable and exhibit low toxicity and ecotoxicity, making them promising compounds for plant protection [20,21].

Nevertheless, even though RLs are known to be synthesized by various bacterial species, they are still mostly produced using *Pseudomonas aeruginosa*, a species that cannot be used as biocontrol agent

because it is an opportunistic human pathogen. In addition, large-scale industrial production is difficult because of low yields obtained with *P. aeruginosa*. To overcome these issues, three methods may be proposed, such as (i) the use of non-pathogenic natural RLs-producing bacteria such as *Burkholderia* sp. [22], (ii) their heterologous synthesis with genetically modified microorganisms generally recognized as safe, such as *Saccharomyces cerevisiae* [23], or (iii) their synthesis using green chemistry. Recently, synthetic environmentally-friendly RLs produced by green chemistry were found to be able to trigger ROS production in *A. thaliana,* showing a promising potential as plant resistance inducers [24]. Moreover, Robineau et al. [25] demonstrated that synthetic mono-RLs confer protection to tomato against *B. cinerea* by both direct antifungal activity and host defense mechanism activation.

So far, biological activity of RLs has never been explored in the wheat-*Z. tritici* pathosystem. The objective of the present study was thus to assess the direct antifungal activity, the plant eliciting effect, as well as the protection efficacy of 19 RLs (either naturals, produced by *P. aeruginosa*, or synthetic (bio-inspired) obtained by green chemistry), as well as lauric acid and dodecanol (C12-carbon chain molecules) on the wheat-*Z. tritici* model. A structure-activity relationship analysis of these compounds was performed in order to highlight the chemical radicals responsible for the RL activities. Moreover, the efficacy of the most active RL was compared between *in vitro* (direct antifungal activity) and *in planta* (disease symptom reduction) conditions. Finally, a possible strain-dependant effect of the RL activity was investigated by examining the *in vitro* antifungal activity of the most active RL toward 21 *Z. tritici* strains that differ in their resistance level to DMI fungicides.

2. Results

2.1. Chemical description of the synthesized RLs

A total of 18 RLs were obtained using green chemistry to investigate their biological activities on the wheat-*Z. tritici* pathosystem (Table 1). Three series of rhamnose derivatives, differing by the function linking the hydrophobic chain (ether, ester, or succinates), were successfully synthesized. A first series of ether rhamnose derivatives (Rh-Eth), synthesized without using solvent from the L-rhamnose and a fatty alcohol with various chain lengths (4 to 18 carbon atoms), was produced (Table 1). Then, a second series of RLs, with an ester link (Rh-Est), was obtained (8 to 12 carbons). Finally, succinate rhamnose derivatives (Rh-Suc), including mono-rhamnosyl (alkenyl)succinate (Rh-Suc-C8, Rh-Suc-C12, and Rh-Suc-C12b) and mono-rhamnosyl (alkenyl)alkylsuccinate (Rh-Suc-C8-C8, Rh-Suc-C8-C12, Rh-Suc-C12-C8, and Rh-Suc-C12-C12) derivatives, were generated (Table 1). Among the synthesized RLs, nine of them (Rh-Eth-C4, Rh-Eth-C6, Rh-Eth-C8, Rh-Eth-C10, Rh-Eth-C12, Rh-Eth-C14, Rh-Eth-C16, Rh-Est-C12, and Rh-Suc-C12) have already been reported [25], while the nine other RLs, belonging for a large part to the new RL family mono-rhamnosyl (alkenyl)alkylsuccinate, were obtained for the first time (Rh-Eth-C18, Rh-Est-C8, Rh-Est-C10, Rh-Suc-C8, Rh-Suc-C12b, Rh-Suc-C8-C8, Rh-Suc-C8-C12, Rh-Suc-C12-C8, Rh-Suc-C12-C12). For mono-rhamnosyl (alkenyl)alkylsuccinate RLs, they were obtained after esterification of L-rhamnose with octenylsuccinic or dodecenylsuccinic anhydrid in *N,N*-dimethylformamide (DMF) in presence of *N,N*-dimethylpyridin-4-amine (DMAP), followed by a second esterification by using alkyl bromide. Then, by combining the use of an alkylated succinic anhydride with 8 or 12 carbon atoms and an octanoic or lauric acid chloride during the synthesis from rhamnose, four new derivatives of rhamnose (Rh-Suc-C8-C8, Rh-Suc-C8-C12, Rh-Suc-C12-C8 and Rh-Suc-C12-C12), with a yield comprised between of 34 and 39%, were successfully developped.

Table 1. List, structure and characteristics of the eighteen synthesized RLs as well as lauric acid, dodecanol and natural RLs.

Scheme	Compound	Name	Molecular weight ($g.moL^{-1}$)
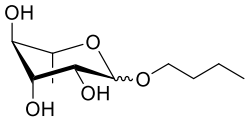	Rh-Eth-C4	Butyl α/β-L-rhamnopyranoside	220
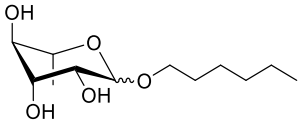	Rh-Eth-C6	Hexyl α/β-L-rhamnopyranoside	248
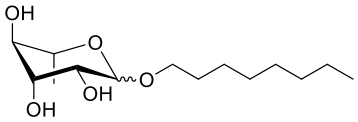	Rh-Eth-C8	Octyl α/β-L-rhamnopyranoside	276
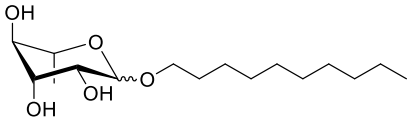	Rh-Eth-C10	Decyl α/β-L-rhamnopyranoside	304
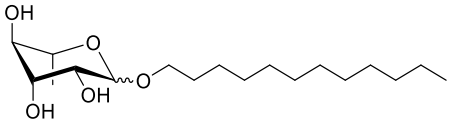	Rh-Eth-C12	Dodecyl α/β-L-rhamnopyranoside	332
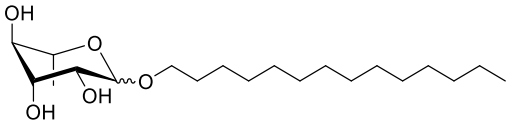	Rh-Eth-C14	Tetradecyl α/β-L-rhamnopyranoside	360
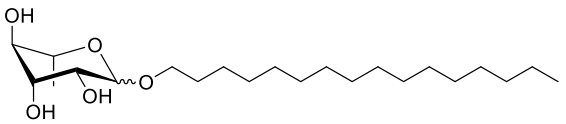	Rh-Eth-C16	Hexadecyl α/β-L-rhamnopyranoside	388
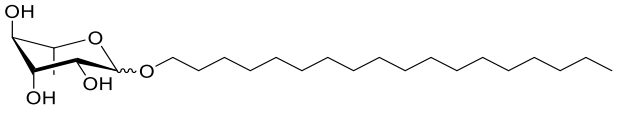	Rh-Eth-C18*	Octadecyl α/β-L-rhamnopyranoside	416
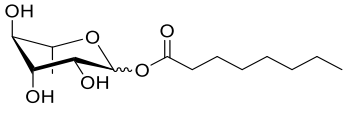	Rh-Est-C8*	Octanoyl α/β-L-rhamnopyranoside	290
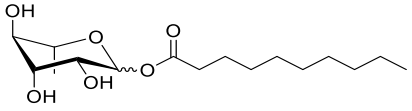	Rh-Est-C10*	Decanoyl α/β-L-rhamnopyranoside	318
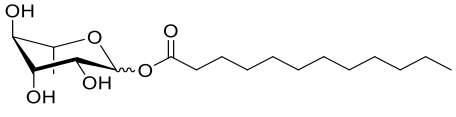	Rh-Est-C12	Dodecanoyl	346

		α/β-L-rhamnopyranoside	
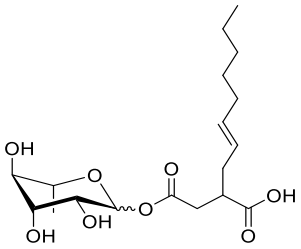	Rh-Suc-C8*	Octenylsuccinate α/β-L-rhamnopyranoside	374
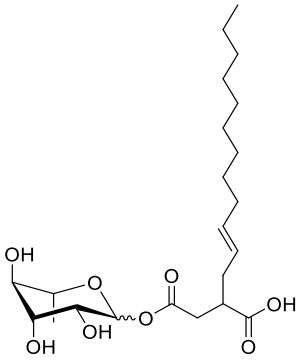	Rh-Suc-C12	Dodecenylsuccinate α/β-L-rhamnopyranoside	430
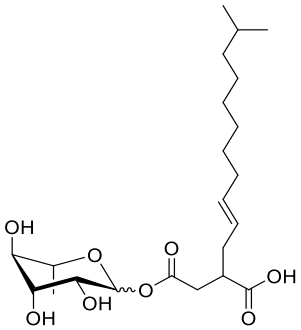	Rh-Suc-C12b*	*Iso*-Dodecenylsuccinate α/β-L-rhamnopyranoside	430
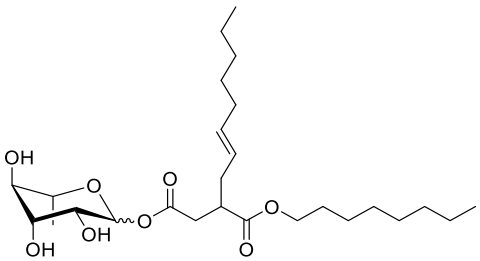	Rh-Suc-C8-C8*	3-Octenyloctylsuccinate α/β-L-rhamnopyranoside	486
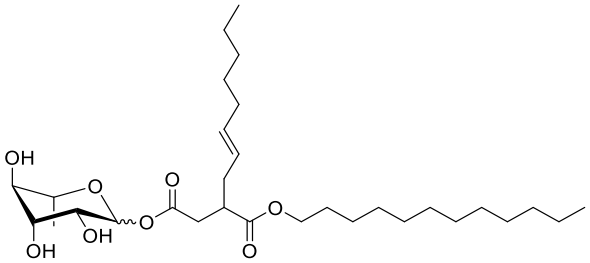	Rh-Suc-C8-C12*	3-Octenyldodecylsuccinate α/β-L-rhamnopyranoside	542

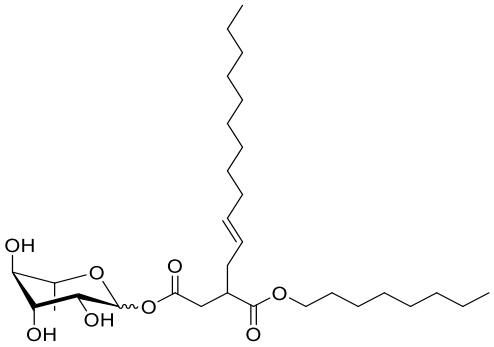	Rh-Suc-C12-C8*	3-Dodecenyloctylsuccinate α/β-L-rhamnopyranoside	542
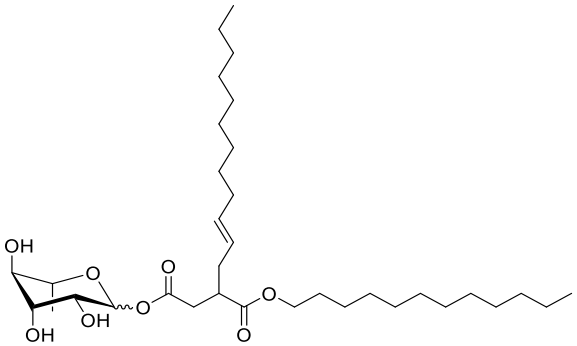	Rh-Suc-C12-C12*	3-Dodecenyldodecylsuccinate α/β-L-rhamnopyranoside	598
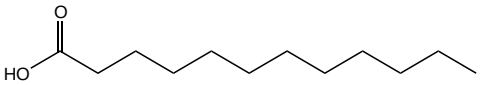	Lauric acid	Lauric acid	200
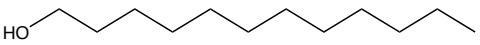	Dodecanol	Dodecanol	186
Mixture of rhamnolipids (data from Agae Technologies LLC)	Nat-Rh	Bacterial rhamnolipids (see "Materials and methods")	578

* Molecules newly synthetized in this study, while the other molecules were already reported in Robineau et al. [25].

2.2. Biological activities of RLs differ according to the length of their carbon chain

A total of 21 molecules, including 18 synthesized RLs and three related molecules (a mixture of natural RLs, lauric acid, and dodecanol) were examined for both their direct (antifungal) and indirect (plant defence elicitation) activities, as well as for their protection efficacy in the greenhouse, on the wheat-*Z. tritici* pathosystem. Regarding the *in vitro* antifungal activity, among all tested RLs, from C4 to C18-derived molecules, only Rh-Eth-C10, Rh-Eth-C12, and Rh-Est-C12 drastically inhibited fungal growth (Table 2, Figure 1). Succinate-RLs did not significantly reduce fungal growth, except for Rh-Suc-C8, which showed an inhibitory effect only at the highest tested concentration of 1500 µM (Table 2). Concerning the ester-RL family, Rh-Est-C10 had no antifungal activity, while Rh-Est-C12 was found to be the most active molecule among all tested RLs (Figure 1). On the other hand, lauric acid and dodecanol displayed a marked *in vitro* antifungal effect againt Z. tritici, with IC_{50} and MIC values close to those of the active RLs. Natural RLs did not show any direct antimicrobial effect.

Concerning the ability of the molecules to elicit plant defenses, activity of two plant enzymes involved in ROS scavenging, catalase (CAT) and peroxidase (POX), was investigated two days after treatment. Only three molecules significantly modified at least one enzymatic activity (Table 2). Rh-Eth-

C12 increased CAT activity by 1.86 fold compared to the control, whereas Rh-Suc-C12b enhanced POX activity by 2.26 fold compared to the control. Rh-Suc-C12, whose chemical structure is close to Rh-Suc-C12b, did not exhibit any induction of the targeted enzymes in our conditions. Finally, Rh-Est-C12 induced both CAT activity and POX activities by 1.71 and 2.27 folds, respectively, when compared to the control. Lauric acid and dodecanol did not cause any significant change in the investigated enzyme activities.

None of the tested molecule displayed *in planta* phytotoxicity at the tested concentration 1.5 mM. Five tested RLs caused a significant reduction in disease symptoms (Table 2). Among them, the four molecules Rh-Eth-C12, Rh-Suc-C12b, Rh-Eth-C10, and Natural-Rh conferred only a slight protection effect, with a decrease in disease severity ranging from 15.5 to 17.4%. On the other hand, disease severity reduction obtained with Rh-Est-C12 treatment was significantly different from all other treatments and exhibited the highest activity, with 35.6% of disease symptom reduction (approximatively 2 fold higher than the protection efficacies conferred by the other active RLs). On the contrary to RLs with C12-carbon chain, lauric acid and dodecanol did not display any significant protection activity.

Table 2. Biological activities, including *in vitro* direct antifungal activity, *in planta* defense activation and *in planta* protection efficacy of the eighteen synthetized RLs, as well as lauric acid, dodecanol and natural RLs, at 1.5 mM, on the wheat-*Zymoseptoria tritici* pathosystem.

Molecule	***In vitro* antifungal activity**		***In planta* defense elicitation activity**		***In planta* protection efficacy**
	IC_{50} (μM)	MIC (μM)	Catalase activity ($U.min^{-1}.g^{-1}$ proteins)	Peroxidase activity ($U.min^{-1}.g^{-1}$ proteins)	Leaf diseased area (%)•
Control	-	-	83.4^{ab}	51.7^{bc}	55.7^{a} (0%)
Natural-Rh	>1500	>1500	71.9^{a}	53.4^{c}	**46.3^{b} (-17.0%)**
Rh-Eth-C4	>1500	>1500	110.4^{abcd}	64.8^{bc}	51.4^{ab} (-7.8%)
Rh-Eth-C6	>1500	>1500	111.7^{abcd}	55.9^{bc}	54.4^{ab} (-2.3%)
Rh-Eth-C8	>1500	>1500	121.1^{abcd}	74.2^{abc}	54.3^{ab} (-2.6%)
Rh-Eth-C10	**158**	**200**	131.6^{bcd}	54.2^{bc}	**46.0^{b} (-17.4%)**
Rh-Eth-C12	**81**	**450**	**155.2^{d}**	71.0^{abc}	**46.2^{b} (-15.5%)**
Rh-Eth-C14	>1500	>1500	99.2^{abcd}	71.2^{abc}	49.4^{ab} (-11.3%)
Rh-Eth-C16	>1500	>1500	130.9^{bcd}	67.7^{bc}	50.3^{ab} (-9.7%)
Rh-Eth-C18	>1500	>1500	Nd*	Nd*	Nd*
Rh-Est-C8	>1500	>1500	112.9^{abcd}	44.9^{c}	50.6^{ab} (-9.1%)
Rh-Est-C10	>1500	>1500	98.4^{abcd}	58.2^{bc}	50.6^{ab} (-9.3%)
Rh-Est-C12	**75**	**133**	**142.5^{cd}**	**117.3^{a}**	**35.9^{c} (-35.6%)**
Rh-Suc-C8	**1399**	**1500**	123.3^{abcd}	60.3^{bc}	54.1^{ab} (-3.0%)
Rh-Suc-C12	>1500	>1500	124.9^{abcd}	76.6^{abc}	50.3^{ab} (-9.7%)
Rh-Suc-C12b	>1500	>1500	96.8^{abc}	**116.9^{a}**	**46.2^{b} (-16.2%)**
Rh-Suc-C8-C8	>1500	>1500	102.4^{abcd}	62.1^{bc}	52.4^{ab} (-6.0%)
Rh-Suc-C8-C12	>1500	>1500	113.7^{abcd}	96.9^{ab}	51.2^{ab} (-8.1%)
Rh-Suc-C12-C8	>1500	>1500	120.1^{abcd}	79.9^{abc}	55.8^{a} (+0.1%)
Rh-Suc-C12-C12	>1500	>1500	Nd*	Nd*	Nd*
Lauric acid	**109**	**200**	94.0^{abc}	76.8^{abc}	50.9^{ab} (-8.7%)
Dodecanol	**164**	**200**	107.4^{abcd}	51.1^{bc}	54.4^{ab} (-2.4%)

(*) No data were obtained for two RLs because of solubilization issues. Different letters indicate significant differences between treatments according to ANOVA followed by Tukey's test at $P \leq 0.05$. Values in bold indicate significant effects. (•) Values between brackets stand for the percentage of disease symptom reduction compared to the control condition.

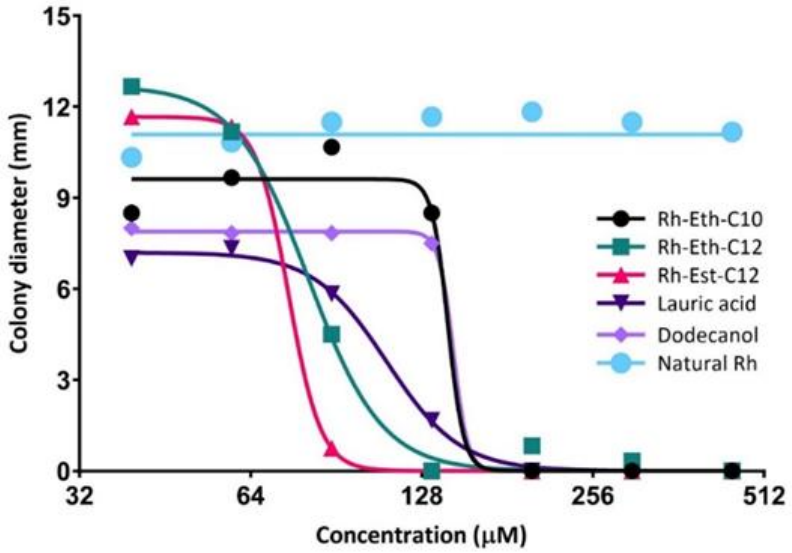

Figure 1. *In vitro* dose-response curves displaying the antifungal effect of the three most efficient RLs, as well as dodecanol and lauric acid, against *Zymoseptoria tritici* (strain T02596) compared to the natural RLs.

2.3. Correlations between in vitro *antifungal activity,* in planta *defence elicitation and protection efficacy*

A correlative analysis was performed to determine whether *in vitro* antifungal and elicitation activities were relevant to explain disease symptom reduction caused by the treatments. The statistical analyses revealed significant positive correlations between both IC_{50} and MIC and the disease severity reduction (r=0.46) (Table 3). However, no significant correlation was found between CAT activity and protection efficacy, while POX activity and disease symptoms were significantly and negatively correlated (r=-0.51).

Table 3. Correlations between protection efficacy and both direct (IC_{50} and MIC) and indirect (plant catalase and peroxidase activities) effects of the tested RLs, as well as dodecanol and lauric acid, obtained on the wheat-*Zymoseptoria tritici* pathosystem.

	IC_{50}	**MIC**	**Catalase activity**	**Peroxidase activity**
IC_{50}	-	-	-	-
MIC	**0.99**	-	-	-
Catalase activity	-0.40	-0.35	-	-
Peroxidase activity	-0.10	-0.10	0.19	-
Leaf diseased area	**0.46**	**0.46**	-0.25	**-0.51**

Significant values according to the Pearson test at $P \leq 0.05$ are indicated in bold

2.4. Comparison of in vitro versus *in planta antifungal effects of Rh-Est-C12*

According to the structure-activity relationship study above, Rh-Est-C12 appeared to be the most active RL for protection efficacy, *in vitro* antifungal effect, and elicitation activity. Hence, we focused on this molecule in order to compare its direct activity *in vitro* and *in planta*. *In planta*, the protective effect of foliar treatment with Rh-Est-C12 on wheat against *Z. tritici* was assessed at different concentrations. There was no significant protection with applications of Rh-Est-C12 at 50, 100, 200, and 400 µM of the RL. However, Rh-Est-C12 treatments with 800, 1600, and 3200 µM significantly reduced disease

symptoms on wheat leaves, with protection rates of 19.9%, 53.3%, and 78.9% respectively (Figure 2). No phytotoxicity was observed at any of the tested concentrations. The *in planta* IC_{50} value of this molecule (the concentration of Rh-Est-C12 reducing by half the disease symptom level compared to the non-treated control) was calculated and was determined as 1510 µM. Rh-Est-C12 exhibited an *in planta* IC_{50} value approximatively 20-fold higher than the IC_{50} value obtained *in vitro* for the molecule, revealing a major difference in the activity of the molecule between the two conditions.

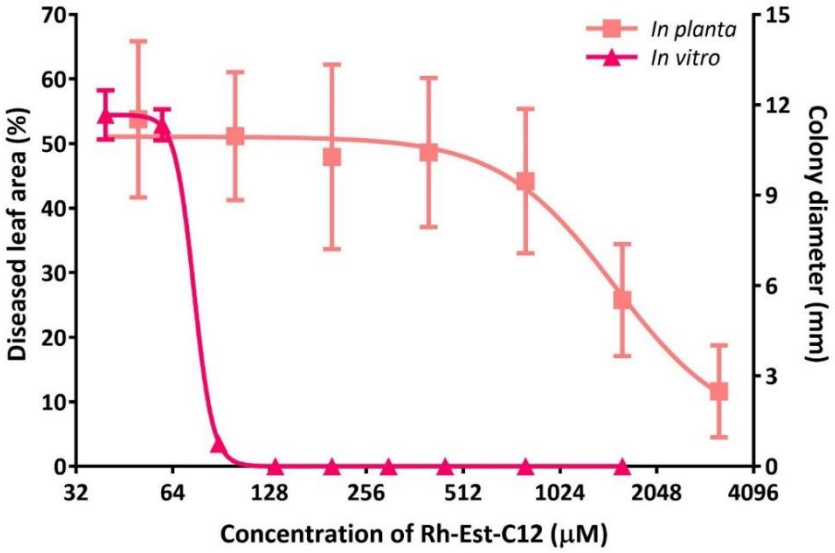

Figure 2. Comparison of *in planta* and *in vitro* dose-response curves of Rh-Est-C12 on the wheat-*Zymoseptoria tritici* pathosystem. Wheat cultivar Alixan and *Z. tritici* strain T02596 were used. The *in planta* activity of the compound was assessed by measuring the percentage of chlorosis and necrosis on the third leaves of each plant at 21 days after inoculation. Bars stand for standard deviations.

Additionally, the effect of Rh-Est-C12 on *in planta* spore germination and fungal hyphal growth was assessed at three different concentrations (50, 400, and 3200 µM) (Figure 3). Whereas no significant activity was observed after application of Rh-Est-C12 at 50 and 400 µM, a strong antifungal effect was highlighted for this compound at 3200 µM. The proportion of non-germinated spores in the treated plants was 2-fold higher than in the control. Moreover, a reduction by 4-fold of the class 4 spore proportion (geminated spores with a strongly developed germ tube) was also scored in the plants treated with 3200 µM Rh-Est-C12 compared to the control (Figure 3). Again, the *in planta* direct activity of Rh-Est-C12 on hyphal growth appeared weaker than its direct antifungal effect obtained *in vitro* on fungal colony development.

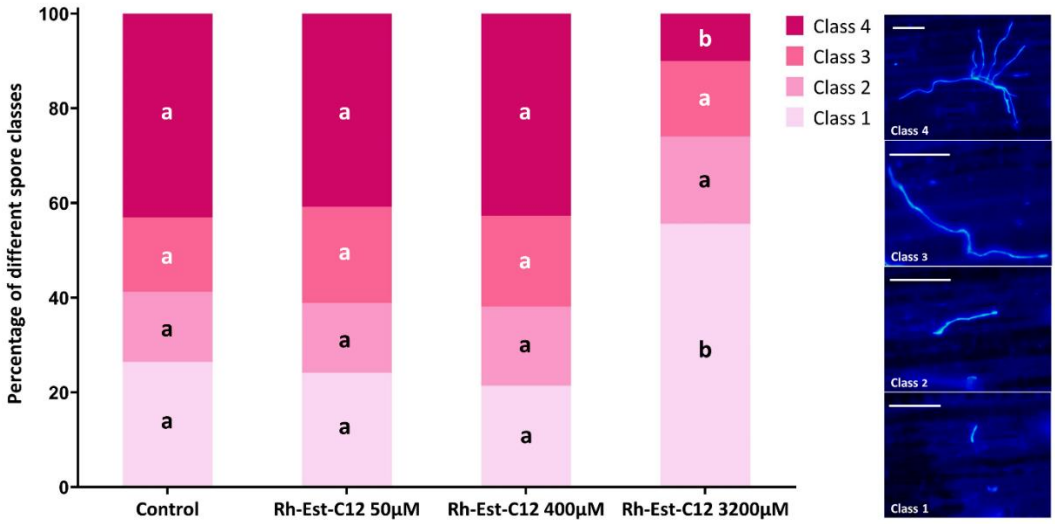

Figure 3. *In planta* spore germination and hyphal growth of *Zymoseptoria tritici* on wheat leaves treated or not with Rh-Est-C12. Wheat cultivar Alixan and *Z. tritici* strain T02596 were used. Percentage of four different classes of Calcofluor-strained spores was assessed three days after inoculation on wheat third leaves. The right panel shows a representative picture of each spore class (scale bar = 25 µm). Class 1: non germinated spore; Class 2: geminated spore with small germ tube; Class 3: geminated spore with developed germ tube; Class 4: geminated spore with a strongly developed germ tube. For each condition, 100 different spores from six different leaves were assessed. Within each class, different letters indicate significant differences between treatments according to ANOVA followed by the Tukey's test at $P \leq 0.05$..

2.5. Direct in vitro *antifungal activity of Rh-Est-C12 does not vary depending on* Z. tritici *strains*

To examine any possible strain effect of Rh-Est-C12 direct *in vitro* antifungal activity, 21 different *Z. tritici* strains showing different resistance levels towards DMI fungicides, were investigated for their resistance level to this RL. Overall, no major difference were observed between all tested strains regarding the IC_{50} values of Rh-Est-C12 (Figure 4A, Supplementary Tables 1 and 2). Resistance factors (ratio between the IC_{50} value of a given strain and the IC_{50} value of the sensitive reference strain IPO323) ranged from 0.7 to 1.2 for Rh-Est-C12, indicating no strain effect on the direct activity of the molecule. By contrast, a strong strain effect was highlighted for the five tested DMI fungicides, with resistance factors ranging from 3.8 to 1071.4 for tebuconazole, from 1.0 to 150.8 for metconazole, from 28.6 to 501.8 for epoxiconazole, 37.4 to 74753.2 for prothioconazole, and from 5.1 to 266.2 for prochloraz (Figure 4A, Supplementary Tables 1 and 2). Rh-Est-C12 displayed similar antifungal activity levels on both (i) non-MDR and non *Cyp51*-overexpressing strains, and (ii) the highly resistant strains with MDR character or overexpressing the *Cyp51* gene (Figure 4B, Supplementary Tables 1 and 2).

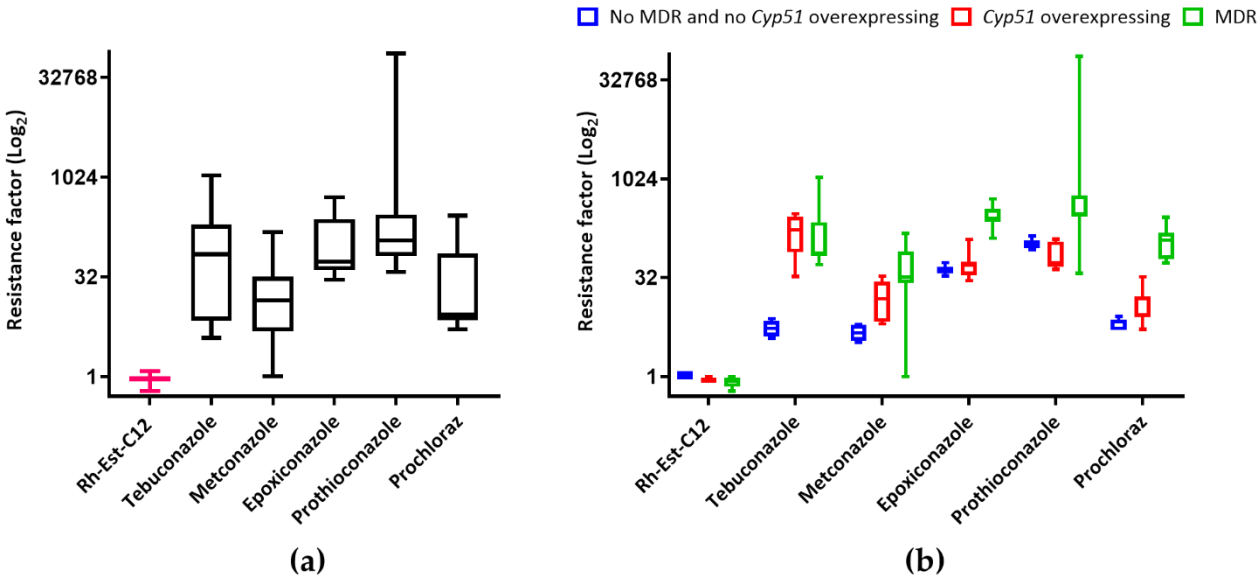

Figure 4. Boxplots showing the resistance factors obtained for 21 different *Zymoseptoria tritici* strains analyzed together (a) or distinguished according to their DMI resistance profiles (seven MDR strains, seven strains overexpressing the *Cyp51* gene, and seven strains without these resistance mechanisms) (b), against five DMI fungicides as well as the RL molecule Rh-Est-C12. Resistance factors correspond to the ratio between the IC_{50} value of a given strain and the IC_{50} value of the sensitive reference strain IPO323.

3. Discussion

We explored here, for the first time, the potential of RLs to protect wheat against *Z. tritici*, a major pathogen on wheat crops, using a panel of 21 molecules, including 18 bioinspired RLs synthesized using green chemistry and three related molecules (a mixture of natural RLs from *P. aeruginosa*, lauric acid, and dodecanol). Natural bacterial RLs have already been reported to show antimicrobial activity against a wide range of plant pathogenic fungi [13]. For instance, Varnier et al. [17] reported a significant antigerminative effect of 0.1 $mg.mL^{-1}$ of bacterial RL against the ascomycete polyphagous fungus *B. cinerea*. Moreover, natural RLs were found particularly effective against certain oomycetes, such as *Phytophthora* sp., by lysing zoospores, hypothetically by intercalating into oomycete cell membranes, leading to their disorganization [14]. However, in our conditions, and even with concentrations up to 0.87 $mg.mL^{-1}$ (*i.e.* 1500 µM) no activity was observed for the tested mixture of natural RLs. Among all tested compounds, only a minority exhibited significant *in vitro* antifungal activity. The structure-activity relationship analysis revealed that bioinspired RLs with 4, 6, 8, 14, 16, and 18 carbon fatty acid tails did not display any significant direct effect. Similarly, succinate-derived molecules were also unable to inhibit fungal *in vitro* growth, except Rh-Suc-C8 which exhibited a very slight effect. The most effective RLs were ether and ester-derived compounds, namely Rh-Eth-C10, Rh-Eth-C12, and Rh-Est-C12. Notably, Robineau et al. [25] also described the antifungal activity of these three compounds against *B. cinerea*. However, they observed a more pronounced effect with Rh-Eth-C10. In the present work, Rh-Eth-C10 was not as effective as Rh-Est-C12 that displayed the lowest IC_{50} among all the tested active compounds (158 and 75 µM, corresponding to 0.048 and 0.026 $mg.mL^{-1}$, for Rh-Eth-C10 and Rh-Est-C12, respectively) (Table 1). Moreover, Rh-Est-C10 did not exhibit any inhibition of fungal growth. Hence, we conclude that 12 carbon is the optimum fatty acid tail length for both ether and ester-RLs regarding their direct activity against *Z. tritici*. Thereafter, we assessed the antifungal potential of chemically simple molecules with 12 carbon chain, lauric acid and dodecanol. Interestingly, these two molecules exhibited a significant direct effect, but their IC_{50} are higher than those of Rh-Est-C12 and Rh-Eth-C12 (Table 2). These results confirm the importance of the 12-carbon chain in the direct activity of RLs towards *Z. tritici*.

We also investigated the elicitor potential of RLs on non-infected wheat using two key enzyme biomarkers of plant defence. Only three molecules significantly enhanced the activity of at least one out of the two targeted plant defense-related enzymes CAT and POX. Rh-Eth-C12 was able to stimulate CAT activity, Rh-Suc-C12b induced POX activity, and Rh-Est-C12 increased both (Table 2). These enzymes are involved in many plant defense responses including ROS scavenging, plant signaling, and hypersensitive response [26,27]. These results suggest an increase of ROS production in wheat plants treated with these three compounds. Since large amounts of ROS in plant tissues can be harmful to the plant, wheat plants likely responded by increasing the activity of ROS scavenging enzymes. Interestingly, natural and synthetic RLs were reported to confer resistance and trigger oxidative burst in other plants such as *A. thaliana* and grapevine [17,24]. Robineau et al. [25] also described a significant increase of ROS production in *A. thaliana* leaf disks treated with Rh-Eth-C12 and Rh-Est-C12. Accumulation of H_2O_2 in wheat leaves during infection with *Z. tritici* was reported to increase plant resistance against the pathogen [28]. While the role of CAT in wheat defense against *Z. tritici* is still unclear, Shetty and colleagues [29] reported an involvement of POX in wheat innate immunity. The authors observed a significant induction of this enzyme in resistant cultivars when infected with *Z. tritici*, compared to susceptible cultivars. This may be explained by the specific roles of POX, such as the reinforcement of cell walls and deposition of polyphenolics [30]. This link between POX and innate resistance of wheat to *Z. tritici* is supported by the positive correlation scored between the induction of POX enzymatic activity and plant protection, *i.e.* negative correlation between POX activity and disease symptoms (Table 3).

As for the *in vitro* direct antifungal activity, interestingly, our results revealed that RLs with C12 fatty acid chain were the most effective regarding the induction of the targeted wheat defense biomarkers (CAT and POX). This dual activity on both the host (wheat) and the pathogen (*Z. tritici*) is more likely due to RL interaction with biological plasma membranes of both organisms. Indeed, Monnier and colleagues [31] demonstrated, using *in silico* models, that RLs can act on both plant and fungal membranes by insertion within the lipid bilayers, near the lipid phosphate group of the phospholipid bilayers, nearby phospholipid glycerol backbones. Even though RLs fit into both membranes, RLs seem to differently affect their fluidity. Indeed, the authors suggested that, in the plant membrane, RLs did not significantly impact lipid dynamics inside the lipid bilayer, whereas, in the fungal membrane, a clear fluidity increase was observed, due probably to the presence of ergosterol. These subtle changes in lipid dynamics could explain why the effect of RLs is less drastic on the plant (only triggering defense reactions) than on the fungus that leads to a strong membrane destabilization causing cell death [31]. The importance of the RL carbon chain in plant defense activation has already been reported in previous studies. For instance, Luzuriaga-Loaiza et al. [24] highlighted different results with synthetic RL bolaforms (SRBs) in *A. thaliana*, where SRBs with 14-carbon fatty acid tails were found to be the most effective to induce ROS production in the plant petioles. Regarding other surfactant agents, it has been shown that for surfactin, a lipopeptide produced by *Bacillus subtilis*, the molecules with chain length of 14 or 15 carbons were found more active than surfactin with 12 carbons to enhance production of H_2O_2 in tobacco cells [32]. On the other hand, we found that lauric acid and dodecanol were not able to elicit POX- and CAT-based defense reactions, suggesting a major role of the sugar head in plant defense induction. Although further investigations are needed to decipher the modes of action of RLs on wheat defense induction, such a result suggests the major importance of both rhamnose head and fatty acid tail in the biological activities of RLs on this plant model. Moreover, the precise structure of the RL carbon chain is also crucial, since we observed a significant enhancement of POX activity when using Rh-Suc-C12b compared to its isoform Rh-Suc-C12, which showed no elicitation activity in the treated wheat plants.

Our results revealed that Rh-Eth-C10, Rh-Eth-C12, Rh-Est-C12, Rh-Suc-C12b, and natural RLs are able to reduce *Z. tritici* disease severity on wheat plants. Overall, four categories of protective RLs were observed: (i) protective RLs exhibiting only antifungal activity (Rh-Eth-C10); (ii) protective RLs displaying only elicitation effect (Rh-Suc-C12b); (iii) protective RLs with both activities (Rh-Eth-C12 and Rh-Est-C12), and (iv) protective RLs displaying neither direct nor indirect effects (Natural-Rh), implying

that this latter compound could induce plant defenses through mechanisms not involving our two targeted enzymatic biomarkers. Statistical analyses revealed a positive correlation between POX activity and protection efficacy, as well as between *in vitro* direct activity and protection efficacy. Surprisingly, even though lauric acid and dodecanol were able to inhibit fungal growth *in vitro* with IC_{50} values closes to those of protective RLs, they were unable to protect wheat against the disease, highlighting again the role of rhamnose head in RL protective activity. As discussed above, our structure-activity relationship study reveals the predominant importance of 12 carbon chain in RL biological activities in the wheat-*Z. tritici* model. Likewise, Robineau et al. [25] also described the important role of 12 carbon fatty acid tails in the bioactivity of RLs on the *A. thaliana-B. cinerea* pathosytem.

The mono-RL Rh-Est-C12 was found to be the most effective RL to protect wheat against *Z. tritici*, displaying a reduction of disease symptoms up to 78.9% when applied at 1.1 $mg.mL^{-1}$ (*i.e.* 3200 µM). This product is able to act dually, by inhibiting fungal growth and eliciting plant defenses by enhancing ROS scavenging enzyme activities. Nevertheless, a significant gap between the *in vitro* and *in planta* efficacies of this molecule was highlighted. A ratio of approximately 20-fold separates the *in vitro* IC_{50} value of Rh-Est-C12 and the needed concentration to reduce disease symptoms by 50% *in planta*. This difference of activity may be explained by several factors, including the adherence level of Rh-Est-C12 on wheat leaves during spraying, biodegradability as well as photodecomposition, and penetration properties of the molecule in wheat leaves. Further studies on formulation may increase and optimize the *in planta* efficacy of Rh-Est-C12. Another explanation of the gap between *in vitro* and *in planta* activities of Rh-Est-C12 is the difference between the physiological state of the fungus *in vitro* and *in planta*. Indeed, the fungus develops *in planta* hyphae which can be considered as more robust (since it is in its wild environment, *i.e.* within its host) than the yeast-like morphotype formed by *Z. tritici in vitro*. Another major difference between *in vitro* and *in planta* conditions is that *Z. tritici* develops *in planta* several specialized structures such as pseudo-appressoria and pycnidia that it cannot form *in vitro*, because of the absence of the host in this latter condition.

Considering the high diversity of *Z. tritici* populations that can be found in a single geographic area [33], we assessed the variability of the direct antifungal activity of Rh-Est-C12 towards 21 different strains of the fungus differing in their resistance level to DMI fungicides, the most used chemical class in the field to control this pathogen. Although the *in vitro* IC_{50} value of Rh-Est-C12 was, as expected, much higher than those of conventional fungicides on the reference strain IPO323 (54.3 $\mu g.mL^{-1}$, *i.e.* 157 µM, for the RL *vs* 0.001 to 0.07 $\mu g.mL^{-1}$ depending on the considered fungicide, Supplementary Table 1), it is notherworthy that no strain effect was observed for Rh-Est-C12. By contrast, strong resistance factors were scored for all tested DMI molecules, thus confirming previous studies reporting high rates of DMI resistance in *Z. tritici* populations [34]. Hence, we could assume that Rh-Est-C12 display a mode of action on *Z. tritici* different from that of DMI fungicides, which inhibit the sterol 14 α-demethylase, CYP51, preventing the fungus to produce ergosterol [35]. Here, we suggest that Rh-Est-C12 interacts directly with *Z. tritici* cell membranes, resulting in an inhibition of the fungal growth, as previously suggested for other fungi [14,18].

The environmentally-friendly properties of RLs, the duality of Rh-Est-C12 biological activities (direct and indirect activities), an absence of strain specific resistance within the examined *Z. tritici* collection, together with the low-cost production and industrial feasibility of bioinspired synthetic RLs compared to bacterial production and purification, makes Rh-Est-C12 a promising candidate to control *Z. tritici* in the field. Nevertheless, additional investigations on the formulation aiming at reducing the concentration of the compound *in planta* are required.

4. Materials and Methods

4.1. Chemical compounds used

A total of 18 RLs varying in their structures (chain length and/or linker) synthetized using green chemistry, as well as lauric acid and dodecanol (Sigma-Aldrich, France), were used in order to investigate the structure-activity relationship of RLs on the wheat-*Z. tritici* pathosystem (Table 1). Moreover, commercial RLs purchased from Agae Technologies LLC (Corvallis, USA) were used as a natural RL reference. This natural RL is a mixture of RLs of different structures, composed by decanoic acid, 3-((6-deoxy-2-O-(6-deoxy-α-L-mannopyranosyl)-α-L-mannopyranosyl)oxy)-, 1-(carboxymethyl)octyl ester (Rh-Rh-C10-C10), and 1-(carboxymethyl)octyl 3-((6-deoxy-α-L-mannopyranosyl)oxy)decanoate (Rh-C10-C10), and produced by *P. aeruginosa* with a purification rate of 90% (data from Agae Technologies LLC). According to the provided information, its average molar mass is estimated to 577.72 $g.mol^{-1}$.

The conversions and the purities of the synthetized products were determined by NMR spectroscopy. NMR spectra were recorded on a Bruker DRX300 spectrometer operating at 300 MHz for ^{1}H nuclei and 75 MHz for ^{13}C nuclei. $CDCl_3$ (99.50% isotopic purity) were purchased from Euriso-Top. The progress of the reactions was checked by thin layer chromatography (TLC) on Merck silica gel 60 glass plates. Detection was carried out by spraying the chromatograms with 10% ethanolic sulfuric acid and heating them to 100 °C. Flash column chromatography was performed with silica gel (40–100 lm, Merck): all chemicals were of reagent grade and used without further purification.

4.2. General procedures for RL synthesis

Among the 18 synthesized RLs, nine belonging to ether (butyl α/β-L-rhamnopyranoside (Rh-Eth-C4), hexyl α/β-L-rhamnopyranoside (Rh-Eth-C6), octyl α/β-L-rhamnopyranoside (Rh-Eth-C8), decyl α/β-L-rhamnopyranoside (Rh-Eth-C10), dodecyl α/β-L-rhamnopyranoside (Rh-Eth-C12), tetradecyl α/β-L-rhamnopyranoside (Rh-Eth-C14), hexadecyl α/β-L-rhamnopyranoside (Rh-Eth-C16)), ester (dodecanoyl α/β-L-rhamnopyranoside (Rh-Est-C12)), and mono-rhamnosyl (alkenyl)succinate (dodecenylsuccinate α/β-L-rhamnopyranoside (Rh-Suc-C12)) families, have already been described in Robineau et al. [25]. The nine new synthesized RLs in the current study were octadecyl α/β-L-rhamnopyranoside (Rh-Eth-C18) (ether family), octanoyl α/β-L-rhamnopyranoside (Rh-Est-C8), decanoyl α/β-L-rhamnopyranoside (Rh-Est-C10) (ester family), octenylsuccinate α/β-L-rhamnopyranoside (Rh-Suc-C8), iso-dodecenylsuccinate α/β-L-rhamnopyranoside (Rh-Suc-C12b) (mono-rhamnosyl (alkenyl)succinate family), 3-octenyloctylsuccinate α/β-L-rhamnopyranoside (Rh-Suc-C8-C8), 3-octenyldodecylsuccinate α/β-L-rhamnopyranoside (Rh-Suc-C8-C12), 3-dodecenyloctylsuccinate α/β-L-rhamnopyranoside (Rh-Suc-C12-C8), and 3-dodecenyldodecylsuccinate α/β-L-rhamnopyranoside (Rh-Suc-C12-C12) (mono-rhamnosyl (alkenyl)alkylsuccinate family).

The general procedures for rhamnose ether, ester and mono-rhamnosyl (alkenyl)succinate molecule syntesesis have been reported in Robineau et al. [25], while the general procedure for mono-rhamnosyl (alkenyl)alkylsuccinate derivative synthesis will be described as follow. First, alkenylsuccinic anhydride (12.2 mmol, 1 eq.) was added dropwise to a stirred solution of L-rhamnose (2.0 g, 12.2 mmol, 1 eq.) and DMAP (1.8 g, 14.6 mmol, 1.2 eq.) in DMF (20 mL). After 16 h at 60°C, DMAP (1.5 g, 12.2 mmol, 1 eq.) and alkyl bromide (14.6 mmol, 1.2 eq.) was added slowly to the reaction mixture and stirred overnight. The reaction was cooled and H_2SO_4 10% was added to reached pH 5. Ethyl acetate was added and the organic phase was washed with a saturated NaCl solution and HCl 1 M. The organic layer was dried with $MgSO_4$ and concentrated under reduced pressure. The rhamnose alkylsuccinate was isolated after purification by column chromatography (EtOAc/Petroleum spirit 5:5).

4.3. RL chemical analysis

The chemical analyses of the previously reported RLs Rh-Eth-C4, Rh-Eth-C6, Rh-Eth-C8, Rh-Eth-C10, Rh-Eth-C12, Rh-Eth-C14, Rh-Eth-C16, Rh-Est-C12, Rh-Suc-C12 were already performed [25]. For the nine new synthesized RLs in the present study, their chemical analyses are described below.

4.3.1. Octadecyl α/β-L-rhamnopyranoside (Rh-Eth-C18)

White solid (β/α ratio 2:8, 30%); Rf 0.70 (AcOEt/MeOH 9/1);^{1}H NMR ($CDCl_3$): 4.73 (m, 2H), 3.91 (m, 2H), 3.77-3.73 (m, 2H), 3.66-3.59 (m, 4H), 3.46-3.34 (m, 4H), 1.57-1.53 (m, 4H), 1.31-1.25 (m, 66H), 0.87 (m, 6H, CH_3) ^{13}C NMR ($CDCl_3$): δ 100.3, 99.6, 73.4, 72.4, 71.4, 70.9, 69.7, 68.2, 68.1, 31.0-21.9 (CH_2 alkyl chain), 17.9, 17.3, 14.4.

4.3.2. Octanoyl α/β-L-rhamnopyranoside (Rh-Est-C8)

Yellowish oil (β/α ratio 3:7, 61%); Rf 0.41 (AcOEt/MeOH 9/1); ^{1}H NMR ($CDCl_3$): 5.06-4.79 (m, 2H), 4.06-3.87 (m, 4H), 3.63-3.41 (m, 4H), 2.41-2.35 (m, 4H), 1.63-1.59 (m, 4H), 1.31-1.23 (m, 22H), 0.92 (m, 6H, CH_3) ^{13}C NMR ($CDCl_3$): δ 174.2, 172.0, 93.2, 92.9, 75.8, 74.2, 73.3, 72.8, 71.1, 69.8, 68.6, 68.1, 34.5, 34,1, 32.0-21.6 (CH_2 alkyl chain), 17.5, 17.1, 13.3.

4.3.3. Decanoyl α/β-L-rhamnopyranoside (Rh-Est-C10)

Yellowish oil (β/α ratio 3:7, 58%); Rf 0.44 (AcOEt/MeOH 9/1); ^{1}H NMR ($CDCl_3$): 5.07-4.78(m, 2H), 4.03-3.89 (m, 4H), 3.65-3.60 (m, 2H), 3.47-3.39 (m, 2H), 2.39-2.34 (m, 4H), 1.63-1.58 (m, 4H), 1.31-1.23 (m, 30H), 0.94 (m, 6H, CH_3) ^{13}C NMR ($CDCl_3$): δ 174.5, 172.1, 93.7, 93.0, 75.9, 74.1, 73.6, 72.6, 71.2, 69.8, 68.6, 68.0, 34.4, 34,3, 32.0-21.6 (CH_2 alkyl chain), 17.7, 17.5, 13.4.

4.3.4. Octenylsuccinate α/β-L-rhamnopyranoside (Rh-Suc-C8)

Colorless oil (β/α ratio 2:8, 59%); Rf 0.19 (AcOEt/MeOH 9/1); ^{1}H NMR ($CDCl_3$): 5.47 (m, 2H), 5.29 (m, 2H), 5.20-5.14 (m, 2H), 4.07-4.03 (m, 2H), 3.69-3.64 (m, 4H), 3.44-3.41 (m, 4H), 2.89-2.84 (m, 2H), 2.71-2.62 (m, 4H), 2.23-1.98 (m, 8H), 1.32-1.08 (m, 18H), 0.91 (m, 6H, CH_3) ^{13}C NMR ($CDCl_3$): δ 178.2, 175.6, 174.8, 134.8, 125.0, 94.4, 91.0, 74.2, 73,8, 73.5, 71.0, 70.7, 44.3, 31.7-21.9 (CH_2 alkyl chain), 16.8, 16.2, 13.8.

4.3.5. Iso-Dodecenylsuccinate α/β-L-rhamnopyranoside (Rh-Suc-C12b)

Yellowish solid (β/α ratio 2:8, 55%); Rf 0.23 (AcOEt/MeOH 9/1); ^{1}H NMR ($CDCl_3$): 5.49 (m, 2H), 5.33 (m, 2H), 5.18-5.11 (m, 2H), 4.09-4.02 (m, 2H), 3.71-3.65 (m, 4H), 3.45-3.41 (m, 4H), 2.90-2.84 (m, 2H), 2.71-2.62 (m, 4H), 2.23-1.98 (m, 8H), 1.65-1.61 (m, 2H), 1.32-1.08 (m, 26H), 0.91 (m, 6H, CH_3) ^{13}C NMR ($CDCl_3$): δ 178.2, 175.6, 174.9, 134.6, 125.2, 94.4, 91.1, 74.1, 73,8, 73.4, 71.0, 70.7, 44.4, 31.8-21.8 (alkyl chain), 17.0, 16.9, 16.7, 16.4, 13.7.

4.3.6. 3-Octenyloctylsuccinate α/β-L-rhamnopyranoside (Rh-Suc-C8-C8)

Yellowish oil (β/α ratio 2:8, 39%); Rf 0.46 (AcOEt/MeOH 9/1); ^{1}H NMR ($CDCl_3$): 5.46 (m, 2H), 5.28 (m, 2H), 5.21-5.12 (m, 2H), 4.09-4.02 (m, 2H), 3.71-3.62 (m, 4H), 3.45-3.40 (m, 4H), 2.90-2.83 (m, 2H), 2.73-2.63 (m, 4H), 2.40-1.98 (m, 12H), 1.61-1.58 (m, 4H), 1.32-1.08 (m, 40H), 0.92 (m, 6H, CH_3), 0.89 (m, 6H, CH_3) ^{13}C NMR ($CDCl_3$): δ 178.2, 175.6, 174.8, 134.8, 125.0, 94.4, 91.0, 74.2, 73,8, 73.5, 71.0, 70.7, 44.3, 34.4, 34,2, 31.7-21.4 (CH_2 alkyl chain), 17.4, 17.2, 16.8, 16.2, 13.8, 13.3.

4.3.7. 3-Octenyldodecylsuccinate α/β-L-rhamnopyranoside (Rh-Suc-C8-C12)

Yellowish oil (β/α ratio 2:8, 38%); Rf 0.45 (AcOEt/MeOH 9/1); ^{1}H NMR ($CDCl_3$): 5.46 (m, 2H), 5.28 (m, 2H), 5.21-5.12 (m, 2H), 4.09-4.02 (m, 2H), 3.71-3.62 (m, 4H), 3.45-3.40 (m, 4H), 2.90-2.83 (m, 2H), 2.72-2.63 (m, 4H), 2.41-1.97 (m, 12H), 1.65-1.57 (m, 4H), 1.32-1.08 (m, 56H), 0.92 (m, 12H, CH_3), ^{13}C NMR ($CDCl_3$): δ 178.2, 175.6, 174.8, 134.8, 125.0, 94.4, 91.0, 74.2, 73,8, 73.5, 71.0, 70.7, 44.3, 34.4, 34,3, 32.0-21.6 (CH_2 alkyl chain), 17.6, 17.3, 16.8, 16.2, 13.8, 13.3.

4.3.8. 3-Dodecenyloctylsuccinate α/β-L-rhamnopyranoside (Rh-Suc-C12-C8)

Yellowish oil (β/α ratio 2:8, 37%); Rf 0.47 (AcOEt/MeOH 9/1); ^{1}H NMR ($CDCl_3$): 5.50 (m, 2H), 5.33 (m, 2H), 5.17-5.10 (m, 2H), 4.09-4.02 (m, 2H), 3.71-3.64 (m, 4H), 3.45-3.41 (m, 4H), 2.92-2.85 (m, 2H), 2.69-2.60 (m, 4H), 2.41-2.34 (m, 4H), 2.23-1.99 (m, 8H), 1.63-1.59 (m, 4H), 1.32-1.06 (m, 56H), 0.92 (m, 12H, CH_3) ^{13}C NMR ($CDCl_3$): δ 178.0, 175.4, 174.6, 134.6, 125.0, 94.4, 91.1, 74.2, 73,9, 73.4, 71.3, 70.9, 44.3, 32.1-21.6 (CH_2 alkyl chain), 17.7, 17.3, 17.0, 16.6, 13.8, 13.4.

4.3.9. 3-Dodecenyldodecylsuccinate α/β-L-rhamnopyranoside (Rh-Suc-C12-C12)

Yellowish oil (β/α ratio 2:8, 34%); Rf 0.43 (AcOEt/MeOH 9/1); ^{1}H NMR ($CDCl_3$): 5.51 (m, 2H), 5.34 (m, 2H), 5.18-5.09 (m, 2H), 4.09-4.03 (m, 2H), 3.70-3.58 (m, 6H), 3.49-3.41 (m, 6H), 2.91-2.84 (m, 2H), 2.71-2.63 (m, 4H), 2.40-2.32 (m, 4H), 2.25-2.00 (m, 8H), 1.66-1.59 (m, 4H), 1.33-1.08 (m, 72H), 0.92 (m, 12H, CH_3) ^{13}C NMR ($CDCl_3$): δ 178.1, 175.5, 174.8, 134.7, 125.1, 94.5, 91.0, 74.2, 73,9, 73.4, 71.1, 70.8, 44.3, 34.5, 34.2, 31.9-21.5 (CH_2 alkyl chain), 17.6, 17.3, 16.9, 16.4, 13.9, 13.7.

4.4. Plant treatment and inoculation

All in *planta* assays were carried out using the pathogenic *Z. tritici* strain T02596 isolated in 2014 from Northern France, and the susceptible wheat cultivar Alixan (Limagrain, France) showing compatible interaction with the strain T02596 [36]. The experiments were performed in the greenhouse at 21 ± 2°C with a 16/8 h day/night cycle. Wheat seeds were pre-germinated in square Petri dishes on moist filter paper, as described by Siah et al. [37]. Germinated grains were placed into 3-L pots filled with universal loam (Gamm Vert, France) and put into the greenhouse. For each condition, three pots containing 12 plants each, meaning 36 plants in total, were used as replicates. Three weeks after sowing, when third-leaves are fully expanded, 30 mL of a solution of 1.5 mM of each RL, as well as lauric acid and dodecanol, were hand-sprayed on the plants of each pot. These molecules were first dissolved in dimethyl sulfoxide (DMSO), with final concentration of DMSO at 0.2%, before being supplemented with 0.05% polyoxyethylene-sorbitan monolaurate (Tween 20, Sigma-Aldrich, USA) as a wetting agent. Control plants were treated with a solution of 0.2% DMSO, supplemented with 0.05% Tween 20. Due to solubilization difficulties at 1.5 mM, treatments with Rh-Eth-C18 and Rh-Suc-C12-C12 were not performed. Two days after treatment, 30 mL of fungal spore suspension (10^6 spores.mL^{-1}), also supplemented with 0.05% of Tween 20, were hand-sprayed on the plants of each pot. *Zymoseptoria tritici* spores were harvested after being cultivated on potato dextrose agar medium (PDA) plates for one week in dark conditions, according to Siah et al. [37]. Immediately after inoculation, each pot was covered with a clear polyethylene bag for 3 days in order to ensure a high humidity level allowing a good plant infection. Three weeks after inoculation, the disease severity was measured on the third leaf by assessing the area covered by lesions (chlorosis or necrosis) bearing or not pycnidia. This experiment was repeated twice. In the case of Rh-Est-C12, the most efficient RL in our conditions, the protection efficacy of this compound was assessed at different concentrations, ranging from 50 μM to 3200 μM (50, 100, 200, 400, 800, 1600, and 3200 μM). This experiment underwent the same conditions as described above, except for DMSO that was used at 0.1% final concentration in the treatment solutions.

4.5. Plant defence-related enzyme assays

Evaluation of the indirect effect of RLs, as well as lauric acid and dodecanol, was performed by assessing the activity of two antioxidant key-enzymes involved in plant defense mechanisms: catalase (CAT; EC: 1.11.1.6) and peroxidase (POX; EC: 1.11.1.7). Wheat plants grown under greenhouse conditions treated or not with 1.5 mM of RLs, as described above, were used to examine the elicitation activity of the compounds. Plant third-leaves were harvested two days after treatment and 100 mg were immediately frozen in liquid nitrogen and stored at -80 °C for further analyses. Three leaves, sampled randomly from three different pots (one leaf per pot), were used as repetitions for each condition. Leaf segments were later ground with a mortar and pestle in liquid nitrogen. The powder obtained was resuspended in 1 mL of 50 mM ice-cold potassium phosphate buffer, pH 7.0, and centrifuged at 12000 g for 10 min at 4°C. The supernatant was used to evaluate the activity of CAT or POX. POX activity was assessed based on the procedure of Mitchell et al. [38] and Shindler et al. [39]. The reactive medium consisted of 0.5 mM 2,2'-azino-bis(3-ethylbenzothiazoline-6-sulfonic acid (ABTS) and 0.25 mM H_2O_2 in 25 mM sodium acetate buffer, pH 4.4. This assay was performed in flat-bottomed polystyrene 96-well microplates (Corning Costar®, Corning, USA). To initiate the reaction, 10 µL of supernatant was added to 190 µL of the reactive mix in plate wells. The increased absorbance at 412 nm, produced by the formation of the radical cation, was monitored kinetically for 5 minutes at 25 °C. POX activity was expressed as change in absorbance at 412 $nm.min^{-1}.g^{-1}$ protein. CAT activity was determined according to Beers and Sizer [40] and García-Limones et al. [41] with slight modifications. To initiate the reaction, 10 µL of wheat leaf supernatant diluted in sterile water 1:4 (v/v) were added to the wells containing 190 µL of reactive medium consisting of 50 mM H_2O_2 in 50 mM potassium phosphate buffer, pH 7.0. 96-well microplates (Greiner UV-Star®, Greiner Bio-One GmbH, Austria), allowing measurements up to 200 nm, were used. The decreased absorbance at 240 nm resulting from the degradation of H_2O_2 was measured kinetically during 5 minutes at 25 °C. CAT activity was expressed as change in absorbance at 240 $nm.min^{-1}.g^{-1}$ protein. Protein content of wheat leaf supernatants was assessed using the method of Bradford [42] with bovin serum albumin (BSA) as a standard.

4.6. In planta *antifungal effect of Rh-Est-C12*

Wheat plants grown under greenhouse conditions, sprayed or not with different concentrations of Rh-Est-C12 (0, 50, 400, and 3200 µM) and inoculated with spore suspension of the T02596 *Z. tritici* strain, were used to assess *in planta* the activity of this molecule on spore germination and hyphal growth of the phytopathogen. The three concentrations 50, 400, and 3200 µM were chosen because they correspond to the lowest, median, and highest concentrations tested *in planta* for this RL, respectively. The chitin staining dye Fluorescent Brightener 28 (Calcofluor, Sigma-Aldrich, USA) was used to stain the fungus on the leaf surfaces, according to Siah et al. [37]. Three days after inoculation, wheat third-leaf segments (2 cm) were harvested and immersed for five minutes in a solution of 0.1% (w/v) Calcofluor and 0.1 M Tris-HCl buffer, pH 8.5. Leaf segments were then washed twice in sterile osmosed water for two minutes. After being dried in dark conditions at room temperature, they were placed on a glass slide, covered with a cover slip and observed microscopically (Nikon, Eclipse 80i) under UV-light. For each leaf segment, the percentage of different spore classes was calculated on 100 observed spores (class 1: non germinated spore; class 2: geminated spore with a small germ tube; class 3 : geminated spore with a developed germ tube; class 4 : geminated spore with a strongly developed germ tube). Six third-leaf segments from three different pots (two segments per pot) were used as replicates for each condition. Pictures were taken with a digital camera (DXM1200C) using image capture software (NIS-Elements BR).

4.7. In vitro *direct antifungal effect of rhamnolipids*

In vitro antifungal activity of all tested RLs, as well as dodecanol and lauric acid, was assessed by measuring the growth of *Z. tritici* colonies on solid medium in sterile 12-well plates (Cellstar standard®, Greiner Bio-One GmbH, Austria). Plate wells were filled with 3 mL of PDA, autoclaved

beforehand, mixed with our molecules of interest at approximatively 40°C. The compounds were first dissolved in DMSO (0.1% final concentration in the wells). After PDA cooling down, 5 µL of the *Z. tritici* strain T02596 spore suspension (5.10^5 spores.mL^{-1}) were added to each well, according to Siah et al. [37]. Ten different concentrations (39.5, 59.3, 88.9, 133.3, 200, 300, 450, 666.7, 1000, and 1500 mM) were used for each molecule. Moreover, control mediums supplemented with 0.1% of DMSO, with or without fungal inoculation, were used. After inoculation, plates were incubated for 10 days in growth chamber in dark conditions at 20 ± 1°C, after which two perpendicular diameters of fungal colonies were measured visually. This experiment was repeated three times and three wells were used as replicates for each condition.

4.8. Fungal strain effect of Rh-Est-C12 antifungal activity

To assess the fungal strain effect of the most active RL Rh-Est-C12 regarding its antifungal direct activity, a total of 21 single-conidial *Z. tritici* strains (Zt.1 to Zt.21) isolated in 2016 from Arras location in northern France, and the reference strain IPO323 isolated in the Netherland in 1981 [41], were assessed for their variability in sensitivity to Rh-Est-C12. These *Z. tritici* strains were chosen because they displayed, in preliminary assays, different resistance levels towards five fungicide molecules belonging to DMI class (tebuconazole, metconazole, epoxiconazole, prothioconazole, prochloraz). The sensitivity of the strains towards these fungicides was evaluated in 96-well microplates, as described in Siah et al. [37], at the concentrations 75, 25, 8.33, 2.78, 0.93, 0.31, 0.10, and 0.03 mg.L^{-1}. The antifungal bioassay for Rh-Est-C12 against the 22 *Z. tritici* strains was performed at the concentrations 450, 300, 200, 133.3, 88.9, 59.3, and 39.5 µM.

4.9. Statistical analyses

Data obtained for *in planta* protection efficacy, enzyme activity, and *in planta* spore germination assays were subjected to analysis of variance (ANOVA) followed by Tukey's test at $P \leq 0.05$, using the XLSTAT software (Addinsoft, Paris, France). For *in vitro* antifungal activity assays, the minimal inhibitory concentration (MIC), defined as the minimal tested concentration totally inhibiting fungal growth, was scored for each molecule. In addition, half-maximal inhibitory concentration (IC_{50}) was calculated using GraphPad Prism software version 8 (GraphPad Software Inc., USA) for each molecule and tested fungal strain. In the strain effect assay, resistance factors were calculated by dividing the IC_{50} of each strain by the IC_{50} of the reference strain IPO323 for each tested compound. Correlations between protection efficacies, *in vitro* direct activity (IC_{50} and MIC), and in *planta* indirect effect (CAT and POX activities) within all the tested molecules, was carried out with principal component analysis (PCA) based on the Pearson correlation test, using XLSTAT software (Addinsoft, Paris, France).

Supplementary Materials: The Supplementary Materials are available online. Supplementary Table 1: Half-maximal inhibitory concentration (IC_{50}) values obtained for 22 *Zymoseptoria tritici* strains differing in their resistance level to DMI fungicides, towards five DMI molecules and the rhamnolipid molecule Rh-Est-C12. Supplementary Table 2: Resistance factors obtained for 22 *Zymoseptoria tritici* strains differing in their resistance level to DMI fungicides, towards five DMI molecules and the rhamnolipid molecule Rh-Est-C12, calculated from the IC_{50} values presented in the Supplementary Table 1. Resistance factors correspond to the ratio between the IC_{50} value of a given strain and the IC_{50} value of the sensitive reference strain IPO323.

Author Contributions: For research articles with several authors, a short paragraph specifying their individual contributions must be provided. Conceptualization, M.M-R., B.R., P.H., P.M., M.H., P.R. and A.S.; methodology, R.P. (Rémi Platel), L.C., S.LG., V.L., N.J. and A.S.; formal analysis, R.P. (Rémi Platel), R.P. (Rutger Pipeleers), L.C., S.LG., P.M., M.H., P.R. and A.S.; writing—original draft preparation, R.P. (Rémi Platel), P.T. and A.S.; writing—review and editing, R.P. (Rémi Platel), R.P. (Rutger Pipeleers), L.C., M.M-R., B.R., P.H., P.M., M.H., P.R. and A.S.; supervision, M.M-R., B.R., P.H., P.M. P.R. and A.S.; project administration, A.S.; funding acquisition, P.H. and A.S. All authors have read and agreed to the published version of the manuscript.

Funding: This research was conducted in the framework of the project Bioscreen (Smartbiocontrol portfolio), funded by the European program Interreg V, and the CPER Alibiotech, funded by the European Union, the French State, and the French Council Hauts-de-France.

Conflicts of Interest: The authors declare no conflict of interest. The funders had no role in the design of the study; in the collection, analyses, or interpretation of data; in the writing of the manuscript, or in the decision to publish the results.

References

FAO Cereal Supply and Demand Brief | World Food Situation | Food and Agriculture Organization of the United Nations [WWW Document], n.d. URL http://www.fao.org/worldfoodsituation/csdb/en/ (accessed 1.18.19).

Fones, H.; Gurr, S. The impact of Septoria tritici Blotch disease on wheat: An EU perspective. *Fungal Genetics and Biology* **2015**, *79*, 3–7, doi:10.1016/j.fgb.2015.04.004.

Torriani, S.F.F.; Melichar, J.P.E.; Mills, C.; Pain, N.; Sierotzki, H.; Courbot, M. *Zymoseptoria tritici*: A major threat to wheat production, integrated approaches to control. *Fungal Genetics and Biology* **2015**, *79*, 8–12, doi:10.1016/j.fgb.2015.04.010.

Cools, H.J.; Hawkins, N.J.; Fraaije, B.A. Constraints on the evolution of azole resistance in plant pathogenic fungi. *Plant Pathology* **2013**, *62*, 36–42, doi:10.1111/ppa.12128.

McDonald, M.C.; Renkin, M.; Spackman, M.; Orchard, B.; Croll, D.; Solomon, P.S.; Milgate, A. Rapid Parallel Evolution of Azole Fungicide Resistance in Australian Populations of the Wheat Pathogen *Zymoseptoria tritici*. *Appl. Environ. Microbiol.* **2019**, *85*, doi:10.1128/AEM.01908-18.

Steinhauer, D.; Salat, M.; Frey, R.; Mosbach, A.; Luksch, T.; Balmer, D.; Hansen, R.; Widdison, S.; Logan, G.; Dietrich, R.A.; et al. A dispensable paralog of succinate dehydrogenase subunit C mediates standing resistance towards a subclass of SDHI fungicides in *Zymoseptoria tritici*. *PLoS Pathog* **2019**, *15*, doi:10.1371/journal.ppat.1007780.

D'aes, J.; De Maeyer, K.; Pauwelyn, E.; Höfte, M. Biosurfactants in plant-*Pseudomonas* interactions and their importance to biocontrol. *Environ Microbiol Rep* **2010**, *2*, 359–372, doi:10.1111/j.1758-2229.2009.00104.x.

Ongena, M.; Jacques, P. *Bacillus* lipopeptides: versatile weapons for plant disease biocontrol. *Trends Microbiol.* **2008**, *16*, 115–125, doi:10.1016/j.tim.2007.12.009.

Sachdev, D.P.; Cameotra, S.S. Biosurfactants in agriculture. *Appl Microbiol Biotechnol* **2013**, *97*, 1005–1016, doi:10.1007/s00253-012-4641-8.

Lourith, N.; Kanlayavattanakul, M. Natural surfactants used in cosmetics: glycolipids. *Int J Cosmet Sci* **2009**, *31*, 255–261, doi:10.1111/j.1468-2494.2009.00493.x.

Chen, J.; Wu, Q.; Hua, Y.; Chen, J.; Zhang, H.; Wang, H. Potential applications of biosurfactant rhamnolipids in agriculture and biomedicine. *Appl. Microbiol. Biotechnol.* **2017**, *101*, 8309–8319, doi:10.1007/s00253-017-8554-4.

Shao, B.; Liu, Z.; Zhong, H.; Zeng, G.; Liu, G.; Yu, M.; Liu, Y.; Yang, X.; Li, Z.; Fang, Z.; et al. Effects of rhamnolipids on microorganism characteristics and applications in composting: A review. *Microbiol. Res.* **2017**, *200*, 33–44, doi:10.1016/j.micres.2017.04.005.

Vatsa, P.; Sanchez, L.; Clement, C.; Baillieul, F.; Dorey, S. Rhamnolipid Biosurfactants as New Players in Animal and Plant Defense against Microbes. *Int J Mol Sci* **2010**, *11*, 5095–5108, doi:10.3390/ijms11125095.

Stanghellini, M.E.; Miller, R.M. BIOSURFACTANTS: Their Identity and Potential Efficacy in the Biological Control of Zoosporic Plant Pathogens. *Plant Disease* **1997**, *81*, 4–12, doi:10.1094/PDIS.1997.81.1.4.

Haba, E.; Pinazo, A.; Jauregui, O.; Espuny, M.J.; Infante, M.R.; Manresa, A. Physicochemical characterization and antimicrobial properties of rhamnolipids produced by *Pseudomonas aeruginosa* 47T2 NCBIM 40044. *Biotechnology and Bioengineering* **2003**, *81*, 316–322, doi:10.1002/bit.10474.

Yoo, D.S. (Inha U.; Lee, B.S. (Inha U.; Kim, E.K. (Inha U. Characteristics of Microbial Biosurfactant as an Antifungal Agent Against Plant Pathogenic Fungus. *Journal of Microbiology and Biotechnology* **2005**.

Varnier, A.-L.; Sanchez, L.; Vatsa, P.; Boudesocque, L.; Garcia-Brugger, A.; Rabenoelina, F.; Sorokin, A.; Renault, J.-H.; Kauffmann, S.; Pugin, A.; et al. Bacterial rhamnolipids are novel MAMPs conferring resistance to *Botrytis cinerea* in grapevine. *Plant, Cell & Environment* **2009**, *32*, 178–193, doi:10.1111/j.1365-3040.2008.01911.x.

Monnier, N.; Furlan, A.; Botcazon, C.; Dahi, A.; Mongelard, G.; Cordelier, S.; Clément, C.; Dorey, S.; Sarazin, C.; Rippa, S. Rhamnolipids From *Pseudomonas aeruginosa* Are Elicitors Triggering *Brassica napus* Protection Against *Botrytis cinerea* Without Physiological Disorders. *Front Plant Sci* **2018**, *9*, doi:10.3389/fpls.2018.01170.

Sanchez, L.; Courteaux, B.; Hubert, J.; Kauffmann, S.; Renault, J.-H.; Clément, C.; Baillieul, F.; Dorey, S. Rhamnolipids elicit defense responses and induce disease resistance against biotrophic, hemibiotrophic, and necrotrophic pathogens that require different signaling pathways in *Arabidopsis* and highlight a central role for salicylic acid. *Plant Physiol.* **2012**, *160*, 1630–1641, doi:10.1104/pp.112.201913.

Johann, S.; Seiler, T.-B.; Tiso, T.; Bluhm, K.; Blank, L.M.; Hollert, H. Mechanism-specific and whole-organism ecotoxicity of mono-rhamnolipids. *Sci. Total Environ.* **2016**, *548–549*, 155–163, doi:10.1016/j.scitotenv.2016.01.066.

Hogan, D.E.; Tian, F.; Malm, S.W.; Olivares, C.; Palos Pacheco, R.; Simonich, M.T.; Hunjan, A.S.; Tanguay, R.L.; Klimecki, W.T.; Polt, R.; et al. Biodegradability and toxicity of monorhamnolipid biosurfactant diastereomers. *Journal of Hazardous Materials* **2019**, *364*, 600–607, doi:10.1016/j.jhazmat.2018.10.050.

Funston, S.J.; Tsaousi, K.; Rudden, M.; Smyth, T.J.; Stevenson, P.S.; Marchant, R.; Banat, I.M. Characterising rhamnolipid production in *Burkholderia thailandensis* E264, a non-pathogenic producer. *Appl Microbiol Biotechnol* **2016**, *100*, 7945–7956, doi:10.1007/s00253-016-7564-y.

Bahia, F.M.; de Almeida, G.C.; de Andrade, L.P.; Campos, C.G.; Queiroz, L.R.; da Silva, R.L.V.; Abdelnur, P.V.; Corrêa, J.R.; Bettiga, M.; Parachin, N.S. Rhamnolipids production from sucrose by engineered *Saccharomyces cerevisiae*. *Scientific Reports* **2018**, *8*, 2905, doi:10.1038/s41598-018-21230-2.

Luzuriaga-Loaiza, W.P.; Schellenberger, R.; De Gaetano, Y.; Obounou Akong, F.; Villaume, S.; Crouzet, J.; Haudrechy, A.; Baillieul, F.; Clément, C.; Lins, L.; et al. Synthetic Rhamnolipid Bolaforms trigger an innate immune response in *Arabidopsis thaliana*. *Sci Rep* **2018**, *8*, 8534, doi:10.1038/s41598-018-26838-y.

Robineau, M.; Le Guenic, S.; Sanchez, L.; Chaveriat, L.; Lequart, V.; Joly, N.; Calonne, M.; Jacquard, C.; Declerck, S.; Martin, P.; et al. Synthetic Mono-Rhamnolipids Display Direct Antifungal Effects and Trigger an Innate Immune Response in Tomato against *Botrytis Cinerea*. *Molecules* **2020**, *25*, doi:10.3390/molecules25143108

Halliwell, B. Reactive Species and Antioxidants. Redox Biology Is a Fundamental Theme of Aerobic Life. *Plant Physiol* **2006**, *141*, 312–322, doi:10.1104/pp.106.077073.

Sun, Y.; Li, P.; Deng, M.; Shen, D.; Dai, G.; Yao, N.; Lu, Y. The *Ralstonia solanacearum* effector RipAK suppresses plant hypersensitive response by inhibiting the activity of host catalases. *Cellular Microbiology* **2017**, *19*, e12736, doi:10.1111/cmi.12736.

Shetty, N.P.; Mehrabi, R.; Lütken, H.; Haldrup, A.; Kema, G.H.J.; Collinge, D.B.; Jørgensen, H.J.L. Role of hydrogen peroxide during the interaction between the hemibiotrophic fungal pathogen *Septoria tritici* and wheat. *New Phytol.* **2007**, *174*, 637–647, doi:10.1111/j.1469-8137.2007.02026.x.

Shetty, N.P.; Kristensen, B.K.; Newman, M.-A.; Møller, K.; Gregersen, P.L.; Jørgensen, H.J.L. Association of hydrogen peroxide with restriction of *Septoria tritici* in resistant wheat. *Physiological and Molecular Plant Pathology* **2003**, *62*, 333–346, doi:10.1016/S0885-5765(03)00079-1.

Lagrimini, L.M. Wound-induced deposition of polyphenols in transgenic plants overexpressing peroxidase. *Plant Physiol.* **1991**, *96*, 577–583, doi:10.1104/pp.96.2.577.

Monnier, N.; Furlan, A.L.; Buchoux, S.; Deleu, M.; Dauchez, M.; Rippa, S.; Sarazin, C. Exploring the Dual Interaction of Natural Rhamnolipids with Plant and Fungal Biomimetic Plasma Membranes through Biophysical Studies. *Int J Mol Sci* **2019**, *20*, doi:10.3390/ijms20051009.

Henry, G.; Deleu, M.; Jourdan, E.; Thonart, P.; Ongena, M. The bacterial lipopeptide surfactin targets the lipid fraction of the plant plasma membrane to trigger immune-related defence responses. *Cell. Microbiol.* **2011**, *13*, 1824–1837, doi:10.1111/j.1462-5822.2011.01664.x.

Siah, A.; Bomble, M.; Tisserant, B.; Cadalen, T.; Holvoet, M.; Hilbert, J.-L.; Halama, P.; Reignault, P. Genetic Structure of *Zymoseptoria tritici* in Northern France at Region, Field, Plant, and Leaf Layer Scales. *Phytopathology* **2018**, *108*, 1114–1123, doi:10.1094/PHYTO-09-17-0322-R.

Huf, A.; Rehfus, A.; Lorenz, K.H.; Bryson, R.; Voegele, R.T.; Stammler, G. Proposal for a new nomenclature for CYP51 haplotypes in *Zymoseptoria tritici* and analysis of their distribution in Europe. *Plant Pathology* **2018**, *67*, 1706–1712, doi:10.1111/ppa.12891.

Price, C.L.; Parker, J.E.; Warrilow, A.G.; Kelly, D.E.; Kelly, S.L. Azole fungicides – understanding resistance mechanisms in agricultural fungal pathogens. *Pest Management Science* **2015**, *71*, 1054–1058, doi:10.1002/ps.4029.

Mejri, S.; Siah, A.; Coutte, F.; Magnin-Robert, M.; Randoux, B.; Tisserant, B.; Krier, F.; Jacques, P.; Reignault, P.; Halama, P. Biocontrol of the wheat pathogen *Zymoseptoria tritici* using cyclic lipopeptides from *Bacillus subtilis*. *Environ Sci Pollut Res Int* **2018**, *25*, 29822–29833, doi:10.1007/s11356-017-9241-9.

Siah, A.; Deweer, C.; Duyme, F.; Sanssené, J.; Durand, R.; Halama, P.; Reignault, P. Correlation of *in planta* endo-beta-1,4-xylanase activity with the necrotrophic phase of the hemibiotrophic fungus *Mycosphaerella graminicola*. *Plant Pathology* **2010**, *59*, 661–670, doi:10.1111/j.1365-3059.2010.02303.x.

Mitchell, H.J.; Hall, J.L.; Barber, M.S. Elicitor-Induced Cinnamyl Alcohol Dehydrogenase Activity in Lignifying Wheat (*Triticum aestivum L.*) Leaves. *Plant Physiol.* **1994**, *104*, 551–556, doi:10.1104/pp.104.2.551.

Shindler, J.S.; Childs, R.E.; Bardsley, W.G. Peroxidase from human cervical mucus. The isolation and characterisation. *Eur. J. Biochem.* **1976**, *65*, 325–331, doi:10.1111/j.1432-1033.1976.tb10345.x.

Beers, R.F.; Sizer, I.W. A spectrophotometric method for measuring the breakdown of hydrogen peroxide by catalase. *J. Biol. Chem.* **1952**, *195*, 133–140.

García-Limones, C.; Hervás, A.; Navas-Cortés, J.A.; Jiménez-Díaz, R.M.; Tena, M. Induction of an antioxidant enzyme system and other oxidative stress markers associated with compatible and incompatible interactions between chickpea (*Cicer arietinum L.*) and *Fusarium oxysporum* f. sp.*ciceris*. *Physiological and Molecular Plant Pathology* **2002**, *61*, 325–337, doi:10.1006/pmpp.2003.0445.

Bradford, M.M. A rapid and sensitive method for the quantitation of microgram quantities of protein utilizing the principle of protein-dye binding. *Analytical Biochemistry* **1976**, *72*, 248–254, doi:10.1016/0003-2697(76)90527-3.

Kema, G.H.; Verstappen, E.C.; Waalwijk, C. Avirulence in the wheat septoria tritici leaf blotch fungus *Mycosphaerella graminicola* is controlled by a single locus. *Mol. Plant Microbe Interact.* **2000**, *13*, 1375–1379, doi:10.1094/MPMI.2000.13.12.1375.

Sample Availability: Samples of the compounds are not available from the authors.

Supplementary Table 1. Half-maximal inhibitory concentration (IC_{50}) values obtained for 22 *Zymoseptoria tritici* strains differing in their resistance level to DMI fungicides, towards five DMI molecules and the rhamnolipid molecule Rh-Est-C12.

***Zymoseptoria tritici* isolates**		**IC_{50} (mg.L^{-1})**					
		Tebuconazole	Metconazole	Epoxiconazole	Prothioconazole	Prochloraz	Rh-Est-C12
Control strain	IPO323	0.07	0.04	0.03	0.001	0.02	**54.3**
No MDR or *Cyp51* gene overexpressing strains	Zt.1	0.26	0.14	1.12	0.10	0.12	**49.9**
	Zt.2	0.54	0.13	1.39	0.10	0.17	**65.4**
	Zt.3	0.49	0.20	1.22	0.09	0.16	**64.1**
	Zt.4	0.48	0.25	1.18	0.14	0.17	**50.3**
	Zt.5	0.38	0.25	1.63	0.12	0.12	**59.0**
	Zt.6	0.36	0.18	1.35	0.08	0.17	**47.4**
	Zt.7	0.29	0.14	1.03	0.12	0.20	**60.3**
***Cyp51* gene overexpressing strains**	Zt.8	5.42	0.25	1.05	0.12	0.19	**49.7**
	Zt.9	9.42	0.61	1.45	0.11	0.12	**49.3**
	Zt.10	15.54	0.56	1.69	0.05	0.39	**44.2**
	Zt.11	12.02	0.72	1.62	0.05	0.20	**51.7**
	Zt.12	18.85	1.10	1.48	0.08	0.25	**48.7**
	Zt.13	21.07	1.35	3.63	0.05	0.79	**49.2**
	Zt.14	2.33	0.27	0.86	0.04	0.20	**45.3**
MDR strains	Zt.15	5.91	1.30	3.82	0.28	3.66	**49.2**
	Zt.16	4.86	1.27	7.47	75.00	3.13	**44.2**
	Zt.17	5.26	0.04	6.72	0.28	1.94	**40.0**
	Zt.18	3.53	1.05	8.03	0.30	1.28	**32.0**
	Zt.19	75.00	6.02	15.05	0.57	1.48	**56.6**
	Zt.20	15.51	3.17	10.56	0.04	6.38	**47.5**
	Zt.21	4.82	1.54	7.61	0.33	2.86	**46.2**

Supplementary Table 2. Resistance factors obtained for 22 *Zymoseptoria tritici* strains differing in their resistance level to DMI fungicides, towards five DMI molecules and the rhamnolipid molecule Rh-Est-C12, calculated from the IC_{50} values presented in the Supplementary Table 1.

***Zymoseptoria tritici* isolates**		**Resistance factors***					
		Tebuconazole	Metconazole	Epoxiconazole	Prothioconazole	Prochloraz	Rh-Est-C12
Control strain	IPO323	1 (0.07)	1 (0.04)	1 (0.03)	1 (0.001)	1 (0.02)	**1 (54.29)**
No MDR or *Cyp51* gene overexpressing strains	Zt.1	3.8	3.6	37.2	102.4	5.1	**0.9**
	Zt.2	7.6	3.3	46.2	104.4	7.2	**1.2**
	Zt.3	7.0	4.9	40.7	89.3	6.7	**1.2**
	Zt.4	6.8	6.2	39.5	137.5	7.2	**0.9**
	Zt.5	5.4	6.1	54.3	117.0	5.1	**1.1**
	Zt.6	5.2	4.6	45.2	84.5	6.9	**0.9**
	Zt.7	4.1	3.5	34.2	117.8	8.2	**1.1**
***Cyp51* gene overexpressing strains**	Zt.8	77.6	6.3	35.0	123.3	8.1	**0.9**
	Zt.9	134.6	15.3	48.2	112.8	5.2	**0.9**
	Zt.10	222.0	14.0	56.3	54.3	16.5	**0.8**
	Zt.11	171.7	18.0	53.9	46.9	8.3	**1.0**
	Zt.12	269.3	27.6	49.3	75.9	10.6	**0.9**
	Zt.13	301.0	33.8	121.1	53.8	33.0	**0.9**
	Zt.14	33.3	6.8	28.6	42.5	8.5	**0.8**
MDR strains	Zt.15	84.4	32.5	127.3	276.5	152.6	**0.9**
	Zt.16	69.5	31.7	249.1	74753.2	130.6	**0.8**
	Zt.17	75.1	1.0	224.1	274.3	80.8	**0.7**
	Zt.18	50.4	26.3	267.5	298.6	53.5	**0.6**
	Zt.19	1071.4	150.8	501.8	564.9	61.8	**1.0**
	Zt.20	221.5	79.3	351.9	37.4	266.2	**0.9**
	Zt.21	68.9	38.6	253.5	328.6	119.2	**0.9**

*Resistance factors correspond to the ratio between the IC50 value of a given strain and the IC50 value of the sensitive reference strain IPO323.

CHAPITRE 2

Le rhamnolipide Rh-Est-C12 protège le blé vis-à-vis de *Zymoseptoria tritici via* principalement une activité antifongique directe sans perturbation majeure de la physiologie foliaire

Lors du précédent chapitre, nous avons montré que le Rh-Est-C12 était le rhamnolipide le plus efficace à notre disposition, présentant une activité antifongique *in vitro* et *in planta* significative, mais aussi d'élicitation des activités CAT et POX chez les feuilles de blé, suggérant que ce composé serait capable de déclencher un *burst* oxydatif chez la plante traitée. Ce rhamnolipide présentait aussi l'efficacité de protection la plus élevée de tous les composés testés, même si des travaux restent encore nécessaires afin de l'améliorer au vu de la différence d'activité conséquente observée entre les conditions *in vitro* et *in planta* (facteur 20). Enfin, nous avons montré que le Rh-Est-C12 présente le même niveau d'activité antifongique vis-à-vis de souches de *Z. tritici* plus ou moins résistantes aux DMI, même vis-à-vis de celles avec un phénotype MDR. En raison de ces résultats encourageants, nous avons mis en place d'autres analyses visant à caractériser plus finement le mode d'action indirect du Rh-Est-C12 sur notre pathosystème. Nous avons cherché à déterminer si, comme le suggère l'induction des activités CAT et POX, ce rhamnolipide bio-inspiré est capable de stimuler les défenses du blé. Dans le but de répondre à cette question, ainsi que pour observer l'effet global de l'application de ce composé sur le métabolisme des feuilles de blé, une approche combinée de transcriptomique et de métabolomique a été menée. Aucune étude ne s'est intéressée, jusque-ici, à l'effet d'un potentiel stimulateur de défenses sur le transcriptome et le métabolome du blé vis-à-vis de *Z. tritici*. Malgré la protection observée avec le traitement, le Rh-Est-C12, dans nos conditions, n'a entraîné que de faibles modifications sur le niveau d'expression des gènes et l'accumulation des métabolites dans les feuilles de blé. Ces résultats indiquent que ce composé ne semble pas entraîner d'altérations coûteuses au niveau énergétique pour l'hôte, ce qui est une propriété bénéfique dans le cadre de son utilisation en tant que composé protecteur du blé. Par ailleurs, ces résultats suggèrent que l'activité de protection du Rh-Est-C12 serait principalement due à son activité antifongique directe, et, dans une moindre mesure, à l'induction des réactions de défense de l'hôte. L'effet de l'infection du blé par *Z. tritici*, durant sa phase biotrophe, sur le transcriptome et le métabolome de l'hôte, sera aussi discuté.

Les résultats obtenus dans le cadre de ce chapitre sont en préparation en vue d'une soumission pour publication dans la revue Frontiers in Plant Science *(IF = 4,30).*

Bioinspired rhamnolipid protects wheat against *Zymoseptoria tritici* through mainly a direct antifugal activity and without major disorganization of the leaf physiology

Rémi Platel[1], Anca Lucau[1], Raymonde Baltenweck[2], Alessandra Maia-Grondard[2], Ludovic Chaveriat[3], Maryline Magnin-Robert[4], Béatrice Randoux[4], Pauline Trapet[1], Rutger Pipeleers[5], Patrice Halama[1], Patrick Martin[3], Jean-Louis Hilbert[1], Monica Höfte[5], Philippe Hugueney[2], Philippe Reignault[4], Ali Siah[1]*

[1] Joint Research Unit N° 1158 BioEcoAgro, Junia, Univ. Lille, INRAE, Univ. Liège, UPJV, Univ. Artois, ULCO, 48, boulevard Vauban, BP 41290, F-59014, Lille cedex, France.

[2] Université de Strasbourg, INRAE, SVQV UMR A1131, Colmar 68000, France.

[3] Univ. Artois, UniLasalle, ULR 7519 – Unité Transformations & Agroressources, F-62408 Béthune, France.

[4] Unité de Chimie Environnementale et Interactions sur le Vivant (EA 4492), Université du Littoral Côte d'Opale, CS 80699, F-62228, Calais cedex, France.

[5] Ghent University, Lab. Phytopathology, Dept. Plants & Crops, B-9000 Ghent, Belgium.

*Corresponding author : ali.siah@junia.com ; Tel.: +33(0)3 28 38 48 48

ABSTRACT

Rhamnolipids (RLs) are glycolipids naturally biosynthesized by bacteria from *Pseudomonas* sp. and *Burkholderia* sp. genera and have been shown to display activities against a wide range of pathogens. Most of previous studies on RLs focused on their direct antimicrobial activity, while only few reports describe the mechanisms by which the RLs induce resistance in plants against pathogens and the related fitness cost on plant physiology. We combined here transcriptomic and metabolomic approaches to unravel the mechanisms underlying a RL-associated induced resistance in wheat against the hemibiotrophic fungus *Zymoseptoria tritici*, a major pathogen on this crop. The investigations were performed by treating wheat plants with a bioinspired synthetic mono-RL with a 12-carbon fatty acid tail (Rh-Est-C12) in both infectious and non-infectious conditions, to assess its potential wheat defence eliciting as well as priming bioactivities. Whereas Rh-Est-C12 conferred to wheat a significant protection against *Z. tritici* (41% disease severity reduction), only a slight effect of the RL on wheat leaf gene expression and metabolite accumulation was obtained. A subset of 24 differentially expressed genes (DEGs) and 11 differentially accumulated metabolites (DAMs) were scored in elicitation modalities examined at two, five and fifteen days post-treatment (dpt), and 25 DEGs and 17 DAMs were recorded in priming modalities tested at five and fifteen dpt. Most of the changes are down-regulations and only few DEGs and DAMs associated with resistance to pathogens were identified, while DEGs and DAMs related to other physiological functions were recorded. Nevertheless, a transient early regulation in gene expression was noticed at two dpt (*e.g.* genes involved in signaling, transcription, translation, cell-wall structure and function), suggesting a perception of the RL by the plant upon treatment. Further *in vitro* and *in planta* bioassays showed that Rh-Est-C12 displays direct antimicrobial activity towards *Z. tritici*, thus confirming previous reports. Taken together, our results suggest that Rh-Est-C12 protects wheat against *Z. tritici* though mainly a direct antifungal activity and to a lesser extent *via* the induction of plant defenses, without causing major alterations on the plant metabolism. This study provides new insights into the modes of action of RLs on the wheat-*Z. tritici* pathosystem and reveals the interest to use this low- fitness cost protective molecule to control the pathogen.

Key words: Wheat, *Zymoseptoria tritici*, plant bioprotection, rhamnolipids, plant defense mechanisms, omics, transcriptomic, metabolomic.

INTRODUCTION

Biosurfactants, also referred to as green surfactants, are amphiphilic surface-active molecules that include a hydrophilic head and a hydrophobic tail (Desai and Banat, 1997). They are produced by a wide range of microorganisms, including bacteria, yeasts, and fungi, and they are classified according to their molecular structure into, mainly, mannosylerythritol lipids, trehalose dimycolate, trehalolipids, sophorolipids, lipopeptides, and rhamnolipids (Crouzet *et al.*, 2020). Biosurfactants have been extensively studied for decades because of their high potential of application in diverse areas, including human health, cosmetic, food industry, petroleum industry, soil and water remediation, nanotechnology, and agriculture (Lourith and Kanlayavattanakul, 2009 ; Sachdev and Cameotra, 2013 ; Shekhar *et al.*, 2015 ; Singh *et al.*, 2019). Besides, these biomolecules are gaining more and more attention due to their high biodegradability as well as their low toxicity and ecotoxicity, making them an ecofriendly alternative to synthetic molecules in several areas, such as for the development of sustainable agriculture (Abdel-Mawgoud *et al.*, 2010 ; Shekhar *et al.*, 2015).

Rhamnolipids (RLs) are glycolipids with biosurfactant properties, naturally biosynthesized as secondary metabolites by bacteria from *Pseudomonas* sp. and *Burkholderia* sp. genera. First report of RLs goes back to 1946, from an *in vitro* culture of *Pseudomonas pyocyanea* (now *P. aeruginosa*) (Bergström *et al.*, 1946). Since then, RLs are one of the most intensively studied classes of surfactant glycolipids. Bacteria often produce RLs as a mixture of molecules with one or two rhamnose residues (mono- or di-RLs), forming a polar hydrophilic head and linked through a beta-glycosylic bond to one or two 3-hydroxy fatty acids, as hydrophobic tails. RL analyses and natural variations in the chemical structures of bacterially produced RLs have led to the identification of a pool of almost 60 differents RLs (Abdel-Mawgoud *et al.*, 2010). The differences among these homologs come from modifications in the glycon and/or the aglycon parts; however, the biodiversity of RLs is mostly due to variations in the aglycon parts (Abdel-Mawgoud *et al.*, 2010). Like other biosurfactants, RLs were explored for their use in several areas, including agriculture and sustainable crop protection. Hence, their potential efficacy for the biocontrol of plant pathogens has been reported in several studies, as recently reviewed by Crouzet *et al.* (2020). Most of the studies described the activities of RLs against a large panel of phytopathogenic fungi and oomycetes, while no direct evidence has been reported about their bioactivities towards bacteria and virus infecting plants (Crouzet et al., 2020b). The mode of action of RLs may be direct towards the pathogen, through an antifungal activity, and/or indirect *via* an induction of plant immunity reactions, as it was, for instance, recently reported for the *Brassica napus-Leptosphaeria maculans* pathosystem using semi-purified RL mixtures from *P. aeruginosa* (Monnier *et al.*, 2020).

The compounds activating plant defense reactions against biotic stress could be distinguished into two categories, elicitors or priming agents, and both can be referred to as resistance inducers. Elicitors induce plant defense responses immediately after their perception by the plant, whereas the priming agents usually activate marked defense responses, not directly after their application, but only once the plant is attacked by a pathogen, making priming agents more suitable than elicitors because of their expected lower fitness cost on the plant physiology (Paré *et al.*, 2005). Primed plants set up stronger and/or faster response patterns and may detect the pathogen attack at a lower threshold, hence reacting in a more sensitized way when compared to naïve (unprimed) plants (Paré *et al.*, 2005; Lämke and Bäurle, 2017). The activation of plant defense responses could rely on either the specific

recognition, by transmembrane plant protein recognition receptors, of conserved molecular motifs from a pathogen, the plant itself or a beneficial microbe (Jones and Dangl, 2006), or be triggered by the exogenous application of natural or synthetic molecules, possibly not perceived by specific plant transmembrane receptors, such as phytohormones and biosurfactants (Siah et al., 2018b). Perception of these initial stimuli by the plant often leads to the onset of numerous defense mechanisms, including earlier (influx of calcium, rapid extracellular alkalinization, mitogen-activated protein kinase cascade involved in phosphorylation, oxidative burst, *etc*.) and subsequent (transcriptional changes in attack-responsive genes, biosynthesis of pathogenesis-related (PR) proteins, production of low-molecular mass secondary metabolites such as phytoalexins or antimicrobial peptides, *etc*.) cellular events (Bolwell *et al.*, 1995 ; Felle, 2001 ; Pedley and Martin, 2005 ; van Loon *et al.*, 2006 ; Galon *et al.*, 2010).

Wheat, along with maize and rice, is one of the most cultivated crops worldwide. It is used as a primary ingredient for both human and livestock foods as well as in several agro-industrial areas. Nevertheless, this crop is challenged in the field by several bio-aggressors, which significantly impact wheat grain quality and quantity (Savary *et al.*, 2019). Septoria tritici blotch, caused by the fungal ascomycete *Zymoseptoria tritici*, is since few decades one of the most frequently occurring and damaging diseases on wheat crop, causing yield losses of up to 50% especially in areas where environmental conditions are suitable for disease establishment (Fones and Gurr, 2015). *Zymoseptoria tritici* is a hemibiotrophic fungus that is characterized by an initial asymptomatic biotrophic phase lasting approximately two weeks, followed by a visually symptomatic necrotrophic phase of around one week (Siah et al., 2010a). However, the duration of these two phases may vary depending on the wheat cultivar, fungal strain, and environmental conditions. The control of *Z. tritici* relies mainly on the use of chemical fungicides, such as in Europe, where 70% of the total applied fungicides target this pathogen (Fones and Gurr, 2015), and to a lower extent on resistant cultivars, as no completely resistant cultivar to *Z. tritici* is available. Meanwhile, the durability of these management strategies is often compromised in the field since *Z. tritici* frequently develops resistances to fungicides and regularly overcomes host resistances (*e.g.* Cowger *et al.*, 2000; Cheval *et al.*, 2017). Hence, looking for new eco-friendly and sustainable protection alternative tools for wheat protection against *Z. tritici*, such as bio-sourced resistance inducers, is strongly encouraged. However, the literature regarding the induced resistance in wheat against this major fungal pathogen is still poor, while defense mechanisms of wheat triggered in response to *Z. tritici* infection are extensively studied at the plant-pathogen interaction level. The objective of the present study was, thus, to unravel defense mechanisms induced, in wheat towards *Z. tritici*, by a bioinspired synthetic mono-RL with a C12-carbon chain (Rh-Est-C12), which was recently shown to be the most active and protective RL among a series of 19 RLs tested on this pathosystem by performing a structure-activity relationship study (Platel *et al.*, 2021). The investigations were performed in greenhouse conditions using a combined transcriptomic and metabolomic approach, in both non-infectious and infectious conditions, to assess the potential eliciting and priming effects of the molecule.

MATERIALS AND METHODS

Bioinspired rhamnolipid synthesis

The RL used in the present study (dodecanoyl α/β-L-rhamnopyranoside, hereafter referred to as Rh-Est-C12) is bioinspired from the RLs naturally produced by *P. aeruginosa* (**Figure 1A**) and was synthesized as described previously by Robineau *et al.* (2020) and Platel *et al.* (2021). The conversion and the purity of the product was assessed using nuclear magnetic resonance (NMR) spectroscopy and confirmatory analyses were performed using elemental analysis (vario MICRO cube CHNS/O, Elementar, Lyon, France) and NMR spectroscopy (NMR, Bruker 400 MHz spectrometer). Briefly, chemical analysis of the obtained molecule Rh-Est-C12 consists of : yellowish oil (β/α ratio 3:7, 52%); Rf 0.48 (AcOEt/MeOH 9/1); ^{1}H NMR (CDCl3): 5.09–4.77 (m, 2H), 4.06–3.87 (m, 4H), 3.66–3.59 (m, 2H), 3.48–3.41 (m, 2H), 2.40–2.33 (m, 4H), 1.65–1.58 (m, 4H), 1.30–1.25 (m, 38H), 0.92 (m, 6H, CH3) 13C NMR (CDCl3): δ 174.7, 172.0, 93.5, 92.8, 75.9, 74.2, 73.4, 72.6, 71.3, 69.9, 68.7, 68.1, 34.4, 34,3, 32.0-21.6 (CH2 alkyl chain), 17.6, 17.4, 13.6. The molecular weight of the obtained molecule is 346 g.mol^{-1}.

Plant and fungal materials

The experiments were conducted using seeds of the wheat cultivar (cv.) Alixan, susceptible to *Z. tritici*, provided by the breeding company Limagrain Europe (Verneuil l'Etang, France). All *in vitro* and *in planta* bioassays were carried out using the pathogenic *Z. tritici* single-spore strain T02596, isolated in 2014 in Northern France from a wheat field non-treated with fungicides. Since its isolation, the strain was stored in cryotube aliquots at -80 °C in order to avoid genetic drift of the strain due to *in vitro* subcultures. The fungal inoculum was produced by growing the strain on potato dextrose agar (PDA) medium during one week in dark conditions.

In vitro antifungal bioactivity assay

The direct activity of Rh-Est-C12 RL towards *Z. tritici* growth was assessed on PDA medium, as described by Platel *et al.* (2021), at different concentrations (1.9, 3.9, 7.8, 15.6, 31.2, 62.5, 125, 250, 500, and 1000 mg.L^{-1}) of the RL. Briefly, the RL was first dissolved in DSMO (0.1 % final DMSO concentration within the medium) before being mixed at approximatively 40°C with an autoclaved PDA medium. The experiment was carried out in sterile 12-well plates (Cellstar standard®, Greiner Bio-One GmbH, Kremsmünster, Austria); each well was filled with 3 mL of the mixture, each treatment was replicated three times. Plate inoculation was performed by spotting a drop of 5 µL of *Z. tritici* spore suspension at 5.10^{5} spores.mL^{-1} at the center of each well. Control wells filled or not with 0.1 % DMSO and inoculated or not with fungal spores were used. After 10-day incubation at 20 ± 1°C in dark conditions, fungal growth was evaluated by measuring the two perpendicular diameters of each fungal colony.

Plant treatment and infection

Wheat seeds were first pregerminated in square Petri dishes (12 × 12 cm) on moist filter paper, as described by Siah *et al.* (2010), before being transferred into three-liter pots filled with universal loam (Gamm Vert, France) and placed in the greenhouse at 21 ± 2°C with a 16/8 h day-night cycle. Three pots of 12 wheat plants each (n=36) were used as replicates for each modality. After three weeks of plant growth, *i.e.* when the third leaves were fully expended (corresponding to day 0, D0), the plants

were pretreated with Rh-Est-C12 at 500 mg.L^{-1} or with a mock treatment as control, using a hand sprayer. A volume of 30 mL was used for the treatment of each pot. Rh-Est-C12 was firstly dissolved in dimethyl sulfoxide (DMSO, Sigma-Aldrich, Saint-Louis, USA), with a final concentration of DMSO of 0.1 % in the treatment solution, supplemented with 0.05% of polyoxyethylene-sorbitan monolaurate (Tween 20, Sigma-Aldrich, Saint-Louis, USA) as a wetting agent. Mock treatment consisted of a solution of 0.1% DMSO supplemented with 0.05% of Tween 20. At two days post-treatment (D2), both RL-treated and mock-treated plants were inoculated by spraying 30 mL of 10^6 spores.mL^{-1} *Z. tritici* suspension. Non-inoculated plants were mock-inoculated by spraying 30 mL of a 0.05 % Tween 20 solution on the plants of each pot. After inoculation, the plants were covered with a clear polyethylene bag for three days, to ensure a high humidity level on the surface of the leaves, a required condition for the disease establishment. Disease severity level was scored on the plant third leaf at 23 days after treatment (D23), corresponding to 21 days post-inoculation, by assessing the leaf areas covered by lesions (chlorosis and necrosis) bearing or not pycnidia.

In planta fungal staining assay

The effect of Rh-Est-C12 on *in planta* spore germination and epiphytic fungal growth on the leaf surface was examined at D5 (*i.e.* three days after inoculation) using the chitin dye Fluorescent Brightener 28 (Calcofluor, Sigma-Aldrich, Saint-Louis, USA). Three-centimeter segments, harvested from third leaves of wheat plants, grown in the greenhouse, inoculated with *Z. tritici* and treated or not with Rh-Est-C12 at 500 mg.L^{-1} as described above, were sampled. The segments were immersed for 5 min in a solution of 0.1% (w/v) Calcofluor with 0.1 M Tris-HCl buffer at pH 8.5, before being rinsed twice in sterile osmosed water for 2 min and dried at room temperature. Leaf segments were then deposited on a glass slide, covered with cover slip, and observed with an optic microscope (Eclipse 80i, Nikon, Champigny-sur-Marne, France) under UV-light. Four germinated spore classes were assessed during notations under the microscope: class 1, non-germinated spore; class 2, germinated spore with a small germ tube; class 3, germinated spore with a developed germ tube; and class 4, germinated spore with a strongly developed germ tube. Nine leaf segments, randomly selected from three different pots (three segments per pot), were used as replicates for each condition. The frequencies of spore classes were determined from the analyses of 100 distinct spores on each leaf segment (n_{spores} = 900). Pictures were obtained using digital camera (DXM1200C, Nikon, Champigny-sur-Marne, France) coupled with the image capture software NIS-Elements BR (Nikon, Champigny-sur-Marne, France).

RNA extraction and transcriptomic analysis

Total RNA from wheat leaves was extracted using RNeasy Plant Mini Kit (Qiagen, Courtaboeuf, France). The quality of RNAs was measured with Nanodrop by analyzing their absorbance ratios A260/280 and A260/230, which were found to range between 2.0 and 2.2. Besides, RNA quality was also examined with Bioanalyzer 2100 (Agilent, France) and a minimal RNA integrity number (RIN) of 0.8 was required for all samples. Non-targeted gene expression analysis was performed using Microarrays GE 4x44 chip purchased from Agilent (Santa Clara, CA, USA). The hybridization for all conditions were carried out in triplicate with three samples of total RNA extracted from bulked wheat leaves (with three different leaves from different pots per bulk). All the nine wheat leaves used for RNA extraction are originating from different pots. All steps of RNA amplification, staining, hybridization, and washing were performed according to the manufacturer's indications. Slides were

scanned at five µm/pixel resolution using the GenePix 4000B scanner (Molecular Devices Corporation, Sunnyvale, CA, USA) and the images were used for grid alignment and expression data digitization by using the software GenePix Pro 6.0 (Molecular Devices Corporation, Sunnyvale, CA, USA).

Metabolite extraction and analysis

Metabolite extraction was performed from powdered freeze-dried wheat leaves (30-50 mg per sample) using 25 µL of methanol per mg dry weight. The extract was then incubated in an ultrasound bath for 10 minutes, before centrifugation at 13000 g at 10 °C for 10 minutes. The supernatant was analyzed using a Dionex Ultimate 3000 UHPLC system (Thermo Fisher Scientific, USA). The chromatographic separations were performed on a Nucleodur C18 HTec column (150 × 2 mm, 1.8 µm particle size; Macherey-Nagel, Germany) maintained at 30 °C. The mobile phase consisted of acetonitrile/formic acid (0.1%, v/v, eluant A) and water/formic acid (0.1%, v/v, eluant B) at a flow rate of 0.3 mL min-1. The gradient elution was programed as follows: 0 to 1 min, 95% B; 1 to 2 min, 95% to 85% B; 2 to 7 min, 85% to 0% B; 7 to 9 min, 100% A. The sample volume injected was 1 µL. The UHPLC system was coupled to an Exactive Orbitrap mass spectrometer (Thermo Fischer Scientific, USA), equipped with an electrospray ionization (ESI) source operating in positive mode. Parameters were set at 300 °C for ion transfer capillary temperature and 2500 V for needle voltages. Nebulization with nitrogen sheath gas and auxiliary gas were maintained at 60 and 15 arbitrary units, respectively. The spectra were acquired within the m/z (mass-to-charge ratio) mass ranging from 100 to 1000 atomic mass units (a.m.u.), using a resolution of 50,000 at m/z 200 a.m.u. The system was calibrated internally using dibutyl-phthalate as lock mass at m/z 279.1591, giving a mass accuracy lower than 1 ppm. The instruments were controlled using the Xcalibur software (Thermo Fischer Scientific, USA). LC-MS grade methanol and acetonitrile were purchased from Roth Sochiel (France); water was provided by a Millipore water purification system. Apigenin and chloramphenicol (Sigma-Aldrich, France) was used as internal standard.

Statistical analyses

Protection efficacy conferred by Rh-Est-C12 on wheat plants in the greenhouse was analyzed using a One-Way analysis of variance (AN0VA) at $P \leq 0.05$, using GraphPad Prism software version 9 (GraphPad Software Inc., San Diego, USA). *In planta* spore germination and hyphal growth were analyzed using the Tukey test at $P \leq 0.05$, using GraphPad Prism software version 9. Half-maximal inhibitory concentration (IC_{50}) was calculated from the dose-response curve of Rh-Est-C12 using the GraphPad Prism software version 9.

Gene expression data in the transcriptomic assay were normalized by Quantile algorithm. The three control samples were filtered for $P < 0.05$ and the average was calculated for each gene. A fold change value was calculated for each gene between individual treated samples and the mean of corresponding controls. Differentially expressed genes (DEGs) were selected for a significant threshold > 2.0 or < 0.5 ($P < 0.05$). Functional annotations of DEGs were based on NCBI GenBank and related-genes physiological processes were assigned with NCBI, AmiGO 2 Gene Ontology and UniProt. Kyoto encyclopedia of genes and genomes (KEGG) pathway analysis was also used to identify relevant biological pathways for the selected genes. However, DEGs may be involved in more than one biological process, especially when it comes to stress responses, hence the determined functional annotation could be subjected to modifications in the future.

In the metabolomic assay, metabolite identification and their classification into different chemical families were based on previously published works on benzoxazinoids (de Bruijn *et al.*, 2016), flavonoids (Wojakowska *et al.*, 2013) and hydroxycinnamic acid amides (Li *et al.*, 2018) from wheat. Besides, the proposed putative metabolite identifications was based on expertized analysis of the corresponding mass spectra and comparison with published reports in literature. Additional information was retrieved from the KEGG and PubChem databases. The relative quantification of the selected metabolites was performed using the software Xcalibur. The identity of some metabolites was confirmed using the corresponding standards provided by Sigma-Aldrich (France). Differential metabolomic analyses among the different conditions were performed using the Tukey's Honest Significant Difference method followed by a false discovery rate (FDR) correction using the Benjamini-Hochberg procedure (Benjamini and Hochberg, 1995). Metabolites of interest were considered differentially accumulated when the false discovery rate was below 5 % (FDR ≤ 0.05).

RESULTS

Rh-Est-C12 displays direct antifungal activity and reduces disease severity caused by *Z. tritici*

Rh-Est-C12 induced-protection in wheat against *Z. tritici* was assessed in the greenhouse. At 23 days after treatment (D23), *i.e* 21 days after inoculation, disease symptom level scored on the third leaves of the non-treated inoculated control plants consisted of 55.7% of diseased leaf area. Preventive treatment two days prior to inoculation with *Z. tritici* with a Rh-Est-C12 solution at 500 $mg.L^{-1}$ resulted in a significant reduction of the disease symptoms caused by the pathogen, with only 32.8% of diseased leaf area on the treated third leaves, corresponding to a reduction of 41.1% **(Figure 1B)**. No phytotoxic effect was observed on wheat leaves at the tested concentration. On the other hand, *in vitro* bioassays were performed in order to assess the direct antifungal effect of Rh-Est-C12 on the fungus. Dose-response curve revealed a total inhibition of the *in vitro* fungal growth by the concentration of 31.2 $mg.L^{-1}$ and an IC_{50} value of 26.8 $mg.L^{-1}$ **(Figure 1C and D)**. Finally, *in planta* cytological staining was carried out to examine the RL effect on *Z. tritici* early infection process. The results revealed that Rh-Est-C12 impacts at D5 (five days after treatment) both spore germination and the epiphytic hyphal growth of the fungus. The proportion of each class of spores was significantly different between Rh-Est-C12-treated and control plants **(Figure 1E)**. On control plants at D5, *Z tritici* spores were mainly germinated with a developed or strongly developed germ tube (class 1 and 2), while on Rh-Est-C12 treated plants, *Z. tritici* spores were less developed and were mostly present as non-germinated spores or germinated spores but only with a small germ tube (class 3 and 4) **(Figure 1E)**.

Rh-Est-C12 did not induce any major modifications in wheat leaf gene expression

RNA microarray chip assay was performed to investigate the effect of Rh-Est-C12 on wheat transcriptome under absence or presence of *Z. tritici*, at two days after treatment (D2) in non-infectious conditions, and at five days after treatment (D5), *i.e* three days after inoculation, in both non-infectious and infectious conditions. These two time points were chosen because they correspond to early stages of both *Z. tritici* infection (D5) and plant defense mechanism induction (D2). The eliciting potential of Rh-Est-C12 was assessed at D2 and D5 by comparing treated and non-treated plants under non-infectious conditions. The priming of plant defenses was evaluated at D5 by comparing treated and non-treated plants under infectious conditions (treated and inoculated plants *vs* non-treated

inoculated plants), by also taking into account the potential elicitation effect of Rh-Est-C12 at D2 and D5. Moreover, additional comparisons were performed (treated and inoculated plants *vs* treated non-inoculated plants, and treated and inoculated plants *vs* non-treated non-inoculated plants) to get a deeper understanding of the potential priming effect of Rh-Est-C12 on wheat plants **(Supplementary Table S2, Supplementary Figures S1 and S2)**. Thereafter, the different comparisons will be referred to as eliciting, fungal, and priming effects, corresponding to the elicitation, fungal infection alone, and priming modalities, respectively.

Overall, out of the 43,803 wheat probes available on the RNA microarray chip, 78 differentially expressed genes (DEGs) were highlighted when taking into account all studied modalities and performed comparisons, and at all time points **(Supplementary Table S1)**. Overall, only a weak regulation of gene expression was observed in both elicitation (24 DEGs, at D2 and D5) and priming (25 DEGs, at D5) modalities, when compared to the transcriptional effect of the fungal infection alone (38 DEGs, D5) **(Figure 2B)**. Only two common DEGs were identified at D5 between priming and fungal effect modalities **(Figure 2A)**. Interestingly, most of the changes observed in gene expression profiles correspond to downregulations, except at D2 in eliciting modality, where a higher number of upregulated genes was found when compared to downregulated ones **(Figure 4)**.

When considering the eliciting modality, at D5, almost no transcriptional effect was observed in the treated wheat plants. We could notice a downregulation of the expression of two DEGs, one encodes for class 1 chitinase, and the other encodes for "rDNA tandem repeat with genes for 18S, 5.8S and 26S rRNA" **(Figure 4)**. However, at an earlier post-treatment stage (D2), 22 DEGs were found. These genes encode for proteins involved in responses to abiotic and oxidative stresses, growth and development, cell-wall structure and function, pigment biosynthesis and chloroplast structure, light-harvesting, photosynthesis and carbohydrate metabolism, protein metabolism, as well as signaling transcription, and translation **(Figure 3)**. Regarding the priming modality at D5, among the 25 DEGs highlighted, only seven were up-regulated, while 18 were down-regulated. All of these DEGs were different from the ones found in eliciting and fungal effect modalities, except two DEGs encoding for heat shock protein 80 and heat shock protein 70-like, which were also deregulated in fungal effect modality **(Figures 2 and 4)**. Genes regulated in the priming modality encode for proteins involved in diverse functions and belong to all targeted functional groups of genes. Finally, fungal infection alone displayed the most important effect on the wheat leaf transcriptome when compared to eliciting and priming modalities. Again, most of the changes observed were due to gene downregulations (six genes upregulated *vs* 32 genes downregulated). All functional groups of genes were represented in this modality, except the gene functional group light-harvesting, photosynthesis and carbohydrate metabolism **(Figure 3 and 4)**.

Rh-Est-C12 also did not cause marked change in wheat leaf metabolite accumulation

An UHPLC-MS analysis was carried out to examine the effect of Rh-Est-C12 on the wheat leaf metabolome, at the same time points as those selected for transcriptomic analysis (D2 and D5) and an additional time point at 15 days after treatment (D15), *i.e* thirteen days after inoculation. This time should coincide with the moment preceding the switch of the fungus from the biotrophic to the necrotrophic phase. All comparisons aiming at investigating the eliciting, priming, and fungal effects were undertaken according to the same pairwise comparison performed above in transcriptomic

assay. A total of 54 metabolites was identified when considering all modalities and performed comparisons, and all time points **(Supplementary Table S3)**. PCA analysis revealed a significant clustering of the treated and/or inoculated plants, indicating that Rh-Est-C12 and/or *Z. tritici* affect wheat metabolite patterns **(Figure 5)**.

When focusing on eliciting modality, only few differentially accumulated metabolites (DAMs) within the treated non-inoculated leaves were highlighted at the three targeted time points **(Figure 6)**. At D2, one amino acid (asparagine) was found under-accumulated, whereas at D5, the concentrations of two phytohormones and precursors (OPDA and MeJA) were significantly decreased. Moreover, two amino acids (valine and proline) were over-accumulated at this later time-point. At D15, six metabolites were significantly under-accumulated, one amino acid (valine), one phytohormone, abscisic acid glucose ester (ABA-Glc), and four flavonoids, luteolin-6-C-hexoside (luteolin-6-C-Glc), luteolin-C-hexosyl-deoxyhexoside (luteolin-C-hexo-O-deoxyhexo), luteolin-C-hexosyl-C-pentoside (luteolin-C-hexo-C-pento) and tricin. In priming modality, more DAMs were observed than in eliciting modality, but at D5 only. At D5, 13 DAMs were under-accumulated, seven of them are amino acids, leucine-isoleucine, phenylalanine, tyrosine, arginine, histidine, lysine, and asparagine, five are benzoxazinoids, HBOA, HBOA-glucoside (HBOAGlc), HMBOA-hexoside (HMBOAGlc), HM2BOA, HM2BOA-hexoside (HM2BOAGlc) and one is an hydroxycinnamic acid amide, feruloylagmatine. It is to notice that most of these under-accumulated DAMs were the same than those found over-accumulated in fungal effect modality. The overaccumulation of only one metabolite, the amino acid aspartic acid, can be associated to the priming modality. No DAMs belonging to the flavonoid and phytohormone families were highlighted at this time point. At D15, however, an increase in the concentration of three flavonoids, luteolin-6-C-Glc, luteolin-C-hexo-C-pento, and chrysoeriol-6-C-hexoside (chrysoeriol-6-C-Glc), was observed. Fungal infection alone caused more changes in leaf metabolite concentrations than eliciting and priming modalities. At D5, among the 54 identified metabolites, 24 were differently accumulated (17 over-accumulated, seven under-accumulated). At D15, considerably less modifications were detected, with seven DAMs only, among them six under-accumulated and one under-accumulated **(Figure6)**.

DISCUSSION

We explored here, using a combined transcriptomic and metabolomic approach, the ability of a bioinspired mono-RL (Rh-Est-C12) to trigger defense reactions in wheat towards *Z. tritici*, a significantly damaging pathogen on this major agroeconomic crop. The results confirmed that Rh-Est-C12 significantly protects wheat against the pathogen by reducing disease severity by almost half, and displays a direct antimicrobial activity towards the fungus both *in vitro* and *in planta*, thus agreeing with a previous report testing the potential activity of this RL, as well as other RLs with different structures, on the wheat-*Z. tritici* pathosystem (Platel *et al.* 2021). The protective and antimicrobial activity of RLs against phytopathogens, including fungi and oomycetes, have been reported in many studies, as reviewed recently by Crouzet *et al.* (2020). However, studies investigating the RL-induced resistance using omics approaches are lacking. Our results reveal that the examined mono-RL, Rh-Est-C12, does not induce major modifications in either the patterns of gene expression or metabolite accumulation, when considering both eliciting and priming modalities.

Surprisingly, only a slight number of DEGs associated with response to pathogens was observed, while a more important set of genes involved in other functions was recorded in both eliciting and priming modalities. Among the DEGs detected in the eliciting modality, a much higher number (22) was scored at D2 than at D5 (2), suggesting that the slight eliciting effect potentially conferred by Rh-Est-C12 at the earlier time point D2 is not persistent and seems to disappear three days later, at D5. Out of the 22 detected DEGs, two encode for heat shock proteins (HSPs), 22.3kDa heat-shock protein and heat shock protein 80. These chaperone proteins are crucial molecules involved in plant defense against abiotic and biotic stresses. As reviewed by ul Haq *et al.* (2019), HSPs may increase ROS scavenging by enhancing plant antioxidant enzymes. Interestingly, we have previously found that Rh-Est-C12 can increase catalase and peroxidase activities in wheat (Platel *et al.*, 2021) Besides, HSPs are also considered to play a role in membrane stability (ul Haq *et al.*, 2019). Remarkably, RLs are supposed to inhibit microbial pathogens and trigger plant immunity defenses by interacting directly with their plasma membranes (Crouzet *et al.*, 2020). Hence, the accumulation of HSP transcripts could suggest that Rh-Est-C12 can affect wheat-cell membrane stability, by mimicking an abiotic stress. This potential "abiotic stress-like" mode of action of Rh-Est-C12 could explain the deregulation of abiotic stress response-associated DEGs observed in this modality, such as cold acclimation protein WCOR518, fasciclin-like protein FLA15, β-carotene hydroxylase, peroxidase 6, β-amylase, and myb-related protein MYBAS1 (Davison *et al.*, 2002 ; Kaplan and Guy, 2004 ; Svensson *et al.*, 2006 ; You and Chan, 2015 ; Zang *et al.*, 2015 ; Peixoto-Junior *et al.*, 2018). At the metabolome level, we detected, at D5, the accumulation of two amino acids, valine and proline, and the under-accumulation of two phytohormones and precursors, OPDA and MeJA. Proline is an osmolyte metabolite involved in adaptation and tolerance to a large variety of abiotic stresses, such as osmotic, freezing, and cold stress (Szabados and Savouré, 2010 ; Lv *et al.*, 2011). The accumulation of this metabolite could likely be a consequence of the Rh-Est-C12 "abiotic stress-like" effect on wheat. At D15 also, the concentration of only a few DAMs was altered. Taken as a whole, these results suggest that Rh-Est-C12 treatment, in the elicitation modality, triggers some modifications in the wheat plant transcriptome and metabolome but its effect is very limited, especially when compared to the deregulation levels induced by other elicitors in other plants. For instance, Landi *et al.* (2017) recently reported, using RNA-seq, that preharvest treatment of strawberry fruit with chitosan and BTH, induced modifications in the expression of 5,062 and 5,210 transcripts, respectively, at 6, 12 and 24 hours post-treatment, compared to control conditions. In grapevine, plant treatment with the beta-glucan laminarin and its sulfated derivative (PS3) induced the regulation of 94 and 132 genes at 12 hours post-treatment, respectively, highlighted Gauthier *et al.* (2014) using a microarray chip. The fact that Rh-Est-C12 induces only slight alterations on the plant transcriptome and metabolome, even with the high used concentration (500 $mg.L^{-1}$), indicates that this RL can provide protection to wheat against *Z. tritici* without a high fitness cost on the plant. Such a positive property is sought after for crop protection compounds, since yield should not be negatively impacted by compounds having insignificant impact on the plant physiology. (Cipollini *et al.*, 2017). At the opposite, elicitors displaying a large extent of alterations on the host physiology, as those presented above, may lead to protection but with, possibly, higher allocation costs within the plant (Tripathi *et al.*, 2019). The suggested neutral effect of Rh-Est-C12 on wheat fitness cost should furthermore be ascertained on wheat grain yield.

In the modality assessing the potential priming effect of Rh-Est-C12, we detected significant downregulation of 18 genes at D5, among them six are involved in response to oxidative stress

(encoding mainly for peroxidases) and five related to light harvesting, photosynthesis, and carbohydrate metabolism (encoding for chlorophyll a/b-binding protein WCAB precursor, chloroplast pigment-binding protein CP24, light-harvesting complex I, light-induced protein 1-like and light-regulated protein precursor). The other downregulated DEGs were associated with other functions. Two of these DEGs are particularly interesting in plant defense against pathogens, (i) the xylanase inhibitor TAXI-III that was reported as being potentially involved in durum wheat resistance against *Fusarium graminearum*, and (ii) the papain-like cysteine peptidase that was often described as a central key-enzyme in plant immunity (Moscetti *et al.*, 2013 ; Misas-Villamil *et al.*, 2016). Additionally, six DEGs were over-expressed (genes encoding for aquaporin PIP1, ATP-dependent RNA helicase, probable pyridoxal biosynthesis protein PDX1.1, sterol desaturase family protein, S-adenosylmethionine synthetase and heat-shock protein 80). Among these genes, some may be involved in plant defense against biotic stress, like those encoding for aquaporin PIP1 and ATP-dependent RNA helicase (Zhang *et al.*, 2014 ; Li *et al.*, 2020). Remarkably, out of all the 24 detected DEGs in the priming modality, only the one encoding for heat-shock protein 80 was found in another condition (*Z. tritici* infection alone) at D5. In addition, the RL effect in priming modality seems weak, with only a few of the detected DEGs thought to be involved in plant resistance to pathogens. On the wheat metabolome, also, only a few changes were observed. At D5, aspartic acid was the only metabolite significantly over-accumulated, whereas 13 DAMs were under-accumulated. Most of them, however, were found over-accumulated in fungal effect modality and totally absent in the comparison treated-inoculated *vs* non-treated non-inoculated (**Supplementary Figure S3**), suggesting that the observed metabolite under-accumulations in the priming modality at D5 are not conferred by the RL treatment but rather by the reduced fungal infection only. Finally, at D15, three flavonoid metabolites were over-accumulated. Flavonoids are secondary metabolites biosynthesized from phenylpropanoid pathway, which have been described as antimicrobial and antioxidant compounds that could be involved in wheat defense against biotic stress (Pietta, 2000).

Insights regarding the effect of *Z. tritici* alone on the wheat transcriptome and metabolome in the case of a compatible interaction have also been acquired. At D5, we observed alterations in the accumulation of transcripts of 43 genes (with all functional groups represented, except light harvesting, photosynthesis, carbohydrate metabolism) and 26 metabolites (all functional or chemical families represented), much more than in the other modalities (*i.e* elicitation and priming ones). The regulation of these DEGs and DAMs may be caused by (i) plant recognition of the fungus and (ii) the subsequent defense response deployment, *i.e* upregulation of genes encoding for pathogenesis-related (PR) proteins, chitinases and thaumatin-like proteins, as well as over-accumulation of specific amino acids, benzoxazinoids, and hydroxycinnamic acid amides. Noteworthy, PR-proteins are key-components of the plant immune system (Ali *et al.*, 2018). Benzoxazinoids are plant defense metabolites found in many *Poaceae* species and are known to display antimicrobial and allelopathic activities, as well as to regulate callose deposition, like in maize (Hashimoto and Shudo, 1996 ; De Bruijn *et al.*, 2018). Hydroxycinnamic acid amides are another family of plant secondary metabolites reported to be positively correlated with plant resistance in several pathosystems (Muroi *et al.*, 2009 ; Gunnaiah *et al.*, 2012 ; Yogendra *et al.*, 2014). Seybold *et al.* (2020) described significant modifications in the accumulation of benzoxazinoids and hydroxycinnamic acid amides during *Z. tritici* infection, between susceptible and resistant cultivars, underlining the potential importance of these metabolites in wheat resistance towards the pathogen. Interestingly, we did not observe any significant

accumulation of benzoxazinoids at D15. Seybold *et al.* (2020) also observed an inhibition of benzoxazinoid accumulation in a susceptible wheat cultivar (Obelisk) at an early stage of *Z. tritici* infection only, hypothetically explained by fungal effector secretion and host-defense manipulation by the pathogen during the studied interaction.

Another possible explanation of the observed modification of DEGs and DAMs in wheat leaves during the infection alone is the "hijacking" of plant metabolism by the fungus to facilitate its invasion. Indeed, still at D5, 37 out of the 43 detected DEGs were downregulated. These genes were particularly associated with response to stress (abiotic, oxidative, pathogens) and secondary metabolism, as well as cell-wall structure and function and amino acid and protein metabolism, suggesting a deleterious effect of the fungus on these functions. Our results suggest that *Z. tritici* could impair cell-wall strengthening in Alixan cultivar. Indeed, the fungal infection induced downregulation of six DEGs associated with cell wall structure and function, including genes encoding for cinnamyl alcohol dehydrogenase and non-specific lipid transfer proteins and precursors. Cinnamyl alcohol dehydrogenase is a key enzyme of lignin biosynthesis pathway, for which encoding genes were also found downregulated by Rudd *et al.* (2015) on wheat at one day after infection with *Z. tritici*. Seybold *et al.* (2020) showed lignin under-accumulation in a susceptible cultivar (Obelisk) compared to a resistant one (Chinese spring), suggesting the role of this crucial monolignol polymer in wheat resistance to *Z. tritici*. Moreover, non-specific lipid transfer proteins (nsLTPs) also play critical roles in protective mechanisms, such as cell-wall organization, against pathogens and have even been classified as part of the PR-14 family. The other functions of this protein family, such as antimicrobial activity or systemic acquired resistance (SAR) signaling, in plant response to biotic stress, have been reviewed by Liu *et al.* (2015). Moreover, we observed, at D15, an under-accumulation of five flavonoids. Flavonoids are known to accumulate in cell walls during infection (Mierziak *et al.*, 2014). Decrease in their concentration may be caused by an overcoming of wheat defense reactions by the fungus. In addition, we observed significant under-accumulation of MeJA and MeSA at D5, suggesting a repression of jasmonic acid (JA) and salicylic acid (SA) pathways at this time point. These phytohormones are particularly crucial in defenses against pathogen attacks. Usually, SA is often considered to be the key hormone regulating defenses against biotrophic pathogens, while JA would trigger defense mechanisms towards necrotrophic invaders. MeSA, a methyl form of SA, would be responsible for SAR (Thaler *et al.*, 2012 ; Chen *et al.*, 2019). In the wheat-*Z. tritici* pathosystem, Rudd *et al.* (2015) also detected a downregulation of SA and JA pathways at the beginning of *Z. tritici* biotrophic phase on the susceptible cultivar Riband. The authors also reported an SA accumulation during the fungal necrotrophic phase, whereas we observed a significant increase in SA concentration in wheat leaves at D15, *i.e* at the end of the biotrophic phase, suggesting that SA regulation during the *Z. tritici* infection is cultivar-dependent.

In conclusion, although Rh-Est-C12 treatment triggers significant regulations, especially on the wheat leaf gene expression at D2, possibly caused by "abiotic stress-like" mimicking due to its interaction with plant plasma membranes, it would appear that the RL protects wheat against *Z. tritici* without causing major alterations on the plant metabolism. Our results suggest that (i) Rh-Est-C12 likely displays a neutral fitness cost on the plant at the tested concentration and (ii) that the protection efficacy conferred by this molecule is mainly due to its direct antifungal activity against the pathogen

and to a lesser extent to an induction of plant defenses. This study also provides new insights into the molecular bases of the wheat-*Z. tritici* interaction.

ACKNOWLEDGEMENTS

This research was conducted in the framework of the project Bioscreen (Smartbiocontrol portfolio), funded by the European program Interreg V, and the CPER Alibiotech, funded by the European Union, the French State, and the French Council Hauts-de-France.

LITERATURE CITED

Abdel-Mawgoud, A.M., Lépine, F., and Déziel, E. (2010). Rhamnolipids: diversity of structures, microbial origins and roles. Appl Microbiol Biotechnol *86*, 1323–1336.

Ali, S., Ganai, B.A., Kamili, A.N., Bhat, A.A., Mir, Z.A., Bhat, J.A., Tyagi, A., Islam, S.T., Mushtaq, M., Yadav, P., et al. (2018). Pathogenesis-related proteins and peptides as promising tools for engineering plants with multiple stress tolerance. Microbiological Research *212–213*, 29–37.

Benjamini, Y., and Hochberg, Y. (1995). Controlling the False Discovery Rate: A Practical and Powerful Approach to Multiple Testing. Journal of the Royal Statistical Society. Series B (Methodological) *57*, 289–300.

Bergström, S., Theorell, H., and Davide, H. (1946). Pyolipic acid, a metabolic product of *Pseudomonas pyocyanea*, active against Mycobacterium tuberculosis. Undefined.

Bolwell, G.P., Butt, V.S., Davies, D.R., and Zimmerlin, A. (1995). The Origin of the Oxidative Burst in Plants. Free Radical Research *23*, 517–532.

De Bruijn, W.J.C., Vincken, J.-P., Duran, K., and Gruppen, H. (2016). Mass Spectrometric Characterization of Benzoxazinoid Glycosides from Rhizopus-Elicited Wheat (*Triticum aestivum*) Seedlings. J Agric Food Chem *64*, 6267–6276.

De Bruijn, W.J.C., Gruppen, H., and Vincken, J.-P. (2018). Structure and biosynthesis of benzoxazinoids: Plant defence metabolites with potential as antimicrobial scaffolds. Phytochemistry *155*, 233–243.

Cheval, P., Siah, A., Bomble, M., Popper, A.D., Reignault, P., and Halama, P. (2017). Evolution of QoI resistance of the wheat pathogen *Zymoseptoria tritici* in Northern France. Crop Protection *92*, 131–133.

Cowger, C., Hoffer, M.E., and Mundt, C.C. (2000). Specific adaptation by *Mycosphaerella graminicola* to a resistant wheat cultivar. Plant Pathology *49*, 445–451.

Crouzet, J., Arguelles-Arias, A., Dhondt-Cordelier, S., Cordelier, S., Pršić, J., Hoff, G., Mazeyrat-Gourbeyre, F., Baillieul, F., Clément, C., Ongena, M., et al. (2020). Biosurfactants in Plant Protection Against Diseases: Rhamnolipids and Lipopeptides Case Study. Front Bioeng Biotechnol *8*.

Davison, P.A., Hunter, C.N., and Horton, P. (2002). Overexpression of beta-carotene hydroxylase enhances stress tolerance in Arabidopsis. Nature *418*, 203–206.

Desai, J.D., and Banat, I.M. (1997). Microbial production of surfactants and their commercial potential. Microbiol. Mol. Biol. Rev. *61*, 47–64.

Felle, H.H. (2001). pH: Signal and Messenger in Plant Cells. Plant Biology *3*, 577–591.

Fones, H., and Gurr, S. (2015). The impact of Septoria tritici Blotch disease on wheat: An EU perspective. Fungal Genet Biol *79*, 3–7.

Galon, Y., Finkler, A., and Fromm, H. (2010). Calcium-Regulated Transcription in Plants. Molecular Plant *3*, 653–669.

Gunnaiah, R., Kushalappa, A.C., Duggavathi, R., Fox, S., and Somers, D.J. (2012). Integrated Metabolo-Proteomic Approach to Decipher the Mechanisms by Which Wheat QTL (Fhb1) Contributes to Resistance against *Fusarium graminearum*. PLOS ONE *7*, e40695.

Ul Haq, S., Khan, A., Ali, M., Khattak, A.M., Gai, W.-X., Zhang, H.-X., Wei, A.-M., and Gong, Z.-H. (2019). Heat Shock Proteins: Dynamic Biomolecules to Counter Plant Biotic and Abiotic Stresses. International Journal of Molecular Sciences *20*, 5321.

Hashimoto, Y., and Shudo, K. (1996). Chemistry of biologically active benzoxazinoids. Phytochemistry *43*, 551–559.

Jones, J.D.G., and Dangl, J.L. (2006). The plant immune system. Nature *444*, 323–329.

Kaplan, F., and Guy, C.L. (2004). β-Amylase Induction and the Protective Role of Maltose during Temperature Shock. Plant Physiology *135*, 1674–1684.

Kunkel, B.N., and Harper, C.P. (2018). The roles of auxin during interactions between bacterial plant pathogens and their hosts. Journal of Experimental Botany *69*, 245–254.

Lämke, J., and Bäurle, I. (2017). Epigenetic and chromatin-based mechanisms in environmental stress adaptation and stress memory in plants. Genome Biology *18*, 124.

Li, G., Chen, T., Zhang, Z., Li, B., and Tian, S. (2020). Roles of Aquaporins in Plant-Pathogen Interaction. Plants *9*, 1134.

Li, Z., Zhao, C., Zhao, X., Xia, Y., Sun, X., Xie, W., Ye, Y., Lu, X., and Xu, G. (2018). Deep Annotation of Hydroxycinnamic Acid Amides in Plants Based on Ultra-High-Performance Liquid Chromatography–High-Resolution Mass Spectrometry and Its *In Silico* Database. Anal. Chem. *90*, 14321–14330.

Van Loon, L.C., Rep, M., and Pieterse, C.M.J. (2006). Significance of Inducible Defense-related Proteins in Infected Plants. Annual Review of Phytopathology *44*, 135–162.

Lourith, N., and Kanlayavattanakul, M. (2009). Natural surfactants used in cosmetics: glycolipids. Int J Cosmet Sci *31*, 255–261.

Lv, W.-T., Lin, B., Zhang, M., and Hua, X.-J. (2011). Proline Accumulation Is Inhibitory to Arabidopsis Seedlings during Heat Stress. Plant Physiology *156*, 1921–1933.

Ma, X., Keller, B., McDonald, B.A., Palma-Guerrero, J., and Wicker, T. (2018). Comparative Transcriptomics Reveals How Wheat Responds to Infection by *Zymoseptoria tritici*. Mol Plant Microbe Interact *31*, 420–431.

Misas-Villamil, J.C., Hoorn, R.A.L. van der, and Doehlemann, G. (2016). Papain-like cysteine proteases as hubs in plant immunity. New Phytologist *212*, 902–907.

Monnier, N., Cordier, M., Dahi, A., Santoni, V., Guénin, S., Clément, C., Sarazin, C., Penaud, A., Dorey, S., Cordelier, S., et al. (2020). Semipurified Rhamnolipid Mixes Protect *Brassica napus* Against *Leptosphaeria maculans* Early Infections. Phytopathology *110*, 834–842.

Moscetti, I., Tundo, S., Janni, M., Sella, L., Gazzetti, K., Tauzin, A., Giardina, T., Masci, S., Favaron, F., and D'Ovidio, R. (2013). Constitutive expression of the xylanase inhibitor TAXI-III delays Fusarium head blight symptoms in durum wheat transgenic plants. Mol Plant Microbe Interact *26*, 1464–1472.

Muroi, A., Ishihara, A., Tanaka, C., Ishizuka, A., Takabayashi, J., Miyoshi, H., and Nishioka, T. (2009). Accumulation of hydroxycinnamic acid amides induced by pathogen infection and identification of agmatine coumaroyltransferase in *Arabidopsis thaliana*. Planta *230*, 517–527.

Nambara, E. (2017). Abscisic Acid. In Encyclopedia of Applied Plant Sciences (Second Edition), B. Thomas, B.G. Murray, and D.J. Murphy, eds. (Oxford: Academic Press), pp. 361–366.

Paré, P.W., Farag, M.A., Krishnamachari, V., Zhang, H., Ryu, C.-M., and Kloepper, J.W. (2005). Elicitors and priming agents initiate plant defense responses. Photosynth Res *85*, 149–159.

Pedley, K.F., and Martin, G.B. (2005). Role of mitogen-activated protein kinases in plant immunity. Current Opinion in Plant Biology *8*, 541–547.

Peixoto-Junior, R.F., Andrade, L.M. de, Brito, M. dos S., Nobile, P.M., Martins, A.P.B., Carlin, S.D., Ribeiro, R.V., Goldman, M.H. de S., Oliveira, J.F.N.C. de, Figueira, A.V. de O., et al. (2018). Overexpression of *ScMYBAS1* alternative splicing transcripts differentially impacts biomass accumulation and drought tolerance in rice transgenic plants. PLOS ONE *13*, e0207534.

Pietta, P.G. (2000). Flavonoids as antioxidants. J Nat Prod *63*, 1035–1042.

Platel, R., Chaveriat, L., Le Guenic, S., Pipeleers, R., Magnin-Robert, M., Randoux, B., Trapet, P., Lequart, V., Joly, N., Halama, P., et al. (2021). Importance of the C12 Carbon Chain in the Biological Activity of Rhamnolipids Conferring Protection in Wheat against *Zymoseptoria tritici*. Molecules *26*, 40.

Robineau, M., Le Guenic, S., Sanchez, L., Chaveriat, L., Lequart, V., Joly, N., Calonne, M., Jacquard, C., Declerck, S., Martin, P., et al. (2020). Synthetic Mono-Rhamnolipids Display Direct Antifungal Effects and Trigger an Innate Immune Response in Tomato against *Botrytis Cinerea*. Molecules *25*.

Rudd, J.J., Kanyuka, K., Hassani-Pak, K., Derbyshire, M., Andongabo, A., Devonshire, J., Lysenko, A., Saqi, M., Desai, N.M., Powers, S.J., et al. (2015). Transcriptome and Metabolite Profiling of the Infection Cycle of *Zymoseptoria tritici* on Wheat Reveals a Biphasic Interaction with Plant Immunity Involving Differential Pathogen Chromosomal Contributions and a Variation on the Hemibiotrophic Lifestyle Definition1[OPEN]. Plant Physiol *167*, 1158–1185.

Sachdev, D.P., and Cameotra, S.S. (2013). Biosurfactants in agriculture. Appl Microbiol Biotechnol *97*, 1005–1016.

Savary, S., Willocquet, L., Pethybridge, S.J., Esker, P., McRoberts, N., and Nelson, A. (2019). The global burden of pathogens and pests on major food crops. Nature Ecology & Evolution *3*, 430–439.

Seybold, H., Demetrowitsch, T.J., Hassani, M.A., Szymczak, S., Reim, E., Haueisen, J., Lübbers, L., Rühlemann, M., Franke, A., Schwarz, K., et al. (2020). A fungal pathogen induces systemic susceptibility and systemic shifts in wheat metabolome and microbiome composition. Nature Communications *11*, 1910.

Shekhar, S., Sundaramanickam, A., and Balasubramanian, T. (2015). Biosurfactant Producing Microbes and their Potential Applications: A Review. Critical Reviews in Environmental Science and Technology *45*, 1522–1554.

Siah, A., Deweer, C., Duyme, F., Sanssené, J., Durand, R., Halama, P., and Reignault, P. (2010). Correlation of in planta endo-beta-1,4-xylanase activity with the necrotrophic phase of the hemibiotrophic fungus *Mycosphaerella graminicola*. Plant Pathology *59*, 661–670.

Siah, A., Magnin-Robert, M., Randoux, B., Choma, C., Rivière, C., Halama, P., and Reignault, P. (2018). Natural Agents Inducing Plant Resistance Against Pests and Diseases. In Natural Antimicrobial Agents, J.-M. Mérillon, and C. Riviere, eds. (Cham: Springer International Publishing), pp. 121–159.

Singh, P., Patil, Y., and Rale, V. (2019). Biosurfactant production: emerging trends and promising strategies. J Appl Microbiol *126*, 2–13.

Svensson, J.T., Crosatti, C., Campoli, C., Bassi, R., Stanca, A.M., Close, T.J., and Cattivelli, L. (2006). Transcriptome Analysis of Cold Acclimation in Barley Albina and Xantha Mutants. Plant Physiol *141*, 257–270.

Szabados, L., and Savouré, A. (2010). Proline: a multifunctional amino acid. Trends in Plant Science *15*, 89–97.

Wojakowska, A., Perkowski, J., Góral, T., and Stobiecki, M. (2013). Structural characterization of flavonoid glycosides from leaves of wheat (*Triticum aestivum L.*) using LC/MS/MS profiling of the target compounds. Journal of Mass Spectrometry *48*, 329–339.

Yogendra, K.N., Pushpa, D., Mosa, K.A., Kushalappa, A.C., Murphy, A., and Mosquera, T. (2014). Quantitative resistance in potato leaves to late blight associated with induced hydroxycinnamic acid amides. Funct Integr Genomics *14*, 285–298.

You, J., and Chan, Z. (2015). ROS Regulation During Abiotic Stress Responses in Crop Plants. Front. Plant Sci. *6*.

Zang, L., Zheng, T., Chu, Y., Ding, C., Zhang, W., Huang, Q., and Su, X. (2015). Genome-Wide Analysis of the Fasciclin-Like Arabinogalactan Protein Gene Family Reveals Differential Expression Patterns, Localization, and Salt Stress Response in Populus. Front. Plant Sci. *6*.

Zhang, X., Zhao, X., Feng, C., Liu, N., Feng, H., Wang, X., Mu, X., Huang, L., and Kang, Z. (2014). The cloning and characterization of a DEAD-Box RNA helicase from stress-responsive wheat. Physiological and Molecular Plant Pathology *88*, 36–42.

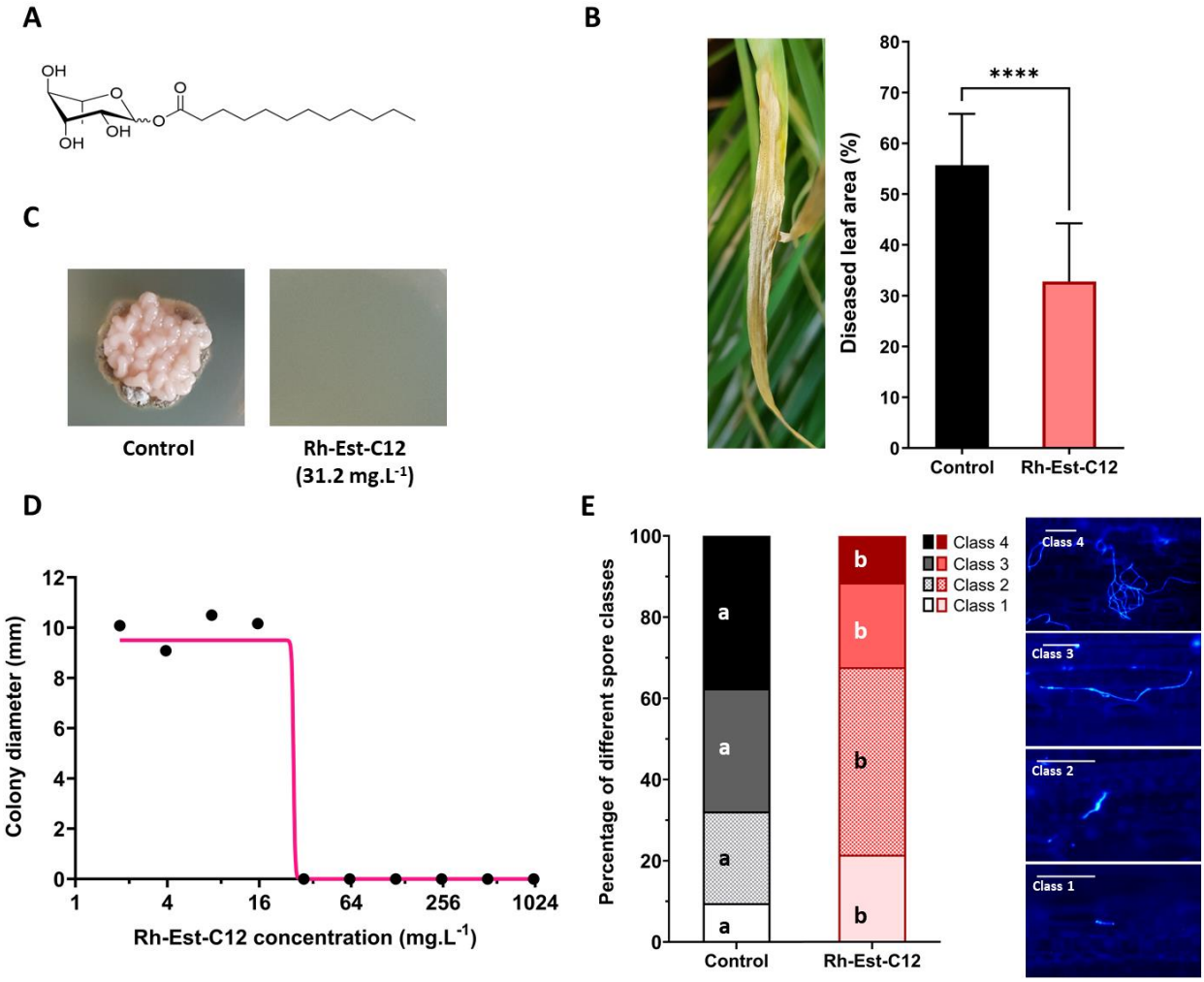

Figure 1. Protective and antifungal effect of the Rh-Est-C12 on wheat (Cv. Alixan) towards *Zymoseptoria tritici* (T02596 strain). (**A**) Molecular structure of the bioinspired synthetic rhamnolipid (RL) Rh-Eth-C12 used in this study. The RL is composed by a rhamnose linked to a C12-carbon chain with an ester bond. (**B**) The disease severity level of septoria tritici blotch was assessed at 23 days after treatment (D23) with Rh-Est-C12 at 500 mg.L^{-1} or mock solution, *i.e* at 21 days after inoculation with the pathogen, by scoring the area chlorosis and necrosis on wheat third-leaves. Results obtained with treated plants were significantly different from control plants according to unpaired t-test ($P \leq 0.05$). Bars stand for standard-deviation (n=36). Representative picture of STB symptoms at D23 on non-treated wheat is shown at the left of the figure. Pictures illustrating colonies in the below *in vitro* assay are presented in (**C**). (**D**) *In vitro* antifungal dose-response curve of Rh-Est-C12 against *Zymoseptoria tritici* (T02596 strain). The direct antifungal activity of the rhamnolipid against the fungal pathogen was assessed by measuring perpendicular diameters of *Z. tritici* colonies after 10 days on PDA medium plates supplemented with different concentrations of the surfactant (n=6). Non-linear regression was designed using GraphPad Prism software version 9. (**E**) *In planta* epiphytic spore development state (class 1: non-germinated spore; class 2: geminated spore with small germ tube; class 3: geminated spore with developed germ tube; class 4: geminated spore with a strongly developed germ tube) was assessed using Calcofluor dye at 5 days after treatment with the Rh-Est-C12 at 500 mg.L^{-1}, *i.e* 3 days after inoculation. The class of 100 distinct spores, selected randomly, was determined, for each condition, on each of the nine third-leaf segments sampled. Within each spore class, the presence of different letters indicates a significant difference according to the Tukey test at $P \leq 0.05$. Scale bar = 25 µm.

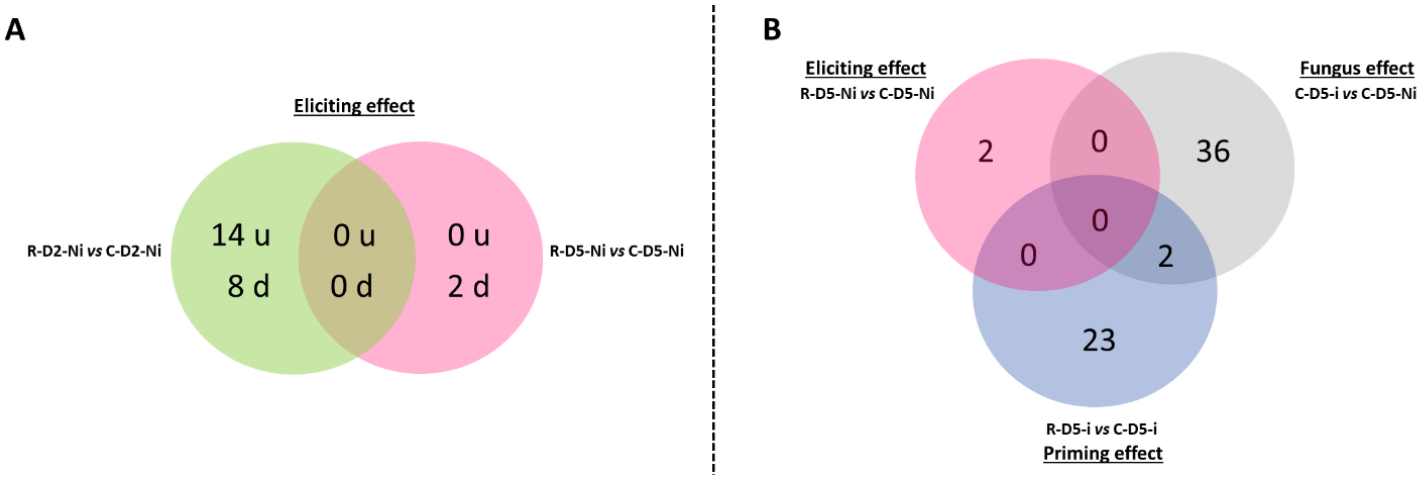

Figure 2: Venn diagrams of the differentially expressed gene number observed during Rh-Est-C12 eliciting, priming as well as *Z. tritici* effects. (A) The effect of the rhamnolipid alone, applied at 500 mg.L^{-1}, on the number of up-regulated (u) and down-regulated (d) was explored at 2 and 5 days after treatment (R-D2-Ni *vs* C-D2-Ni and R-D5-Ni *vs* C-D5-Ni respectively). (B) The eliciting (R-D5-Ni *vs* C-D5-Ni), fungal (C-D5-i *vs* C-D5-Ni) and priming effects (R-D5-i *vs* C-D5-i) on significantly deregulated gene number in wheat third-leaves (Cv. Alixan) were compared at five days after treatment with Rh-Est-C12, *i.e* at three days after infection with *Z. tritici* (T02596 strain)About the codification, C stands for treatment with mock solution while R is for Rh-Est-C12 application. Ni concerns mock inoculated wheat while i means inoculated plants with *Z. tritici*. D2 or D5 indicate that third-leaves were respectively collected at 2 or 5 days after treatment.

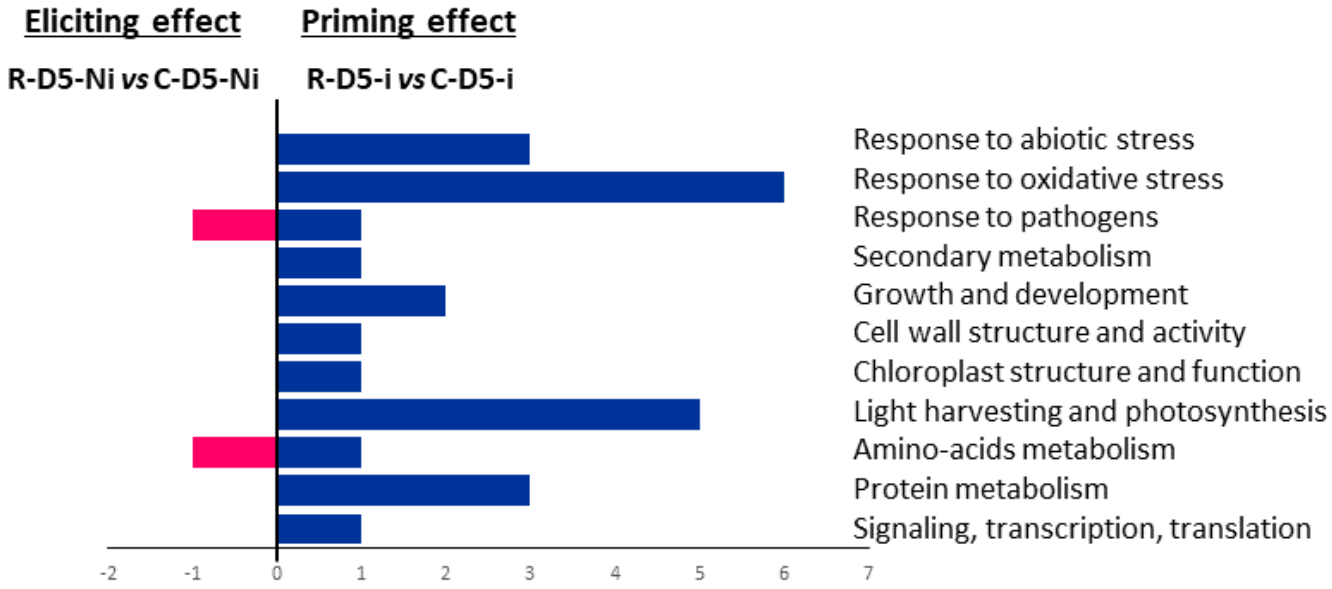

Figure 3: Functional groups of differentially expressed gene number observed in eliciting conditions (R-D5-Ni *vs* C-D5-Ni) compared to priming (R-D5-i *vs* C-D5-i). DEGs were classified in the different functional groups according to NCBI GenBank. About the codification, C stands for treatment with mock solution while R is for Rh-Est-C12 application. Ni concerns mock inoculated wheat while i means inoculated plants with *Z. tritici*. D2 and D5 indicate that third-leaves were respectively collected at 2 and 5 days after treatment.

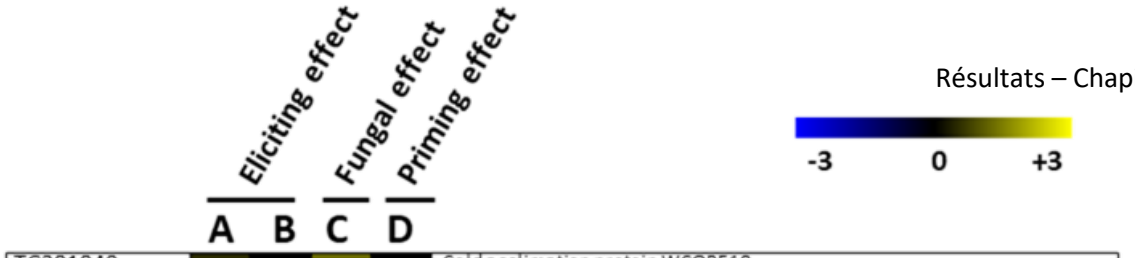

TC381840	Cold acclimation protein WCOR518	Response to abiotic stress
TA54418_4565	Cold acclimation protein WCOR413	
CA624093	Low temperature induced protein	
EF028787	CBFIVd-D22	
EF028785	CBFIVd-A22	
EF028775	CBFIVb-21.1	
AY428036	Dehydration response element binding protein	
TC436852	Hly-III related protein	
TA78527_4565	BZIP transcription factor bZIP110	
TC369712	Salt stress root protein RS1	
TA62779_4565	Aquaporin PIP1	
TA73273_4565	ATP-dependent RNA helicase	
TA61073_4565	Zinc-containing alcohol dehydrogenase superfamily	Response to oxidative stress
CA600821	Metallothioneine type2	
TA84010_4565	Nodulin-like protein	
TA61435_4565	Peroxidase 6	
BQ161851	Peroxidase	
CK212695	Class III peroxidase 62 precursor	
TA66389_4565	Peroxidase precursor	
AF532972	chromosome 6BL thylakoid-bound ascorbate peroxidase	
TA54666_4565	Class I chitinase	Response to pathogens and secondary metabolism
TC426538	Chitinase 2	
TA72415_4565	Chitinase	
TA55707_4565	Thaumatin-like protein TLP4	
TC392855	Protein WIR1A	
TA70475_4565	RGA2	
TA65444_4565	Reticulon	
TA53249_4565	IPS1 riboregulator	
TC442947	ENOD40-like protein	
TA76681_4565	HS1-like protein	
TA50072_4565	Probable pyridoxal biosynthesis protein PDX1.1	
TA84120_4565	Protein EGG APPARATUS-1	Growth and development
DQ435671	alpha tubulin-1D (TUBA-1D)	
TA86474_4565	Auxin Efflux Carrier	
TA56474_4565	Auxin-repressed protein	
TA56454_4565	Auxin-repressed protein	
TA67195_4565	Protein cab-1	
TA72187_4565	Cell Division Protein AAA ATPase family	
TA61883_4565	Sterol desaturase family protein	
TA70788_4565	Dormancy/auxin associated protein	
TA56367_4565	Exoglucanase precursor	Cell wall structure and function
TA56367_4565	Beta-D-glucan exohydrolase isoenzyme ExoI	
TA66611_4565	Fasciclin-like protein FLA15	
TA68562_4565	Glycoside hydrolase, family 19	
CK205454	Non-specific lipid transfer protein 1 precursor	
TA61828_4565	Non-specific lipid-transfer protein	
CK152333	Type 1 non specific lipid transfer protein precursor	
TA87087_4565	Cinnamyl alcohol dehydrogenase	
AB114627	Taxi-III mRNA for xylanase inhibitor TAXI-III	
TA56529_4565	Glutamyl-tRNA reductase 2	Pigment biosynthesis and chloroplast structure
TA92426_4565	Beta-carotene hydroxylase	
TA92734_4565	Diap1 protein	
TA69442_4565	Plastid-specific 30S ribosomal protein 1, chloroplast precursor	
TA56048_4565	Ribulose bisphosphate carboxylase small chain	Light harvesting, photosynthesis, carbohydrate metabolism
TC371150	Chlorophyll a/b-binding protein WCAB precursor	
CK217674	Chloroplast pigment-binding protein CP24	
TA55816_4565	Light-harvesting complex I	
TA53867_4565	Light-induced protein 1-like	
TA59583_4565	Light-regulated protein precursor	
TA72052_4565	Beta-amylase	
TA64535_4565	Glycine decarboxylase P subunit	Amino acid metabolism
TC430171	Indole-3-glycerol phosphate lyase	
TA69140_4565	L-allo-threonine aldolase-related protein	
TA69994_4565	Glutamate dehydrogenase	
TC393988	Glycine/proline-rich protein	
TA60889_4565	S-adenosylmethionine synthetase	
TA59594_4565	22.3kDa heat-shock protein	Protein metabolism
TA64099_4565	Heat shock protein 80	
HM209063	Heat shock protein 70-like (HSP70)	
TC414782	Asparaginase	
TA53535_4565	Ubiquitin carrier protein	
TA78844_4565	Papain-like cysteine peptidase XBCP3	
TA82476_4565	HAP3-like transcriptional-activator	Signaling, transcription, translation
TA52984_4565	Histone H1 WH1B.1	
TC447945	Myb-related protein MYBAS1	
TC450123	rDNA tandem repeat with genes for 18S, 5.8S and 26S rRNA	
CA721206	Zinc finger protein 219	
D16416	Zinc-finger protein WZF1	

Figure 4: Heatmap representation of gene expression deregulation in wheat leaves (Cv. Alixan) caused by the foliar application of 500 mg.L^{-1} Rh-Est-C12 and/or inoculation with *Z. tritici* (T02596 strain) at two (A) and five days after treatment (B, C, D). Columns (A) and (B) illustrate the effect of the rhamnolipid without further inoculation with the fungus, *i.e* the eliciting effect, respectively at two (R-D2-Ni *vs* C-D2-Ni) and five days (R-D5-Ni *vs* C-D5-Ni) after treatment. In (C) is represented the fungal action alone (C-D5-i *vs* C-D5-Ni) while (D) shows the potential priming activity of Rh-Est-C12 (R-D5-i *vs* C-D5-i). Gene-related physiological processes are represented on the right part of the heatmap and were determined using NCBI, AmiGO 2 Gene Ontology, KEGG and UniProt. Significant relative change in gene transcription is expressed in Log2 ratio, according to the yellow-blue color scale, using the WebMev software. C stands for treatment with mock solution while R is for Rh-Est-C12 application. Ni concerns mock inoculated wheat while i means inoculated plants with *Z. tritici*. D2 and D5 indicate that third-leaves were respectively collected at 2 and 5 days after treatment.

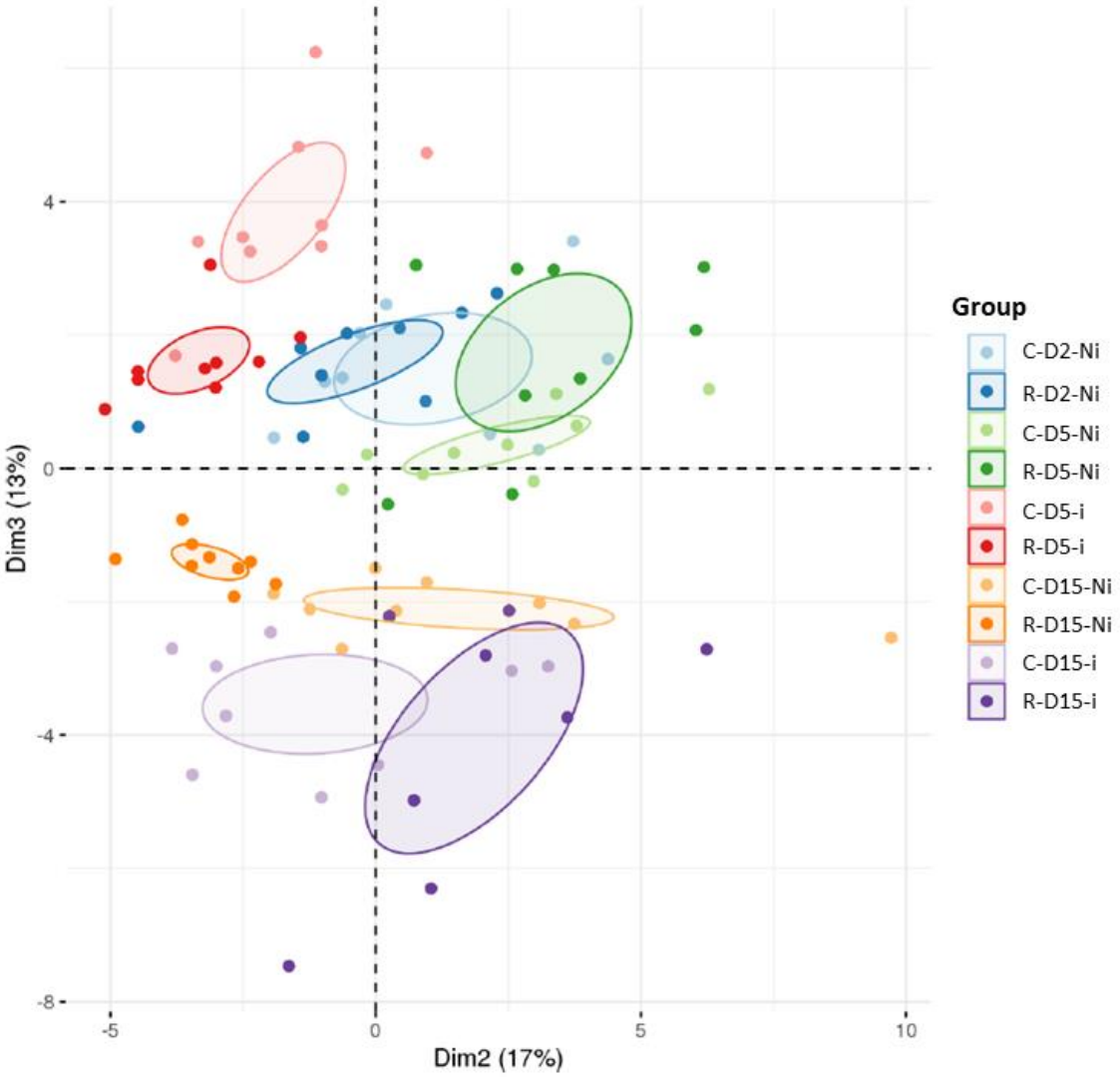

Figure 5: Principal component analysis (PCA) of targeted metabolomic data sets from wheat leaves treated or not with Rh-Est-C12 and/or inoculated with *Z. tritici*. For each modality, nine biological replicates were used. C stands for treatment with mock solution while R is for Rh-Est-C12 application. Ni concerns mock inoculated wheat while i means inoculated plants with *Z. tritici*. D2, D5 and D15 indicate that third-leaves were respectively collected at 2, 5 and 15 days after treatment.

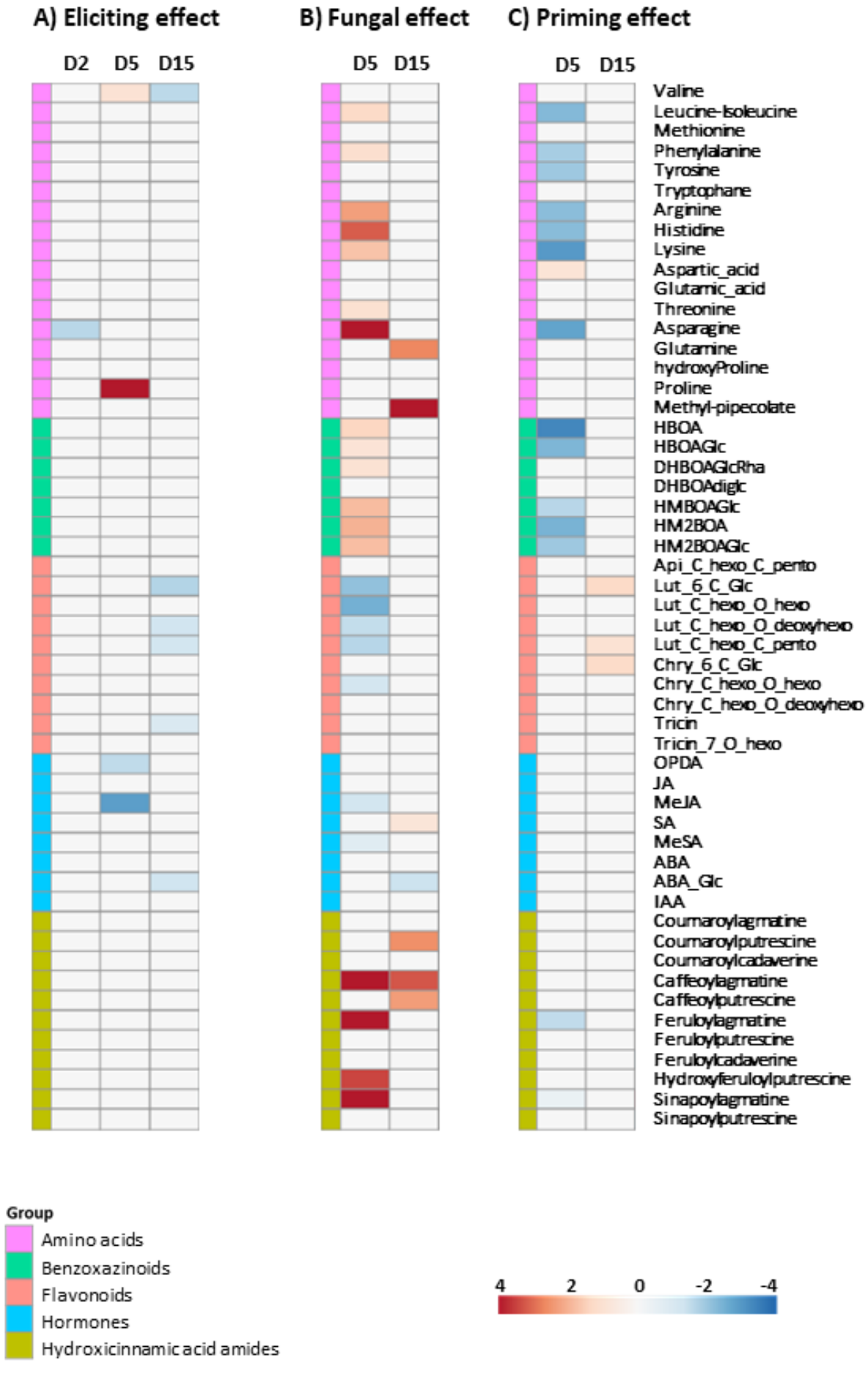
A) Eliciting effect
B) Fungal effect
C) Priming effect
D2
D5
D15
D5
D15
D5
D15
Valine
Leucine-Isoleucine
Methionine
Phenylalanine
Tyrosine
Tryptophane
Arginine
Histidine
Lysine
Aspartic_acid
Glutamic_acid
Threonine
Asparagine
Glutamine
hydroxyProline
Proline
Methyl-pipecolate
HBOA
HBOAGlc
DHBOAGlcRha
DHBOAdiglc
HMBOAGlc
HM2BOA
HM2BOAGlc
Api_C_hexo_C_pento
Lut_6_C_Glc
Lut_C_hexo_O_hexo
Lut_C_hexo_O_deoxyhexo
Lut_C_hexo_C_pento
Chry_6_C_Glc
Chry_C_hexo_O_hexo
Chry_C_hexo_O_deoxyhexo
Tricin
Tricin_7_O_hexo
OPDA
JA
MeJA
SA
MeSA
ABA
ABA_Glc
IAA
Coumaroylagmatine
Coumaroylputrescine
Coumaroylcadaverine
Caffeoylagmatine
Caffeoylputrescine
Feruloylagmatine
Feruloylputrescine
Feruloylcadaverine
Hydroxyferuloylputrescine
Sinapoylagmatine
Sinapoylputrescine
Group
Amino acids
Benzoxazinoids
Flavonoids
Hormones
Hydroxicinnamic acid amides
4
2
0
-2
-4

Figure 6: Heatmap representation of differentially accumulated metabolites within wheat third-leaves (Cv. Alixan) treated or not with Rh-Est-C12 and infected with *Z. tritici* (T02596 strain) or not, at different time-points. With metabolite relative accumulation changes in the (A) eliciting modalities, from the left to the right, R-D2-Ni *vs* C-D2-Ni, R-D5-Ni *vs* C-D5-Ni and R-D15-Ni *vs* C-D15-Ni; (B) fungal modalities, C-D5-i *vs* C-D5-Ni and C-D15-i *vs* C-D15-Ni; (C) priming modalities, R-D5-i *vs* C-D5-i and R-D15-i *vs* C-D15-i. C stands for treatment with mock solution while R is for Rh-Est-C12 application. Ni concerns mock inoculated wheat while i means inoculated plants with *Z. tritici*. D2, D5 and D15 indicate that third-leaves were respectively collected at 2, 5 and 15 days after treatment. Log2 of significant metabolite fold changes for indicated pairwise comparisons are given by shades of red or blue colors according to the corresponding scale bar. Metabolites were grouped according to their functional or chemical family as amino acids, benzoxazinoids, flavonoids, hormones and hydroxycinnamic acid amides. Data represent mean values of nine biological replicates for each condition and time point. Statistical analyses were performed using the Tukey's Honest Significant Difference method followed by a false discovery rate (FDR) correction, with FDR < 0.05. For FDR ≥ 0.05, Log2 fold changes were set to 0.

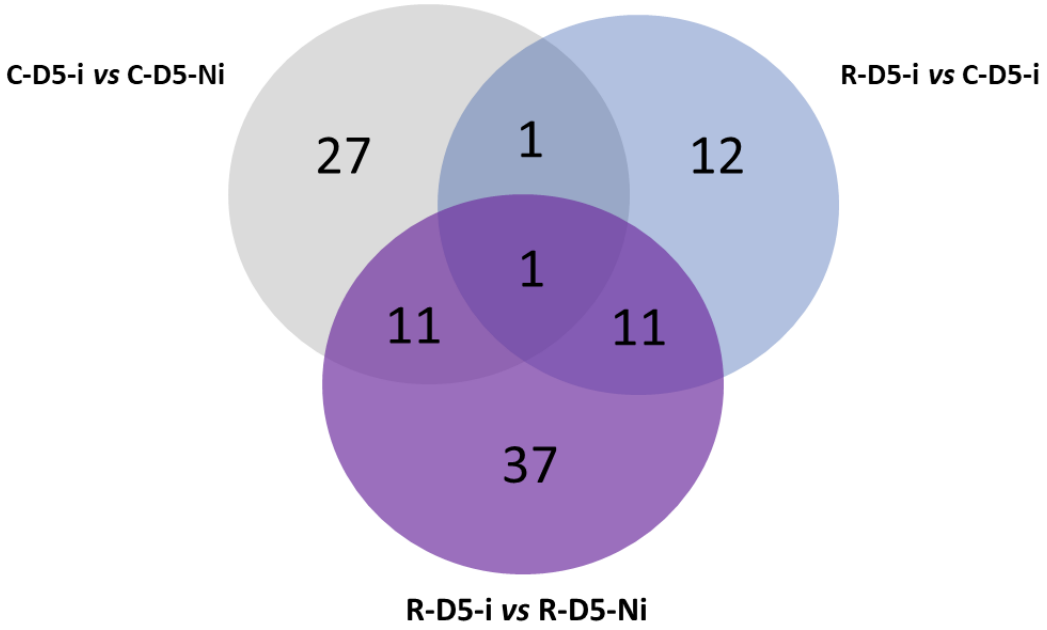

Supplementary Figure S1: Venn diagram of the number of DEGs observed during the fungus effect (C-D5-i *vs* C-D5-Ni), the priming effect (R-D5-i vs C-D5-i) and the whole deregulation on gene expression caused by the rhamnolipid treatment followed by *Z. tritici* infection (R-D5-i *vs* C-D5-Ni) at five days after treatment. Wheat cultivar Alixan, *Z. tritici* T02596 strain and a rhamnolipid concentration of 500 $mg.L^{-1}$ were used. C stands for treatment with mock solution while R is for Rh-Est-C12 application. Ni concerns mock inoculated wheat while i means inoculated plants with *Z. tritici*. D5 indicate that third-leaves were respectively collected at 5 days after treatment.

	A	B		
TA54418_4565			Cold acclimation protein WCOR413	Response to abiotic stress
U73211			Cold acclimation protein WCOR410c (Wcor410c)	
CA624093			Low temperature induced protein	
AF058794			COR39 (cor39)	
TA73273_4565			ATP-dependent RNA helicase	
TA84187_4565			Protein phosphatase type 2-C	
TA92949_4565			Efflux transporter, RND family, MFP subunit	
TA62230_4565			NAC transcription factor	
CF133748			Myb-related protein	
DQ286566			WRKY transcription factor (WRKY)	
TC421665			Transcription factor Myb2	
AY781354			DREB transcription factor 4A (DREB4)	
EF028787			CBFIVd-D22	
EF028785			CBFIVd-A22	
TC369712			Salt stress root protein RS1	
TC436852			Hly-III related proteins	
TA59927_4565			Monodehydroascorbate reductase	
TA59060_4565			22 kDa drought-inducible protein	
TA102260_4565			Nitrite reductase apoprotein	Response to oxidative stress
TC401354			Metallothionein-like protein type 3	
BQ161851			Peroxidase	
CK212695			Class III peroxidase 62 precursor	
TA61435_4565			Peroxidase 6	
TC384087			Glutathione S-transferase	
TA61129_4565			Glutathione transferase	
CA600821			Metallothioneine type2	
TC429241			Peptide methionine sulfoxide reductase	
TA51226_4565			Glutaredoxin	
TC426538			Chitinase 2	Response to pathogens
TA72415_4565			Chitinase	
TC442947			ENOD40-like protein	
EF570122			Pathogen-inducible transcription factor ERF3	
TA76681_4565			HS1-like protein	
TA57993_4565			MutT/nudix-like	
TA84120_4565			Protein EGG APPARATUS-1	Flowering and seed maturation
TC404192			AAA ATPase, central region (50.1 kD)-like protein	
TA70093_4565			U2AF small subunit	
TA86268_4565			CONSTANS interacting protein 5	
TA70788_4565			Dormancy/auxin associated protein	Growth and development
TA61980_4565			Abscisic stress ripening-like protein	
DQ435671			Alpha tubulin-1D (TUBA-1D)	
TC405303			Mitogen-activated protein kinase 7	
L27516			Wcs66	
TA61828_4565			Non-specific lipid-transfer protein	Cell wall structure and function
TA66611_4565			Fasciclin-like protein FLA15	
CK152333			Type 1 non specific lipid transfer protein precursor	
TA87087_4565			Cinnamyl alcohol dehydrogenase	
CK207368			Cellulose synthase BoCesA7	
TA77295_4565			3-ketoacyl-CoA synthase	
TA77906_4565			Hydroxyproline-rich glycoprotein-like	
TA60114_4565			UDP-D-xylose epimerase 2	
TA61116_4565			Non-specific lipid-transfer protein 4.3 precursor	
TA92734_4565			Diap1 protein	Chloroplast structure, light harvesting, carbohydrate metabolism
TC371150			Chlorophyll a/b-binding protein WCAB precursor	
CK217674			Chloroplast pigment-binding protein CP24	
TA55816_4565			Light-harvesting complex I	
TA61423_4565			Chloroplast pigment-binding protein CP24	
TA59583_4565			Light-regulated protein precursor	
EU492898			Ribulose-1,5-bisphosphate carboxylase	
TA70102_4565			Phosphoenolpyruvate carboxykinase	
TA91251_4565			Isoform ERG1b of A2WWV5	
TA52838_4565			Glycine rich protein	Amino acid metabolism
TC393988			Glycine/proline-rich protein	
TA69140_4565			L-allo-threonine aldolase-related protein	
TA69994_4565			Glutamate dehydrogenase	
TA82049_4565			Bifunctional aspartokinase/homoserine dehydrogenase 2	
TA67255_4565			Heat-shock protein precursor	Protein metabolism
HM209063			Heat shock protein 70-like (HSP70)	
TC391450			ATP-dependent Clp protease ATP-binding subunit	
JX104551			SNAP34	
TA53535_4565			Ubiquitin carrier protein	
TA58123_4565			Fatty acid desaturase	Lipid metabolism
TA87662_4565			Acyl-ACP thioesterase	
TA52495_4565			Lysophospholipase-like protein	
TA81385_4565			Phosphoenolpyruvate carboxylase	Signaling, transcription, translation, etc.
TA68843_4565			Exonuclease family protein	
TA54635_4565			EF-hand Ca2+-binding protein CCD1	
TA73684_4565			Serine/threonine protein kinase	
D16416			Zinc-finger protein WZF1	
AY881102			Putative MAPK protein kinase (MAPK1a)	
TA74203_4565			Receptor-like protein kinase	
TA85618_4565			DEAD-box ATP-dependent RNA helicase 26	
CA721206			Zinc finger protein 219	
EF040602			ZIM motif-containing protein	
TA51878_4565			Susceptibility homeodomain transciption factor	
TC389894			Tetratricopeptide repeat (TPR)-containing protein-like	

Supplementary Figure S2: Heatmap representation of differentially expressed genes in (A) wheat leaves treated with Rh-Est-C12 consecutively infected with *Z. tritici*, at five days after treatment, compared to non-infected-leaves that underwent only rhamnolipid application (R-D5-i *vs* R-D5-Ni). In (B), the whole response specter of differential gene expression in wheat leaves caused by foliar application of Rh-Est-C12 and infection with *Z. tritici* compared to control plants is shown (R-D5-i *vs* C-D5-Ni). Wheat cultivar Alixan, *Z. tritici* T02596 strain and a rhamnolipid concentration of 500 $mg.L^{-1}$ were used. Gene-related physiological processes are represented on the right part of the heatmap and were determined using NCBI, AmiGO 2 Gene Ontology, KEGG and UniProt. Significant relative change in gene transcription is expressed in Log2 ratio, according to the yellow-blue color scale, using the WebMev software. C stands for treatment with mock solution while R is for Rh-Est-C12 application. Ni concerns mock inoculated wheat while i means inoculated plants with *Z. tritici*. D5 indicate that third-leaves were respectively collected at 5 days after treatment.

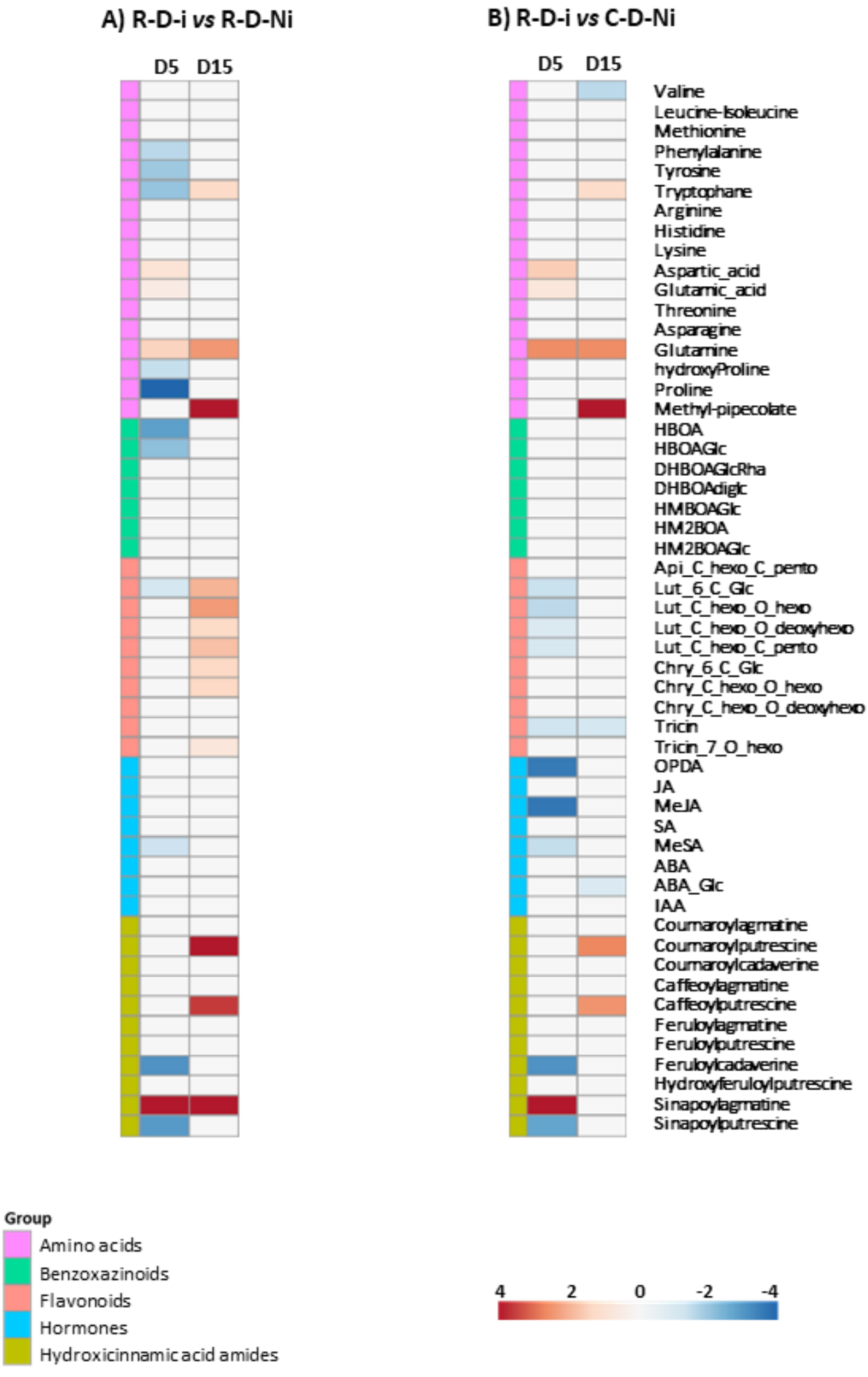
A) R-D-i vs R-D-Ni
D5
D15
B) R-D-i vs C-D-Ni
D5
D15
Valine
Leucine-Isoleucine
Methionine
Phenylalanine
Tyrosine
Tryptophane
Arginine
Histidine
Lysine
Aspartic_acid
Glutamic_acid
Threonine
Asparagine
Glutamine
hydroxyProline
Proline
Methyl-pipecolate
HBOA
HBOAGlc
DHBOAGlcRha
DHBOAdiglc
HMBOAGlc
HM2BOA
HM2BOAGlc
Api_C_hexo_C_pento
Lut_6_C_Glc
Lut_C_hexo_O_hexo
Lut_C_hexo_O_deoxyhexo
Lut_C_hexo_C_pento
Chry_6_C_Glc
Chry_C_hexo_O_hexo
Chry_C_hexo_O_deoxyhexo
Tricin
Tricin_7_O_hexo
OPDA
JA
MeJA
SA
MeSA
ABA
ABA_Glc
IAA
Coumaroylagmatine
Coumaroylputrescine
Coumaroylcadaverine
Caffeoylagmatine
Caffeoylputrescine
Feruloylagmatine
Feruloylputrescine
Feruloylcadaverine
Hydroxyferuloylputrescine
Sinapoylagmatine
Sinapoylputrescine
Group
Amino acids
Benzoxazinoids
Flavonoids
Hormones
Hydroxicinnamic acid amides
4
2
0
-2
-4

Supplementary Figure S3: Heatmap of significant relative changes in metabolite accumulation pattern within wheat third-leaves (Cv. Alixan) following Rh-Est-C12 application at different time-points. Pairwise comparisons performed, from the left to the right, correspond to (A) R-D5-i *vs* R-D5-Ni, R-D15-i *vs* R-D15-Ni and (B) R-D5-i *vs* C-D5-Ni, R-D15-i *vs* C-D15-Ni. C stands for treatment with mock solution while R is for Rh-Est-C12 application. Ni concerns mock inoculated wheat while i means inoculated plants with *Z. tritici*. D2, D5 and D15 indicate that third-leaves were respectively collected at 2, 5 and 15 days after treatment. Log2 of significant metabolite fold changes for indicated pairwise comparisons are given by shades of red or blue colors according to the corresponding scale bar. Metabolites were grouped according to their functional or chemical family as amino acids, benzoxazinoids, flavonoids, hormones and hydroxycinnamic acid amides. Data represent mean values of nine biological replicates for each condition and time point. Statistical analyses were performed using the Tukey's Honest Significant Difference method followed by a false discovery rate (FDR) correction, with FDR < 0.05. For FDR ≥ 0.05, Log2 fold changes were set to 0.

Supplementary Table S1: Alterations in gene expression pattern responses of wheat leaves caused by the eliciting effect of Rh-Est-C12 at two (A) and five (B) days after treatment, respectively (R-D2-Ni *vs* C-D2-Ni) and (R-D5-Ni *vs* C-D5-Ni), the *Zymoseptoria tritici* infection (C-D5-i *vs* C-D5-Ni) and observed during (D) rhamnolipid priming conditions (R-D5-i *vs* C-D5-i). This table is related to Figure 4. Wheat cultivar Alixan, *Z. tritici* T02596 strain and a rhamnolipid concentration of 500 $mg.L^{-1}$ were used. Gene-related physiological processes are represented on the right part of the table and were determined using NCBI, AmiGO 2 Gene Ontology, KEGG and UniProt. C stands for treatment with mock solution while R is for Rh-Est-C12 application. Ni concerns mock inoculated wheat while i means inoculated plants with *Z. tritici*. D2 and D5 indicate that third-leaves were respectively collected at 2 and 5 days after treatment. Top Hit, ID and reference numbers are also presented.

	Eliciting effect		Fungal effect	Priming effect				
	A	B	C	D				
Name	R-D2-Ni *vs* C-D2-Ni	R-D5-Ni vs C-D5-Ni	C-D5-i *vs* C-D5-Ni	R-D5-i *vs* C-D5-i	Description	TopHit	ID	RefNumber
Response to abiotic stress								
TC381840	2,4760	1,0000	3,0605	1,0000	Cold acclimation protein WCOR518	tc|TC381840	A_99_P421457	19082
TA54418_4565	1,0000	1,0000	2,5297	1,0000	Cold acclimation protein WCOR413	ta|TA54418_4565|	A_99_P210931	43524
CA624093	1,0000	1,0000	8,8824	1,0000	Low temperature induced protein	ta|CA624093|ta|C	A_99_P459967	11840
EF028787	1,0000	1,0000	0,3043	1,0000	CBFIVd-D22	gb|EF028787|ta|T	A_99_P405352	948
EF028785	1,0000	1,0000	0,2543	1,0000	CBFIVd-A22	gb|EF028785|gb|E	A_99_P140518	15660
EF028775	1,0000	1,0000	0,2535	1,0000	CBFIVb-21.1	gb|EF028775|tc|T	A_99_P012439	20101
AY428036	1,0000	1,0000	0,3768	1,0000	Dehydration response element binding protein	gb|AY428036|gb|E	A_99_P074325	23922
TC436852	1,0000	1,0000	0,2955	1,0000	Hly-III related protein	tc|TC436852	A_99_P511722	6696
TA78527_4565	1,0000	1,0000	0,4594	1,0000	BZIP transcription factor bZIP110	ta|TA78527_4565|	A_99_P289066	42528
TC369712	1,0000	1,0000	1,0000	0,4755	Salt stress root protein RS1	tc|TC369712	A_99_P407642	6772
TA62779_4565	1,0000	1,0000	1,0000	3,4587	Aquaporin PIP1	ta|TA62779_4565|	A_99_P234106	9903
TA73273_4565	1,0000	1,0000	1,0000	2,8643	ATP-dependent RNA helicase	ta|TA73273_4565|	A_99_P430447	24209
Response to oxidative stress								
TA61073_4565	1,0000	1,0000	0,3344	1,0000	Zinc-containing alcohol dehydrogenase superfamily	ta|TA61073_4565|	A_99_P408522	21811
CA600821	1,0000	1,0000	0,2760	1,0000	Metallothioneine type2	ta|CA600821|tc|T	A_99_P460107	16140
TA84010_4565	2,9456	1,0000	1,0000	0,3796	Nodulin-like protein	ta|TA84010_4565|	A_99_P307876	15025
TA61435_4565	0,3348	1,0000	1,0000	0,1487	Peroxidase 6	ta|TA61435_4565|	A_99_P415477	32597
BQ161851	1,0000	1,0000	1,0000	0,2850	Peroxidase	ta|BQ161851|tc|T	A_99_P431937	25512
CK212695	1,0000	1,0000	1,0000	0,3180	Class III peroxidase 62 precursor	ta|CK212695|tc|T	A_99_P407997	44165
TA66389_4565	1,0000	1,0000	1,0000	0,2922	Peroxidase precursor	ta|TA66389_4565|	A_99_P247391	14997
AF532972	1,0000	1,0000	1,0000	0,4802	chromosome 6BL thylakoid-bound ascorbate peroxidase	gb|AF532972|gb|A	A_99_P259786	38976
Response to pathogens								
TA54666_4565	1,0000	0,2924	1,0000	1,0000	Class I chitinase	ta|TA54666_4565|	A_99_P211671	41435
TC426538	1,0000	1,0000	13,5307	1,0000	Chitinase 2	tc|TC426538	A_99_P488752	20923
TA72415_4565	1,0000	1,0000	4,8597	1,0000	Chitinase	ta|TA72415_4565|	A_99_P268406	11345
TA55707_4565	1,0000	1,0000	3,4425	1,0000	Thaumatin-like protein TLP4	ta|TA55707_4565|	A_99_P509202	23176
TC392855	1,0000	1,0000	0,5507	1,0000	Protein WIR1A	tc|TC392855	A_99_P060636	28568
TA70475_4565	1,0000	1,0000	0,4104	1,0000	RGA2	ta|TA70475_4565|	A_99_P433007	20640
TA65444_4565	1,0000	1,0000	0,3907	1,0000	Reticulon	ta|TA65444_4565|	A_99_P412857	7188
TA53249_4565	1,0000	1,0000	0,2556	1,0000	IPS1 riboregulator	ta|TA53249_4565|	A_99_P207336	20707
TC442947	1,0000	1,0000	0,3281	1,0000	ENOD40-like protein	tc|TC442947	A_99_P525387	1183
TA76681_4565	1,0000	1,0000	1,0000	0,2666	HS1-like protein	ta|TA76681_4565|	A_99_P194333	16022
Secondary metabolism								
TA50072_4565	1,0000	1,0000	1,0000	3,6839	Probable pyridoxal biosynthesis protein PDX1.1	ta|TA50072_4565|	A_99_P197801	18956
Flowering and seed maturation								
TA84120_4565	1,0000	1,0000	0,2751	1,0000	Protein EGG APPARATUS-1	ta|TA84120_4565|	A_99_P308216	36050
Growth and development								
DQ435671	4,0224	1,0000	1,0000	1,0000	alpha tubulin-1D (TUBA-1D)	gb|DQ435671|ta|T	A_99_P012999	6685
TA86474_4565	4,6137	1,0000	1,0000	1,0000	Auxin Efflux Carrier	ta|TA86474_4565|	A_99_P192117	12326
TA56474_4565	0,3507	1,0000	1,0000	1,0000	Auxin-repressed protein	ta|TA56474_4565|	A_99_P215841	35480
TA56454_4565	0,2896	1,0000	1,0000	1,0000	Auxin-repressed protein	ta|TA56454_4565|	A_99_P215761	27870
TA67195_4565	0,3445	1,0000	1,0000	1,0000	Protein cab-1	ta|TA67195_4565|	A_99_P250166	16476
TA72187_4565	1,0000	1,0000	0,2876	1,0000	Cell Division Protein AAA ATPase family	ta|TA72187_4565|	A_99_P267636	41732
TA61883_4565	1,0000	1,0000	1,0000	3,5486	Sterol desaturase family protein	ta|TA61883_4565|	A_99_P231241	32885
TA70788_4565	1,0000	1,0000	1,0000	0,2813	Dormancy/auxin associated protein	ta|TA70788_4565|	A_99_P262826	45151

	Eliciting effect		Fungal effect	Priming effect				
	A	B	C	D				
Name	R-D2-Ni *vs* C-D2-Ni	R-D5-Ni vs C-D5-Ni	C-D5-i *vs* C-D5-Ni	R-D5-i *vs* C-D5-i	Description	TopHit	ID	RefNumber
Cell wall structure and function								
TA56367_4565	0,5407	1,0000	1,0000	1,0000	Exoglucanase precursor	ta|TA56367_456	A_99_P215601	6504
TA56367_4565	0,4738	1,0000	1,0000	1,0000	Beta-D-glucan exohydrolase isoenzyme ExoI	ta|TA56367_456	A_99_P433432	15270
TA66611_4565	8,6860	1,0000	0,3372	1,0000	Fasciclin-like protein FLA15	ta|TA66611_456	A_99_P248201	22500
TA68562_4565	1,0000	1,0000	0,3766	1,0000	Glycoside hydrolase, family 19	ta|TA68562_456	A_99_P255031	1863
CK205454	1,0000	1,0000	0,3699	1,0000	Non-specific lipid transfer protein 1 precursor	ta|CK205454|tc|	A_99_P427502	36085
TA61828_4565	1,0000	1,0000	0,3668	1,0000	Non-specific lipid-transfer protein	ta|TA61828_456	A_99_P231006	27677
CK152333	1,0000	1,0000	0,3202	1,0000	Type 1 non specific lipid transfer protein precursor	ta|CK152333|tc|	A_99_P446157	36915
TA87087_4565	1,0000	1,0000	0,0592	1,0000	Cinnamyl alcohol dehydrogenase	ta|TA87087_456	A_99_P318481	8569
AB114627	1,0000	1,0000	1,0000	0,3116	Taxi-III mRNA for xylanase inhibitor TAXI-III	gb|AB114627|gb	A_99_P195998	22657
Pigment biosynthesis								
TA56529_4565	2,1599	1,0000	1,0000	1,0000	Glutamyl-tRNA reductase 2	ta|TA56529_456	A_99_P216016	43656
TA92426_4565	4,5534	1,0000	1,0000	1,0000	Beta-carotene hydroxylase	ta|TA92426_456	A_99_P336181	23802
Chloroplast structure and function								
TA92734_4565	1,0000	1,0000	0,3150	1,0000	Diap1 protein	ta|TA92734_456	A_99_P337136	42984
TA69442_4565	1,0000	1,0000	1,0000	0,2943	Plastid-specific 30S ribosomal protein 1, chloroplast precursor	ta|TA69442_456	A_99_P258121	37451
Light harvesting and photosynthesis								
TA56048_4565	2,3370	1,0000	1,0000	1,0000	Ribulose bisphosphate carboxylase small chain	ta|TA56048_456	A_99_P444042	23343
TC371150	4,0099	1,0000	1,0000	0,1805	Chlorophyll a/b-binding protein WCAB precursor	tc|TC371150	A_99_P409112	19146
CK217674	3,3076	1,0000	1,0000	0,3216	Chloroplast pigment-binding protein CP24	ta|CK217674|tc|	A_99_P437157	39278
TA55816_4565	1,0000	1,0000	1,0000	0,5050	Light-harvesting complex I	ta|TA55816_456	A_99_P214401	27084
TA53867_4565	1,0000	1,0000	1,0000	0,3512	Light-induced protein 1-like	ta|TA53867_456	A_99_P209081	23883
TA59583_4565	1,0000	1,0000	1,0000	0,3590	Light-regulated protein precursor	ta|TA59583_456	A_99_P223636	16866
Carbohydrate metabolism								
TA72052_4565	0,4187	1,0000	1,0000	1,0000	Beta-amylase	ta|TA72052_456	A_99_P009886	12260
Amino-acids metabolism								
TA64535_4565	1,0000	1,0000	0,3402	1,0000	Glycine decarboxylase P subunit	ta|TA64535_456	A_99_P240211	15342
TC430171	1,0000	1,0000	0,0893	1,0000	Indole-3-glycerol phosphate lyase	tc|TC430171	A_99_P496502	8009
TA69140_4565	1,0000	1,0000	0,3061	1,0000	L-allo-threonine aldolase-related protein	ta|TA69140_456	A_99_P449637	41850
TA69994_4565	1,0000	1,0000	0,3764	1,0000	Glutamate dehydrogenase	ta|TA69994_456	A_99_P259951	10977
TC393988	1,0000	1,0000	0,1308	1,0000	Glycine/proline-rich protein	tc|TC393988	A_99_P543657	7174
TA60889_4565	1,0000	1,0000	1,0000	2,8554	S-adenosylmethionine synthetase	ta|TA60889_456	A_99_P227511	9678
Protein metabolism								
TA59594_4565	3,2559	1,0000	1,0000	1,0000	22.3kDa heat-shock protein	ta|TA59594_456	A_99_P223676	44575
TA64099_4565	2,6016	1,0000	0,1519	3,4096	Heat shock protein 80	ta|TA64099_456	A_99_P238761	26
HM209063	1,0000	1,0000	0,2354	2,1997	Heat shock protein 70-like (HSP70)	gb|HM209063|g	A_99_P234541	16785
TC414782	1,0000	1,0000	0,2639	1,0000	Asparaginase	tc|TC414782	A_99_P466942	23822
TA53535_4565	1,0000	1,0000	0,1923	1,0000	Ubiquitin carrier protein	ta|TA53535_456	A_99_P208256	24763
TA78844_4565	1,0000	1,0000	1,0000	0,4606	Papain-like cysteine peptidase XBCP3	ta|TA78844_456	A_99_P290171	29285
Signaling, transcription, translation								
TA82476_4565	3,7353	1,0000	1,0000	1,0000	HAP3-like transcriptional-activator	ta|TA82476_456	A_99_P302726	42546
TA52984_4565	3,6271	1,0000	1,0000	1,0000	Histone H1 WH1B.1	ta|TA52984_456	A_99_P497187	27663
TC447945	0,4220	1,0000	1,0000	1,0000	Myb-related protein MYBAS1	tc|TC447945	A_99_P538902	19305
TC450123	1,0000	0,0664	1,0000	1,0000	rDNA tandem repeat with genes for 18S, 5.8S and 26S rRNA	tc|TC450123	A_99_P544312	866
CA721206	1,0000	1,0000	0,3296	1,0000	Zinc finger protein 219	ta|CA721206|tc|	A_99_P533942	44850
D16416	1,0000	1,0000	1,0000	0,5072	Zinc-finger protein WZF1	gb|D16416|ta|T	A_99_P489622	10858

Supplementary Table S2: Alterations in gene expression pattern responses illustrating (A) R-D5-i *versus* R-D5-Ni as well as (B), the whole response of wheat to the rhamnolipid and the pathogen, R-D5-i *versus* C-D5-Ni. This table is related to Supplementary Figure S4 . Wheat cultivar Alixan, *Z. tritici* T02596 strain and a rhamnolipid concentration of 500 $mg.L^{-1}$ were used. Gene-related physiological processes are represented on the right part of the table and were determined using NCBI, AmiGO 2 Gene Ontology, KEGG and UniProt. C stands for treatment with mock solution while R is for Rh-Est-C12 application. Ni concerns mock inoculated wheat while i means inoculated plants with *Z. tritici*. D5 indicate that third-leaves were collected at 5 days after treatment. Top Hit, ID and reference numbers are also presented.

	A	B				
Name	R-D5-i *vs* R-D5-Ni	R-D5-i *vs* C-D5-Ni	Description	TopHit	ID	RefNumber
Response to abiotic stress						
TA54418_4565	7,4785	1,0000	Cold acclimation protein WCOR413	ta|TA54418_456	A_99_P210931	43524
U73211	2,6271	1,0000	Cold acclimation protein WCOR410c (Wcor410c)	gb|U73211|gb|U	A_99_P509672	30914
CA624093	3,1237	6,3201	Low temperature induced protein	ta|CA624093|ta	A_99_P459967	11840
AF058794	3,2216	2,8069	COR39 (cor39)	gb|AF058794|gb	A_99_P000281	39752
TA73273_4565	4,6451	4,6272	ATP-dependent RNA helicase	ta|TA73273_456	A_99_P430447	24209
TA84187_4565	0,3340	1,0000	Protein phosphatase type 2-C	ta|TA84187_456	A_99_P308421	21815
TA92949_4565	0,2647	1,0000	Efflux transporter, RND family, MFP subunit	ta|TA92949_456	A_99_P144213	15689
TA62230_4565	0,3470	1,0000	NAC transcription factor	ta|TA62230_456	A_99_P232346	6986
CF133748	0,5054	1,0000	Myb-related protein	ta|CF133748|tc|	A_99_P453952	5264
DQ286566	0,3439	0,4157	WRKY transcription factor (WRKY)	gb|DQ286566|ta	A_99_P455767	42312
TC421665	0,4667	0,5449	Transcription factor Myb2	tc|TC421665|tc|	A_99_P479147	37654
AY781354	0,4658	0,4330	DREB transcription factor 4A (DREB4)	gb|AY781354|gb	A_99_P197071	14918
EF028787	0,3331	0,2706	CBFIVd-D22	gb|EF028787|ta	A_99_P405352	948
EF028785	0,3488	0,2629	CBFIVd-A22	gb|EF028785|gb	A_99_P140518	15660
TC369712	0,2693	0,2597	Salt stress root protein RS1	tc|TC369712	A_99_P407642	6772
TC436852	1,0000	0,3734	Hly-III related proteins	tc|TC436852	A_99_P511722	6696
TA59927_4565	1,0000	0,4435	Monodehydroascorbate reductase	ta|TA59927_456	A_99_P224741	7355
TA59060_4565	1,0000	0,3945	22 kDa drought-inducible protein	ta|TA59060_456	A_99_P222071	24327
Response to oxidative stress						
TA102260_4565	7,7725	7,2280	Nitrite reductase apoprotein	ta|TA102260_45	A_99_P366657	8326
TC401354	0,4472	1,0000	Metallothionein-like protein type 3	tc|TC401354	A_99_P446677	44649
BQ161851	0,4760	0,4200	Peroxidase	ta|BQ161851|tc	A_99_P431937	25512
CK212695	0,4174	0,3184	Class III peroxidase 62 precursor	ta|CK212695|tc|	A_99_P407997	44165
TA61435_4565	0,1741	0,2027	Peroxidase 6	ta|TA61435_456	A_99_P415477	32597
TC384087	0,4739	0,4275	Glutathione S-transferase	tc|TC384087	A_99_P411017	6865
TA61129_4565	0,4062	0,4092	Glutathione transferase	ta|TA61129_456	A_99_P228341	15064
CA600821	0,4414	0,3408	Metallothioneine type2	ta|CA600821|tc|	A_99_P460107	16140
TC429241	1,0000	0,4463	Peptide methionine sulfoxide reductase	tc|TC429241	A_99_P494392	29872
TA51226_4565	1,0000	0,4196	Glutaredoxin	ta|TA51226_456	A_99_P200897	45008
Response to pathogens						
TC426538	3,2690	6,6861	Chitinase 2	tc|TC426538	A_99_P488752	20923
TA72415_4565	1,0000	3,1080	Chitinase	ta|TA72415_456	A_99_P268406	11345
TC442947	0,3054	0,3054	ENOD40-like protein	tc|TC442947	A_99_P525387	1183
EF570122	0,3191	0,3950	Pathogen-inducible transcription factor ERF3	gb|EF570122|gb	A_99_P177974	11088
TA76681_4565	0,3038	1,0000	HS1-like protein	ta|TA76681_456	A_99_P194333	16022
TA57993_4565	0,3685	1,0000	MutT/nudix-like	ta|TA57993_456	A_99_P219466	4113
Flowering and seed maturation						
TA84120_4565	0,3312	0,3269	Protein EGG APPARATUS-1	ta|TA84120_456	A_99_P308216	36050
TC404192	1,0000	0,4137	AAA ATPase, central region (50.1 kD)-like protein	tc|TC404192	A_99_P450607	15744
TA70093_4565	1,0000	0,4476	U2AF small subunit	ta|TA70093_456	A_99_P260356	14065
TA86268_4565	1,0000	6,3553	CONSTANS interacting protein 5	ta|TA86268_456	A_99_P315626	21018

	A	B				
Name	R-D5-i *vs* R-D5-Ni	R-D5-i *vs* C-D5-Ni	Description	TopHit	ID	RefNumber
Growth and development						
TA70788_4565	0,3873	0,4173	Dormancy/auxin associated protein	ta|TA70788_456	A_99_P262826	45151
TA61980_4565	1,0000	0,3849	Abscisic stress ripening-like protein	ta|TA61980_456	A_99_P231656	43647
DQ435671	1,0000	0,3752	Alpha tubulin-1D (TUBA-1D)	gb|DQ435671|ta	A_99_P012999	6685
TC405303	0,3142	1,0000	Mitogen-activated protein kinase 7	tc|TC405303	A_99_P452302	22398
L27516	3,3956	1,0000	Wcs66	gb|L27516|gb|M	A_99_P167734	4367
Cell wall structure and activity						
TA61828_4565	1,0000	0,3999	Non-specific lipid-transfer protein	ta|TA61828_456	A_99_P231006	27677
TA66611_4565	1,0000	0,2492	Fasciclin-like protein FLA15	ta|TA66611_456	A_99_P248201	22500
CK152333	1,0000	0,2855	Type 1 non specific lipid transfer protein precursor	ta|CK152333|tc|	A_99_P446157	36915
TA87087_4565	1,0000	0,0944	Cinnamyl alcohol dehydrogenase	ta|TA87087_456	A_99_P318481	8569
CK207368	1,0000	0,5232	Cellulose synthase BoCesA7	ta|CK207368|tc|	A_99_P424332	22342
TA77295_4565	1,0000	0,4688	3-ketoacyl-CoA synthase	ta|TA77295_456	A_99_P284791	23697
TA77906_4565	0,4527	0,4223	Hydroxyproline-rich glycoprotein-like	ta|TA77906_456	A_99_P286926	32415
TA60114_4565	0,4000	0,4045	UDP-D-xylose epimerase 2	ta|TA60114_456	A_99_P412027	14821
TA61116_4565	0,4933	0,3082	Non-specific lipid-transfer protein 4.3 precursor	ta|TA61116_456	A_99_P228291	22943
Chloroplast structure and function						
TA92734_4565	1,0000	0,1752	Diap1 protein	ta|TA92734_456	A_99_P337136	42984
Light harvesting and photosynthesis						
TC371150	0,2371	0,2858	Chlorophyll a/b-binding protein WCAB precursor	tc|TC371150	A_99_P409112	19146
CK217674	0,3347	0,3749	Chloroplast pigment-binding protein CP24	ta|CK217674|tc|	A_99_P437157	39278
TA55816_4565	1,0000	0,4759	Light-harvesting complex I	ta|TA55816_456	A_99_P214401	27084
TA61423_4565	1,0000	0,4533	Chloroplast pigment-binding protein CP24	ta|TA61423_456	A_99_P229541	44166
TA59583_4565	0,4288	1,0000	Light-regulated protein precursor	ta|TA59583_456	A_99_P223636	16866
EU492898	0,4845	1,0000	Ribulose-1,5-bisphosphate carboxylase	gb|EU492898|ta	A_99_P625436	18029
Carbohydrate metabolism						
TA70102_4565	0,2493	0,3105	Phosphoenolpyruvate carboxykinase	ta|TA70102_456	A_99_P260386	18755
TA91251_4565	0,2911	0,3341	Isoform ERG1b of A2WWV5	ta|TA91251_456	A_99_P332361	17064
Amino-acids metabolism						
TA52838_4565	4,0093	4,5867	Glycine rich protein	ta|TA52838_456	A_99_P163692	5193
TC393988	0,2677	0,2183	Glycine/proline-rich protein	tc|TC393988	A_99_P543657	7174
TA69140_4565	0,2624	0,2234	L-allo-threonine aldolase-related protein	ta|TA69140_456	A_99_P449637	41850
TA69994_4565	0,2422	0,2621	Glutamate dehydrogenase	ta|TA69994_456	A_99_P259951	10977
TA82049_4565	1,0000	2,7976	Bifunctional aspartokinase/homoserine dehydrogenase 2, chloroplast prec	ta|TA82049_456	A_99_P163227	42192

	A	B				
Name	R-D5-i *vs* R-D5-Ni	R-D5-i *vs* C-D5-Ni	Description	TopHit	ID	RefNumber
Protein metabolism						
TA67255_4565	3,3495	3,5074	Heat-shock protein precursor	ta|TA67255_456	A_99_P250376	10187
HM209063	0,5698	0,5177	Heat shock protein 70-like (HSP70)	gb|HM209063|g	A_99_P234541	16785
TC391450	0,2458	1,0000	ATP-dependent Clp protease ATP-binding subunit	tc|TC391450	A_99_P433687	20222
JX104551	0,3942	1,0000	SNAP34	gb|JX104551|ta|	A_99_P292561	27821
TA53535_4565	1,0000	0,3973	Ubiquitin carrier protein	ta|TA53535_456	A_99_P208256	24763
Lipid metabolism						
TA58123_4565	0,4510	1,0000	Fatty acid desaturase	ta|TA58123_456	A_99_P219611	11349
TA87662_4565	1,0000	0,4479	Acyl-ACP thioesterase	ta|TA87662_456	A_99_P437477	32120
TA52495_4565	1,0000	0,4527	Lysophospholipase-like protein	ta|TA52495_456	A_99_P204796	24058
Signaling, transcription, translation						
TA81385_4565	5,0694	4,3236	Phosphoenolpyruvate carboxylase	ta|TA81385_456	A_99_P299011	44004
TA68843_4565	0,4674	0,3908	Exonuclease family protein	ta|TA68843_456	A_99_P256071	41928
TA54635_4565	0,2322	0,3794	EF-hand Ca2+-binding protein CCD1	ta|TA54635_456	A_99_P165947	28159
TA73684_4565	0,3243	0,3771	Serine/threonine protein kinase	ta|TA73684_456	A_99_P423972	31763
D16416	0,2334	0,2611	Zinc-finger protein WZF1	gb|D16416|ta|T	A_99_P489622	10858
AY881102	0,4348	1,0000	Putative MAPK protein kinase (MAPK1a)	gb|AY881102|ta	A_99_P014394	16503
TA74203_4565	0,3949	1,0000	Receptor-like protein kinase	ta|TA74203_456	A_99_P274251	4201
TA85618_4565	1,0000	3,9979	DEAD-box ATP-dependent RNA helicase 26	ta|TA85618_456	A_99_P313296	14881
CA721206	1,0000	0,4445	Zinc finger protein 219	ta|CA721206|tc|	A_99_P533942	44850
EF040602	1,0000	0,4563	ZIM motif-containing protein	gb|EF040602|ta	A_99_P614787	18006
TA51878_4565	1,0000	0,4278	Susceptibility homeodomain transciption factor	ta|TA51878_456	A_99_P202881	23811
Other functions						
TC389894	3,9449	4,0264	Tetratricopeptide repeat (TPR)-containing protein-like	tc|TC389894	A_99_P431697	38421

Supplementary Table S3: List of the 54 metabolites detected in wheat leaves (cv. Alixan) with ultra-high-performance liquid chromatography-mass spectrometry (UHPLC-MS), using a targeted metabolomic approach. Metabolites were classified according to KEGG (Kyoto Encyclopedia of Genes and Genomes; http://www.genome.ad.jp/kegg) and PubChem (http://pubchem.ncbi.nlm.nih.gov) databases. Id: identifier; m/z: mass-to-charge ratio; m/z error (difference between the measured m/z and the calculated m/z of an ion, in ppm); RT: retention time. (*) correspond to metabolites confirmed with authentic standards.

Id	Metabolite	Formula	Class [a]	Detected *m/z*	*m/z* error (ppm)	RT (min)	KEGG ID	PubChem CID
1	**Arginine**	$C_6H_{14}N_4O_2$	Amino acids	175.1190	0.20	0,85	C00062	6322
2	**Asparagine**	$C_4H_8N_2O_3$	Amino acids	133.0609	0.86	0,98	C00152	6267
3	**Aspartic acid**	$C_4H_7NO_4$	Amino acids	134.0449	0.69	1,02	C00049	5960
4	**Glutamic acid**	$C_5H_9NO_4$	Amino acids	148.0604	0,77	1,01	C00025	4525487
5	**Glutamine**	$C_5H_{10}N_2O_3$	Amino acids	147.0764	0,09	0,99	C00064	5961
6	**Histidine**	$C_6H_9N_3O_2$	Amino acids	156.0769	0.68	1,01	C00135	6274
7	**Hydroxyproline**	$C_5H_9NO_3$	Amino acids	132.0656	0.70	1,01	C01157	5810
8	**Isoleucine**	$C_6H_{13}NO_2$	Amino acids	132.1020	0.76	1,56	C00407	6306
9	**Leucine**	$C_6H_{13}NO_2$	Amino acids	132.1020	0.76	1,62	C00123	6106
10	**Lysine**	$C_6H_{14}N_2O_2$	Amino acids	147.1129	0.44	0.84	C00047	5962
11	**Methionine**	$C_5H_{11}NO_2S$	Amino acids	150.0584	0.36	2.04	C00073	6137
12	**Phenylalanine**	$C_9H_{11}NO_2$	Amino acids	166.0862	-0.53	4.30	C00079	6140
13	**Proline**	$C_5H_9NO_2$	Amino acids	116.0708	1.69	1.23	C00148	145742
14	**Threonine**	$C_4H_9NO_3$	Amino acids	120.0657	1.22	1.08	C00188	6288
15	**Tryptophan**	$C_{11}H_{12}N_2O_2$	Amino acids	205.0973	0.51	4.75	C00078	6305
16	**Tyrosine**	$C_9H_{11}NO_3$	Amino acids	182.0813	0.54	3.20	C00082	6057
17	**Valine**	$C_5H_{11}NO_2$	Amino acids	118.0863	0.48	1.14	C00183	6287
18	Methylpipecolic acid	$C_7H_{13}NO_2$	Amino acid derivatives	144.1019	0.27	1,08	C10172	115244
19	DHBOA-hexosyl-hexoside	$C_{14}H_{17}NO_9$	Benzoxazinoids	523.1773	0.59	4.48		
20	DHBOA-hexosyl-deoxyhexoside	$C_8H_7NO_4$	Benzoxazinoids	490.1557	0.59	4.71		
21	HBOA	$C_8H_7NO_3$	Benzoxazinoids	166.0499	0.34	5.92	C15769	322636
22	HBOA-glucoside	$C_{14}H_{17}NO_8$	Benzoxazinoids	328.1027	0.09	4.71		14605136
23	HM2BOA	$C_{10}H_{11}NO_5$	Benzoxazinoids	226.0709	-0.61	5.51		11064107
24	HMBOA-hexoside	$C_{10}H_{11}NO_5$	Benzoxazinoids	358.1241	-0.61	5.06		
25	HM2BOA-hexoside	$C_{16}H_{21}NO_{10}$	Benzoxazinoids	388.1245	1.86	5.36		
26	Apigenin-6-C-hexoside-C-pentoside	$C_{26}H_{28}O_{14}$	Flavonoids	565,1553	0,09	4,66		
27	Chrysoeriol-6-C-hexoside	$C_{22}H_{22}O_{11}$	Flavonoids	463.1237	0.43	5.35	C05990	442611
28	Chrysoeriol-C-hexosyl-O-deoxyhexoside	$C_{28}H_{32}O_{15}$	Flavonoids	609.1817	0.50	5.24		
29	Chrysoeriol-C-hexosyl-O-hexoside	$C_{28}H_{32}O_{16}$	Flavonoids	625.1766	0.42	5.17		72193674
30	Luteolin-C-hexosyl-deoxyhexoside	$C_{27}H_{30}O_{15}$	Flavonoids	595.1660	0.45	5.02		
31	Luteolin-C-hexosyl-C-pentoside	$C_{26}H_{28}O_{15}$	Flavonoids	581,1504	0.51	4.97		44258081
32	Luteolin-C-hexosyl-O-hexoside	$C_{27}H_{30}O_{16}$	Flavonoids	611,1608	0,23	4,98		
33	Luteolin-6-C-hexoside	$C_{21}H_{20}O_{11}$	Flavonoids	449,108	0,36	5.00	C01750	5280459
34	Tricin	$C_{17}H_{14}O_7$	Flavonoids	331.0812	0,09	6.45	C10193	5281702
35	Tricin-7-O-hexoside	$C_{23}H_{24}O_{12}$	Flavonoids	493,1343	0,5	5.56		5322022
36	**Abscisic acid**	C15H20O4	Phytohormones	265,14343	0,53	6,06		
37	Abscisic acid glucose ester	C21H30O9	Phytohormones	427,19625	0,35	4,33		
38	**Indole acetic acid**	C10H9NO2	Phytohormones	176,0706	1,16	1,71		
39	**OPDA**	C18H28O3	Phytohormones	293,211121	0,89	7,42		
40	**Jasmonic acid**	$C_{12}H_{18}O_3$	Phytohormones	211,1329	0,14	6.27	C08491	5281166
41	**Methyljasmonate**	C13H20O3	Phytohormones	225,148521	0,31	6,88		
42	**Salicylic acid**	$C_7H_6O_3$	Phytohormones	139,039	0,21	**4,5**	C00805	338
43	**Methylsalicylate**	$C_8H_8O_3$	Phytohormones	153,05462	0,56	5,39		
44	Coumaroylagmatine	$C_{14}H_{20}N_4O_2$	Hydroxycinnamic acid amides	277,1659	0,01	4,66	C04498	5280691
45	Coumaroylputrescine	$C_{13}H_{18}N_2O_2$	Hydroxycinnamic acid amides	235,1441	0,02	4.50		
46	Coumaroylcadaverine	$C_{14}H_{20}N_2O_2$	Hydroxycinnamic acid amides	249,15975	0,56	3,97		
47	Caffeoylagmatine	$C_{14}H_{20}N_4O_3$	Hydroxycinnamic acid amides	293,1608	0,06	4.52		
48	Caffeoylputrescine	$C_{13}H_{18}N_2O_3$	Hydroxycinnamic acid amides	251,139	0,08	4.47	C03002	
49	Feruloylagmatine	$C_{15}H_{22}N_4O_3$	Hydroxycinnamic acid amides	307,1765	0,11	4.57	C18325	46173376
50	Feruloylputrescine	$C_{14}H_{20}N_2O_3$	Hydroxycinnamic acid amides	265,1548	0,49	4.70	C10497	5281796
51	Feruloylcadaverine	$C_{15}H_{22}N_2O_3$	Hydroxycinnamic acid amides	279,1702	0,43	4.85		
52	Hydroxyferuloylputrescine	$C_{14}H_{20}N_2O_4$	Hydroxycinnamic acid amides	281,14955	0,12	3,81		
53	Sinapoylagmatine	$C_{16}H_{24}N_4O_4$	Hydroxycinnamic acid amides	337,187	0,09	4.65		
54	Sinapoylputrescine	$C_{15}H_{22}N_2O_4$	Hydroxycinnamic acid amides	295,1653	0,22	4.56		

[a] Metabolites was classified according to KEGG (Kyoto Encyclopedia of Genes and Genomes; http://www.genome.ad.jp/kegg/) and PubChem (http://pubchem.ncbi.nlm.nih.gov) databases. Id: identifier; *m/z* : mass-to-charge ratio; *m/z* error (difference between the measured *m/z* and the calculated *m/z* of an ion, represented in ppm); RT: retention time. Compounds indicated in bold were confirmed with authentic standards.

CHAPITRE 3

Le lipopeptide mycosubtiline potentialise les réponses immunitaires du blé vis-à-vis de *Zymoseptoria tritici*

Dans le chapitre précédent, nous avions montré que le Rh-Est-C12 protégeait le blé vis-à-vis de *Z. tritici* sans entraîner d'altérations majeures chez l'hôte, que ce soit au niveau de l'expression de gènes, ou de l'accumulation de métabolites dans les feuilles de blé. Les résultats obtenus suggèrent que la protection conférée par le rhamnolipide provenait majoritairement de son activité antifongique et, plus minoritairement, de son activité d'induction des défenses du blé. Dans ce chapitre, nous avons cherché à déterminer si la mycosubtiline, un autre composé surfactant, était capable d'induire des réactions de défense chez le blé, toujours dans le cadre d'une interaction compatible avec *Z. tritici*. La mycosubtiline est un lipopeptide cyclique (CLP), produit notamment par *Bacillus subtilis* et présentant une activité antifongique directe vis-à-vis de *Z. tritici* (Mejri *et al*., 2018). Par ailleurs, Farace et al. (2015) ont montré que ce CLP induisait des réactions de défense *in vitro* chez des cellules de vigne. Ici, nous avons voulu déterminer si la mycosubtiline présentait, ou non, un double mode d'action pour protéger le blé vis-à-vis de l'agent phytopathogène (antifongique et stimulation des défenses de la plante). Pour ce faire, nous avons mené une approche combinée de transcriptomique et de métabolomique, comme dans le chapitre précédent, mais aussi associée à des analyses cytologiques. Contrairement au Rh-Est-C12, le traitement foliaire du blé avec la mycosubtiline a entraîné des modifications conséquentes dans l'accumulation de transcrits et de métabolites dans les conditions traitées. En particulier, nos résultats suggèrent que la mycosubtiline serait capable de *primer* le blé, ce qui est généralement reconnu comme plus avantageux en termes de coûts énergétiques que l'élicitation des défenses de la plante (Martinez-Medina *et al.*, 2016). Le mécanisme par lequel la mycosubtiline déclenche la potentialisation du blé sera discuté. Celle-ci pourrait être causée par l'interaction de la mycosubtiline avec les membranes cytoplasmiques de l'hôte modifiant sa fluidité, comme un stress abiotique-*like*. Ce stimulus permettrait de déclencher des réactions de défense chez le blé, notamment les voies de réponses associées à la phytohormone acide abscissique (ABA).

Les résultats obtenus dans le cadre de ce chapitre sont en préparation en vue de leur publication dans la revue Plant Phyisology *(IF = 6,90).*

Deciphering defense mechanisms primed by the *Bacillus subtilis* lipopeptide mycosubtilin in wheat towards *Zymoseptoria tritici*

Rémi Platel[1], Anca Lucau[1], Raymonde Baltenweck[2], Alessandra Maia-Grondard[2], Pauline Trapet[1], Maryline Magnin-Robert[3], Béatrice Randoux[3], Morgane Duret[1], Patrice Halama[1], Jean-Louis Hilbert[1], François Coutte[1], Philippe Jacques[4], Philippe Hugueney[2], Philippe Reignault[3] and Ali Siah[1]*

[1] Joint Research Unit 1158 BioEcoAgro, Junia, Univ. Lille, Université Liège, UPJV, Univ. Artois, ULCO, INRAE, 59000 Lille, France.

[2] Université de Strasbourg, INRAE, SVQV UMR A1131, 68000 Colmar, France.

[3] Unité de Chimie Environnementale et Interactions sur le Vivant (EA 4492), Université du Littoral Côte d'Opale, CS 80699, 62228 Calais Cedex, France.

[4] Joint Research Unit 1158 BioEcoAgro, TERRA Teaching and Research Centre, MiPI, Gembloux Agro-Bio Tech, Université Liège, 5030 Gembloux, Belgium.

*Corresponding author : ali.siah@junia.com ; Tel.: +33(0)3 28 38 48 48

ABSTRACT

Induced immunity in plants is a valuable eco-friendly tool that fits with sustainable agriculture and healthy food. However, despite the agroeconomic significance of a major crop as wheat, the mechanisms underlying the induction of its defense responses are still unclear. Here, we show that mycosubtilin, a lipopeptide from *Bacillus subtilis*, protects wheat against the hemibiotrophic fungal pathogen *Zymoseptoria tritici* through dual (direct and indirect) modes of action and that the indirect one relies mainly on priming rather than the elicitation of plant defense-related mechanisms. Indeed, foliar application of the biomolecule primed, during the early stages of infection, the expression of 80 genes associated with sixteen functional groups, including responses to pathogens, abiotic and oxidative stresses, secondary metabolism, cell-wall structure and function, and primary metabolic pathways (carbohydrate, amino acid, protein, lipid, and energy metabolisms). More specifically, genes involved in abscisic acid (ABA) biosynthesis and ABA-associated signaling pathways are regulated, suggesting a role of this phytohormone in the indirect activity of mycosubtilin. Interestingly, mycosubtilin also primed the accumulation of several flavonoids during the period preceding the fungal switch to the necrotrophic phase. This priming-based bioactivity of mycosubtilin against a biotic stress could result from an interaction of the biomolecule with leaf cell plasma membranes that may mimic an abiotic stress-like stimulus in wheat plants, as supported by cytological bioassays, as well as the regulation of genes associated with abiotic stress-responses and early signal transduction in the treated plants. Further bioassays showed that mycosubtilin displays a direct antifungal activity against *Z. tritici in vitro* and *in planta* and reduces disease severity caused by the pathogen. This study provides new insights into induced immunity in wheat and opens new perspectives for the use of mycosubtilin lipopeptide as a biocontrol compound with two distinct modes of action against *Z. tritici*.

INTRODUCTION

Wheat is one of the most cultivated cereal crops worldwide, serving as primary ingredient in human diet, food industry, and livestock feed. Wheat cultivation has to cope with a wide range of phytopathogenic microorganisms impacting its growth, productivity and quality of production (Savary *et al.*, 2019). The most frequently occurring and damaging pathogen on wheat crop is the hemibiotrophic fungus *Zymoseptoria tritici*, responsible for Septoria tritici blotch (STB) disease, causing severe yield losses of up to 50 % during high-level pressure years (Fones and Gurr, 2015). The infection process of hemibiotrophic pathogens consists of an initial asymptomatic biotrophic phase followed by a necrotrophic phase, the latter being characterized by visual symptom apparition (Koeck *et al.*, 2011). Even if progresses have been accomplished in wheat resistance breeding during the last decades, with 21 resistance genes described against *Z. tritici*, disease control of STB relies mainly on synthetic fungicides (Brown *et al*., 2015 ; Torriani *et al*., 2015). In Europe, 70 % of the total currently applied fungicides are used to protect wheat against *Z. tritici* (Fones and Gurr, 2015). Nevertheless, fungicide resistance developed by *Z. tritici* populations is an increasing concern for wheat producers *(Cools et al*., 2013 ; Cools and Fraaije, 2013 ; McDonald *et al*., 2019 ; Steinhauer *et al*., 2019). Therefore, a strong need for substitutes and alternatives have emerged in the recent years, reinforced by all the concerns around the potential impacts of chemical inputs on the environment and human health.

Biosurfactants, or green surfactants, have been reported as ecofriendly promised candidates for biocontrol of crop diseases (Ongena and Jacques, 2008 ; D'aes *et al*., 2010 ; Vatsa *et al*., 2010 ; Sachdev and Cameotra, 2013 ; Shekhar *et al*., 2015 ; Chen *et al*., 2017 ; Crouzet *et al*., 2020). They are surface-active biomolecules produced by a broad range of microorganisms, including bacteria and fungi. These molecules are often classified according to their chemical structure, such as mannosylerythritol lipids, trehalose dimycolate, trehalolipids, sophorolipids, rhamnolipids, and lipopeptides (Crouzet *et al.*, 2020). Even though they may be very diverse both in their structure and origin, they all are amphiphilic molecules, composed by hydrophilic and hydrophobic moieties. They also exhibit a high potential of application in numerous fields, including human health, cosmetic, food industry, petroleum industry, soil and water remediation, nanotechnology, and agriculture (Lourith and Kanlayavattanakul, 2009 ; Sachdev and Cameotra, 2013 ; Shekhar *et al*., 2015 ; Singh *et al*., 2019). Regarding their use in crop protection, many studies have reported their significant efficacy in plant protection against pathogens (Ongena and Jacques, 2008 ; D'aes *et al*., 2010 ; Vatsa *et al*., 2010 ; Sachdev and Cameotra, 2013 ; Chen *et al*., 2017 ; Crouzet *et al*., 2020). Moreover, green surfactants have been described as displaying high biodegradability, as well as low toxicity and ecotoxicity, two major advantages required for the development of sustainable agriculture (Shekhar *et al*., 2015).

The possible modes of action of biosurfactants in plant protection against pathogens are diverse. For instance, they can display direct antimicrobial activity towards pathogens, modify the bio-availability of nutrients used by the pathogens, and/or induce plant immune defenses (D'aes *et al*., 2010). The compounds inducing the plant immune defenses may be distinguished into two categories, including elicitors, that directly activate host defense responses after their application, and priming agents, that require additional signals, such as pathogen recognition, to trigger the full defense responses (Paré *et al*., 2005). Primed plants may develop a stronger and/or faster response pattern than so-called naïve (unprimed) plants. They also may detect the pathogen invasion at a lower

threshold and hence react in a more sensitized way. Finally, primed plants may exhibit other response networks, involving specific defense pathways (Paré *et al*., 2005; Lämke and Bäurle, 2017).

Bacillus spp. are considered as microbial factories for the production of metabolites of interest, especially biosurfactant molecules such as lipopeptides. Lipopeptides consist of hydrophobic fatty acid tail linked to a short linear or cyclic oligopeptide (CLPs), and were, at first, mostly studied for their direct antimicrobial activities against phytopathogenic agents. However, many investigations were also performed on their stimulating effect of host defense mechanisms (Ongena and Jacques, 2008 ; Raaijmakers *et al*., 2010; Rabbee *et al*., 2019 ; Crouzet *et al*., 2020). Three main groups of CLPs were reported to exhibit significant biological activities, including surfactins, iturins and fengycins. These CLPs possess a significant antimicrobial activity against a wide range of fungi and oomycetes, due probably to their ability to interact directly with pathogen plasma membranes, hence resulting in their destabilization, pore formation and cytoplasmic leakage, leading *in fine* to cell death or to an inhibition of spore germination (Chitarra *et al.*, 2003 ; Romero *et al*., 2007 ; Etchegaray *et al*., 2008; Pérez-García *et al*., 2011 ; Qian *et al*., 2016 ; Desmyttere *et al*., 2019). However, some authors suggest that CLPs could also display antifungal activity by interacting with fungal intracellular targets (Qi *et al.*, 2010). Concerning their ability to induce plant immunity system, many studies have highlighted the potential of mainly two families of CLPs, fengycin and surfactin, to trigger defense reactions in various plants, such as bean, citrus, grapevine, lettuce, tomato, melon, rye grass, sugar beet, and wheat, as reviewed by Crouzet *et al*. (2020). Mycosubtilin, another CLP was also shown to induce defense responses in grapevine cells (Farace *et al*., 2015). Supposedly, CLPs are able to fit into the lipid bilayer of host plant plasma membranes, slightly altering the lipid dynamics, hence leading to the activation of defense reactions, as eliciting or priming agents (Deleu *et al.*, 2008 ; Nasir *et al*., 2010 ; Schellenberger *et al*., 2019).

Although the innate immunity of wheat towards *Z. tritici* is extensively studied (*e.g.* Rudd *et al*., 2015; Seybold *et al*., 2020), the literature regarding the induced resistance in wheat against this major fungal pathogen, with exogenous treatments, is relatively poor. Regarding CLPs, only one study showing the potential of surfactin to activate defense mechanisms in wheat against *Z. tritici* has been recently reported (Le Mire *et al*., 2018). Nevertheless, the ability of mycosubtilin, a CLP from the iturin family, to induce defense reactions in wheat against this disease has never been investigated, while its direct antimicrobial activity against *Z. tritici* has already been examined (Mejri *et al*., 2018). Omics tools, including transcriptomics and metabolomics, have significantly improved these later years the understanding of plant-pathogen cross-talks. Although such approaches have already been used to investigate the interactions between wheat and *Z. tritici*, they have not been deployed so far to examine the induced resistance in this pathosystem. The aim of the present study was thus to determine whether mycosubtilin is able to trigger immunity reactions in wheat towards *Z. tritici* as an elicitation (in absence of infection) or a priming (in presence of infection) molecule, by using transcriptomic and metabolomic tools. The analyses allowed to decipher the mechanisms as well as the plant-defense related pathways induced by the biomolecule. Cytological bioassays were also performed to better understand the mode of action of mycosubtilin on both the fungus and the host plant.

MATERIALS AND METHODS

Plant growth, treatment and inoculation

Seeds of the cultivar (cv.) Alixan (Limagrain, France), susceptible to STB, were pregerminated in square Petri dishes (12 × 12 cm) on moist filter paper as described by Siah *et al*. (2010), and germinated grains were delicately transferred into three-liter pots filled with universal loam (Gamm Vert, France). The prepared pots were then placed in the greenhouse at 21 ± 2°C with a 16/8 h day-night cycle. For each condition and each sampling modality, three pots harboring 12 wheat plants each (n=36), were used. At day 0 (DO), corresponding to three weeks after sowing, plants of each pot were hand-sprayed with 30 mL of either a solution of 100 $mg.L^{-1}$ mycosubtilin from *Bacillus subtilis* (Lipofabrik, Lesquin, France) or mock (control) treatment. Mycosubtilin was firstly dissolved in dimethyl sulfoxide (DMSO, Sigma-Aldrich, Saint-Louis, USA), leading to a final DMSO concentration of 0.1 % in the treatment solution, also supplemented with 0.05 % of polyoxyethylene-sorbitan monolaurate (Tween 20, Sigma-Aldrich, Saint-Louis, USA) serving as wetting agent. Mock treatment consisted of a solution of 0.1 % DMSO supplemented with 0.05 % of Tween 20. At two days after treatment (D2), half of the plants treated with mycosubtilin, as well as control plants, were inoculated by hand-spraying 30 mL of *Z. tritici* spore suspension (10^6 $spores.mL^{-1}$), mixed with 0.05 % of Tween 20, on the plants of each pot. Fungal spores were obtained by growing the *Z. tritici* single-spore strain T02596 (isolated in 2014 in Northern France) on potato dextrose agar (PDA) medium during one week in dark conditions, according to Siah *et al*. (2010). The other half of the plants were mock inoculated by hand spraying 30 mL of a 0.05 % Tween 20 solution on the plants of each pot. All pots, even the mock inoculated ones, were then immediately covered with a clear polyethylene bag for three days in order to ensure a high humidity level on the surface of the leaves, a required condition for the success of the infection. At 23 days after treatment (D23), the disease severity level was assessed by scoring, on the plant third leaves, the area of lesions (chlorosis and necrosis) bearing or not pycnidia. Leaf samples were harvested at two (D2), five (D5) and fifteen (D15) days after treatment for further cytological, biochemical, or molecular analyses. In addition to the protection efficacy assay, a phytotoxicity biotest was performed in order to evaluate the impact of mycosubtilin at different concentrations (0, 0.8, 4, 20, 100, and 500 mg L^{-1}) on leaf appearance and plant fresh biomass. The assay was carried out in the greenhouse using the same conditions of plant growth and treatment described above. Leaf appearance was assessed on the third leaves at two, seven, and 15 days after treatment, while the plant fresh biomass was determined at 15 days after treatment. Three pots of nine plants each (27 plants in total) were used as replicates for each molecule concentration condition. The global design of the whole study is presented in **Supplementary Figure S1**.

In vitro antifungal activity assay in solid medium

In vitro antifungal effect of mycosubtilin was determined by measuring the growth of the *Z. tritici* strain T02596 on PDA medium, as described by Platel *et al*. (2021). Briefly, mycosubtilin was dissolved in DMSO (0.1 % final DMSO concentration) and different concentrations of this biomolecule (0.19, 0.39, 0.78, 1.56, 3.125, 6.25, 12.5, 25, 50, and 100 $mg.L^{-1}$) were mixed at approximatively 40°C with an autoclaved PDA medium. Each well of sterile 12-well plates (Cellstar standard®, Greiner Bio-One GmbH, Kremsmünster, Austria) were filled with three mL of the mixture. After PDA polymerization, a drop of 5 µL of *Z. tritici* spore suspension at 5.10^5 $spores.mL^{-1}$ was spotted on the center of each plate

well. After drop drying in sterile conditions, the plates were incubated in a growth chamber at 20 ± 1°C in dark conditions. Ten days later, the growth of fungal colonies was assessed by measuring their two perpendicular diameters. Control wells supplemented or not with 0.1 % DMSO and inoculated or not with fungal spores were also used. This experiment was repeated twice and three wells were used as replicates for each condition.

In vitro direct activity bioassays in liquid medium

In vitro direct antifungal activity of mycosubtilin in liquid medium was assessed by measuring cell viability of the *Z. tritici* strain T02596 using resazurin staining, as proposed by Siah *et al*. (2010b). Sterile 12-well plates (Cellstar standard®, Greiner Bio-One GmbH, Austria) were used for the bioassay. Plate wells were filled with 2 mL of autoclaved glucose peptone medium supplemented with mycosubtilin at different concentrations (0.8, 4, 20, 100, and 500 $mg.L^{-1}$), before inoculation with fungal spore suspension already prepared in sterile glucose peptone medium, for a final concentration of 5.10^4 $spores.mL^{-1}$. Mycosubtilin was first dissolved in DMSO at a final concentration of 0.5 % in the wells. Controls with and without 0.5 % DMSO and with or without the fungus, were also used. After incubation for ten days at 20 ± 1 °C under agitation at 150 rpm in dark conditions, 140 µL of the content of each well were sampled and deposited in flat-bottomed polystyrene 96-well microplates (Corning Costar®, Corning, USA). Then, 10 µL Alamar blue (AbD Serotec, UK) were added to each well before incubating the microplates for 4h in the same conditions described above. Cell viability was evaluated by measuring the absorbance at 540 nm using a microplate reader (Multiskan GO, Thermo Fischer Scientific, France). Six biological replicates were used as repetitions for each condition.

The inhibitory effect of mycosubtilin towards unique wheat cells (cv. Alixan) was assessed in sterile 12-well plates (Cellstar standard®, Greiner Bio-One GmbH, Austria). Wheat unique cells were obtained using the protocol of Biesaga-Kościelniak *et al.* (2008), with few modifications. Briefly, wheat caryopses were plunged for five minutes in 70% ethanol, rinsed twice with sterile osmotic water, and disinfected for 20 min in a 15% calcium hypochlorite solution, before being cleansed again at least twice. Mature embryos were delicately separated from the rest of the grain and were gently ground in a mortar. Fifty embryos were required to initiate wheat-cell suspension in 200 mL Erlenmeyer flask. These flasks contained 20 mL of autoclaved Gamborg B5 medium including vitamins (Duchefa Biochemie B.V, Netherlands), supplemented with 20 $g.L^{-1}$ sucrose and 3.5 $mg.L^{-1}$ 2,4-dichlorophenoxyacetic acid (Thermo Fischer Scientific, France). Wheat cell suspensions were incubated at 20 ± 1 °C in dark conditions under agitation at 80 rpm. At three and six days after inoculation, 20 mL of sterile medium were added to each flask. At 10 days, the mixture was filtered through a one mm sieve, to get rid of ungrounded agglomerate tissue. Fresh medium was added to the filtrates to obtain 80 mL suspension in each flask. Seven days later, 20 mL of Gamborg B5 fresh medium were supplemented. Finally, every week, 25 % of the suspension was discarded and replaced by fresh medium. After two months of subculture, 12-well plate wells were filled with two mL of wheat cell suspension as well as two mL of fresh Gamborg B5 medium supplemented with mycosubtilin at different concentrations (0.8, 4, 20, 100, and 500 $mg.L^{-1}$). The plates were, then, placed into growth chamber at 20 ± 1 °C in the dark with an agitation of 80 rpm. Three weeks after incubation, the number of wheat cells were counted for each condition using a Malassez hemocytometer under a light microscope (Nikon, Champigny-sur-Marne, France). Representative pictures were obtained using

digital camera (DXM1200C, Nikon, Champigny-sur-Marne, France) coupled with the image capture software NIS-Elements BR (Nikon, Champigny-sur-Marne, France).

In planta cytological assays

The direct antifungal activity of mycosubtilin at 100 mg.L^{-1} on *Z. tritici* spore germination as well as on the epiphytic hyphal growth of the fungus on the leaf surface was assessed *in planta* at D5 using Fluorescent Brightener 28 (Calcofluor, Sigma-Aldrich, Saint-Louis, USA), a chitin staining dye. Third-leaf segments (2 cm) harvested from wheat plants grown in the greenhouse, inoculated with *Z. tritici* and treated or not with mycosubtilin in the same conditions described above, were sampled and immersed for five minutes in a solution of 0.1 % (w/v) Calcofluor buffered with 0.1 M Tris-HCl, pH 8.5. Leaf segments were then rinsed twice in sterile osmosed water for two minutes before being dried in dark conditions at room temperature. Finally, they were deposited on a glass slide, covered with cover slip, and observed with an optic microscope (Eclipse 80i, Nikon, Champigny-sur-Marne, France) under UV-light. The proportion of different spore classes was determined from 100 distinct spores on each third-leaf segment. Spore classes were defined as followed; class 1, non-germinated spore; class 2, germinated spore with a small germ tube; class 3, geminated spore with developed germ tube; and class 4, geminated spore with a strongly developed germ tube. Nine leaf segments, randomly selected from three different pots (three segments per pot), were used as replicates for each condition. Pictures were obtained using digital camera (DXM1200C, Nikon, Champigny-sur-Marne, France) coupled with the image capture software NIS-Elements BR (Nikon, Champigny-sur-Marne, France).

Sampling design for transcriptomic and metabolomic analyses

Samples were collected at two days (D2) and five days (D5) after treatment for transcriptomic analyses. For each condition, *i.e.* plants treated with mycosubtilin (M) or not (control, C), and inoculated with *Z. tritici* (i) or not (Ni), nine third leaves sampled from three different pots (three leaves per pot), were randomly harvested, bulked per pot, immediately frozen in liquid nitrogen and stored at -80°C for further analyses. Thereafter, 100 mg of frozen pooled leaves were ground in a mortar with liquid nitrogen for RNA extraction. Regarding metabolomic analyses, samples were collected at D2, D5, as well as fifteen days after treatment (D15). For each modality, nine third leaves were randomly harvested from three different pots (three leaves per pot), immediately frozen in liquid nitrogen, and stored at -80°C for further analyses. Leaves were later freeze-dried using Alpha 2-4 LSCplus lyophilizer (Martin Christ Gefriertrocknungsanlagen GmbH, Osterode am Harz, Germany) and ground with iron beads using a MM2 Retsch mixer-mill (Retsch GmbH, Haan, Germany) in order to obtain a fine powder, suitable for analyses. Sampling design for both transcriptomic and metabolomic analyses is illustrated in **Supplementary Figure S1**.

RNA extraction and microarray analyses

Total RNA was extracted from wheat leaves using RNeasy Plant Mini Kit (Qiagen, Courtaboeuf, France). RNA quality was determined with Nanodrop by analyzing their absorbance ratios A260/280 and A260/230, which were found to range between 2.0 and 2.2. Moreover, RNA quality was also examined with Bioanalyzer 2100 (Agilent, France) and a minimal RNA integrity number (RIN) of 0.8 was required for all samples. For microarray analyses, hybridization for all conditions were performed in

triplicate with three sets of total RNA extracted from bulked wheat leaves (see above Sampling design section). Wheat Gene Expression Microarrays GE 4x44 (Agilent, Santa Clara, CA, USA) were used to study the gene expression profile between the different conditions. RNA amplification, staining, hybridization, and washing steps were conducted according to the manufacturer's specifications. Slides were scanned at five µm/pixel resolution using the GenePix 4000B scanner (Molecular Devices Corporation, Sunnyvale, CA, USA). Images were used for grid alignment and expression data digitization with GenePix Pro 6.0 software (Molecular Devices Corporation, Sunnyvale, CA, USA). Gene expression data were normalized by Quantile algorithm. The three control samples were filtered for $P < 0.05$ and the average was calculated for each gene. A fold change (FC) value was calculated for each gene between individual treated samples and the mean of corresponding controls. Differentially expressed genes (DEGs) were selected for a significant threshold > 2.0 or < 0.5 ($P < 0.05$). Functional annotation of DEGs was based on NCBI GenBank and related-genes physiological processes were assigned with NCBI, AmiGO 2 Gene Ontology and UniProt. KEGG pathway analysis was also used to identify relevant biological pathways for the selected genes. All microarray data have been submitted to the NCBI GEO: archive for functional genomics data with the accession number.

Metabolite extraction and UHPLC-MS analyses

Metabolites were extracted from powdered freeze-dried wheat leaves (30-50 mg per sample) using 25 µL of methanol per mg dry weight. The extract was then incubated in an ultrasound bath for 10 minutes, before centrifugation at 13000 g at 10 °C for 10 minutes. The supernatant was analyzed using a Dionex Ultimate 3000 UHPLC system (Thermo Fisher Scientific, USA). The chromatographic separations were performed on a Nucleodur C18 HTec column (150 × 2 mm, 1.8 µm particle size; Macherey-Nagel, Germany) maintained at 30 °C. The mobile phase consisted of acetonitrile/formic acid (0.1%, v/v, eluant A) and water/formic acid (0.1%, v/v, eluant B) at a flow rate of 0.3 mL min^{-1}. The gradient elution was programed as follows: 0 to 1 min, 95% B; 1 to 2 min, 95% to 85% B; 2 to 7 min, 85% to 0% B; 7 to 9 min, 100% A. The sample volume injected was 1 µL. The UHPLC system was coupled to an Exactive Orbitrap mass spectrometer (Thermo Fischer Scientific, USA), equipped with an electrospray ionization (ESI) source operating in positive mode. Parameters were set at 300 °C for ion transfer capillary temperature and 2500 V for needle voltages. Nebulization with nitrogen sheath gas and auxiliary gas were maintained at 60 and 15 arbitrary units, respectively. The spectra were acquired within the m/z (mass-to-charge ratio) mass ranging from 100 to 1000 atomic mass units (a.m.u.), using a resolution of 50,000 at m/z 200 a.m.u. The system was calibrated internally using dibutyl-phthalate as lock mass at m/z 279.1591, giving a mass accuracy lower than 1 ppm. The instruments were controlled using the Xcalibur software (Thermo Fischer Scientific, USA). LC-MS grade methanol and acetonitrile were purchased from Roth Sochiel (France); water was provided by a Millipore water purification system. Apigenin and chloramphenicol (Sigma-Aldrich, France) was used as internal standard.

Metabolites belonging to different chemical families were identified based on published works about benzoxazinoids (de Bruijn *et al*., 2016), flavonoids (Wojakowska *et al*., 2013) and hydroxycinnamic acid amides (Li *et al*., 2018) from wheat. Putative metabolite identifications were proposed based on expertized analysis of the corresponding mass spectra and comparison with published literature. Further information was retrieved from the KEGG (Kyoto Encyclopedia of Genes and Genomes, http://www.genome.ad.jp/kegg/) and PubChem (http://pubchem.ncbi.nlm.nih.gov)

databases. Relative quantification of the selected metabolites was performed using the Xcalibur software. For some metabolites, identity was confirmed with the corresponding standard provided by Sigma-Aldrich (France).

Statistical analyses

Protection efficacy data set was analyzed using One-Way analysis of variance (AN0VA) at $P \leq 0.05$, while data obtained for *in planta* spore germination and hyphal growth were analyzed using ANOVA followed by the Tukey's test at $P \leq 0.05$, using GraphPad Prism software version 9 (GraphPad Software Inc., San Diego, USA). Regarding the *in vitro* antifungal activity assay, the half-maximal inhibitory concentration (IC_{50}) was also determined with the GraphPad Prism software version 9. For transcriptomic assay, DEGs were selected for a significant threshold > 2.0 or < 0.5 ($P < 0.05$). Functional annotations of DEGs were determined based on NCBI GenBank, AmiGO 2 Gene Ontology, UniProt and KEGG pathways. However, DEGs may be involved in more than one biological process, especially when it comes to stress responses, hence the determined functional annotation could be subjected to modifications in the future. Differential metabolomic analyses were performed with the W4M platform (Guitton *et al*., 2017), using the Tukey's Honest Significant Difference method followed by a false discovery rate (FDR) correction using the Benjamini-Hochberg procedure (Benjamini and Hochberg, 1995). Metabolites of interest were considered differentially accumulated when the false discovery rate was below 5 % (FDR ≤ 0.05).

RESULTS

Foliar application of mycosubtilin protects wheat against *Z. tritici* and reduces fungal spore germination and leaf epithetic growth

The ability of mycosubtilin to confer protection to wheat against *Z. tritici* was assessed in the greenhouse using the wheat cv. Alixan and the pathogenic *Z. tritici* strain T02596. At 21 days after inoculation, the level of disease severity consisted of 55.7% of diseased leaf area in the non-treated inoculated plants. Preventive foliar application of mycosubtilin at 100 $mg.L^{-1}$ two days before inoculation resulted in a significant disease reduction (23.3% of diseased leaf area, corresponding to a 58.1% decrease) at 21 days after inoculation, *i.e.* 23 days after treatment (D23) in treated plants when compared to non-treated inoculated plants **(Figure 1A)**. *In planta* fungal staining assays using Calcofluor revealed that the treatment with mycosubtilin significantly reduces the rates of both spore germination and epithetic growth of *Z. tritici* at three days after inoculation, *i.e* five days after treatment (D5) **(Figure 1B)**. In treated wheat plants, non-germinated spores (class 1) were significantly more abundant (approximatively five-fold) than in the control plants. Moreover, the numbers of germinated spores with either developed germ tube (class 3) or strongly developed germ tube (class 4) were significantly reduced (by three- and seven-folds, respectively) on treated plants when compared to the control ones.

Mycosubtilin impacts the *in vitro* growth of both *Z. tritici* spores and wheat single cells, but at different concentration thresholds

The effect of mycosubtilin on the *Z. tritici in vitro* growth was evaluated on solid PDA medium in 12-well plates. The biomolecule exhibited a strong antifungal activity against the pathogen, with IC_{50} and MIC values of 0.57 and 0.78 $mg.L^{-1}$, respectively **(Supplementary Figure S2)**. In order to gain more insights into the mode of action of mycosubtilin on the host plant as well as on the pathogen, further bioassays were performed in liquid medium to examine the effect of the lipopeptide on the development (cell multiplication) of either wheat single cells or *Z. tritici* spores. Microscopic observation of the fungal spores grown in glucose peptone liquid medium showed that mycosubtilin totally inhibits the fungal growth from the concentration of 4 $mg.L^{-1}$. Besides, the lipopeptide exhibits also an effect on the growth of wheat single cells cultivated in suspension in MS liquid medium, but with a total inhibiting concentration of 500 $mg.L^{-1}$ **(Figure 2)**. Hence, the activity threshold of mycosubtilin seems to be 125-fold higher towards wheat single cells than against *Z. tritici* spores in liquid medium. However, no phytotoxic effect of mycosubtilin was observed at this concentration when the biomolecule is applied on wheat leaves. Indeed, no visible leaf necrosis and no significant effect on the total fresh biomass were noticed on the treated plants at all tested concentrations **(Figure 2)**.

Mycosubtilin regulates several defense-associated genes in wheat against *Z. tritici*

Transcriptomic analyses using RNA microarray assay were performed in order to examine both eliciting and priming effects of mycosubtilin in wheat towards *Z. tritici* during the early stages of the fungal infection. The bioassay was performed in non-infectious conditions at two days after treatment (D2), and in both non-infectious and infectious conditions at five days after treatment (D5), *i.e* three days after inoculation. The eliciting effect was examined at D2 and D5 by comparing the treated non-inoculated plants to non-treated and non-inoculated plants. The priming effect was investigated at D5 by comparing treated and inoculated plants to non-treated inoculated plants, by taking into account the elicitation modality at both D2 and D5. Moreover, in order to have a reliable conclusion and comprehensive view on the data linked to the priming effect, additional comparisons (treated and inoculated plants *versus* treated non-inoculated plants, and treated and inoculated plants *versus* non-treated non-inoculated plants), were also performed **(Supplementary Table S2, Supplementary Figure S4)**. The fungal effect was investigated at D5 by comparing non-treated and inoculated plants to non-treated and non-inoculated ones. The different comparisons will thereafter be referred to as eliciting, fungal, and priming effects, corresponding to eliciting, infection alone, and priming modalities, respectively.

Among the 43,803 wheat probes represented in the RNA microarray chip, a total of 130 genes were regulated (*i.e.* when taking into account both up and down regulations) when examining eliciting, fungal, and priming effects and considering all time points **(Supplementary Table S1)**. Overall, treatment with mycosubtilin led to a broader gene regulation response in priming modality at D5 when compared to both elicitation modalities at D2 or D5 **(Figures 3, 4 and 5)**. When considering the eliciting effect at both D2 and D5, only 40 differentially expressed genes (DEGs) were highlighted, with 18, 6, and 16 DEGs specifically scored at D2, both D2 and D5, and D5, respectively. Among them, 28 were upregulated and 12 were downregulated **(Figure 3A)**. At D5, priming modality displayed considerably

more DEGs (80) when compared to the eliciting effect at D5 (22), with 13 DEGs found in common among the two modalities. Globally, when considering all investigated modalities at D5 (eliciting, fungal, and priming effects), a total of 116 DEGs were recorded **(Figure 3B)**. Out of the detected 116 DEGs, 8, 27 and 59, were specifically noticed during either elicitation, fungal or priming effect modalities, respectively. **(Figure 3B)**.

Functional groups of DEGs recorded during wheat eliciting or priming by mycosubtilin at D5 were compared **(Figure 4)**. Consistently with the findings highlighted above in Venn diagrams, priming conditions clearly exhibited more DEGs annotated in the highlighted functional groups when compared to the eliciting conditions at D5. Among the sixteen identified functional groups of DEGs, those linked to responses to stress were the most regulated upon treatment with mycosubtilin, especially in priming conditions, followed by those involved in growth and development, and chloroplast and light harvesting. Few functional groups of DEGs were found only in priming modality, including those related to pigment biosynthesis, photosynthesis, flowering and seed maturation, cell wall structure and function, and primary metabolic pathways (carbohydrate, amino acid, protein, and lipid metabolisms). Moreover, a relative strong increase in the number of DEGs involved in transcription regulation, RNA-processing and translation, as well as secondary metabolism, was observed in priming when compared to elicitation modalities **(Figures 4)**.

When examining the gene regulation in detail, mycosubtilin-induced eliciting effect observed at D2 mainly involved DEGs associated to responses to pathogens, oxidative stress, and abiotic stress; most of them were significantly upregulated, except *peroxidase* and *peroxidase 2*, which were significantly downregulated **(Figures 5, Supplementary Table S1)**. Noticeably, three DEGs involved in signaling, transcription, and translation (*Ca^{2+}/H^{+} exchanging protein*, *zinc finger protein WZF1*, and *histone H1 WH1A.3*) were found overexpressed at D2 **(Figure 5)**. Additionally, at D5, a downregulation of eight others DEGs, three associated with responses to pathogens (*thaumatin-like protein TL4, chitinase*, and *chitinase*2), as well as an upregulation of eight DEGs, with, among them, two linked with responses to pathogens, were recorded. In the priming modality at D5, mycosubtilin induced the regulation of a substantial number of genes related to several physiological pathways. Among them, a subset of 26 genes are linked to responses to stresses, including thirteen to oxidative stress, nine to pathogens, and four to abiotic stress. Interestingly, several genes involved in abscisic acid (ABA) phytohormone biosynthesis (*beta-carotene hydroxylase* and *lycopene β-cyclase*) and ABA-associated signaling pathways (*ARK protein*, *aquaporins*, *aldose reductase*, *ABC1 family protein-like*, *glutathione peroxidase-like protein GPX15Hv*, *nicotianamine synthase 3*, *chlorophyll a/b binding protein of LHCII type III choloroplast precursor*, *light-harvesting complex 1* and *S-adenosylmethionine synthetase*) were also regulated in priming modality at D5 **(Figure 5)**. Regarding the effect of the fungal infection alone on the wheat leaf transcriptome at D5, only an upregulation of six DEGs involved in response to abiotic stress and pathogens was obtained, whereas a set of 32 DEGs was downregulated by the fungus alone at this time point, among them some are also related to responses to abiotic stress and pathogens. However, the most remarkable effect of *Z. tritici* is the downregulation of an important number of genes involved in cell-wall structure, amino acid metabolism, and protein metabolism **(Figure 5)**.

Mycosubtilin primes flavonoid accumulation in wheat against *Z. tritici*

Metabolomic analyses using UHPLC-MS was undertaken to assess the effect of mycosubtilin on the wheat leaf metabolome in both non-infectious and infectious conditions, and at the same time points than those targeted in the above transcriptomic assay (D2 and D5), with an additional time point corresponding to 15 days after treatment (D15), *i.e* 13 days after inoculation, corresponding to the late stage of *Z. tritici* biotrophic phase. The eliciting effect was investigated at D2, D5, and D15 by comparing the treated non-inoculated plants to non-treated and non-inoculated plants. The priming effect was examined at D5 as well as D15, on the one hand, by comparing treated and inoculated plants to non-treated inoculated plants, and on the other hand, by considering the elicitation modalities at D2, D5, and D15. Besides, further comparisons (treated and inoculated plants *versus* treated non-inoculated plants, and treated and inoculated plants *versus* non-treated non-inoculated plants), were also carried out in order to have a comprehensive picture on the data linked to the priming effect on leaf metabolome **(Supplementary Figure 5)**. As described in the transcriptomic assay, the different comparisons in the metabolomic assay will also be referred to as eliciting, fungal, and priming effects, corresponding to eliciting, infection alone, and priming modalities, respectively.

The analyses were targeted on 54 metabolites belonging to major chemical families that were detected and identified using UHPLC-MS **(Figure 6, Supplementary Table S3)**. Plant treatment with mycosubtilin and/or inoculation with *Z. tritici* resulted in marked differentiations among wheat leaf metabolite patterns, as highlighted by the PCA analysis **(Supplementary Figure S6)**. The largest changes in the accumulation of the selected metabolites were observed during fungal infection alone or during priming modalities, whereas only minor modifications were scored in eliciting modalities **(Figure 6)**. In all eliciting modalities, only eight differentially accumulated metabolites (DAMs) were recorded, among them four were under-accumulated at D2 (asparagine and chry-C-hexo-O-hexo), D5 (MeJA), and D15 (tricin), and four were over-accumulated at D15, including three amino acids (glutamic acid, threonine and proline) and one hormone (ABA_Glc). However, in the priming modalities, a higher number of DAMs was scored, including 16 DAMs at D5 and 16 DAMs at D15 **(Figure 6)**. At D5, only metabolite down-accumulation was detected (corresponding mainly to those over-accumulated in the fungal modalities), whereas at D15, both increases and decreases in metabolite concentration were observed. At D15, a decrease in the concentration of three hydroxycinnamic acid amides (coumaroylputrescine, coumaroylcadaverine, and caffeoylputrescine) and five amino acids and derivatives (leucine-isoleucine, arginine, threonine, glutamine, and methyl-pipecolate) were found. Interestingly, seven metabolites belonging to flavonoids and one benzoxazinoid were over-accumulated specifically in the priming modality at D15 **(Figure 6)**.

Fungal infection alone induced substantial modifications in metabolite accumulation patterns at D5 and D15, with marked changes at D5, corresponding to the early stages of infection **(Figure 6)**. Indeed, at D15, only significant changes in the concentration of glutamine, methyl-pipecoalte, salicylic acid, and four hydroxycinnamic acid amides were noticed. However, at D5, a total of 26 DAMs, about half of the quantified molecules, were significantly regulated, with 18 molecules over-accumulated and eight under-accumulated. Seven amino acids, six benzoxazinoids, and five hydroxycinnamic acid amides were more concentrated, while three phytohormone precursors or derivatives (OPDA, MeJA and MeSA), five flavonoids, four luteolin derivatives, and one chrysoeriol derivative were down-accumulated **(Figure 6)**. The proposed model on the effects of mycosubtilin-induced priming and *Z.*

tritici infection at D5 and D15 on both hydroxycinnamic acid amide and flavonoid biosynthesis pathways within wheat leaves is illustrated **(Figure 7)**.

DISCUSSION

We combined here transcriptomic and metabolomic approaches to unravel the resistance mechanisms induced in wheat, by using the *B. subtills* lipopeptide mycosubtilin as a treatment and *Z. tritici* as a phytopathogen model. Only few previous works have used Omics when characterizing induced resistance in plants, whilst such tools could be helpful and informative on the molecular and physiological changes occurring during plant resistance activation using exogenous treatments (*e.g.* Gauthier *et al*., 2014 ; Fiorilli *et al*., 2018). Our results revealed that mycosubtilin likely acts on the wheat-*Z. tritici* pathosystem through a double (direct and indirect) activity and that the indirect activity relies mainly on the priming rather than the elicitation of wheat defense mechanisms.

Mycosubtilin displays direct antifungal towards *Z. tritici* and likely interacts with wheat leaf cells without causing *in planta* phytotoxicity

Foliar application of mycosubtilin at 100 mg.L^{-1} decreased by more than half (58.1%) *Z. tritici* symptoms on wheat plants, thus agreeing with previous results obtained on this pathosystem (Mejri *et al*., 2018). Mycosubtilin has also been reported to biocontrol other pathogens, such as *Bremia lactucae* on lettuce, *Botrytis cinerea* on grapevine, and *Fusarium oxysporum* f. sp. *iridacearum* on *Iris* sp. (Deravel *et al*., 2014; Farace *et al*., 2015; Mihalache *et al*., 2018). Our *in vitro* and *in planta* bioassays showed that mycosubtilin exhibits a direct antifungal effect on both spore germination and epiphytic growth of *Z. tritici* on wheat leaves, hence corroborating previous findings on this fungus (Mejri *et al*., 2018). Interestingly, our results revealed that mycosubtilin exhibits growth inhibiting activity on fungal as well as wheat single cells grown in suspension, suggesting that the lipopeptide interacts with the cells of both organisms with a common process. Indeed, it has been reported that the mode of action of mycosubtilin may rely on the destabilization of cytoplasmic membranes (Nasir *et al.*, 2010 ; Nasir and Besson, 2012), that could lead to the loss of cell integrity, cytoplasm leakage, and ultimately cell death. We can, thus, hypothesize that the biological activities of mycosubtilin on both *Z. tritici* and wheat cells may be associated with its ability to interact with the plasma membranes of both organisms. Nevertheless, the *in vitro* threshold concentration of the molecule activity on both species varies strongly, with a difference of 125-fold between *Z. tritici* and wheat cells, despite that fungal cells growing in contact with the biomolecule during the bioassay were protected by cell-walls, while wheat cells grown in suspension didn't likely develop cell-walls. However, no visible phytotoxicity caused by mycosubtilin on the whole plants was observed even at the highest tested concentration (500 mg.L^{-1}), presumably because leaves are overall more robust (presence of cuticle, etc.) than single wheat cells growing *in vitro*. An effect of mycosubtilin at 50 mg.L^{-1} on the growth of grapevine single cells has already been observed, with a significant increase in the amounts of cell death (23% of the total cells compared with 11% in the control) observed at 24h post-treatment, thus agreeing with our results (Farace *et al*., 2015). Taken together, these results suggest that, when applied on wheat plants at 100 mg.L^{-1}, mycosubtilin is able, on the one hand, to display a direct antimicrobial activity towards the pathogen and, on the other hand, to interact with the plasma membranes of plant leaf cells without causing damages that could lead to their death. More likely, this interaction of the molecule with the

plant cell plasma membranes could be the initial stimulus triggering the downstream defense reactions highlighted in the wheat plants in the transcriptomic and metabolomic assays. This defense-initiating stimulus could be attributed, as suggested in other plant models, to the potential biophysical and biochemical interactions of mycosubtilin with the lipid bilayer of the leaf cell plasma membranes, hence modifying their fluidity as an "abiotic stress-like" agent, like thermal or drought stress (Uemura and Yoshida, 1986 ; Niu and Xiang, 2018 ; Couchoud *et al*., 2019 ; Crouzet *et al*., 2020). This "abiotic stress-like" mechanism could, hence, explain the accumulation of gene transcripts involved in plant defenses against abiotic and oxidative stresses found in eliciting conditions.

Perception of mycosubtilin by wheat leaves leads to the elicitation of few genes associated with plant defense

Transcriptomic analyses revealed that in wheat plant treated with mycosubtilin (100 $mg.L^{-1}$), the expression of genes involved in plant responses to stresses and other biological functions was significantly regulated. At D2, in the elicitation modality, 24 DEGs were recorded, among them three, involved in signaling, transcription and translation were upregulated, including gene encoding for Ca^{2+}/H^{+} exchanging protein, a crucial regulator protein of cytoplasm calcium homeostasis. Moreover, we found in the same modality and time point an overexpression of a *CBL-interacting protein kinase* (*CIPK*) gene, encoding for a protein functioning as a calcium sensor displaying a large range of activity in plant responses against stresses (Wang *et al*., 2016; Cui *et al*., 2018). Calcium influx into the cytoplasm is considered as one of the first cellular reactions after stress signal perception, that can trigger subsequent downstream defense reactions upon detection of the elevation of calcium concentration, by calcium-dependent protein kinases (CDPKs) (Harmon *et al*., 2000). The accumulation of *Ca2+/H+ exchanging protein* and *CIPK* transcripts detected in our conditions could likely be linked to the mycosubtilin-induced initial stimulus suggested above on the wheat cell plasma membranes, leading to a modification in Ca^{2+} concentration inside wheat cells and hence to the subsequent triggered defense reactions observed in wheat leaves. In addition, among the DEGs still highlighted at D2 in the elicitation modality, 14 are associated to responses to either oxidative, pathogen, or abiotic stresses, suggesting that mycosubtilin confers to wheat an increased resistance level to these stresses. Notably, the upregulation of three genes encoding for a *Pathogenesis-related (PR) protein* or precursors (*pathogen-related protein*, c*hitinase II precursor*, and *PR17d precursor*), known to play a major role in plant resistance to pathogens, was observed. Chitinases are enzymes known to be involved in wheat defenses against *Z. tritici* by degrading the fungal cell-wall chitin (Kettles and Kanyuka, 2016). PR-17 is a class of PR proteins with an unknown mode of action, discovered by Christensen *et al*. (2002) and which could be involved in wheat defense against powdery mildew (Görlach et al., 1996b). WIR1 is a membrane protein able to fortify plant cell wall and that was reported to contribute to wheat defense responses against fungal infections, including powdery mildew and stripe rust (Bull *et al*., 1992 ; Coram *et al*., 2008). The accumulation of these transcripts at D2, *i.e* just before the moment of plant inoculation, may contribute to wheat protection against *Z. tritici*. Nevertheless, further investigations are needed to determine the role of these proteins during the studied compatible interaction.

At D5, still in the elicitation context, 22 DEGs were found, among them six were also reported at D2, including three involved in responses to oxidative stress (*peroxidase*, *peroxidase 6* and

metallothionein-like protein type 3) and two in growth and development (*ZIM motif family protein* and *auxin-repressed protein*). Genes encoding for ZIM motif family protein were described as key repressors of the jasmonic acid (JA) signaling pathway (Chini *et al*., 2009), being, hence, involved in the regulation of many physiological processes, especially in the mediation of plant responses to biotic and abiotic stresses (Sun *et al*., 2017; Ruan *et al*., 2019). A large number of genes belonging to this family were found to be regulated by other hormones such as gibberellins and ABA (Zheng *et al*., 2020). Considering DEGs involved in the growth and development functional group, the upregulation of 1-*aminocyclopropane-1-carboxylate (ACC) oxidase* is to be noticed. This enzyme has been shown to be of prior importance for ethylene (ETH) production in plants (Houben and Van de Poel, 2019). As ETH is a gaseous plant hormone playing a crucial role in several biological processes, including tolerance to stresses, wheat responses to mycosubtilin could hence include ETH-responses (B. Adie et al., 2007). Remarkably, Chandler *et al*. (2015) showed that mycosubtilin induces gene expression modifications *in vitro* in rice cells, with, especially, an increase in the quantity of *ACC synthase* (*ACS1*) transcripts, another key enzyme in ETH synthesis. Regarding DEGs involved in response to pathogens, genes encoding for PR proteins (*thaumatin-like protein TLP4* and *chitinases*) were found downregulated, whereas *MLA7*, an homolog of a resistance gene against powdery mildew in barley (Caldo *et al*., 2004), and *hydrolase alpha/beta fold family-like*, encoding for a protein family displaying large varieties of functions in plants (Mindrebo *et al*., 2016), were upregulated. In addition to this ability of mycosubtilin to regulate wheat defenses against biotic stress, we also observed significant modifications in the expression of genes involved in responses to abiotic stress, suggesting that mycosubtilin triggers multifaceted cross-talks in wheat defense pathways. In fact, three DEGs involved in response to abiotic stress were upregulated in the elicitation modality at D5, including genes encoding for transcription factor (TF) MYB2 (myeloblastosis), MYB-related protein, and ATP-dependent RNA helicase. MYB TFs were particularly studied for their critical importance in plant growth and stress tolerance, as reviewed by Ambawat *et al*., (2013). More precisely, a MYB2 was reported to participate in rice tolerance to salt, cold, and dehydration stress (Yang *et al*., 2012). The authors also showed that this TF was regulated by ABA. ATP-dependent helicases are major actors involved in RNA whole life, such as RNA splicing and decay as well as translation initiation (Nakamura *et al*., 2004). Zhang *et al*. (2014) reported that wheat RNA helicase 1 (*TaRH1*) may play a regulatory role during plant responses to both biotic and abiotic stress.

Mycosubtilin primes genes associated with several metabolic pathways in wheat

In the priming modality at D5, we observed different DEG patterns than those detected in the elicitation ones at D2 and D5, with a number of DEGs drastically higher than in the other tested modalities, suggesting that mycosubtilin would act on wheat as a priming compound. This hypothesis is supported by the upregulation of the gene encoding for histone H1 WH1A.3 recorded at D2 in elicitation modality. Indeed, histone modifications are supposed to play a central role in priming memorization and transcription reprogramming after the stressing cue, corresponding here to mycosubtilin application (Lämke and Bäurle, 2017). Out of the 80 DEGs noticed in the priming modality, 26 are involved in responses to stresses (oxidative, pathogen and abiotic stresses). Among them, we observed significant downregulation of the expression of genes encoding for chitinases, glucan endo-1,3- beta glucosidase isoenzyme 1 and a germin-like protein. In addition, as observed in elicitation modalities, transcripts of *peroxidase* were also downregulated, suggesting that mycosubtilin may

negatively regulate peroxidase-related defense mechanisms. On the other hand, mycosubtilin priming led to the overexpression of DEGs involved in responses to pathogens such as *harpin binding protein (HrBP1-1)*, a gene encoding for a protein located in plant cell walls known to promote anti-pathogen responses and SAR in plants (Chen *et al*., 2012). We also found DEGs potentially involved in carotenoids and ABA biosynthesis, such as *beta-carotene hydroxylase* and *lycopene β-cyclase* (Du *et al*., 2010 ; Kang *et al*., 2018 ; Finkelstein, 2013). Remarkably, a significant number of DEGs described to play a part in ABA signaling and response pathways were regulated, such as genes encoding for ARK protein, aquaporins, aldose reductase, ABC1 family protein-like, glutathione peroxidase-like protein GPX15Hv, nicotianamine synthase 3, chlorophyll a/b binding protein of LHCII type III choloroplast precursor, light-harvesting complex 1 and S-adenosylmethionine synthetase (Karuna Sree *et al*., 2000 ; Inoue *et al*., 2003 ; Liu *et al*., 2013 ; Zhai *et al*., 2013 ; Kim *et al*., 2015 ; Saruhashi *et al*., 2015 ; Hwang *et al*., 2016 ; Fang *et al*., 2019). The expression of some of these genes could potentially lead to significant protective activity in wheat. For instance, aquaporins (AQPs) are membrane proteins, existing in a large variety of organisms, mainly known for their role in water transport (Verkman, 2013). As reviewed recently by Li *et al*. (2020), a member of AQP subfamily PIP1, AtPIP1;4, found in *Arabidopsis thaliana*, was shown to play a central part in pathogen associated-molecular patterns (PAMPs)-triggered immunity (PTI) and SAR in the plant, by regulating H_20_2 transport across plasma membrane, from apoplast to cytoplasm, hence playing an active role in triggering H_20_2-dependent host defenses. Another AQP, AtPIP1;2, has been reported to be involved in PTI and ABA-dependent stomatal closure in *A. thaliana (Rodrigues et al*., 2017). Another identified relevant DEG in the priming modality is *ABC1-family like*. Indeed, Wang *et al*. (2013) have recently reported that *TaAbc1* upregulation is associated with hypersensitive response against stripe rust in wheat. Additionally, genes involved in carbohydrate metabolism were over-transcribed in the priming modality. ABA has been described as primordial in the regulation of carbohydrate metabolism during plant stresses (Kempa *et al*., 2008). We also found an overexpression of DEGs involved in amino acid, protein, lipid and energy metabolisms, that could be regulated by mycosubtilin to compensate the potential deleterious effect of *Z. tritici* infection on wheat metabolism. Finally, four DEGs associated with signaling, transcription and translation were upregulated in the priming modality, highlighting the significant broader amplitude of responses displayed in mycosubtilin-primed and infected wheat plants than in naïve infected plants.

Mycosubtilin did not elicit marked metabolite regulation but primes flavonoid accumulation in wheat leaves

Metabolomic analyses showed a substantially higher number of DAMs in the priming modality than in the elicitation ones, thus agreeing with transcriptomic findings. Indeed, only few metabolites were regulated upon treatment with mycosubtilin in the elicitation modality, such as methyl jasmonate (MeJA) at D5 belonging to jasmonate family, hence corroborating with transcriptomic findings suggesting the involvement of JA pathway in mycosubtilin-induced defenses. At D15, a flavonoid (tricin) was found under-accumulated, whereas four metabolites were detected in higher concentrations, *i.e* glutamic acid, threonine as well as, remarkably, ABA-glucoside (ABA-Glc), and proline. Proline is an osmolyte amino acid involved in adaptation to abiotic stress, especially salt, osmotic, and freezing stresses (Szabados and Savouré, 2010 ; Lv *et al.*, 2011). Proline accumulation is supposed to be biosynthesized from glutamic acid and regulated by ABA (Stewart, 1980 ; Cao *et al*., 2020). Although the concentration of ABA and derivatives was not significantly regulated in treated

wheat leaves, except at D15 for ABA-Glc, many DEGs and DAMs associated to ABA-dependent pathways were scored, suggesting that wheat responses to mycosubtilin may involve this hormone (both in elicitation and priming modalities). Whereas the role of ABA in plant tolerance to abiotic stress, such as drought, salinity, cold, and heavy metals has been extensively investigated, its effect on plant pathogen resistance remains obscure (Asselbergh *et al*., 2008 ; Vishwakarma *et al*., 2017). As reviewed by Lievens *et al*. (2017), a negative effect of this phytohormone on plant resistance was reported for many pathosystems, such as tomato-*B. cinerea* and rice-*Magnaporthe oryzae*. In the rice-*M. grisea* pathosystem, ABA was shown to compromise rice resistance against the pathogen by acting antagonistically towards SA-dependent pathway (Jiang *et al*., 2010). Some phytopathogens were even able to biosynthesize their own ABA, such as *B. cinerea* and *M. oryzae*, most likely to modulate host defenses and enhance their pathogenicity (Ding *et al*., 2015 ; Spence *et al*., 2015). However, in the later years, this phytohormone was described to also display positive effect on plant resistance in other pathosystems, such as *A. thaliana-Pythium irregulare* and *Brassica napus-Leptosphaeria maculans* (Adie *et al*., 2007b ; Kaliff *et al*., 2007). Two ABA-dependent modes of action on plant resistance against pathogens were highlighted, including regulation of stomatal closure in order to prevent pathogens from invading the plant, and callose deposition (Ton *et al*., 2009). In addition, ABA was also recently proposed as a potential key actor in molecular cross-talks for plant-microbe symbiosis at the rhizosphere level (Stec *et al*., 2016). In the wheat-*Z. tritici* pathosystem, the role of ABA, as well as ethylene, in the host resistance mechanisms has, up to now, been clearly overlooked. Hence, further investigations focusing on this phytohormone may provide new insights into its role in wheat resistance against *Z. tritici*.

In the priming modality at D5, only an under-accumulation of metabolites was observed, with patterns of amino acids and benzoxazinoids in opposition to those scored in the fungal effect modality at the same time point. This result suggests that mycosubtilin treatment (weakening the fungus pathogenicity) may reduce the expected fungal effect on wheat benzoxazinoid and amino acid pathways, likely due (i) to its direct antifungal activity and/or (ii) to a countering by the plant of *Z. tritici* effect on these two pathways thanks to a compensatory mechanism. However, at D15, we observed remarkable significant changes in metabolite accumulation. The most remarkable result was clearly the increased accumulation of almost all targeted flavonoids, especially luteolin-derivatives **(Figure 6 and 7)**. Indeed, we detected an over-accumulation of lut-6-C-Glc, lut-C-hexo-O-hexo, lut-C-hexo-O-deoxyhexo, lut-C-hexo-C-pento, chry-6-C-Glc, chry-C-hexo-O-hexo, and tricin-7-O-hexo **(Figure 6 and 7)**. Remarkably, at D5 in the priming modality, genes encoding for chalcone synthase 1 and 2, enzymes involved in flavonoid biosynthesis, were significantly upregulated **(Figure 7)**. Flavonoids are known to exhibit a range of biological activities in plant protection, not only antimicrobial activity but also strong antioxidant activity and cell-wall reinforcing (Lam *et al*., 2015 ; Lan *et al*., 2015 ; Al Aboody and Mickymaray, 2020). Accumulation of compounds displaying these three activities may be greatly beneficial for the host, especially just at the moment preceding the *Z. tritici* switch to necrotrophic phase. Indeed, at this time, *Z. tritici* growth increases, and the fungus produces toxins to induce wheat cell apoptosis, in order to feed on the released nutrients (Steinberg, 2015b). Hence, cell-wall strengthening and the increase in antioxidant capacity may very likely help wheat mesophyll cells to resist to the pathogen attack as well as apoptotic-like cell death initiating symptom development. On the other hand, hydroxycinnamic acid amides (coumaroylputrescine, coumaroylcadaverine, and caffeoylputrescine) were significantly under-accumulated. The decrease in the concentration of these

metabolites in wheat leaves may be linked with the hypotheses regarding mycosubtilin effect on plant metabolome during the priming modality emitted above (due to direct mycosubtilin antifungal effect and/or plant compensatory mechanism). Nevertheless, another reason would be the reorganization of metabolic pathways due to the mycosubtilin priming effect, as illustrated in **Figure 7**. Hence, during infection, flavonoid biosynthesis pathway would be enhanced at the detriment of the hydroxycinnamic acid amide pathway, leading to this differential accumulation in wheat leaves in the priming modalities. Interestingly, flavonoid biosynthesis may be induced by ABA, highlighting once more that ABA-dependent responses may be crucial to understand wheat responses to mycosubtilin (Gai *et al*., 2020). Finally, other metabolomic responses associated with the mycosubtilin-primed effect is the under-accumulation of leucine-isoleucine, arginine, threonine, glutamine, methyl-pipecolate and DHBOAdiglc, likely explained by the antifungal and/or compensatory hypotheses launched above **(Figure 6)**.

In conclusion, this study provides new insights into the mechanisms underlying the bioactivity of the *B. subtilis* lipopeptide mycosubtilin on the wheat-*Z. tritici* pathosystem. This promising biomolecule likely confers protection through a double activity, *i.e.* directly by displaying an antimicrobial activity against the fungus, and indirectly by priming defense responses in wheat that can help the plant to deal with the pathogen. Taken together, these findings reveal that mycosubtilin acts on wheat as a priming agent rather than an eliciting agent, likely by involving ABA, JA, ETH biosynthesis and signaling pathways. The stimulation of the plant immune system by mycosubtilin probably results from the interaction of the biomolecule with plasma membranes of leaf cells leading to the activation of abiotic stress-like responses in the plant. However, further investigations are required to unravel the precise mechanisms by which wheat leaf cells perceive mycosubtilin within the membranes.

ACKNOWLEDGEMENTS

This research was conducted in the framework of the project Bioscreen (Smartbiocontrol portfolio), funded by the European program Interreg V, and the CPER Alibiotech, funded by the European Union, the French State, and the French Council Hauts-de-France.

CONFLICT OF INTEREST

Philippe Jacques is a co-founder of Lipofabrik and Lipofabrik Belgium and a member of the scientific advisory board of both companies.

LITERATURE CITED

Adie, B., Chico, J.M., Rubio-Somoza, I., and Solano, R. (2007a). Modulation of Plant Defenses by Ethylene. J Plant Growth Regul *26*, 160–177.

Adie, B.A.T., Pérez-Pérez, J., Pérez-Pérez, M.M., Godoy, M., Sánchez-Serrano, J.-J., Schmelz, E.A., and Solano, R. (2007b). ABA Is an Essential Signal for Plant Resistance to Pathogens Affecting JA Biosynthesis and the Activation of Defenses in Arabidopsis. Plant Cell *19*, 1665–1681.

Al Aboody, M.S., and Mickymaray, S. (2020). Anti-Fungal Efficacy and Mechanisms of Flavonoids. Antibiotics (Basel) *9*.

Ambawat, S., Sharma, P., Yadav, N.R., and Yadav, R.C. (2013). MYB transcription factor genes as regulators for plant responses: an overview. Physiol Mol Biol Plants *19*, 307–321.

Asselbergh, B., De Vleesschauwer, D., and Höfte, M. (2008). Global Switches and Fine-Tuning—ABA Modulates Plant Pathogen Defense. MPMI *21*, 709–719.

Benjamini, Y., and Hochberg, Y. (1995). Controlling the False Discovery Rate: A Practical and Powerful Approach to Multiple Testing. Journal of the Royal Statistical Society. Series B (Methodological) *57*, 289–300.

Biesaga-Kościelniak, J., Kościelniak, J., Filek, M., and Janeczko, A. (2008). Rapid production of wheat cell suspension cultures directly from immature embryos. Plant Cell Tiss Organ Cult *94*, 139.

Brown, J.K.M., Chartrain, L., Lasserre-Zuber, P., and Saintenac, C. (2015). Genetics of resistance to Zymoseptoria tritici and applications to wheat breeding. Fungal Genet Biol *79*, 33–41.

de Bruijn, W.J.C., Vincken, J.-P., Duran, K., and Gruppen, H. (2016). Mass Spectrometric Characterization of Benzoxazinoid Glycosides from Rhizopus-Elicited Wheat (Triticum aestivum) Seedlings. J Agric Food Chem *64*, 6267–6276.

Bull, J., Mauch, F., Hertig, C., Rebmann, G., and Dudler, R. (1992). Sequence and expression of a wheat gene that encodes a novel protein associated with pathogen defense. Mol Plant Microbe Interact *5*, 516–519.

Cao, X., Wu, L., Wu, M., Zhu, C., Jin, Q., and Zhang, J. (2020). Abscisic acid mediated proline biosynthesis and antioxidant ability in roots of two different rice genotypes under hypoxic stress. BMC Plant Biology *20*, 198.

Chandler, S., Van Hese, N., Coutte, F., Jacques, P., Höfte, M., and De Vleesschauwer, D. (2015). Role of cyclic lipopeptides produced by Bacillus subtilis in mounting induced immunity in rice (Oryza sativa L.). Physiological and Molecular Plant Pathology *91*, 20–30.

Chen, J., Wu, Q., Hua, Y., Chen, J., Zhang, H., and Wang, H. (2017). Potential applications of biosurfactant rhamnolipids in agriculture and biomedicine. Appl. Microbiol. Biotechnol. *101*, 8309–8319.

Chen, Z., Zeng, M., Song, B., Hou, C., Hu, D., Li, X., Wang, Z., Fan, H., Bi, L., Liu, J., et al. (2012). Dufulin Activates HrBP1 to Produce Antiviral Responses in Tobacco. PLoS One *7*.

Chini, A., Fonseca, S., Chico, J.M., Fernández-Calvo, P., and Solano, R. (2009). The ZIM domain mediates homo- and heteromeric interactions between Arabidopsis JAZ proteins. Plant J *59*, 77–87.

Chitarra, G.S., Breeuwer, P., Nout, M.J.R., van Aelst, A.C., Rombouts, F.M., and Abee, T. (2003). An antifungal compound produced by Bacillus subtilis YM 10-20 inhibits germination of Penicillium roqueforti conidiospores. J Appl Microbiol *94*, 159–166.

Christensen, A.B., Cho, B.H., Næsby, M., Gregersen, P.L., Brandt, J., Madriz-Ordeñana, K., Collinge, D.B., and Thordal-Christensen, H. (2002). The molecular characterization of two barley proteins establishes the novel PR-17 family of pathogenesis-related proteins. Mol Plant Pathol *3*, 135–144.

Cools, H.J., and Fraaije, B.A. (2013). Update on mechanisms of azole resistance in Mycosphaerella graminicola and implications for future control. Pest Management Science *69*, 150–155.

Cools, H.J., Hawkins, N.J., and Fraaije, B.A. (2013). Constraints on the evolution of azole resistance in plant pathogenic fungi. Plant Pathology *62*, 36–42.

Coram, T.E., Settles, M.L., and Chen, X. (2008). Transcriptome analysis of high-temperature adult-plant resistance conditioned by Yr39 during the wheat–Puccinia striiformis f. sp. tritici interaction. Molecular Plant Pathology *9*, 479–493.

Crouzet, J., Arguelles-Arias, A., Dhondt-Cordelier, S., Cordelier, S., Pršić, J., Hoff, G., Mazeyrat-Gourbeyre, F., Baillieul, F., Clément, C., Ongena, M., et al. (2020a). Biosurfactants in Plant Protection Against Diseases: Rhamnolipids and Lipopeptides Case Study. Front Bioeng Biotechnol *8*.

Crouzet, J., Arguelles-Arias, A., Dhondt-Cordelier, S., Cordelier, S., Pršić, J., Hoff, G., Mazeyrat-Gourbeyre, F., Baillieul, F., Clément, C., Ongena, M., et al. (2020b). Biosurfactants in Plant Protection Against Diseases: Rhamnolipids and Lipopeptides Case Study. Front. Bioeng. Biotechnol. *8*.

D'aes, J., De Maeyer, K., Pauwelyn, E., and Höfte, M. (2010). Biosurfactants in plant-Pseudomonas interactions and their importance to biocontrol. Environ Microbiol Rep *2*, 359–372.

Deleu, M., Paquot, M., and Nylander, T. (2008). Effect of Fengycin, a Lipopeptide Produced by Bacillus subtilis, on Model Biomembranes. Biophys J *94*, 2667–2679.

Deravel, J., Lemière, S., Coutte, F., Krier, F., Van Hese, N., Béchet, M., Sourdeau, N., Höfte, M., Leprêtre, A., and Jacques, P. (2014). Mycosubtilin and surfactin are efficient, low ecotoxicity molecules for the biocontrol of lettuce downy mildew. Appl Microbiol Biotechnol *98*, 6255–6264.

Desmyttere, H., Deweer, C., Muchembled, J., Sahmer, K., Jacquin, J., Coutte, F., and Jacques, P. (2019). Antifungal Activities of Bacillus subtilis Lipopeptides to Two Venturia inaequalis Strains Possessing Different Tebuconazole Sensitivity. Front. Microbiol. *10*.

Ding, Z.-T., Zhang, Z., Luo, D., Zhou, J.-Y., Zhong, J., Yang, J., Xiao, L., Shu, D., and Tan, H. (2015). Gene Overexpression and RNA Silencing Tools for the Genetic Manipulation of the S-(+)-Abscisic Acid Producing Ascomycete Botrytis cinerea. Int J Mol Sci *16*, 10301–10323.

Du, H., Wang, N., Cui, F., Li, X., Xiao, J., and Xiong, L. (2010). Characterization of the beta-carotene hydroxylase gene DSM2 conferring drought and oxidative stress resistance by increasing xanthophylls and abscisic acid synthesis in rice. Plant Physiol *154*, 1304–1318.

Etchegaray, A., de Castro Bueno, C., de Melo, I.S., Tsai, S.M., Fiore, M. de F., Silva-Stenico, M.E., de Moraes, L.A.B., and Teschke, O. (2008). Effect of a highly concentrated lipopeptide extract of Bacillus subtilis on fungal and bacterial cells. Arch Microbiol *190*, 611–622.

Fang, L., Abdelhakim, L.O.A., Hegelund, J.N., Li, S., Liu, J., Peng, X., Li, X., Wei, Z., and Liu, F. (2019). ABA-mediated regulation of leaf and root hydraulic conductance in tomato grown at elevated CO 2 is associated with altered gene expression of aquaporins. Horticulture Research *6*, 1–10.

Farace, G., Fernandez, O., Jacquens, L., Coutte, F., Krier, F., Jacques, P., Clément, C., Barka, E.A., Jacquard, C., and Dorey, S. (2015). Cyclic lipopeptides from Bacillus subtilis activate distinct patterns of defence responses in grapevine. Mol Plant Pathol *16*, 177–187.

Finkelstein, R. (2013). Abscisic Acid Synthesis and Response. Arabidopsis Book *11*.

Fiorilli, V., Vannini, C., Ortolani, F., Garcia-Seco, D., Chiapello, M., Novero, M., Domingo, G., Terzi, V., Morcia, C., Bagnaresi, P., et al. (2018). Omics approaches revealed how arbuscular mycorrhizal symbiosis enhances yield and resistance to leaf pathogen in wheat. Scientific Reports *8*, 9625.

Fones, H., and Gurr, S. (2015a). The impact of Septoria tritici Blotch disease on wheat: An EU perspective. Fungal Genet Biol *79*, 3–7.

Fones, H., and Gurr, S. (2015b). The impact of Septoria tritici Blotch disease on wheat: An EU perspective. Fungal Genet Biol *79*, 3–7.

Gai, Z., Wang, Y., Ding, Y., Qian, W., Qiu, C., Xie, H., Sun, L., Jiang, Z., Ma, Q., Wang, L., et al. (2020). Exogenous abscisic acid induces the lipid and flavonoid metabolism of tea plants under drought stress. Scientific Reports *10*, 12275.

Gauthier, A., Trouvelot, S., Kelloniemi, J., Frettinger, P., Wendehenne, D., Daire, X., Joubert, J.-M., Ferrarini, A., Delledonne, M., Flors, V., et al. (2014). The Sulfated Laminarin Triggers a Stress Transcriptome before Priming the SA- and ROS-Dependent Defenses during Grapevine's Induced Resistance against Plasmopara viticola. PLOS ONE *9*, e88145.

Görlach, J., Volrath, S., Knauf-Beiter, G., Hengy, G., Beckhove, U., Kogel, K.H., Oostendorp, M., Staub, T., Ward, E., Kessmann, H., et al. (1996). Benzothiadiazole, a novel class of inducers of systemic acquired resistance, activates gene expression and disease resistance in wheat. The Plant Cell *8*, 629–643.

Guitton, Y., Tremblay-Franco, M., Le Corguillé, G., Martin, J.-F., Pétéra, M., Roger-Mele, P., Delabrière, A., Goulitquer, S., Monsoor, M., Duperier, C., et al. (2017). Create, run, share, publish, and reference your LC-MS, FIA-MS, GC-MS, and NMR data analysis workflows with the Workflow4Metabolomics 3.0 Galaxy online infrastructure for metabolomics. Int J Biochem Cell Biol *93*, 89–101.

Harmon, A.C., Gribskov, M., and Harper, J.F. (2000). CDPKs – a kinase for every Ca2+ signal? Trends in Plant Science *5*, 154–159.

Houben, M., and Van de Poel, B. (2019). 1-Aminocyclopropane-1-Carboxylic Acid Oxidase (ACO): The Enzyme That Makes the Plant Hormone Ethylene. Front. Plant Sci. *10*.

Hwang, J.-U., Song, W.-Y., Hong, D., Ko, D., Yamaoka, Y., Jang, S., Yim, S., Lee, E., Khare, D., Kim, K., et al. (2016). Plant ABC Transporters Enable Many Unique Aspects of a Terrestrial Plant's Lifestyle. Mol Plant *9*, 338–355.

Inoue, H., Higuchi, K., Takahashi, M., Nakanishi, H., Mori, S., and Nishizawa, N.K. (2003). Three rice nicotianamine synthase genes, OsNAS1, OsNAS2, and OsNAS3 are expressed in cells involved in long-distance transport of iron and differentially regulated by iron. The Plant Journal *36*, 366–381.

Jiang, C.-J., Shimono, M., Sugano, S., Kojima, M., Yazawa, K., Yoshida, R., Inoue, H., Hayashi, N., Sakakibara, H., and Takatsuji, H. (2010). Abscisic acid interacts antagonistically with salicylic acid signaling pathway in rice-Magnaporthe grisea interaction. Mol Plant Microbe Interact *23*, 791–798.

Kaliff, M., Staal, J., Myrenås, M., and Dixelius, C. (2007). ABA is required for Leptosphaeria maculans resistance via ABI1- and ABI4-dependent signaling. Mol Plant Microbe Interact *20*, 335–345.

Kang, C., Zhai, H., Xue, L., Zhao, N., He, S., and Liu, Q. (2018). A lycopene β-cyclase gene, IbLCYB2, enhances carotenoid contents and abiotic stress tolerance in transgenic sweetpotato. Plant Science *272*, 243–254.

Karuna Sree, B., Rajendrakumar, C.S.V., and Reddy, A.R. (2000). Aldose reductase in rice (Oryza sativa L.): stress response and developmental specificity. Plant Sci *160*, 149–157.

Kempa, S., Krasensky, J., Santo, S.D., Kopka, J., and Jonak, C. (2008). A Central Role of Abscisic Acid in Stress-Regulated Carbohydrate Metabolism. PLOS ONE *3*, e3935.

Kettles, G.J., and Kanyuka, K. (2016). Dissecting the Molecular Interactions between Wheat and the Fungal Pathogen Zymoseptoria tritici. Front Plant Sci *7*.

Kim, S.H., Kim, S.H., Palaniyandi, S.A., Yang, S.H., and Suh, J.-W. (2015). Expression of potato S-adenosyl-L-methionine synthase (SbSAMS) gene altered developmental characteristics and stress responses in transgenic Arabidopsis plants. Plant Physiol Biochem *87*, 84–91.

Koeck, M., Hardham, A.R., and Dodds, P.N. (2011). The role of effectors of biotrophic and hemibiotrophic fungi in infection. Cell Microbiol *13*, 1849–1857.

Lam, P.Y., Liu, H., and Lo, C. (2015). Completion of Tricin Biosynthesis Pathway in Rice: Cytochrome P450 75B4 Is a Unique Chrysoeriol 5'-Hydroxylase. Plant Physiol *168*, 1527–1536.

Lämke, J., and Bäurle, I. (2017). Epigenetic and chromatin-based mechanisms in environmental stress adaptation and stress memory in plants. Genome Biology *18*, 124.

Lan, W., Lu, F., Regner, M., Zhu, Y., Rencoret, J., Ralph, S.A., Zakai, U.I., Morreel, K., Boerjan, W., and Ralph, J. (2015). Tricin, a Flavonoid Monomer in Monocot Lignification. Plant Physiology *167*, 1284–1295.

Le Mire, G., Siah, A., Brisset, M.-N., Gaucher, M., Deleu, M., and Jijakli, M.H. (2018). Surfactin Protects Wheat against Zymoseptoria tritici and Activates Both Salicylic Acid- and Jasmonic Acid-Dependent Defense Responses. Agriculture *8*, 11.

Li, G., Chen, T., Zhang, Z., Li, B., and Tian, S. (2020). Roles of Aquaporins in Plant-Pathogen Interaction. Plants *9*, 1134.

Li, Z., Zhao, C., Zhao, X., Xia, Y., Sun, X., Xie, W., Ye, Y., Lu, X., and Xu, G. (2018). Deep Annotation of Hydroxycinnamic Acid Amides in Plants Based on Ultra-High-Performance Liquid Chromatography–High-Resolution Mass Spectrometry and Its In Silico Database. Anal. Chem. *90*, 14321–14330.

Lievens, L., Pollier, J., Goossens, A., Beyaert, R., and Staal, J. (2017). Abscisic Acid as Pathogen Effector and Immune Regulator. Front. Plant Sci. *8*.

Liu, R., Xu, Y.-H., Jiang, S.-C., Lu, K., Lu, Y.-F., Feng, X.-J., Wu, Z., Liang, S., Yu, Y.-T., Wang, X.-F., et al. (2013). Light-harvesting chlorophyll a/b-binding proteins, positively involved in abscisic acid signalling, require a transcription repressor, WRKY40, to balance their function. J Exp Bot *64*, 5443–5456.

Lourith, N., and Kanlayavattanakul, M. (2009). Natural surfactants used in cosmetics: glycolipids. Int J Cosmet Sci *31*, 255–261.

Lv, W.-T., Lin, B., Zhang, M., and Hua, X.-J. (2011). Proline Accumulation Is Inhibitory to Arabidopsis Seedlings during Heat Stress. Plant Physiology *156*, 1921–1933.

McDonald, M.C., Renkin, M., Spackman, M., Orchard, B., Croll, D., Solomon, P.S., and Milgate, A. (2019). Rapid Parallel Evolution of Azole Fungicide Resistance in Australian Populations of the Wheat Pathogen Zymoseptoria tritici. Appl. Environ. Microbiol. *85*.

Mejri, S., Siah, A., Coutte, F., Magnin-Robert, M., Randoux, B., Tisserant, B., Krier, F., Jacques, P., Reignault, P., and Halama, P. (2018). Biocontrol of the wheat pathogen Zymoseptoria tritici using cyclic lipopeptides from Bacillus subtilis. Environ Sci Pollut Res Int *25*, 29822–29833.

Mihalache, G., Balaes, T., Gostin, I., Stefan, M., Coutte, F., and Krier, F. (2018). Lipopeptides produced by Bacillus subtilis as new biocontrol products against fusariosis in ornamental plants. Environ Sci Pollut Res *25*, 29784–29793.

Mindrebo, J.T., Nartey, C.M., Seto, Y., Burkart, M.D., and Noel, J.P. (2016). Unveiling the functional diversity of the Alpha-Beta hydrolase fold in plants. Curr Opin Struct Biol *41*, 233–246.

Nakamura, T., Muramoto, Y., Yokota, S., Ueda, A., and Takabe, T. (2004). Structural and transcriptional characterization of a salt-responsive gene encoding putative ATP-dependent RNA helicase in barley. Plant Science *167*, 63–70.

Nasir, M.N., and Besson, F. (2012). Interactions of the antifungal mycosubtilin with ergosterol-containing interfacial monolayers. Biochimica et Biophysica Acta (BBA) - Biomembranes *1818*, 1302–1308.

Nasir, M.N., Thawani, A., Kouzayha, A., and Besson, F. (2010). Interactions of the natural antimicrobial mycosubtilin with phospholipid membrane models. Colloids Surf B Biointerfaces *78*, 17–23.

Ongena, M., and Jacques, P. (2008). Bacillus lipopeptides: versatile weapons for plant disease biocontrol. Trends Microbiol. *16*, 115–125.

Paré, P.W., Farag, M.A., Krishnamachari, V., Zhang, H., Ryu, C.-M., and Kloepper, J.W. (2005). Elicitors and priming agents initiate plant defense responses. Photosynth Res *85*, 149–159.

Pérez-García, A., Romero, D., and de Vicente, A. (2011). Plant protection and growth stimulation by microorganisms: biotechnological applications of Bacilli in agriculture. Curr Opin Biotechnol *22*, 187–193.

Platel, R., Chaveriat, L., Le Guenic, S., Pipeleers, R., Magnin-Robert, M., Randoux, B., Trapet, P., Lequart, V., Joly, N., Halama, P., et al. (2021). Importance of the C12 Carbon Chain in the Biological Activity of Rhamnolipids Conferring Protection in Wheat against Zymoseptoria tritici. Molecules *26*, 40.

Qi, G., Zhu, F., Du, P., Yang, X., Qiu, D., Yu, Z., Chen, J., and Zhao, X. (2010). Lipopeptide induces apoptosis in fungal cells by a mitochondria-dependent pathway. Peptides *31*, 1978–1986.

Qian, S., Lu, H., Sun, J., Zhang, C., Zhao, H., Lu, F., Bie, X., and Lu, Z. (2016). Antifungal activity mode of Aspergillus ochraceus by bacillomycin D and its inhibition of ochratoxin A (OTA) production in food samples. Food Control *60*, 281–288.

Raaijmakers, J.M., De Bruijn, I., Nybroe, O., and Ongena, M. (2010). Natural functions of lipopeptides from Bacillus and Pseudomonas: more than surfactants and antibiotics. FEMS Microbiology Reviews *34*, 1037–1062.

Rabbee, M.F., Ali, M.S., Choi, J., Hwang, B.S., Jeong, S.C., and Baek, K. (2019). Bacillus velezensis: A Valuable Member of Bioactive Molecules within Plant Microbiomes. Molecules *24*, 1046.

Rodrigues, O., Reshetnyak, G., Grondin, A., Saijo, Y., Leonhardt, N., Maurel, C., and Verdoucq, L. (2017). Aquaporins facilitate hydrogen peroxide entry into guard cells to mediate ABA- and pathogen-triggered stomatal closure. PNAS *114*, 9200–9205.

Romero, D., de Vicente, A., Rakotoaly, R.H., Dufour, S.E., Veening, J.-W., Arrebola, E., Cazorla, F.M., Kuipers, O.P., Paquot, M., and Pérez-García, A. (2007). The iturin and fengycin families of lipopeptides are key factors in antagonism of Bacillus subtilis toward Podosphaera fusca. Mol Plant Microbe Interact *20*, 430–440.

Ruan, J., Zhou, Y., Zhou, M., Yan, J., Khurshid, M., Weng, W., Cheng, J., and Zhang, K. (2019). Jasmonic Acid Signaling Pathway in Plants. Int J Mol Sci *20*.

Rudd, J.J., Kanyuka, K., Hassani-Pak, K., Derbyshire, M., Andongabo, A., Devonshire, J., Lysenko, A., Saqi, M., Desai, N.M., Powers, S.J., et al. (2015). Transcriptome and Metabolite Profiling of the Infection Cycle of Zymoseptoria tritici on Wheat Reveals a Biphasic Interaction with Plant Immunity Involving Differential Pathogen Chromosomal Contributions and a Variation on the Hemibiotrophic Lifestyle Definition1[OPEN]. Plant Physiol *167*, 1158–1185.

Sachdev, D.P., and Cameotra, S.S. (2013). Biosurfactants in agriculture. Appl Microbiol Biotechnol *97*, 1005–1016.

Saruhashi, M., Kumar Ghosh, T., Arai, K., Ishizaki, Y., Hagiwara, K., Komatsu, K., Shiwa, Y., Izumikawa, K., Yoshikawa, H., Umezawa, T., et al. (2015). Plant Raf-like kinase integrates abscisic acid and

hyperosmotic stress signaling upstream of SNF1-related protein kinase2. Proc Natl Acad Sci U S A *112*, E6388-6396.

Savary, S., Willocquet, L., Pethybridge, S.J., Esker, P., McRoberts, N., and Nelson, A. (2019). The global burden of pathogens and pests on major food crops. Nature Ecology & Evolution *3*, 430–439.

Schellenberger, R., Touchard, M., Clément, C., Baillieul, F., Cordelier, S., Crouzet, J., and Dorey, S. (2019). Apoplastic invasion patterns triggering plant immunity: plasma membrane sensing at the frontline. Mol Plant Pathol *20*, 1602–1616.

Seybold, H., Demetrowitsch, T.J., Hassani, M.A., Szymczak, S., Reim, E., Haueisen, J., Lübbers, L., Rühlemann, M., Franke, A., Schwarz, K., et al. (2020). A fungal pathogen induces systemic susceptibility and systemic shifts in wheat metabolome and microbiome composition. Nature Communications *11*, 1910.

Shekhar, S., Sundaramanickam, A., and Balasubramanian, T. (2015). Biosurfactant Producing Microbes and their Potential Applications: A Review. Critical Reviews in Environmental Science and Technology *45*, 1522–1554.

Siah, A., Deweer, C., Duyme, F., Sanssené, J., Durand, R., Halama, P., and Reignault, P. (2010a). Correlation of in planta endo-beta-1,4-xylanase activity with the necrotrophic phase of the hemibiotrophic fungus Mycosphaerella graminicola. Plant Pathology *59*, 661–670.

Siah, A., Deweer, C., Morand, E., Reignault, Ph., and Halama, P. (2010b). Azoxystrobin resistance of French Mycosphaerella graminicola strains assessed by four in vitro bioassays and by screening of G143A substitution. Crop Protection *29*, 737–743.

Singh, P., Patil, Y., and Rale, V. (2019). Biosurfactant production: emerging trends and promising strategies. J Appl Microbiol *126*, 2–13.

Spence, C.A., Lakshmanan, V., Donofrio, N., and Bais, H.P. (2015). Crucial Roles of Abscisic Acid Biogenesis in Virulence of Rice Blast Fungus Magnaporthe oryzae. Front. Plant Sci. *6*.

Stec, N., Banasiak, J., and Jasiński, M. (2016). Abscisic acid - an overlooked player in plant-microbe symbioses formation? Acta Biochim Pol *63*, 53–58.

Steinberg, G. (2015). Cell biology of Zymoseptoria tritici: Pathogen cell organization and wheat infection. Fungal Genet Biol *79*, 17–23.

Steinhauer, D., Salat, M., Frey, R., Mosbach, A., Luksch, T., Balmer, D., Hansen, R., Widdison, S., Logan, G., Dietrich, R.A., et al. (2019). A dispensable paralog of succinate dehydrogenase subunit C mediates standing resistance towards a subclass of SDHI fungicides in Zymoseptoria tritici. PLoS Pathog *15*.

Stewart, C.R. (1980). The Mechanism of Abscisic Acid-induced Proline Accumulation in Barley Leaves. Plant Physiol *66*, 230–233.

Sun, H., Chen, L., Li, J., Hu, M., Ullah, A., He, X., Yang, X., and Zhang, X. (2017). The JASMONATE ZIM-Domain Gene Family Mediates JA Signaling and Stress Response in Cotton. Plant and Cell Physiology *58*, 2139–2154.

Szabados, L., and Savouré, A. (2010). Proline: a multifunctional amino acid. Trends in Plant Science *15*, 89–97.

Ton, J., Flors, V., and Mauch-Mani, B. (2009). The multifaceted role of ABA in disease resistance. Trends Plant Sci *14*, 310–317.

Torriani, S.F.F., Melichar, J.P.E., Mills, C., Pain, N., Sierotzki, H., and Courbot, M. (2015). Zymoseptoria tritici: A major threat to wheat production, integrated approaches to control. Fungal Genetics and Biology *79*, 8–12.

Vatsa, P., Sanchez, L., Clement, C., Baillieul, F., and Dorey, S. (2010). Rhamnolipid Biosurfactants as New Players in Animal and Plant Defense against Microbes. Int J Mol Sci *11*, 5095–5108.

Verkman, A.S. (2013). Aquaporins. Curr Biol *23*, R52-55.

Vishwakarma, K., Upadhyay, N., Kumar, N., Yadav, G., Singh, J., Mishra, R.K., Kumar, V., Verma, R., Upadhyay, R.G., Pandey, M., et al. (2017). Abscisic Acid Signaling and Abiotic Stress Tolerance in Plants: A Review on Current Knowledge and Future Prospects. Front Plant Sci *8*.

Wang, X., Wang, X., Duan, Y., Yin, S., Zhang, H., Huang, L., and Kang, Z. (2013). TaAbc1, a Member of Abc1-Like Family Involved in Hypersensitive Response against the Stripe Rust Fungal Pathogen in Wheat. PLoS One *8*.

Wojakowska, A., Perkowski, J., Góral, T., and Stobiecki, M. (2013). Structural characterization of flavonoid glycosides from leaves of wheat (Triticum aestivum L.) using LC/MS/MS profiling of the target compounds. Journal of Mass Spectrometry *48*, 329–339.

Yang, A., Dai, X., and Zhang, W.-H. (2012). A R2R3-type MYB gene, OsMYB2, is involved in salt, cold, and dehydration tolerance in rice. J Exp Bot *63*, 2541–2556.

Zhai, C.-Z., Zhao, L., Yin, L.-J., Chen, M., Wang, Q.-Y., Li, L.-C., Xu, Z.-S., and Ma, Y.-Z. (2013). Two Wheat Glutathione Peroxidase Genes Whose Products Are Located in Chloroplasts Improve Salt and H2O2 Tolerances in Arabidopsis. PLOS ONE *8*, e73989.

Zhang, X., Zhao, X., Feng, C., Liu, N., Feng, H., Wang, X., Mu, X., Huang, L., and Kang, Z. (2014). The cloning and characterization of a DEAD-Box RNA helicase from stress-responsive wheat. Physiological and Molecular Plant Pathology *88*, 36–42.

Zheng, Y., Chen, X., Wang, P., Sun, Y., Yue, C., and Ye, N. (2020). Genome-wide and expression pattern analysis of JAZ family involved in stress responses and postharvest processing treatments in Camellia sinensis. Scientific Reports *10*, 2792.

Figures

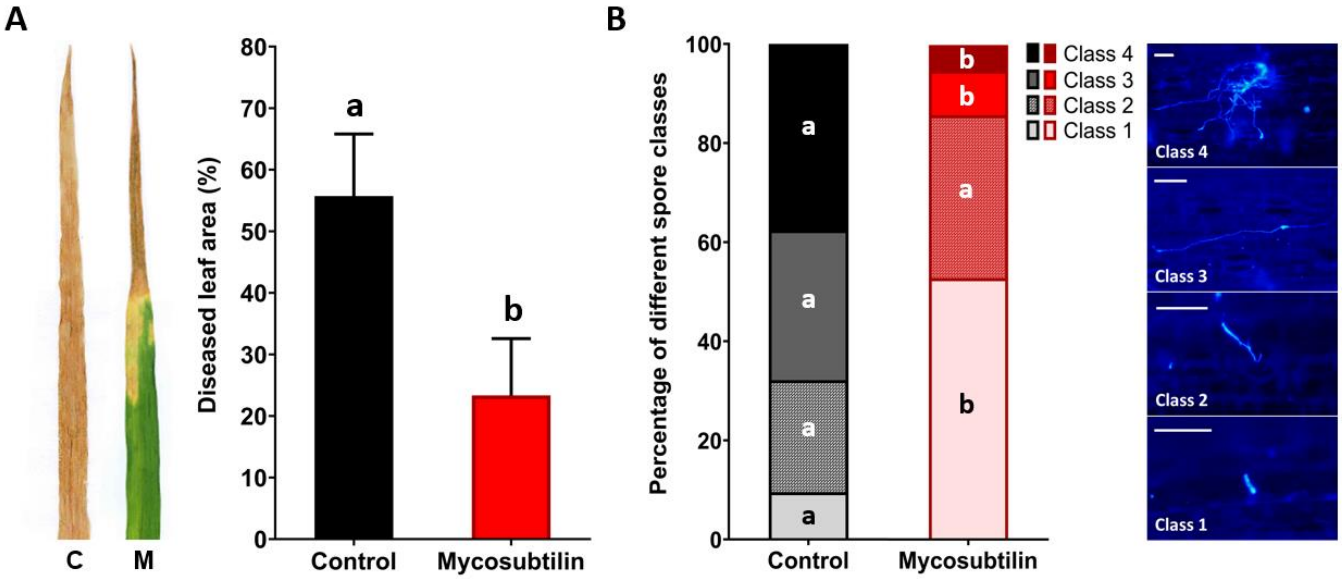

Figure 1. Disease severity level (**A**) and rates of *in planta* spore germination and epiphytic growth (**B**) of *Zymoseptoria tritici* (T02596 strain) on wheat leaves (cv. Alixan) pre-treated with mycosubtilin (M) at 100 mg.L^{-1} or not (C, control). (**A**) Disease severity level was scored at 21 day safter inoculation (*i.e* 23 days after mycosubtilin treatment) by assessing the area of lesions (chlorosis and necrosis) on wheat third leaf of each plant (n=36). Means tagged with the same letter are not significantly different according to One-way ANOVA test ($P \leq 0.05$). (**B**) Proportions of four different development stages of fungal spores was assessed by using Calcofluor staining recorded at three days after inoculation (*i.e.* five days after mycosubtilin treatment). The different spore development classes are defined as followed: Class 1, non-germinated spore; Class 2, geminated spore with small germ tube; Class 3, geminated spore with developed germ tube; Class 4, geminated spore with a strongly developed germ tube. For each condition, the different classes were determined from 100 distinct spores chosen randomly on each third-leaf segment. Within each spore class, the presence of different letters indicates a significant difference according to the Tukey test at $P \leq 0.05$. Scale bar = 25 µm.

Mycosubtilin (mg. L^{-1})	Control	DMSO	0.8	4	20	100	500
Fungal cell suspension							
ΔDO (540 nm)	1.39 (± 0.10)	1.47 (± 0.20)	1.36 (± 0.23)	1.36 (± 0.23)	~0	~0	~0
Wheat cell suspension	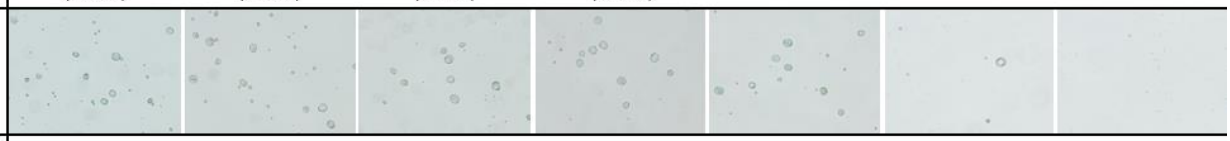						
Wheat cell (cells mL^{-1})	$12x10^4$ ($\pm$ $11,4x10^4$)	$10x10^4$ ($\pm$ $8,2x10^4$)	$11x10^4$ ($\pm$ $11,0x10^4$)	$12x10^4$ ($\pm$ $10,3x10^4$)	$7x10^4$ ($\pm$ $10,6x10^4$)	$1x10^4$ ($\pm$ $3,2x10^4$)	< $1x10^4$
Wheat leaf surface							
Visible tissue damage	No necrosis	No necrosis	No necrosis	No necrosis	No necrosis	No necrosis	No necrosis
Wheat plant biomass							
Fresh weight (g per pot)	10.2.3 (± 11.5)	102.0 (± 15.6)	103.7 (± 6.7)	102.0 (± 7.2)	98.9 (± 8.5)	101.4 (± 8.8)	102.5 (± 10.2)

Figure 2. Effect of mycosubtilin at different concentrations on the growth of either *Z. tritici* or wheat cells grown *in vitro* in liquid medium in twelve well microplates, and on leaf appearance and plant fresh biomass of whole plants grown in the greenhouse. Fungal growth was assessed using resazurin staining and optical density measurement at 10 days after inoculation (dai) of glucose peptone medium with *Z. tritici* spores (n=6), while wheat cell growth was evaluated using Malassez hemocytometer at 21 days after inoculation of Gamborg B5 medium with wheat cell suspension (n=10). Leaf appearance was assessed visually at two, seven and fifteen days after plant treatment (n=27), while the fresh biomass was determined by weighting nine whole plants from each pot (n=3). Representative pictures of either *Z. tritici* or wheat cell cultures observed under light microscope at magnification 10x and 20x respectively, as well as the microplate wells used for *Z. tritici* culture medium staining with resazurin, are shown. Likewise, representative pictures of leaf appearance and aerial plant fresh biomass, at fifteen days after treatment, are also presented.

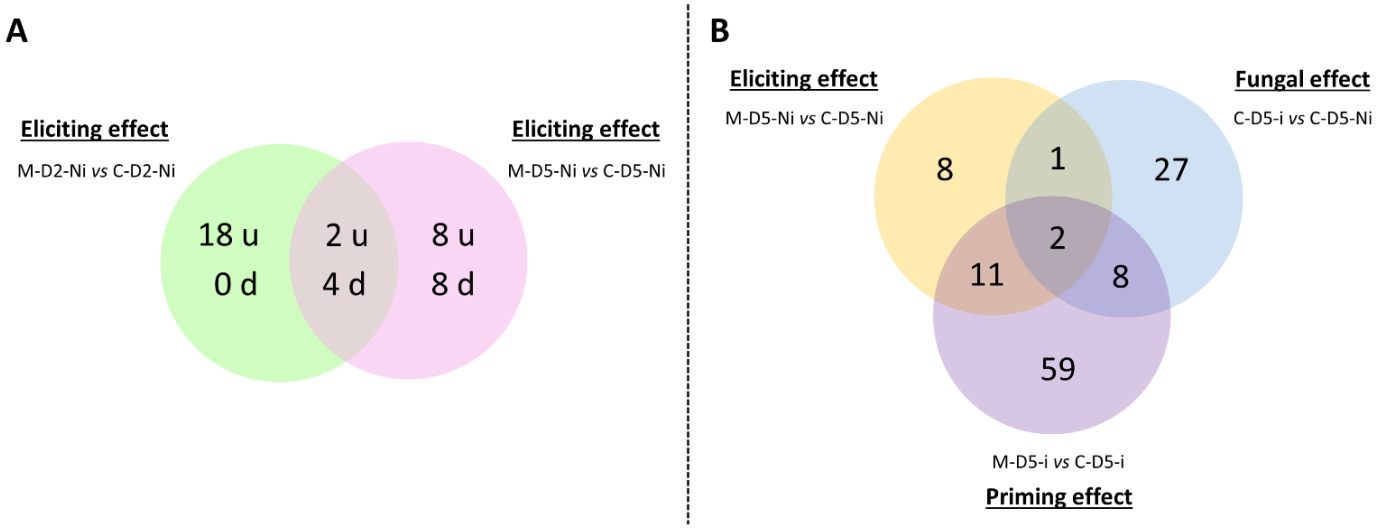

Figure 3. Venn diagrams underlying (**A**) the number of up-regulated (u) or down-regulated (d) genes observed after mycosubtilin treatment in non-infectious conditions by *Zymoseptoria tritici* as well as (**B**) the number of differentially expressed genes in the different tested conditions at five days after treatment with mycosubtilin (*i.e.* three days after wheat inoculation with *Z. tritici*). In (**A**), the potential early elicitation effect of mycosubtilin at two days after treatment (M-D2-Ni *vs* C-D2-Ni) on the levels of wheat leaf gene expression is compared to the later one at five days after treatment (M-D5-Ni *vs* C-D5-Ni). In (**B**), The eliciting effect of mycosubtilin (M-D5-Ni *vs* C-D5-Ni) is compared to the fungus effect (C-D5-i *vs* C-D5-Ni) and to the priming effect of mycosubtilin (M-D5-i *vs* C-D5-i). M means treated with mycosubtilin towards mock treated C. Ni stands for mock inoculated whereas i indicates that plants were infected with *Z. tritici*. D2 and D5 means that leaves were sampled respectively at two and five days after mycosubtilin treatment.

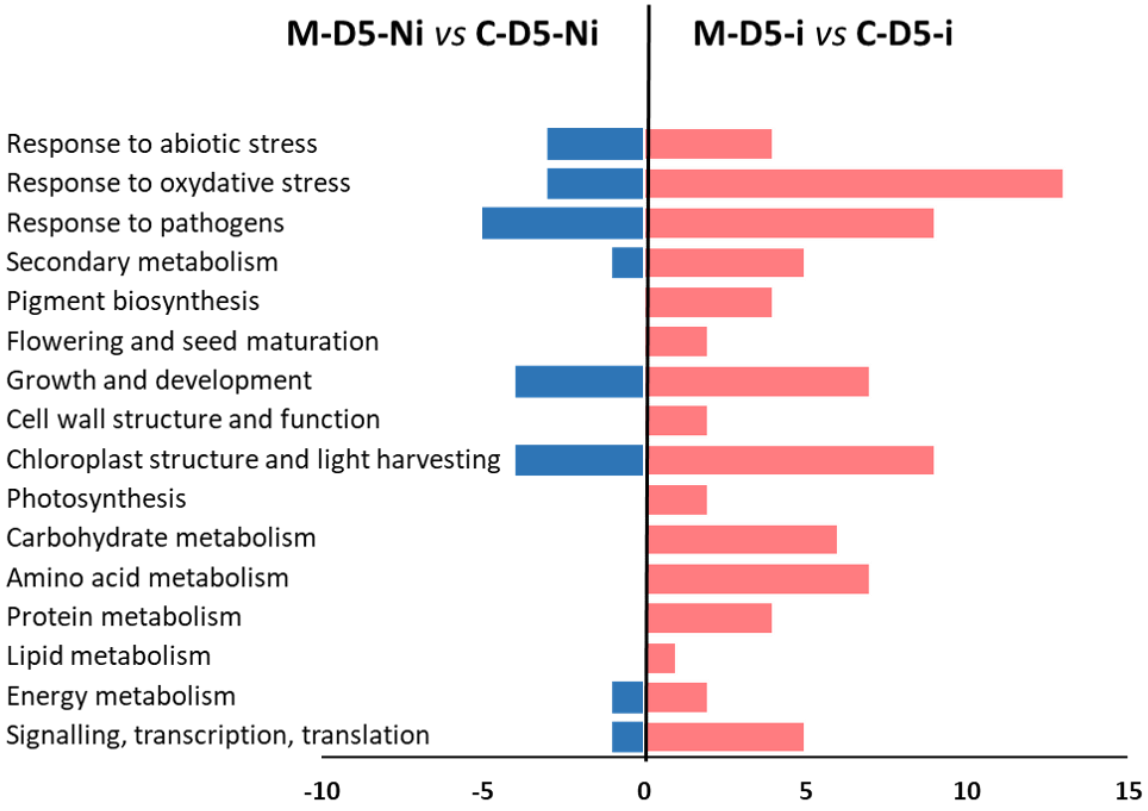

Figure 4. Functional groups of differentially expressed genes highlighting eliciting (M-D5-Ni *vs* C-D5-Ni) or priming (M-D-5i *vs* C-D5-i) effect of wheat defenses after treatment with mycosubtilin. Functional annotation of DEGs was performed based on NCBI GenBank and related-gene physiological processes were assigned with NCBI, AmiGO 2 Gene Ontology and UniProt. M means treated with mycosubtilin towards mock treated C. Ni stands for mock inoculated whereas i indicates that plants were infected with *Z. tritici*. D5 means that leaves were sampled at five days after mycosubtilin treatment.

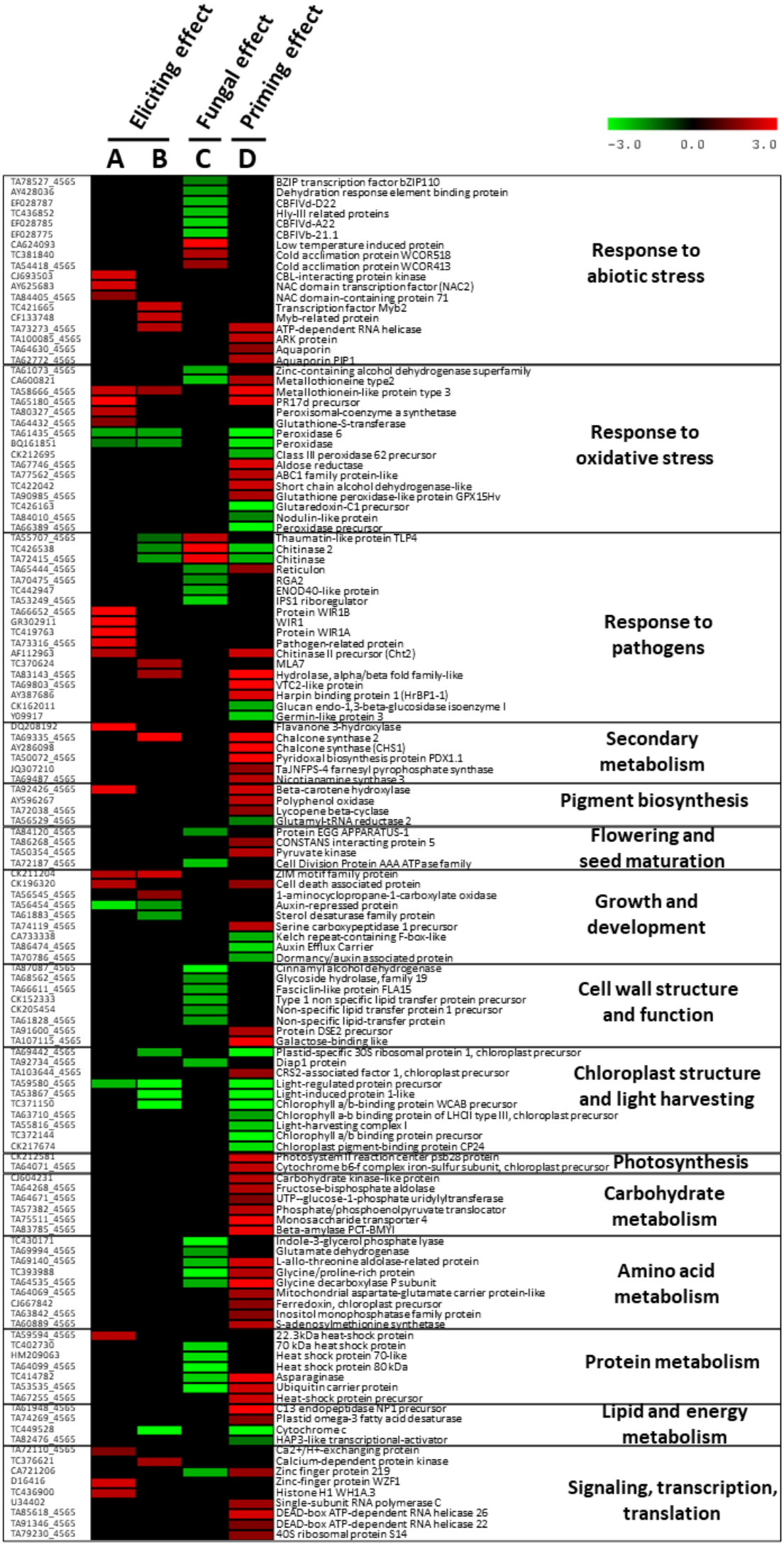
Eliciting effect
Fungal effect
Priming effect
A
B
C
D
-3.0
0.0
3.0
TA78527_4565 BZIP transcription factor bZIP110
AY428036 Dehydration response element binding protein
EF028787 CBFIVd-D22
TC436852 Hly-III related proteins
EF028785 CBFIVd-A22
EF028775 CBFIVb-21.1
CA624093 Low temperature induced protein
TC381840 Cold acclimation protein WCOR518
TA54418_4565 Cold acclimation protein WCOR413
CJ693503 CBL-interacting protein kinase
AY625683 NAC domain transcription factor (NAC2)
TA84405_4565 NAC domain-containing protein 71
TC421665 Transcription factor Myb2
CF133748 Myb-related protein
TA73273_4565 ATP-dependent RNA helicase
TA100085_4565 ARK protein
TA64630_4565 Aquaporin
TA62772_4565 Aquaporin PIP1
Response to abiotic stress
TA61073_4565 Zinc-containing alcohol dehydrogenase superfamily
CA600821 Metallothioneine type2
TA58666_4565 Metallothionein-like protein type 3
TA65180_4565 PR17d precursor
TA80327_4565 Peroxisomal-coenzyme a synthetase
TA64432_4565 Glutathione-S-transferase
TA61435_4565 Peroxidase 6
BQ161851 Peroxidase
CK212695 Class III peroxidase 62 precursor
TA67746_4565 Aldose reductase
TA77562_4565 ABC1 family protein-like
TC422042 Short chain alcohol dehydrogenase-like
TA90985_4565 Glutathione peroxidase-like protein GPX15Hv
TC426163 Glutaredoxin-C1 precursor
TA84010_4565 Nodulin-like protein
TA66389_4565 Peroxidase precursor
Response to oxidative stress
TA55707_4565 Thaumatin-like protein TLP4
TC426538 Chitinase 2
TA72415_4565 Chitinase
TA65444_4565 Reticulon
TA70475_4565 RGA2
TC442947 ENOD40-like protein
TA53249_4565 IPS1 riboregulator
TA66652_4565 Protein WIR1B
GR302911 WIR1
TC419763 Protein WIR1A
TA73316_4565 Pathogen-related protein
AF112963 Chitinase II precursor (Cht2)
TC370624 MLA7
TA83143_4565 Hydrolase, alpha/beta fold family-like
TA69803_4565 VTC2-like protein
AY387686 Harpin binding protein 1 (HrBP1-1)
CK162011 Glucan endo-1,3-beta-glucosidase isoenzyme I
Y09917 Germin-like protein 3
Response to pathogens
DQ208192 Flavanone 3-hydroxylase
TA69335_4565 Chalcone synthase 2
AY286098 Chalcone synthase (CHS1)
TA50072_4565 Pyridoxal biosynthesis protein PDX1.1
JQ307210 TaJNFPS-4 farnesyl pyrophosphate synthase
TA69487_4565 Nicotianamine synthase 3
Secondary metabolism
TA92426_4565 Beta-carotene hydroxylase
AY596267 Polyphenol oxidase
TA72038_4565 Lycopene beta-cyclase
TA56529_4565 Glutamyl-tRNA reductase 2
Pigment biosynthesis
TA84120_4565 Protein EGG APPARATUS-1
TA86268_4565 CONSTANS interacting protein 5
TA50354_4565 Pyruvate kinase
TA72187_4565 Cell Division Protein AAA ATPase family
Flowering and seed maturation
CK211204 ZIM motif family protein
CK196320 Cell death associated protein
TA56545_4565 1-aminocyclopropane-1-carboxylate oxidase
TA56454_4565 Auxin-repressed protein
TA61883_4565 Sterol desaturase family protein
TA74119_4565 Serine carboxypeptidase 1 precursor
CA733338 Kelch repeat-containing F-box-like
TA86474_4565 Auxin Efflux Carrier
TA70786_4565 Dormancy/auxin associated protein
Growth and development
TA87087_4565 Cinnamyl alcohol dehydrogenase
TA68562_4565 Glycoside hydrolase, family 19
TA66611_4565 Fasciclin-like protein FLA15
CK152333 Type 1 non specific lipid transfer protein precursor
CK205454 Non-specific lipid transfer protein 1 precursor
TA61828_4565 Non-specific lipid-transfer protein
TA91600_4565 Protein DSE2 precursor
TA107115_4565 Galactose-binding like
Cell wall structure and function
TA69442_4565 Plastid-specific 30S ribosomal protein 1, chloroplast precursor
TA92734_4565 Diap1 protein
TA103644_4565 CRS2-associated factor 1, chloroplast precursor
TA59580_4565 Light-regulated protein precursor
TA53867_4565 Light-induced protein 1-like
TC371150 Chlorophyll a/b-binding protein WCAB precursor
TA63710_4565 Chlorophyll a-b binding protein of LHCII type III, chloroplast precursor
TA55816_4565 Light-harvesting complex I
TC372144 Chlorophyll a/b binding protein precursor
CK217674 Chloroplast pigment-binding protein CP24
Chloroplast structure and light harvesting
CK212581 Photosystem II reaction center psb28 protein
TA64071_4565 Cytochrome b6-f complex iron-sulfur subunit, chloroplast precursor
Photosynthesis
CJ604231 Carbohydrate kinase-like protein
TA64268_4565 Fructose-bisphosphate aldolase
TA64671_4565 UTP--glucose-1-phosphate uridylyltransferase
TA57382_4565 Phosphate/phosphoenolpyruvate translocator
TA75511_4565 Monosaccharide transporter 4
TA83785_4565 Beta-amylase PCT-BMY1
Carbohydrate metabolism
TC430171 Indole-3-glycerol phosphate lyase
TA69994_4565 Glutamate dehydrogenase
TA69140_4565 L-allo-threonine aldolase-related protein
TC393988 Glycine/proline-rich protein
TA64535_4565 Glycine decarboxylase P subunit
TA64069_4565 Mitochondrial aspartate-glutamate carrier protein-like
CJ667842 Ferredoxin, chloroplast precursor
TA63842_4565 Inositol monophosphatase family protein
TA60889_4565 S-adenosylmethionine synthetase
Amino acid metabolism
TA59594_4565 22.3kDa heat-shock protein
TC402730 70 kDa heat shock protein
HM209063 Heat shock protein 70-like
TA64099_4565 Heat shock protein 80 kDa
TC414782 Asparaginase
TA53535_4565 Ubiquitin carrier protein
TA67255_4565 Heat-shock protein precursor
Protein metabolism
TA61948_4565 C13 endopeptidase NP1 precursor
TA74269_4565 Plastid omega-3 fatty acid desaturase
TC449528 Cytochrome c
TA82476_4565 HAP3-like transcriptional-activator
Lipid and energy metabolism
TA72110_4565 Ca2+/H+-exchanging protein
TC376621 Calcium-dependent protein kinase
CA721206 Zinc finger protein 219
D16416 Zinc-finger protein WZF1
TC436900 Histone H1 WH1A.3
U34402 Single-subunit RNA polymerase C
TA85618_4565 DEAD-box ATP-dependent RNA helicase 26
TA91346_4565 DEAD-box ATP-dependent RNA helicase 22
TA79230_4565 40S ribosomal protein S14
Signaling, transcription, translation

Figure 5. Heatmap showing significantly up- or down-regulated genes in wheat third-leaves (cv. Alixan) treated or not with 100 mg.L^{-1} mycosubtilin and infected or not with *Zymoseptoria tritici* (strain T02596), recorded at two days after treatment in noninfectious conditions (**A** and **B**) and at five days after treatment (*i.e.* three days after inoculation) in infectious conditions (**C** and **D**). A and B highlight the eliciting effect, C shows the fungal effect, while D reveals the priming effect induced by mycosubtilin. Gene-related physiological processes are represented on the right part of the graph and were determined using NCBI, AmiGO 2 Gene Ontology, KEGG and UniProt. **A**, M-D2-Ni *vs* C-D2-Ni; **B**, M-D5-Ni *vs* C-D5-Ni; **C**, C-D5-i *vs* C-D5-Ni; **D**, M-D5-i *vs* C-D5-i. Significant relative change in gene expression is presented in Log2 ratio, according to the color scale, using the WebMev software. M means treated with mycosubtilin towards mock treated C. Ni stands for mock inoculated whereas i indicated that plants were infected with *Z. tritici*. D2 and D5 means that leaves were sampled respectively at two and five days after mycosubtilin treatment.

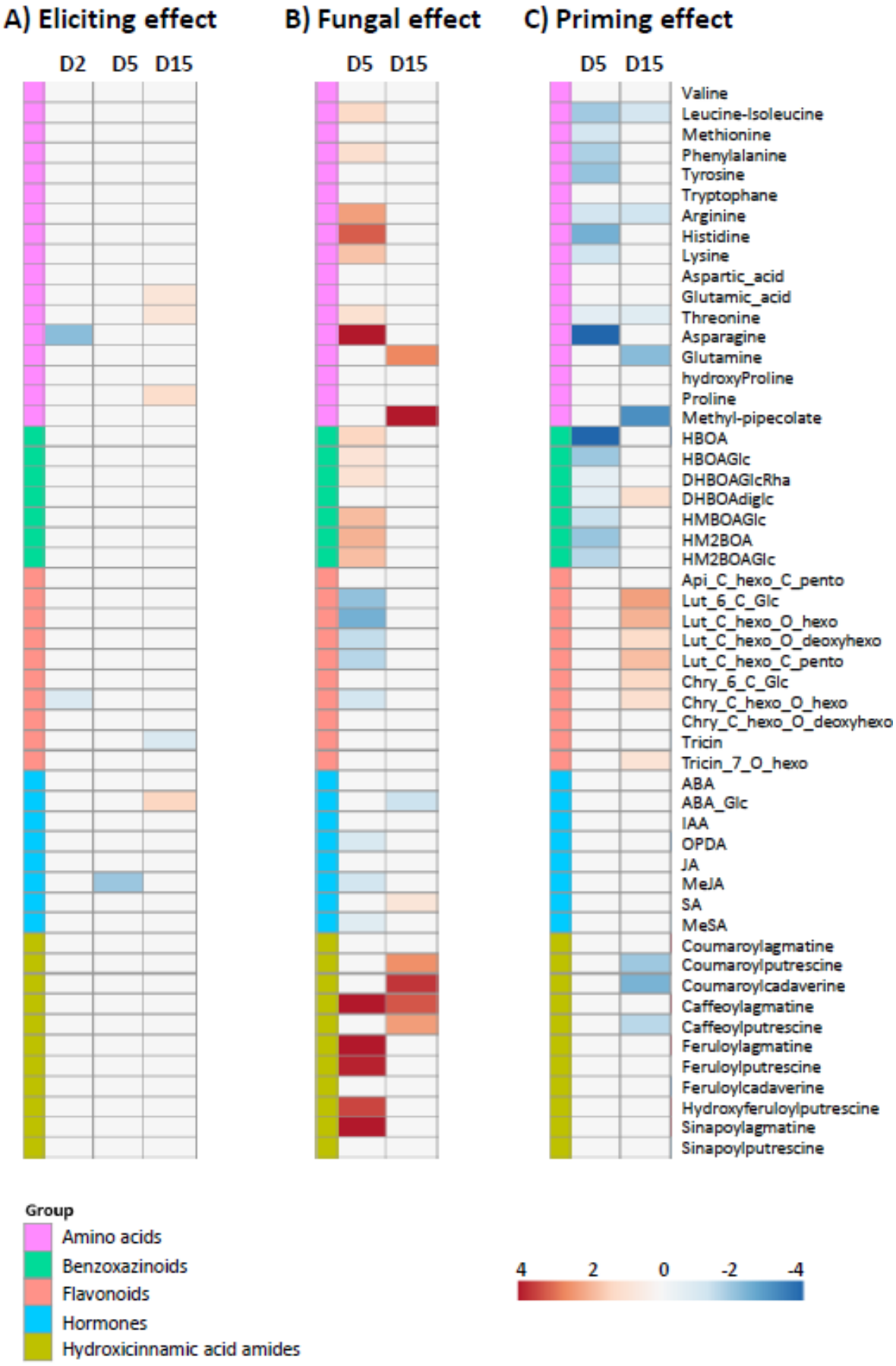
A) Eliciting effect
D2
D5
D15
B) Fungal effect
D5
D15
C) Priming effect
D5
D15
Valine
Leucine-Isoleucine
Methionine
Phenylalanine
Tyrosine
Tryptophane
Arginine
Histidine
Lysine
Aspartic_acid
Glutamic_acid
Threonine
Asparagine
Glutamine
hydroxyProline
Proline
Methyl-pipecolate
HBOA
HBOAGlc
DHBOAGlcRha
DHBOAdiglc
HMBOAGlc
HM2BOA
HM2BOAGlc
Api_C_hexo_C_pento
Lut_6_C_Glc
Lut_C_hexo_O_hexo
Lut_C_hexo_O_deoxyhexo
Lut_C_hexo_C_pento
Chry_6_C_Glc
Chry_C_hexo_O_hexo
Chry_C_hexo_O_deoxyhexo
Tricin
Tricin_7_O_hexo
ABA
ABA_Glc
IAA
OPDA
JA
MeJA
SA
MeSA
Coumaroylagmatine
Coumaroylputrescine
Coumaroylcadaverine
Caffeoylagmatine
Caffeoylputrescine
Feruloylagmatine
Feruloylputrescine
Feruloylcadaverine
Hydroxyferuloylputrescine
Sinapoylagmatine
Sinapoylputrescine
Group
Amino acids
Benzoxazinoids
Flavonoids
Hormones
Hydroxicinnamic acid amides
4
2
0
-2
-4

Figure 6. Heatmap of significant relative changes in metabolite patterns within wheat third-leaves (cv. Alixan) treated or not with 100 mg.L^{-1} mycosubtilin and infected or not with *Zymoseptoria tritici* (strain T02596) at different time points (n = 9 plants). (A), potential elicitation effect of mycosubtilin in noninfectious conditions at 2 (M-D2-Ni *vs* C-D2-Ni), 5 (M-D5-Ni *vs* C-D5-Ni) and 15 (M-D15-Ni *vs* C-D15-Ni) days after treatment (dat). B, Fungal effect on wheat leaf metabolome at 5 (C-D5-i *vs* C-D5-Ni) and 15 (C-D15-i *vs* C-D15-Ni) dat, *i.e.* at 3 and 13 days after wheat inoculation (dai) with *Z. tritici*, respectively. C, Priming effect of mycosubtilin in infectious conditions at 5 (MD5i *vs* CD5i) and 15 (MD15i *vs* CD15i) dat (*i.e.* at 3 and 13 dai, respectively). M means treated with mycosubtilin towards mock treated C. Ni stands for mock inoculated whereas i indicates that plants were infected with *Z. tritici*. D2, D5 and D15 mean that leaves were sampled respectively at two, five and fifteen days after mycosubtilin treatment. Log2 of significant metabolite fold changes for indicated pairwise comparisons are given by shades of red or blue colors according to the scale bar. Metabolites were grouped according to their functional or chemical family as amino acids, benzoxazinoids, flavonoids, hormones and hydroxycinnamic acid amides. Data represent mean values of nine biological replicates for each condition and time point. Statistical analyses were performed using the Tukey's Honest Significant Difference method followed by a false discovery rate (FDR) correction, with FDR < 0.05. For FDR ≥ 0.05, Log2 fold changes were set to 0.

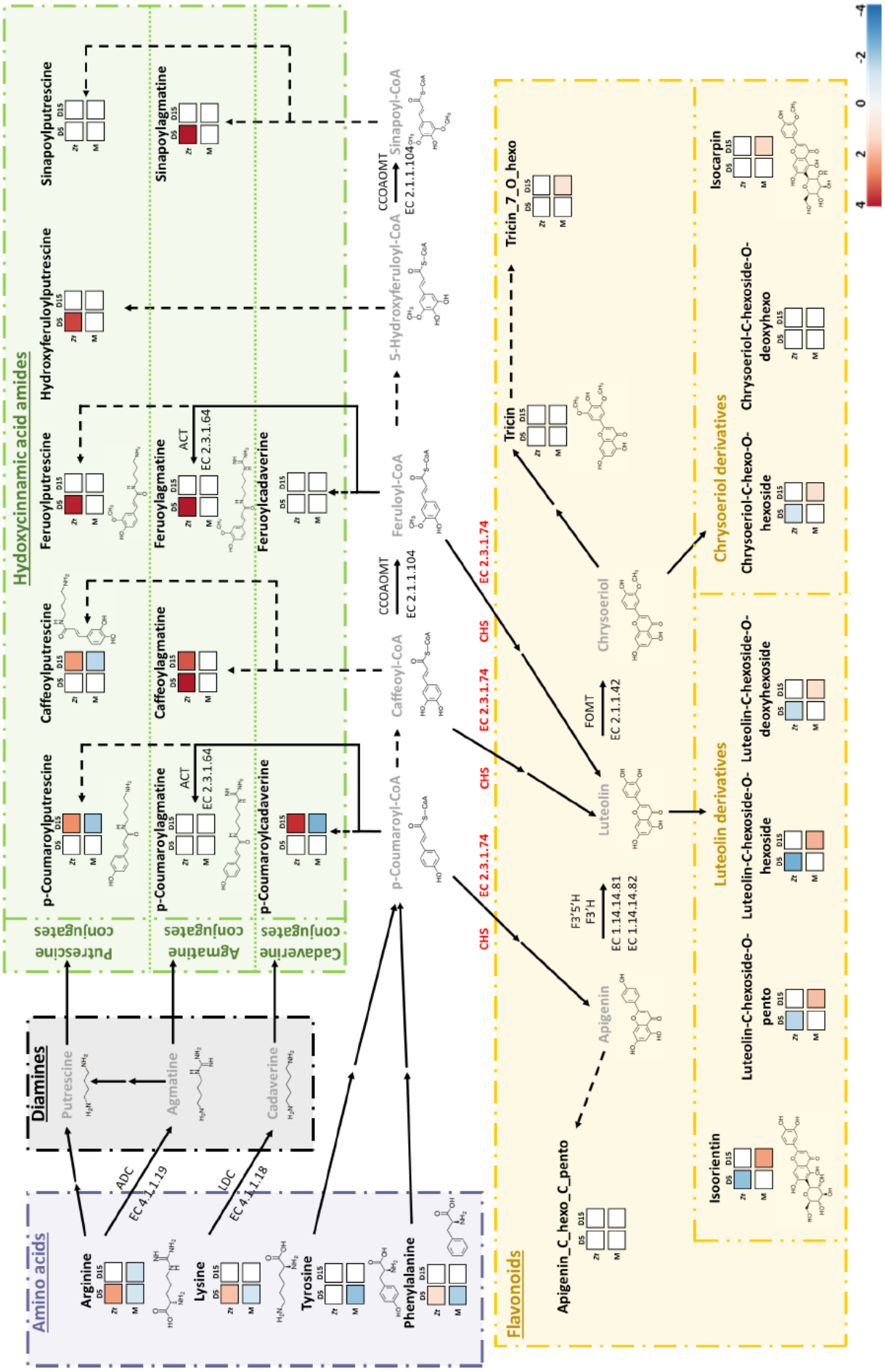
Amino acids
Arginine
Lysine
Tyrosine
Phenylalanine
ADC
EC 4.1.1.19
LDC
EC 4.1.1.18
Diamines
Putrescine
Agmatine
Cadaverine
Putrescine conjugates
Agmatine conjugates
Cadaverine conjugates
Hydoxycinnamic acid amides
p-Coumaroylputrescine
Caffeoylputrescine
Feruoylputrescine
Hydroxyferuloylputrescine
Sinapoylputrescine
p-Coumaroylagmatine
Caffeoylagmatine
Feruoylagmatine
Sinapoylagmatine
p-Coumaroylcadaverine
Feruoylcadaverine
ACT
EC 2.3.1.64
p-Coumaroyl-CoA
Caffeoyl-CoA
Feruloyl-CoA
5-Hydroxyferuloyl-CoA
Sinapoyl-CoA
CCOAOMT
EC 2.1.1.104
CHS
EC 2.3.1.74
F3'5'H
F3'H
EC 1.14.14.81
EC 1.14.14.82
FOMT
EC 2.1.1.42
Flavonoids
Apigenin
Luteolin
Chrysoeriol
Tricin
Apigenin_C_hexo_C_pento
Luteolin derivatives
Isoorientin
Luteolin-C-hexoside-O-pento
Luteolin-C-hexoside-O-hexoside
Luteolin-C-hexoside-O-deoxyhexoside
Chrysoeriol derivatives
Isocarpin
Chrysoeriol-C-hexoside-O-hexoside
Chrysoeriol-C-hexoside-O-deoxyhexo
Tricin_7_O_hexo
D5
D15
Zt
M
4
2
0
-2
-4

Figure 7. Metabolic map of the biosynthesis pathways and patterns of accumulation of major hydroxycinnamic acid amides and flavonoids within wheat third leaves (cv. Alixan) inoculated with *Zymoseptoria tritici* (strain T02596) pre-treated or not with mycosubtilin. Metabolic pathways are based on KEGG pathways (map00310, map00330, map00940, map00941, map00944). Amino acids, diamines, hydroxycinnamic acid amides and flavonoids metabolite families are separated and indicated in block of different colors, respectively purple, black, green and orange. Heatmaps show significant Log2 fold changes in metabolite accumulation, according to the corresponding scale bar. For each analyzed metabolite, the two upper squares represent the fungus effect on the relative accumulation of the compound, from the left to the right, at five (C-D5-i *vs* C-D5-Ni) and fifteen (C-D15-i *vs* C-D15-Ni) days after treatment (dat), *i.e* 13 days after inoculation (dai). The two lower squares represent the effect of application of mycosubtilin (priming) prior to infection with *Z. tritici* on the wheat metabolome at five (M-D5-i *vs* C-D5-i) and fifteen (M-D15-i *vs* C-D15-i) dat. Metabolites in grey were not analyzed in this study. Solid arrows stand for enzymatic reactions completely described in the abovementioned KEGG pathways whereas dashed arrows are for suggested ones. Double arrows represent two or more metabolic steps. With ACT: agmatine N4-coumaroyltransferase, ADC: arginine decarboxylase, CCOAOMT: caffeoyl-CoA O-methyltransferase, CHS: chalcone synthase, F3’5’H: flavonoid 3',5'-hydroxylase, F3’H: flavonoid 3'-monooxygenase, FOMT: flavone 3'-O-methyltransferase, LDC: lysine decarboxylase. Genes coding for chalcone synthase were significantly upregulated when plants were primed with mycosubtilin at five days after treatment (M-D5-i *vs* C-D5-i), hence CHS is presented in red. M means treated with mycosubtilin towards mock treated C. Ni stands for mock inoculated whereas i indicates that plants were infected with *Z. tritici*. D5 and D15 mean that leaves were sampled respectively at five and fifteen days after mycosubtilin treatment.

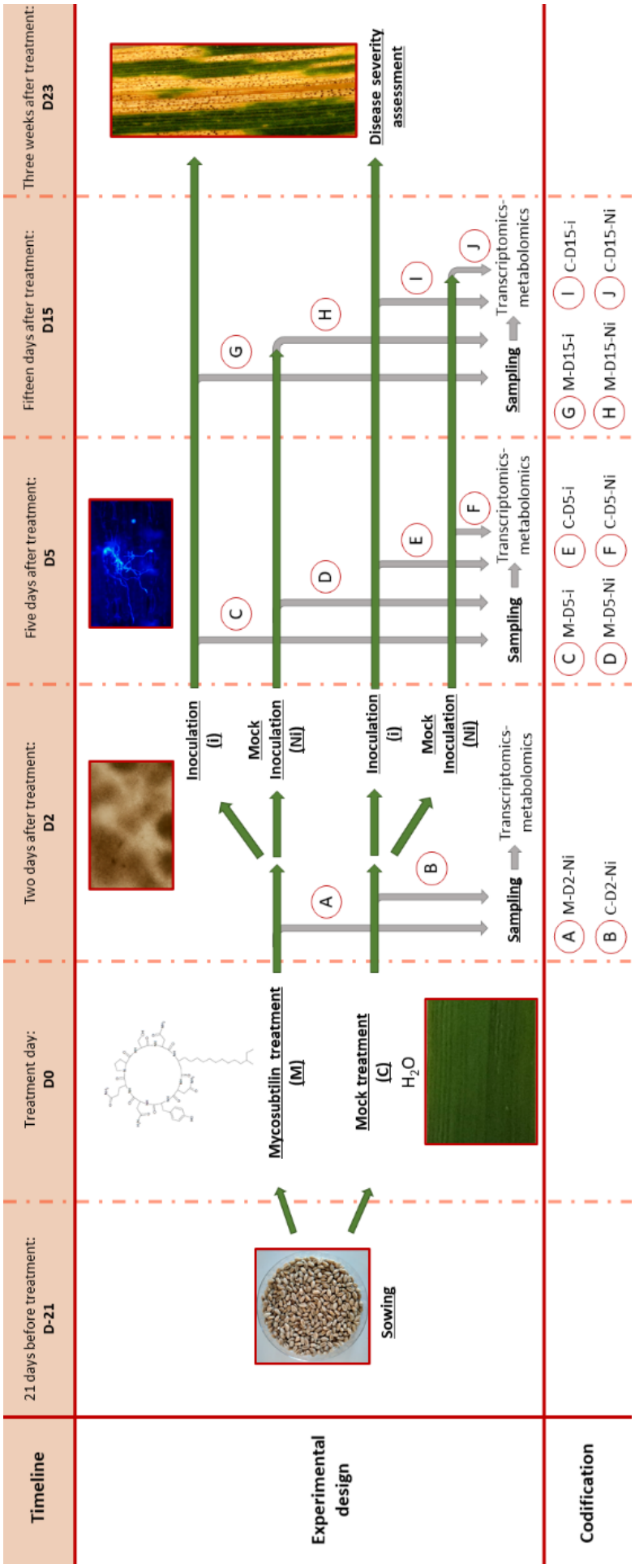
Timeline
Experimental design
Codification
21 days before treatment: D-21
Treatment day: D0
Two days after treatment: D2
Five days after treatment: D5
Fifteen days after treatment: D15
Three weeks after treatment: D23
Sowing
Mycosubtilin treatment (M)
Mock treatment (C)
H2O
Inoculation (i)
Mock Inoculation (Ni)
Sampling
Transcriptomics-metabolomics
Disease severity assessment
A M-D2-Ni
B C-D2-Ni
C M-D5-i
D M-D5-Ni
E C-D5-i
F C-D5-Ni
G M-D15-i
H M-D15-Ni
I C-D15-i
J C-D15-Ni

Supplementary figure S1. Experimental design illustrating the main steps of the whole study. After pre-germination in square petri dishes, wheat seeds (cv. Alixan) were grown in greenhouse for 21 days. At days 0 (DO), plants were either sprayed with a solution of mycosubtilin at 100 $mg.L^{-1}$ or with a mock treatment. Photography of wheat third-leaves epidermis observed with an optic microscope is shown. At two days after treatment (D2), third leaves were harvested for each condition and were used for further analyses (transcriptomics and metabolomics). After this, remaining plants were inoculated, or not, with a spore suspension of the *Zymoseptoria tritici* strain T02596 (concentration: 10^6 spores mL^{-1}). Photography of *Z. tritici* growing on PDA medium and observed microscopically is presented. At five days (D5) and fifteen days (D15) after treatment, wheat third leaves were sampled for further analyses; assessment of the *in planta* infection process of the fungus at D5 was investigated as well as transcriptomic analyses whereas metabolomic assays were performed at D5 and D15. Finally, at 23 days after treatment (D23), disease severity level was scored by measuring the third-leaf area with disease lesions. Codification used for each modality in the present study is shown at the bottom of the figure.

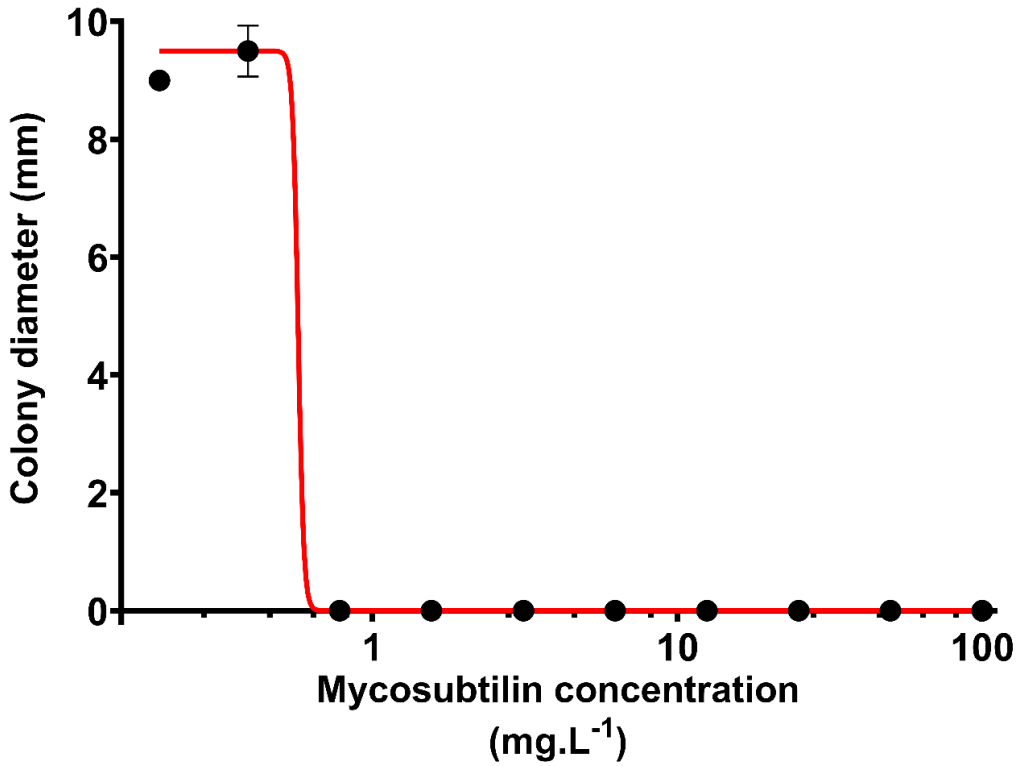

Supplementary figure S2. Dose-response curve obtained *in vitro* for mycosubtilin towards the *Zymoseptoria tritici* strain T02596. The fungal growth was assessed on PDA medium amended or not with different concentrations of mycosubtilin and scored 10 days of incubation by measuring fungal colony perpendicular diameters (n=6 colonies)**.** Non-linear regression was performed and IC_{50} was determined at 0.57 $mg.L^{-1}$ using GraphPad Prism software version 9.

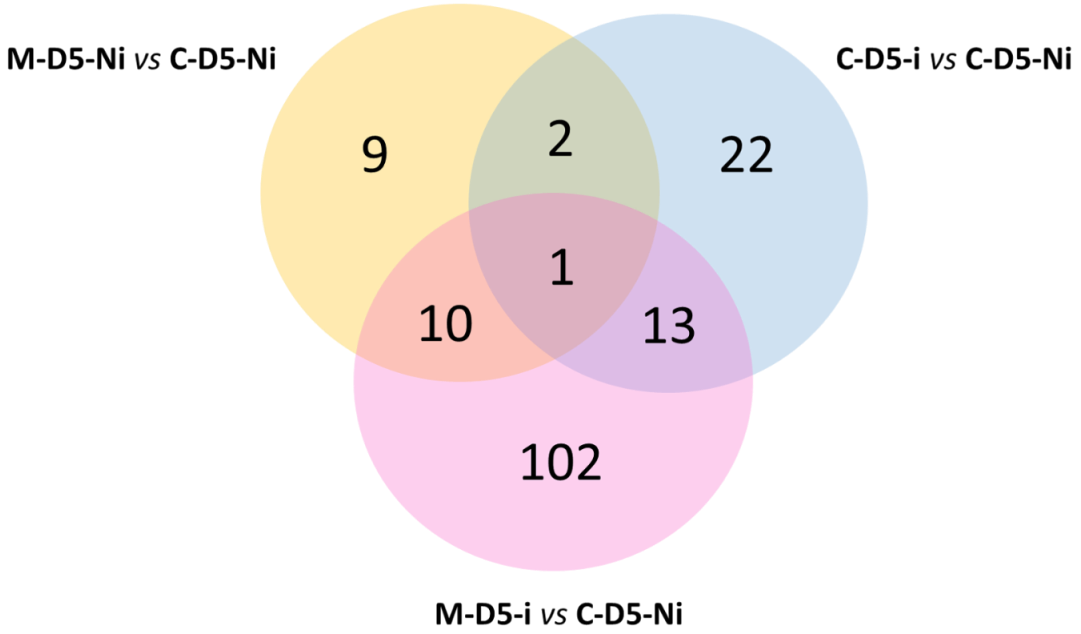

Supplementary figure S3. Venn diagram of the number of differentially expressed genes observed when investigating the eliciting effect of mycosubtilin (M-D5-Ni *vs* C-D5-Ni), *Zymoseptoria tritici* effect (C-D5-i vs C-D5-Ni) and the combined effect of both mycosubtilin and *Z. tritici* (M-D5-i vs M-D5-Ni) at five days after treatment with mycosubtilin (*i.e.* three days after wheat inoculation with *Z. tritici*). M means treated with mycosubtilin towards mock treated C. Ni stands for mock inoculated whereas i indicates that plants were infected with *Z. tritici*. D5 mean that leaves were sampled at five days after mycosubtilin treatment.

	A	B		
CA624093			Low temperature induced protein	Response to abiotic stress
TA73273_4565			ATP-dependent RNA helicase	
TA54418_4565			Cold acclimation protein WCOR413	
TA84187_4565			Protein phosphatase type 2-C	
TA92949_4565			Efflux transporter, RND family, MFP subunit	
AY785903			TaCBF6	
TA67331_4565			Proline-rich protein precursor	
TC381840			Cold acclimation protein WCOR518	
TA100085_4565			ARK protein	
TA79737_4565			Importin beta-like protein	
TA57180_4565			Actin	
TA74058_4565			Serine hydroxymethyltransferase	
TA58666_4565			Metallothionein-like protein type 3	Response to oxidative stress
TA102260_4565			Nitrite reductase apoprotein	
TA77625_4565			Chloroplast glutathione reductase	
TA65180_4565			PR17d precursor	
TA67746_4565			Aldose reductase	
TA64544_4565			Mitochondrial lipoamide dehydrogenase	
TA100790_4565			Cytochrome P450 family protein	
TA65542_4565			GMC oxidoreductase	
TA61435_4565			Peroxidase 6	
BQ161851			Peroxidase	
CK212695			Class III peroxidase 62 precursor	
TA55707_4565			Thaumatin-like protein TLP4	Response to pathogens
TA69803_4565			VTC2-like protein	
TC426538			Chitinase 2	
TA72415_4565			Chitinase	
GR302911			WIR1	
TC419763			Protein WIR1A	
TA76681_4565			HS1-like protein	
EF570122			Pathogen-inducible transcription factor ERF3	
AF112963			Chitinase II precursor (Cht2)	
TC370624			MLA7	
TA83143_4565			Hydrolase, alpha/beta fold family-like	
AY387686			Harpin binding protein 1 (HrBP1-1)	
TC404042			Phytosulfokine	
TA53249_4565			IPS1 riboregulator	
DQ208192			Flavanone 3-hydroxylase	Secondary metabolism
TA69335_4565			Chalcone synthase 2	
AY286098			Chalcone synthase (CHS1)	
TA50072_4565			Pyridoxal biosynthesis protein PDX1.1	
JQ307210			TaJNFPS-4 farnesyl pyrophosphate synthase	
TA83418_4565			GGDP synthase	
TA83418_4565			Isochorismate synthetase	
TA86268_4565			CONSTANS interacting protein 5	Flowering and seed maturation
TA84120_4565			Protein EGG APPARATUS-1	
TA50354_4565			Pyruvate kinase	
TA99155_4565			DNA replication and repair protein RecF	Growth and development
TC405303			Mitogen-activated protein kinase 7	
CK211204			ZIM motif family protein	
CK196320			Cell death associated protein	
TA84990_4565			CDK5RAP1-like protein	
TC380019			SAP-like protein BP-73	
CA612835			Abscisic stress ripening protein-like protein	
TA87087_4565			Cinnamyl alcohol dehydrogenase	Cell wall structure and function
TA66611_4565			Fasciclin-like protein FLA15	
CK152333			Type 1 non specific lipid transfer protein precursor	
CK205454			Non-specific lipid transfer protein 1 precursor	
TA61828_4565			Non-specific lipid-transfer protein	
TC383836			Nucleosome assembly protein 1-like protein 2	
TA102372_4565			Hydroxyproline-rich glycoprotein DZ-HRGP precursor	
TA91600_4565			Protein DSE2 precursor	
TA66617_4565			Plastid-specific 30S ribosomal protein 3, chloroplast precursor	Chloroplast structure and pigment biosynthesis
TA95179_4565			Amidophosphoribosyl-transferase	
CD879285			Triosephosphate isomerase, chloroplast precursor	
TA103644_4565			CRS2-associated factor 1, chloroplast precursor	
TA92734_4565			Diap1 protein	
TA92426_4565			Beta-carotene hydroxylase	
AY596267			Polyphenol oxidase	
TA70845_4565			Porphobilinogen deaminase	
TA58881_4565			Glutamate-1-semialdehyde 2,1-aminomutase, chloroplast precursor	
TA89084_4565			S-adenosyl-L-methionine Mg-protoporphyrin IX methyltranserase	
TA72038_4565			Lycopene beta-cyclase	
TC371150			Chlorophyll a/b-binding protein WCAB precursor	Light harvesting
TA63710_4565			Chlorophyll a-b binding protein of LHCII type III, chloroplast precursor	
TA55816_4565			Light-harvesting complex I	
TC372144			Chlorophyll a/b binding protein precursor	
CK217674			Chloroplast pigment-binding protein CP24	
CK212381			Photosystem II reaction center psb28 protein	Photosynthesis
TA64071_4565			Cytochrome b6-f complex iron-sulfur subunit, chloroplast precursor	
AF251264			Ribulose bisphosphate carboxylase activase B (RcaB)	
CJ604231			Carbohydrate kinase-like protein	Carbohydrate metabolism
TA83009_4565			FKBP-type peptidyl-prolyl cis-trans isomerase 3, chloroplast precursor	
TA64268_4565			Fructose-bisphosphate aldolase	
TA64671_4565			UTP--glucose-1-phosphate uridylyltransferase	
TA57382_4565			Phosphate/phosphoenolpyruvate translocator	
TA75511_4565			Monosaccharide transporter 4	
TA83785_4565			Beta-amylase PCT-BMY1	
DQ139267			4-hydroxyphenylpyruvate dioxygenase	Amino acid metabolism
TA82049_4565			Bifunctional aspartokinase/homoserine dehydrogenase 2, chloroplast precursor	
TC430171			Indole-3-glycerol phosphate lyase	
TA69994_4565			Glutamate dehydrogenase	
TA64535_4565			Glycine decarboxylase P subunit	
EU236151			Arginine decarboxylase	
TA64069_4565			Mitochondrial aspartate-glutamate carrier protein-like	
CJ667842			Ferredoxin, chloroplast precursor	
TA63842_4565			Inositol monophosphatase family protein	
TC369894			Glycine/D-amino acid oxidases-like	
TC448142			Glycine cleavage system H protein, mitochondrial precursor	
TC413834			S-adenosylmethionine:2-demethylmenaquinone methyltransferase-like	
TA79034_4565			3-dehydroquinate dehydratase/shikimate 5-dehydrogenase	
TA67255_4565			Heat-shock protein precursor	Protein metabolism
TA70500_4565			ATP-dependent Clp protease proteolytic subunit	
TA61948_4565			C13 endopeptidase NP1 precursor	
TC402730			70 kDa heat shock protein	
HM209063			Heat shock protein 70-like	
TA64099_4565			Heat shock protein 80	
TA74269_4565			Plastid omega-3 fatty acid desaturase	Lipid and energy metabolism
TC449528			Cytochrome c	
TA82827_4565			GTP-binding protein-related	Signaling, transcription, translation
TA51150_4565			Serine/threonine kinase	
U34402			Single-subunit RNA polymerase C	
TA85618_4565			DEAD-box ATP-dependent RNA helicase 26	
TA91346_4565			DEAD-box ATP-dependent RNA helicase 22	
D38485			Ps16 protein	
TA71493_4565			Elongation factor Ts	
TA88703_4565			Elongation factor G, mitochondrial precursor	
TA85526_4565			Translation initiation factor IF-2	
CA502352			Elongation factor	
TA79230_4565			40S ribosomal protein S14	
TA53517_4565			Ribosomal protein l34	
TA70216_4565			30S ribosomal protein S17, chloroplast precursor	
TA68774_4565			50S ribosomal protein L1, chloroplast precursor	
TA71488_4565			50S ribosomal protein L35	
TA61485_4565			Ribosomal protein s6 RPS6-2	
TA66609_4565			Ribosome-like protein	
TA50993_4565			Large subunit 26S ribosomal RNA gene	
TA56520_4565			Ribosomal protein L35A	
TA61855_4565			Ribosomal protein L13a	
TA58672_4565			Ribosomal protein	
TA58281_4565			60S ribosomal protein L44	
CV767873			60S ribosomal protein L27	
TA61981_4565			Large subunit 26S ribosomal RNA gene	
CK214923			Ribosomal protein L11	
TA64720_4565			50S ribosomal protein L21, chloroplast precursor	
TC413718			60S acidic ribosomal protein P3	
TA61076_4565			60S ribosomal protein L10-2	
TA68490_4565			50S ribosomal protein L28, chloroplast precursor	
TA58879_4565			Ribosomal protein L37	
TA54070_4565			Ribosomal protein L10A	
TA91877_4565			C3meo4	Other functions
TC389894			Tetratricopeptide repeat (TPR)-containing protein-like	
AF110180			High-affinity phosphate transporter PT1	

Supplementary figure S4. Heatmap of differentially expressed genes in wheat leaves (Cv.Alixan) after *Zymoseptoria tritici* (T02596 strain) infection in presence of mycosubtilin, at five days after treatment (*i.e.* three days after inoculation). (A) Comparison in gene expression between wheat leaves treated with mycosubtilin and inoculated with the fungus *versus* leaves treated with mycosubtilin and non-inoculated (M-D5-i *vs* M-D5-Ni). (B) whole specter of gene regulation induced by the combined effect of both mycosubtilin and *Z. tritici* (MD5i *vs* CD5Ni). Gene-related physiological processes are represented on the right part of the graph and were determined using NCBI, AmiGO 2 Gene Ontology, KEGG and UniProt. Significant relative changes in gene expression are presented in Log2 ratio, according to the corresponding color scale, using the WebMev software. M means treated with mycosubtilin towards mock treated C. Ni stands for mock inoculated whereas i indicates that plants were infected with *Z. tritici*. D5 means that leaves were sampled at five days after mycosubtilin treatment.

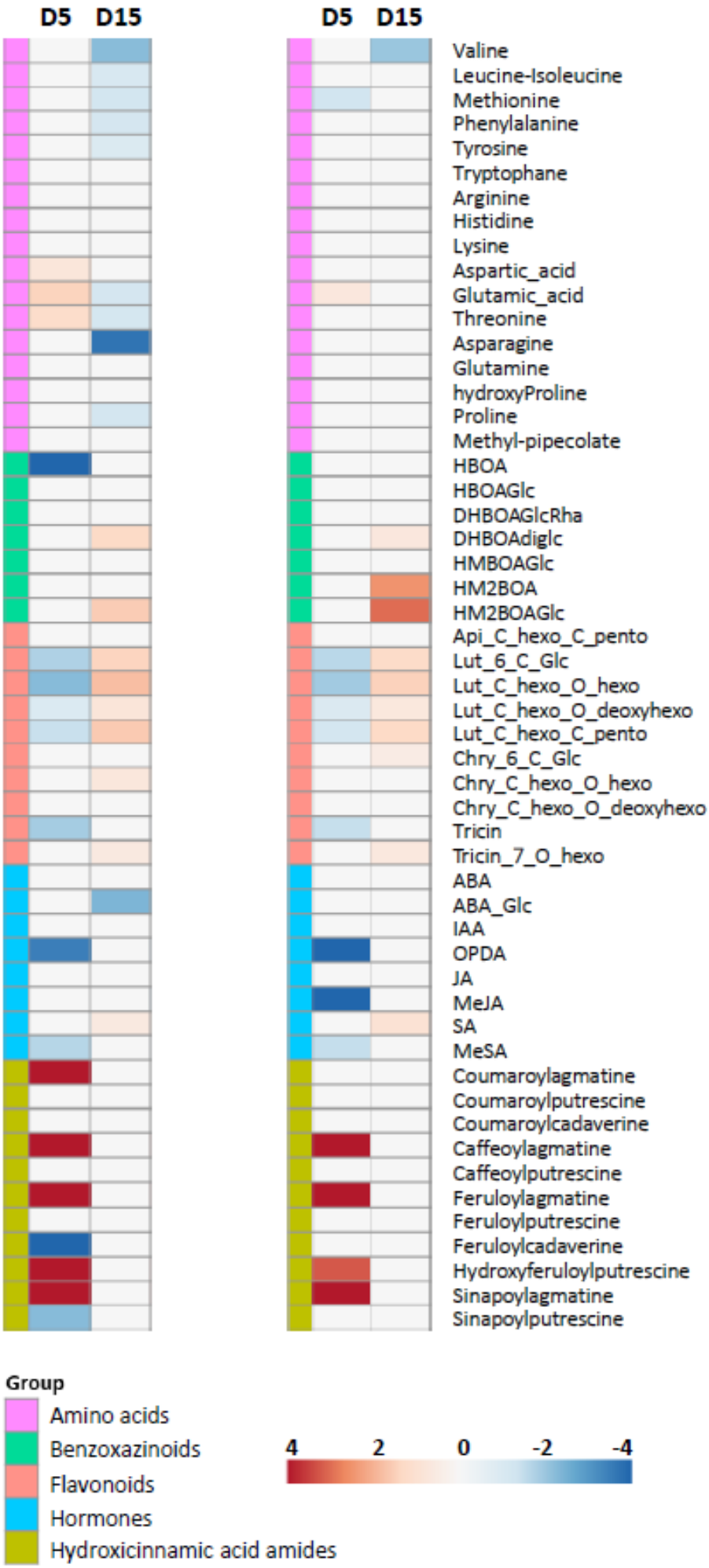
D5
D15
D5
D15
Valine
Leucine-Isoleucine
Methionine
Phenylalanine
Tyrosine
Tryptophane
Arginine
Histidine
Lysine
Aspartic_acid
Glutamic_acid
Threonine
Asparagine
Glutamine
hydroxyProline
Proline
Methyl-pipecolate
HBOA
HBOAGlc
DHBOAGlcRha
DHBOAdiglc
HMBOAGlc
HM2BOA
HM2BOAGlc
Api_C_hexo_C_pento
Lut_6_C_Glc
Lut_C_hexo_O_hexo
Lut_C_hexo_O_deoxyhexo
Lut_C_hexo_C_pento
Chry_6_C_Glc
Chry_C_hexo_O_hexo
Chry_C_hexo_O_deoxyhexo
Tricin
Tricin_7_O_hexo
ABA
ABA_Glc
IAA
OPDA
JA
MeJA
SA
MeSA
Coumaroylagmatine
Coumaroylputrescine
Coumaroylcadaverine
Caffeoylagmatine
Caffeoylputrescine
Feruloylagmatine
Feruloylputrescine
Feruloylcadaverine
Hydroxyferuloylputrescine
Sinapoylagmatine
Sinapoylputrescine
Group
Amino acids
Benzoxazinoids
Flavonoids
Hormones
Hydroxicinnamic acid amides
4
2
0
-2
-4

Supplementary figure S5. Heatmap of significant relative changes in metabolite pattern accumulation within wheat third-leaves (Cv. Alixan) following mycosubtilin application and/or *Zymoseptoria tritici* (T02596 strain) infection, at different time points (n=9 plants). (A) From the left to the right, the following conditions are presented, M-D5-i *vs* M-D5-Ni and M-D15-i *vs* M-D15-Ni. (B) Whole specter of metabolite accumulation modifications induced by the combined effect of mycosubtilin treatment and *Z. tritici* infection (from the left to the right M-D5-i *vs* C-D5-Ni and M-D15-i *vs* C-D15-Ni). M means treated with mycosubtilin towards mock treated C. Ni stands for mock inoculated whereas i indicates that plants were infected with *Z. tritici*. D5 and D15 mean that leaves were sampled respectively at five and fifteen days after mycosubtilin treatment. Log2 of significant metabolite fold changes for indicated pairwise comparisons are given by shades of red or blue colors according to the scale bar. Metabolites were grouped according to their functional or chemical family as amino acids, benzoxazinoids, flavonoids, hormones and hydroxycinnamic acid amides. Data represent mean values of nine biological replicates for each condition and time point. Statistical analyses were performed using the Tukey's Honest Significant Difference method followed by a false discovery rate (FDR) correction, with FDR < 0.05. For FDR ≥ 0.05, Log2 fold changes were set to 0.

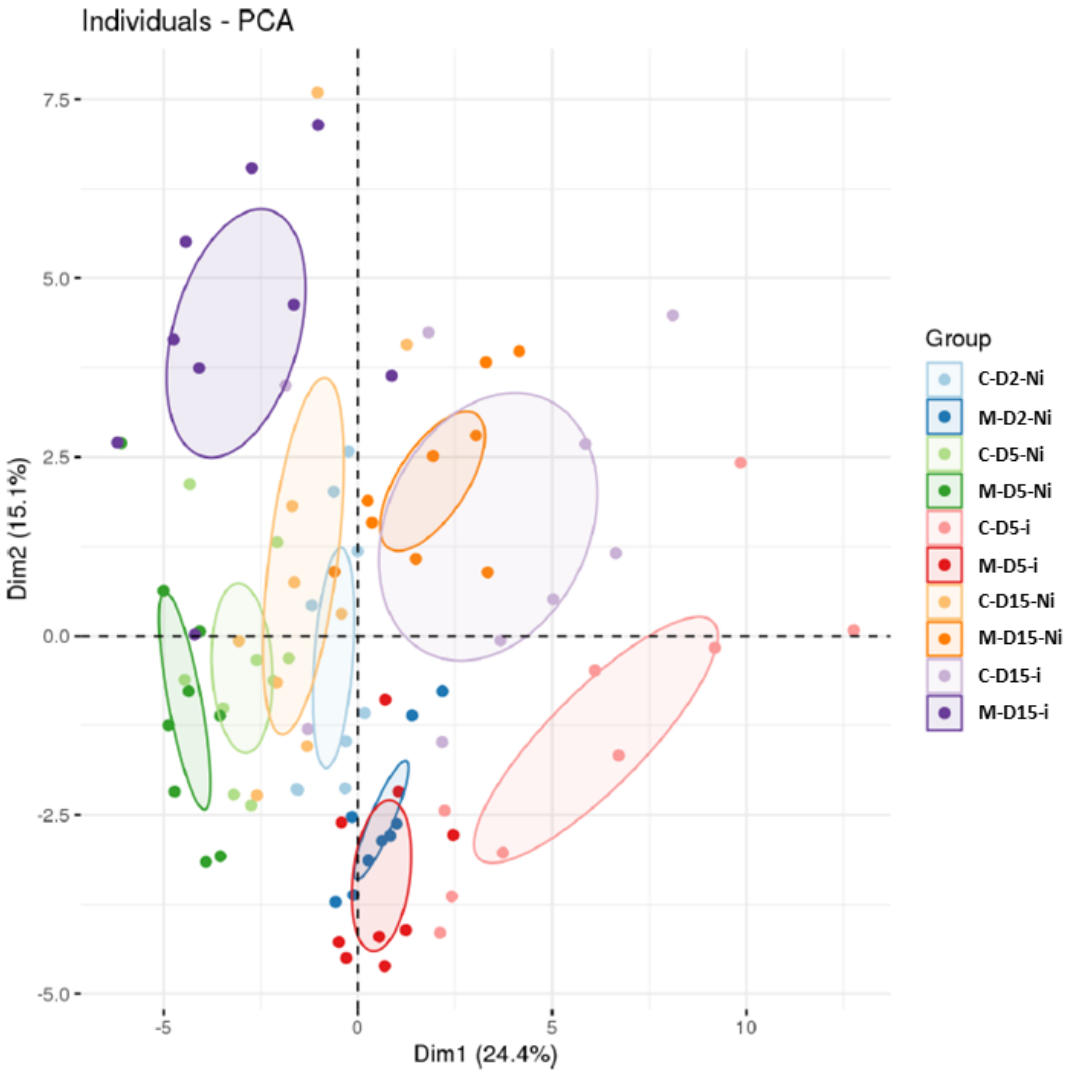

Supplementary Figure S6. Principal component analysis (PCA) displaying the global impact of mycosubtilin treatment and infection with *Zymoseptoria tritici* on wheat leaf metabolome. PCA was performed on relative amounts of all analyzed compounds in the different groups of samples. For each group, nine biological replicates were used. The first two principal components explain 24.4% and 15.1% of the variance separating the groups of samples, respectively.

Supplementary Table S1. Relative gene expression profiles in wheat third-leaves for mycosubtilin early (A) or later elicitation (B), fungus inoculation (C) and priming (D). This table is related to figure 6. Gene-related physiological processes are represented on the right part of the table and were determined using NCBI, AmiGO 2 Gene Ontology, KEGG and UniProt. With A: M-D2-Ni *vs* C-D2-Ni; B: M-D5-Ni *vs* C-D5-Ni; C: C-D5-i *vs* C-D5-Ni and D: M-D5-i *vs* C-D5-i. Log2 ratios >2 correspond to up-regulated genes (in red) and log2 ratios <0.5 to down-regulated genes (in green). Log2 ratios <2 and >0.5 were conventionally referred to 1. M means treated with mycosubtilin towards mock treated C. Ni stands for mock inoculated whereas i indicates that plants were infected with *Z. tritici*. D2 and D5 mean that leaves were sampled respectively at two and five days after mycosubtilin treatment.

	A	B	C	D				
Name	MNiD0 vs CNiD0	MNiD3 vs CNiD3	CiD3 vs CNiD3	MiD3 vs CiD3	Description	TopHit	ID	RefNumber
Response to abiotic stress								
TA78527_4565	1,0000	1,0000	0,4594	1,0000	BZIP transcription factor bZIP110	ta|TA78527_4565|	A_99_P289066	42528
AY428036	1,0000	1,0000	0,3768	1,0000	Dehydration response element binding protein	gb|AY428036|gb|E	A_99_P074325	23922
EF028787	1,0000	1,0000	0,3043	1,0000	CBFIVd-D22	gb|EF028787|ta|T/	A_99_P405352	948
TC436852	1,0000	1,0000	0,2955	1,0000	Hly-III related proteins	tc|TC436852	A_99_P511722	6696
EF028785	1,0000	1,0000	0,2543	1,0000	CBFIVd-A22	gb|EF028785|gb|E	A_99_P140518	15660
EF028775	1,0000	1,0000	0,2535	1,0000	CBFIVb-21.1	gb|EF028775|tc|TC	A_99_P012439	20101
CA624093	1,0000	1,0000	8,8824	1,0000	Low temperature induced protein	ta|CA624093|ta|C	A_99_P459967	11840
TC381840	1,0000	1,0000	3,0605	1,0000	Cold acclimation protein WCOR518	tc|TC381840	A_99_P421457	19082
TA54418_4565	1,0000	1,0000	2,5297	1,0000	Cold acclimation protein WCOR413	ta|TA54418_4565|	A_99_P210931	43524
CJ693503	3,9743	1,0000	1,0000	1,0000	CBL-interacting protein kinase	ta|CJ693503|tc|TC	A_99_P431532	1799
AY625683	3,9232	1,0000	1,0000	1,0000	NAC domain transcription factor (NAC2)	gb|AY625683|ta|T	A_99_P425752	32825
TA84405_4565	2,3672	1,0000	1,0000	1,0000	NAC domain-containing protein 71	ta|TA84405_4565|	A_99_P423302	13839
TC421665	1,0000	3,6317	1,0000	1,0000	Transcription factor Myb2	tc|TC421665|tc|TC	A_99_P479147	37654
CF133748	1,0000	3,5665	1,0000	1,0000	Myb-related protein	ta|CF133748|tc|TC	A_99_P453952	5264
TA73273_4565	1,0000	3,1435	1,0000	3,4706	ATP-dependent RNA helicase	ta|TA73273_4565|	A_99_P271141	28142
TA100085_4565	1,0000	1,0000	1,0000	3,4983	ARK protein	ta|TA100085_4565	A_99_P360266	21911
TA64630_4565	1,0000	1,0000	1,0000	2,3547	Aquaporin	ta|TA64630_4565|	A_99_P240586	20137
TA62772_4565	1,0000	1,0000	1,0000	3,1293	Aquaporin PIP1	ta|TA62772_4565|	A_99_P234076	10538
Response to oxydative stress								
TA61073_4565	1,0000	1,0000	0,3344	1,0000	Zinc-containing alcohol dehydrogenase superfamily	ta|TA61073_4565|	A_99_P408522	21811
CA600821	1,0000	1,0000	0,2760	3,0496	Metallothioneine type2	ta|CA600821|tc|TC	A_99_P460107	16140
TA58666_4565	3,5920	2,6363	1,0000	4,7939	Metallothionein-like protein type 3	ta|TA58666_4565|	A_99_P446552	19674
TA65180_4565	11,1557	1,0000	1,0000	4,6107	PR17d precursor	ta|TA65180_4565|	A_99_P242791	20412
TA80327_4565	3,3133	1,0000	1,0000	1,0000	Peroxisomal-coenzyme a synthetase	ta|TA80327_4565|	A_99_P295351	41985
TA64432_4565	2,2668	1,0000	1,0000	1,0000	Glutathione-S-transferase	ta|TA64432_4565|	A_99_P239886	42661
TA61435_4565	0,3513	0,3554	1,0000	0,0971	Peroxidase 6	ta|TA61435_4565|	A_99_P552147	16980
BQ161851	0,4950	0,4049	1,0000	0,2188	Peroxidase	ta|BQ161851|tc|TC	A_99_P431937	25512
CK212695	1,0000	1,0000	1,0000	0,3268	Class III peroxidase 62 precursor	ta|CK212695|tc|TC	A_99_P407997	44165
TA67746_4565	1,0000	1,0000	1,0000	4,1175	Aldose reductase	ta|TA67746_4565|	A_99_P252121	11372
TA77562_4565	1,0000	1,0000	1,0000	3,2047	ABC1 family protein-like	ta|TA77562_4565|	A_99_P285771	37317
TC422042	1,0000	1,0000	1,0000	3,6762	Short chain alcohol dehydrogenase-like	tc|TC422042	A_99_P152847	16834
TA90985_4565	1,0000	1,0000	1,0000	2,8981	Glutathione peroxidase-like protein GPX15Hv	ta|TA90985_4565|	A_99_P491687	28365
TC426163	1,0000	1,0000	1,0000	0,1801	Glutaredoxin-C1 precursor	tc|TC426163	A_99_P487912	11412
TA84010_4565	1,0000	1,0000	1,0000	0,4558	Nodulin-like protein	ta|TA84010_4565|	A_99_P307876	15025
TA66389_4565	1,0000	1,0000	1,0000	0,1906	Peroxidase precursor	ta|TA66389_4565|	A_99_P247391	14997
Response to pathogens								
TA55707_4565	1,0000	0,5486	3,4425	1,0000	Thaumatin-like protein TLP4	ta|TA55707_4565|	A_99_P509202	23176
TC426538	1,0000	0,4366	13,5307	0,2663	Chitinase 2	tc|TC426538	A_99_P488752	20923
TA72415_4565	1,0000	0,3820	4,8597	0,3235	Chitinase	ta|TA72415_4565|	A_99_P268406	11345
TA65444_4565	1,0000	1,0000	0,3907	2,4595	Reticulon	ta|TA65444_4565|	A_99_P412857	7188
TA70475_4565	1,0000	1,0000	0,4104	1,0000	RGA2	ta|TA70475_4565|	A_99_P433007	20640
TC442947	1,0000	1,0000	0,3281	1,0000	ENOD40-like protein	tc|TC442947	A_99_P525387	1183
TA53249_4565	1,0000	1,0000	0,2556	1,0000	IPS1 riboregulator	ta|TA53249_4565|	A_99_P207336	20707
TA66652_4565	17,1386	1,0000	1,0000	1,0000	Protein WIR1B	ta|TA66652_4565|	A_99_P248341	33427
GR302911	13,8584	1,0000	1,0000	1,0000	WIR1	gb|GR302911|tc|T	A_99_P488332	14017
TC419763	10,4972	1,0000	1,0000	1,0000	Protein WIR1A	tc|TC419763	A_99_P475682	36715
TA73316_4565	4,4605	1,0000	1,0000	1,0000	Pathogen-related protein	ta|TA73316_4565|	A_99_P271256	41870
AF112963	3,1035	1,0000	1,0000	3,6904	Chitinase II precursor (Cht2)	gb|AF112963|ta|T/	A_99_P000381	24453
TC370624	1,0000	2,7363	1,0000	1,0000	MLA7	tc|TC370624	A_99_P408547	22360
TA83143_4565	1,0000	2,7211	1,0000	5,7061	Hydrolase, alpha/beta fold family-like	ta|TA83143_4565|	A_99_P304906	15369
TA69803_4565	1,0000	1,0000	1,0000	5,8659	VTC2-like protein	ta|TA69803_4565|	A_99_P259271	42520
AY387686	1,0000	1,0000	1,0000	4,1747	Harpin binding protein 1 (HrBP1-1)	gb|AY387686|ta|T	A_99_P645996	44828
CK162011	1,0000	1,0000	1,0000	0,3420	Glucan endo-1,3-beta-glucosidase isoenzyme I	ta|CK162011|tc|TC	A_99_P492787	8899
Y09917	1,0000	1,0000	1,0000	0,2637	Germin-like protein 3	gb|Y09917|gb|FJ8:	A_99_P546587	21507
Secondary metabolism								
DQ208192	9,6489	1,0000	1,0000	1,0000	Flavanone 3-hydroxylase	gb|DQ208192|ta|T	A_99_P163772	30321
TA69335_4565	1,0000	11,9472	1,0000	10,5210	Chalcone synthase 2	ta|TA69335_4565|	A_99_P174849	25042
AY286098	1,0000	1,0000	1,0000	6,3104	Chalcone synthase (CHS1)	gb|AY286098|gb|A	A_99_P163037	29628
TA50072_4565	1,0000	1,0000	1,0000	5,7942	Pyridoxal biosynthesis protein PDX1.1	ta|TA50072_4565|	A_99_P197801	18956
JQ307210	1,0000	1,0000	1,0000	2,4647	TaJNFPS-4 farnesyl pyrophosphate synthase	gb|JQ307210|ta|T/	A_99_P255071	6487
TA69487_4565	1,0000	1,0000	1,0000	3,2033	Nicotianamine sythase 3	ta|TA69487_4565|	A_99_P258261	20065
Pigment biosynthesis								
TA92426_4565	4,6192	1,0000	1,0000	3,7490	Beta-carotene hydroxylase	ta|TA92426_4565|	A_99_P336181	23802
AY596267	1,0000	1,0000	1,0000	3,3863	Polyphenol oxidase	gb|AY596267|ta|T	A_99_P081185	22056
TA72038_4565	1,0000	1,0000	1,0000	2,4004	Lycopene beta-cyclase	ta|TA72038_4565|	A_99_P267096	33927
TA56529_4565	1,0000	1,0000	1,0000	0,4659	Glutamyl-tRNA reductase 2	ta|TA56529_4565|	A_99_P216016	43656
Flowering and seed maturation								
TA84120_4565	1,0000	1,0000	0,4140	1,0000	Protein EGG APPARATUS-1	ta|TA84120_4565|	A_99_P308216	36050
TA86268_4565	1,0000	1,0000	1,0000	2,4193	CONSTANS interacting protein 5	ta|TA86268_4565|	A_99_P315626	21018
TA50354_4565	1,0000	1,0000	1,0000	3,1442	Pyruvate kinase	ta|TA50354_4565|	A_99_P558877	37866
Growth and development								
TA72187_4565	1,0000	1,0000	0,2876	1,0000	Cell Division Protein AAA ATPase family	ta|TA72187_4565|	A_99_P267636	41732
CK211204	3,1279	3,8023	1,0000	1,0000	ZIM motif family protein	ta|CK211204|ta|BI	A_99_P469812	31070
CK196320	3,0527	1,0000	1,0000	2,4193	Cell death associated protein	ta|CK196320|tc|TC	A_99_P536337	8482
TA56545_4565	1,0000	2,3451	1,0000	1,0000	1-aminocyclopropane-1-carboxylate oxidase	ta|TA56545_4565|	A_99_P216071	11632
TA56454_4565	0,2222	0,3825	1,0000	1,0000	Auxin-repressed protein	ta|TA56454_4565|	A_99_P215761	27870
TA61883_4565	1,0000	0,3739	1,0000	1,0000	Sterol desaturase family protein	ta|TA61883_4565|	A_99_P231241	32885
TA74119_4565	1,0000	1,0000	1,0000	3,2686	Serine carboxypeptidase 1 precursor	ta|TA74119_4565|	A_99_P273981	5019
CA733338	1,0000	1,0000	1,0000	0,3309	Kelch repeat-containing F-box-like	ta|CA733338|tc|TC	A_99_P568977	2248
TA86474_4565	1,0000	1,0000	1,0000	0,2405	Auxin Efflux Carrier	ta|TA86474_4565|	A_99_P192117	12326
TA70786_4565	1,0000	1,0000	1,0000	0,3417	Dormancy/auxin associated protein	ta|TA70786_4565|	A_99_P262816	1345

	A	B	C	D				
Name	MNiD0 vs CNiD0	MNiD3 vs CNiD3	CiD3 vs CNiD3	MiD3 vs CiD3	Description	TopHit	ID	RefNumber
Cell wall structure and function								
TA87087_4565	1,0000	1,0000	0,0592	1,0000	Cinnamyl alcohol dehydrogenase	ta|TA87087_4565|	A_99_P318481	8569
TA68562_4565	1,0000	1,0000	0,3766	1,0000	Glycoside hydrolase, family 19	ta|TA68562_4565|	A_99_P255031	1863
TA66611_4565	1,0000	1,0000	0,3372	1,0000	Fasciclin-like protein FLA15	ta|TA66611_4565|	A_99_P248201	22500
CK152333	1,0000	1,0000	0,3202	1,0000	Type 1 non specific lipid transfer protein precursor	ta|CK152333|tc|TC	A_99_P446157	36915
CK205454	1,0000	1,0000	0,3699	1,0000	Non-specific lipid transfer protein 1 precursor	ta|CK205454|tc|TC	A_99_P427502	36085
TA61828_4565	1,0000	1,0000	0,3668	1,0000	Non-specific lipid-transfer protein	ta|TA61828_4565|	A_99_P231006	27677
TA91600_4565	1,0000	1,0000	1,0000	2,9867	Protein DSE2 precursor	ta|TA91600_4565|	A_99_P333491	35745
TA107115_4565	1,0000	1,0000	1,0000	5,0040	Galactose-binding like	ta|TA107115_4565	A_99_P386442	35996
Chloroplast structure and function								
TA69442_4565	1,0000	0,3415	1,0000	0,1868	Plastid-specific 30S ribosomal protein 1, chloroplast pr	ta|TA69442_4565|	A_99_P258121	37451
TA92734_4565	1,0000	1,0000	0,3150	1,0000	Diap1 protein	ta|TA92734_4565|	A_99_P337136	42984
TA103644_4565	1,0000	1,0000	1,0000	2,5178	CRS2-associated factor 1, chloroplast precursor	ta|TA103644_4565	A_99_P010186	14454
Light harvesting								
TA59580_4565	0,3099	0,1806	1,0000	0,1687	Light-regulated protein precursor	ta|TA59580_4565|	A_99_P223621	14346
TA53867_4565	1,0000	0,1549	1,0000	0,1783	Light-induced protein 1-like	ta|TA53867_4565|	A_99_P209081	23883
TC371150	1,0000	0,1464	1,0000	0,0368	Chlorophyll a/b-binding protein WCAB precursor	tc|TC371150	A_99_P409112	19146
TA63710_4565	1,0000	1,0000	1,0000	0,3636	Chlorophyll a-b binding protein of LHCII type III, chloro	ta|TA63710_4565|	A_99_P237481	36780
TA55816_4565	1,0000	1,0000	1,0000	0,2774	Light-harvesting complex I	ta|TA55816_4565|	A_99_P214401	27084
TC372144	1,0000	1,0000	1,0000	0,1915	Chlorophyll a/b binding protein precursor	tc|TC372144	A_99_P410077	391
CK217674	1,0000	1,0000	1,0000	0,2346	Chloroplast pigment-binding protein CP24	ta|CK217674|tc|TC	A_99_P437157	39278
Photosynthesis								
CK212581	1,0000	1,0000	1,0000	4,1967	Photosystem II reaction center psb28 protein	ta|CK212581|tc|TC	A_99_P424262	24845
TA64071_4565	1,0000	1,0000	1,0000	3,4588	Cytochrome b6-f complex iron-sulfur subunit, chloropl	ta|TA64071_4565|	A_99_P238726	35747
Carbohydrate metabolism								
CJ604231	1,0000	1,0000	1,0000	3,2506	Carbohydrate kinase-like protein	ta|CJ604231|tc|TC	A_99_P441937	19794
TA64268_4565	1,0000	1,0000	1,0000	3,0694	Fructose-bisphosphate aldolase	ta|TA64268_4565|	A_99_P239376	27725
TA64671_4565	1,0000	1,0000	1,0000	2,1494	UTP--glucose-1-phosphate uridylyltransferase	ta|TA64671_4565|	A_99_P004441	24422
TA57382_4565	1,0000	1,0000	1,0000	3,2052	Phosphate/phosphoenolpyruvate translocator	ta|TA57382_4565|	A_99_P217791	33087
TA75511_4565	1,0000	1,0000	1,0000	5,1904	Monosaccharide transporter 4	ta|TA75511_4565|	A_99_P278701	5738
TA83785_4565	1,0000	1,0000	1,0000	4,6539	Beta-amylase PCT-BMYI	ta|TA83785_4565|	A_99_P307146	32293
Amino acid metabolism								
TC430171	1,0000	1,0000	0,0893	1,0000	Indole-3-glycerol phosphate lyase	tc|TC430171	A_99_P496502	8009
TA69994_4565	1,0000	1,0000	0,3764	1,0000	Glutamate dehydrogenase	ta|TA69994_4565|	A_99_P259951	10977
TA69140_4565	1,0000	1,0000	0,3061	3,9418	L-allo-threonine aldolase-related protein	ta|TA69140_4565|	A_99_P449637	41850
TC393988	1,0000	1,0000	0,1308	3,1335	Glycine/proline-rich protein	tc|TC393988	A_99_P543657	7174
TA64535_4565	1,0000	1,0000	0,3402	6,8149	Glycine decarboxylase P subunit	ta|TA64535_4565|	A_99_P240211	15342
TA64069_4565	1,0000	1,0000	1,0000	2,7421	Mitochondrial aspartate-glutamate carrier protein-like	ta|TA64069_4565|	A_99_P238716	33459
CJ667842	1,0000	1,0000	1,0000	2,2975	Ferredoxin, chloroplast precursor	ta|CJ667842|tc|TC	A_99_P436607	43120
TA63842_4565	1,0000	1,0000	1,0000	2,2437	Inositol monophosphatase family protein	ta|TA63842_4565|	A_99_P237761	10378
TA60889_4565	1,0000	1,0000	1,0000	3,1980	S-adenosylmethionine synthetase	ta|TA60889_4565|	A_99_P227511	9678
Protein metabolism								
TA59594_4565	3,2151	1,0000	1,0000	1,0000	22.3 kDa heat-shock protein	ta|TA59594_4565|	A_99_P223676	44575
TC402730	1,0000	1,0000	0,2499	1,0000	70 kDa heat shock protein	tc|TC402730	A_99_P448647	36262
HM209063	1,0000	1,0000	0,2354	1,0000	Heat shock protein 70-like	gb|HM209063|gb|	A_99_P234541	16785
TA64099_4565	1,0000	1,0000	0,1519	1,0000	Heat shock protein 80 kDa	ta|TA64099_4565|	A_99_P238761	26
TC414782	1,0000	1,0000	0,2639	4,7982	Asparaginase	tc|TC414782	A_99_P466942	23822
TA53535_4565	1,0000	1,0000	0,1923	3,8264	Ubiquitin carrier protein	ta|TA53535_4565|	A_99_P208256	24763
TA67255_4565	1,0000	1,0000	1,0000	3,7019	Heat-shock protein precursor	ta|TA67255_4565|	A_99_P250376	10187
TA61948_4565	1,0000	1,0000	1,0000	5,9779	C13 endopeptidase NP1 precursor	ta|TA61948_4565|	A_99_P231506	7777
Lipid metabolism								
TA74269_4565	1,0000	1,0000	1,0000	2,2655	Plastid omega-3 fatty acid desaturase	ta|TA74269_4565|	A_99_P274486	33811
Energy metabolism								
TC449528	1,0000	0,1814	1,0000	0,0777	Cytochrome c	tc|TC449528	A_99_P542662	24896
TA82476_4565	1,0000	1,0000	1,0000	0,5086	HAP3-like transcriptional-activator	ta|TA82476_4565|	A_99_P302726	42546
Signaling								
TA72110_4565	2,1573	1,0000	1,0000	1,0000	Ca2+/H+-exchanging protein	ta|TA72110_4565|	A_99_P267366	40677
TC376621	1,0000	2,7894	1,0000	1,0000	Calcium-dependent protein kinase	tc|TC376621	A_99_P415112	24028
Transcription regulation								
CA721206	1,0000	1,0000	0,3296	2,5283	Zinc finger protein 219	ta|CA721206|tc|TC	A_99_P533942	44850
D16416	3,8660	1,0000	1,0000	1,0000	Zinc-finger protein WZF1	gb|D16416|ta|TA7	A_99_P489622	10858
TC436900	3,1349	1,0000	1,0000	1,0000	Histone H1 WH1A.3	tc|TC436900	A_99_P511852	5211
Transcription, RNA-processing and translation								
U34402	1,0000	1,0000	1,0000	2,6546	Single-subunit RNA polymerase C	gb|U34402|ta|TA8	A_99_P000396	29420
TA85618_4565	1,0000	1,0000	1,0000	3,9276	DEAD-box ATP-dependent RNA helicase 26	ta|TA85618_4565|	A_99_P313296	14881
TA91346_4565	1,0000	1,0000	1,0000	2,1117	DEAD-box ATP-dependent RNA helicase 22	ta|TA91346_4565|	A_99_P332671	20451
TA79230_4565	1,0000	1,0000	1,0000	2,3422	40S ribosomal protein S14	ta|TA79230_4565|	A_99_P165432	22492

Supplementary Table S2. Relative gene expression profiles illustrating fungus effect in presence of mycosubtilin (M-D5-i vs M-D5-Ni) and the whole specter of plant responses to mycosubtilin and fungus (M-D5-i vs C-D5-Ni). This table is related to supplementary figure S5. Gene-related physiological processes are represented on the right part of the graph and were determined using NCBI, AmiGO 2 Gene Ontology, KEGG and UniProt. Log2 ratios >2 correspond to up-regulated genes (in red) and log2 ratios <0.5 to down-regulated genes (in green). Log2 ratios <2 and >0.5 were conventionally referred to 1. M means treated with mycosubtilin towards mock treated C. Ni stands for mock inoculated whereas i indicates that plants were infected with *Z. tritici*. D5 means that leaves were sampled at five days after mycosubtilin treatment.

	A	B				
Name	MiD3 vs MniD3	MiD3 vs CNiD3	Description	TopHit	ID	RefNumber
Response to abiotic stress						
CA624093	10,8866	7,9255	Low temperature induced protein	ta|CA624093|ta|C	A_99_P459967	11840
TA73273_4565	3,1771	10,1871	ATP-dependent RNA helicase	ta|TA73273_4565|	A_99_P271141	28142
TA54418_4565	5,3330	1,0000	Cold acclimation protein WCOR413	ta|TA54418_4565|	A_99_P210931	43524
TA84187_4565	0,4464	1,0000	Protein phosphatase type 2-C	ta|TA84187_4565|	A_99_P308421	21815
TA92949_4565	0,2966	1,0000	Efflux transporter, RND family, MFP subunit	ta|TA92949_4565|	A_99_P144213	15689
AY785903	0,3354	1,0000	TaCBF6	gb|AY785903|gb|C	A_99_P000681	22350
TA67331_4565	0,3060	1,0000	Proline-rich protein precursor	ta|TA67331_4565|	A_99_P498102	7990
TC381840	1,0000	2,6078	Cold acclimation protein WCOR518	tc|TC381840	A_99_P421457	19082
TA100085_4565	1,0000	3,6298	ARK protein	ta|TA100085_4565	A_99_P360266	21911
TA79737_4565	1,0000	3,9456	Importin beta-like protein	ta|TA79737_4565|	A_99_P293321	35865
TA57180_4565	1,0000	2,7545	Actin	ta|TA57180_4565|	A_99_P217276	4091
TA74058_4565	1,0000	2,5253	Serine hydroxymethyltransferase	ta|TA74058_4565|	A_99_P008296	33374
Response to oxydative stress						
TA58666_4565	4,1559	8,3937	Metallothionein-like protein type 3	ta|TA58666_4565|	A_99_P446552	19674
TA102260_4565	7,2071	5,8849	Nitrite reductase apoprotein	ta|TA102260_4565	A_99_P366657	8326
TA77625_4565	1,0000	3,3397	Chloroplast glutathione reductase	ta|TA77625_4565|	A_99_P285981	31266
TA65180_4565	1,0000	6,9092	PR17d precursor	ta|TA65180_4565|	A_99_P242791	20412
TA67746_4565	1,0000	3,0000	Aldose reductase	ta|TA67746_4565|	A_99_P252121	11372
TA64544_4565	1,0000	2,9082	Mitochondrial lipoamide dehydrogenase	ta|TA64544_4565|	A_99_P240241	32379
TA100790_4565	1,0000	2,8398	Cytochrome P450 family protein	ta|TA100790_4565	A_99_P362271	32984
TA65542_4565	1,0000	2,7234	GMC oxidoreductase	ta|TA65542_4565|	A_99_P244206	18477
TA61435_4565	1,0000	0,1966	Peroxidase 6	ta|TA61435_4565|	A_99_P552147	16980
BQ161851	1,0000	0,4719	Peroxidase	ta|BQ161851|tc|T(	A_99_P431937	25512
CK212695	1,0000	0,4214	Class III peroxidase 62 precursor	ta|CK212695|tc|TC	A_99_P407997	44165
Response to pathogens						
TA55707_4565	7,4080	3,7743	Thaumatin-like protein TLP4	ta|TA55707_4565|	A_99_P509202	23176
TA69803_4565	6,4953	5,3893	VTC2-like protein	ta|TA69803_4565|	A_99_P259271	42520
TC426538	4,2133	1,0000	Chitinase 2	tc|TC426538	A_99_P488752	20923
TA72415_4565	5,5826	1,0000	Chitinase	ta|TA72415_4565|	A_99_P268406	11345
GR302911	5,8764	1,0000	WIR1	gb|GR302911|tc|T	A_99_P488332	14017
TC419763	9,3819	1,0000	Protein WIR1A	tc|TC419763	A_99_P475682	36715
TA76681_4565	0,4121	1,0000	HS1-like protein	ta|TA76681_4565|	A_99_P194333	16022
EF570122	0,3030	1,0000	Pathogen-inducible transcription factor ERF3	gb|EF570122|gb|H	A_99_P177974	11088
AF112963	1,0000	4,3880	Chitinase II precursor (Cht2)	gb|AF112963|ta|T	A_99_P000381	24453
TC370624	1,0000	3,4177	MLA7	tc|TC370624	A_99_P408547	22360
TA83143_4565	1,0000	3,0760	Hydrolase, alpha/beta fold family-like	ta|TA83143_4565|	A_99_P304906	15369
AY387686	1,0000	4,0090	Harpin binding protein 1 (HrBP1-1)	gb|AY387686|ta|T	A_99_P645996	44828
TC404042	1,0000	3,8154	Phytosulfokine	tc|TC404042	A_99_P450387	20130
TA53249_4565	1,0000	0,2250	IPS1 riboregulator	ta|TA53249_4565|	A_99_P207336	20707
Secondary metabolism						
DQ208192	12,9069	7,4518	Flavanone 3-hydroxylase	gb|DQ208192|ta|T	A_99_P163772	30321
TA69335_4565	1,0000	10,9130	Chalcone synthase 2	ta|TA69335_4565|	A_99_P174849	25042
AY286098	1,0000	5,4080	Chalcone synthase (CHS1)	gb|AY286098|gb|A	A_99_P163037	29628
TA50072_4565	1,0000	5,9485	Pyridoxal biosynthesis protein PDX1.1	ta|TA50072_4565|	A_99_P197801	18956
JQ307210	1,0000	2,2196	TaJNFPS-4 farnesyl pyrophosphate synthase	gb|JQ307210|ta|TA	A_99_P255071	6487
TA83418_4565	1,0000	2,8848	GGDP synthase	ta|TA83418_4565|	A_99_P305831	14702
TA83418_4565	1,0000	2,3471	Isochorismate synthetase	ta|TA83418_4565|	A_99_P565517	1945
Flowering and seed maturation						
TA86268_4565	5,3738	11,9770	CONSTANS interacting protein 5	ta|TA86268_4565|	A_99_P315626	21018
TA84120_4565	0,4894	0,5134	Protein EGG APPARATUS-1	ta|TA84120_4565|	A_99_P308216	36050
TA50354_4565	1,0000	4,0211	Pyruvate kinase	ta|TA50354_4565|	A_99_P558877	37866
Growth and development						
TA99155_4565	6,4739	7,5675	DNA replication and repair protein RecF	ta|TA99155_4565|	A_99_P357521	34334
TC405303	0,2207	1,0000	Mitogen-activated protein kinase 7	tc|TC405303	A_99_P452302	22398
CK211204	0,4144	1,0000	ZIM motif family protein	ta|CK211204|ta|BI	A_99_P469812	31070
CK196320	1,0000	2,3513	Cell death associated protein	ta|CK196320|tc|TC	A_99_P536337	8482
TA84990_4565	1,0000	2,8643	CDK5RAP1-like protein	ta|TA84990_4565|	A_99_P311161	19118
TC380019	1,0000	2,5327	SAP-like protein BP-73	tc|TC380019	A_99_P419147	17470
CA612835	1,0000	0,5152	Abscisic stress ripening protein-like protein	ta|CA612835|tc|T(	A_99_P512357	23935
Cell wall structure and activity						
TA87087_4565	0,2972	1,0000	Cinnamyl alcohol dehydrogenase	ta|TA87087_4565|	A_99_P318481	8569
TA66611_4565	0,2902	0,2694	Fasciclin-like protein FLA15	ta|TA66611_4565|	A_99_P248201	22500
CK152333	0,4777	0,3021	Type 1 non specific lipid transfer protein precurso	ta|CK152333|tc|TC	A_99_P446157	36915
CK205454	1,0000	0,4856	Non-specific lipid transfer protein 1 precursor	ta|CK205454|tc|TC	A_99_P427502	36085
TA61828_4565	1,0000	0,3846	Non-specific lipid-transfer protein	ta|TA61828_4565|	A_99_P231006	27677
TC383836	1,0000	2,4738	Nucleosome assembly protein 1-like protein 2	tc|TC383836	A_99_P423887	18218
TA102372_4565	1,0000	3,1164	Hydroxyproline-rich glycoprotein DZ-HRGP precurs	ta|TA102372_4565	A_99_P039309	28910
TA91600_4565	1,0000	3,1924	Protein DSE2 precursor	ta|TA91600_4565|	A_99_P333491	35745
Chloroplast structure and function						
TA66617_4565	1,0000	2,8274	Plastid-specific 30S ribosomal protein 3, chloropla	ta|TA66617_4565|	A_99_P248226	33266
TA95179_4565	1,0000	2,9719	Amidophosphoribosyl-transferase	ta|TA95179_4565|	A_99_P345026	40498
CD879285	1,0000	2,6638	Triosephosphate isomerase, chloroplast precurso	ta|CD879285|tc|TC	A_99_P434992	19245
TA103644_4565	1,0000	3,0541	CRS2-associated factor 1, chloroplast precursor	ta|TA103644_4565	A_99_P010186	14454
TA92734_4565	1,0000	0,4010	Diap1 protein	ta|TA92734_4565|	A_99_P337136	42984

	A	B				
Name	MiD3 vs MniD3	MiD3 vs CNiD3	Description	TopHit	ID	RefNumber
Pigment biosynthesis						
TA92426_4565	1,0000	3,3226	Beta-carotene hydroxylase	ta|TA92426_4565|	A_99_P258181	23802
AY596267	1,0000	3,8471	Polyphenol oxidase	gb|AY596267|ta|T	A_99_P081185	22056
TA70845_4565	1,0000	3,2178	Porphobilinogen deaminase	ta|TA70845_4565|	A_99_P155942	10728
TA58881_4565	1,0000	2,8977	Glutamate-1-semialdehyde 2,1-aminomutase, chl	ta|TA58881_4565|	A_99_P419897	32620
TA89084_4565	1,0000	2,4213	S-adenosyl-L-methionine Mg-protoporphyrin IX m	ta|TA89084_4565|	A_99_P494142	24157
TA72038_4565	1,0000	2,7744	Lycopene beta-cyclase	ta|TA72038_4565|	A_99_P267096	33927
Light harvesting						
TC371150	1,0000	0,0737	Chlorophyll a/b-binding protein WCAB precursor	tc|TC371150	A_99_P409112	19146
TA63710_4565	1,0000	0,4580	Chlorophyll a-b binding protein of LHCII type III, cl	ta|TA63710_4565|	A_99_P237481	36780
TA55816_4565	1,0000	0,3900	Light-harvesting complex I	ta|TA55816_4565|	A_99_P214401	27084
TC372144	1,0000	0,3827	Chlorophyll a/b binding protein precursor	tc|TC372144	A_99_P410077	391
CK217674	1,0000	0,3345	Chloroplast pigment-binding protein CP24	ta|CK217674|tc|TC	A_99_P437157	39278
Photosynthesis						
CK212581	1,0000	3,3828	Photosystem II reaction center psb28 protein	ta|CK212581|tc|TC	A_99_P424262	24845
TA64071_4565	1,0000	3,5968	Cytochrome b6-f complex iron-sulfur subunit, chl	ta|TA64071_4565|	A_99_P238726	35747
AF251264	1,0000	3,8899	Ribulose bisphosphate carboxylase activase B (Rc	gb|AF251264|ta|T	A_99_P449812	42320
Carbohydrate metabolism						
CJ604231	1,0000	3,5308	Carbohydrate kinase-like protein	ta|CJ604231|tc|TC	A_99_P441937	19794
TA83009_4565	1,0000	2,6181	FKBP-type peptidyl-prolyl cis-trans isomerase 3, cl	ta|TA83009_4565|	A_99_P430677	38537
TA64268_4565	1,0000	2,7123	Fructose-bisphosphate aldolase	ta|TA64268_4565|	A_99_P239376	27725
TA64671_4565	1,0000	2,0409	UTP--glucose-1-phosphate uridylyltransferase	ta|TA64671_4565|	A_99_P004441	24422
TA57382_4565	1,0000	4,1155	Phosphate/phosphoenolpyruvate translocator	ta|TA57382_4565|	A_99_P217791	33087
TA75511_4565	1,0000	4,8683	Monosaccharide transporter 4	ta|TA75511_4565|	A_99_P278701	5738
TA83785_4565	1,0000	4,4735	Beta-amylase PCT-BMYI	ta|TA83785_4565|	A_99_P307146	32293
Amino-acids metabolism						
DQ139267	2,7893	4,3191	4-hydroxyphenylpyruvate dioxygenase	gb|DQ139267|ta|T	A_99_P637271	37769
TA82049_4565	4,4783	2,7594	Bifunctional aspartokinase/homoserine dehydrog	ta|TA82049_4565|	A_99_P163227	42192
TC430171	0,4417	1,0000	Indole-3-glycerol phosphate lyase	tc|TC430171	A_99_P496502	8009
TA69994_4565	0,5428	1,0000	Glutamate dehydrogenase	ta|TA69994_4565|	A_99_P259951	10977
TA64535_4565	1,0000	3,1452	Glycine decarboxylase P subunit	ta|TA64535_4565|	A_99_P240211	15342
EU236151	1,0000	3,3617	Arginine decarboxylase	gb|EU236151|ta|T	A_99_P229841	38415
TA64069_4565	1,0000	5,2741	Mitochondrial aspartate-glutamate carrier protei	ta|TA64069_4565|	A_99_P238716	33459
CJ667842	1,0000	3,3303	Ferredoxin, chloroplast precursor	ta|CJ667842|tc|TC	A_99_P436607	43120
TA63842_4565	1,0000	2,3311	Inositol monophosphatase family protein	ta|TA63842_4565|	A_99_P237761	10378
TC369894	1,0000	3,3870	Glycine/D-amino acid oxidases-like	tc|TC369894	A_99_P427247	29953
TC448142	1,0000	2,8702	Glycine cleavage system H protein, mitochondrial	tc|TC448142	A_99_P538777	8089
TC413834	1,0000	2,5071	S-adenosylmethionine:2-demethylmenaquinone r	tc|TC413834	A_99_P465342	10889
TA79034_4565	1,0000	2,2333	3-dehydroquinate dehydratase/shikimate 5-dehy	ta|TA79034_4565|	A_99_P290801	15040
Protein metabolism						
TA67255_4565	1,0000	6,2782	Heat-shock protein precursor	ta|TA67255_4565|	A_99_P250376	10187
TA70500_4565	1,0000	4,3298	ATP-dependent Clp protease proteolytic subunit	ta|TA70500_4565|	A_99_P261831	33261
TA61948_4565	1,0000	3,5141	C13 endopeptidase NP1 precursor	ta|TA61948_4565|	A_99_P231506	7777
TC402730	0,4696	0,3776	70 kDa heat shock protein	tc|TC402730	A_99_P448647	36262
HM209063	1,0000	0,3461	Heat shock protein 70-like	gb|HM209063|gb|	A_99_P234541	16785
TA64099_4565	1,0000	0,3827	Heat shock protein 80 kDa	ta|TA64099_4565|	A_99_P238761	26
Lipid metabolism						
TA74269_4565	1,0000	2,9766	Plastid omega-3 fatty acid desaturase	ta|TA74269_4565|	A_99_P274486	33811
Energy metabolism						
TC449528	1,0000	0,2457	Cytochrome c	tc|TC449528	A_99_P542662	24896
Signaling						
TA82827_4565	1,0000	3,5853	GTP-binding protein-related	ta|TA82827_4565|	A_99_P303856	12334
TA51150_4565	1,0000	3,0011	Serine/threonine kinase	ta|TA51150_4565|	A_99_P200651	28794
Transcription, RNA-processing, translation						
U34402	1,0000	5,1196	Single-subunit RNA polymerase C	gb|U34402|ta|TA8	A_99_P000396	29420
TA85618_4565	3,8503	8,0637	DEAD-box ATP-dependent RNA helicase 26	ta|TA85618_4565|	A_99_P313296	14881
TA91346_4565	1,0000	2,9475	DEAD-box ATP-dependent RNA helicase 22	ta|TA91346_4565|	A_99_P332671	20451
D38485	1,0000	3,8436	Ps16 protein	gb|D38485|ta|TA6	A_99_P243491	32092
TA71493_4565	1,0000	4,3047	Elongation factor Ts	ta|TA71493_4565|	A_99_P265276	14490
TA88703_4565	1,0000	2,1987	Elongation factor G, mitochondrial precursor	ta|TA88703_4565|	A_99_P323926	25452
TA85526_4565	1,0000	3,4363	Translation initiation factor IF-2	ta|TA85526_4565|	A_99_P426897	36495
CA502352	1,0000	3,3990	Elongation factor	ta|CA502352|tc|TC	A_99_P433232	2769
TA79230_4565	1,0000	4,0916	40S ribosomal protein S14	ta|TA79230_4565|	A_99_P165432	22492
TA53517_4565	1,0000	3,7743	Ribosomal protein l34	ta|TA53517_4565|	A_99_P428417	18198
TA70216_4565	1,0000	3,6376	30S ribosomal protein S17, chloroplast precursor	ta|TA70216_4565|	A_99_P260786	41398
TA68774_4565	1,0000	3,5124	50S ribosomal protein L1, chloroplast precursor	ta|TA68774_4565|	A_99_P255791	32662
TA71488_4565	1,0000	3,4800	50S ribosomal protein L35	ta|TA71488_4565|	A_99_P265261	23498
TA61485_4565	1,0000	3,4580	Ribosomal protein s6 RPS6-2	ta|TA61485_4565|	A_99_P229796	30672
TA66609_4565	1,0000	3,3720	Ribosome-like protein	ta|TA66609_4565|	A_99_P441707	27111
TA50993_4565	1,0000	3,2869	Large subunit 26S ribosomal RNA gene	ta|TA50993_4565|	A_99_P568177	38089
TA56520_4565	1,0000	3,2492	Ribosomal protein L35A	ta|TA56520_4565|	A_99_P215981	843
TA61855_4565	1,0000	3,1757	Ribosomal protein L13a	ta|TA61855_4565|	A_99_P231131	34917
TA58672_4565	1,0000	2,9515	Ribosomal protein	ta|TA58672_4565|	A_99_P221126	44143
TA58281_4565	1,0000	2,7390	60S ribosomal protein L44	ta|TA58281_4565|	A_99_P220136	28679
CV767873	1,0000	2,5830	60S ribosomal protein L27	ta|CV767873|tc|TC	A_99_P424047	37514
TA61981_4565	1,0000	2,5522	Large subunit 26S ribosomal RNA gene	ta|TA61981_4565|	A_99_P410577	31986
CK214923	1,0000	2,5427	Ribosomal protein L11	ta|CK214923|ta|CI	A_99_P479112	18063
TA64720_4565	1,0000	2,5323	50S ribosomal protein L21, chloroplast precursor	ta|TA64720_4565|	A_99_P240931	20989
TC413718	1,0000	2,4327	60S acidic ribosomal protein P3	tc|TC413718|tc|TC	A_99_P421697	43054
TA61076_4565	1,0000	2,3721	60S ribosomal protein L10-2	ta|TA61076_4565|	A_99_P228111	36378
TA68490_4565	1,0000	2,3161	50S ribosomal protein L28, chloroplast precursor	ta|TA68490_4565|	A_99_P254736	20009
TA58879_4565	1,0000	2,2323	Ribosomal protein L37	ta|TA58879_4565|	A_99_P221536	19773
TA54070_4565	1,0000	2,1438	Ribosomal protein L10A	ta|TA54070_4565|	A_99_P209766	19576
Other functions						
TA91877_4565	1,0000	2,5423	C3meo4	ta|TA91877_4565|	A_99_P334381	24012
TC389894	5,7677	5,7787	Tetratricopeptide repeat (TPR)-containing protein	tc|TC389894	A_99_P431697	38421
AF110180	4,6138	1,0000	High-affinity phosphate transporter PT1	gb|AF110180	A_99_P026169	24145

Supplementary Table S3. List of the 56 metabolites detected in wheat leaves (cv. Alixan) with ultra-high-performance liquid chromatography-mass spectrometry (UHPLC-MS), using a targeted metabolomic approach. Metabolites were classified according to KEGG (Kyoto Encyclopedia of Genes and Genomes; http://www.genome.ad.jp/kegg) and PubChem (http://pubchem.ncbi.nlm.nih.gov) databases. Id: identifier; m/z: mass-to-charge ratio; m/z error (difference between the measured m/z and the calculated m/z of an ion, in ppm); RT: retention time. * indicates that compounds were confirmed with authentic standards.

Id	Metabolite	Formula	Class [a]	Detected *m/z*	*m/z* error (ppm)	RT (min)	KEGG ID	PubChem CID
1	**Arginine**	$C_6H_{14}N_4O_2$	Amino acids	175.1190	0.20	0,85	C00062	6322
2	**Asparagine**	$C_4H_8N_2O_3$	Amino acids	133.0609	0.86	0,98	C00152	6267
3	**Aspartic acid**	$C_4H_7NO_4$	Amino acids	134.0449	0.69	1,02	C00049	5960
4	**Glutamic acid**	$C_5H_9NO_4$	Amino acids	148.0604	0,77	1,01	C00025	4525487
5	**Glutamine**	$C_5H_{10}N_2O_3$	Amino acids	147.0764	0,09	0,99	C00064	5961
6	**Histidine**	$C_6H_9N_3O_2$	Amino acids	156.0769	0.68	1,01	C00135	6274
7	**Hydroxyproline**	$C_5H_9NO_3$	Amino acids	132.0656	0.70	1,01	C01157	5810
8	**Isoleucine**	$C_6H_{13}NO_2$	Amino acids	132.1020	0.76	1,56	C00407	6306
9	**Leucine**	$C_6H_{13}NO_2$	Amino acids	132.1020	0.76	1,62	C00123	6106
10	**Lysine**	$C_6H_{14}N_2O_2$	Amino acids	147.1129	0.44	0.84	C00047	5962
11	**Methionine**	$C_5H_{11}NO_2S$	Amino acids	150.0584	0.36	2.04	C00073	6137
12	**Phenylalanine**	$C_9H_{11}NO_2$	Amino acids	166.0862	-0.53	4.30	C00079	6140
13	**Proline**	$C_5H_9NO_2$	Amino acids	116.0708	1.69	1.23	C00148	145742
14	**Threonine**	$C_4H_9NO_3$	Amino acids	120.0657	1.22	1.08	C00188	6288
15	**Tryptophan**	$C_{11}H_{12}N_2O_2$	Amino acids	205.0973	0.51	4.75	C00078	6305
16	**Tyrosine**	$C_9H_{11}NO_3$	Amino acids	182.0813	0.54	3.20	C00082	6057
17	**Valine**	$C_5H_{11}NO_2$	Amino acids	118.0863	0.48	1.14	C00183	6287
18	Methylpipecolic acid	$C_7H_{13}NO_2$	Amino acid derivatives	144.1019	0.27	1,08	C10172	115244
19	DHBOA-hexosyl-hexoside	$C_{14}H_{17}NO_9$	Benzoxazinoids	523.1773	0.59	4.48		
20	DHBOA-hexosyl-deoxyhexoside	$C_8H_7NO_4$	Benzoxazinoids	490.1557	0.59	4.71		
21	HBOA	$C_8H_7NO_3$	Benzoxazinoids	166.0499	0.34	5.92	C15769	322636
22	HBOA-glucoside	$C_{14}H_{17}NO_8$	Benzoxazinoids	328.1027	0.09	4.71		14605136
23	HM2BOA	$C_{10}H_{11}NO_5$	Benzoxazinoids	226.0709	-0.61	5.51		11064107
24	HMBOA-hexoside	$C_{10}H_{11}NO_5$	Benzoxazinoids	358.1241	-0.61	5.06		
25	HM2BOA-hexoside	$C_{16}H_{21}NO_{10}$	Benzoxazinoids	388.1245	1.86	5.36		
26	Apigenin-6-C-hexoside-C-pentoside	$C_{26}H_{28}O_{14}$	Flavonoids	565,1553	0,09	4,66		
27	Chrysoeriol-6-C-hexoside	$C_{22}H_{22}O_{11}$	Flavonoids	463.1237	0.43	5.35	C05990	442611
28	Chrysoeriol-C-hexosyl-O-deoxyhexoside	$C_{28}H_{32}O_{15}$	Flavonoids	609.1817	0.50	5.24		
29	Chrysoeriol-C-hexosyl-O-hexoside	$C_{28}H_{32}O_{16}$	Flavonoids	625.1766	0.42	5.17		72193674
30	Luteolin-C-hexosyl-deoxyhexoside	$C_{27}H_{30}O_{15}$	Flavonoids	595.1660	0.45	5.02		
31	Luteolin-C-hexosyl-C-pentoside	$C_{26}H_{28}O_{15}$	Flavonoids	581,1504	0.51	4.97		44258081
32	Luteolin-C-hexosyl-O-hexoside	$C_{27}H_{30}O_{16}$	Flavonoids	611,1608	0,23	4,98		
33	Luteolin-6-C-hexoside	$C_{21}H_{20}O_{11}$	Flavonoids	449,108	0,36	5.00	C01750	5280459
34	Tricin	$C_{17}H_{14}O_7$	Flavonoids	331.0812	0,09	6.45	C10193	5281702
35	Tricin-7-O-hexoside	$C_{23}H_{24}O_{12}$	Flavonoids	493,1343	0,5	5.56		5322022
36	**Abscisic acid**	C15H20O4	Phytohormones	265,14343	0,53	6,06		
37	Abscisic acid glucose ester	C21H30O9	Phytohormones	427,19625	0,35	4,33		
38	**Indole acetic acid**	C10H9NO2	Phytohormones	176,0706	1,16	1,71		
39	**OPDA**	C18H28O3	Phytohormones	293,211121	0,89	7,42		
40	**Jasmonic acid**	$C_{12}H_{18}O_3$	Phytohormones	211,1329	0,14	6.27	C08491	5281166
41	**Methyljasmonate**	C13H20O3	Phytohormones	225,148521	0,31	6,88		
42	**Salicylic acid**	$C_7H_6O_3$	Phytohormones	139,039	0,21	**4,5**	C00805	338
43	**Methylsalicylate**	$C_8H_8O_3$	Phytohormones	153,05462	0,56	5,39		
44	Coumaroylagmatine	$C_{14}H_{20}N_4O_2$	Hydroxycinnamic acid amides	277,1659	0,01	4,66	C04498	5280691
45	Coumaroylputrescine	$C_{13}H_{18}N_2O_2$	Hydroxycinnamic acid amides	235,1441	0,02	4.50		
46	Coumaroylcadaverine	$C_{14}H_{20}N_2O_2$	Hydroxycinnamic acid amides	249,15975	0,56	3,97		
47	Caffeoylagmatine	$C_{14}H_{20}N_4O_3$	Hydroxycinnamic acid amides	293,1608	0,06	4.52		
48	Caffeoylputrescine	$C_{13}H_{18}N_2O_3$	Hydroxycinnamic acid amides	251,139	0,08	4.47	C03002	
49	Feruloylagmatine	$C_{15}H_{22}N_4O_3$	Hydroxycinnamic acid amides	307,1765	0,11	4.57	C18325	46173376
50	Feruloylputrescine	$C_{14}H_{20}N_2O_3$	Hydroxycinnamic acid amides	265,1548	0,49	4.70	C10497	5281796
51	Feruloylcadaverine	$C_{15}H_{22}N_2O_3$	Hydroxycinnamic acid amides	279,1702	0,43	4.85		
52	Hydroxyferuloylputrescine	$C_{14}H_{20}N_2O_4$	Hydroxycinnamic acid amides	281,14955	0,12	3,81		
53	Sinapoylagmatine	$C_{16}H_{24}N_4O_4$	Hydroxycinnamic acid amides	337,187	0,09	4.65		
54	Sinapoylputrescine	$C_{15}H_{22}N_2O_4$	Hydroxycinnamic acid amides	295,1653	0,22	4.56		

[a] Metabolites was classified according to KEGG (Kyoto Encyclopedia of Genes and Genomes; http://www.genome.ad.jp/kegg/) and PubChem (http://pubchem.ncbi.nlm.nih.gov) databases. Id: identifier; *m/z* : mass-to-charge ratio; *m/z* error (difference between the measured *m/z* and the calculated *m/z* of an ion, represented in ppm); RT: retention time. Compounds indicated in bold were confirmed with authentic standards.

CHAPITRE 4

Isolement et identification de souches de *Bacillus velezensis* produisant des lipopeptides et présentant une activité antifongique vis-à-vis de *Zymoseptoria tritici*

Dans le chapitre précédent, nous avons montré que la mycosubtiline, un lipopeptide cyclique, était capable de protéger le blé vis-à-vis de *Z. tritici* grâce à un double mode d'action (activité antifongique directe et stimulation des défenses de l'hôte *via* la potentialisation). Ici, deux souches de bactéries (S1 et S6) provenant de la phyllosphère de blé, ont été isolées au Maroc. Ces bactéries été identifiées comme appartenant à l'espèce de *Bacillus velezensis* et se sont révélées prometteuses pour le biocontrôle de *Z. tritici*. Les deux souches bactériennes sélectionnées, S1 et S6, ont montré une activité antagoniste significative vis-à-vis de *Z. tritici in vitro*. Nous avons ensuite produit les filtrats de culture dont l'activité antifongique a ensuite été déterminée. Les résultats obtenus sont très encourageants et l'activité antifongique *in vitro*, en particulier du surnageant produit avec la souche S1, vis-à-vis de l'agent phytopathogène, était forte. La caractérisation des métabolites produits par ces souches a été réalisée et a permis de montrer que la souche S1 biosynthétisait différents types de lipopeptides, notamment plusieurs bacillomycines D putatives. Le rôle potentiel de ces composés dans l'activité antifongique des surnageants sera discuté.

Cette étude a été menée en collaboration avec plusieurs partenaires ayant réalisé un certain nombre de travaux :

- INRA de Kenitra (Maroc) : Isolement des souches
- URCA Reims : Identification des souches
- Université de Lille : Caractérisation des lipopeptides produits par les souches
- ULCO Calais et Junia Lille : Activités biologiques, coordination et rédaction du manuscrit

Les résultats obtenus dans le cadre de ce chapitre sont en cours de consolidation et de préparation en vue de leur publication dans la revue Agronomy *(IF = 2,60).*

Isolation and Identification of lipopeptide-producing *Bacillus velezensis* strains from wheat phyllosphere with antifungal activity against the wheat pathogen *Zymoseptoria tritici*

Rémi Platel[1†], Mélodie Sawiki[2†], Qassim Esmaeel[3], Béatrice Randoux[2], Pauline Trapet[1], Mohamed El Guili[4], Noureddine Chtaina[5], Ségolène Arnauld[1], Alexandre Bricout[1], Alice Rochex[1], Patrice Halama[1], Cédric Jacquard[3], Essaid Ait Barka[3], Philippe Reignault[2], Maryline Magnin-Robert[2†], Ali Siah[1†]

[1] Joint Research Unit 1158 BioEcoAgro, Junia, Univ. Lille, Université Liège, UPJV, Univ. Artois, ULCO, INRAE, F-59000 Lille, France.

[2] Unité de Chimie Environnementale et Interactions sur le Vivant (EA 4492), Université du Littoral Côte d'Opale, CS 80699, F-62228 Calais Cedex, France.

[3] Unité de Résistance Induite et Bioprotection des Plantes (EA4707 - USC INRAe 1488), Université de Reims-Champagne-Ardenne, Reims, France

[4] Laboratory of Phytopathology and Post-Harvest Quality, Regional Centre for Agronomic Research, Kenitra 14070, Morocco.

[5] Laboratory of Phytopathology, Department of Production, Protection and Biotechnology, Hassan II Institute of Agronomic and Veterinary medicine, Rabat 10010, Morocco.

*Corresponding author : ali.siah@junia.com ; Tel.: +33(0)3 28 38 48 48

†These authors contributed equally to this work.

ABSTRACT

Septoria tritici blotch, caused by the fungal pathogen *Zymoseptoria tritici*, is a highly significant disease on wheat crops worldwide, causing yield losses of up to 50% during severe epidemics. Disease management relies mainly on the use of chemical fungicides and to a lower extent on the use of resistant cultivars. Because of the potential negative impacts of agrochemicals on both the environment and human health, a development of ecofriendly crop protection tools, such as the use of compounds with biocontrol properties, is hence strongly recommended. The objective of the present study was thus to search for new bacterial strains with promising antimicrobial activity against *Z. tritici*. Two phyllospheric bacteria (S1 and S6) were isolated from wheat ears in Morocco and were identified as *Bacillus velezensis* strains according to 16s rRNA sequencing. Antagonistic assays performed with either living strains or cell-free culture filtrates showed significant antifungal effects against *Z. tritici*. For the culture filtrate, the half-maximal inhibitory dilution and the minimal inhibitory dilution consisted of 1.4% and 3.7 % for the strain S1, and 7.4% and 15% for the strain S6, respectively. Matrix assisted laser desorption Ionization-time of flight (MALDI-ToF) analysis revealed that both strains synthesize cyclic lipopeptides from different families. The strain S1 produces surfactins, iturins as well as fengycins, while the strain S6 seems to synthetize only surfactins and iturins. Interestingly, iturins produced by the strain S1 are putative bacillomycin D, while those from the strain S6 are putative iturin A or mycosubtilin. Such patterns could explain the difference observed in the activity of the culture filtrates from the two strains. This study allows the identification of new lipopeptide-producing strains of *B. velezensis* with a high potential of application for the biocontrol of *Z. tritici*.

Keywords : *Zymoseptoria tritici*, *Bacillus velezensis*, antimicrobial agents, cyclic lipopeptides, Bacillomycin D.

INTRODUCTION

Bacillus sp. are ubiquitous Gram-positive bacteria occurring in diverse ecological niches and are known for their ability to produce a wide array of metabolites with applications in several areas, like crop bio-protection against pests and diseases. *Bacillus* genus harbors more than 300 described species (www.bacterio.net/bacillus.html) but constitutes a phylogenetically incoherent group with two main reported clades (*B. subtilis* and *B. cereus* clades) (Bhandari *et al*., 2013). Most of the exploited *Bacillus* species for the production of biologically active lipopeptides are *B. subtilis*, *B. pumilus*, *B. licheniformis, B. velezensis*, and *B. amyloliquefaciens*, although the classification of these later species is confusing and still not unanimous within the scientific community (Fan *et al.*, 2017). *Bacillus* species dedicate approximatively 5 to 8% of their total genome to the biosynthesis of bioactive secondary metabolites, such as peptides and lipopeptides, polyketides, bacteriocins, and siderophores (Hamley *et al*. 2015). Lipopeptides from *Bacillus* sp. are synthesized by multi-enzymatic proteins named non-ribosomal peptide synthetases, which confer substantial structural diversity to the molecules and results in the production of linear, branched, or cyclic compounds usually considered as low toxic (Strieker *et al*., 2010 ; Deravel *et al*., 2014). Lipopeptides are classified into three main families according to their amino acid sequence, including iturins (mycosubtilin, iturin A, and bacillomycin D), surfactin, and fengycin (Xunchao *et al*., 2013; Guo *et al*. 2014). The surfactin family consists of heptapeptides containing a β-hydroxy fatty acid, while iturin family includes heptapeptides with a β-amino fatty acid (Romero *et al*., 2007 ; Jacques, 2011). Molecules belonging to the fengycin family, as well as the related plipastatin, are decapeptides linked to a β-hydroxy fatty acid. Lipopeptides have been demonstrated to show a broad spectrum of antimicrobial activity towards a wide range of phytopathogenic fungi, oomycetes, bacteria, and viruses through direct antagonistic effect and/or *via* the stimulation of the plant immunity (Crouzet et al., 2020a). These modes of action seem to result mainly from the interaction of the lipopeptides with the cell plasma membranes of the targeted organisms, because of their amphiphilic properties conferring them an affinity with cell membranes (Fira *et al.,* 2018 ; Crouzet *et al*., 2020) .

Wheat is one of the most cultivated and consumed cereals worldwide, used as basic human and livestock foods in several regions around the world. *Zymoseptoria tritici*, causing Septoria tritici blotch, is one of the most occurring and devastating pathogens on wheat crops, able to induce grain yield losses up to 50%, especially in regions where the environmental conditions are favorable for disease development (Ponomarenko *et al*., 2011 ; Fones and Gurr, 2015). *Zymoseptoria tritici* is a hemibiotrophic fungus, with a biotrophic phase of about two weeks, followed by a necrotrophic phase of one week (Siah *et al*., 2010). However, this time lapse varies depending on the host cultivar, the fungal strain, and the environmental conditions (Lovell *et al.*, 2004). Since host resistance to *Z. tritici* is not fully effective in most wheat cultivars, disease control relies mainly of the use of synthetic chemical fungicides. However, the use of such products is increasingly controversial because of their potential negative and harmful impacts on both the environment and human health. Besides, *Z. tritici* frequently develops resistance to fungicides and regularly overcomes host-resistance genes, making it one of the most difficult plant pathogens to control in the field (Cowger *et al*., 2000; Cheval *et al*., 2017). In this context and in the framework of sustainable agriculture, it is urgent to develop and promote alternative control strategies against this disease. One of the most promising alternatives to allow a reduction of chemical pesticides is the biocontrol of plant pathogens using microorganisms or natural

substances. Such an eco-friendly solution received increasing attention because of its potential improved safety when compared to conventional pesticides (Beneduzi *et al*., 2012). The main objective of the present study was thus to isolate new biocontrol agents producing metabolites with antimicrobial bioactivity against *Z. tritici*, by focusing on the bacterial species *B. velezensis*, which has never been investigated for its antifungal activity towards the pathogen. Although previous reports on *B. velezensis* were performed with strains collected mainly from soil or rhizosphere, we isolated here bacterial strains from wheat phyllosphere (plant ear). The assays consisted to isolate, identify, and characterize the antimicrobial activity of the isolated strains against *Z. tritici*. Moreover, the lipopeptide metabolites produced by the bacteria were also identified using matrix assisted laser desorption Ionization-time of flight (MALDI-ToF) analysis.

MATERIALS AND METHODS

Bacillus sp. strain isolation

Both S1 and S6 *B. velezensis* strains used in the present study were isolated from wheat ears in August 2016 in Morocco. The strain S1 was isolated in Ait Mellol location (GPS coordinates 033°14’44 006°22’52 251,33’) while the strain S6 was isolated in Marrakech location (GPS coordinates 031°26’61 006°50’50 716,81). One wheat ear was sampled from unknown cultivar in each location and then immediately immersed in laboratory conditions in a solution of 250 mL of physiological water, before being submitted for agitation for 2h. Serial dilution was then performed from each sample until reaching 10^{-6} of the mother solution, then 100 µL of the obtained diluted solution (10^{-6}) was spread on a Petri plate amended with potato dextrose agar (PDA) medium. After an incubation period of 24h at 25°C in dark conditions, characteristic colonies of *B. velezensis* were collected under sterile conditions and transferred into new PDA plates, before conservation at -80 C° in cryotubes for further analyses.

Culture filtrate production and preparation

Culture filtrates (free cell supernatants) from the S1 and S6 *B. velezensis* strains were produced in sterile conditions using a modified Landy's liquid medium (Landy *et al.*, 1948), containing 20 $g.L^{-1}$ glucose, 5 $g.L^{-1}$ glutamic acid, 1 $g.L^{-1}$ yeast extract, 1 $g.L^{-1}$ K_2HPO_4, 0.5 $g.L^{-1}$ $MgSO_4.7H_2O$, 0.5 $g.L^{-1}$ KCl, 1.6 $mg.L^{-1}$ $CuSO_4.5H_2O$, 0.4 $mg.L^{-1}$ $FeSO_4.7H_2O$, 1.2 $mg.L^{-1}$ $MnSO_4.H_2O$, and 3-(N-morpholino)propanesulfonic acid buffer at 100 mM pH 7.0. A preculture of each strain was prepared in 100 mL Erlenmeyer containing 10 mL of modified Landy's medium inoculated with frozen stocked cells of each bacterial strain and incubated at 30 C° under 160 rpm shaking for 16h. Then, 10 mL of each preculture were used to inoculate 250 mL Erlenmeyer amended with 100 mL of modified Landy's medium, which then were incubated at 30 C° and 160 rpm shaking for 48h. The first step of the filtration consisted to adjust the concentration of the cultures regarding the bacterial cells into 0.8 optical density at 600 nm using a Spectrophotometer, in order to allow a better and reliable further filtration process. The adjusted cultures were then centrifuged at 10,000 g for 10 min before being sterilized by filtration across a 0.22 mm cellulose acetate membrane and stored at -20 C°.

In vitro bacterial antagonism activity and antifungal activity bioassays of culture filtrates

Antagonism activity of both *B. velezensis* strains S1 and S6 and the antifungal activity of their culture filtrates were assessed using the *Z. tritici* single-conidial strain T02596 isolated in 2014 from northern France (Platel *et al*., 2021). The antagonism assays were performed by plate confrontation between the bacterial strains and the fungus. The fungus was grown on PDA medium in Petri dishes incubated at 20°C. After five days of incubation, fungal spores were collected by washing the cultures with 10 mL of sterile distilled water, and then, the concentration of spore suspensions was adjusted to $1x10^6$ spores.mL^{-1}. An aliquot of 0.5 mL of spore suspension was spread on PDA Petri dish before being incubated at 20°C for 24h in the dark. Then, 10 µL of bacterial suspension (0.8 optical density, corresponding to 7.10^6 CFU/mL) were deposited on the center of the dish. This bacterial suspension was obtained with a pre-culture of each strain in 25 mL Erlenmeyer containing 5 mL of lysogeny broth (LB) medium inoculated with frozen stocked cells of each bacterial strain (300 µL) and incubated at 28 C° for 24h under 180 rpm shaking. The antagonism effect was evaluated by observing an inhibition zone after 13 days of incubation at 28°C in the dark. Three Petri dishes were used as replicates for each condition.

The assays regarding the antifungal activity of the bacterial filtrates were performed in 12-well plates amended with PDA medium supplemented with different concentrations of each culture filtrate (final dilutions in PDA medium corresponding to 0.9, 1.9, 3.8, 7.5, 15, and 30% of culture filtrate). The plates were prepared, inoculated, and incubated according to Platel *et al*. (2021). Three plate wells were used as repetitions for each condition, including the control without culture filtrate. The effect of the culture filtrate on fungal growth was noticed by measuring visually the two perpendicular diameters of each developed *Z. tritici* colony. Dose-response curve and half-maximal inhibitory dilution (ID_{50}) value of each strain were performed using the GraphPad Prism software version 9 (GraphPad Software Inc., San Diego, USA).

MALDI-ToF assay

Bacterial colonies grown on PDA medium at 30 °C for 72h h were spread onto a MALDI ground steel target plate (Bruker Daltonik, Bremen, Germany). They were washed twice with a 99.9/0.1 (v/v) H2O:Trifluoroacetic acid (TFA) solution and treated with a 70/30 (v/v) formic acid:H2O solution. They were then coated with a solution of α-cyano-4-hydroxycinnamic acid matrix (10mg/mL in H2O:acetonitrile:TFA, 50/47.5/2.5 v/v/v). Analyses were realized with the Bruker Daltonik Autoflex Speed MALDI-ToF/ToF mass spectrometer. Calibration of the device was performed with the Peptide Calibration Standard II kit from Bruker Daltonik composed of bradykinin 1-7, angiotensin I, angiotensin II, substance P, bombesin, rening substrate, ACTH clip 1-17, ACTH clip 18-39, and somatostatin. Analyses were carried out in the reflector and positive mode in the m/z 700-5000 mass range. Mass spectra were obtained by accumulating 2000 lasers shots at 50% of intensity.

Molecular identification of S1 and S6 strains

Genomic DNA from exponentially growing S1 and S6 cultures was extracted using the Wizard Genomic Purification DNA Kit (Promega Corp., Madison, WI, USA) following instructions from the supplier. The strains S1 and S6 were identified by sequencing the 16S rRNA gene using 16S forward 5'AGAGTTTGATCATGGCTCAG and 16S reverse 5'ACGGTTACCTTGTTACGACTT primers (Esmaeel *et al*., 2020), and the following PCR cycles: one cycle at 94°C for 5min, 30 cycles (94°C, 1min; 56°C, 30s; 72°C, 2min), and a final extension at 72°C for 10 min. The resulting PCR product sizes were purified with the

GeneJET Gel Extraction Kit (Thermo Scientific Fermentas, Waltham, USA) and then sequenced at GENWIZ Co., Ltd. (Leipzig, Germany) using Sanger sequencing technology. The sequencing reaction was performed in two directions using the forward and reverse primers (FD1, RP1) to cover the length of the 16S rRNA gene. After trimming, forward and reverse sequences were aligned and then assembled to obtain the full contiguous sequence. The sequences were then submitted to blast basic using local alignment search tool (BLAST) provided online by the national center for biotechnology information (NCBI, Bethesda, MD, USA). The nearest 16S rRNA gene sequences were downloaded and the phylogenetic tree was constructed using the neighbor-joining algorithms and kimura two-parameter model *via* MEGA version X (Kumar *et al*., 2018). The dataset was boot-strapped 1000 times. The 16S rRNA gene sequences of strains S1 and S6 have been deposited in GenBank under accession numbers MW931521 and MW931522, respectively.

RESULTS

S1 and S6 strains are new unique *B. velezensis* genotypes

Based on the obtained 16S rRNA gene sequences, strains S1 and S6 shared high sequence similarity (>99%) with *B. velezensis*. The phylogenetic analysis constructed using MEGA version X with neighbor-joining method indicated that strains S1 and S6 belong to the genus *Bacillus* and form a monophyletic cluster with *B. velezensis* with a high bootstrap score (>95%) (**Figure 1**). Moreover, sequence alignment of 16S rRNA gene sequence between strains S1 and S6 showed that both strains shared 99.86% sequence identity. Therefore, the following names *B. velezensis* strain S1 and *B. velezensis* strain S6 are proposed. They also shared high sequence identity with other species of *Bacillus* sp., including *B. vallismortis*, *B. subtilis*, *B. mojavensis*, and *B. halotolerans* (**Figure 1**).

S1 strain shows stronger antifungal activity towards *Z. tritici* compared to S6 strain

The antagonistic activity of S1 and S6 strains towards *Z. tritici* was performed by depositing a bacterial suspension on the center of PDA-amended Petri plates already inoculated with *Z. tritici*. Results revealed that both strains exbibit antagonistic activity against the pathogen and form a visible halo around the formed bacterium colonies (**Figure 2A,B**), which revealing a release and diffusion of antimicrobial compounds into the surrounding medium. On the other hand, culture filtrates from the two strains were produced and tested for their antimicrobial activity against the fungus on PDA medium. Dose-response curves revealed that culture filtrates from both strains are able to inhibit fungal growth, but the S1 culture filtrate showed higher antifungal activity when compared to S6 culture filtrate (**Figure 2C,D**). The minimal-inhibitory dilution (MID) values for S1 and S6 culture filtrates correspond to 3.75% and 15%, while the half-maximal inhibitory dilution (ID_{50}) values for S1 and S6 culture filtrates correspond to 1.4% and 7.4%, respectively (**Figure 2C,D**). In order to examine the effect of culture media on the growth of the two bacterial strains, three growth media were tested (King's B medium, KB; plate count agar, PCA, and lysogeny broth, LB). Results highlighted that LB is the most suitable among the three tested media for *in vitro* growth of both *B. velezensis* strains (**Supplementary Figure S1**).

Both S1 and S6 strains produce cyclic lipopeptides but with distinct patterns

Lipopeptides produced by the two *B. velezensis* strains S1 and S6 grown on solid medium were assessed using MALDI-ToF analysis. Both strains produced cyclic lipopeptides from different families, with several putative chemical structures within each family (**Table 1, Figure 3**). Even if common metabolites were detected among the two bacterial strains, they overall displayed different putative metabolite patterns (**Table 1**). The strain S1 produced surfactins, iturins as well as fengycins, while the strain S6 biosynthetized only surfactins and iturins. Interestingly, iturins produced by the strain S1 are, putatively, bacillomycin D, while those produced by the strain S6 are iturin A or mycosubtilin. Surfactins produced by both strains are surfactin or pumilacidin (**Table 1**).

DISCUSSION

We isolated here two wheat phyllosphere-associated bacterial strains identified as two strains of *B. velezensis* (S1 and S6), and exhibiting potent antagonistic activity against *Z. tritici*, a major pathogen on wheat crops. Our results are in agreements with previous reports showing that this beneficial bacterial species can display antagonistic activity against crop phytopathogens. For instance, the *B. velezensis* strain FZB42 (previously named as *B. amyloliquefaciens* strain FZB42) has been shown to exhibit antagonistic activity against another wheat pathogen, *Fusarium graminearum*, as well as the phytopathogenic bacterium *Ralstonia solanacearum* (Gu *et al*., 2017). We suggest that the antagonistic activity of the *B. velezensis* strains S1 and S6 observed here against *Z. tritici* is due to the capacity of the strains to produce antimicrobial compounds, such as lipopeptides. Indeed, lipopeptides are known to be the major contributor to *Bacillus* sp. biocontrol activity (Abderrahmani *et al*., 2011). Various strains of *B. velezensis* have recently received considerable attention since this species can produce different types of biologically active secondary metabolites that can suppress plant pathogens (Rabbee *et al*., 2019). It has been reported *B. velezensis* strains are able to synthesize various bioactive lipopeptides, like amylocyclicin, bacilysin, bacillomycin D, bacillibactin, bacillaene, difficidin, fengycin, macrolactin, plantazolicin, and surfactin (Chen *et al*., 2017). Today, several products based on *Bacillus* spp., such as *B. amyloliquefaciens, B. pumilus* or *B. subtilis*, are marketed as a biopesticides (Pérez-García *et al*., 2011; Rabbee *et al.*, 2019).

Our results showed that the culture filtrate from the *B. velezensis* strain S1 displayed a strong and a higher antifungal activity against *Z. tritici* when compared to the strain S6. This marked difference could be explained by the differential composition in the lipopeptides synthetized by the two strains. Indeed, MALDI-ToF analysis revealed a presence of fengycin and bacillomycin D (an antimicrobial lipopeptide belonging to the iturin family) only in the most active filtrate, from the strain S1. The importance of these two lipopeptides in the antifungal activity of *B. velezensis* has already been reported with the *B. velezensis* strain FZB42, in which a double mutant that was deficient in both bacillomycin D and fengycin synthesis (ΔbmyA ΔfenA) heavily impaired its ability to inhibit the growth of *F. oxysporum*, thereby indicating synergistic effects among such lipopeptides against this targeted fungal pathogen (Koumoutsi *et al*., 2004). In the same way, Romero and colleagues (2007) reported that the lipopeptides from iturin and fengycin families have a major role in the antimicrobial activity of *Bacillus* sp. strains on *Podosphaera fusca*. However, other studies seem to point out that the presence of bacillomycin as being solely responsible for the antifungal activity. For instance, bacillomycin D deficient mutant strains of *B. velezensis* strain FZB42 or strain SQR9 exhibited severely impaired antifungal activities, which indicated that the bacillomycin D appear to be the major

contributor to the antifungal activity against *F. oxysporum* (Chen *et al*., 2009; Xu *et al*., 2013). *Cao et al*., (2018) suggest that the relative contribution of each lipopeptide to the antimicrobial activity may also be dependent on the species of the targeted plant pathogen. These authors have reported that iturin and fengycin are functionally redundant in antagonism against the bacterium *Ralstonia solanacearum*, when only iturin family metabolites appear to have an antagonism activity against the fungus *Fusarium oxysporum*.

The effect of purified lipopeptides from *B. subtilis* have been previously examined against *Z. tritici*. It has been shown that mycosubtilin, a lipopeptide belonging to iturin family, displayed a strong antifungal activity against *Z. tritici* (half-maximal inhibitory concentration of 1.4 mg L^{-1}), while neither surfactin nor fengycin showed significant activity towards the pathogen (Mejri *et al*., 2018). On the other hand, bacterium cell-free filtrates of a mutant strain of *B. subtilis* overproducing mycosubtilin showed an antagonistic activity against several phytopathogenic fungi, including *Pythium aphanidermatum*, *Botrytis cinerea*, and *F. oxysporum*, with growth inhibition zones significantly larger than those induced by the wild-type supernatant (Leclère *et al*., 2005). Taken together, these results suggest that lipopeptides of the iturin family may display an interesting antifungal activity towards plant phytopathogens. Moyne *et al*. (2001) reported that analogues of bacillomycin and/or length of the lipid chain may have an influence on the antifungal activity of this lipopeptide on various phytopathogenic fungi, such as *Alternaria solani*, *Aspergillus flavus*, *Colletotrichum gloeosporioides*, *Phomopsis gossypii*, and *Sclerotium rolfsii*. The mechanism underlying the bacillomycin D antifungal activity was performed on *F. graminearum* and revealed an inhibition of the formation and germination of conidia (Gu *et al*., 2017). In details, the mycelia structure swollen in the presence of Bacillomycin D. Moreover, observations with electronic microscopy revealed substantial destruction of hyphae and conidia, with loose of cell walls and irregular shapes, which indicate that the cytoplasm was leaking out of the cells (Gu *et al*., 2017).

This study highlighted that the two strains isolated from wheat plant ears and identified as *B. velezensis* strains S1 and S6 exhibit antimicrobial activity against the wheat pathogen *Z. tritici*, and that their biological activity seems to be related to the production of lipopeptides. The higher antifungal activity observed for the culture filtrate S1 could, thus, be due to the different lipopeptides it may produce, in particular the various analogues of bacillomycin D. Hence, further investigations using purified lipopeptides are needed to confirm the antifungal activity of bacillomycin D, alone or in mixture with other lipopeptides, against *Z. tritici*. On the other hand, (Chowdhury et al., 2015a) have suggested that *B. velezensis*, and notably the strain FBZ42, may trigger pathways of induced systemic resistance (ISR) which can also contribute to the biocontrol activity of FZB42. Indeed, sub-lethal concentrations of lipopeptides and volatiles produced by plant-associated *Bacilli* trigger pathways of ISR, which protect plants against attacks of pathogenic microbes, viruses, and nematodes (Chowdury *et al*., 2015). In this sense, the ability of the S1 and S6 *B. velezensis* strains to induce ISR in wheat against *Z. tritici* should be investigated.

ACKNOWLEDGEMENTS

This research was conducted in the framework of the projects Bacplant, funded by the European program Arimnet and l'Agence Nationale de la Recherche (ANR) and the CPER Alibiotech, funded by

the European Union, the French State, and the French Region Hauts-de-France. The authors thank Océane Bueno for technical support.

REFERENCES

Abderrahmani, A., Tapi, A., Nateche, F., Chollet, M., Leclère, V., Wathelet, B., Hacene, H., Jacques, P., 2011. Bioinformatics and molecular approaches to detect NRPS genes involved in the biosynthesis of kurstakin from *Bacillus thuringiensis*. *Appl Microbiol Biotechnol* 92, 571–581.

Beneduzi, A., Ambrosini, A., Passaglia, L.M.P., 2012. Plant growth-promoting rhizobacteria (PGPR): their potential as antagonists and biocontrol agents. *Genetics and Molecular Biology* 35, 1044–1051.

Bhandari V, Ahmod NZ, Shah HN, Gupta RS. (2013). Molecular signatures for *Bacillus* species: demarcation of the *Bacillus subtilis* and *Bacillus cereus* clades in molecular terms and proposal to limit the placement of new species into the genus Bacillus. *Int J Syst Evol Microbiol*. 63:2712-2726.

Cao Y, Pi H, Chandrangsu P, Li Y, Zhou H, Xiong H, Helmann JD, Cai Y. (2018) Antagonism of two plant-growth promoting *Bacillus velezensis* isolates against *Ralstonia solanacearum* and *Fusarium oxysporum*. *Scientific Reports* 8: 4360.

Chen, X.H.; Koumoutsi, A.; Scholz, R.; Eisenreich, A.; Schneider, K.; Heinemeyer, I.; Morgenstern, B.; Voss, B.; Hess, W.R.; Reva, O.; et al. Comparative analysis of the complete genome sequence of the plant growth-promoting bacterium *Bacillus amyloliquefaciens* FZB42. *Nat. Biotechnol*. 2007, 25, 1007–1014.

Chen, X.H.; Koumoutsi, A.; Scholz, R.; Schneider, K.; Vater, J.; Süssmuth, R.; Piel, J.; Borriss, R. Genome analysis of *Bacillus amyloliquefaciens* FZB42 reveals its potential for biocontrol of plant pathogens. *J. Biotechnol*. 2009, 140, 27–37.

Chen, Jianwei, Wu, Q., Hua, Y., Chen, Jun, Zhang, H., Wang, H., 2017. Potential applications of biosurfactant rhamnolipids in agriculture and biomedicine. *Appl. Microbiol. Biotechnol*. 101, 8309–8319.

Cheval, P., Siah, A., Bomble, M., Popper, A.D., Reignault, P., Halama, P., 2017. Evolution of QoI resistance of the wheat pathogen *Zymoseptoria tritici* in Northern France. *Crop Protection* 92, 131–133.

Chowdury SP, Hartmann A, Gao X, Borriss R (2015) Biocontrol mechanism by root-associated *Bacillus amyloliquefaciens* FZB42 – a review. *Front. Microbiol*.

Cowger, C., Hoffer, M.E., Mundt, C.C., 2000. Specific adaptation by *Mycosphaerella graminicola* to a resistant wheat cultivar. *Plant Pathology* 49, 445–451.

Crouzet J, Arguelles-Arias A., Dhondt-Cordelier S., Cordelier S., Pršic J., Mazeyrat-Goubeyre F, Baillieul F, Clément C., Ongena M., Dorey S. 2020. Biosurfactants in plant protection against diseases: rhamnolipids and lipopeptides case study. *Front. Bioeng. Biotechnol*. 8, 1040.

Deravel, J., Lemière, S., Coutte, F., Krier, F., Van Hese, N., Béchet, M., Sourdeau, N., Höfte, M., Leprêtre, A., Jacques, P., 2014. Mycosubtilin and surfactin are efficient, low ecotoxicity molecules for the biocontrol of lettuce downy mildew. *Appl Microbiol Biotechnol* 98, 6255–6264.

Fan, B., Blom, J., Klenk, H.-P., Borriss, R., 2017. *Bacillus amyloliquefaciens*, *Bacillus velezensis*, and *Bacillus siamensis* Form an "Operational Group *B. amyloliquefaciens*" within the *B. subtilis* Species Complex. *Front. Microbiol*. 8.

Fira, D., Dimkić, I., Berić, T., Lozo, J., Stanković, S., 2018. Biological control of plant pathogens by *Bacillus* species. *Journal of Biotechnology* 285, 44–55.

Fones, H., Gurr, S., 2015. The impact of Septoria tritici Blotch disease on wheat: An EU perspective. *Fungal Genet Biol* 79, 3–7.

Gu, Q.; Yang, Y.; Yuan, Q.; Shi, G.; Wu, L.; Lou, Z.; Huo, R.; Wu, H.; Borriss, R.; Gao, X. Bacillomycin D produced by *Bacillus amyloliquefaciens* is involved in the antagonistic interaction with the plant-pathogenic fungus *Fusarium graminearum*. *Appl. Environ. Microbiol*. 2017, 83, 1–17.

Guo, Q., Dong, W., Li, S., Lu, X., Wang, P., Zhang, X., Wang, Y., Ma, P., (2014). Fengycin produced by *Bacillus subtilis* NCD-2 plays a major role in biocontrol of cotton seedling damping-off disease. *Microbiol. Res*. 169, 533–540.

Hamley L.W. (2015). Lipopeptides: from self-assembly to bioactivity. *Chem. Commun*., 51, 8574.

Jacques P. (2011). Surfactin and other lipopeptides from *Bacillus* spp. In: Soberon-Chavez G (ed) Biosurfactants microbiology monographs, vol 20. Springer-Verlag, Heidelberg, pp 57-91.

Koumoutsi, A.; Chen, X.H.; Henne, A.; Liesegang, H.; Hitzeroth, G.; Franke, P.; Vater, J.; Borriss, R. Structural and functional characterization of gene clusters directing nonribosomal synthesis of bioactive cyclic lipopeptides in *Bacillus amyloliquefaciens* strain FZB42. *J. Bacteriol*. 2004, 186, 1084–1096.

Kumar, S., Stecher, G., Li, M., Knyaz, C., Tamura, K., 2018. MEGA X: Molecular Evolutionary Genetics Analysis across Computing Platforms. *Molecular Biology and Evolution* 35, 1547–1549.

Landy M, Warren GH, Rosenman SB, Colio LG. (1948) Bacillomycin: an antibiotic from *Bacillus subtilis* active against pathogenic fungi. *Proc Soc Exp Biol Med*, 67:539e41.

Leclère V, Béchet M, Adam A, Guez J-S, Wathelet B, Ongena M, Thonart P, Gancel F, Chollet-Imbert M, Jacques P (2005) Mycosubtilin overproduction by *Bacillus subtilis* BBG100 enhances the organism's antagonistic and biocontrol activities. *Appl Environ Microbiol* 71:4577–4584.

Lovell, D.J., Hunter, T., Powers, S.J., Parker, S.R., Bosch, F.V. den, 2004. Effect of temperature on latent period of septoria leaf blotch on winter wheat under outdoor conditions. *Plant Pathology* 53, 170–181.

Mejri S, Siah A, Coutte F, Magnin-Robert M, Randoux B, Tisserant B, Krier F, Jacques P, Reignault Ph, Halama P. 2018. Biocontrol of the wheat pathogen *Zymoseptoria tritici* using cyclic lipopeptides from *Bacillus subtilis*. *Environ. Sci. Pollut. Res.* 25(30):29822-29833.

Moyne AL, Shelby R, Cleveland TE, Tuzun S (2001) Bacillomycin D: an iturin with antifungal activity against *Aspergillus flavus*. *J. Appl. Microbiol*. 90, 622-629.

Pérez-García, A.; Romero, D.; de Vicente, A. Plant protection and growth stimulation by microorganisms: Biotechnological applications of *Bacilli* in agriculture. *Curr. Opin. Biotechnol*. 2011, 22, 187–193.

Ponomarenko, A., Goodwin, S.B., Kema, G.H.J., 2011. Septoria tritici blotch (STB) of wheat. Septoria tritici blotch (STB) of wheat.

Platel, R., Chaveriat, L., Le Guenic, S., Pipeleers, R., Magnin-Robert, M., Randoux, B., Trapet, P., Lequart, V., Joly, N., Halama, P., Martin, P., Höfte, M., Reignault, P., Siah, A., 2021. Importance of the C12 Carbon Chain in the Biological Activity of Rhamnolipids Conferring Protection in Wheat against *Zymoseptoria tritici*. *Molecules* 26, 40.

Rabbee MF, Ali MS, Choi J, Hwang BS, Jeong SC, Baek KH. 2019. *Bacillus velezensis*: a valuable member of bioactive molecules within plant microbiomes. *Molecules* 24:46.

Romanazzi, G.; Feliziani, E. *Botrytis cinerea* (Gray Mold). In Postharvest Decay: Control Strategies; Bautista-Banos, S., Ed.; Elsevier: Amsterdam, The Netherlands, 2014; pp. 131–146.

Romero D, de Vicente A, Rakotoaly RH, Dufour SE, Veening J-W, Arrebola E, Cazorla FM, Kuipers OP, Paquot M, Pérez-Garcia A (2007) The iturin and fenngycin families of lipopeptides are key factors in antagonism of *Bacillus subtilis* toward *Podospaera fusca*. *Mol Plant Microbe Interact* 20, 430-440.

Strieker, M., Tanović, A., Marahiel, M.A., 2010. Nonribosomal peptide synthetases: structures and dynamics. *Current Opinion in Structural Biology, Theory and simulation / Macromolecular assemblages* 20, 234–240.

Xu, Z., Shao, J., Li, B., Yan, X., Shen, Q., and Zhang, R. (2013). Contribution of bacillomycin D in *Bacillus amyloliquefaciens* SQR9 to antifungal activity and biofilm formation. *Appl. Environ. Microbiol*. 79, 808-815.

Xunchao, C., Hui, L., Ya-rong, X., Chang-hong, L., 2013. Study of endophytic *Bacillus amyloliquefaciens* CC09 and its antifungal cyclic lipopeptides. https://doi.org/10.7324/jabb.2013.1101.

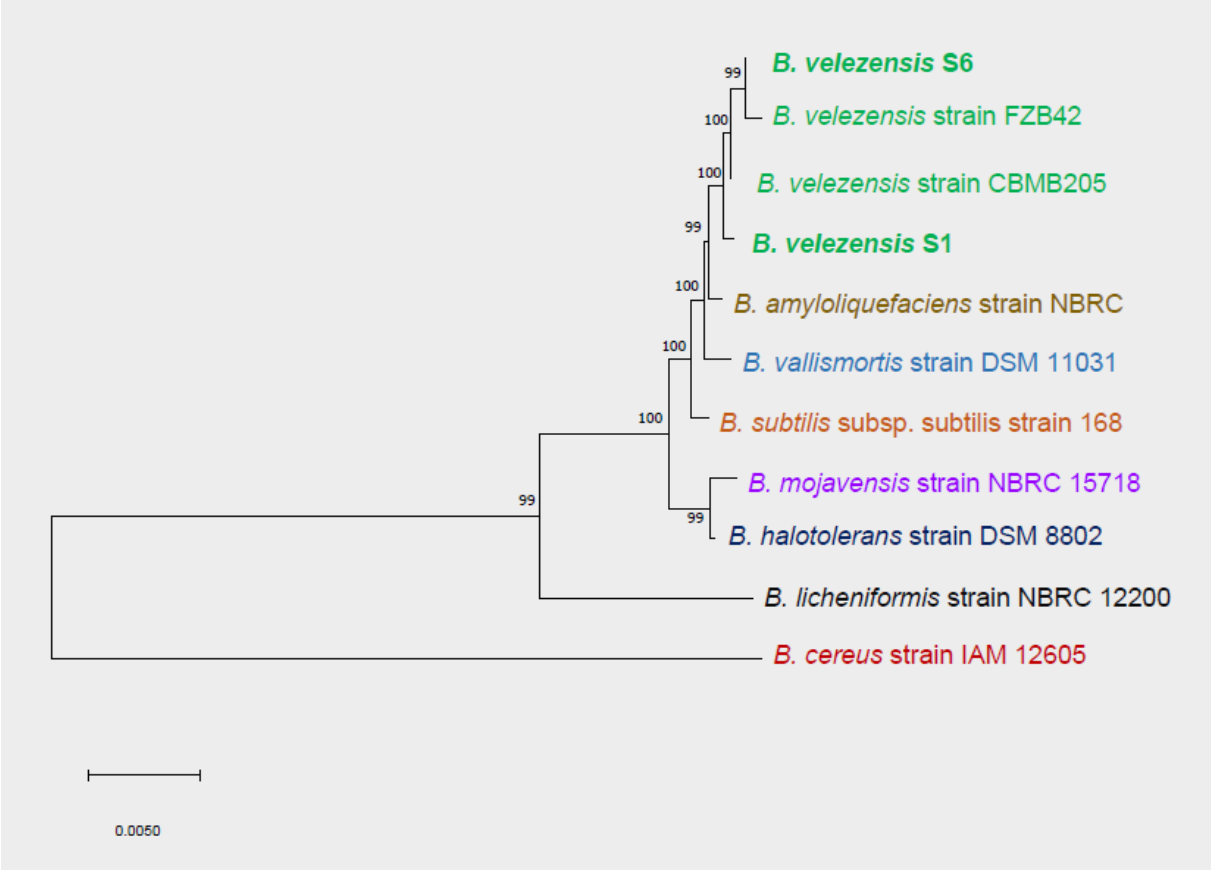

Figure 1. Phylogenetic tree of the S1 and S6 *Bacillus velezensis* strains. The tree was built based on 16S rRNA gene sequences using MEGA version X with neighbor-joining method. Values at nodes indicate bootstrap values out of 1000 resampling. *Bacillus cereus* IAM 12605 was used as an outgroup. S1 and S6 are shown in bold.

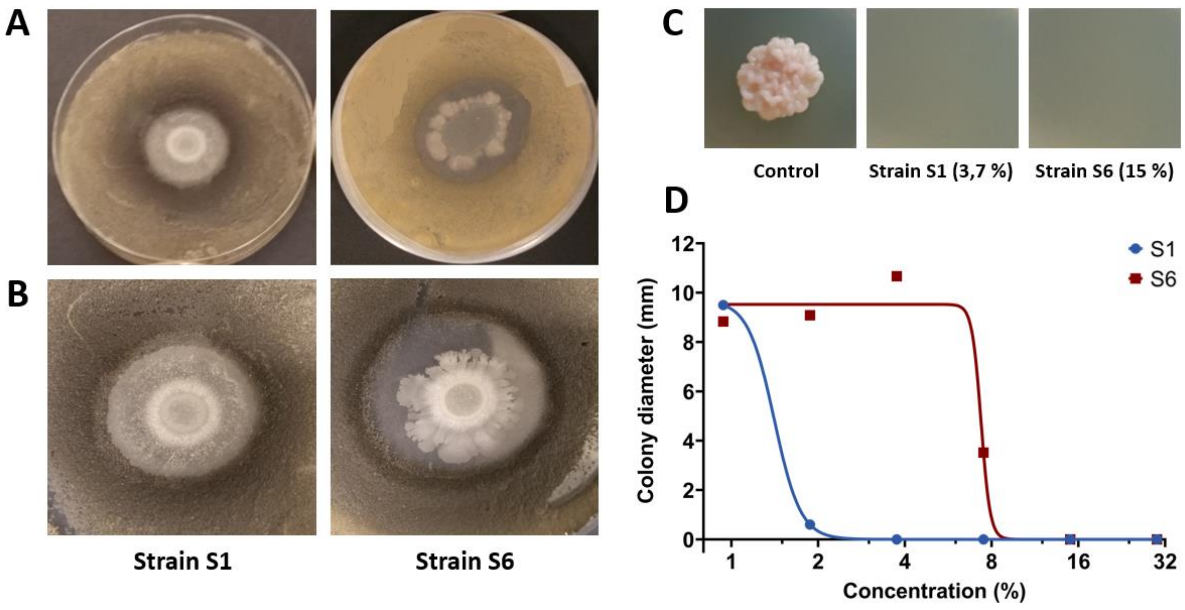

Figure 2. Antifungal activity of S1 and S6 *Bacillus velezensis* strains against the *Zymoseptoria tritici* strain T02596. **A and B**, Antagonistic activity of S1 and S6 strains on solid PDA medium at 13 days after Petri plate inoculation (B is a zoom of A). The inhibiting effect is visualized by the formation of a halo around the bacterial colonies. **C**, illustration of the antifungal effect of the S1 and S6 culture filtrates on *Z. tritici* observed on PDA medium. **D**, *in vitro* dose-response curves of the antifungal effect of the S1 and S6 culture filtrates on *Z. tritici* growth assessed by measuring the fungal colony diameters at 10 days after plate inoculation. Dose-response curves were performed using GraphPad Prism software v 9.0. Three repetitions were used as replicates for each concentration of tested culture filtrate.

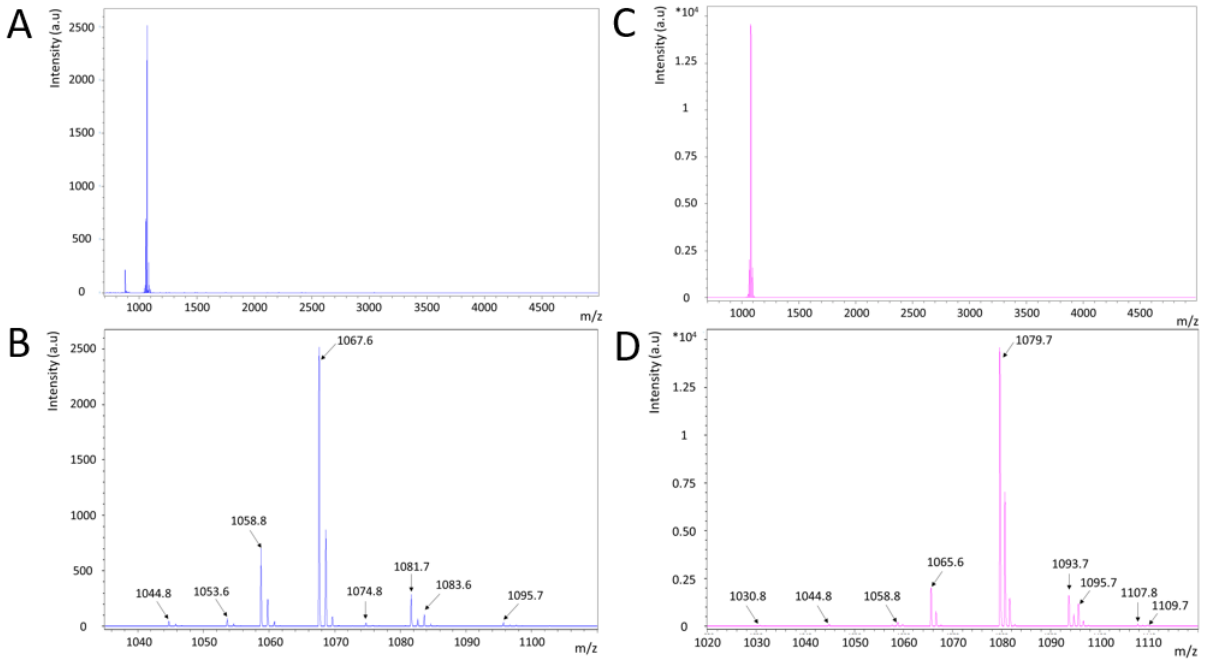

Figure 3. Whole-cell MALDI-ToF mass spectra of the two *Bacillus velezensis* strains S1 (A, B) and S6 (C, D). B and D are a zoom on A and D, respectively.

Table 1. Putative metabolites produced by the two *Bacillus velezensis* bacterial strains S1 and S6 grown on PDA medium, detected by MALDI-TOF.

Bacillus velezensis S1		
m/z	**Putative assigned lipopeptide**	**Lipopeptide family**
1044.8	Surfactin C14 or [Ile7] Surfactin C14 or [Val7] Surfactin C15 or [Val7] Pumilacidin C14 $[M+Na]^+$	Surfactin
1058.8	Surfactin C15 or [Ile7] Surfactin C15 or [Ile7] Pumilacidin C14 or [Val7] Pumilacidin C15 $[M+Na]^+$	Surfactin
1074.8	[Ile7] Surfactin C15 or [Ile7] Pumilacidin C14 or [Val7] Pumilacidin C15 $[M+K]^+$	Surfactin
1053.6	Bacillomycin D C14 $[M+Na]^+$	Iturin
1067.7	Bacillomycin D C15 $[M+Na]^+$	Iturin
1083.7	Bacillomycin D C15 $[M+K]^+$	Iturin
1081.7	Bacillomycin D C16 $[M+Na]^+$	Iturin
1095.7	Bacillomycin D C17 $[M+Na]^+$	Iturin
1486.0	Fengycin A C16 $[M+Na]^+$ or Fengycin A C15 (insat) $[M+K]^+$	Fengycin
1499.8	Fengycin A C17 $[M+Na]^+$ or Fengycin AC16 (insat) $[M+K+]^+$ or Fengycin B C15 (insat) $[M+Na]^+$	Fengycin
Bacillus velezensis S6		
m/z	**Putative assigned lipopeptide**	**Lipopeptide family**
1030.8	Surfactin C13 or [Val7] Surfactin C14 or [Ile7] Surfactin C13 or [Ala4] Surfactin C15 $[M+Na]^+$	Surfactin
1044.8	Surfactin C14 or [Val7] Surfactin C15 or [Ile7] Surfactin C14 or [Val7] Pumilacidin C14 $[M+Na]^+$	Surfactin
1058.8	Surfactin C15 or [Ile7] Surfactin C15 or [Ile7] Pumilacidin C14 or [Val7] Pumilacidin C15 $[M+Na]^+$	Surfactin
1065.6	Iturin A C14 or Mycosubtilin C14 $[M+Na]^+$	Iturin
1079.6	Iturin A C15 or Mycosubtilin C15 $[M+Na]^+$	Iturin
1095.6	Iturin A C15 or Mycosubtilin C15 $[M+K]^+$	Iturin
1093.6	Iturin A C16 or Mycosubtilin C16 $[M+Na]^+$	Iturin
1109.6	Iturin A C16 or Mycosubtilin C16 $[M+K]^+$	Iturin
1107.6	Iturin A C17 or Mycosubtilin C17 $[M+Na]^+$	Iturin

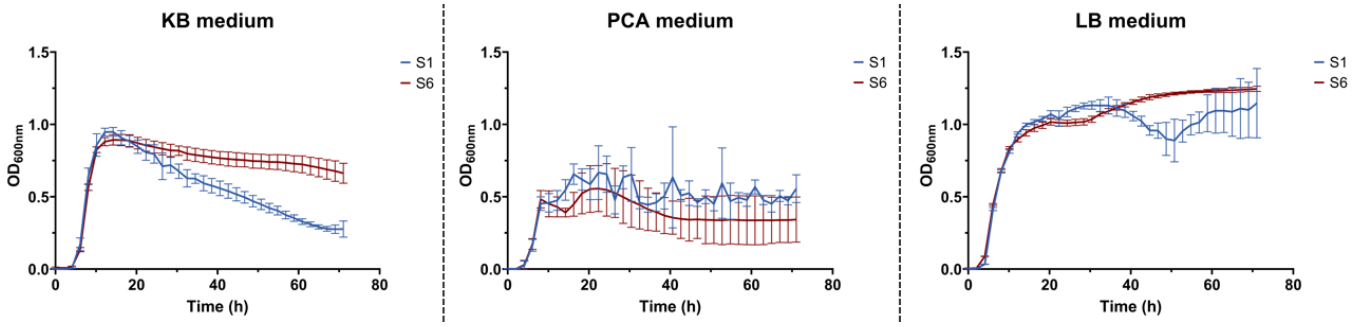

Supplementary Figure S1. Kinetics of S1 and S6 *Bacillus velezensis* strains growth in different liquid media. These two strains were inoculated in Erlenmeyer containing one of the three different media, from the left to the right, King's B (KB), Plate Count Agar (PCA) and lysogeny broth (LB) for three days. Bacterium growth was assessed by measuring the optical density in each well at 600 nm. Three repetitions were used for each condition. Optical density was also measured for controls (i.e media without bacteria) and these data were used to correct optical density means presented in this figure. Bars stand for standard deviation (n=3).

DISCUSSION GÉNÉRALE ET PERSPECTIVES

Dans le cadre de ce projet de thèse, nous avons démarré les travaux avec une bibliothèque de 181 métabolites (d'origines naturelles ou synthétiques) ou extraits microbiens. Nous avons initié les travaux par le criblage de ces composés sur la base de leur activité antifongique directe *in vitro* vis-à-vis de *Z. tritici*. Cette étape a permis de mettre en évidence plusieurs biomolécules et extraits microbiens prometteurs. Parmi les 146 extraits fongiques testés, huit (provenant de *Penicillium griseofulvum*, *Trichoderma virens*, *Aspergillus niger*, *Myrothecium verrucaria*, *Lecanicillium longisporum*, *P. cyclopium*, *Trichothecium roseum*, *Emericella rugulosa*) se sont révélés significativement actifs *in vitro* vis-à-vis de l'agent pathogène, avec des CI_{50} inférieures à 10% (v/v). Néanmoins, certains surnageants présentaient le risque de contenir des mycotoxines dangereuses pour la santé humaine (Sorenson *et al.*, 1975 ; Northolt *et al*., 1979 ; Nielsen *et al*., 2009 ; Banani *et al*., 2016 ; Siciliano *et al*., 2017), et ont donc été écartés du criblage. Finalement, trois extraits provenant des espèces fongiques *T. virens, L. longisporum* et *E. rugulosa*, ne comprenant pas, à notre connaissance, de composés toxiques ou écotoxiques majeurs, et inhibant de manière significative la croissance de *Z. tritici*, se sont révélés être les plus prometteurs parmi les surnageants d'origine fongique obtenus à l'issu de ce criblage. *Trichoderma virens* est un champignon filamenteux tellurique bien connu pour produire des métabolites antibiotiques, parasiter des champignons pathogènes et déclencher des phénomènes d'ISR chez certains hôtes (Burns and Benson, 2000 ; Djonović *et al*., 2006). Il est d'ores et déjà utilisé en tant qu'agent de biocontrôle pour lutter contre *Rhizoctonia solani*, *Sclerotium rolfsii*, et *Pythium* spp (Mukherjee and Kenerley, 2010). Si plusieurs travaux ont montré l'efficacité d'autres espèces de *Trichoderma* dans la lutte contre la septoriose du blé, en particulier *T. harzanium*, le potentiel de *T. virens* en tant que solution de biocontrôle n'avait jusqu'alors jamais été rapporté sur notre pathosystème d'étude. *L. longisporum* est un champignon entomopathogène commercialisé en tant qu'agent de biocontrôle pour lutter contre les pucerons. Plusieurs études ont aussi démontré sa capacité à agir contre des agents phytopathogènes responsables de l'oïdium chez plusieurs espèces cultivées dont le concombre (Kim *et al*., 2008), mais aucune n'a visé des espèces fongiques pathogènes infectant le blé. Peu d'informations sont disponibles dans la littérature à propos d'*E. rugulosa*, mais il semblerait que celui-ci produise des composés fongicides efficaces contre l'agent responsable de la fusariose de la tomate *Fusarium oxysporum* f.sp. *lycopersici* (Sibounnavong *et al.*, 2011). De plus amples analyses ont été initiées afin de déterminer l'effet de ces extraits *in planta*, notamment dans le but de déterminer leur efficacité de protection ainsi que leur potentiel effet éliciteur *via* l'étude de l'activité d'enzymes-clés impliquées dans les voies de défense du blé (catalase, peroxydase, β-1,3-glucanase et chitinase). Les résultats de ces expériences n'étaient toutefois pas concluants et ne seront pas présentés dans le présent manuscrit. En effet, nous avons observé des différences significatives majeures entre les activités des différents lots d'extraits fournis par l'UCLouvain. Les analyses concernant les activités biologiques de ces extraits sont donc en hiatus le temps d'obtenir une répétabilité de production satisfaisante. Des études complémentaires visant à caractériser les composants majoritaires des différents extraits d'intérêt pourraient ici avoir un double rôle, permettre de comprendre les différences d'efficacité entre les lots et identifier les biomolécules responsables de leurs activités.

Aucun des lipodepsipeptides cycliques testés (N1, N2, N8, WLIP, orfamide, putisolvin, lokisin et xantholysin) n'a montré d'activité significative directe *in vitro* vis-à-vis de *Z. tritici* à l'issu de ce criblage, alors que plusieurs de ceux-ci ont déjà été rapportés comme présentant des activités antimicrobiennes, notamment vis-à-vis des agents phytopathogènes *Botrytis cinerea* et *Magnaporthe*

oryzae (Geudens and Martins, 2018; Omoboye *et al*., 2019). Omoboye *et al.* (2019) ont aussi récemment démontré que les métabolites suivants, WLIP et lokisin, étaient capables de déclencher des mécanismes d'ISR chez le riz contre *M. oryzae* lorsqu'appliqués au niveau racinaire. Il pourrait donc être intéressant de réaliser des expériences similaires sur le pathosystème blé-*Z. tritici* afin de faire avancer nos connaissances sur le potentiel de ces métabolites en tant que composés de biocontrôle dans le cadre de la lutte contre ce pathogène.

D'un point de vue global, sélectionner les composés d'intérêt uniquement selon ce criblage *in vitro* ne nous a permis de discerner que ceux présentant une activité antifongique, mais pas ceux capables d'induire les réactions de défense de l'hôte. Afin d'obtenir le plus large panel de composés prometteurs pour protéger le blé contre la septoriose, il aurait aussi été pertinent de réaliser un criblage de ceux-ci selon leur activité indirecte. Cette étape était initialement prévue dans le cadre de cette thèse et aurait dû permettre d'identifier les biomolécules ou extraits capables d'influer sur les voies de défenses de la plante. Pour ce faire, nous avions prévu de déterminer leur effet *in planta* sur l'activité de six enzymes présentes dans les feuilles de blé et jouant un rôle-clé dans les réactions de défense chez les plantes, avec deux impliquées dans la détoxification des ROS, la CAT et la SOD ; la LOX, qui intervient dans la biosynthèse du JA ; la PAL, enzyme centrale de la voie de biosynthèse des phénylpropanoïdes ; et deux protéines PR, chitinase et β-1,3-glucanase (Halliwell, 2006 ; Huang *et al*., 2010 ; Wasternack and Hause, 2013 ; Gill *et al*., 2015). En raison du nombre élevé de composés à tester, nous avons cherché à mettre en place une méthode de criblage à haut-débit utilisant la station de pipetage automatisée de la plateforme Realcat (Université de Lille). Des protocoles automatisés utilisant ces robots ont donc été établis pour toutes ces enzymes. Ceux-ci ont demandé un nombre extrêmement conséquent de sous-étapes d'optimisation et de validation. Finalement, à cause de contraintes techniques, l'optimisation des protocoles visant à déterminer les activités de la lipoxygénase et de la phénylalanine-ammonia lyase n'a pas été concluante. Ces enzymes ont été abandonnées en tant que biomarqueurs et ont été substituées par la POX, une enzyme impliquée dans la détoxification des ROS, mais aussi la lignification, ainsi que l'oxydation de composés phénoliques (Pandey *et al*., 2017). Néanmoins, en raison de nombreuses contraintes techniques, de temps, et finalement sanitaires, le criblage des composés selon leur activité indirecte n'a pas pu être réalisé. Les travaux effectués pour la mise en place de cette méthode automatisée et innovante de criblage pourraient être utiles dans d'autres futurs projets. Les compétences acquises dans l'analyse des activités enzymatiques du blé m'ont aussi été utiles dans l'étude des activités biologiques des rhamnolipides sur le pathosystème blé-*Z. tritici*.

Lors de l'étape de criblage des rhamnolipides selon leur activité directe contre *Z. tritici*, nous avons pu remarquer une grande diversité dans leur efficacité d'inhibition alors même que ces molécules ne présentaient souvent entres elles que de faibles différences structurelles. Nous avons alors décidé d'étudier la relation entre leurs structures et leurs activités biologiques (antifongique, élicitation des défenses, protection) sur notre pathosystème, comme présenté dans le **chapitre 1**. Nous avons pu montrer que parmi les 19 rhamnolipides à notre disposition, ceux présentant des chaines carbonées à 12 carbones ainsi que des liaisons éthers ou esters étaient les plus efficaces pour les différentes activités biologiques étudiées. Aucun rhamnolipide avec un nombre impair de carbones dans leur chaîne carbonée n'a été synthétisé par les partenaires de l'Université d'Artois, il aurait pourtant été judicieux de déterminer les activités de mono-rhamnolipides avec des chaines carbonées

à 11 ou 13 carbones pour déterminer quelle longueur de chaîne était vraiment la plus optimale sur notre pathosystème. Par ailleurs, l'absence de protection et d'élicitation des défenses du blé observée après traitement avec l'acide laurique et le dodécanol, respectivement un acide gras et un alcool à 12 carbones, ont permis de mettre en évidence le rôle capital du groupement rhamnose dans l'activité des rhamnolipides. Il pourrait être pertinent de déterminer si d'autres familles de molécules présentant des queues hydrophobes (comme les lipopeptides) seraient plus efficaces pour protéger le blé vis-à-vis de la septoriose si elles présentaient des chaines carbonées de 12 carbones. Le mélange de rhamnolipides naturels produit par *P. aeruginosa* n'a, quant à lui, montré aucun effet antifongique direct *in vitro* vis-à-vis de *Z. tritici* et aucune induction des activités CAT et POX du blé, même à des concentrations allant jusqu'à 1,5 mM. Toutefois, à cette même concentration, nous avons observé une réduction significative de la sévérité de la maladie sur les feuilles de blé. Plusieurs hypothèses pourraient expliquer cela. Une des plus plausibles est que ce composé serait capable de stimuler les défenses de l'hôte sans modifier l'activité des deux enzymes susmentionnées, soulignant les faiblesses de n'utiliser qu'un faible nombre de biomarqueurs différents à un seul moment, deux jours après traitement. Des analyses plus poussées ciblant les modes d'action de ce composé pourraient nous fournir plus d'informations sur son activité protectrice. Enfin, nous avons pu mettre en évidence que le Rh-Est-C12 était le rhamnolipide le plus efficace, à notre disposition, pour protéger le blé de la septoriose. Ce rhamnolipide est d'autant plus intéressant dans la lutte contre cette maladie qu'il est aussi actif sur des souches hautement résistantes aux DMI, une famille de fongicides de synthèse largement utilisée sur la culture du blé (Cools *et al*., 2013 ; McDonald *et al*., 2019). En raison de l'induction des activités de la catalase et de la peroxydase observée chez le blé après traitement avec cette molécule, notre hypothèse était que le mode d'action du Rh-Est-C12 était double (activité directe antifongique et indirecte *via* élicitation des défenses de l'hôte).

Nous avons donc cherché à caractériser de manière plus fine, dans le **chapitre 2**, le mode d'action indirect du rhamnolipide Rh-Est-C12, à l'aide d'une approche combinée de transcriptomique et de métabolomique ciblée. Nous avons pu montrer que le traitement foliaire du blé avec le Rh-Est-C12 déclenchait des altérations significatives au niveau du transcriptome des feuilles de blé deux jours après traitement, avec une modification de l'expression de 20 gènes, dont un certain nombre était lié à des réponses de la plante aux stress abiotiques. Ces altérations pourraient être causées par l'interaction du rhamnolipide avec les membranes plasmiques végétales, conduisant à leur déstabilisation et à ces réponses de la part du blé. En effet, plusieurs auteurs ont suggéré que l'induction des défenses des plantes par les rhamnolipides étaient déclenchée selon ce mécanisme (Crouzet et al., 2020). Néanmoins, que ce soit en conditions élicitation (feuilles traitées mais non-inoculées) ou *priming* (feuilles traitées puis inoculées), l'effet du traitement sur l'accumulation des métabolites détectés et sur le niveau de transcription des gènes était globalement faible. Les résultats ainsi obtenus suggèrent que l'activité protectrice de ce rhamnolipide, lorsqu'appliqué préventivement sur les feuilles de blé, serait principalement liée à son activité antifongique directe. Une autre possibilité, toutefois, est que ce rhamnolipide serait capable d'induire des phénomènes de résistance chez le blé sans entraîner de modifications physiologiques majeures.

Pour aller plus loin dans l'exploration du potentiel des rhamnolipides en protection des cultures, d'autres travaux ont été réalisés. Ainsi, nous avons, en collaboration avec l'Université de Gand, comparé l'effet de l'application des rhamnolipides produits par *P. aeruginosa* (rhamnolipides dits

« naturels ») ou du Rh-Est-12, entre les deux pathosystèmes blé-*Zymoseptoria tritici* et riz-*Magnaporthe oryzae*. Ces derniers présentent plusieurs caractéristiques communes. En effet, le riz (*Oryza sativa* L.) est, tout comme le blé, une espèce appartenant à la famille des *Poaceae*, massivement cultivée au niveau mondial. *M. Oryzae* (anamorphe : *Pyricularia oryzae*) est, comme *Z. tritici*, un champignon phytopathogène hémibiotrophe majeur de cette culture. Cet agent pathogène est responsable de pertes de rendement annuelles dans les pays producteurs estimées entre 10% et 30% en moyenne (Skamnioti and Gurr, 2009). Plusieurs analyses comparatives ont ainsi été menées, et les résultats obtenus sont résumés en **annexe 2 (Tableau supplémentaire 2)**. Globalement, les rhamnolipides naturels n'ont présenté aucune activité bénéfique pour la protection du blé **(Annexe 2).** A l'inverse, sur le pathosystème riz-*M. oryzae*, ces rhamnolipides étaient beaucoup plus intéressants. Au niveau de leurs propriétés antifongiques, ceux-ci étaient capables d'inhiber la germination des spores et la croissance mycélienne de *M. oyzae in vitro* **(Annexe 2 ; Tableau supplémentaire 2, Figure supplémentaire 2)**. Aussi, la co-application de ces rhamnolipides naturels avec les spores lors de l'infection foliaire du riz diminuait le nombre des lésions causées par la maladie, même à la concentration la plus basse testée (50 µM). Nous avons, de plus, observé une réduction significative des symptômes lorsque ce composé était appliqué au niveau racinaire. L'efficacité de ce composé varie donc grandement entre les deux pathosystèmes. Le Rh-Est-C12 s'est montré, quant à lui, actif sur les deux pathosystèmes (i) au niveau antifongique, (ii) lorsqu'appliqué au niveau racinaire et (iii) en co-application avec les spores du champignon alors que les concentrations utilisées pour la co-application étaient plus faibles que celles efficaces dans le cadre du **chapitre 1**, où le Rh-Est-C12 ne présentait une activité de protection significative sur le blé qu'à partir de 800 µM. Notre hypothèse actuelle pour expliquer les raisons de la protection observée lors des expériences de co-application rhamnolipides/spores est que les rhamnolipides, en s'intercalant dans les membranes fongiques, induiraient des fuites cellulaires chez les spores de *Z. tritici* et *M. oryzae*, conduisant à la libération de signaux moléculaires de type PAMP, qui déclencheraient la résistance chez les plantes-hôtes étudiées. Afin de tester cette hypothèse, des travaux supplémentaires visant à étudier l'effet de cette co-application (rhamnolipides avec les spores de *Z. tritici* ou M. *Oryzae*) sur la production de marqueurs cytologiques de l'induction des défenses des hôtes, comme la production de ROS ou le dépôt de callose, vont bientôt être initiés. L'ensemble des travaux réalisés sur les deux pathosystèmes sera valorisé sous forme d'article scientifique une fois les résultats complémentaires obtenus.

Un autre surfactant d'intérêt dont le mode d'action a été particulièrement étudié dans le cadre de cette thèse est la mycosubtiline, un lipopeptide cyclique produit notamment par *Bacillus subtilis*. Nous avons pu, dans le **chapitre 3**, montrer que ce composé, lorsqu'appliqué au niveau foliaire, protégeait le blé vis-à-vis de *Z. tritici* grâce à un double mode d'action, antifongique direct et indirect *via* potentialisation. Ainsi, nous avons observé, après traitement et dans les premières phases de l'infection, la modification significative du niveau d'expression de 80 gènes, dont une partie est impliquée dans les réponses aux stress abiotiques et biotiques. Plusieurs gènes d'intérêt impliqués dans ces réactions de défense ont ainsi été mis en évidence, notamment des gènes impliqués dans les voies de réponse à l'ABA. Une accumulation de flavonoïdes, une famille de molécules connue pour présenter des activités antifongiques, antioxydantes, et de renforcement des parois des cellules végétales, a aussi été observée (Al Aboody and Mickymaray, 2020; Lam *et al*., 2015; Lan *et al*., 2015). Ces travaux ont permis d'identifier des gènes et métabolites potentiellement centraux dans la résistance induite du blé vis-à-vis de la septoriose et qui mériteraient sans aucun doute de voir leur

rôle étudié plus en détail dans des projets futurs (*e.g* l'ABA, la famille des flavonoïdes, les gènes codants pour la protéine WIR1, le précurseur de la protéine PR17d, MLA7, et bien d'autres). Si nous avons pu mettre en évidence l'effet potentialisateur de la mycosubtiline lorsqu'appliqué en traitement foliaire, il serait pertinent de déterminer ultérieurement si les mécanismes de résistance impliqués peuvent être catégorisés de type LAR ou SAR à l'aide d'un protocole expérimental adapté. Notre hypothèse est que la mycosubtiline potentialiserait le blé *via* son interaction avec les membranes plasmiques du blé, déclenchant un stimulus semblable à celui causé par un stress abiotique, ce qui expliquerait les nombreuses modifications métaboliques liés aux réponses à ces types de stress, dont

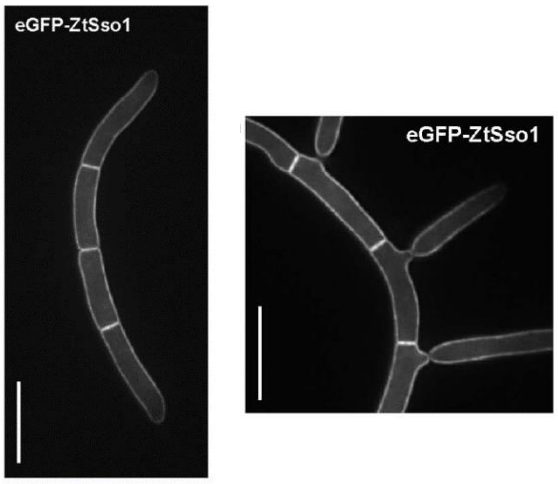

Figure 26 : Cellules de *Zymoseptoria tritici* exprimant le marqueur de membrane plasmique eGFP-ZtSso1. Barres d'échelle = 10 µM

les réponses à l'ABA (Vishwakarma *et al*., 2017). Les lipopeptides et les rhamnolipides supposément agissent vis-à-vis des champignons pathogènes en s'intercalant dans leur membrane, les déstabilisant et conduisant *in fine* à leur mort cellulaire. Ils stimuleraient aussi les défenses de l'hôte *via* des mécanismes similaires d'interaction avec les membranes végétales mais avec des impacts différents en raison des différences de compositions membranaires (Crouzet et al., 2020). Dans notre cas, si le Rh-Est-C12 et la mycosubtiline présentent tous deux des activités antifongiques significatives, et que leur traitement semble avoir déclenché un stimulus semblable à un stress abiotique dans les deux cas, seul la mycosubtiline semble stimuler de façon marquée les défenses. Une des perspectives possibles de ces travaux serait de vérifier l'hypothèse concernant les interactions rhamnolipide et lipopeptide avec les membranes du blé ou de *Z. tritici*, par exemple en produisant des composés d'intérêt marqués pour déterminer, par autoradiographie, leurs cibles cellulaires. Il pourrait aussi être possible de travailler avec des cellules modifiées génétiquement pour produire des marqueurs fluorescents des membranes plasmiques, comme cela a récemment été effectué avec la souche de *Z. tritici* IPO323_eGFP-Sso1 transformée pour exprimer une protéine membranaire marquée (Kilaru *et al*., 2017 ; Steinberg *et al*., 2020).

Ainsi, la mycosubtiline et le Rh-Est-C12 partagent un certain nombre de points communs. Bien que les démarches aient pu différer concernant l'analyse des activités biologiques de ces composés, nous tenterons de comparer de manière non exhaustive le potentiel de ces composés pour lutter contre *Z. tritici* chez le blé. Pour commencer, il convient de rappeler que la mycosubtiline est produite à partir de *Bacillus subtilis* alors que le Rh-Est-C12 l'est par chimie verte. Comme mentionné ci-dessus,

ces deux composés présentent une activité antifongique significative vis-à-vis de *Z. tritici* due, supposément, à leur capacité à interagir avec les membranes plasmiques fongiques. La mycosubtiline s'est néanmoins révélée plus efficace pour inhiber la croissance de l'agent pathogène *in vitro* que le Rh-Est-C12, avec des CMI de 0.78 $mg.L^{-1}$ et 31.2 $mg.L^{-1}$ et des CI_{50} de 0.57 $mg.L^{-1}$ et 26.8 $mg.L^{-1}$, respectivement. Aussi, l'activité de protection conférée par la mycosubtiline (58,1%) après application foliaire était supérieure à celle obtenue après traitement avec le Rh-Est-C12 (41,1%), alors même que la concentration testée pour le lipopeptide (100 mg.L-1) était inférieure à celle pour le rhamnolipide (500 mg.L-1). Cette différence entre activités de protection pourrait s'expliquer, en partie, par les modes d'action des deux composés. En effet, contrairement au Rh-Est-C12, la mycosubtiline présenterait un double mode d'action : antifongique et potentialisateur des défenses du blé, rendant ce composé particulièrement prometteur pour lutter contre *Z. tritici*. Le rhmanolipide présente toutefois d'autres activités biologiques d'intérêt. Nous avons ainsi mis en évidence que son application racinaire, à de faibles concentrations, était capable de réduire significativement la sévérité de la maladie sur les feuilles de blé. Par ailleurs, il était aussi efficace pour inhiber la croissance de souches de l'agent pathogène hautement résistantes aux DMI. Ce composé, pourrait ainsi, selon son utilisation, présenter d'autres avantages dans la lutte contre ce champignon. L'étude des dernières activités biologiques décrites n'a pas été réalisée avec la mycosubtiline dans le cadre de ce projet de thèse. Afin d'aller plus loin dans ce travail de comparaison, il pourrait être pertinent d'étudier, cette fois, l'effet d'un mélange Rh-Est-C12 et mycosubtiline pour protéger le blé, ce qui permettrait d'en apprendre plus sur leurs possibles cibles cellulaires communes. Une autre possibilité pourrait être de suivre une approche d'évolution expérimentale *in vitro* en mettant en contact des souches de *Z. tritici* avec le Rh-Est-C12 et/ou la mycosubtiline. Ces travaux pourraient permettre, d'une part, de comprendre et, potentiellement, prévenir l'apparition de phénomènes de résistance chez le champignon vis-à-vis de ces composés, mais aussi de déterminer si les résistances développées contre l'un ou l'autre de ces surfactants apporteraient des avantages évolutifs vis-à-vis de l'autre, ce qui supporterait l'hypothèse d'une cible cellulaire commune.

Enfin, dans le cadre du **chapitre 4**, deux souches de *Bacillus velezensis* provenant de la phyllosphère de blé, ont été isolées et identifiées. Celles-ci, nommées S1 et S6, présentaient une activité antagoniste significative vis-à-vis de *Z. tritici*. Leurs surnageants ont, tous les deux, significativement inhibé la croissance de l'agent pathogène *in vitro*, et celui provenant de la souche S1 était le plus efficace des deux, avec une CI_{50} de 1,4%. Les métabolites produits par ces deux souches ont été caractérisés par MALDI-TOF et nous avons pu mettre en évidence que la S1 biosynthétise probablement des bacillomycines D, un lipopeptide membre de la famille des iturines, dont l'activité antimicrobienne a déjà été rapportée vis-à-vis d'autres agents phytopathogènes mais jamais vis-à-vis de *Z. tritici* (Moyne *et al*., 2001 ; Gu *et al*., 2017). Des travaux additionnels concernant cette souche sont prévus et viseront notamment à purifier les métabolites qu'elle produit afin de déterminer leurs activités biologiques, notamment de protection *in planta*.

Plusieurs composés d'intérêt sur le pathosystème blé-*Z. tritici* ont donc été mis en évidence dans le cadre de ce projet de thèse, et les modes d'action de deux d'entre eux, le Rh-Est-C12 et la mycosubtiline, deux molécules amphiphiles surfactantes, ont été particulièrement étudiées. Certains mécanismes liés à la résistance induite chez le blé ont aussi été mis en lumière. Les résultats obtenus ainsi que la philosophie suivie tout au long de cette thèse s'inscrivent dans une démarche globale

d'identification d'outils durables pour lutter contre *Z. tritici*, en particulier en raison des résistances déployés par celui-ci contre les fongicides de synthèse (Leroux *et al*., 2007; Cheval *et al.*, 2017). L'étude des composés d'intérêt devra, par la suite, se poursuivre au champ afin de déterminer leur efficacité de protection en conditions non-contrôlées, celle-ci pouvant grandement différer de celle observée en serre. Dans ce cadre, et même si les lipopeptides et rhamnolipides sont généralement décrits comme respectueux de l'environnement (Crouzet et al., 2020), il sera primordial de vérifier la toxicité et l'éco-toxicité de ces composés ainsi que leur rémanence dans l'environnement et leur accumulation dans les parties comestibles des plantes cultivées. En effet, il convient de rappeler que produits d'origine « naturelle » n'est pas antinomique de toxique pour la santé humaine et l'environnement. Une analyse de leur cycle de vie, allant de leur production jusqu'à leur purification et en passant par la gestion des déchets pourrait aussi être envisagée afin de déterminer leur impact sur l'environnement au sens large. Des travaux visant à améliorer la formulation des composés d'intérêts surfactants seront aussi nécessaires, au vu de la différence d'activité significative notamment observée avec le Rh-Est-C12 *in vitro* et *in planta*. Ceux-ci devraient être mis en place prochainement au laboratoire en collaboration avec l'Université de Gand. Des travaux complémentaires visant à déterminer la durée d'efficacité des traitements, ainsi qu'à optimiser les conditions et modes d'application des différents composés, pourraient aussi être imaginés. En particulier, des concentrations trop élevées de mycosubtiline et du Rh-Est-C12 pourraient se révéler néfastes sur le blé et sa production en raison de leur mode d'action qui, supposément, pourrait agir comme un stress abiotique. Une gestion parcimonieuse des traitements sera aussi à mettre en place afin de limiter l'apparition de phénomènes de résistance de la part du champignon pathogène. Aussi, il conviendra de chercher à limiter les pertes d'efficacité souvent observés lors du passage de la serre au champ avec les produits de biocontrôle. Malgré tout cela, il semble peu probable que ces composés de biocontrôle, pris indépendamment, se révèlent aussi efficaces que les fongicides de synthèse pour lutter contre la septoriose du blé dans les années à venir. Ceux-ci pourraient toutefois faire partie d'une combinaison de leviers agroécologiques, incluant par exemple, le recours à des variétés plus résistantes ou le recours à des mesures prophylactiques (*e.g.* décalage des dates de semis, association de variétés, enfouissement des résidus de culture, *etc*.) qui pourraient ainsi limiter la pression et la nuisibilité de la maladie.

RÉFÉRENCES BIBLIOGRAPHIQUES

Abalos, A., Pinazo, A., Infante, M.R., Casals, M., García, F., Manresa, A., 2001. Physicochemical and Antimicrobial Properties of New Rhamnolipids Produced by *Pseudomonas aeruginosa* AT10 from Soybean Oil Refinery Wastes. Langmuir 17, 1367–1371. https://doi.org/10.1021/la0011735

Adhikari, T.B., Balaji, B., Breeden, J., Goodwin, S.B., 2007. Resistance of wheat to *Mycosphaerella graminicola* involves early and late peaks of gene expression. Physiological and Molecular Plant Pathology 71, 55–68. https://doi.org/10.1016/j.pmpp.2007.10.004

Al Aboody, M.S., Mickymaray, S., 2020. Anti-Fungal Efficacy and Mechanisms of Flavonoids. Antibiotics (Basel) 9. https://doi.org/10.3390/antibiotics9020045

Ali, Md.S., Baek, K.-H., 2020. Jasmonic Acid Signaling Pathway in Response to Abiotic Stresses in Plants. Int J Mol Sci 21. https://doi.org/10.3390/ijms21020621

Ali, S., Ganai, B.A., Kamili, A.N., Bhat, A.A., Mir, Z.A., Bhat, J.A., Tyagi, A., Islam, S.T., Mushtaq, M., Yadav, P., Rawat, S., Grover, A., 2018. Pathogenesis-related proteins and peptides as promising tools for engineering plants with multiple stress tolerance. Microbiological Research 212–213, 29–37. https://doi.org/10.1016/j.micres.2018.04.008

Alippi, A.M., Perelló, A.E., Sisterna, M.N., Greco, N.M., Cordo, C.A., 2000. Potential of Spore-forming bacteria as biocontrol agents of wheat foliar diseases under laboratory and greenhouse conditions / Das Potential der sporenbildenden Bakterien bei der biologischen Bekämpfung von Blattkrankheiten der Weizenpflanzen under Labor- und Gewächshausbedingungen. Zeitschrift für Pflanzenkrankheiten und Pflanzenschutz / Journal of Plant Diseases and Protection 107, 155–169.

ANSES, Retrait des produits à base de chlorothalonil | ephy [WWW Document], n.d. URL https://ephy.anses.fr/actualites/retrait-produits-base-chlorothalonil (accessed 11.25.20).

Ao, H.C., Griffiths, E., 1976. Change in virulence of *Septoria nodorum* and *S. tritici* after passage through alternative hosts. Transactions of the British Mycological Society 66, 337–340. https://doi.org/10.1016/S0007-1536(76)80067-8

Arraiano, L.S., Balaam, N., Fenwick, P.M., Chapman, C., Feuerhelm, D., Howell, P., Smith, S.J., Widdowson, J.P., Brown, J.K.M., 2009. Contributions of disease resistance and escape to the control of septoria tritici blotch of wheat. Plant Pathology 58, 910–922. https://doi.org/10.1111/j.1365-3059.2009.02118.x

Arvalis-Institut du végétal, Septoriose, miser sur le choix variétal et les seuils d'intervention (2013a) [WWW Document], n.d. URL https://www.arvalis-infos.fr/maladies-des-cereales-a-paille-septoriose-quelle-nuisibilite-et-quelle-strategie-de-protection--@/view-20824-arvarticle.html (accessed 9.21.20).

Arvalis-Institut du végétal, Septoriose - Maladie sur Blé tendre, blé dur, triticale, ARVALIS Résultats (2013b) [WWW Document], n.d. . Les Fiches Accidents - ARVALIS-infos.fr. URL http://www.fiches.arvalis-infos.fr (accessed 1.19.19).

Aziz, A., Poinssot, B., Daire, X., Adrian, M., Bézier, A., Lambert, B., Joubert, J.-M., Pugin, A., 2003. Laminarin Elicits Defense Responses in Grapevine and Induces Protection Against *Botrytis cinerea* and *Plasmopara viticola.* MPMI 16, 1118–1128. https://doi.org/10.1094/MPMI.2003.16.12.1118

Banani, H., Marcet-Houben, M., Ballester, A.-R., Abbruscato, P., González-Candelas, L., Gabaldón, T., Spadaro, D., 2016. Genome sequencing and secondary metabolism of the postharvest pathogen *Penicillium griseofulvum*. BMC Genomics 17. https://doi.org/10.1186/s12864-015-2347-x

Banke, S., Mcdonald, B.A., 2005. Migration patterns among global populations of the pathogenic fungus *Mycosphaerella graminicola*. Molecular Ecology 14, 1881–1896. https://doi.org/10.1111/j.1365-294X.2005.02536.x

Barriuso, J., Solano, B.R., Gutiérrez Mañero, F.J., 2008. Protection Against Pathogen and Salt Stress by Four Plant Growth-Promoting Rhizobacteria Isolated from *Pinus* sp. on *Arabidopsis thaliana*. Phytopathology® 98, 666–672. https://doi.org/10.1094/PHYTO-98-6-0666

Bektas, Y., Eulgem, T., 2015. Synthetic plant defense elicitors. Front Plant Sci 5. https://doi.org/10.3389/fpls.2014.00804

Betsuyaku, S., Katou, S., Takebayashi, Y., Sakakibara, H., Nomura, N., Fukuda, H., 2018. Salicylic Acid and Jasmonic Acid Pathways are Activated in Spatially Different Domains Around the Infection Site During Effector-Triggered Immunity in *Arabidopsis thaliana*. Plant Cell Physiol 59, 8–16. https://doi.org/10.1093/pcp/pcx181

Bingham, I.J., Walters, D.R., Foulkes, M.J., Paveley, N.D., 2009. Crop traits and the tolerance of wheat and barley to foliar disease. Annals of Applied Biology 154, 159–173. https://doi.org/10.1111/j.1744-7348.2008.00291.x

Bocquet, L., Rivière, C., Dermont, C., Samaillie, J., Hilbert, J.-L., Halama, P., Siah, A., Sahpaz, S., 2018. Antifungal activity of hop extracts and compounds against the wheat pathogen *Zymoseptoria tritici*. Industrial Crops and Products 122, 290–297. https://doi.org/10.1016/j.indcrop.2018.05.061

Bonawitz, N.D., Chapple, C., 2010. The genetics of lignin biosynthesis: connecting genotype to phenotype. Annual review of genetics. https://doi.org/10.1146/annurev-genet-102209-163508

Bouma, E., 2005. Development of comparable agro-climatic zones for the international exchange of data on the efficacy and crop safety of plant protection products. EPPO Bulletin 35, 233–238. https://doi.org/10.1111/j.1365-2338.2005.00830.x

Brandt, W., Gürke, M., Köhler, F.E., Pabst, G., Schellenberg, G., Vogtherr, M., 1883. Köhler's Medizinal-Pflanzen in naturgetreuen Abbildungen mit kurz erläuterndem Texte : Atlas zur Pharmacopoea germanica, austriaca, belgica, danica, helvetica, hungarica, rossica, suecica, Neerlandica, British pharmacopoeia, zum Codex medicamentarius, sowie zur Pharmacopoeia of the United States of America. Fr. Eugen Köhler, Gera-Untermhaus : https://doi.org/10.5962/bhl.title.623

Bricout, A., 2020. Mise en évidence d'une forte diversité structurale de lipopeptides chez *P. syringae*, un complexe bactérien aux activités antifongiques prometteuses (These de doctorat). Lille 1.

Brown, J.K.M., Chartrain, L., Lasserre-Zuber, P., Saintenac, C., 2015. Genetics of resistance to *Zymoseptoria tritici* and applications to wheat breeding. Fungal Genet Biol 79, 33–41. https://doi.org/10.1016/j.fgb.2015.04.017

Bruce, T., Matthes, M.C., Napier, J., Pickett, J., 2007. Stressful "memories" of plants: evidence and possible mechanisms. https://doi.org/10.1016/J.PLANTSCI.2007.09.002

Brunner, P.C., Torriani, S.F.F., Croll, D., Stukenbrock, E.H., McDonald, B.A., 2013. Coevolution and Life Cycle Specialization of Plant Cell Wall Degrading Enzymes in a Hemibiotrophic Pathogen. Mol Biol Evol 30, 1337–1347. https://doi.org/10.1093/molbev/mst041

Burns, J.R., Benson, D.M., 2000. Biocontrol of Damping-off of Catharanthus roseus Caused by *Pythium ultimum* with *Trichoderma virens* and Binucleate Rhizoctonia Fungi. Plant Disease 84, 644–648. https://doi.org/10.1094/PDIS.2000.84.6.644

Castro, A.C., Simón, M.R., 2016. Effect of tolerance to Septoria tritici blotch on grain yield, yield components and grain quality in Argentinean wheat cultivars. Crop Protection 90, 66–76. https://doi.org/10.1016/j.cropro.2016.08.015

Caulier, S., Nannan, C., Gillis, A., Licciardi, F., Bragard, C., Mahillon, J., 2019. Overview of the Antimicrobial Compounds Produced by Members of the *Bacillus subtilis* Group. Front. Microbiol. 10. https://doi.org/10.3389/fmicb.2019.00302

Chain, F., Côté-Beaulieu, C., Belzile, F., Menzies, J.G., Bélanger, R.R., 2009. A Comprehensive Transcriptomic Analysis of the Effect of Silicon on Wheat Plants Under Control and Pathogen Stress Conditions. MPMI 22, 1323–1330. https://doi.org/10.1094/MPMI-22-11-1323

Chartrain, L., Brading, P.A., Widdowson, J.P., Brown, J.K.M., 2004. Partial Resistance to Septoria Tritici Blotch (*Mycosphaerella graminicola*) in Wheat Cultivars Arina and Riband. Phytopathology® 94, 497–504. https://doi.org/10.1094/PHYTO.2004.94.5.497

Chen, J., Liu, X., Fu, S., An, Z., Feng, Y., Wang, R., Ji, P., 2020. Effects of sophorolipids on fungal and oomycete pathogens in relation to pH solubility. Journal of Applied Microbiology 128, 1754–1763. https://doi.org/10.1111/jam.14594

Cheval, P., Siah, A., Bomble, M., Popper, A.D., Reignault, P., Halama, P., 2017. Evolution of QoI resistance of the wheat pathogen *Zymoseptoria tritici* in Northern France. Crop Protection 92, 131–133. https://doi.org/10.1016/j.cropro.2016.10.017

Choi, Y.-E., Goodwin, S.B., 2010. Gene Encoding a c-Type Cyclin in *Mycosphaerella graminicola* Is Involved in Aerial Mycelium Formation, Filamentous Growth, Hyphal Swelling, Melanin Biosynthesis, Stress Response, and Pathogenicity. MPMI 24, 469–477. https://doi.org/10.1094/MPMI-04-10-0090

Chowdhury, S.P., Uhl, J., Grosch, R., Alquéres, S., Pittroff, S., Dietel, K., Schmitt-Kopplin, P., Borriss, R., Hartmann, A., 2015. Cyclic Lipopeptides of *Bacillus amyloliquefaciens* subsp. plantarum Colonizing the Lettuce Rhizosphere Enhance Plant Defense Responses Toward the Bottom Rot Pathogen *Rhizoctonia solani*. MPMI 28, 984–995. https://doi.org/10.1094/MPMI-03-15-0066-R

Chungu, C., Gilbert, J., Townley-Smith, F., 2001. Septoria tritici Blotch Development as Affected by Temperature, Duration of Leaf Wetness, Inoculum Concentration, and Host. Plant Disease 85, 430–435. https://doi.org/10.1094/PDIS.2001.85.4.430

Cipollini, D., Walters, D., Voelckel, C., 2017. Costs of Resistance in Plants: From Theory to Evidence, in: Annual Plant Reviews Online. American Cancer Society, pp. 263–307. https://doi.org/10.1002/9781119312994.apr0512

Conrath, U., Beckers, G.J.M., Flors, V., García-Agustín, P., Jakab, G., Mauch, F., Newman, M.-A., Pieterse, C.M.J., Poinssot, B., Pozo, M.J., Pugin, A., Schaffrath, U., Ton, J., Wendehenne, D., Zimmerli, L., Mauch-Mani, B., 2006. Priming: getting ready for battle. Mol Plant Microbe Interact 19, 1062–1071. https://doi.org/10.1094/MPMI-19-1062

Conrath, U., Beckers, G.J.M., Langenbach, C.J.G., Jaskiewicz, M.R., 2015. Priming for Enhanced Defense. Annu. Rev. Phytopathol. 53, 97–119. https://doi.org/10.1146/annurev-phyto-080614-120132

Consortium (IWGSC), T.I.W.G.S., Appels, R., Eversole, K., Stein, N., Feuillet, C., Keller, B., Rogers, J., Pozniak, C.J., Choulet, F., Distelfeld, A., Poland, J., Ronen, G., Sharpe, A.G., Barad, O., Baruch, K., Keeble-Gagnère, G., Mascher, M., Ben-Zvi, G., Josselin, A.-A., Himmelbach, A., Balfourier, F., Gutierrez-Gonzalez, J., Hayden, M., Koh, C., Muehlbauer, G., Pasam, R.K., Paux, E., Rigault, P., Tibbits, J., Tiwari, V., Spannagl, M., Lang, D., Gundlach, H., Haberer, G., Mayer, K.F.X., Ormanbekova, D., Prade, V., Šimková, H., Wicker, T., Swarbreck, D., Rimbert, H., Felder, M., Guilhot, N., Kaithakottil, G., Keilwagen, J., Leroy, P., Lux, T., Twardziok, S., Venturini, L., Juhász, A., Abrouk, M., Fischer, I., Uauy, C., Borrill, P., Ramirez-Gonzalez, R.H., Arnaud, D., Chalabi, S., Chalhoub, B., Cory, A., Datla, R., Davey, M.W., Jacobs, J., Robinson, S.J., Steuernagel, B., Ex, F. van, Wulff, B.B.H., Benhamed, M., Bendahmane, A., Concia, L., Latrasse, D., Bartoš, J., Bellec, A., Berges, H., Doležel, J., Frenkel, Z., Gill, B., Korol, A., Letellier, T., Olsen, O.-A., Singh, K., Valárik, M., Vossen, E. van der, Vautrin, S., Weining, S., Fahima, T., Glikson, V., Raats, D., Číhalíková, J., Toegelová, H., Vrána, J., Sourdille, P., Darrier, B., Barabaschi, D., Cattivelli, L., Hernandez, P., Galvez, S., Budak, H., Jones, J.D.G., Witek, K., Yu, G., Small, I., Melonek, J., Zhou, R., Belova, T., Kanyuka, K., King, R., Nilsen, K., Walkowiak, S., Cuthbert, R., Knox, R., Wiebe, K., Xiang, D., Rohde, A., Golds, T., Čížková, J., Akpinar, B.A., Biyiklioglu, S., Gao, L., N'Daiye, A., Kubaláková, M., Šafář, J., Alfama, F., Adam-Blondon, A.-F., Flores, R., Guerche, C., Loaec, M., Quesneville, H., Condie, J., Ens, J., Maclachlan, R., Tan, Y., Alberti, A., Aury, J.-M., Barbe, V., Couloux, A., Cruaud, C., Labadie, K., Mangenot, S., Wincker, P., Kaur, G., Luo, M., Sehgal, S., Chhuneja, P., Gupta, O.P., Jindal, S., Kaur, P., Malik, P., Sharma, P., Yadav, B., Singh, N.K., Khurana, J.P., Chaudhary, C., Khurana, P., Kumar, V., Mahato, A., Mathur, S., Sevanthi, A., Sharma, N., Tomar, R.S., Holušová, K., Plíhal, O., Clark, M.D., Heavens, D., Kettleborough, G., Wright, J., Balcárková, B., Hu, Y., Salina, E., Ravin, N., Skryabin, K., Beletsky, A., Kadnikov, V., Mardanov, A., Nesterov, M., Rakitin, A., Sergeeva, E., Handa, H., Kanamori, H., Katagiri, S., Kobayashi, F., Nasuda, S., Tanaka, T., Wu, J., Cattonaro, F., Jiumeng, M., Kugler, K., Pfeifer, M., Sandve, S., Xun, X., Zhan, B., Batley, J., Bayer, P.E., Edwards, D., Hayashi, S., Tulpová, Z., Visendi, P., Cui, L., Du, X., Feng, K., Nie, X., Tong, W., Wang, L.,

2018. Shifting the limits in wheat research and breeding using a fully annotated reference genome. Science 361. https://doi.org/10.1126/science.aar7191

Cools, H.J., Hawkins, N.J., Fraaije, B.A., 2013. Constraints on the evolution of azole resistance in plant pathogenic fungi. Plant Pathology 62, 36–42. https://doi.org/10.1111/ppa.12128

Cordo, C.A., Monaco, C.I., Segarra, C.I., Simon, M.R., Mansilla, A.Y., Perello, A.E., Kripelz, N.I., Bayo, D., Conde, R.D., 2007. *Trichoderma* sp. as elicitors of wheat plant defense responses against *Septoria tritici*. Biocontrol science and technology.

Cousin, A., Mehrabi, R., Guilleroux, M., Dufresne, M., VAN DER Lee, T., Waalwijk, C., Langin, T., Kema, G.H.J., 2006. The MAP kinase-encoding gene *MgFus3* of the non-appressorium phytopathogen *Mycosphaerella graminicola* is required for penetration and in vitro pycnidia formation. Mol. Plant Pathol. 7, 269–278. https://doi.org/10.1111/j.1364-3703.2006.00337.x

Croll, D., McDonald, B.A., 2012. The Accessory Genome as a Cradle for Adaptive Evolution in Pathogens. PLoS Pathogens 8. https://doi.org/10.1371/journal.ppat.1002608

Crouzet, J., Arguelles-Arias, A., Dhondt-Cordelier, S., Cordelier, S., Pršić, J., Hoff, G., Mazeyrat-Gourbeyre, F., Baillieul, F., Clément, C., Ongena, M., Dorey, S., 2020. Biosurfactants in Plant Protection Against Diseases: Rhamnolipids and Lipopeptides Case Study. Front. Bioeng. Biotechnol. 8. https://doi.org/10.3389/fbioe.2020.01014

Dean, R., Van Kan, J.A.L., Pretorius, Z.A., Hammond-Kosack, K.E., Di Pietro, A., Spanu, P.D., Rudd, J.J., Dickman, M., Kahmann, R., Ellis, J., Foster, G.D., 2012. The Top 10 fungal pathogens in molecular plant pathology. Mol. Plant Pathol. 13, 414–430. https://doi.org/10.1111/j.1364-3703.2011.00783.x

Deepak, S., Shailasree, S., Kini, R.K., Muck, A., Mithöfer, A., Shetty, S.H., 2010. Hydroxyproline-rich Glycoproteins and Plant Defence. Journal of Phytopathology 158, 585–593. https://doi.org/10.1111/j.1439-0434.2010.01669.x

Delisle, G., Champoux, M., Houde, M., 2001. Characterization of Oxalate Oxidase and Cell Death in Al-Sensitive and Tolerant Wheat Roots. Plant Cell Physiol 42, 324–333. https://doi.org/10.1093/pcp/pce041

Derridj, S., 1996. Nutrients on the Leaf Surface, in: Morris, C.E., Nicot, P.C., Nguyen-The, C. (Eds.), Aerial Plant Surface Microbiology. Springer US, Boston, MA, pp. 25–42. https://doi.org/10.1007/978-0-585-34164-4_2

Desoignies, N., Schramme, F., Ongena, M., Legrève, A., 2013. Systemic resistance induced by *Bacillus* lipopeptides in *Beta vulgaris* reduces infection by the rhizomania disease vector *Polymyxa betae*. Molecular Plant Pathology 14, 416–421. https://doi.org/10.1111/mpp.12008

Ding, P., Ding, Y., 2020. Stories of Salicylic Acid: A Plant Defense Hormone. Trends in Plant Science 25, 549–565. https://doi.org/10.1016/j.tplants.2020.01.004

Djonović, S., Pozo, M.J., Dangott, L.J., Howell, C.R., Kenerley, C.M., 2006. Sm1, a Proteinaceous Elicitor Secreted by the Biocontrol Fungus *Trichoderma virens* Induces Plant Defense Responses and Systemic Resistance. MPMI 19, 838–853. https://doi.org/10.1094/MPMI-19-0838

Dobler, L., Vilela, L.F., Almeida, R.V., Neves, B.C., 2016. Rhamnolipids in perspective: gene regulatory pathways, metabolic engineering, production and technological forecasting. New Biotechnology 33, 123–135. https://doi.org/10.1016/j.nbt.2015.09.005

Drummond, J.B., Craigie, R.A., Braithwaite, M., Gillum, A.T., McCloy, B.L., 2015. The effect of fungicide dose rate and mixtures on *Zymoseptoria tritici* in two cultivars of autumn sown wheat. NZPP 68, 420–427. https://doi.org/10.30843/nzpp.2015.68.5822

Du Fall, L.A., Solomon, P.S., 2013. The necrotrophic effector SnToxA induces the synthesis of a novel phytoalexin in wheat. New Phytol 200, 185–200. https://doi.org/10.1111/nph.12356

Duba, A., Goriewa-Duba, K., Wachowska, U., 2018. A Review of the Interactions between Wheat and Wheat Pathogens: *Zymoseptoria tritici*, *Fusarium* spp. and *Parastagonospora nodorum*. Int J Mol Sci 19. https://doi.org/10.3390/ijms19041138

Duncan, K.E., Howard, R.J., 2000. Cytological analysis of wheat infection by the leaf blotch pathogen *Mycosphaerella graminicola*. Mycological Research 104, 1074–1082. https://doi.org/10.1017/S0953756299002294

Ecophyto, Optimiser les traitements fongicides sur les maladies du feuillage de blé tendre au moyen d'un outil d'aide à la décision (2018) | Ecophytopic [WWW Document], n.d. URL https://ecophytopic.fr/piloter/optimiser-les-traitements-fongicides-sur-les-maladies-du-feuillage-de-ble-tendre-au-moyen (accessed 11.26.20).

Ecophyto II : réduire l'utilisation des produits phytopharmaceutiques progressivement - Ecophyto PRO : réduire et améliorer l'utilisation des phytos [WWW Document], n.d. URL https://www.ecophyto-pro.fr/n/ecophyto-ii-reduire-l-utilisation-des-produits-phytopharmaceutiques-progressivem/n:104 (accessed 3.1.21).

Eriksen, L., Borum, F., Jahoor, A., 2003. Inheritance and localisation of resistance to *Mycosphaerella graminicola* causing septoria tritici blotch and plant height in the wheat (*Triticum aestivum* L.) genome with DNA markers. Theor Appl Genet 107, 515–527. https://doi.org/10.1007/s00122-003-1276-2

Eriksen, L., Munk, L., 2003. The Occurrence of *Mycosphaerella graminicola* and its Anamorph *Septoria tritici* in Winter Wheat during the Growing Season. European Journal of Plant Pathology 109, 253–259. https://doi.org/10.1023/A:1022851502770

Evans, J.K., 1981. Wheat Production and its Social Consequences in the Roman World. The Classical Quarterly 31, 428–442. https://doi.org/10.1017/S0009838800009769

Eyal, Z., Center, I.M. and W.I., 1987. The Septoria Diseases of Wheat: Concepts and Methods of Disease Management. CIMMYT.

Farace, G., Fernandez, O., Jacquens, L., Coutte, F., Krier, F., Jacques, P., Clément, C., Barka, E.A., Jacquard, C., Dorey, S., 2015. Cyclic lipopeptides from *Bacillus subtilis* activate distinct patterns of defence responses in grapevine. Mol Plant Pathol 16, 177–187. https://doi.org/10.1111/mpp.12170

FAO Cereal Supply and Demand Brief (2020) | World Food Situation | Food and Agriculture Organization of the United Nations [WWW document], n.d. URL http://www.fao.org/worldfoodsituation/csdb/en/ (accessed 8.31.20)

FAO Save and Grow in practice: maize, rice, wheat [WWW Document], n.d. URL http://www.fao.org/ag/save-and-grow/MRW/index_en.html (accessed 9.7.20).

Figueroa, M., Hammond-Kosack, K.E., Solomon, P.S., 2018. A review of wheat diseases—a field perspective. Molecular Plant Pathology 19, 1523–1536. https://doi.org/10.1111/mpp.12618

Fiorilli, V., Vannini, C., Ortolani, F., Garcia-Seco, D., Chiapello, M., Novero, M., Domingo, G., Terzi, V., Morcia, C., Bagnaresi, P., Moulin, L., Bracale, M., Bonfante, P., 2018. Omics approaches revealed how arbuscular mycorrhizal symbiosis enhances yield and resistance to leaf pathogen in wheat. Scientific Reports 8, 9625. https://doi.org/10.1038/s41598-018-27622-8

Fj, G., Ts, L., 1985. Moisture effects on the discharge and survival of conidia of *Septoria tritici*. Phytopathology 75, 180–182. https://doi.org/10.1094/phyto-75-180

Flaishman, M.A. (Tel A.U., Eyal, Z., Zilberstein, A., Voisard, C., Haas, D., 1996. Suppression of Septoria tritici blotch and leaf rust of wheat by recombinant cyanide-producing strains of *Pseudomonas putida*. Molecular plant-microbe interactions : MPMI (USA).

Flicek, P., Amode, M.R., Barrell, D., Beal, K., Billis, K., Brent, S., Carvalho-Silva, D., Clapham, P., Coates, G., Fitzgerald, S., Gil, L., Girón, C.G., Gordon, L., Hourlier, T., Hunt, S., Johnson, N., Juettemann, T., Kähäri, A.K., Keenan, S., Kulesha, E., Martin, F.J., Maurel, T., McLaren, W.M., Murphy, D.N., Nag, R., Overduin, B., Pignatelli, M., Pritchard, B., Pritchard, E., Riat, H.S., Ruffier, M., Sheppard, D., Taylor, K., Thormann, A., Trevanion, S.J., Vullo, A., Wilder, S.P., Wilson, M., Zadissa, A., Aken, B.L., Birney, E., Cunningham, F., Harrow, J., Herrero, J., Hubbard, T.J.P., Kinsella, R., Muffato, M., Parker, A., Spudich, G., Yates, A., Zerbino, D.R., Searle, S.M.J., 2014. Ensembl 2014. Nucleic Acids Res 42, D749–D755. https://doi.org/10.1093/nar/gkt1196

Flor, H.H., 1971. Current Status of the Gene-For-Gene Concept. Annual Review of Phytopathology 9, 275–296. https://doi.org/10.1146/annurev.py.09.090171.001423

Fones, H., Gurr, S., 2015. The impact of Septoria tritici Blotch disease on wheat: An EU perspective. Fungal Genet Biol 79, 3–7. https://doi.org/10.1016/j.fgb.2015.04.004

Fones, H.N., Eyles, C.J., Kay, W., Cowper, J., Gurr, S.J., 2017. A role for random, humidity-dependent epiphytic growth prior to invasion of wheat by *Zymoseptoria tritici*. Fungal Genet Biol 106, 51–60. https://doi.org/10.1016/j.fgb.2017.07.002

Fraaije, B.A., Bayon, C., Atkins, S., Cools, H.J., Lucas, J.A., Fraaije, M.W., 2012. Risk assessment studies on succinate dehydrogenase inhibitors, the new weapons in the battle to control Septoria leaf blotch in wheat. Molecular Plant Pathology 13, 263–275. https://doi.org/10.1111/j.1364-3703.2011.00746.x

FranceAgriMer - établissement national des produits de l'agriculture et de la mer, Variétés des céréales à paille - Récolte (2019) | [WWW Document], n.d. URL https://www.franceagrimer.fr (accessed 8.31.20)

FranceAgriMer - établissement national des produits de l'agriculture et de la mer, Bilans céréaliers 2018/19 allemand, autrichien et français (2020) | [WWW Document], n.d. URL https://www.franceagrimer.fr/Actualite/Filieres/Cereales/2019/Bilans-cerealiers-2018-19-allemand-autrichien-et-francais (accessed 8.31.20).

Francisco, C.S., Ma, X., Zwyssig, M.M., McDonald, B.A., Palma-Guerrero, J., 2019. Morphological changes in response to environmental stresses in the fungal plant pathogen *Zymoseptoria tritici*. Scientific Reports 9, 9642. https://doi.org/10.1038/s41598-019-45994-3

Freeman, B., Beattie, G., 2008. An Overview of Plant Defenses against Pathogens and Herbivores. The Plant Health Instructor. https://doi.org/10.1094/PHI-I-2008-0226-01

Frei, M., 2013. Lignin: Characterization of a Multifaceted Crop Component. ScientificWorldJournal 2013. https://doi.org/10.1155/2013/436517

Friesen, T.L., 2017. *Nicotiana benthamiana* as a nonhost of *Zymoseptoria tritici*. New Phytologist 213, 7–9. https://doi.org/10.1111/nph.14299

Gaffney, T., Friedrich, L., Vernooij, B., Negrotto, D., Nye, G., Uknes, S., Ward, E., Kessmann, H., Ryals, J., 1993. Requirement of salicylic Acid for the induction of systemic acquired resistance. Science 261, 754–756. https://doi.org/10.1126/science.261.5122.754

García-Gutiérrez, L., Zeriouh, H., Romero, D., Cubero, J., Vicente, A. de, Pérez-García, A., 2013. The antagonistic strain *Bacillus subtilis* UMAF6639 also confers protection to melon plants against cucurbit powdery mildew by activation of jasmonate- and salicylic acid-dependent defence responses. Microbial Biotechnology 6, 264–274. https://doi.org/10.1111/1751-7915.12028

Garcion, C., Lohmann, A., Lamodière, E., Catinot, J., Buchala, A., Doermann, P., Métraux, J.-P., 2008. Characterization and Biological Function of the ISOCHORISMATE SYNTHASE2 Gene of Arabidopsis. Plant Physiology 147, 1279–1287. https://doi.org/10.1104/pp.108.119420

Gayon, J., 2016. From Mendel to epigenetics: History of genetics. Comptes Rendus Biologies, Trajectories of genetics, 150 years after Mendel / Trajectoire de la génétique, 150 après Mendel Guest Editors /

Rédacteurs en chef invités : Bernard Dujon, Georges Pelletier 339, 225–230. https://doi.org/10.1016/j.crvi.2016.05.009

Gechev, T.S., Hille, J., 2005. Hydrogen peroxide as a signal controlling plant programmed cell death. J Cell Biol 168, 17–20. https://doi.org/10.1083/jcb.200409170

Geudens, N., Martins, J.C., 2018. Cyclic Lipodepsipeptides From *Pseudomonas* spp. – Biological Swiss-Army Knives. Front. Microbiol. 9. https://doi.org/10.3389/fmicb.2018.01867

Gigot, C., Saint-Jean, S., Huber, L., Maumené, C., Leconte, M., Kerhornou, B., Vallavieille-Pope, C. de, 2013. Protective effects of a wheat cultivar mixture against splash-dispersed septoria tritici blotch epidemics. Plant Pathology 62, 1011–1019. https://doi.org/10.1111/ppa.12012

Gill, S.S., Anjum, N.A., Gill, R., Yadav, S., Hasanuzzaman, M., Fujita, M., Mishra, P., Sabat, S.C., Tuteja, N., 2015. Superoxide dismutase--mentor of abiotic stress tolerance in crop plants. Environ Sci Pollut Res Int 22, 10375–10394. https://doi.org/10.1007/s11356-015-4532-5

Girousse, C., Roche, J., Guerin, C., Le Gouis, J., Balzegue, S., Mouzeyar, S., Bouzidi, M.F., 2018. Coexpression network and phenotypic analysis identify metabolic pathways associated with the effect of warming on grain yield components in wheat. PLoS One 13. https://doi.org/10.1371/journal.pone.0199434

Gladders, P., Paveley, N.D., Barrie, I.A., Hardwick, N.V., Hims, M.J., Langton, S., Taylor, M.C., 2001. Agronomic and meteorological factors affecting the severity of leaf blotch caused by *Mycosphaerella graminicola* in commercial wheat crops in England. Annals of Applied Biology 138, 301–311. https://doi.org/10.1111/j.1744-7348.2001.tb00115.x

Glazebrook, J., 2005. Contrasting mechanisms of defense against biotrophic and necrotrophic pathogens. Annu Rev Phytopathol 43, 205–227. https://doi.org/10.1146/annurev.phyto.43.040204.135923

Godwin, R.J., Wood, G.A., Taylor, J.C., Knight, S.M., Welsh, J.P., 2003. Precision Farming of Cereal Crops: a Review of a Six Year Experiment to develop Management Guidelines. Biosystems Engineering, Precision Agriculture - Managing Soil and Crop Variability for Cereals 84, 375–391. https://doi.org/10.1016/S1537-5110(03)00031-X

Goodwin, S.B., M'Barek, S.B., Dhillon, B., Wittenberg, A.H.J., Crane, C.F., Hane, J.K., Foster, A.J., Lee, T.A.J.V. der, Grimwood, J., Aerts, A., Antoniw, J., Bailey, A., Bluhm, B., Bowler, J., Bristow, J., Burgt, A. van der, Canto-Canché, B., Churchill, A.C.L., Conde-Ferràez, L., Cools, H.J., Coutinho, P.M., Csukai, M., Dehal, P., Wit, P.D., Donzelli, B., Geest, H.C. van de, Ham, R.C.H.J. van, Hammond-Kosack, K.E., Henrissat, B., Kilian, A., Kobayashi, A.K., Koopmann, E., Kourmpetis, Y., Kuzniar, A., Lindquist, E., Lombard, V., Maliepaard, C., Martins, N., Mehrabi, R., Nap, J.P.H., Ponomarenko, A., Rudd, J.J., Salamov, A., Schmutz, J., Schouten, H.J., Shapiro, H., Stergiopoulos, I., Torriani, S.F.F., Tu, H., Vries, R.P. de, Waalwijk, C., Ware, S.B., Wiebenga, A., Zwiers, L.-H., Oliver, R.P., Grigoriev, I.V., Kema, G.H.J., 2011. Finished Genome of the Fungal Wheat Pathogen *Mycosphaerella graminicola* Reveals Dispensome Structure, Chromosome Plasticity, and Stealth Pathogenesis. PLOS Genetics 7, e1002070. https://doi.org/10.1371/journal.pgen.1002070

Görlach, A., Bertram, K., Hudecova, S., Krizanova, O., 2015. Calcium and ROS: A mutual interplay. Redox Biology 6, 260–271. https://doi.org/10.1016/j.redox.2015.08.010

Görlach, J., Volrath, S., Knauf-Beiter, G., Hengy, G., Beckhove, U., Kogel, K.H., Oostendorp, M., Staub, T., Ward, E., Kessmann, H., Ryals, J., 1996. Benzothiadiazole, a novel class of inducers of systemic acquired resistance, activates gene expression and disease resistance in wheat. The Plant Cell 8, 629–643. https://doi.org/10.1105/tpc.8.4.629

Groenewald, M., Groenewald, J.Z., Linde, C.C., Crous, P.W., 2007. Development of polymorphic microsatellite and single nucleotide polymorphism markers for *Cercospora beticola* (Mycosphaerellaceae). Molecular Ecology Notes 7, 890–892. https://doi.org/10.1111/j.1471-8286.2007.01739.x

Gu, Q., Yang, Y., Yuan, Q., Shi, G., Wu, L., Lou, Z., Huo, R., Wu, H., Borriss, R., Gao, X., 2017a. Bacillomycin D Produced by *Bacillus amyloliquefaciens* Is Involved in the Antagonistic Interaction with the Plant-Pathogenic Fungus *Fusarium graminearum*. Appl. Environ. Microbiol. 83. https://doi.org/10.1128/AEM.01075-17

Habig, M., Quade, J., Stukenbrock, E.H., 2017. Forward Genetics Approach Reveals Host Genotype-Dependent Importance of Accessory Chromosomes in the Fungal Wheat Pathogen *Zymoseptoria tritici*. mBio 8. https://doi.org/10.1128/mBio.01919-17

Haghdel, M., Banihashemi, Z., 2005. Survival and host range of *Mycosphaerella graminicola* the causal agent of Septoria leaf blotch of wheat. Iranian Journal of Plant Pathology 41.

Halama, P., 1996. The occurrence of *Mycosphaerella graminicola*, teleomorph of *Septoria tritici* in France. Plant Pathology 45, 135–138. https://doi.org/10.1046/j.1365-3059.1996.d01-103.x

Halliwell, B., 2006. Reactive Species and Antioxidants. Redox Biology Is a Fundamental Theme of Aerobic Life. Plant Physiol 141, 312–322. https://doi.org/10.1104/pp.106.077073

Hamley, I.W., Dehsorkhi, A., Jauregi, P., Seitsonen, J., Ruokolainen, J., Coutte, F., Chataigné, G., Jacques, P., 2013. Self-assembly of three bacterially-derived bioactive lipopeptides. Soft Matter 9, 9572–9578. https://doi.org/10.1039/C3SM51514A

Han, Q., Wu, F., Wang, X., Qi, H., Shi, L., Ren, A., Liu, Q., Zhao, M., Tang, C., 2015. The bacterial lipopeptide iturins induce *Verticillium dahliae* cell death by affecting fungal signalling pathways and mediate plant defence responses involved in pathogen-associated molecular pattern-triggered immunity. Environ Microbiol 17, 1166–1188. https://doi.org/10.1111/1462-2920.12538

Hassine, M., Siah, A., Hellin, P., Cadalen, T., Halama, P., Hilbert, J.-L., Hamada, W., Baraket, M., Yahyaoui, A., Legrève, A., Duvivier, M., 2019. Sexual reproduction of *Zymoseptoria tritici* on durum wheat in Tunisia revealed by presence of airborne inoculum, fruiting bodies and high levels of genetic diversity. Fungal Biology 123, 763–772. https://doi.org/10.1016/j.funbio.2019.06.006

Henry, G., Deleu, M., Jourdan, E., Thonart, P., Ongena, M., 2011. The bacterial lipopeptide surfactin targets the lipid fraction of the plant plasma membrane to trigger immune-related defence responses. Cell. Microbiol. 13, 1824–1837. https://doi.org/10.1111/j.1462-5822.2011.01664.x

Henry, G., Thonart, P., Ongena, M., 2012. PAMPs, MAMPs, DAMPs and others: an update on the diversity of plant immunity elicitors. Biotechnol. Agron. Soc. Environ.

Hilker, M., Schwachtje, J., Baier, M., Balazadeh, S., Bäurle, I., Geiselhardt, S., Hincha, D.K., Kunze, R., Mueller-Roeber, B., Rillig, M.C., Rolff, J., Romeis, T., Schmülling, T., Steppuhn, A., van Dongen, J., Whitcomb, S.J., Wurst, S., Zuther, E., Kopka, J., 2016. Priming and memory of stress responses in organisms lacking a nervous system. Biol Rev Camb Philos Soc 91, 1118–1133. https://doi.org/10.1111/brv.12215

Hiraga, S., Sasaki, K., Ito, H., Ohashi, Y., Matsui, H., 2001. A large family of class III plant peroxidases. Plant Cell Physiol 42, 462–468. https://doi.org/10.1093/pcp/pce061

Holmes, S.J.I., Colhoun, J., 1974. Infection of wheat by *Septoria nodorum* and *S. tritici* in relation to plant age, air temperature and relative humidity. Transactions of the British Mycological Society 63, 329–338. https://doi.org/10.1016/S0007-1536(74)80178-6

Huang, J., Gu, M., Lai, Z., Fan, B., Shi, K., Zhou, Y.-H., Yu, J.-Q., Chen, Z., 2010. Functional Analysis of the Arabidopsis PAL Gene Family in Plant Growth, Development, and Response to Environmental Stress. Plant Physiology 153, 1526–1538. https://doi.org/10.1104/pp.110.157370

IBMA, Positions (2017), URL https://www.ibmafrance.com/positions/ (accessed 11.30.20).

INRAE, l'origine des blés modernes révélée [WWW Document], 2016 . INRAE Institutionnel. URL https://www.inrae.fr/actualites/lorigine-bles-modernes-revelee (accessed 2.23.21).

Jones, J.D.G., Dangl, J.L., 2006. The plant immune system. Nature 444, 323–329. https://doi.org/10.1038/nature05286

Kawagoe, Y., Shiraishi, S., Kondo, H., Yamamoto, S., Aoki, Y., Suzuki, S., 2015. Cyclic lipopeptide iturin A structure-dependently induces defense response in Arabidopsis plants by activating SA and JA signaling pathways. Biochem Biophys Res Commun 460, 1015–1020. https://doi.org/10.1016/j.bbrc.2015.03.143

Kema, G., Yu, D., Rijkenberg, F., Shaw, M., Baayen, R.P., 1996. Histology of the pathogenesis of Mycosphaerella graminicola in wheat. https://doi.org/10.1094/Phyto-86-777

Kema, G.H.J., van Silfhout, C.H., 1997. Genetic Variation for Virulence and Resistance in the Wheat-*Mycosphaerella graminicola* Pathosystem III. Comparative Seedling and Adult Plant Experiments. Phytopathology® 87, 266–272. https://doi.org/10.1094/PHYTO.1997.87.3.266

Kema, G.H.J., Verstappen, E.C.P., Todorova, M., Waalwijk, C., 1996. Successful crosses and molecular tetrad and progeny analyses demonstrate heterothallism in *Mycosphaerella graminicola*. Curr Genet 30, 251–258. https://doi.org/10.1007/s002940050129

Keon, J., Antoniw, J., Carzaniga, R., Deller, S., Ward, J.L., Baker, J.M., Beale, M.H., Hammond-Kosack, K., Rudd, J.J., 2007. Transcriptional adaptation of *Mycosphaerella graminicola* to programmed cell death (PCD) of its susceptible wheat host. Mol. Plant Microbe Interact. 20, 178–193. https://doi.org/10.1094/MPMI-20-2-0178

Kettles, G.J., Kanyuka, K., 2016. Dissecting the Molecular Interactions between Wheat and the Fungal Pathogen *Zymoseptoria tritici*. Front Plant Sci 7. https://doi.org/10.3389/fpls.2016.00508

Kilaru, S., Schuster, M., Ma, W., Steinberg, G., 2017. Fluorescent markers of various organelles in the wheat pathogen *Zymoseptoria tritici*. Fungal Genetics and Biology 105, 16–27. https://doi.org/10.1016/j.fgb.2017.05.001

Kildea, S., Marten-Heick, T., Grant, J., Mehenni-Ciz, J., Dooley, H., 2019. A combination of target-site alterations, overexpression and enhanced efflux activity contribute to reduced azole sensitivity present in the Irish *Zymoseptoria tritici* population. Eur J Plant Pathol 154, 529–540. https://doi.org/10.1007/s10658-019-01676-4

Kildea, S., Ransbotyn, V., Khan, M.R., Fagan, B., Leonard, G., Mullins, E., Doohan, F.M., 2008. *Bacillus megaterium* shows potential for the biocontrol of septoria tritici blotch of wheat. Biological Control 47, 37–45. https://doi.org/10.1016/j.biocontrol.2008.07.001

Kim, J.J., Goettel, M.S., Gillespie, D.R., 2008. Evaluation of *Lecanicillium longisporum*, Vertalec® for simultaneous suppression of cotton aphid, *Aphis gossypii*, and cucumber powdery mildew, *Sphaerotheca fuliginea*, on potted cucumbers. Biological Control 45, 404–409. https://doi.org/10.1016/j.biocontrol.2008.02.003

King, R., Urban, M., Lauder, R.P., Hawkins, N., Evans, M., Plummer, A., Halsey, K., Lovegrove, A., Hammond-Kosack, K., Rudd, J.J., 2017. A conserved fungal glycosyltransferase facilitates pathogenesis of plants by enabling hyphal growth on solid surfaces. PLoS Pathog. 13, e1006672. https://doi.org/10.1371/journal.ppat.1006672

Klarzynski, O., Plesse, B., Joubert, J.-M., Yvin, J.-C., Kopp, M., Kloareg, B., Fritig, B., 2000. Linear β-1,3 Glucans Are Elicitors of Defense Responses in Tobacco. Plant Physiology 124, 1027–1038. https://doi.org/10.1104/pp.124.3.1027

Kramer, B., Thines, E., Foster, A.J., 2009. MAP kinase signalling pathway components and targets conserved between the distantly related plant pathogenic fungi *Mycosphaerella graminicola* and *Magnaporthe grisea*. Fungal Genetics and Biology 46, 667–681. https://doi.org/10.1016/j.fgb.2009.06.001

Lam, P.Y., Liu, H., Lo, C., 2015. Completion of Tricin Biosynthesis Pathway in Rice: Cytochrome P450 75B4 Is a Unique Chrysoeriol 5'-Hydroxylase. Plant Physiol 168, 1527–1536. https://doi.org/10.1104/pp.15.00566

Lämke, J., Bäurle, I., 2017. Epigenetic and chromatin-based mechanisms in environmental stress adaptation and stress memory in plants. Genome Biology 18, 124. https://doi.org/10.1186/s13059-017-1263-6

Lan, W., Lu, F., Regner, M., Zhu, Y., Rencoret, J., Ralph, S.A., Zakai, U.I., Morreel, K., Boerjan, W., Ralph, J., 2015. Tricin, a Flavonoid Monomer in Monocot Lignification. Plant Physiology 167, 1284–1295. https://doi.org/10.1104/pp.114.253757

Lancashire, P.D., Bleiholder, H., Boom, T.V.D., Langelüddeke, P., Stauss, R., Weber, E., Witzenberger, A., 1991. A uniform decimal code for growth stages of crops and weeds. Annals of Applied Biology 119, 561–601. https://doi.org/10.1111/j.1744-7348.1991.tb04895.x

Latoud, C., Peypoux, F., Michel, G., 1987. Action of iturin A, an antifungal antibiotic from *Bacillus subtilis*, on the yeast *Saccharomyces cerevisiae*: modifications of membrane permeability and lipid composition. J Antibiot (Tokyo) 40, 1588–1595. https://doi.org/10.7164/antibiotics.40.1588

Le Mire, G., Siah, A., Brisset, M.-N., Gaucher, M., Deleu, M., Jijakli, M.H., 2018. Surfactin Protects Wheat against *Zymoseptoria tritici* and Activates Both Salicylic Acid- and Jasmonic Acid-Dependent Defense Responses. Agriculture 8, 11. https://doi.org/10.3390/agriculture8010011

Le Mire, G., Siah, A., Marolleau, B., Gaucher, M., Maumené, C., Brostaux, Y., Massart, S., Brisset, M.-N., Jijakli, M.H., 2019. Evaluation of λ-Carrageenan, CpG-ODN, Glycine Betaine, Spirulina platensis, and Ergosterol as Elicitors for Control of *Zymoseptoria tritici* in Wheat. Phytopathology PHYTO11170367R. https://doi.org/10.1094/PHYTO-11-17-0367-R

Lee, W.-S., Rudd, J.J., Hammond-Kosack, K.E., Kanyuka, K., 2014. *Mycosphaerella graminicola* LysM effector-mediated stealth pathogenesis subverts recognition through both CERK1 and CEBiP homologues in wheat. Mol Plant Microbe Interact 27, 236–243. https://doi.org/10.1094/MPMI-07-13-0201-R

Lefevere, H., Bauters, L., Gheysen, G., 2020. Salicylic Acid Biosynthesis in Plants. Front. Plant Sci. 11. https://doi.org/10.3389/fpls.2020.00338

Lehmann, S., Serrano, M., L'haridon, F., Tjamos, S.E., Métraux, J.-P., 2015. Reactive oxygen species and plant resistance to fungal pathogens. Phytochemistry. https://doi.org/10.1016/j.phytochem.2014.08.027

Leroux, P., Albertini, C., Gautier, A., Gredt, M., Walker, A.-S., 2007. Mutations in the *CYP51* gene correlated with changes in sensitivity to sterol 14 alpha-demethylation inhibitors in field isolates of *Mycosphaerella graminicola*. Pest Manag Sci 63, 688–698. https://doi.org/10.1002/ps.1390

Levy, E., Eyal, Z., Chet, I., 1988. Suppression of septoria tritici blotch and leaf rust on wheat seedling leaves by *Pseudomonas*. Plant Pathology 37, 551–557. https://doi.org/10.1111/j.1365-3059.1988.tb02114.x

Levy, E., Gough, F.J., Berlin, K.D., Guiana, P.W., Smith, J.T., 1992. Inhibition of *Septoria tritici* and other phytopathogenic fungi and bacteria by *Pseudomonas fluorescens* and its antibiotics. Plant Pathology 41, 335–341. https://doi.org/10.1111/j.1365-3059.1992.tb02355.x

Li, G., Chen, T., Zhang, Z., Li, B., Tian, S., 2020. Roles of Aquaporins in Plant-Pathogen Interaction. Plants 9, 1134. https://doi.org/10.3390/plants9091134

Li, Y., Héloir, M.-C., Zhang, X., Geissler, M., Trouvelot, S., Jacquens, L., Henkel, M., Su, X., Fang, X., Wang, Q., Adrian, M., 2019. Surfactin and fengycin contribute to the protection of a *Bacillus subtilis* strain against grape downy mildew by both direct effect and defence stimulation. Molecular Plant Pathology 20, 1037–1050. https://doi.org/10.1111/mpp.12809

Lin, X., Alspaugh, J.A., Liu, H., Harris, S., 2015. Fungal Morphogenesis. Cold Spring Harb Perspect Med 5. https://doi.org/10.1101/cshperspect.a019679

Linley, E., Denyer, S.P., McDonnell, G., Simons, C., Maillard, J.-Y., 2012. Use of hydrogen peroxide as a biocide: new consideration of its mechanisms of biocidal action. J Antimicrob Chemother 67, 1589–1596. https://doi.org/10.1093/jac/dks129

Lobell, D.B., Schlenker, W., Costa-Roberts, J., 2011. Climate Trends and Global Crop Production Since 1980. Science 333, 616–620. https://doi.org/10.1126/science.1204531

Lourith, N., Kanlayavattanakul, M., 2009. Natural surfactants used in cosmetics: glycolipids. Int J Cosmet Sci 31, 255–261. https://doi.org/10.1111/j.1468-2494.2009.00493.x

Luna, E., Pastor, V., Robert, J., Flors, V., Mauch-Mani, B., Ton, J., 2011. Callose deposition: a multifaceted plant defense response. Mol Plant Microbe Interact 24, 183–193. https://doi.org/10.1094/MPMI-07-10-0149

Luzuriaga-Loaiza, W.P., Schellenberger, R., De Gaetano, Y., Obounou Akong, F., Villaume, S., Crouzet, J., Haudrechy, A., Baillieul, F., Clément, C., Lins, L., Allais, F., Ongena, M., Bouquillon, S., Deleu, M., Dorey,

S., 2018. Synthetic Rhamnolipid Bolaforms trigger an innate immune response in *Arabidopsis thaliana*. Sci Rep 8, 8534. https://doi.org/10.1038/s41598-018-26838-y

Lynch, K.M., Zannini, E., Guo, J., Axel, C., Arendt, E.K., Kildea, S., Coffey, A., 2016. Control of *Zymoseptoria tritici* cause of septoria tritici blotch of wheat using antifungal *Lactobacillus* strains. Journal of Applied Microbiology 121, 485–494. https://doi.org/10.1111/jam.13171

Madlung, A., Comai, L., 2004. The Effect of Stress on Genome Regulation and Structure. Ann Bot 94, 481–495. https://doi.org/10.1093/aob/mch172

Malamy, J., Carr, J.P., Klessig, D.F., Raskin, I., 1990. Salicylic Acid: a likely endogenous signal in the resistance response of tobacco to viral infection. Science 250, 1002–1004. https://doi.org/10.1126/science.250.4983.1002

Marshall, R., Kombrink, A., Motteram, J., Loza-Reyes, E., Lucas, J., Hammond-Kosack, K.E., Thomma, B.P.H.J., Rudd, J.J., 2011. Analysis of Two in Planta Expressed LysM Effector Homologs from the Fungus *Mycosphaerella graminicola* Reveals Novel Functional Properties and Varying Contributions to Virulence on Wheat. Plant Physiology 156, 756–769. https://doi.org/10.1104/pp.111.176347

Martinez-Medina, A., Flors, V., Heil, M., Mauch-Mani, B., Pieterse, C.M.J., Pozo, M.J., Ton, J., van Dam, N.M., Conrath, U., 2016. Recognizing Plant Defense Priming. Trends in Plant Science 21, 818–822. https://doi.org/10.1016/j.tplants.2016.07.009

M'Barek, S.B., Cordewener, J.H.G., Tabib Ghaffary, S.M., van der Lee, T.A.J., Liu, Z., Mirzadi Gohari, A., Mehrabi, R., America, A.H.P., Robert, O., Friesen, T.L., Hamza, S., Stergiopoulos, I., de Wit, P.J.G.M., Kema, G.H.J., 2015. FPLC and liquid-chromatography mass spectrometry identify candidate necrosis-inducing proteins from culture filtrates of the fungal wheat pathogen *Zymoseptoria tritici*. Fungal Genet Biol 79, 54–62. https://doi.org/10.1016/j.fgb.2015.03.015

McCartney, C., Mercer, P.C., Cooke, L.R., Fraaije, B.A., 2007. Effects of a strobilurin-based spray programme on disease control, green leaf area, yield and development of fungicide-resistance in *Mycosphaerella graminicola* in Northern Ireland. Crop Protection 26, 1272–1280. https://doi.org/10.1016/j.cropro.2006.10.027

McDonald, M.C., Renkin, M., Spackman, M., Orchard, B., Croll, D., Solomon, P.S., Milgate, A., 2019. Rapid Parallel Evolution of Azole Fungicide Resistance in Australian Populations of the Wheat Pathogen *Zymoseptoria tritici*. Appl. Environ. Microbiol. 85. https://doi.org/10.1128/AEM.01908-18

McKendry, A.L. (University of M., Henke, G.E., Finney, P.L., 1995. Effects of Septoria leaf blotch on soft red winter wheat milling and baking quality. Cereal chemistry (USA).

Mehrabi, R., Kema, G.H.J., 2006. Protein kinase A subunits of the ascomycete pathogen *Mycosphaerella graminicola* regulate asexual fructification, filamentation, melanization and osmosensing. Molecular Plant Pathology 7, 565–577. https://doi.org/10.1111/j.1364-3703.2006.00361.x

Mehrabi, R., M'Barek, S.B., van der Lee, T.A.J., Waalwijk, C., de Wit, P.J.G.M., Kema, G.H.J., 2009. Gα and Gβ Proteins Regulate the Cyclic AMP Pathway That Is Required for Development and Pathogenicity of the Phytopathogen *Mycosphaerella graminicola*. Eukaryot Cell 8, 1001–1013. https://doi.org/10.1128/EC.00258-08

Mehrabi, R., Taga, M., Kema, G.H.J., 2007. Electrophoretic and cytological karyotyping of the foliar wheat pathogen *Mycosphaerella graminicola* reveals many chromosomes with a large size range. Mycologia 99, 868–876. https://doi.org/10.1080/15572536.2007.11832518

Mehrabi, R., van der Lee, T., Waalwijk, C., Kema, G.H.J., 2006a. *MgSlt2*, a Cellular Integrity MAP Kinase Gene of the Fungal Wheat Pathogen *Mycosphaerella graminicola*, Is Dispensable for Penetration but Essential for Invasive Growth. MPMI 19, 389–398. https://doi.org/10.1094/MPMI-19-0389

Mehrabi, R., Zwiers, L.-H., de Waard, M.A., Kema, G.H.J., 2006b. MgHog1 Regulates Dimorphism and Pathogenicity in the Fungal Wheat Pathogen *Mycosphaerella graminicola*. MPMI 19, 1262–1269. https://doi.org/10.1094/MPMI-19-1262

Mejri, S., Siah, A., Coutte, F., Magnin-Robert, M., Randoux, B., Tisserant, B., Krier, F., Jacques, P., Reignault, P., Halama, P., 2018. Biocontrol of the wheat pathogen *Zymoseptoria tritici* using cyclic lipopeptides from *Bacillus subtilis*. Environ Sci Pollut Res Int 25, 29822–29833. https://doi.org/10.1007/s11356-017-9241-9

Meng, X., Zhang, S., 2013. MAPK cascades in plant disease resistance signaling. Annu Rev Phytopathol 51, 245–266. https://doi.org/10.1146/annurev-phyto-082712-102314

Mierziak, J., Kostyn, K., Kulma, A., 2014. Flavonoids as Important Molecules of Plant Interactions with the Environment. Molecules 19, 16240–16265. https://doi.org/10.3390/molecules191016240

Ministère de l'agriculture et de l'alimentation, Qu'est-ce que le biocontrôle ? [WWW Document], 2021 . URL https://agriculture.gouv.fr/quest-ce-que-le-biocontrole (accessed 3.12.21).

Mirzadi Gohari, A., Mehrabi, R., Robert, O., Ince, I.A., Boeren, S., Schuster, M., Steinberg, G., de Wit, P.J.G.M., Kema, G.H.J., 2014. Molecular characterization and functional analyses of *ZtWor1*, a transcriptional regulator of the fungal wheat pathogen *Zymoseptoria tritici*. Mol. Plant Pathol. 15, 394–405. https://doi.org/10.1111/mpp.12102

Monnier, N., Furlan, A., Botcazon, C., Dahi, A., Mongelard, G., Cordelier, S., Clément, C., Dorey, S., Sarazin, C., Rippa, S., 2018. Rhamnolipids From *Pseudomonas aeruginosa* Are Elicitors Triggering *Brassica napus* Protection Against *Botrytis cinerea* Without Physiological Disorders. Front Plant Sci 9. https://doi.org/10.3389/fpls.2018.01170

Monnier, N., Furlan, A.L., Buchoux, S., Deleu, M., Dauchez, M., Rippa, S., Sarazin, C., 2019. Exploring the Dual Interaction of Natural Rhamnolipids with Plant and Fungal Biomimetic Plasma Membranes through Biophysical Studies. Int J Mol Sci 20. https://doi.org/10.3390/ijms20051009

Motteram, J., Küfner, I., Deller, S., Brunner, F., Hammond-Kosack, K.E., Nürnberger, T., Rudd, J.J., 2009. Molecular characterization and functional analysis of MgNLP, the sole NPP1 domain-containing protein, from the fungal wheat leaf pathogen *Mycosphaerella graminicola*. Mol Plant Microbe Interact 22, 790–799. https://doi.org/10.1094/MPMI-22-7-0790

Motteram, J., Lovegrove, A., Pirie, E., Marsh, J., Devonshire, J., van de Meene, A., Hammond-Kosack, K., Rudd, J.J., 2011. Aberrant protein N-glycosylation impacts upon infection-related growth transitions of the haploid plant-pathogenic fungus *Mycosphaerella graminicola*. Mol. Microbiol. 81, 415–433. https://doi.org/10.1111/j.1365-2958.2011.07701.x

Moyne, A.L., Shelby, R., Cleveland, T.E., Tuzun, S., 2001. Bacillomycin D: an iturin with antifungal activity against *Aspergillus flavus*. J Appl Microbiol 90, 622–629. https://doi.org/10.1046/j.1365-2672.2001.01290.x

Mukherjee, P.K., Kenerley, C.M., 2010. Regulation of Morphogenesis and Biocontrol Properties in *Trichoderma virens* by a VELVET Protein, Vel1. Appl. Environ. Microbiol. 76, 2345–2352. https://doi.org/10.1128/AEM.02391-09

Nadal, M., García-Pedrajas, M.D., Gold, S.E., 2008. Dimorphism in fungal plant pathogens. FEMS Microbiol Lett 284, 127–134. https://doi.org/10.1111/j.1574-6968.2008.01173.x

Nielsen, K.F., Mogensen, J.M., Johansen, M., Larsen, T.O., Frisvad, J.C., 2009. Review of secondary metabolites and mycotoxins from the *Aspergillus niger* group. Anal Bioanal Chem 395, 1225–1242. https://doi.org/10.1007/s00216-009-3081-5

Northolt, M.D., Egmond, H.P. van, Paulsch, W.E., 1979. Ochratoxin A production by some fungal species [*Aspergillus ochraceus, Penicillium cyclopium, and Penicillium viridicatum*] in relation to water activity and temperature [on cheese and barley]. Journal of Food Protection (USA).

O'Driscoll, A., Kildea, S., Doohan, F., Spink, J., Mullins, E., 2014. The wheat-Septoria conflict: a new front opening up? Trends Plant Sci. 19, 602–610. https://doi.org/10.1016/j.tplants.2014.04.011

Omoboye, O.O., Oni, F.E., Batool, H., Yimer, H.Z., De Mot, R., Höfte, M., 2019. *Pseudomonas* Cyclic Lipopeptides Suppress the Rice Blast Fungus *Magnaporthe oryzae* by Induced Resistance and Direct Antagonism. Front Plant Sci 10. https://doi.org/10.3389/fpls.2019.00901

Ongena, M., Jacques, P., 2008. *Bacillus* lipopeptides: versatile weapons for plant disease biocontrol. Trends Microbiol. 16, 115–125. https://doi.org/10.1016/j.tim.2007.12.009

Ongena, M., Jourdan, E., Adam, A., Paquot, M., Brans, A., Joris, B., Arpigny, J.-L., Thonart, P., 2007. Surfactin and fengycin lipopeptides of *Bacillus subtilis* as elicitors of induced systemic resistance in plants. Environmental Microbiology 9, 1084–1090. https://doi.org/10.1111/j.1462-2920.2006.01202.x

Optimiser les traitements fongicides sur les maladies du feuillage de blé tendre au moyen d'un outil d'aide à la décision | Ecophytopic [WWW Document], n.d. URL https://ecophytopic.fr/piloter/optimiser-les-traitements-fongicides-sur-les-maladies-du-feuillage-de-ble-tendre-au-moyen (accessed 11.26.20).

Ors, M., Randoux, B., Siah, A., Couleaud, G., Maumené, C., Sahmer, K., Reignault, P., Halama, P., Selim, S., 2019. A Plant Nutrient- and Microbial Protein-Based Resistance Inducer Elicits Wheat Cultivar-Dependent Resistance Against *Zymoseptoria tritici*. Phytopathology® 109, 2033–2045. https://doi.org/10.1094/PHYTO-03-19-0075-R

Palma-Guerrero, J., Torriani, S.F.F., Zala, M., Carter, D., Courbot, M., Rudd, J.J., McDonald, B.A., Croll, D., 2016. Comparative transcriptomic analyses of *Zymoseptoria tritici* strains show complex lifestyle transitions and intraspecific variability in transcription profiles. Mol. Plant Pathol. 17, 845–859. https://doi.org/10.1111/mpp.12333

Pandey, V.P., Awasthi, M., Singh, S., Tiwari, S., Dwivedi, U.N., 2017. A Comprehensive Review on Function and Application of Plant Peroxidases. Biochemistry & Analytical Biochemistry 06.

Park, S.-W., Kaimoyo, E., Kumar, D., Mosher, S., Klessig, D.F., 2007. Methyl Salicylate Is a Critical Mobile Signalfor Plant Systemic Acquired Resistance. Science 318, 113–116. https://doi.org/10.1126/science.1147113

Parker, J.E., Warrilow, A.G.S., Price, C.L., Mullins, J.G.L., Kelly, D.E., Kelly, S.L., 2014. Resistance to antifungals that target CYP51. J Chem Biol 7, 143–161. https://doi.org/10.1007/s12154-014-0121-1

Perelló, A.E., Moreno, M.V., Mónaco, C., Simón, M.R., Cordo, C., 2009. Biological control of Septoria tritici blotch on wheat by *Trichoderma* spp. under field conditions in Argentina. BioControl 54, 113–122. https://doi.org/10.1007/s10526-008-9159-8

Pérez-Montaño, F., Alías-Villegas, C., Bellogín, R.A., del Cerro, P., Espuny, M.R., Jiménez-Guerrero, I., López-Baena, F.J., Ollero, F.J., Cubo, T., 2014. Plant growth promotion in cereal and leguminous agricultural important plants: From microorganism capacities to crop production. Microbiological Research 169, 325–336. https://doi.org/10.1016/j.micres.2013.09.011

Pieterse, C.M.J., Wees, S.C.M. van, Pelt, J.A. van, Knoester, M., Laan, R., Gerrits, H., Weisbeek, P.J., Loon, L.C. van, 1998. A Novel Signaling Pathway Controlling Induced Systemic Resistance in Arabidopsis. The Plant Cell 10, 1571–1580. https://doi.org/10.1105/tpc.10.9.1571

Pilet-Nayel, M.-L., Moury, B., Caffier, V., Montarry, J., Kerlan, M.-C., Fournet, S., Durel, C.-E., Delourme, R., 2017. Quantitative Resistance to Plant Pathogens in Pyramiding Strategies for Durable Crop Protection. Front. Plant Sci. 8. https://doi.org/10.3389/fpls.2017.01838

Poppe, S., Dorsheimer, L., Happel, P., Stukenbrock, E.H., 2015. Rapidly Evolving Genes Are Key Players in Host Specialization and Virulence of the Fungal Wheat Pathogen *Zymoseptoria tritici* (*Mycosphaerella graminicola*). PLOS Pathogens 11, e1005055. https://doi.org/10.1371/journal.ppat.1005055

Ptashne, M., 2008. Transcription: a mechanism for short-term memory. Curr Biol 18, R25-27. https://doi.org/10.1016/j.cub.2007.11.017

Qi, G., Zhu, F., Du, P., Yang, X., Qiu, D., Yu, Z., Chen, J., Zhao, X., 2010. Lipopeptide induces apoptosis in fungal cells by a mitochondria-dependent pathway. Peptides 31, 1978–1986. https://doi.org/10.1016/j.peptides.2010.08.003

Quaedvlieg, W., Kema, G.H.J., Groenewald, J.Z., Verkley, G.J.M., Seifbarghi, S., Razavi, M., Mirzadi Gohari, A., Mehrabi, R., Crous, P.W., 2011. *Zymoseptoria* gen. nov.: a new genus to accommodate *Septoria*-like species occurring on graminicolous hosts. Persoonia 26, 57–69. https://doi.org/10.3767/003158511X571841

Radojičić, A., Li, X., Zhang, Y., 2018. Salicylic Acid: A Double-Edged Sword for Programed Cell Death in Plants. Front. Plant Sci. 9. https://doi.org/10.3389/fpls.2018.01133

Rahman, A., Uddin, W., Wenner, N.G., 2015. Induced systemic resistance responses in perennial ryegrass against *Magnaporthe oryzae* elicited by semi-purified surfactin lipopeptides and live cells of *Bacillus amyloliquefaciens*. Molecular Plant Pathology 16, 546–558. https://doi.org/10.1111/mpp.12209

Ray, S., Anderson, J.M., Urmeev, F.I., Goodwin, S.B., 2003. Rapid induction of a protein disulfide isomerase and defense-related genes in wheat in response to the hemibiotrophic fungal pathogen *Mycosphaerella graminicola*. Plant Mol Biol 53, 741–754. https://doi.org/10.1023/B:PLAN.0000019120.74610.52

Reignault, P., Sancholle, M., 2005. Plant–pathogen interactions: will the understanding of common mechanisms lead to the unification of concepts? Comptes Rendus Biologies 328, 821–833. https://doi.org/10.1016/j.crvi.2005.07.002

Reimers, P.J., Guo, A., Leach, J.E., 1992. Increased Activity of a Cationic Peroxidase Associated with an Incompatible Interaction Between *Xanthomonas oryzae pv oryzae* and Rice (*Oryza sativa*). Plant Physiol 99, 1044–1050.

Renard-Merlier, D., Randoux, B., Nowak, E., Farcy, F., Durand, R., Reignault, P., 2007. Iodus 40, salicylic acid, heptanoyl salicylic acid and trehalose exhibit different efficacies and defence targets during a wheat/powdery mildew interaction. Phytochemistry 68, 1156–1164. https://doi.org/10.1016/j.phytochem.2007.02.011

Robert-Seilaniantz, A., Grant, M., Jones, J.D.G., 2011. Hormone crosstalk in plant disease and defense: more than just jasmonate-salicylate antagonism. Annu Rev Phytopathol 49, 317–343. https://doi.org/10.1146/annurev-phyto-073009-114447

Robineau, M., Le Guenic, S., Sanchez, L., Chaveriat, L., Lequart, V., Joly, N., Calonne, M., Jacquard, C., Declerck, S., Martin, P., Dorey, S., Ait Barka, E., 2020. Synthetic Mono-Rhamnolipids Display Direct Antifungal Effects and Trigger an Innate Immune Response in Tomato against *Botrytis Cinerea*. Molecules 25. https://doi.org/10.3390/molecules25143108

Rohel, E.A., Payne, A.C., Fraaije, B.A., Hollomon, D.W., 2001. Exploring infection of wheat and carbohydrate metabolism in *Mycosphaerella graminicola* transformants with differentially regulated green fluorescent protein expression. Mol. Plant Microbe Interact. 14, 156–163. https://doi.org/10.1094/MPMI.2001.14.2.156

Rudd, J.J., Kanyuka, K., Hassani-Pak, K., Derbyshire, M., Andongabo, A., Devonshire, J., Lysenko, A., Saqi, M., Desai, N.M., Powers, S.J., Hooper, J., Ambroso, L., Bharti, A., Farmer, A., Hammond-Kosack, K.E., Dietrich, R.A., Courbot, M., 2015. Transcriptome and Metabolite Profiling of the Infection Cycle of *Zymoseptoria tritici* on Wheat Reveals a Biphasic Interaction with Plant Immunity Involving Differential Pathogen Chromosomal Contributions and a Variation on the Hemibiotrophic Lifestyle Definition. Plant Physiol 167, 1158–1185. https://doi.org/10.1104/pp.114.255927

Rudd, J.J., Keon, J., Hammond-Kosack, K.E., 2008. The Wheat Mitogen-Activated Protein Kinases TaMPK3 and TaMPK6 Are Differentially Regulated at Multiple Levels during Compatible Disease Interactions with *Mycosphaerella graminicola*. Plant Physiol 147, 802–815. https://doi.org/10.1104/pp.108.119511

Ruiz-Herrera, J., León, C.G., Guevara-Olvera, L., Cárabez-Trejo, A., 1995. Yeast-mycelial dimorphism of haploid and diploid strains of *Ustilago maydis*. Microbiology, 141, 695–703. https://doi.org/10.1099/13500872-141-3-695

Sachdev, D.P., Cameotra, S.S., 2013. Biosurfactants in agriculture. Appl Microbiol Biotechnol 97, 1005–1016. https://doi.org/10.1007/s00253-012-4641-8

Sahli, R., Rivière, C., Siah, A., Smaoui, A., Samaillie, J., Hennebelle, T., Roumy, V., Ksouri, R., Halama, P., Sahpaz, S., 2018. Biocontrol activity of effusol from the extremophile plant, *Juncus maritimus*, against the wheat pathogen *Zymoseptoria tritici*. Environ Sci Pollut Res Int 25, 29775–29783. https://doi.org/10.1007/s11356-017-9043-0

Saintenac, C., Lee, W.-S., Cambon, F., Rudd, J.J., King, R.C., Marande, W., Powers, S.J., Bergès, H., Phillips, A.L., Uauy, C., Hammond-Kosack, K.E., Langin, T., Kanyuka, K., 2018. Wheat receptor-kinase-like protein Stb6 controls gene-for-gene resistance to fungal pathogen *Zymoseptoria tritici*. Nature Genetics 50, 368–374. https://doi.org/10.1038/s41588-018-0051-x

Samain, E., Aussenac, T., Selim, S., 2019. The Effect of Plant Genotype, Growth Stage, and *Mycosphaerella graminicola* Strains on the Efficiency and Durability of Wheat-Induced Resistance by *Paenibacillus* sp. Strain B2. Front. Plant Sci. 10. https://doi.org/10.3389/fpls.2019.00587

Sanchez, L., Courteaux, B., Hubert, J., Kauffmann, S., Renault, J.-H., Clément, C., Baillieul, F., Dorey, S., 2012. Rhamnolipids elicit defense responses and induce disease resistance against biotrophic, hemibiotrophic, and necrotrophic pathogens that require different signaling pathways in Arabidopsis and highlight a central role for salicylic acid. Plant Physiol. 160, 1630–1641. https://doi.org/10.1104/pp.112.201913

Sánchez, M., Aranda, F.J., Teruel, J.A., Espuny, M.J., Marqués, A., Manresa, A., Ortiz, A., 2010. Permeabilization of biological and artificial membranes by a bacterial dirhamnolipid produced by *Pseudomonas aeruginosa*. J Colloid Interface Sci 341, 240–247. https://doi.org/10.1016/j.jcis.2009.09.042

Sánchez-Vallet, A., Mesters, J.R., Thomma, B.P.H.J., 2015. The battle for chitin recognition in plant-microbe interactions. FEMS Microbiol Rev 39, 171–183. https://doi.org/10.1093/femsre/fuu003

Sanderson, F.R., 1972. A *Mycosphaerella* species as the Ascogenous state of *Septoria tritici* Rob. and Desm. New Zealand Journal of Botany 10, 707–709. https://doi.org/10.1080/0028825X.1972.10430256

Schellenberger, R., Touchard, M., Clément, C., Baillieul, F., Cordelier, S., Crouzet, J., Dorey, S., 2019. Apoplastic invasion patterns triggering plant immunity: plasma membrane sensing at the frontline. Mol Plant Pathol 20, 1602–1616. https://doi.org/10.1111/mpp.12857

Sen, S., Borah, S.N., Bora, A., Deka, S., 2017. Production, characterization, and antifungal activity of a biosurfactant produced by *Rhodotorula babjevae* YS3. Microb Cell Fact 16. https://doi.org/10.1186/s12934-017-0711-z

Septo-LIS® - ARVALIS - Institut du végétal [WWW Document], n.d. URL http://www.septolis.arvalisinstitutduvegetal.fr/ (accessed 11.26.20).

Serrano, M., Wang, B., Aryal, B., Garcion, C., Abou-Mansour, E., Heck, S., Geisler, M., Mauch, F., Nawrath, C., Métraux, J.-P., 2013. Export of Salicylic Acid from the Chloroplast Requires the Multidrug and Toxin Extrusion-Like Transporter EDS5. Plant Physiology 162, 1815–1821. https://doi.org/10.1104/pp.113.218156

Seybold, H., Demetrowitsch, T.J., Hassani, M.A., Szymczak, S., Reim, E., Haueisen, J., Lübbers, L., Rühlemann, M., Franke, A., Schwarz, K., Stukenbrock, E.H., 2020. A fungal pathogen induces systemic susceptibility and systemic shifts in wheat metabolome and microbiome composition. Nature Communications 11, 1910. https://doi.org/10.1038/s41467-020-15633-x

Shaw, M.W., 1987. Assessment of upward movement of rain splash using a fluorescent tracer method and its application to the epidemiology of cereal pathogens. Plant Pathology 36, 201–213. https://doi.org/10.1111/j.1365-3059.1987.tb02222.x

Shaw, M.W., Royle, D.J., 1989. Airborne inoculum as a major source of *Septoria tritici* (*Mycosphaerella graminicola*) infections in winter wheat crops in the UK. Plant Pathology 38, 35–43. https://doi.org/10.1111/j.1365-3059.1989.tb01425.x

Shetty, N.P., Jensen, J.D., Knudsen, A., Finnie, C., Geshi, N., Blennow, A., Collinge, D.B., Jørgensen, H.J.L., 2009. Effects of beta-1,3-glucan from *Septoria tritici* on structural defence responses in wheat. J. Exp. Bot. 60, 4287–4300. https://doi.org/10.1093/jxb/erp269

Shetty, N.P., Kristensen, B.K., Newman, M.-A., Møller, K., Gregersen, P.L., Jørgensen, H.J.L., 2003. Association of hydrogen peroxide with restriction of *Septoria tritici* in resistant wheat. Physiological and Molecular Plant Pathology 62, 333–346. https://doi.org/10.1016/S0885-5765(03)00079-1

Shetty, N.P., Mehrabi, R., Lütken, H., Haldrup, A., Kema, G.H.J., Collinge, D.B., Jørgensen, H.J.L., 2007. Role of hydrogen peroxide during the interaction between the hemibiotrophic fungal pathogen *Septoria tritici* and wheat. New Phytol. 174, 637–647. https://doi.org/10.1111/j.1469-8137.2007.02026.x

Shewry, P.R., 2009. Wheat. J. Exp. Bot. 60, 1537–1553. https://doi.org/10.1093/jxb/erp058

Shimizu, T., Nakano, T., Takamizawa, D., Desaki, Y., Ishii-Minami, N., Nishizawa, Y., Minami, E., Okada, K., Yamane, H., Kaku, H., Shibuya, N., 2010. Two LysM receptor molecules, CEBiP and OsCERK1, cooperatively

regulate chitin elicitor signaling in rice. Plant J 64, 204–214. https://doi.org/10.1111/j.1365-313X.2010.04324.x

Shipton, W.A., Boyd, W.R.J., Rosielle, A.A., Shearer, B.I., 1971. The common Septoria diseases of wheat. Bot. Rev 37, 231–262. https://doi.org/10.1007/BF02858957

Shtienberg, D. (The H.U. of J., 1992. Effects of foliar diseases on gas exchange processes: a comparative study. Phytopathology (USA).

Siah, A., Bomble, M., Tisserant, B., Cadalen, T., Holvoet, M., Hilbert, J.-L., Halama, P., Reignault, P., 2018a. Genetic Structure of *Zymoseptoria tritici* in Northern France at Region, Field, Plant, and Leaf Layer Scales. Phytopathology 108, 1114–1123. https://doi.org/10.1094/PHYTO-09-17-0322-R

Siah, A., Deweer, C., Duyme, F., Sanssené, J., Durand, R., Halama, P., Reignault, P., 2010. Correlation of in planta endo-beta-1,4-xylanase activity with the necrotrophic phase of the hemibiotrophic fungus *Mycosphaerella graminicola*. Plant Pathology 59, 661–670. https://doi.org/10.1111/j.1365-3059.2010.02303.x

Siah, A., Magnin-Robert, M., Randoux, B., Choma, C., Rivière, C., Halama, P., Reignault, P., 2018b. Natural Agents Inducing Plant Resistance Against Pests and Diseases, in: Mérillon, J.-M., Riviere, C. (Eds.), Natural Antimicrobial Agents, Sustainable Development and Biodiversity. Springer International Publishing, Cham, pp. 121–159. https://doi.org/10.1007/978-3-319-67045-4_6

Sibounnavong, P., Charoenporn, C., Kanokmedhakul, S., Soytong, K., 2011. Antifungal metabolites from antagonistic fungi used to control tomato wilt fungus *Fusarium oxysporum* f. sp. *lycopersici*. African Journal of Biotechnology 10, 19714–19722. https://doi.org/10.4314/ajb.v10i85

Siciliano, I., Bosio, P., Gilardi, G., Gullino, M.L., Garibaldi, A., 2017. Verrucarin A and roridin E produced on spinach by *Myrothecium verrucaria* under different temperatures and CO2 levels. Mycotoxin Res 33, 139–146. https://doi.org/10.1007/s12550-017-0273-2

Simón, M.R., Cordo, C.A., Perelló, A.E., Struik, P.C., 2003. Influence of Nitrogen Supply on the Susceptibility of Wheat to *Septoria tritici*. Journal of Phytopathology 151, 283–289. https://doi.org/10.1046/j.1439-0434.2003.00720.x

Singh, P., Patil, Y., Rale, V., 2019. Biosurfactant production: emerging trends and promising strategies. J Appl Microbiol 126, 2–13. https://doi.org/10.1111/jam.14057

Skamnioti, P., Gurr, S.J., 2009. Against the grain: safeguarding rice from rice blast disease. Trends in Biotechnology 27, 141–150. https://doi.org/10.1016/j.tibtech.2008.12.002

Smartbiocontrol : Présentation générale, n.d. URL http://www.smartbiocontrol.eu/fr/presentation-generale/ (accessed 3.1.21)

Snape, J.W., Pánková, K., 2013. *Triticum Aestivum L* (Wheat), in: ELS. American Cancer Society. https://doi.org/10.1002/9780470015902.a0003691.pub2

Sorenson, W.G., Sneller, M.R., Larsh, H.W., 1975. Qualitative and Quantitative Assay of Trichothecin: a Mycotoxin Produced by *Trichothecium roseum*. Appl. Environ. Microbiol. 29, 653–657.

Souza, A.C.O., Taborda, C.P., 2020. Epidemiology of Dimorphic Fungi☆, in: Reference Module in Life Sciences. Elsevier. https://doi.org/10.1016/B978-0-12-809633-8.12056-4

Stanghellini, M.E., Miller, R.M., 1997. BIOSURFACTANTS: Their Identity and Potential Efficacy in the Biological Control of Zoosporic Plant Pathogens. Plant Disease 81, 4–12. https://doi.org/10.1094/PDIS.1997.81.1.4

Steinberg, G., 2015. Cell biology of *Zymoseptoria tritici*: Pathogen cell organization and wheat infection. Fungal Genet Biol 79, 17–23. https://doi.org/10.1016/j.fgb.2015.04.002

Steinberg, G., Schuster, M., Gurr, S.J., Schrader, T.A., Schrader, M., Wood, M., Early, A., Kilaru, S., 2020. A lipophilic cation protects crops against fungal pathogens by multiple modes of action. Nature Communications 11, 1608. https://doi.org/10.1038/s41467-020-14949-y

Steppuhn, A., Baldwin, I.T., 2008. Induced Defenses and the Cost-Benefit Paradigm, in: Schaller, A. (Ed.), Induced Plant Resistance to Herbivory. Springer Netherlands, Dordrecht, pp. 61–83. https://doi.org/10.1007/978-1-4020-8182-8_3

Stergiopoulos, I., Zwiers, L.-H., De Waard, M.A., 2003. The ABC Transporter MgAtr4 Is a Virulence Factor of *Mycosphaerella graminicola* that Affects Colonization of Substomatal Cavities in Wheat Leaves. MPMI 16, 689–698. https://doi.org/10.1094/MPMI.2003.16.8.689

Stewart, E. l, Croll, D., Lendenmann, M.H., Sanchez-Vallet, A., Hartmann, F.E., Palma-Guerrero, J., Ma, X., McDonald, B.A., 2018. Quantitative trait locus mapping reveals complex genetic architecture of quantitative virulence in the wheat pathogen *Zymoseptoria tritici*. Molecular Plant Pathology 19, 201–216. https://doi.org/10.1111/mpp.12515

Stocco, M.C., Mónaco, C.I., Abramoff, C., Lampugnani, G., Salerno, G., Kripelz, N., Cordo, C.A., Consolo, V.F., 2016. Selection and characterization of Argentine isolates of *Trichoderma harzianum* for effective biocontrol of Septoria leaf blotch of wheat. World J Microbiol Biotechnol 32, 49. https://doi.org/10.1007/s11274-015-1989-9

Strawn, M.A., Marr, S.K., Inoue, K., Inada, N., Zubieta, C., Wildermuth, M.C., 2007. Arabidopsis Isochorismate Synthase Functional in Pathogen-induced Salicylate Biosynthesis Exhibits Properties Consistent with a Role in Diverse Stress Responses. J. Biol. Chem. 282, 5919–5933. https://doi.org/10.1074/jbc.M605193200

Strieker, M., Tanović, A., Marahiel, M.A., 2010. Nonribosomal peptide synthetases: structures and dynamics. Current Opinion in Structural Biology, Theory and simulation / Macromolecular assemblages 20, 234–240. https://doi.org/10.1016/j.sbi.2010.01.009

Stukenbrock, E.H., Banke, S., Javan-Nikkhah, M., McDonald, B.A., 2007. Origin and domestication of the fungal wheat pathogen *Mycosphaerella graminicola* via sympatric speciation. Mol. Biol. Evol. 24, 398–411. https://doi.org/10.1093/molbev/msl169

Suffert, F., Sache, I., Lannou, C., 2011. Early stages of septoria tritici blotch epidemics of winter wheat: build-up, overseasoning, and release of primary inoculum. Plant Pathology 60, 166–177. https://doi.org/10.1111/j.1365-3059.2010.02369.x

Tabib Ghaffary, S.M., Faris, J.D., Friesen, T.L., Visser, R.G.F., van der Lee, T.A.J., Robert, O., Kema, G.H.J., 2012. New broad-spectrum resistance to septoria tritici blotch derived from synthetic hexaploid wheat. Theor Appl Genet 124, 125–142. https://doi.org/10.1007/s00122-011-1692-7

Tackenberg, M., Volkmar, C., Dammer, K.-H., 2016. Sensor-based variable-rate fungicide application in winter wheat. Pest Manag Sci 72, 1888–1896. https://doi.org/10.1002/ps.4225

Testa, A., Oliver, R., Hane, J., 2015. Overview of genomic and bioinformatic resources for *Zymoseptoria tritici*. Fungal Genetics and Biology, Septoria tritici blotch disease of wheat: Tools and techniques to study the pathogen Zymoseptoria tritici 79, 13–16. https://doi.org/10.1016/j.fgb.2015.04.011

Thaler, J.S., Humphrey, P.T., Whiteman, N.K., 2012. Evolution of jasmonate and salicylate signal crosstalk. Trends in Plant Science, Special Issue: Specificity of plant–enemy interactions 17, 260–270. https://doi.org/10.1016/j.tplants.2012.02.010

Thordal-Christensen, H., Zhang, Z., Wei, Y., Collinge, D.B., 1997. Subcellular localization of H2O2 in plants. H2O2 accumulation in papillae and hypersensitive response during the barley—powdery mildew interaction. The Plant Journal 11, 1187–1194. https://doi.org/10.1046/j.1365-313X.1997.11061187.x

Tiley, A.M.M., White, H.J., Foster, G.D., Bailey, A.M., 2019. The *ZtvelB* Gene Is Required for Vegetative Growth and Sporulation in the Wheat Pathogen *Zymoseptoria tritici*. Front Microbiol 10. https://doi.org/10.3389/fmicb.2019.02210

Torriani, S.F.F., Melichar, J.P.E., Mills, C., Pain, N., Sierotzki, H., Courbot, M., 2015. *Zymoseptoria tritici*: A major threat to wheat production, integrated approaches to control. Fungal Genetics and Biology, Septoria tritici blotch disease of wheat: Tools and techniques to study the pathogen Zymoseptoria tritici 79, 8–12. https://doi.org/10.1016/j.fgb.2015.04.010

UMR Transfrontalière BioEcoAgro (www.bioecoagro.eu) - Gouvernance [WWW Document], n.d. URL https://www.bioecoagro.eu/umrt-bioecoagro_fre/Gouvernance (accessed 4.22.21).

Van Loon, L.C., Pierpoint, W.S., Boller, Th., Conejero, V., 1994. Recommendations for naming plant pathogenesis-related proteins. Plant Mol Biol Rep 12, 245–264. https://doi.org/10.1007/BF02668748

Varnier, A.-L., Sanchez, L., Vatsa, P., Boudesocque, L., Garcia-Brugger, A., Rabenoelina, F., Sorokin, A., Renault, J.-H., Kauffmann, S., Pugin, A., Clement, C., Baillieul, F., Dorey, S., 2009. Bacterial rhamnolipids are novel MAMPs conferring resistance to *Botrytis cinerea* in grapevine. Plant Cell Environ. 32, 178–193. https://doi.org/10.1111/j.1365-3040.2008.01911.x

Vatsa, P., Sanchez, L., Clement, C., Baillieul, F., Dorey, S., 2010. Rhamnolipid Biosurfactants as New Players in Animal and Plant Defense against Microbes. Int J Mol Sci 11, 5095–5108. https://doi.org/10.3390/ijms11125095

Veses, V., Gow, N.A.R., 2009. Pseudohypha budding patterns of *Candida albicans*. Med Mycol 47, 268–275. https://doi.org/10.1080/13693780802245474

Vidhyasekaran, P., 2015. Salicylic Acid Signaling in Plant Innate Immunity, in: Vidhyasekaran, P. (Ed.), Plant Hormone Signaling Systems in Plant Innate Immunity, Signaling and Communication in Plants. Springer Netherlands, Dordrecht, pp. 27–122. https://doi.org/10.1007/978-94-017-9285-1_2

Vishwakarma, K., Upadhyay, N., Kumar, N., Yadav, G., Singh, J., Mishra, R.K., Kumar, V., Verma, R., Upadhyay, R.G., Pandey, M., Sharma, S., 2017. Abscisic Acid Signaling and Abiotic Stress Tolerance in Plants: A Review on Current Knowledge and Future Prospects. Front Plant Sci 8. https://doi.org/10.3389/fpls.2017.00161

Waewthongrak, W., Leelasuphakul, W., McCollum, G., 2014. Cyclic Lipopeptides from *Bacillus subtilis* ABS–S14 Elicit Defense-Related Gene Expression in Citrus Fruit. PLOS ONE 9, e109386. https://doi.org/10.1371/journal.pone.0109386

Walters, D.R., Bennett, A.E., 2014. Microbial Induction of Resistance to Pathogens, in: Induced Resistance for Plant Defense. John Wiley & Sons, Ltd, pp. 149–170. https://doi.org/10.1002/9781118371848.ch8

Walters, D.R., Havis, N.D., Oxley, S.J.P., 2008. *Ramularia collo-cygni*: the biology of an emerging pathogen of barley. FEMS Microbiol Lett 279, 1–7. https://doi.org/10.1111/j.1574-6968.2007.00986.x

Wang, X., Tang, C., Deng, L., Cai, G., Liu, X., Liu, B., Han, Q., Buchenauer, H., Wei, G., Han, D., Huang, L., Kang, Z., 2010. Characterization of a pathogenesis-related thaumatin-like protein gene *TaPR5* from wheat induced by stripe rust fungus. Physiol Plant 139, 27–38. https://doi.org/10.1111/j.1399-3054.2009.01338.x

Wasternack, C., Hause, B., 2013. Jasmonates: biosynthesis, perception, signal transduction and action in plant stress response, growth and development. An update to the 2007 review in Annals of Botany. Ann Bot 111, 1021–1058. https://doi.org/10.1093/aob/mct067

Wenham, H.T., 1959. Studies on septaria leaf blotch disease of wheat (*Triticum aestivum L.*) caused by *Septoria tritici* Desm. New Zealand Journal of Agricultural Research 2, 208–213. https://doi.org/10.1080/00288233.1959.10420304

Williams, J.R., Jones, D.G., 1973. Infection of grasses by *Septoria nodorum* and *S. tritici*. Transactions of the British Mycological Society 60, 355–358. https://doi.org/10.1016/S0007-1536(73)80019-1

Wittenberg, A.H.J., Lee, T.A.J. van der, M'Barek, S.B., Ware, S.B., Goodwin, S.B., Kilian, A., Visser, R.G.F., Kema, G.H.J., Schouten, H.J., 2009. Meiosis Drives Extraordinary Genome Plasticity in the Haploid Fungal Plant Pathogen *Mycosphaerella graminicola*. PLOS ONE 4, e5863. https://doi.org/10.1371/journal.pone.0005863

Yamamoto, S., Shiraishi, S., Suzuki, S., 2015. Are cyclic lipopeptides produced by *Bacillus amyloliquefaciens* S13-3 responsible for the plant defence response in strawberry against *Colletotrichum gloeosporioides*? Lett Appl Microbiol 60, 379–386. https://doi.org/10.1111/lam.12382

Yang, F., Li, W., Jørgensen, H.J.L., 2013. Transcriptional reprogramming of wheat and the hemibiotrophic pathogen *Septoria tritici* during two phases of the compatible interaction. PLoS One 8, e81606. https://doi.org/10.1371/journal.pone.0081606

Yang, H., Yu, H., Ma, L.-J., 2020. Accessory Chromosomes in *Fusarium oxysporum*. Phytopathology® 110, 1488–1496. https://doi.org/10.1094/PHYTO-03-20-0069-IA

Yemelin, A., Brauchler, A., Jacob, S., Laufer, J., Heck, L., Foster, A.J., Antelo, L., Andresen, K., Thines, E., 2017. Identification of factors involved in dimorphism and pathogenicity of *Zymoseptoria tritici*. PLOS ONE 12, e0183065. https://doi.org/10.1371/journal.pone.0183065

Yoshida, S., Koitabashi, M., Nakamura, J., Fukuoka, T., Sakai, H., Abe, M., Kitamoto, D., Kitamoto, H., 2015. Effects of biosurfactants, mannosylerythritol lipids, on the hydrophobicity of solid surfaces and infection behaviours of plant pathogenic fungi. Journal of Applied Microbiology 119, 215–224. https://doi.org/10.1111/jam.12832

Zadoks, J.C., Chang, T.T., Konzak, C.F., 1974. A decimal code for the growth stages of cereals. Weed Research 14, 415–421.

Zhan, J., Pettway, R.E., McDonald, B.A., 2003. The global genetic structure of the wheat pathogen *Mycosphaerella graminicola* is characterized by high nuclear diversity, low mitochondrial diversity, regular recombination, and gene flow. Fungal Genetics and Biology 38, 286–297. https://doi.org/10.1016/S1087-1845(02)00538-8

Zhan, J., Stefanato, F.L., McDonald, B.A., 2006. Selection for increased cyproconazole tolerance in *Mycosphaerella graminicola* through local adaptation and in response to host resistance. Molecular Plant Pathology 7, 259–268. https://doi.org/10.1111/j.1364-3703.2006.00336.x

ANNEXES

ANNEXE 1 : RÉSULTATS DU CRIBLAGE DES COMPOSÉS POUR LEUR ACTIVITÉ ANTIFONGIQUE *IN VITRO*

L'activité antifongique des surnageants fongiques et bactériens ainsi que des métabolites purifiés ou synthétisés par chimie verte a été déterminée *in vitro*. Les tests concernant les extraits fongiques ont été réalisés en plaques 96-puits **(Figure 1)** alors que ceux pour les autres composés ont été effectués en boîtes de Petri. L'ensemble des résultats est présenté dans le **Tableau 1.**

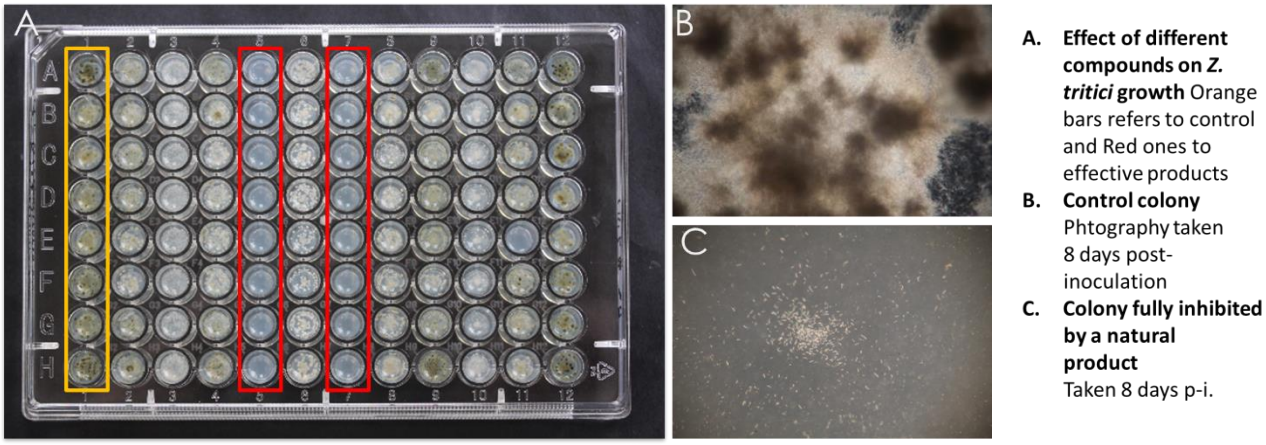

Figure supplémentaire 1 : Photographie illustrant l'évaluation *in vitro* de l'activité antifongique des extraits fongiques fournis par l'Université Catholique de Louvain en microplaque 96-puits.

Tableau supplémentaire 1 : Activité antifongique *in vitro* des 181 composés testés à une seule concentration.

Composés	Concentration	Inhibition de la croissance de *Z. tritici in vitro*
Extraits fongiques		
Aspergillus niger	30%	100%
Lecanicillium longisporum	30%	100%
Paecilomyces lilacinus	30%	100%
Penicillium aurantiogriseum	30%	100%
Penicillium brevicompactum	30%	100%
Penicillium griseofulvum	30%	100%
Trichoderma Virens	30%	100%
Trichothecium roseum	30%	100%
Myrothecium verrucaria	30%	100%
Laetiporus sulphureus	30%	100%
Penicillium cyclopium	30%	100%
Chaetomium globosum	30%	80%-99%
Emericella rugulosa	30%	80%-99%
Penicillium purpurogenum	30%	80%-99%
Sporothrix insectorum	30%	80%-99%
Talaromyces flavus	30%	80%-99%
Aspergillus flavus	30%	80%-99%
Beauveria brongniartii	30%	80%-99%
Hypomyces chrysospermus	30%	80%-99%

Chaetomium globosum2	30%	80%-99%
Hypomyces rosellus	30%	80%-99%
Penicillium funiculosum	30%	80%-99%
Penicillium viridicatum	30%	80%-99%
Dacrymyces stillatus	30%	50%-79%
Paecilomyces farinosus	30%	50%-79%
Chaetomium cochliodes	30%	50%-79%
Chondrostereum purpureum	30%	50%-79%
Fusarium proliferatum	30%	50%-79%
Fusarium oxysporum	30%	50%-79%
Metarhizium anisopliae	30%	50%-79%
Sordaria fimicola	30%	50%-79%
Trichoderma koningii	30%	50%-79%
Trichoderma polysporum	30%	50%-79%
Ulocladium atrum	30%	50%-79%
Candida ethanolica	30%	50%-79%
Colletotrichum coccodes	30%	50%-79%
Trichoderma pseudokoningii	30%	50%-79%
Trichoderma arundinaceum	30%	50%-79%
Acremonium alternatum	30%	0%-49%
Alternaria alternata	30%	0%-49%
Ascoidea hylecoeti	30%	0%-49%
Aspergillus ustus	30%	0%-49%
Aureobasidium pullulans	30%	0%-49%
Beauveria bassiana	30%	0%-49%
Beauveria felina	30%	0%-49%
Botrytis cinerea	30%	0%-49%
Bulleromyces albus	30%	0%-49%
Candida glabrata	30%	0%-49%
Candida melibiosica	30%	0%-49%
Candida parapsilosis	30%	0%-49%
Candida tenuis	30%	0%-49%
Candida butyri	30%	0%-49%
Candida oleophila	30%	0%-49%
Candida saitoana	30%	0%-49%
Candida sake	30%	0%-49%
Cephaloascus fragrans	30%	0%-49%
Chaetomium cupreum	30%	0%-49%
Chaetomium cupreum2	30%	0%-49%
Cladosporium cladosporioides	30%	0%-49%
Cladosporium fulvum	30%	0%-49%
Clonostachys compactiuscula	30%	0%-49%
Coniothyrium concentricum	30%	0%-49%
Cryptococcus flavescens	30%	0%-49%
Dioszegia hungarica	30%	0%-49%
Drechslera poae	30%	0%-49%
Emericella nidulans	30%	0%-49%
Epicoccum nigrum	30%	0%-49%
Epicoccum purpurascens	30%	0%-49%
Fellomyces polyborus	30%	0%-49%
Filobasidium floriforme	30%	0%-49%
Fusarium chlamydosporum	30%	0%-49%

Fusarium culmorum	30%	0%-49%
Fusarium graminearum	30%	0%-49%
Galactomyces geotrichum	30%	0%-49%
Gliocladium catenulatum	30%	0%-49%
Hanseniaspora uvarum	30%	0%-49%
Hansfordia pulvinata	30%	0%-49%
Hyalodendron lignicola	30%	0%-49%
Hypholoma fasciculare	30%	0%-49%
Hypocrea pachybasioides	30%	0%-49%
Irpex lacteus	30%	0%-49%
Lecanicillium dimorphum	30%	0%-49%
Melanospora argentinensis	30%	0%-49%
Metarhizium anisopliae var. majus	30%	0%-49%
Metschnikowia fructicola	30%	0%-49%
Microdochium bolleyi	30%	0%-49%
Nectria ochroleuca	30%	0%-49%
Nigrospora sacchari	30%	0%-49%
Metschnikowia pulcherrima	30%	0%-49%
Paecilomyces fumorosoroseus	30%	0%-49%
Galactomyces geotrichum	30%	0%-49%
Penicillium striatisporum	30%	0%-49%
Pestalotiopsis disseminata	30%	0%-49%
Phlebiopsis spissa	30%	0%-49%
Phytophthora cryptogea	30%	0%-49%
Pleurotus ostreatus	30%	0%-49%
Pseudozyma fusiformata	30%	0%-49%
Pyricularia oryzae	30%	0%-49%
Pythium aphanidermatum	30%	0%-49%
Rhizoctonia solani	30%	0%-49%
Rhodosporidium paludigenum	30%	0%-49%
Rhodotorula glutinis	30%	0%-49%
Laetarsia fuciformis	30%	0%-49%
Rhodotorula mucilaginosa	30%	0%-49%
Saccharomyces cerevisiae	30%	0%-49%
Sclerotinia minor	30%	0%-49%
Trametes versicolor	30%	0%-49%
Trichoderma asperellum	30%	0%-49%
Trichoderma atroviride	30%	0%-49%
Trichoderma hamatum	30%	0%-49%
Trichoderma harzianum	30%	0%-49%
Trichoderma longibrachiatum	30%	0%-49%
Ulocladium oudemansii	30%	0%-49%
Verticillium chlamydosporium	30%	0%-49%
Verticillium lecanii	30%	0%-49%
Alternaria longipes	30%	0%-49%
Aphanocladium album	30%	0%-49%
Chaetomium piluliferum	30%	0%-49%
Cladosporium herbarum	30%	0%-49%
Clonostachys rosea	30%	0%-49%
Rhodosporidium diobovatum	30%	0%-49%
Cylindrocarpon destructans	30%	0%-49%
Heteroconium chaetospira	30%	0%-49%

Nomuraea rileyi	30%	0%-49%
Ochroconis constricta	30%	0%-49%
Penicillium frequentans	30%	0%-49%
Penicillium oxalicum	30%	0%-49%
Waitea circinata	30%	0%-49%
Tilletiopsis pallescens	30%	0%-49%
Trichoderma reesei	30%	0%-49%
Trichoderma viride	30%	0%-49%
Pythium ultimum	30%	0%-49%
Pleurotus eryngii	30%	0%-49%
Pleurotus pulmonarius	30%	0%-49%
Coprinus comatus	30%	0%-49%
Oudemansiella mucida	30%	0%-49%
Nigrospora sphaerica	30%	0%-49%
Acremonium sordidulum	30%	0%-49%
Ampelomyces quisqualis	30%	0%-49%
Coniothyrium minitans	30%	0%-49%
Moesziomyces rugulosus	30%	0%-49%
Pythium oligandrum	30%	0%-49%
Phlebiopsis gigantea	30%	0%-49%
Iriformospora indica	30%	0%-49%
Verticillium biguttatum	30%	0%-49%
Stachybotrys bisbyi	30%	0%-49%
Extraits bactériens		
***Bacillus velezensis* S1**	30%	100%
***Bacillus velezensis* S6**	30%	100%
***Paenibacillus polymyxa* M2**	30%	100%
***Paenibacillus polymyxa* AMESA**	30%	100%
***Bacillus amyloliquefaciens* I3**	30%	100%
Lipodepsipeptides cycliques purifiés		
N1	50 $\mu g.ml^{-1}$	0%
N2	50 $\mu g.ml^{-1}$	0%
N8	50 $\mu g.ml^{-1}$	0%
WLIP	50 $\mu g.ml^{-1}$	0%
Orfamide	50 $\mu g.ml^{-1}$	0%
Putisolvin	50 $\mu g.ml^{-1}$	0%
Lokisin	50 $\mu g.ml^{-1}$	0%
Xantholysin	50 $\mu g.ml^{-1}$	0%
Rhamnolipides et molécules associées		
Rhamnolipides naturels	1500 µM	0%
Rh-Eth-C4	1500 µM	0%
Rh-Eth-C6	1500 µM	0%
Rh-Eth-C8	1500 µM	0%
Rh-Eth-C10	1500 µM	100%
Rh-Eth-C12	1500 µM	100%
Rh-Eth-C14	1500 µM	0%
Rh-Eth-C16	1500 µM	0%
Rh-Eth-C18	1500 µM	0%
Rh-Est-C8	1500 µM	0%
Rh-Est-C10	1500 µM	0%
Rh-Est-C12	1500 µM	100%
Rh-Suc-C8	1500 µM	100%

Rh-Suc-C12	1500 µM	0%
Rh-Suc-C12b	1500 µM	0%
Rh-Suc-C8-C8	1500 µM	0%
Rh-Suc-C8-C12	1500 µM	0%
Rh-Suc-C12-C8	1500 µM	0%
Rh-Suc-C12-C12	1500 µM	0%
Acide laurique	1500 µM	100%
Dodécanol	1500 µM	100%
Liopeptide cyclique purifié		
Mycosubtiline	50 $\mu g.ml^{-1}$	100%

ANNEXE 2 : COMPARAISON DES ACTIVITÉS BIOLOGIQUES DES RHAMNOLIPIDES ENTRE LES PATHOSYSTÈMES BLÉ-*ZYMOSEPTORIA TRITICI* ET RIZ-*MAGNAPORTE ORYZAE*

Tableau supplémentaire 2 : Résumé des activités biologiques du mix de rhamnolipides produits par *Pseudomonas aeruginosa* et du Rh-Est-C12 observées sur les pathosystèmes riz-*Magnaporte oryzae* et blé-*Zymoseptoria tritici*

Compound	**Natural Rhamnolipids**				**Rh-Est-C12**			
Pathosystem	Rice-*M. oryzae*		Wheat-*Z. tritici*		Rice-*M. oryzae*		Wheat-*Z. tritici*	
Concentration (µM)	50	200	50	200	50	200	50	200
***In vitro* antifungal assays**								
Spore germination	+	+	0	0	0	+	0	+
Appressorium formation	+/0	+/0	Nd*	Nd*	+	+	Nd*	Nd*
Mycelium growth	+	+	Nd*	Nd*	0	+	Nd*	Nd*
Spore cell leakage	0	0	0	0	0	0	0	+
Mycelium cell leakage	0	0	Nd*	Nd*	0	+	Nd*	Nd*
***In planta* fungal spore and rhamnolipid co-application**								
Spore germination	In progress	In progress	0	0	In progress	In progress	+	+
Disease severity	+	+	0	0	+	+	+	+
Callose deposition	In progress	In progress	In progress	In progress	In progress	In progress	In progress	In progress
ROS production	In progress	In progress	In progress	In progress	In progress	In progress	In progress	In progress
***In planta* rhamnolipid root application**								
Disease severity	+	+	0	0	+	+	+	+

Avec (+) effet significatif observé, (0) sans effet significatif observé et (+/0) effet à vérifier. (Nd*) Les analyses indiquées n'ont pas pu être réalisées avec *Z. tritici* car ce champignon ne forme pas d'appressorium et se développe *in vitro* avec une morphologie de type levure, ne produisant pas de mycélium dans ces conditions.

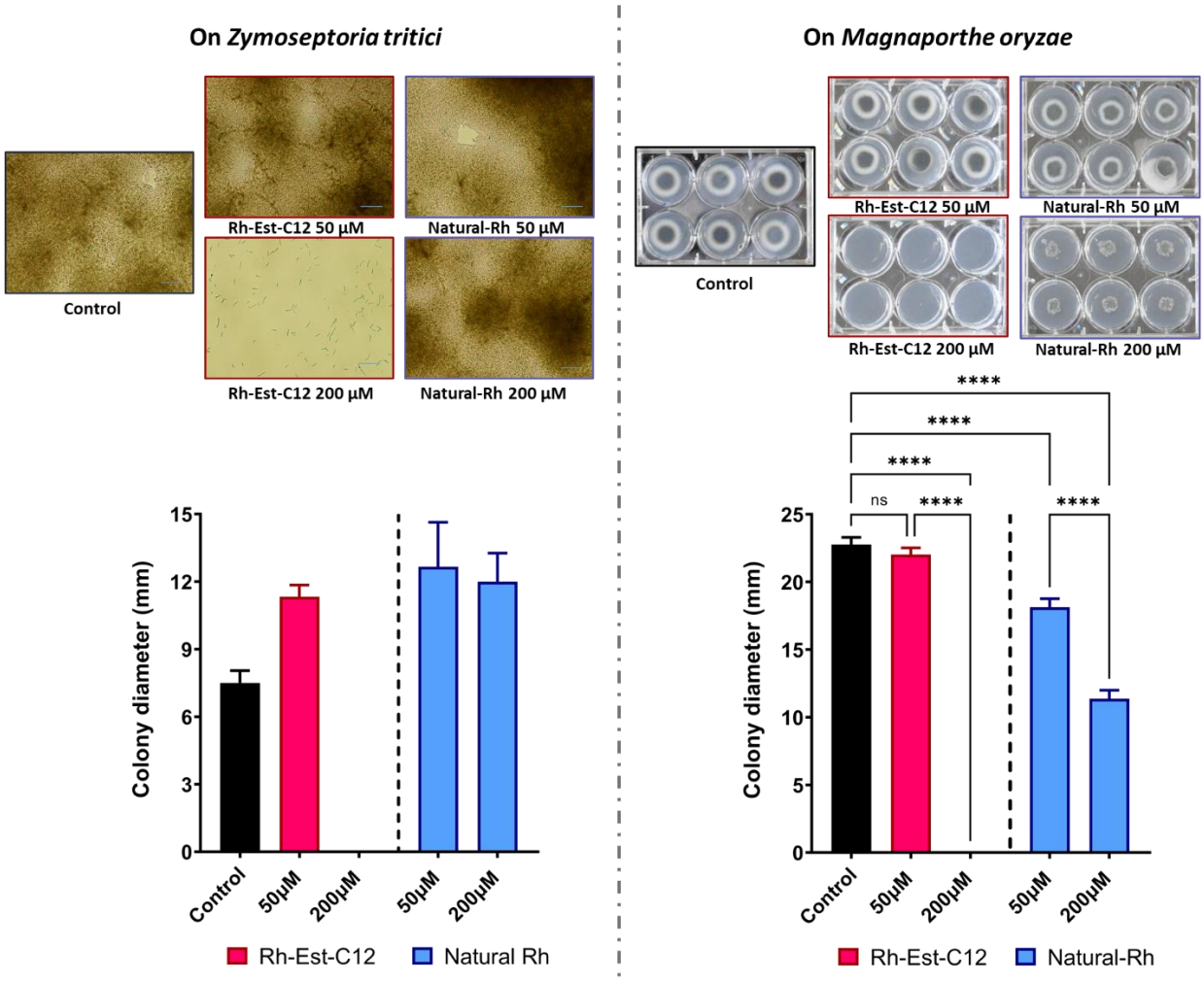

Figure supplémentaire 2 : Activité antifongique in vitro du Rh-Est-C12 et du mix de rhamnolipides produits par *Pseudomonas aeruginosa* vis-à-vis de *Z. tritici* (à gauche) et *M. oryzae* (à droite). Les photographies de *Z. tritici* ont été prises 3 jours après inoculation au microscope avec une magnification X10 et les mesures des diamètres des colonies de ce champignon ont été réalisées 10 jours après inoculation avec des spores de *Z. tritici* ($5x10^5$ spores.mL^{-1}). Les photographies et mesures des diamètres des colonies de *M. oryzae* ont été réalisées 5 jours après inoculation ($5x10^4$ spores.mL^{-1}). Les barres d'erreur des graphiques représentent les écarts-types. Les analyses statistiques ont consisté en une Anova One-way sur chaque jeu de données suivi par un test de Tukey. Les **** correspondent à des différences significatives ($P < 0.0001$).

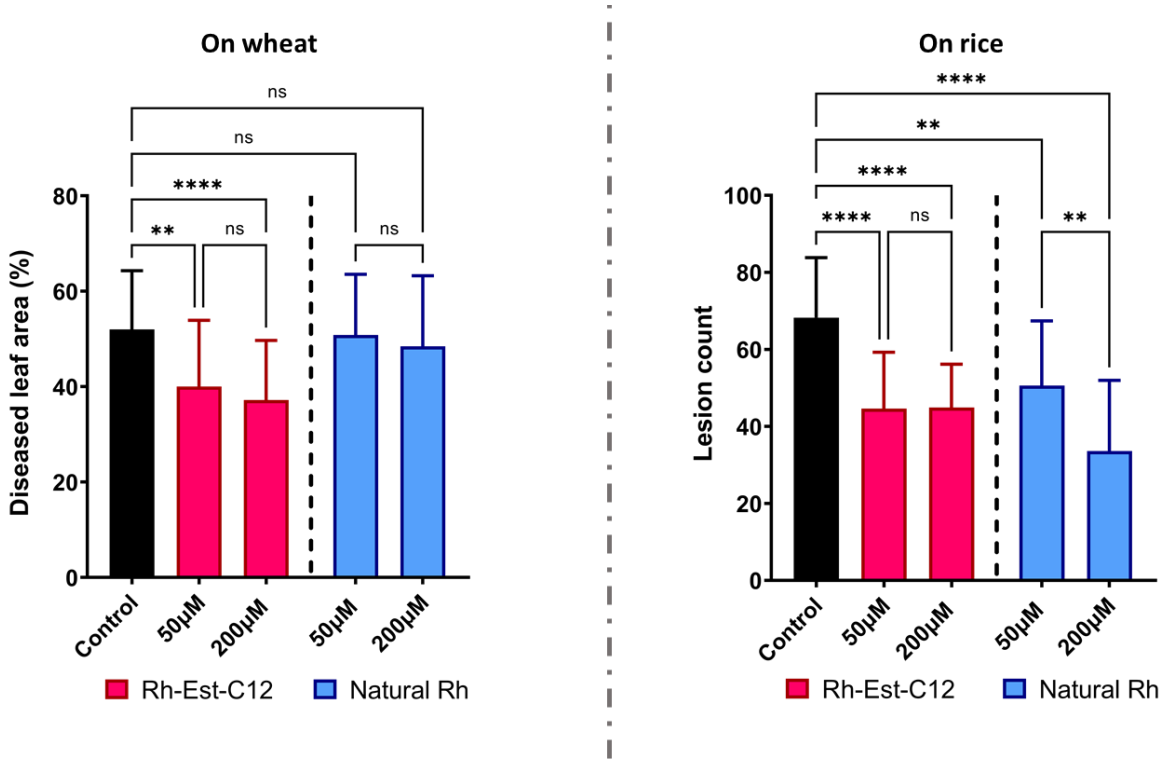

Figure supplémentaire 3 : Effet de la co-inoculation de spores de *Z. tritici* ou de *M. oryzae* avec différents rhamnolipides sur la sévérité de leur infection. L'activité in planta des composés sur blé a été déterminée 21 jours après leur co-application avec les spores fongiques ($10x10^5$ spores.mL^{-1}) en mesurant le pourcentage de lésions chlorotiques et nécrotiques sur les troisièmes feuilles de chaque plante. La quantité de lésions sur les feuilles de riz a été déterminée 6 jours après co-application des spores de M. oryzae ($5x10^4$ spores.mL^{-1}) avec les rhamnolipides sur les deuxièmes feuilles de chaque plante. Les barres d'erreur des graphiques représentent les écarts-types. Les analyses statistiques ont consisté en une Anova One-way sur chaque jeu de données suivi par un test de Tukey. Les ** correspondent aux différences significatives entre conditions ($P < 0.01$) et **** ($P < 0.0001$).

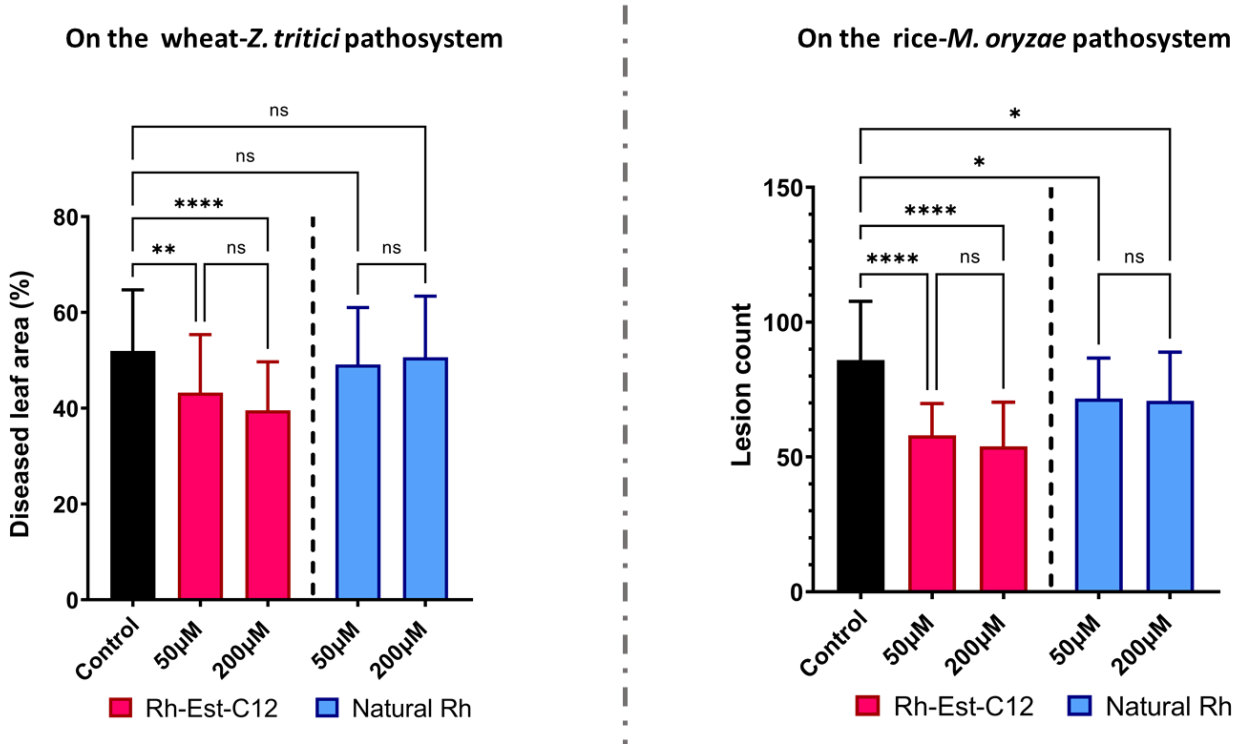

Figure supplémentaire 4 : Effet de l'application racinaire du Rh-Est-C12 et du mix de rhamnolipides produits par *Pseudomonas aeruginosa* sur la protection du blé et du riz vis-à-vis, respectivement, de *Z. tritici* (à gauche) et *M. oryzae* (à droite). Avant semis, le sol a été mélangé avec les rhamnolipides aux concentrations indiquées et les graines pré-germées de blé comme de riz ont été plongées dans une solution contentant le rhamnolipide à la concentration testée. Trois jours avant inoculation avec l'agent pathogène, les rhamnolipides ont été appliqués une nouvelle fois au niveau du sol. Le pourcentage de lésions chlorotiques et nécrotiques sur les troisièmes feuilles de chaque plant de blé a été déterminé 21 jours après infection avec les spores de *Z. tritici* ($10x10^5$ spores.mL^{-1}). La quantité de lésions sur les feuilles de riz a été déterminée 6 jours après infection avec les spores de *M. oryzae* ($5x10^4$ spores.mL^{-1}) sur les deuxièmes feuilles de chaque plante. Les barres d'erreur des graphiques représentent les écarts-types. Les analyses statistiques ont consisté en une Anova One-way sur chaque jeu de données suivi par un test de Tukey. Les * correspondent aux différences significatives entre conditions ($P < 0.05$), ** ($P < 0.05$) et **** ($P < 0.0001$).